COLLAPSE OF STEAM BUBBLES

IN SUBCOOLED WATER

by

MUSTAFA OSMAN ISIKAN

Department of Thermodynamics and Fluid Mechanics,
University of Strathclyde,
Glasgow,
SCOTLAND

A thesis submitted for the degree of Doctor of Philosophy in accordance with the regulations of the University of Strathclyde, Department of Thermodynamics and Fluid Mechanics.

March 1986

ABSTRACT

Condensation, of steam bubbles generated at an orifice and rising freely through water, subcooled from 5 K to 36.6 K at pressures of 1 bar and 2 bar, has been analysed theoretically and experimentally. Orifice diameters were 1 mm and 2 mm, and steam flow rates of 0.5, 1 and 1.5 g/min were used.

The data indicate a decrease in collapse Fourier number with increase in either Jakob number or steam flow rate, or with a decrease in pressure, while change in orifice diameter does not have a significant effect on collapse Fourier number.

Average values of heat transfer coefficient around the collapsing bubbles have been determined to be between $0.15 \cdot 10^5 - 0.35 \cdot 10^5$ W/m^{2}K.

The effect of bubble distortion and of local heating of the liquid, close to the orifice, due to condensation of the bubbles, have both been included in the quasi-steady state theory which has been presented. The experimental data is compared with the theoretical predictions.

A semi-empirical correlation for bubble rise height has been proposed, which is also based on the quasi-steady theory combined with a correlation for the velocity of steam bubbles condensing in subcooled water.

ACKNOWLEDGEMENTS

The author wishes to express his gratitude to the following:

Professor Hugh C. Simpson, SM, ScD, FInstP, AMAIChE, CEng, FIMechE, FRSE, Chairman of the Mechanical Engineering Group, for the use of equipment and research facilities and his useful guidance.

Mr. George C. Beggs, BSc, CEng, MIMechE, for his supervision, help and encouragement during the entire period of this work.

Dr. David H. Rooney, BSc, PhD, ARCST, CEng, MIMechE, MIED, for his help and guidance.

All the technical staff of the Heat Engines Laboratory, especially Messrs J. Lowe and E. Duncan for their assistance during the experimental work.

The Ministry of Education of Turkey for the scholarship grant during the early period of study.

TABLE OF CONTENTS

APPENDICES

PORTFOLIO

NOMENCLATURE

Ar	Archimedes number $= \frac{gR_o^3}{\nu^2}$
A_r	the surface area at the rear of the bubble, m^2
B	parameter defined as $B = Ja^2.\frac{\alpha}{R_o}.\sqrt{\frac{\rho_f}{\Delta P}}$
B_{eff}	parameter defined by equation (2.10)
C_1	variable defined by equation (A 6.19)
C_b	constant defined by equation (A 6.16)
C_l	the centre line of the inlet orifice
CX	horizontal distance of the centroid of the bubble from the orifice centre line, mm
CY	vertical distance of the centroid of the bubble above the orifice, mm
c_p	specific heat, J/kg.K
D	diffusion coefficient, m^2/s
d	orifice diameter, mm
Ec	Eckert number $= \frac{\dot{m}^2}{d^4.c_p.\rho_o.(T_o-T_w)}$
Eu	Euler number $= \frac{P.\rho_o.d^4}{\dot{m}^2}$
F	number of frames in cine film

Fo Fourier number for the collapse region = $\frac{\alpha_f . t}{4R_o^2}$

Fo_2 Fourier number for the growth and collapse regions = $\frac{\alpha_f . t}{4R_m^2}$

Fo_c collapse Fourier number = $\frac{\alpha_f . t_c}{4R_o^2}$

Fr Froude number = $\frac{\dot{m}^2}{gd^5\rho_o^2}$

g gravitational acceleration, m/s^2

h instantaneous heat transfer coefficient ; heat transfer coefficient, W/m^2K

h_{fg} specific enthalpy of evaporation, J/kg

Ja Jakob number = $\frac{\rho_f . c_{pf} . \Delta T}{\rho_g . h_{fg}}$

k thermal conductivity, W/mK

k_m mass transfer coefficient, m/s

LE distance of leading edge (i.e. top most point) of the bubble above the orifice, mm

LP distance of lowest point of the bubble above the orifice, mm

$\dot{m}, \dot{m}_s$ steam mass flow rate, g/min

Nu instantaneous Nusselt number = $\frac{2hR}{k_f}$

P pressure in the bubble chamber, bar ; pressure, N/m^2

Pe Peclet number = $\frac{2RU}{\alpha}$

Pe_o Peclet number = $\frac{2R_oU}{\alpha}$

Pr Prandtl number = $\frac{\nu}{\alpha}$

Q rate of heat transfer from the bubble at time t, W

q_θ heat flux at angular position θ on the surface of the bubble, W/m^2

R equivalent bubble radius, mm; bubble radius, m

$\dot{R}$ bubble wall radial velocity = $\frac{dR}{dt}$, m/s

Re Reynolds number = $\frac{2RU}{\nu} = \frac{2RU\rho}{\mu}$

Re_o Reynolds number = $\frac{2R_oU}{\nu}$

R_o bubble radius at detachment, m

r radial coordinate, m

s surface renewal rate, 1/s

T temperature, K

ΔT subcooling or superheating of water relative to steam, K

t time from the beginning of bubble growth or bubble detachment, ms; time, s

$\bar{t}$ time from detachment to a mean point between successive frames, ms

Δt time interval between alternate frames in cine film, ms

U average vertical velocity of bubble during condensation (after detachment), mm/s; bubble rise velocity, m/s

u_r velocity in the radial direction, m/s

u_θ velocity in the tangential direction, m/s

V bubble volume, m^3

V_s steam volume flow rate, mm^3/s

We Weber number $= \frac{\dot{m}^2}{d^3 \cdot \sigma \cdot \rho_0}$

w velocity of subcooled liquid in bubble chamber or flow channel, mm/s

y radial distance from the bubble surface $= r-R$, m

Z dimensionless bubble volume $= \frac{V}{\frac{4}{3} \cdot \pi R_0^3}$

α thermal diffusivity, m^2/s

β dimensionless radius based on bubble radius at detachment $= \frac{R}{R_o}$

β_2 dimensionless radius based on maximum radius $= \frac{R}{R_m}$

γ polar angle from vertical defining the base of the spherical-cap bubble, radians

δ thermal boundary layer thickness, m

ε dimensionless variable $= (\frac{\delta}{R})^2$; rate of energy dissipation by turbulence per unit of mass, W/kg or m^2/s^3

ε_T total rate of energy dissipation per unit of mass, W/kg or m^2/s^3

θ polar angle from vertical, radians

μ dynamic viscosity, Ns/m^2

ν kinematic viscosity $= \mu/\rho$, m^2/s

ρ density, kg/m^3

σ surface tension, N/m

ϕ dimensionless temperature ratio $= \frac{T-T_\infty}{T_i-T_\infty}$

ψ bubble shape factor defined by equation (5.50)

Subscripts

a average

b bubble ; back

c condensation or collapse region

d detachment

f fluid ; front

g growth region

i vapour water interface

l liquid

m maximum ; mean

o value at detachment ; initial value

r rear

s steam ; separation

sat saturation

T,t total

v vapour

w water ; wake

∞ bulk liquid value

γ to define heat transfer from spherical-cap bubbles

Note: The nomenclature for experimental parameters and the experimental results on the test data sheets are given in section 4.2.

CHAPTER 1

INTRODUCTION

1.1 General aspects of direct contact condensation

Direct contact condensation is important in the design of equipment such as condensers, cooling towers, feed water heaters and deaerators. It is of current importance in the development of economic water desalination units, utilisation of geothermal brine for energy production and emergency cooling of nuclear reactors.

The advantages of direct contact condensation over conventional processes using metallic transfer surfaces, are due to relative simplicity of design, reduced corrosion and scaling problems, lower maintenance costs, greater heat transfer area for a given volume, higher heat transfer rates and lower temperature driving forces.

The limitations of direct contact condensation are due to the physical properties of the fluids in contact; low solubility, low viscosity and surface tension, differences in the specific gravities for ease of separation with no affinity for stable emulsions, chemical inertness and stability being required for economical and trouble free operation.

While condensation on a solid surface is limited only by the extent of the surface and the rate of cooling of the surface, direct contact condensation is naturally limited by the balance between the latent heat of condensation and the sensible heat that the liquid can absorb until saturation is attained.

1.2 Emergency cooling of nuclear reactors

When a loss of coolant accident (LOCA) occurs in a nuclear reactor, due for example to the fracture of a main pipe in a Pressurised Water Reactor (PWR), various types of direct contact condensation may occur, dependent on the methods adopted to counteract the effects of the fracture (see Fig. 1.1 for a typical PWR loop). The resultant direct contact condensation between vapour and water may be :

1) Condensation of steam bubbles or jets in a pool of water : e.g.,
   i) In the upper plenum and/or reactor core when hot leg emergency core cooling (ECC) injection is employed,
   ii) In parts of the downcomer,
   iii) In the containment vessel.

2) Steam condensed by a spray of water : e.g., in the upper plenum with hot leg ECC injection.

3) Steam condensed in a parallel stream with water: e.g.,
   i) As a falling film from the upper plenum,
   ii) In the downcomer,
   iii) In the lower plenum.

When the emergency core coolant is injected through a hot leg during a LOCA in a PWR, water enters the upper plenum of the reactor vessel and falls on to an upper core plate (adapter plate or tie plate) and tries to penetrate to the reactor core against a flow of rising steam. In the safety analysis and prediction, information is required on the effectiveness with which the water penetrates to the core and on the steam water interactions in the upper plenum and at the core plate.

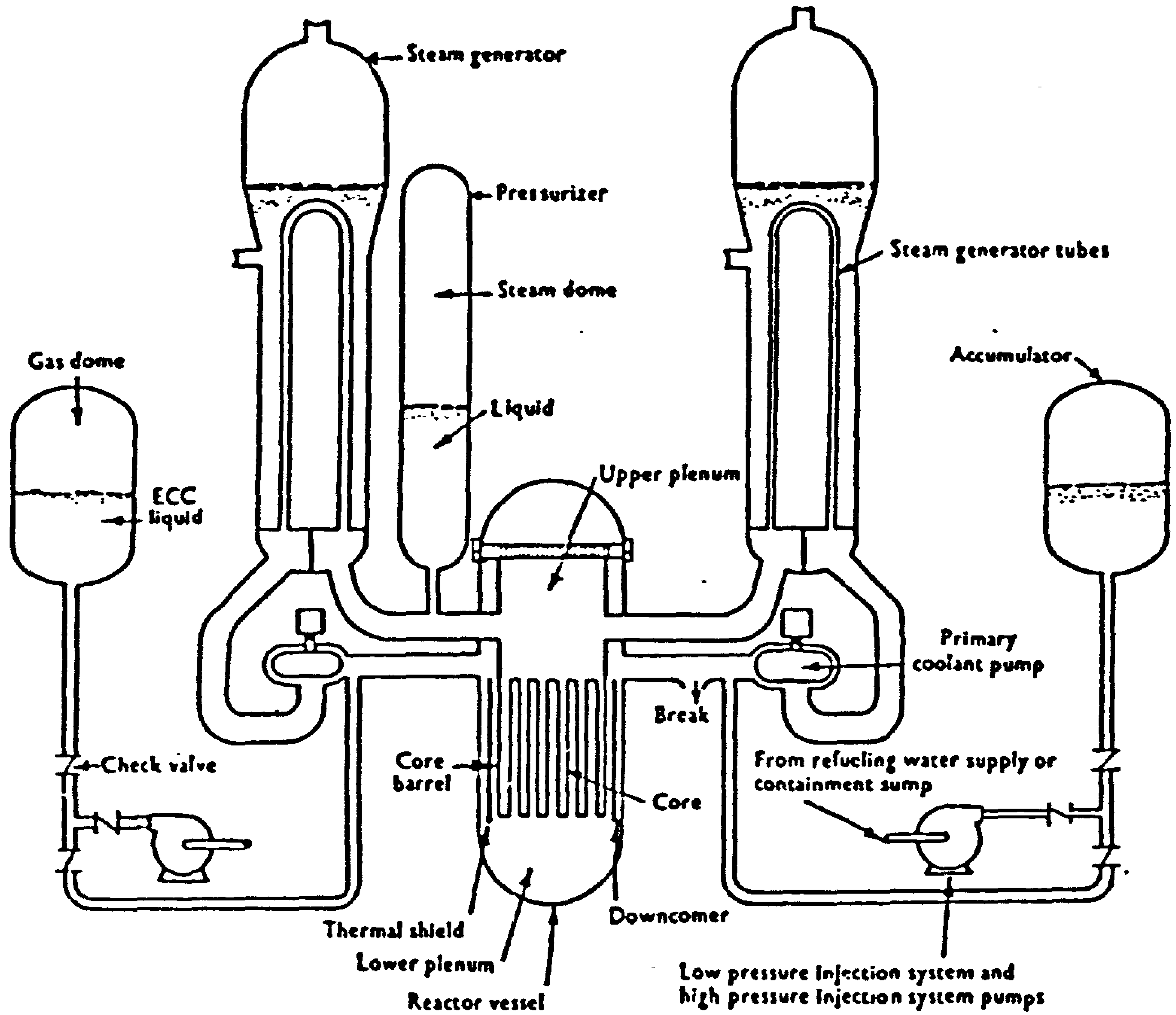

Fig. 1.1 Multiple Loop PWR system [42]

1.3 Project description

This work is a study of the behaviour of steam bubbles generated at an orifice and passing upward through a water pool in a bubble chamber. The experiments were carried out to find out whether the bubbles condensed completely within a prescribed liquid pool height or whether they escaped through the pool.

The main variables in the tests are, the height of the liquid pool, the water subcooling relative to the steam, the steam mass flow rate, the orifice diameter and the system pressure. The experimental results are compared with predicted bubble collapse rates obtained through a theoretical analysis.

CHAPTER 2

LITERATURE REVIEW

2.1 Introduction

The processes governing the growth or collapse of vapour bubbles in a liquid pool are determined mainly by the temperature of the liquid and by interactions resulting from the hydrodynamic behaviour of the bubbles in the liquid pool. The precise effects of these parameters can involve both heat transfer between bubble and liquid, and liquid inertia. In some cases liquid inertia may be the dominant feature while in others heat transfer may be the main factor controlling growth or collapse. Many research workers, using an extended form of the Rayleigh equation, originally developed for the collapse of a cavity in a liquid, have demonstrated the close relationship between the phenomena of bubble growth and those of bubble collapse.

This, of course, implies that many of the features noted by these workers in bubble growth may also be important factors in the field of bubble collapse.

2.2 Growth of vapour bubbles

An extensive amount of work has been carried out into the growth of vapour bubbles in a superheated liquid and much of this has been the subject of a comprehensive review in a book on boiling phenomena by Stralen and Cole [1]. In addition, Bankoff [7] has given an extensive review of heat transfer controlled bubble growth.

As mentioned earlier much of this work owes a great deal to Rayleigh [3]. In his work on the collapse of a spherical cavity in a liquid under a constant pressure difference, he derived an equation giving the time for the inertia controlled collapse of a bubble as

$$t = R_o \sqrt{\frac{3\rho_l}{2\Delta P}} \int_{\beta}^{1} \frac{\beta^{3/2}\, d\beta}{(1-\beta^3)^{1/2}} \qquad (2.1)$$

Further work by Forster and Zuber [4], Plesset and Zwich [5] and others led to an extended form for the equation of motion as

$$R\ddot{R} + \frac{3}{2}\dot{R}^2 = \frac{\Delta P(t)}{\rho_l} - \frac{2\sigma}{\rho_l R} - 4\nu\frac{\dot{R}}{R} \qquad (2.2)$$

the last two terms being included to account for surface tension and viscous effects.

In boiling, the initial stage of bubble growth, when the vapour temperature equals the temperature of the superheated liquid around it, is controlled mainly by liquid inertia effects and a solution can be obtained corresponding to that given by equation (2.1). As growth continues, heat transfer effects become more significant and, towards the later stages of growth, when the vapour pressure inside the bubble is approximately the same as the system pressure outside the bubble, growth is controlled by heat transfer. In general after a few microseconds of inertia controlled growth the remaining bubble growth takes place in a few milliseconds and in most of the work reported in the next paragraph heat transfer effectively controls the growth.

Stralen and Cole [1] reported that Bosnjakovic [38], by assuming a conduction layer surrounding a spherical bubble and by equating the heat conducted through this layer to the heat absorbed by evaporation, showed that the bubble radius was given by

$$R(t) = C\ Ja\ (\alpha t)^{1/2} \qquad (2.3)$$

where the value of C depended on the time dependent thickness assumed for the conduction layer, and Stralen suggested

$$C = \frac{2}{\pi^{1/2}} .$$

The same result was obtained by Forster and Zuber [4] who considered the bubble boundary as a moving sink. A different value,

$$C = \left(\frac{12}{\pi}\right)^{1/2} ,$$

was obtained by Plesset and Zwick [5] who assumed a thin boundary layer between the vapour bubble and the liquid and applied a perturbation technique to a stationary growing bubble. This value of

$$C = \left(\frac{12}{\pi}\right)^{1/2}$$

was also obtained, by Birkhoff, Margulies and Horning [39], in a detailed solution for a growing bubble and by Scriven [6] for large superheats. Scriven [6] also gave an equation which he suggested was more accurate for small superheats as

$$R(t) \cong (2Ja)^{1/2}\ (\alpha t)^{1/2} \qquad (2.4)$$

Ruckenstein [8] investigated the effect of a constant translational velocity on the bubble growth rate. He reduced the energy equation in the liquid to the diffusion problem solved by Levich [9] giving the temperature distribution around the bubble as

$$\frac{T-T_i}{T_\infty - T_i} = \frac{2}{\sqrt{\pi}} \operatorname{erf} \frac{\frac{3}{2} \, UR \, y \, \sin^2\theta}{2\sqrt{\frac{3}{2} \, UR^3 \alpha \left(\frac{2}{3} - \cos\theta + \frac{1}{3}\cos^3\theta\right)}} \tag{2.5}$$

and gave a correlation for the heat transfer rate as

$$Nu = \left(\frac{4}{\pi}\right)^{1/2} Pe^{1/2} \tag{2.6}$$

A further theoretical analysis by Ruckenstein and Davis [31] assumed potential flow around a spherical bubble and showed that for zero translational velocity, apart from the effect of an initial radius, the growth rates conformed closely to the values given by Plesset and Zwick [5], (equation (2.3) with $C = (12/\pi)^{1/2}$), but noted that, at lower values of Jakob number the growth rates increased with increasing velocity although this effect reduced with increase in Jakob number as radial convection increased, being of no significance for $Ja > 50$. They also pointed out that caution should be exercised in applying this analysis to low Jakob numbers, especially at low translational velocities because, under these conditions, the assumption of a thin boundary layer became questionable. The theory was in good agreement with Florschuetz et al's [40] data on growing and translating vapour bubbles at uniform superheats in the low Jakob number range ($3 < Ja < 10$).

Growth and collapse of vapour bubbles in liquid nitrogen was studied by Hewitt and Parker [41]. Their experimental data for bubble growth in boiling was in good agreement with the Plesset and Zwick [5] theory (equation (2.3) with $C = (12/\pi)^{1/2}$).

2.3 Condensation of vapour bubbles

Although it was implied in the previous section that, for bubble growth in a liquid of small superheat, liquid inertia effects soon became negligible and thereafter growth was controlled by heat transfer, the same conditions do not necessarily apply throughout bubble collapse. Thus, in highly subcooled boiling, where the temperature driving force remains relatively large, bubble collapse appears to be dominated by liquid inertia.

Florschuetz and Chao [10] investigated the relative importance of liquid inertia and heat transfer on the spherically symmetrical collapse rate of vapour bubbles (see table (2.1) in the attached portfolio for experimental values).

Bubble collapse was classified into 3 regions :

i) Where the Jakob number was high, so that the wall temperature was approximately equal to the bulk liquid temperature so that the vapour pressure remained constant at the initial value throughout collapse, this implying liquid inertia controlled collapse and conforming to the simple Rayleigh solution (see equ. (2.1)), the solution for the dimensionless collapse time being given as

$$\tau_I = \frac{t}{R_o}\sqrt{\frac{2\Delta P}{3\rho_L}} \qquad (2.7)$$

ii) Where the vapour pressure in the bubble remained equal to the system pressure, so that liquid inertia effects were negligible and collapse was dominated by heat transfer. Neglecting the effects of surface curvature, a plane interface solution was derived for heat transfer controlled collapse as

$$\beta = 1 - \tau_H^{\frac{1}{2}} \qquad (2.8)$$

where $\tau_H = \frac{4}{\pi} Ja^2 \frac{\alpha t}{R_o^2}$

The Plesset and Zwick temperature integral was solved leading to a solution for the dimensionless time, τ, in heat transfer controlled collapse as

$$\tau_H = \frac{1}{3} \left(\frac{2}{\beta} + \beta^2 - 3 \right) \qquad (2.9)$$

Although both equations (2.8) and (2.9) were approximate results, nevertheless it was concluded that these two equations should represent lower and upper limits to the collapse time for heat transfer controlled collapse and that in each case the nature of the collapse was quite different from the inertia controlled collapse of equation (2.1).

iii) In general cases, where both liquid inertia and heat transfer affected the collapse, the relative importance of the two effects was considered to depend on the value of a parameter,

$$B = Ja^2 \frac{\alpha}{R_o} \sqrt{\frac{\rho_f}{\Delta P}}, \text{ heat transfer effects}$$

becoming more important as B decreased and liquid inertia effects more important as B increased. They also included an interesting indication that, for certain intermediate values of B ($0.05 < B < 10.0$) the combined effects of liquid inertia and heat transfer could produce a range of alternate collapse and regrowth periods before collapse finally continued.

An effective value of B was defined as

$$B_{eff} = \psi^2 B \left(\frac{\rho_{vsat}}{\bar{\rho}_V}\right)^2 \tag{2.10}$$

where ψ was a factor introduced to account for the non-linearity of the vapour pressure and temperature relation and used an average mean value of reference density, $\bar{\rho}_V$ for the temperature range T_∞ to T_{sat}.

They suggested that collapse would be heat transfer controlled for $B_{eff} < 0.05$, and liquid inertia controlled for $B_{eff} > 10.0$ with both effects present in varying amounts between these values. However it may be noted that, in the example given for heat transfer controlled collapse of water vapour bubbles at atmospheric pressure, for $40 \leq Ja \leq 100$ the value of B_{eff} was always greater than 0.05 while for inertia controlled collapse with $150 \leq Ja \leq 250$ B_{eff} was always less than 10.

For heat transfer controlled collapse, the collapse rates were, in general, faster than given by equation (2.9) although agreement was reasonably good with theoretical predictions for low translational velocities, but the collapse rates increased if translational velocities were significant, in some cases collapse being more rapid than that given by the plane interface solution of equation (2.8). It was suggested that deviation from the slow collapse rate of equation (2.9) would be greater for small values of Jakob number, due to the relatively earlier breakdown of the thin thermal boundary layer approximation for slowly collapsing bubbles. They noted that results published by Levenspiel [21] gave a more rapid collapse rate than any of the above and showed a markedly faster collapse even than that indicated by the lower bound equation (2.8). However these collapse rates were still very much slower than for purely inertia controlled collapse and it was suggested that the rapidity of collapse in this case was due to the high translational velocities of the bubble and that liquid inertia effects were insignificant.

Wittke and Chao [11] used the same apparatus as Florschuetz and Chao [10], modified to study the effects of translational velocity and the presence of noncondensables in the collapsing bubbles (see table (2.1)). As it was considered that translational velocity would have little effect in liquid inertia controlled collapse, attention was directed solely at heat transfer controlled collapse, but they rejected the thin boundary layer assumption of Plesset and Zwick as unsatisfactory and obtained a numerical solution of the governing equations. Their experimental results showed reasonably good agreement with their theory. It was shown that, at any value of Jakob number, an increase in translational velocity not only increased the collapse rate, but in the absence of noncondensables caused it to increase with time. However, the presence of noncondensables, except for stationary bubbles at very low Jakob numbers, caused a reduction in the collapse rate, with the collapse rate decreasing as collapse continued. They found that the Florschuetz and Chao upper bound solution was theoretically valid for large Jakob numbers but the applicability was restricted as heat transfer controlled collapse would only occur at low values of Jakob number.

Brucker and Sparrow [12] investigated the collapse of water vapour bubbles of about 3 mm initial diameter, at pressures in the range 10.3 to 62.1 bar, subcoolings from 15 to 100 K (see table (2.1)). They found the bubble translational velocities approximately constant, with a range from 150 to 220 mm/s, and also that the bubbles followed a pattern of spherical at detachment, changing to hemispherical, then to ellipsoidal at which condition the shorter lived bubbles collapsed, while longer lived bubbles changed again to spherical shape before final collapse. It was noted that, irrespective of the total bubble collapse time, the times of change to hemispherical and then to ellipsoidal were essentially constant at about 0.010 and 0.020 seconds respectively. The average heat transfer coefficients obtained were about 10^4 W/m^{2}K and both collapse time and height to collapse increased with increasing pressure and decreasing temperature difference.

Empirical relations were given for both the collapse time and the height to collapse in the form

$$Fo_c = 13.9/Ja^{3/4}.Ra^{1/2} \tag{2.11}$$

and $$\frac{Z_c}{R_o} = 1536/Ja^{3/5}.Ra^{1/4} \tag{2.12}$$

where $Ra = [8g(\rho_l - \rho_v)R_o^3/\rho_f \nu_f^2].Pr_f$.

Nordmann [13] studied the heat transfer around bubbles supplied through an orifice into a slightly downwards flow of water (see table (2.1)). Using sensitive pressure transducers, coupled with high speed film of the emerging bubbles, pressure fluctuations were recorded near the surface of the condensing bubbles. These measurements, showed that the maximum pressure fluctuations occurred at detachment, with a further slightly lower amplitude fluctuation towards the end of collapse. It was noted that the magnitude of the fluctuation depended on the Jakob number, the effect being much greater for Ja > 100 than for lower values of Ja.

The amplitude of the fluctuation against condensation time was plotted as shown in Fig. 2.1, which clearly indicated, that for Ja > 100, the amplitude increased rapidly as the condensation time was reduced, while for Ja < 100 there was comparatively little change of amplitude with change in condensation time.

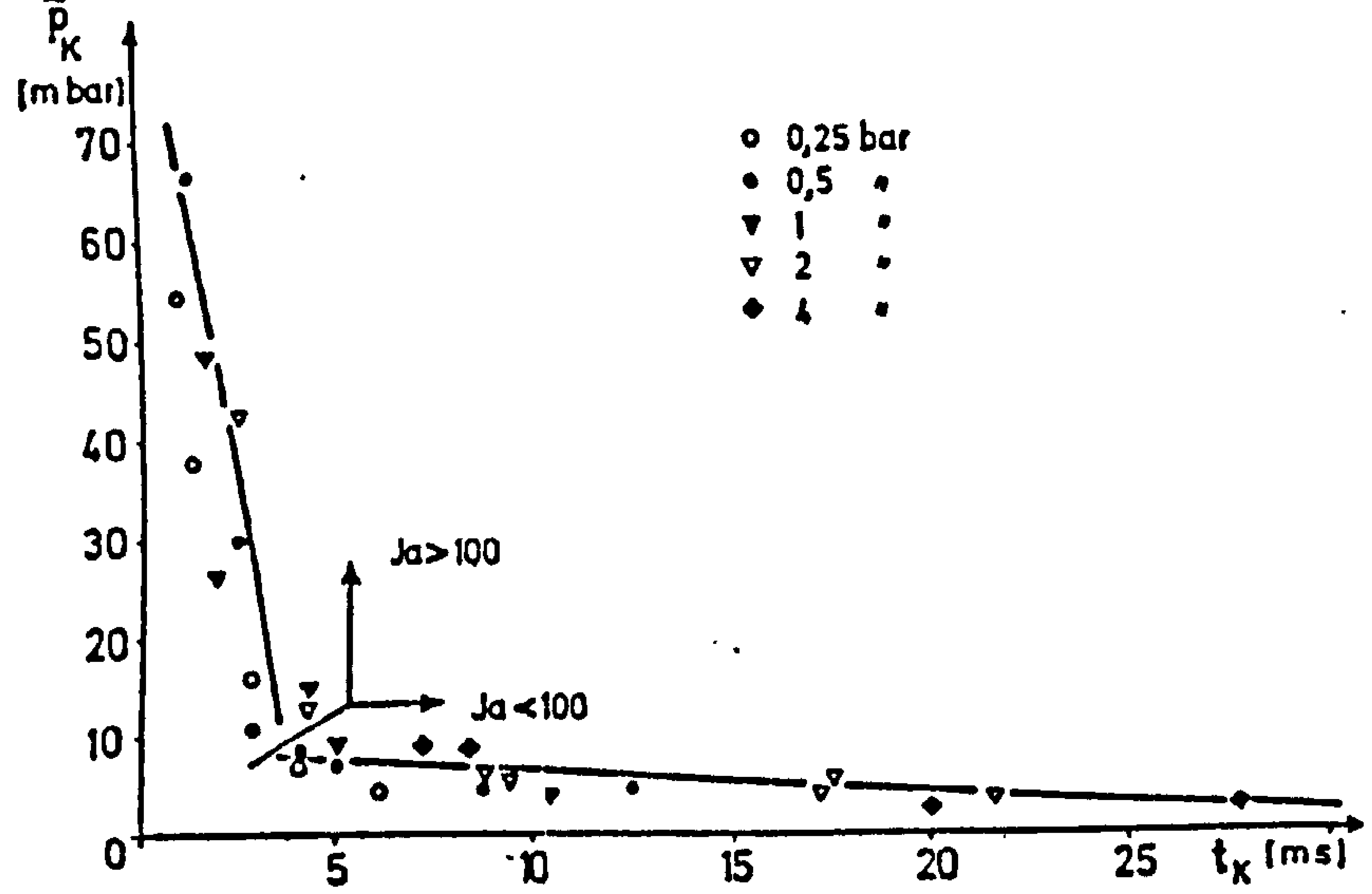

Fig. 2.1 Maximum pressure amplitude - $\tilde{P}_K$ at the end of condensation as a function of condensation time, t_K [13].

Holographic interferometry was also used, this being only feasible while a stable smooth boundary layer prevailed at the phase boundary of the condensing bubbles. This was the case for Ja < 30, the irregularity of the surface increasing as the Jakob number increased, eliminating the regularity of the fringe pattern around the bubbles. It was concluded that the presence of the thermal boundary layer indicated that the bubble collapse was dominated by heat transfer for Ja < 30, while the pressure fluctuation pattern indicated that for Ja > 100, the collapse was dominated by liquid inertia effects, and for 30 < Ja < 100 there was a transition region in which both effects were present.

Values of B_{eff}, as defined by Florschuetz and Chao [10], were obtained as B_{eff} < 0.025 for heat transfer controlled collapse and $B_{eff} > 0.44$ for liquid inertia controlled collapse compared with the values of $B_{eff} < 0.05$ and $B_{eff} > 10$ given by Florschuetz and Chao.

In the heat transfer controlled region, it was observed that the bubble formed a long neck before detaching as hemispherical, changing to pear-shaped and back to hemispherical before collapsing as horizontal ellipsoids. Also, after detachment the bottom of the bubble rose rapidly, passing through the bubble volume, penetrating and deforming the top of the bubble. This sometimes caused entrainment of water into the bubble and the emergence of tiny water droplets or steam bubbles at the top of the bubble.

In the transition region, the turbulence at the phase boundary increased with increase in Jakob number and the detached bubble shape alternated between hemispherical and ellipsoidal. The neck at detachment became shorter, condensation occurred more around the bubble, the translational movement of the centre of gravity was greatly reduced. The top of a bubble frequently penetrated the preceding bubble producing a toroidal volume with rapid collapse.

In the inertia controlled region, the turbulent bubble surface continually changed shape during growth. Detachment occurred with a short neck and after detachment condensation took place all around the bubble, with no apparent translational movement of the centre of gravity.

Nordmann [13] applied the Nusselt equation for a solid sphere, $Nu = cRe^{m}.Pr^{n}$ [14] and, using the bubble wall velocity as the characteristic velocity, obtained for the heat transfer controlled and transitional regions the equation

$$\beta = (1-2.95.10^2\ Pr^{0.26}\ Ja^{0.87}\ Fo)^s \qquad (2.13)$$

where $s = 1-0.005.Ja$ (for $0 < Ja < 100$).

For the heat transfer controlled region, heat transfer coefficients were determined from the fringe patterns around the bubbles, and the disturbance in these fringes meant that in only a few cases was it possible to calculate the coefficients after detachment and even then only for one or two frames. This meant that in most cases the heat transfer coefficients were determined just before detachment.

The heat transfer around the top half of the bubble was related to the equation $Nu = cRe^m Pr^n$, modified by inclusion of the Jakob number and the density ratio, ρ_v/ρ_l with the downward velocity of water as the characteristic velocity. Two values of Nusselt number were determined; one at the top of the bubble ($\theta = 0°$) Nu_t and one at the side of the bubble ($\theta = 90°$) Nu_s, and these were expressed as

$$Nu_t = 4000.Re^{0.25}\ Pr^{0.66}.Ja^{0.27}\ \left(\frac{\rho_v}{\rho_L}\right)^{0.75} \qquad (2.14)$$

$$Nu_s = 253.Re^{0.48}.Pr^{0.66}.Ja^{0.36}.\left(\frac{\rho_v}{\rho_L}\right)^{0.75} \qquad (2.15)$$

where $Re = \dfrac{2Rw}{\nu_f}$

A mean Nusselt number defined as $Nu_m = \sqrt{Nu_t.Nu_s}$ was thus given as

$$Nu_m = 1000.Re^{0.33}Pr^{0.66}.Ja^{0.27}.\left(\frac{\rho_v}{\rho_L}\right)^{0.79} \qquad (2.16)$$

The values of heat transfer coefficient calculated were up to 65000 W/m^2K, with a maximum value at the top of the bubble gradually decreasing down towards the 90° position. The mean value around the bubble surface increased with increase in pressure. Thick thermal boundary layers formed around the neck of the attached bubble reducing the heat transfer in that region.

Mayinger and Chen [15], using the same apparatus as Nordmann, carried out experiments on the collapse of bubbles of R113 vapour having initial diameters about 2 mm (see table (2.1)). The tests were carried out over a range of pressures from 0.4 to 4 bar with subcoolings from 5 to 60 K. The experimental data were correlated, together with those of Nordmann [13] and Brucker and Sparrow [12], to show that the heat transfer coefficient was apparently unaffected by the value of Jakob number in the range $1.6 \leq Ja \leq 60$, and agreement, within the range of the experimental data, was obtained, to within ± 50%, with the Nusselt equations for a solid sphere

$$Nu = 0.37\ Re^{0.6}\ Pr^{1/3} \tag{2.17}$$

and

$$Nu = 2.0 + 0.6\ Re^{0.5}\ Pr^{1/3} \tag{2.18}$$

where $Re = \dfrac{2R_O w}{\nu_f}$

Denekamp et al [16] carried out a study into the behaviour of water vapour bubbles, injected under sub-atmospheric conditions into a co-current flow of water subcooled by 1-5 K (see table(2.1)). Their main interest lay in the behaviour of the bubble prior to detachment. It was observed that the bubbles left the orifice in pairs, and that after detachment, the second and smaller bubble was sucked into the leading bubble so that the combined bubble formed a mushroom shape. Values of condensed mass, detachment diameter and bubble frequency were presented related to subcooling, with water temperature and water level above the orifice as parameters. Approximately half of the vapour was condensed before detachment. The governing conservation equations were solved numerically, and attention was directed at the leading bubble of each pair to derive a theoretical prediction for detachment radius and amount of condensation before detachment.

Delmas et al [17] investigated the influence of noncondensable gas on the collapse of vapour bubbles (see table (2.1)). The bubbles were obtained by boiling under vacuum and collapse initiated by increasing the pressure to atmospheric. Collapse rates were compared with the inertia controlled collapse of Rayleigh modified by assuming an isentropic pressure change within the bubble. This resulted in a much slower collapse, together with a significant oscillation in bubble radius, these oscillations also appearing in the experimental measurements, with a time lag of 0.4 to 0.8 ms. The collapse rates were, in general, between the values given by Florschuetz and Chao [10] (equations (2.8) and (2.9)) although as the nitrogen content increased, the collapse rates were much slower than those indicated by equation (2.9). The effect of the noncondensable gas on bubble stability was also noted and four regions indicated depending on bubble initial radius and on pressure difference :

i) Stable region at low initial radius and low pressure difference,

ii) At high initial radius and high pressure difference, considerable oscillation occurred during collapse with a sudden explosive rupture when the bubble attained a minimum size,

iii) At high initial radius but low pressure difference, bubble rupture by progressive division due to condensation in preferential sites,

iv) A mixed region, between (ii) and (iii) at medium pressure difference and high initial radius.

Bankoff and Mason [18] measured turbulent heat transfer coefficients at the surface of bubbles collapsing in a counter current stream of subcooled water (see table (2.1)) and observed three different types of bubble depending on steam flow rate and water temperature :

i) At low steam flow rates and high subcoolings (50-73 K); essentially ellipsoidal bubbles of smooth surface with initial diameter of about 0.5 mm and a frequency of about 2500 Hz corresponding to the bubbles observed by Gunther [43] in subcooled nucleate boiling. These bubbles were correlated to within ± 20% by the equation,

$$Nu = 0.000374\ Pe^{1.74}\ St^{1.5} \qquad (2.19)$$

where the Strouhal number, St, is the ratio of mean bubble wall velocity and liquid jet velocity

ii) At increased steam flow rates and decreased subcoolings (about 50 K) the bubbles had a frequency of about 720 Hz and collapsed as irregular ellipsoids conforming, to within ± 20%, to the equation

$$Nu = 21.1\ Pe^{0.404}\ St^{0.2} \qquad (2.20)$$

iii) At even lower subcoolings (18-30 K) the bubbles were of irregular shape, of initial diameter from about 1.2 to 4.5 mm, with large volume oscillations, had a frequency range of 200 to 1000 Hz, did not collapse completely and conformed, to within ± 50%, to the equation

$$Nu = 63.7\ Pe^{0.265}\ St^{-0.1} \tag{2.21}$$

The authors also concluded that a much larger proportion of the heat transfer was due to latent heat transport than had been previously estimated, this fraction decreasing with increase in subcooling and increase in liquid jet velocity but increasing with heat flux and dominating near burn-out (max. heat flux).

Dimić [19] carried out a theoretical investigation into the collapse of one component vapour bubbles with translatory motion in subcooled liquid. The differential energy equation was solved to obtain an expression for the thickness of the thermal boundary layer around the bubble and hence a general solution was derived for the variation in bubble radius with time, qualitatively similar to that of Ruckenstein's [31] for bubble growth. A solution was then derived for the collapse of a stationary bubble as

$$\beta = 2\left(1+\frac{16}{\pi}\ Ja^2Fo\right)^{1/2} .\cos\left[\frac{1}{3}\left[\pi+\arccos\left(1+\frac{16}{\pi}\ Ja^2Fo\right)^{-3/2}\right]\right] \tag{2.22}$$

which agreed, to within ± 6%, with equation (2.9) of Florschuetz and Chao and equation (2.24) of Voloshko and Vurgaft [20], and was in qualitative agreement with the bubble growth solution of Skinner and Bankoff [44].

By assuming quasi steady state conditions throughout collapse and assuming a range of functional relationships between translational velocity and bubble radius, a range of solutions was derived for bubble radius versus time.

It is interesting to note that the solution for constant translational velocity, i.e.

$$\beta = \left(1 - \frac{6}{\sqrt{\pi}}\, Ja Pe^{0.5} Fo\right)^{2/3}$$

was also obtained by Isenberg, Moalem and Sideman [23].

Four other solutions were given for different radius dependent relationships in the form

$$\beta = (1 - C\, Ar^{a}\, Pr^{b}\, Ja\, Fo)^{e} \qquad (2.23)$$

where Ar is the Archimedes number.
Voloshko and Vurgaft [20] presented an empirical correlation for the collapse of steam bubbles in subcooled water for $40 \leq Ja \leq 75$ (see table (2.2) in the attached portfolio),

$$\beta = 1 - 6.776.10^{4}.Fo \qquad (2.24)$$

which agreed with the experimental data to within ± 30%. When compared with the Florschuetz and Chao [10] equation (2.8), the collapse rate was slower for the early part (down to $\beta = 0.8$) of the collapse time, but accelerated during the later part to give a more rapid collapse, this being possibly associated with the effect of translational velocity.

Using equation (2.24) they obtained the equation for heat transfer coefficient as

$$h = 1.694.10^4 \frac{k_f}{JaR_o} \tag{2.25}$$

Levenspiel [21] studied the collapse of steam bubbles in water by sudden pressurisation while boiling under vacuum conditions (see table (2.2)). Considering a differential heat balance for the condensing bubble, he derived a correlation for the instantaneous heat transfer coefficient for his experimental data :

$$h = 14163.R.h_{fg}.\rho_v \tag{2.26}$$

He then deduced the mean heat transfer coefficient over the collapse period as

$$h_m = \frac{\int_0^Q h dQ}{Q}$$

where Q was the total heat transferred during the collapse, and concluded that the mean value was 0.75 times the instantaneous initial value, h_o.

Prisnyakov [22] applied the first law of thermodynamics, for stationary condensing bubbles assuming the vapour obeyed the perfect gas laws, and obtained the following equation,

$$\beta = 1-2\varepsilon \left(\frac{16}{\pi} Ja^2 \, Fo\right)^{1/2} \tag{2.27}$$

where ε is a physical constant to be calculated for the experimental condition, having values 1 to 0.96 for water subcoolings 0 to 22 K.

Isenberg et al [23], assuming potential flow and quasi-steady state conditions around condensing bubbles derived an approximate analytical solution, including the effect of noncondensables. As the solution related to low Jakob numbers, the effect of bubble wall velocity was neglected compared with that of translational velocity. Using Ruckenstein's [8] heat transfer equation for spherical bubbles rising independently in boiling liquid they obtained the solution

$$Ja\,Pe^{1/2}Fo = \frac{\pi}{4}^{1/2}\left[\frac{2}{3}(1-\beta^{3/2}) + \frac{\beta_f^{3/2}}{3}\ln\left[\frac{(1-\beta_f)^{3/2}(\beta^{3/2}+\beta_f^{3/2})}{(1+\beta_f^{3/2})(\beta^{3/2}-\beta_f^{3/2})}\right]\right] \tag{2.28}$$

For a pure vapour $\beta_f = 0$, and the equation reduces to

$$\beta = \left\{1 - \frac{6}{\sqrt{\pi}} Ja.Pe^{1/2}\ Fo\right\}^{2/3} \tag{2.29}$$

Isenberg and Sideman [24] also presented a finite difference numerical solution for bubbles with noncondensables, condensing either in their own liquid or in another immiscible liquid. Their experimental data with pentane and steam bubbles condensing in their own liquids agreed well with equation (2.28) especially at high values of Peclet number. The agreement between the numerical and analytical solutions was better at high Peclet numbers and at low Jakob numbers but correlation of the experimental data was better with the numerical solution for Ja > 30.

In the above analysis, involving noncondensables, it has been assumed that the noncondensables have been homogeneously mixed with the vapour. Moalem and Sideman [25] extended the analysis to include the build up of a concentration of noncondensables near the phase boundary, which is likely to occur in two component systems where internal circulation is restricted, indicating that this would slow down the collapse process. Moalem and Sideman [26] also included the effects of translational velocity, taken as constant for 2 mm < Ro < 4 mm, the solution corresponding to equation (2.28), and for Ro < 1 mm assuming $U \propto \sqrt{R}$, obtained the relation

$$JaPe_o^{1/2} \;.\; dFo = -\frac{\sqrt{\pi}}{4}\frac{\beta^{13/4}}{(\beta^3-\beta_f^{\;3})}\,d\beta \tag{2.30}$$

which in the case of noncondensables reduced to

$$\beta = \left(1-\frac{5}{\sqrt{\pi}}JaPe_o^{1/2}\;.\;Fo\right)^{4/5} \tag{2.31}$$

where $Pe_o = \frac{2R_oU_o}{\alpha}$.

It is clear that, with increase in noncondensables the rate of collapse would decrease, and in such cases the radius dependent velocity changes would be slower, so that the effect of the velocity would decrease with increase in noncondensable content. This is borne out by equations (2.28) and (2.30). When the analysis was extended to forced flow boiling, where the bubbles detaching from the surface were subject to a transverse flow of velocity U_L, while rising with the velocity $U_b = c\sqrt{R}$, the equation resulted as

$$JaPe_o^{1/2}dFo = -\frac{\sqrt{\pi}}{4(\beta+U_R^2)^{1/4}}\cdot\frac{\beta^{7/2}}{\beta^3-\beta_f^{\;3}}d\beta \tag{2.32}$$

where $U_R = U_L/U_m$ and U_m was the rise velocity corresponding to the maximum radius at detachment, which for the case of zero translational velocity reduced to equation (2.30).

Equation (2.32) gave good agreement with the experimental data of Abdelmessih et al [27] for a noncondensable content corresponding to $\beta_f = 0.4$.

Moalem et al [29] presented an approximate analytical solution, related to the changes in temperature field and flow velocity in bubble trains, for pentane bubbles, with or without noncondensables, condensing in liquid pentane or in water. They showed the effect of bubble frequency and the number of bubbles in a train on both the temperature field and the flow velocity. The results predicted the amount of liquid subcooling to maintain a bubble train and the liquid height for complete condensation, for different numbers of bubbles in a train at given frequencies.

For a given number of bubbles in a train, increase in frequency necessitated higher bulk liquid subcooling and this effect was increased by the presence of noncondensables for a given frequency. For a given bulk liquid subcooling, frequency did not have any significant influence on condensation height but the presence of noncondensables increased the condensation height. Moalem et al [30] also presented an exact numerical analysis, solving the potential flow field and the energy equation simultaneously for a bubble train. The solution in the case of one bubble was in good agreement with the previous analysis of Isenberg and Sideman [24] confirming the reliability of the theory.

The agreement between the approximate analytical [29] and the exact numerical [30] solutions was good, especially at frequencies above 10 bubbles per second. The assumption of the energy balance in the analytical solution, that all the heat accumulated within the liquid envelope between the condensing bubble and the bubble following it, was not completely fulfilled at low frequencies when bubbles were far apart.

Moalem et al [30] showed that the bubble frequency affected the condensation rate in two ways : (1) by reducing the effective subcooling (due to condensation of the preceding bubbles) leading to a reduction in the condensation rate, and (2) by increasing the bubble rise velocity leading to an increase in the condensation rate. At low frequencies (up to 12-14 bubbles per second), increase in frequency reduced the effective subcooling and had little effect on the rise velocity, and thus decreased the condensation rate. However, at high frequencies, each bubble entered the wake region of the preceding bubble, increasing the rise velocity and hence increased the convection effects and the collapse rate which, for 26 bubbles per second, approached that of a single bubble. If noncondensables were present, they had little effect on the rise velocity but affected the temperature field tending to reduce the condensation rate even more.

The experimental data for pentane-pentane and pentane-water systems were in good agreement with the analytical solution except at high frequencies and/or high noncondensable content. The bubbles deviated from the assumed axial symmetry and, at high frequencies, different interaction effects occurred as the bubbles approached each other. The assumption of homogeneous distribution of noncondensables was considered inappropriate when the noncondensable content was high.

Schmidt [35] carried out a range of tests in which highly superheated steam (100-200 K) was injected into saturated water at high system pressures (see table (2.2)). In such conditions, in contrast to those where saturated steam is injected into subcooled water, the main thermal resistance is inside the bubble, where a thermal boundary layer forms on the steam side of the steam-water interface. He defined an average heat transfer coefficient, in the range of 0.5 - 7.5 kW/m²K, as

$$h = \frac{\dot{m} c_p}{S} \ln \frac{T_o - T_w}{T_s - T_w} \tag{2.33}$$

where S is average bubble surface area during growth, $\dot{m}$ is steam mass flow rate. T_s and T_o are the respective steam temperatures at orifice outlet and inside the bubble at detachment. The values obtained were about one order of magnitude lower than values reported for the collapse of saturated steam bubbles in subcooled water (see tables (2.1) and (2.2) for values reported in the literature), this indicating a better heat transfer when the main thermal resistance was on the water side of the interface rather than on the steam side.

Schmidt [35] reported an increase in heat transfer coefficient with increased pressure (due to changes in enthalpy of evaporation and in steam viscosity and thermal conductivity). The coefficient also increased with increase in orifice diameter and mass flow rate, the rate of increase being greater for Re < 1300, at which value there was a transition from steady state to unsteady state bubble generation. There was no significant effect on the heat transfer rate due to increase in the amount of superheat in the bubble. The heat transfer coefficients were presented as Stanton number against Reynolds number, to within ± 20%, in the form

$$St = \frac{h\ d}{\dot{m} c_p} \sqrt{\frac{\sigma}{g(\rho_w - \rho_s)}} = \text{constant}.Re^{0.766} \qquad (2.34)$$

where the constant depends on orifice diameter (ranging from 8 at d = 3 mm to 12 at d = 1.5 mm).

Schmidt [34] also noted that the bubble volume at detachment and the bubble frequency both increased with steam mass flow rate, the volume also increasing with decrease in system pressure and increase in orifice diameter, while, for a given mass flow rate, the frequency increased with decrease in orifice diameter.

The bubble surface area at detachment was given, to within ± 30%, as

$$S = 1.913.10^{-3} .d^2 \left[\frac{Fr}{Re^2We^2} \left(\frac{(Eu.Ec)^{1/2}}{Re}\right)^{5.35}\right]^{1/3} \qquad (2.35)$$

and the frequency of formation, to within ± 10%, as

$$f = 3.08.10^{-2} \left(\frac{g}{d}\right)^{1/2} . Re^{0.426} \qquad (2.36)$$

where $Re = \dot{m}/d\mu_o$.

Akiyama [36] investigated growth and collapse of vapour bubbles in subcooled boiling (see table (2.2)). Employing the heat transfer correlation, given by Grigull [37], for solid spheres in laminar flow

$$Nu = 0.37.Re^{0.6}.Pr^{1/3} \qquad (2.37)$$

and from a heat balance for a collapsing bubble he derived the equation,

$$\beta = (1 - 1.036.\ JaPe^{0.6}\ Pr^{-0.27}\ Fo)^{5/7} \qquad (2.38)$$

This correlation overpredicted bubble collapse rates when compared with the experimental data.

2.4 Review findings

The following conclusions may be drawn from the preceding literature review :

There is a limited amount of experimental data and theoretical study on vapour bubbles condensing in subcooled liquids. When such experiments were performed, no extensive or accurate analysis of the cine-films was carried out because the necessary electronic equipment was not in general use.

None of the existing quasi-steady state theories take account of radial velocities, bubble distortion or local temperature differences produced around the condensing bubbles. Each of these may have some effect on the collapse rate of the bubble although the relative magnitude of the different effects should depend on the parameters controlling the collapse. For example, radial velocities may be comparable with the bubble rise velocity especially at high subcoolings, there may be bubble distortion especially early in the collapse and the condensation of the bubble must lead to local heating of the water around the bubble.

Ruckenstein and Davis [31] presented a general solution for a growing bubble, with allowance made for radial velocity effects but with no allowance made for either distortion or local temperature changes. This gave the bubble radius R at any time t in terms of a complicated integral equation, which was solved iteratively for certain cases of the growth of vapour bubbles, but the result is found to be too complicated for ready engineering use.

It would therefore be desirable to obtain a more complete solution, easier to use, and including the effects of the three variables mentioned.

CHAPTER 3

EXPERIMENTAL APPARATUS AND TEST PROCEDURE

3.1 Test rig

A schematic layout of the bubble chamber test rig is shown in fig. 3.1. It consisted of three main parts; a steam boiler, a steam flow measuring section, and a bubble test chamber, including an injection orifice.

3.1.1 The steam boiler

The stainless steel boiler was a vertical cylinder of 230 mm inside diameter, 380 mm height and 12.7 mm thickness. It was enclosed in another cylindrical steel container insulated by two layers of bricks at the bottom. The boiler was placed on top of a 3 kW external ring heater embedded, in a layer of Kaowool ceramic fibre ($k = 0.08$ W/mK), on the bricks. The sides and top of the boiler were insulated by fibre glass ($k = 0.03$ W/mK). An additional 325 W immersion heater, controlled by a variac transformer, was used during the experiments, to maintain the pressure in the boiler constant for different steam flow rates. A sight glass, to observe the water level inside the boiler, and a safety valve, to prevent unwanted high pressures, were fitted to the boiler. Two pressure gauges were fitted, one for subatmospheric and the other for elevated pressures.

3.1.2 Flow measuring section and calibration

Steam, generated from distilled water in the boiler, was passed through a 6 mm diameter copper pipe to the flow measuring section. This part consisted of a 1.5 mm diameter, 200 mm long stainless steel pipe. Another 6 mm diameter copper pipe carried steam from the flow measuring section to the bubble chamber. The two copper pipes and

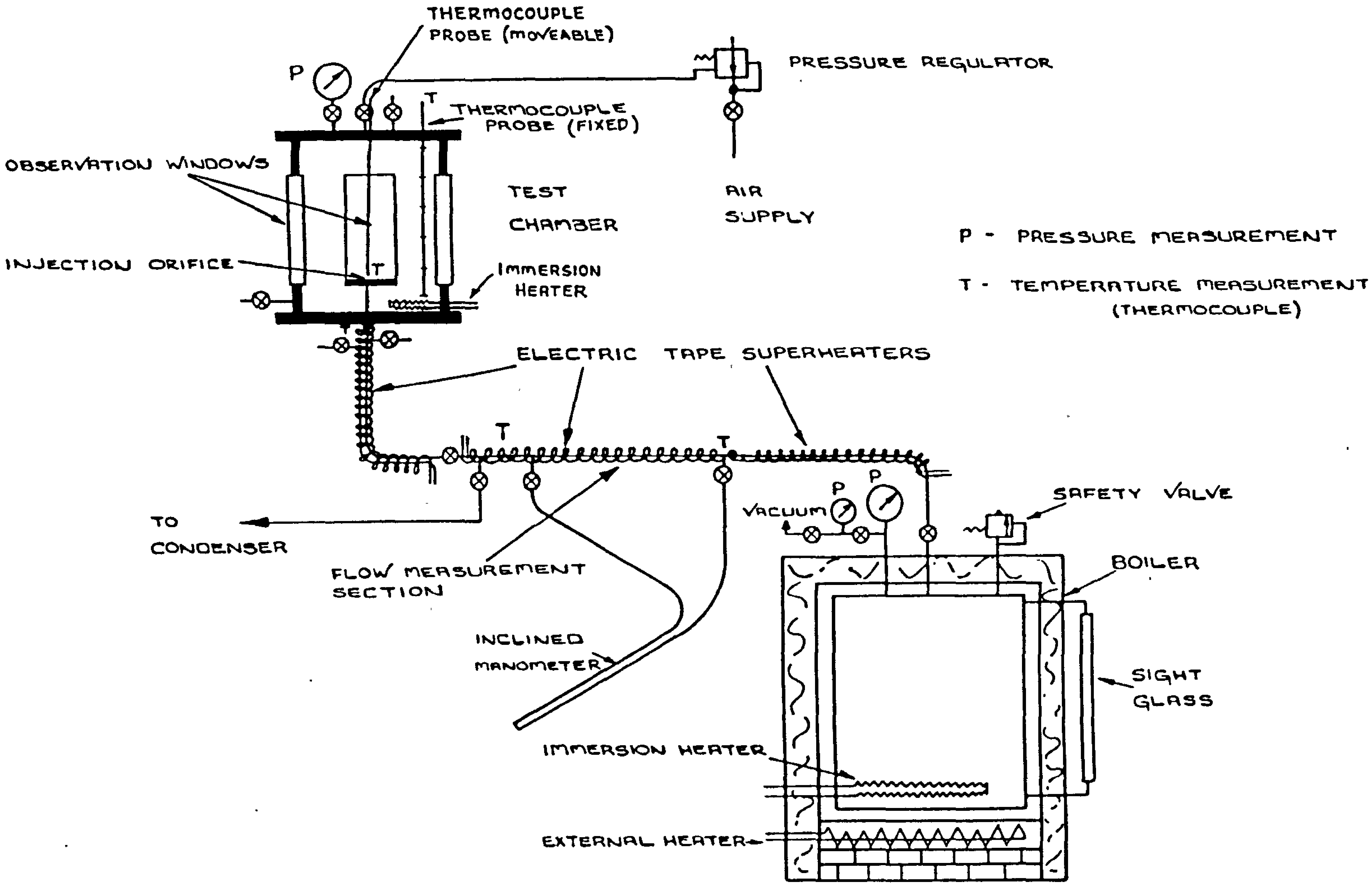

Fig. 3.1 Layout of steam bubble condensation rig

the stainless steel pipe were each wrapped by a 260 watt electric tape heater controlled by variac transformers to superheat the steam before it reached the bubble chamber.

Two pressure tappings at each end of the measuring section were connected to a 30° inclined manometer. Carbon tetrachloride (CCl_4) (ρ = 1594 kg/m^3), dyed red to differentiate it from water, was used as the manometric fluid. Two copper constantan thermocouples, one before and one after the measuring section, were installed on the copper pipes to indicate steam temperatures. The tape heater was adjusted to maintain the steam temperature constant and ensure single phase superheated steam throughout the measuring pipe.

During the calibration the temperatures at both ends of the copper pipes were kept at 160°C. In order to establish the relationship between the temperature on the pipe and the steam pressure inside the pipe, tests were carried out, at different pressures, using saturated steam and it was found that the steam temperature was about 4 K above the temperature of the pipe surface. Therefore the steam temperature inside the pipe during calibration was assumed to be 164°C. Apart from the manometric liquid - CCl_4, the arms of the inclined manometer and the copper pipes connecting them to the pressure tappings were filled with water. The valve to the test chamber was closed and differences in steam flow rate were obtained by adjustment of the valve leading to the condenser.

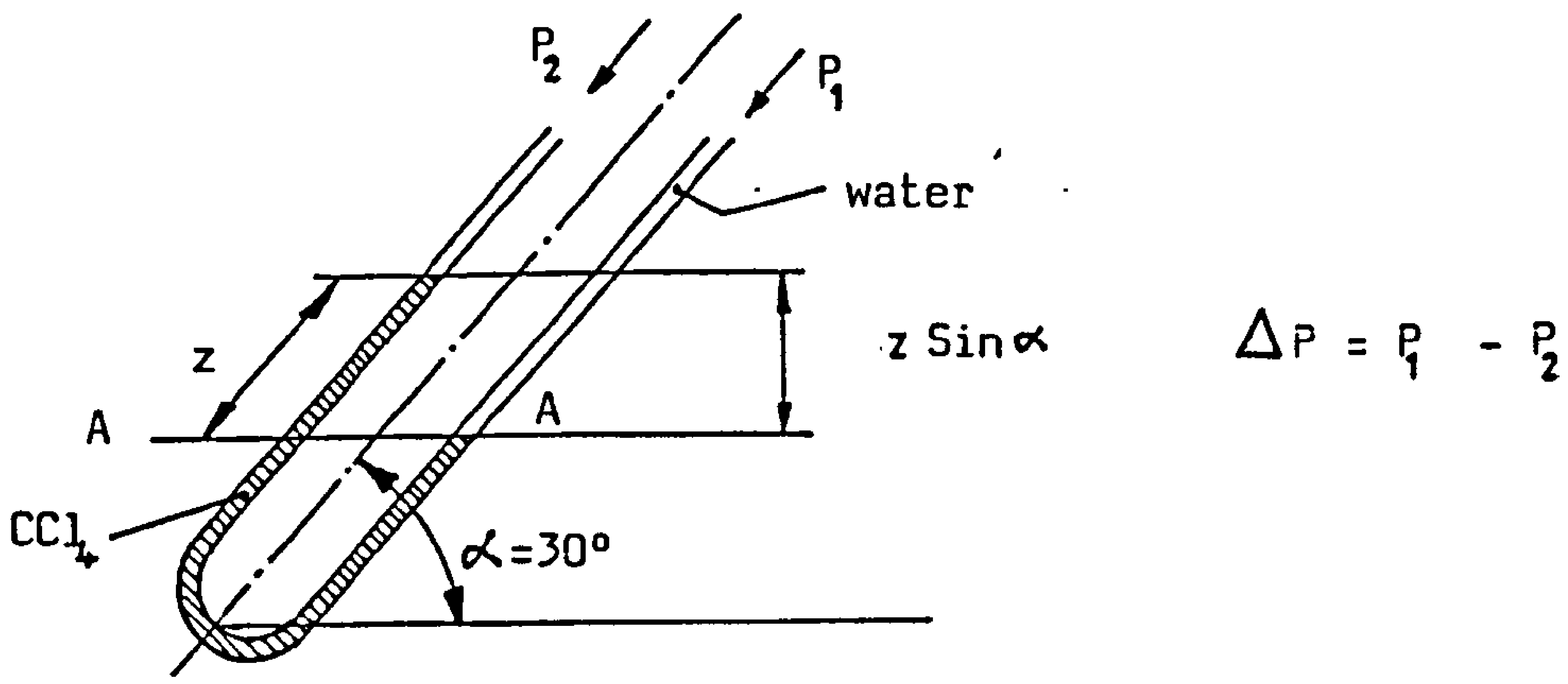

Fig. 3.2 Pressure drop in inclined manometer

As illustrated in fig. 3.2, pressures on both arms of the manometer should be equal at plane A-A.

$$P_1 + \rho_W gz\mathrm{Sin}\alpha = P_2 + \rho_C gz\mathrm{Sin}\alpha$$

$$\therefore \quad \Delta P = P_1 - P_2 = gz\mathrm{Sin}\alpha(\rho_C - \rho_W) \qquad (3.1)$$

with the density of water, ρ_W = 998 kg/m³ and of CCl_4, ρ_C = 1594 kg/m³ (both at 16°C). ΔP is the pressure drop in the pipe, which for a manometer inclination of 30° is given as

$$\Delta P = 2.922.z \quad N/m^2 \qquad (3.2)$$

where z(mm) is the difference in CCl_4 levels in the limbs of the manometer.

While carrying out the calibration, the steam flow rate ($\dot{m}$) was measured in g/min by collection of condensate while, at the same time, recording the corresponding pressure difference (z) on the manometer.

The pressure drop in a pipe having a diameter d and length l is given by

$$\Delta P = \lambda \frac{l}{d} \frac{\rho U^2}{2} \tag{3.3}$$

where $\lambda = \lambda(Re)$ is the flow resistance coefficient and U the mean velocity of flow.

Multiplying both sides by $\frac{\rho d^2}{\mu^2}$ in eqn. (3.3),

$$\frac{\rho d^2 \Delta P}{\mu^2} = \frac{\lambda l}{2d} \cdot \frac{U^2 \rho^2 d^2}{\mu^2} = \frac{\lambda l}{2d} Re^2 = \frac{l}{2d} f(Re) \tag{3.4}$$

This indicates that for a given pipe length and diameter, the dimensionless group

$B = \frac{\rho d^2 \Delta P}{\mu^2}$ is a function of Reynolds number (Re) only.

This is applicable for all fluids and conditions (temperatures and pressures).

From the measurement of condensate and manometric pressure difference, the values of

B and Re $\left(= \frac{4\dot{m}}{\pi d \mu}\right)$ were determined and the calibration

curve was plotted as shown in Fig. 3.3. As a check on the calibration curve, measurements were also taken using air, with the mass flow rate determined by a rotameter.

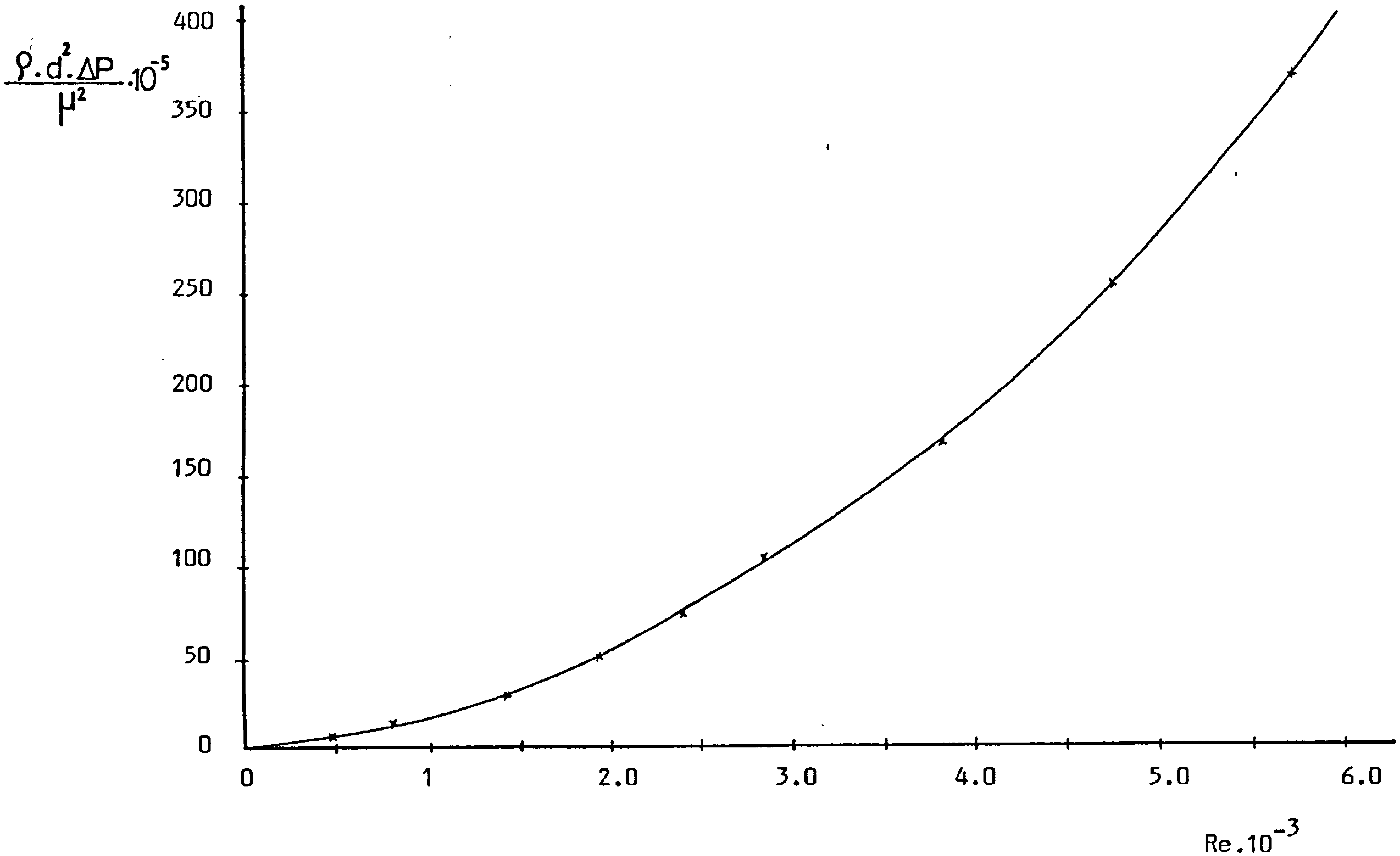

Fig. 3.3 The calibration curve

3.1.3 Bubble test chamber

After passing through the flow measuring section, steam passed to the injection orifice situated at the base of the bubble chamber, where bubbles were formed which then rose into the subcooled distilled water. The steel chamber was 180 mm square x 240 mm high with borosilicate glass windows installed in three of the sides to permit observation and photography of the condensation process. A layer of low conductivity polycarbonate was fitted to the base of the test chamber to house the injection orifice, the intention being to minimise heat losses from the steam in the orifice before bubble formation and to reduce convection currents in the region surrounding the issuing steam.

Apart from the windows, the sides of the chamber were insulated by a layer of low conductivity cement. The top and the base were also insulated using fibre glass. A 325 W immersion heater was installed at the wall, near the base, to heat up the water in the chamber to near boiling temperature and hence to obtain different degrees of subcooling. A valve situated near the base was used to drain water from the chamber.

The test chamber could be filled to any required level with distilled water and could be pressurised up to 4 bar by means of a pressure regulator, using compressed air from the main supply. A pressure gauge and a valve, to release pressure if required, were situated at the top of the chamber. A thermocouple probe was installed for measuring the water temperature in the chamber at six different levels in 38 mm intervals, the first one being 6.3 mm away from the base. A valve, situated before the orifice on the copper pipe, was used to adjust the steam flow rate.

The injection orifice was initially manufactured from brass with the tip just emerging above the layer of polycarbonate and with two thermocouples embedded into the brass wall. However, due to the relatively high thermal conductivity of the brass, excessive convection currents were set up, particularly at low steam flow rates, in the region surrounding the emerging bubble. In addition, and especially at high water subcoolings, significant pre-detachment condensation occurred. To minimise these effects, the orifice material was changed from brass to PTFE which has a thermal conductivity of 0.25 W/mK and could be used at temperatures up to 250°C. A sketch of the 2 mm diameter orifice is shown in Fig. 3.4.

Due to the low conductivity of PTFE it was not practicable to embed thermocouples in the orifice walls. Hence a thermocouple was fixed to the wall of the copper supply pipe just before entry to the orifice. In order to relate the temperature indicated by this thermocouple to the actual temperature of the emerging steam bubbles, provision was made for a thermocouple probe to be inserted through the roof of the bubble chamber, capable of being lowered into the steam bubbles at the orifice mouth. After some tests, at different steam flow rates and water subcoolings, it was found that a temperature of 165°C on the copper wall before the orifice would provide steam, either slightly superheated or saturated, at the orifice mouth. Therefore the temperature on the copper wall was maintained at 165°C during the experiments.

3.2 Photographic technique

A shadowgraph (direct shadow) optical system, illustrated in Fig. 3.5, was used to obtain photographic

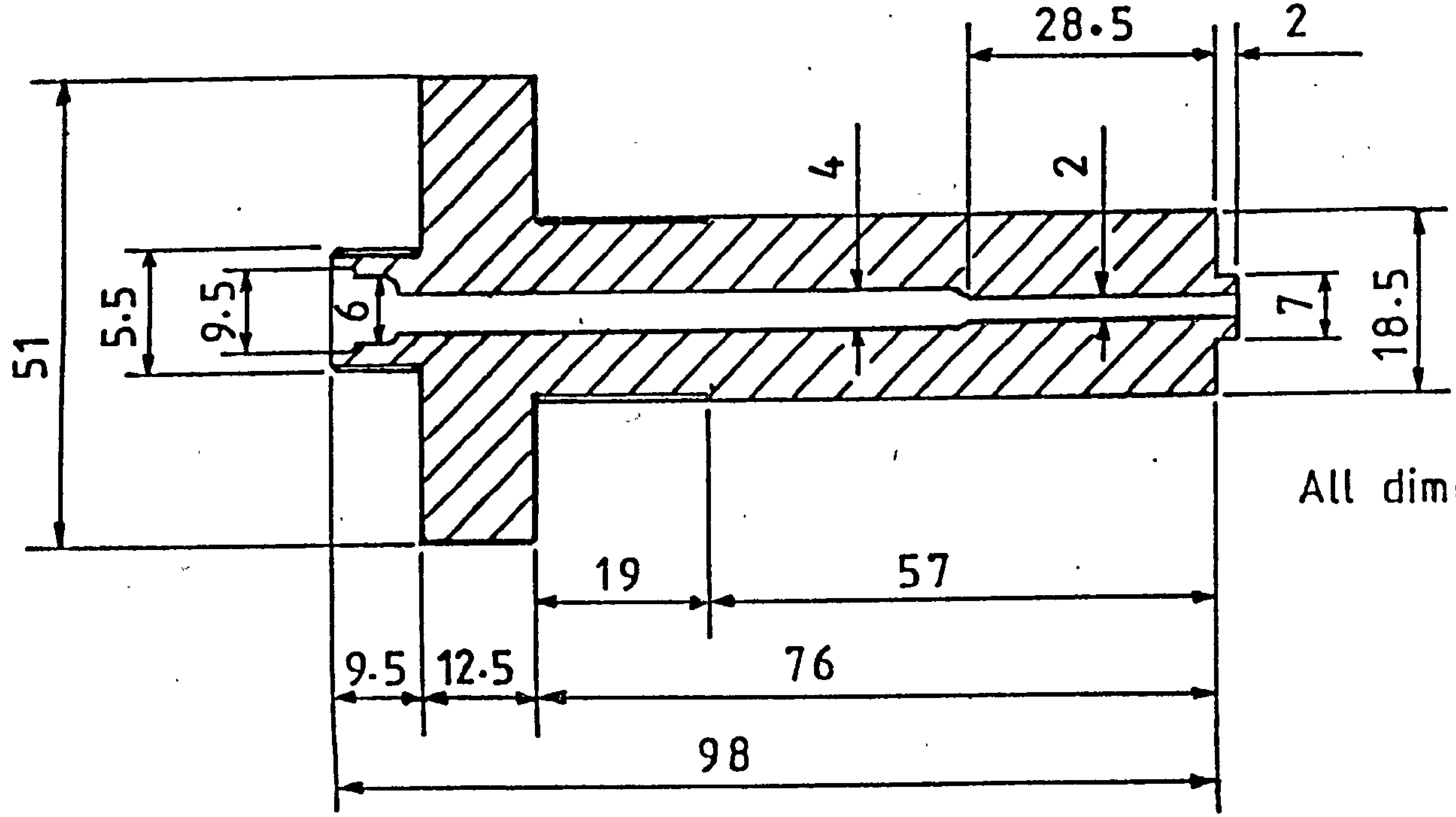

All dimensions in mm.

Fig. 3.4 Axial cross-section of injection orifice

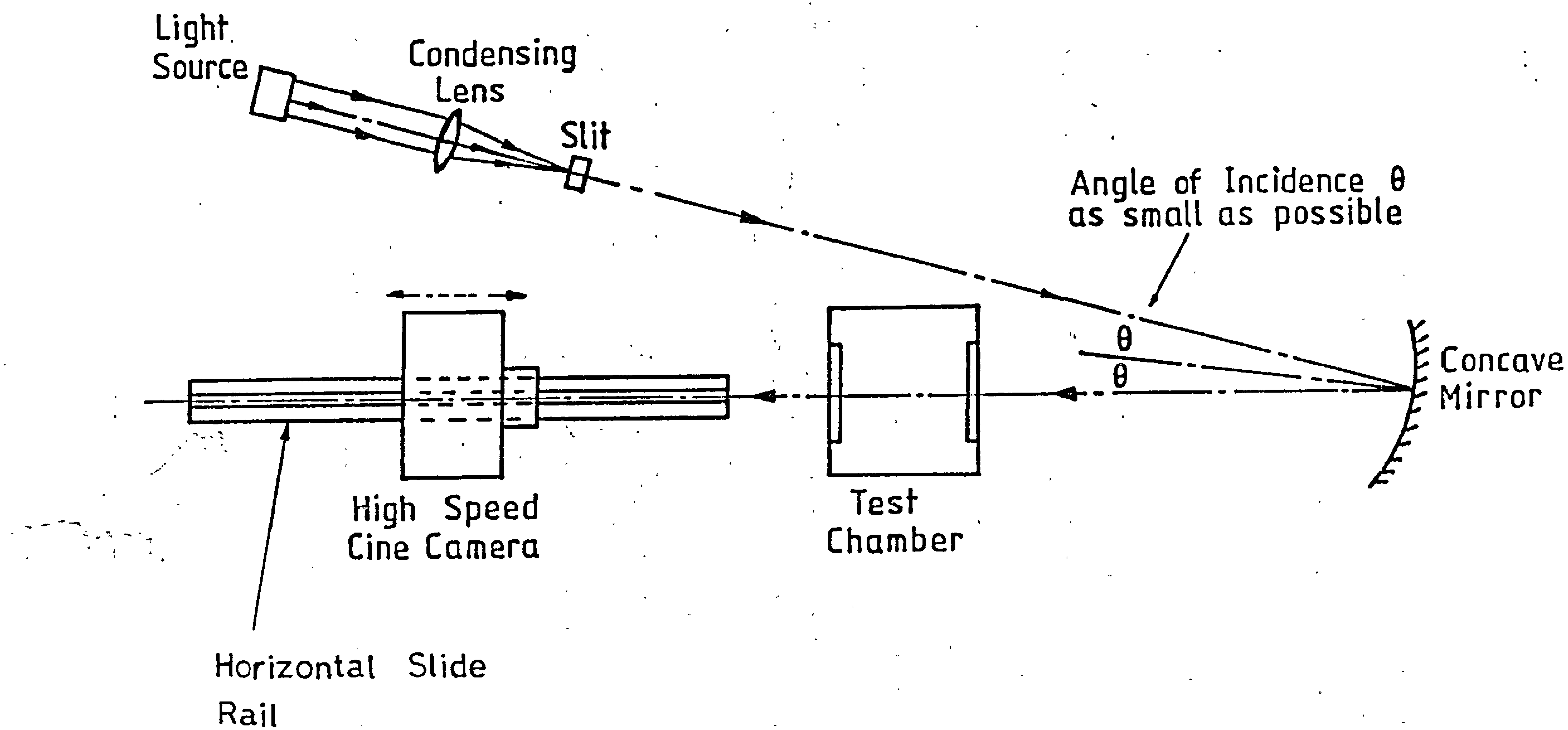

Fig. 3.5 Shadowgraph optical system

recordings of growing and collapsing bubbles. The theory of the direct-shadow method to detect density gradients in colourless fluids is well documented and will not be presented here. A thorough discussion and review is given by Holder and North [33].

The light source used was a 250-watt mercury vapour discharge lamp having a 250 volt D.C. supply. The condensing lens was positioned to give a sharp image of the arc at a slit located at the focus of a spherical concave mirror, having 8 inches diameter and a focal length of 6 feet, this reflecting a parallel beam of light through the test chamber. All the light passing outside the lens was cut off by a 4-sided covering fitted around the lamp and the lens. To minimise aberrations the reflection angle, θ at the mirror was kept as small as possible ($\theta < 10$ degrees).

A Hitachi 16 HM high speed camera with a speed range of up to 20,000 frames per second was located on a horizontal rail which had a vertical adjustment over a range of 60 mm. The camera could be moved horizontally along the rail to give either distant or close up images of the emerging bubbles and the associated convection currents. Close up views gave useful detail of bubble growth, detachment and collapse at high and medium subcoolings; distant views were useful, particularly, for studying bubble train effects, when condensation effects were small, or for more extensive pictorial records of bubble movement. During filming, the camera was focussed at the plane passing through the tip of the orifice to get a sharp image of the bubble and the tip, the diameter of the tip being used as a reference measure to calculate bubble dimensions during analysis of the cine films.

A camera speed of 500 frames per second was used for zero and low water subcoolings, this being increased up to 2500 frames per second as subcooling increased and bubbles condensed more quickly. 16 mm Kodak Tri-X reversal film of 30.5 m length (Type No. 7278) was used. The films were processed to the negative and used in that form during the analysis. A timing light generator connected to the camera produced marks on the film in time intervals of 10 milliseconds.

3.3 Test procedure and programme

A considerable effort was spent to obtain effective evacuation of air from the apparatus and finally the following procedure was adopted :

The boiler was filled with distilled water to the prescribed level and then a vacuum pump was connected to the boiler and run for about three hours without any heating. The external and immersion heaters were then switched on and, when steam formation started (still under vacuum), the valve connected to the vacuum pump was turned down to a minimum level to prevent steam going to the pump and damaging it. When atmospheric pressure inside the boiler was reached, the vacuum pump was switched off and the pressure allowed to rise. During the pressure rise, a purge valve on the boiler was opened to remove any residual air.

The vacuum pump was then used to evacuate the pipes leading to the test chamber and, after several hours, the supply valve from the boiler was opened and the pipe system allowed to fill with steam. The vacuum pump was once more disconnected and the steam again purged to atmosphere. The boiler and the pipe systems were thereafter maintained at a pressure higher than atmospheric (about 1.5 bar), by suitable regulation of the immersion heater in the boiler, to compensate for heat losses from the system.

In the tests, a water level of 40 mm above the orifice was maintained in the test chamber, with the water being heated up to boiling point by the immersion heater and by steam injected via the orifice plate, the former being switched off when the required conditions were attained. After convection currents around the heater disappeared and while the water temperature was still near boiling, suitable cine films were recorded while all the other relevant measurements were taken.

The water in the chamber was then allowed to cool progressively, to give where possible Jakob numbers up to 75, in increments of 15, with cine film and measurements recorded at each Jakob number. In each case, whenever bubbles formed, cine film recording was continued throughout bubble collapse. However, at high subcoolings the intensity of pre-detachment condensation meant that,in some cases,no bubbles detached from the orifice.

The range of test conditions covered is as follows :

Steam flow rates	:	3 steps ranging from 0.5 to 1.5 g/min
Subcoolings	:	at 1 bar, range from 5 K to 29.7 K to give Jakob numbers of 15, 30, 45, 60 and 75 and at 2 bar, range from 9.3 K to 36.6 K to give Jakob numbers of 15, 30, 45 and 60
Pressures	:	1 bar and 2 bar
Orifice diameters	:	1 mm and 2 mm

3.4 Analysis of films

A DT-11A HIPAD digitiser, interfaced to an Apple-II micro-computer, was used to obtain, from the cine films, measured values of bubble volume, bubble surface area and bubble position (all related to time), throughout both growth and collapse periods. The speed at a particular section of film was determined from timing marks on the film.

To carry out the measurements, the cine film was projected on to the tablet of the digitiser via a mirror (silverised on the front face to avoid image distortion) inclined at 45° to the horizontal. The cursor of the digitiser was then traversed around the bubble outline and the resulting X and Y coordinates fed to the computer for transformation to the required bubble volume, surface area, centroid position, etc., using a computer program written specially for the purpose. To facilitate the coordinate measurements, the tablet was covered with paper printed with a 1 mm square grid. The arrangement of digitiser and computer together with projector and mirror is illustrated in Fig. 3.6.

The bubble projected on the graph paper was assumed to be comprised of frustums of cones, each having a height of either 10 mm or in some cases 5 mm. The computer program took 4 coordinates of a frustum and calculated volume, surface area, and position of centroid. An illustration of bubble projection on graph paper is given in Fig. 3.7.

The calculations were carried out as follows :

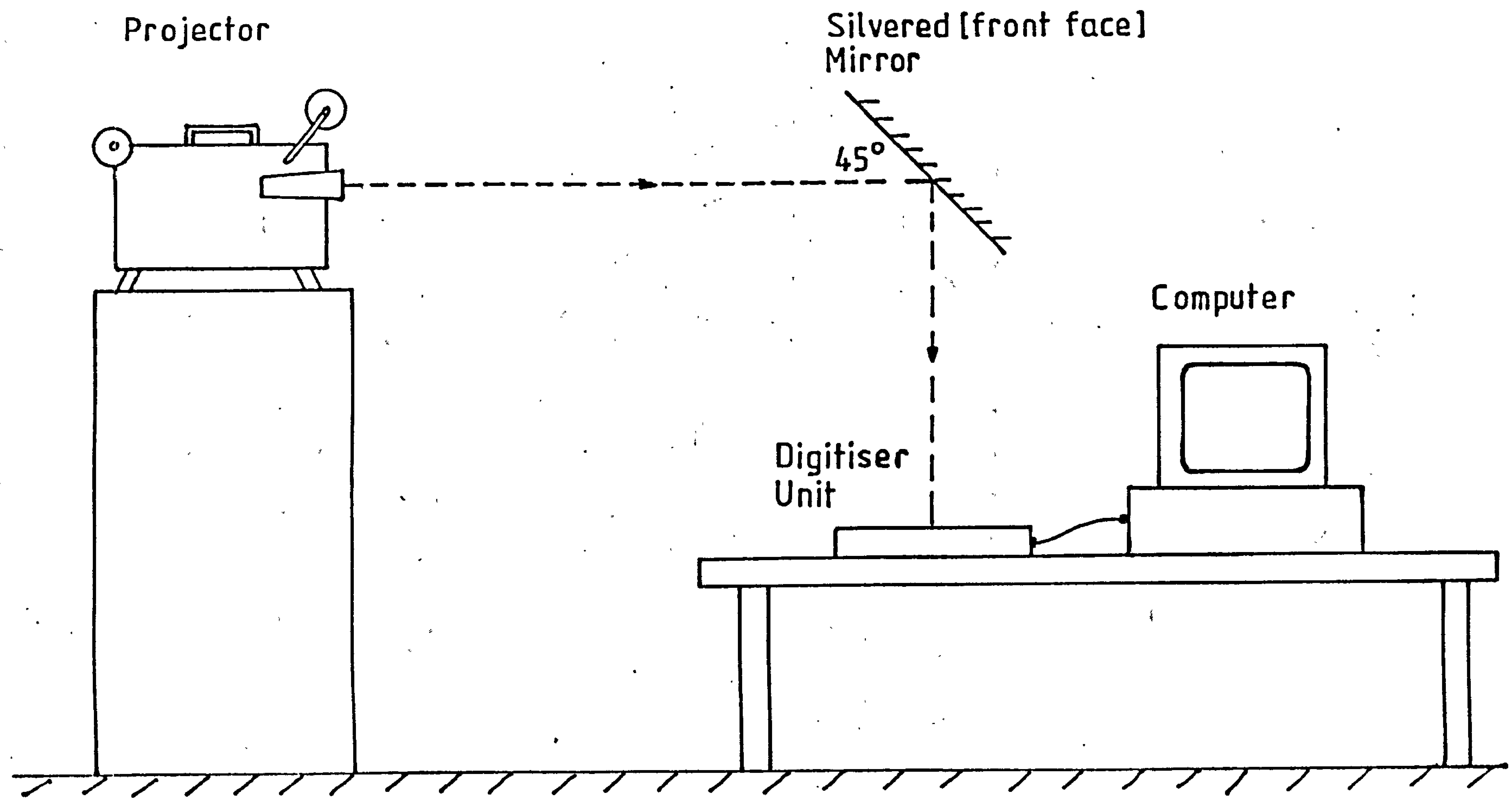

Fig. 3.6 Arrangement of digitiser and computer

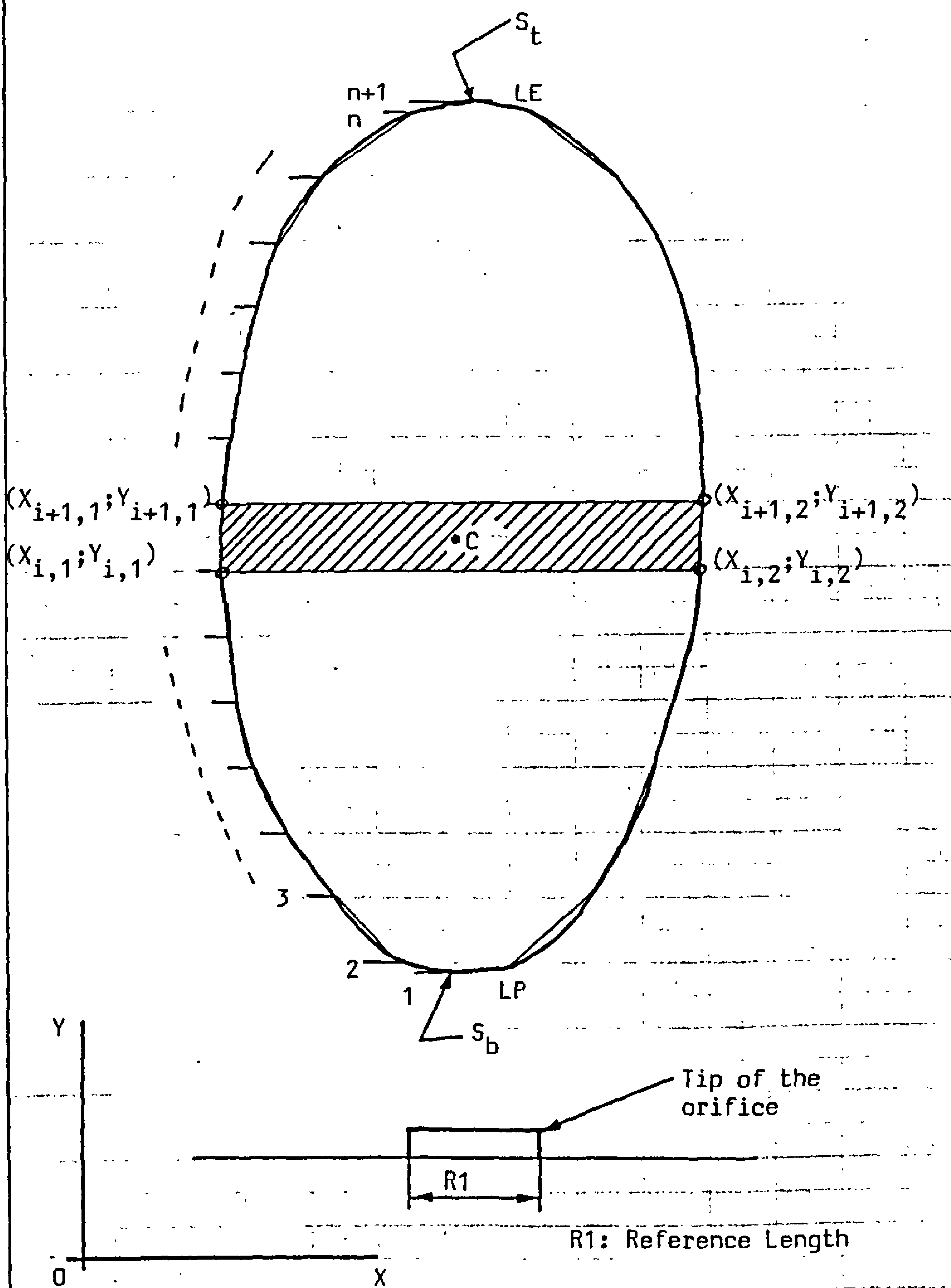

Fig. 3.7 Bubble projection on graph paper

i) The volume of the i th frustum (hatched in Fig. 3.7) was calculated from the coordinate measurements, X and Y as

$$V_i = \frac{\pi}{3} h_i \left(R_{ti}^2 + R_{ti} R_{bi} + R_{bi}^2\right) \qquad (3.5)$$

where R_b and R_t are respectively the radii of the bottom and top surfaces, and h is the height of the frustum. Hence the total volume of the bubble :

$$V_B = \sum_{i=1}^{n} V_i \qquad (3.6)$$

(ii) The lateral area of the i th frustum was

$$A_i = \pi \, (R_{bi} + R_{ti}) \sqrt{h_i^2 + (R_{ti} - R_{bi})^2} \qquad (3.7)$$

Hence the total surface area of the bubble was

$$S_B = \sum_{i=1}^{n} A_i + S_b + S_t \qquad (3.8)$$

where S_b & S_t are the respective areas at the bottom of the first frustum and at the top of the last frustum.

iii) The equivalent radius of the bubble,

$$R = \left(\frac{3V_B}{4\pi}\right)^{1/3} \qquad (3.9)$$

iv) Location of the centroid of each frustum was calculated according to the formula,

$$c = \frac{1}{4} \, d \left(\frac{1+2k+3k^2}{1+k+k^2}\right) \qquad (3.10)$$

where d is the distance between the centroids of the bases of frustum, and

$k = \frac{R_t}{R_b}$ is the ratio of the radius of the top surface to the radius of the base.

The centroid of each frustum is at a distance c from the centroid of the base along the line of length joining the centroids of the base and the top surface as illustrated in Fig. 3.8.

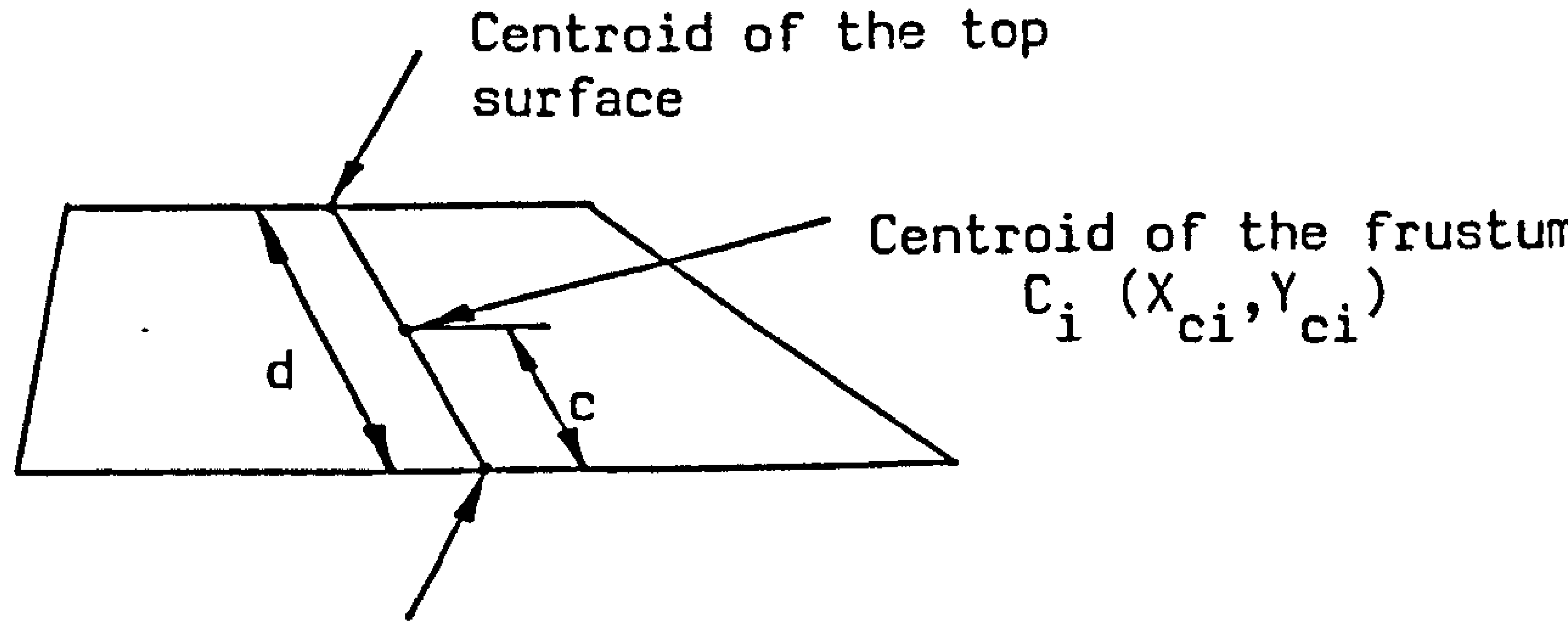

Fig. 3.8 The centroid of the frustum of a cone

Hence the bubble centroid position (X_{CB}, Y_{CB}) was calculated as

$$X_{CB} = \frac{\sum_{i=1}^{n} V_i \, X_{ci}}{\sum_{i=1}^{n} V_i}, \quad Y_{CB} = \frac{\sum_{i=1}^{n} V_i \, Y_{ci}}{\sum_{i=1}^{n} V_i} \qquad (3.11)$$

CHAPTER 4

EXPERIMENTAL RESULTS AND DATA ANALYSIS

4.1 Introduction

The test results are typified by the set shown in Figures 4.1 and 4.2, these being printed by the plotter. These results relate to a particular steam flow rate (0.45 g/min) and water subcooling (9.3 K) at 2 bar pressure with a 2 mm diameter orifice and include :

(i) An artistic impression of the bubble shape over a range of frames in the cine film
(ii) A table of experimental parameters
(iii) A table of experimental results
(iv) 10 plots of experimental or derived data

4.2 Format of Test Results

4.2.1 Impressions of Bubble Shape

For any particular test condition, several sequences of bubble growth and collapse were photographed. The impressions illustrated are typical of the events at that particular test condition.

4.2.2 Experimental Parameters

The identification of parameters and other details relevant to Fig.4.1 is as follows:

d : orifice diameter, mm
$\dot{m}_s$: steam mass flow rate, g/min
V_s : steam volume flow rate, mm³/s
ΔT : water subcooling, K
Z : water level above orifice in chamber (=40 mm in all tests)
P : pressure in bubble chamber steam space, bar

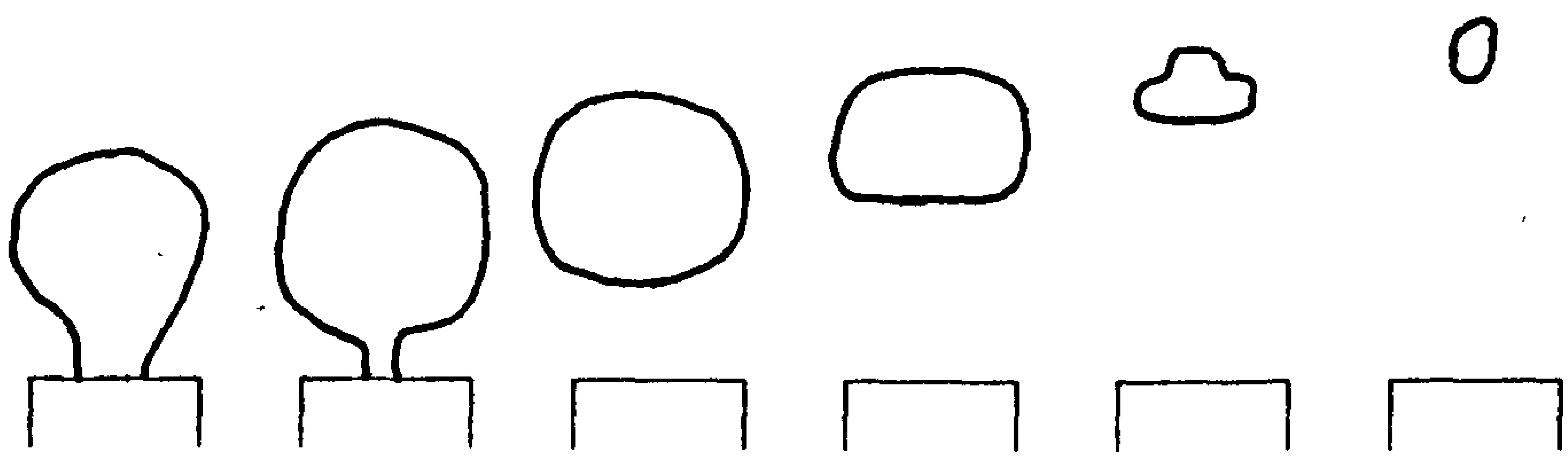

FRAME NUMBERS :	1 -9	10-11	12-13	14-18	19	20-24

EXPERIMENTAL PARAMETERS :

d	2	Z	40	F	24
$\dot{m}_s$	.45	P	2.005	Ja	15
(V_s	6643)	Δt	2.37	T_p	165
ΔT	9.3	(CS	422)		

EXPERIMENTAL RESULTS :

t_g	28.46	h_c	17086	Pe_o	7210
t_c	24.7	Nu_c	63		
t_t	53.16	Z_d	4.22		
f_s	38	Z_c	11.36		
R_m	2.51	U	250		
R_o	2.45	Fo_c	1.749E-04		

TEST NO : (4.1).2 FILM NO : 44-2/4

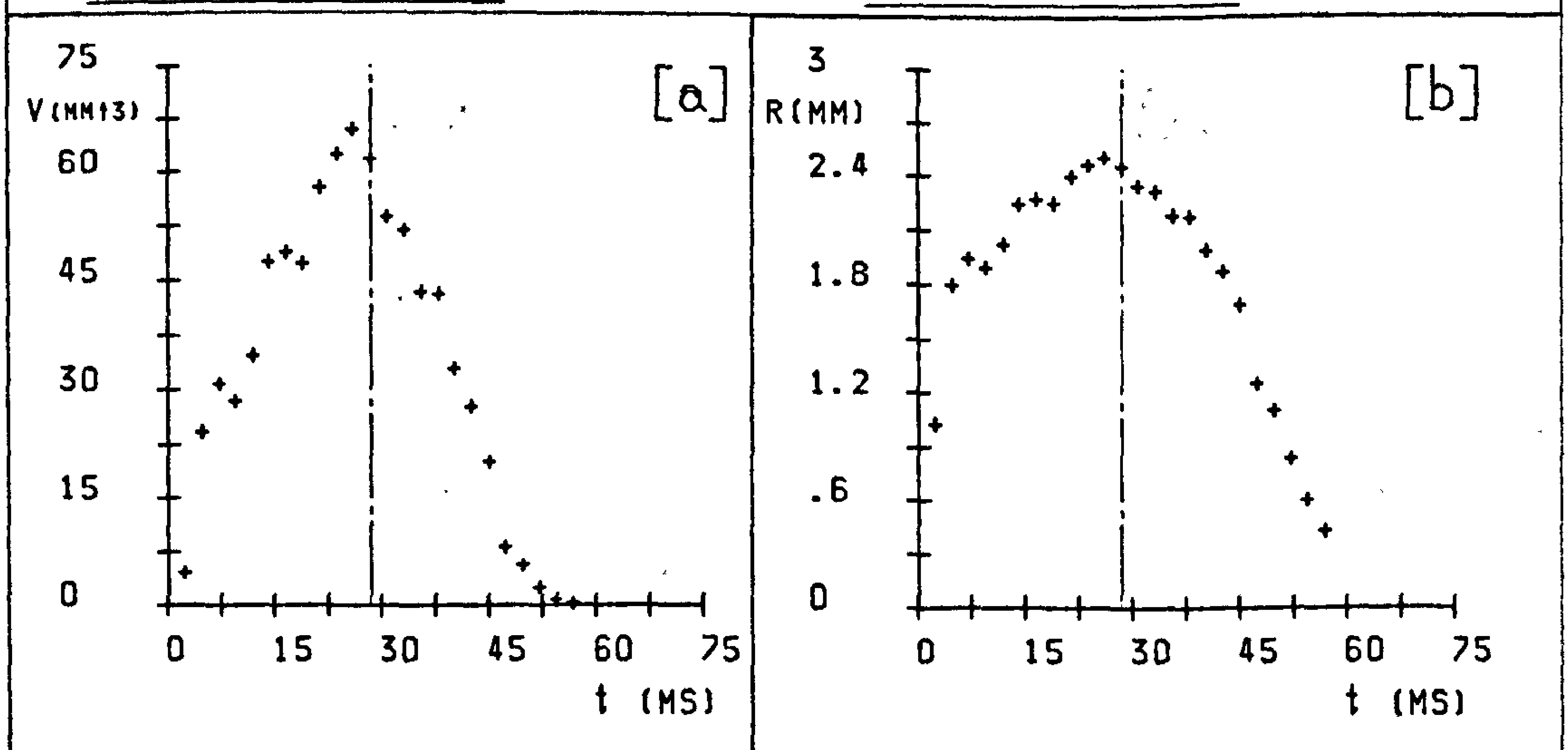

Fig. 4.1 Experimental parameters and results

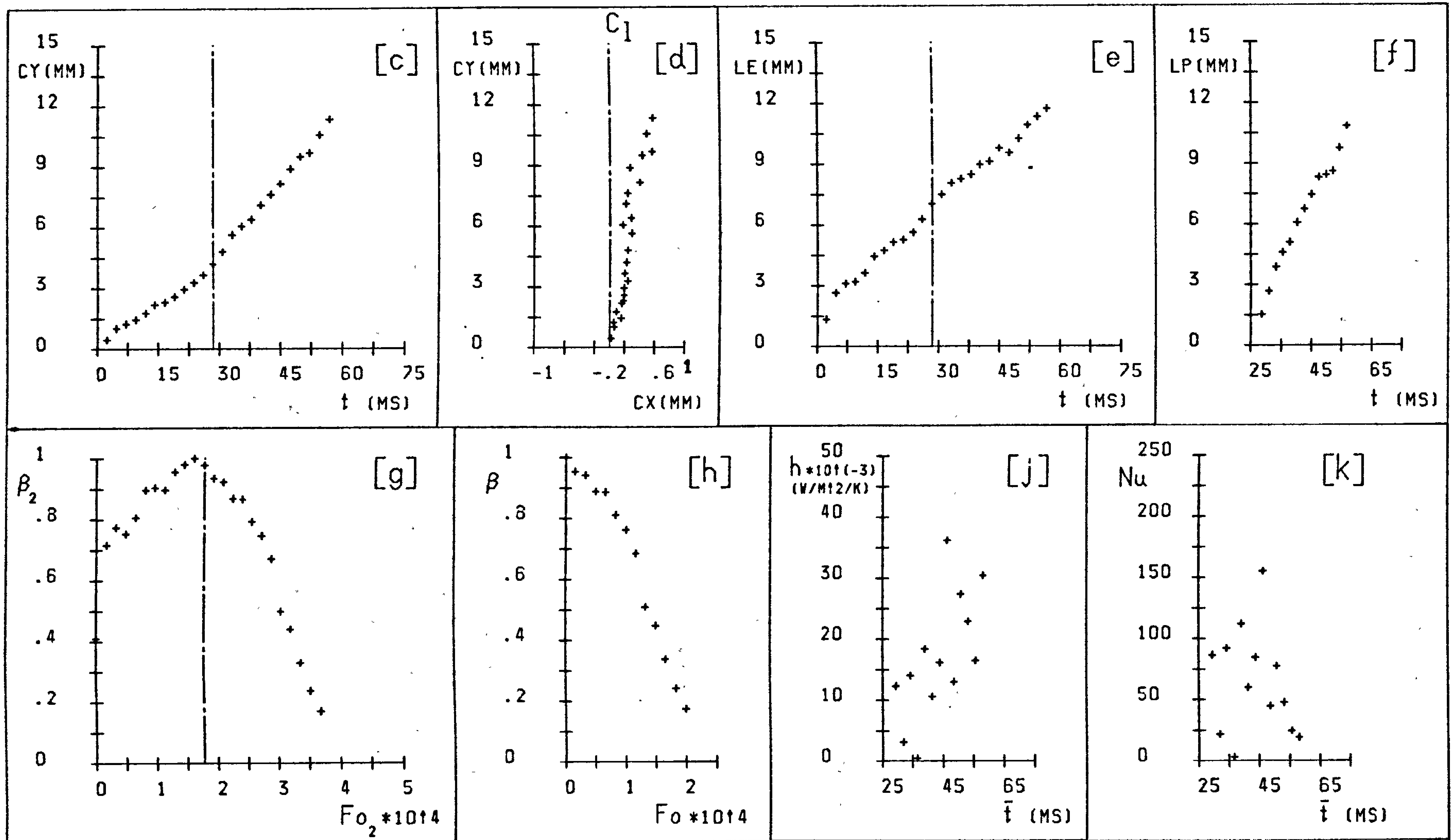

Fig. 4.2 Experimental results

(4.1).2

Δt : time interval between alternate frames in cine film, ms

Cs : camera speed, frames per sec

F : number of frames

Ja : Jakob number $= \frac{\rho_w c_{pw} \Delta T}{\rho_s h_{fg}}$

T_p : steam temperature at copper pipe before orifice (= 165°C in all tests)

Pe_o : Peclet number $= \frac{2R_o U}{\alpha}$

4.2.3 Experimental results

The identification of the items in Fig.4.1 is as follows :

tg : time from bubble initiation to detachment from orifice, ms

t_c : time from bubble detachment to complete collapse due to condensation, ms

t_t : total time from initiation to complete collapse = tg + t_c, ms

f_s : bubble frequency, 1/s

R_m : maximum radius of bubble, mm

R_o : bubble radius at detachment, mm

h_c : average heat transfer coefficient during condensation (after detachment), W/m²K

Nu_c : average Nusselt number during condensation

Z_d : bubble centroid height at detachment (above orifice), mm

Z_c : bubble centroid height at collapse, mm

U : average vertical velocity of bubble during condensation (after detachment), mm/s

Fo_c : collapse Fourier number $= \frac{\alpha_w t_c}{4R_o^2}$

4.2.4 Data Plots

There are 10 separate data plots (identified as 'a' to 'k' over Figs. 4.1 and 4.2), the data points on which relate to computed values. The vertical chaindotted line on plot (d) indicates the centre line of the orifice while the vertical chaindotted line on plots (a), (b), (c), (e) and (g) indicates the point of detachment and thereby separates the bubble growth and bubble collapse (condensation) regions.

4.3 Comments on individual data plots

Plot (a) : This is a plot of bubble volume versus time, as obtained from the cine film analysis. The data clearly show the bubble growth period, the bubble volume reaching a maximum value just before detachment, i.e. just before detachment the reduction in volume due to condensation is apparently beginning to overcome the growth due to steam flow.* For this subcooling value of 9.3 K, the data indicate that, after detachment, bubble collapse due to condensation is fairly rapid.

Plot (b) : This shows bubble radius R to a base of time and is an alternate form of plot (a) since R was evaluated from $V = \frac{4}{3} \pi R^3$.

Plot (c) : This shows the position of the Y coordinate of the centroid of the bubble with respect to time. It shows the bubble centroid rising fairly uniformly throughout bubble growth, with a slight acceleration at detachment and with a more rapid centroid movement after detachment than during growth.

* It was not possible to sustain a constant steady steam flow rate,unaffected by fluctuations, throughout the experiment .

Plot (d) : This is a spatial plot of the X and Y coordinates of the centroid of the bubble during growth and collapse. In this plot, the vertical chaindotted line represents the centre line of the inlet orifice and the data indicate the bubble movement relative to this from initiation to collapse. The plot clearly shows that, during bubble growth, the bubble centroid position deviates only slightly from the orifice centreline. After detachment, however, the bubble does not travel straight upwards, but deviates from the centre line by up to about 0.6 mm, (or perhaps more since these are X-projected values and the radial deviation may be greater), which is much less than the bubble diameter at detachment. The height above the inlet orifice at which complete collapse occurred is about 12 mm, which means the bubble rose about 8 mm between detachment and complete collapse.

Plot (e) : This is a plot of the position of the "leading edge" (LE) of the bubble (i.e. top most point) against time and, as such, is an alternative to plot (c).

Plot (f) : This is a similar plot to (e) but with the "lowest point" (LP) of the bubble being plotted against time, for the collapse region only. A comparison of plots (c), (e) and (f) gives some indication of the distortion in bubble shape from the spherical and also suggests that, after detachment, condensation occurs mainly on the upper part of the bubble.

Plot (g) : This is a dimensionless plot which shows $\beta_2 = \frac{R}{R_m}$ against Fourier number $Fo_2 = \frac{\alpha_w . t}{4R_m^2}$ and is an attempt to physically relate the bubble growth and collapse to the heat conduction through the bubble boundary layer.

Plot (h) : This is another dimensionless plot of the data, similar to plot (g), but using the bubble radius at detachment R_o, instead of the maximum bubble radius R_m, in the expressions for β and F_o, and with time t being measured from the point of detachment. Here

$$\beta = \frac{R}{R_o} \text{ and } F_o = \frac{\alpha_w . t}{4R_o^2} \qquad (4.1)$$

and the data are plotted only for the collapse region.

Plot (j) : This is a plot of instantaneous heat transfer coefficient h, between the steam bubble and the water, versus time for the collapse region. The values of h were evaluated as

$$h = \frac{\frac{\Delta V}{\Delta t} \cdot \rho_s \cdot h_{fg}}{A \; . \; \Delta T} \qquad (4.2)$$

where $\Delta V = V_i - V_{i+1}$, the difference in bubble volume between two successive frames

$A = \frac{A_i + A_{i+1}}{2}$, the average bubble surface area between two successive frames.*

In the plot, $\bar{t} = \frac{t_i + t_{i+1}}{2}$ indicates the time to a point between two successive frames. The data show condensation heat transfer coefficients ranging up to about 35 kW/m^2K.

Plot (k) : This shows the instantaneous Nusselt number plotted against time for the collapse region. The Nusselt number was calculated as

$$Nu = \frac{2h.R}{k_w} \qquad (4.3)$$

* ΔT is taken as the nominal temperature difference between steam and water ,$T_s - T_\infty$.

where $R = \frac{R_i+R_{i+1}}{2}$, the average bubble equivalent radius between two successive frames.

4.4 Experimental Results

The grid of the test conditions together with the corresponding test numbers is given in Table 4.1. Water subcoolings, corresponding to Jakob numbers at different pressures, are also presented in Table 4.1. For example, Test '5.2' indicates a 2 mm diameter orifice being used, at 2 bar pressure with a steam mass flow rate of 0.92 g/min and a water subcooling of 18.5 K (corresponding to a Jakob number value of 30). Three bubbles were analysed for each of the 38 conditions. Experimental results, for one bubble in each condition, are given in the following pages. The numerical values of some of the variables are given in Appendix 4.

In each case the bubble is represented by one of the following symbols (X, + and *), each of which relates to the same bubble in all plots. In the following chapters all 3 bubbles in each condition are plotted in dimensionless form as β vs Fo.

4.5 Determination of bubble rise velocity, Peclet number and collapse Fourier number

The bubble rise velocities, U were determined for each bubble from the slopes of the 'CY versus t' curves. The detachment radius of the bubble, R_o and the collapse time after detachment, t_c were determined, in most cases, from the 'V versus t' curves as they showed more clearly the effect of noncondensables towards the end of collapse

d (mm)	P (bar)	$\dot{m}$ (g/min) \ Ja	15	30	45	60	75
			Test number				
2	1	0.5	1.1	1.2	-	-	-
		1.0	2.1	2.2	2.3	-	-
		1.5	3.1	3.2	3.3	3.4	-
	2	0.45	4.1	4.2	-	-	-
		0.92	5.1	5.2	5.3	-	-
		1.42	6.1	6.2	6.3	6.4	-
1	1	0.42	7.1	7.2	7.3	-	-
		1.0	8.1	8.2	8.3	8.4	-
		1.42	-	9.2	9.3	9.4	9.5
	2	0.45	10.1	10.2	-	-	-
		0.82	11.1	11.2	11.3	-	-
		1.39	12.1	12.2	12.3	12.4	-

Ja	15	30	45	60	75	P (bar)
ΔT (K)	5	10	14.9	19.8	24.7	1
	9.3	18.5	27.6	36.6	45.6	2

Table 4.1 The grid of the test conditions , and water subcoolings corresponding to Jakob numbers

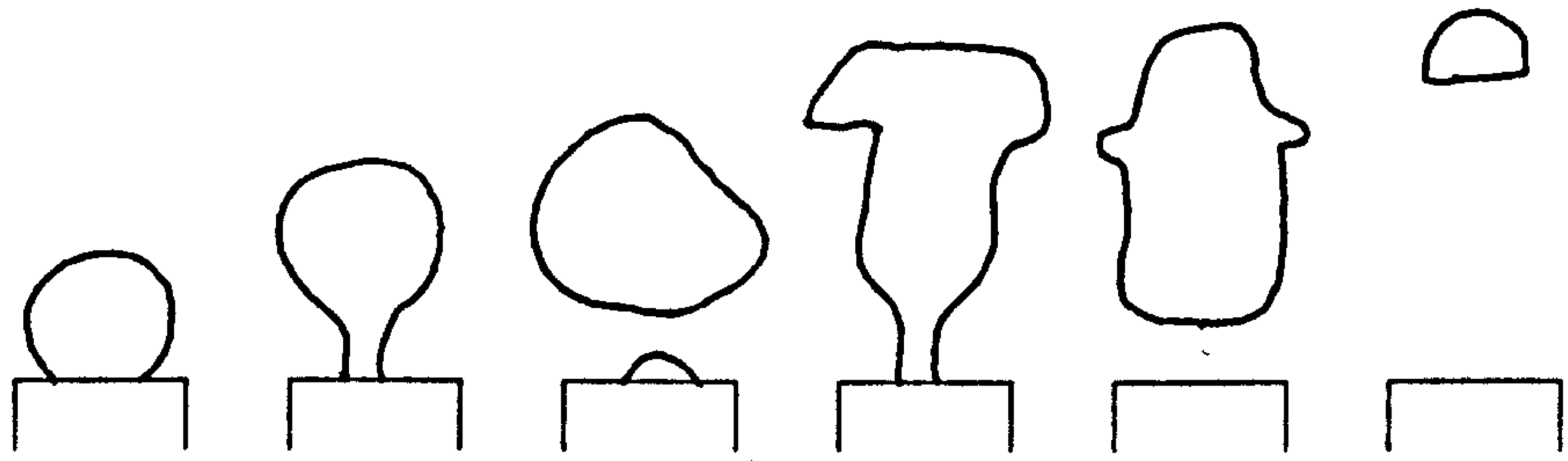

FRAME NUMBERS : 1 -7 8 -12 13-14 15-22 23-28 29-34

EXPERIMENTAL PARAMETERS :

d	2
$\dot{m}_s$	.5
(V_s	13935)
ΔT	5

Z	40
P	.991
Δt	2.29
(CS	436)

F	34
Ja	15
T_p	165

EXPERIMENTAL RESULTS :

t_g	50.46
t_c	26
t_t	76.46
f_s	20
R_m	3.84
R_o	3.46

h_c	21285
Nu_c	121
Z_d	7.76
Z_c	18.12
U	480
Fo_c	9.09E-05

Pe_o	19840

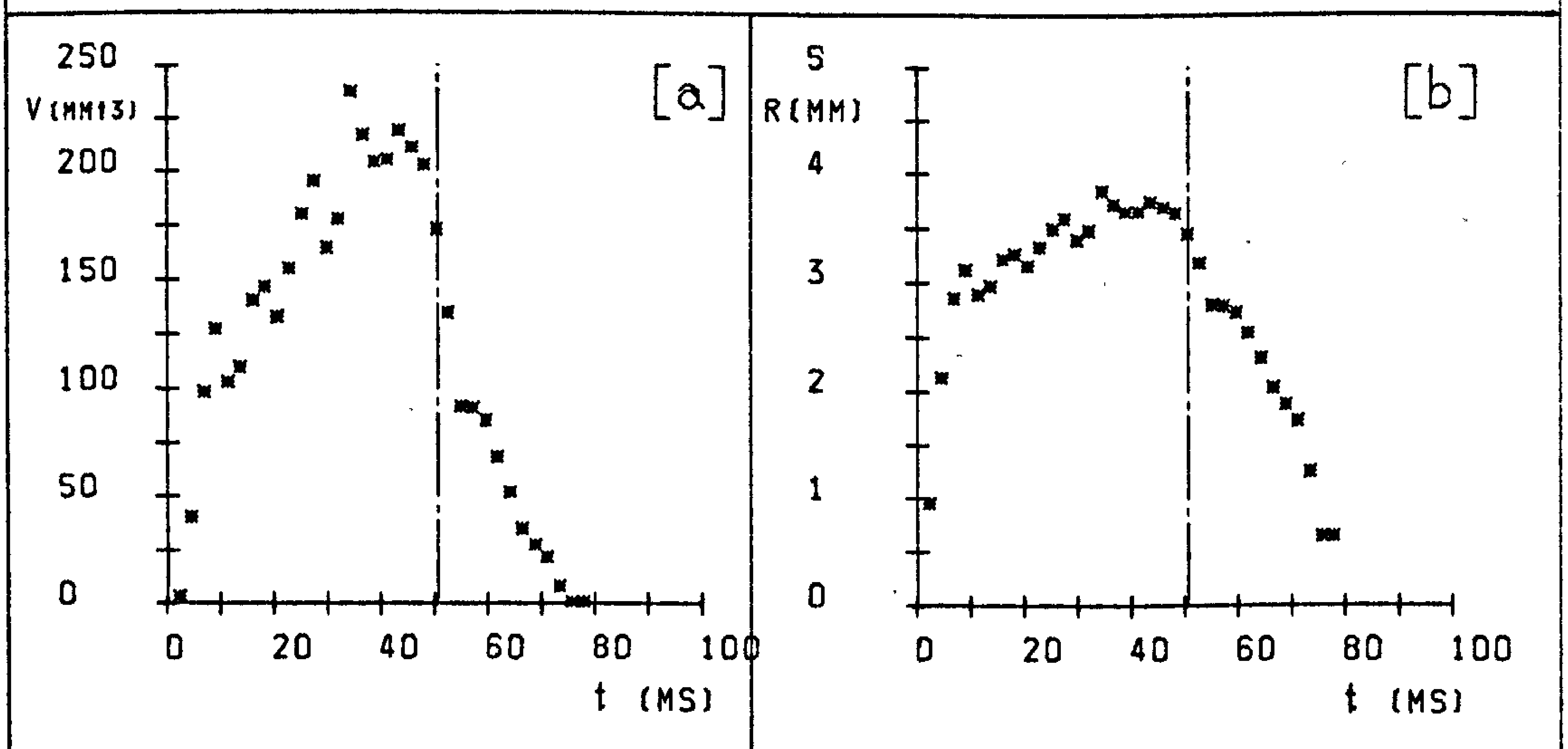

TEST NO : (1.1).3 FILM NO : 34-2/5

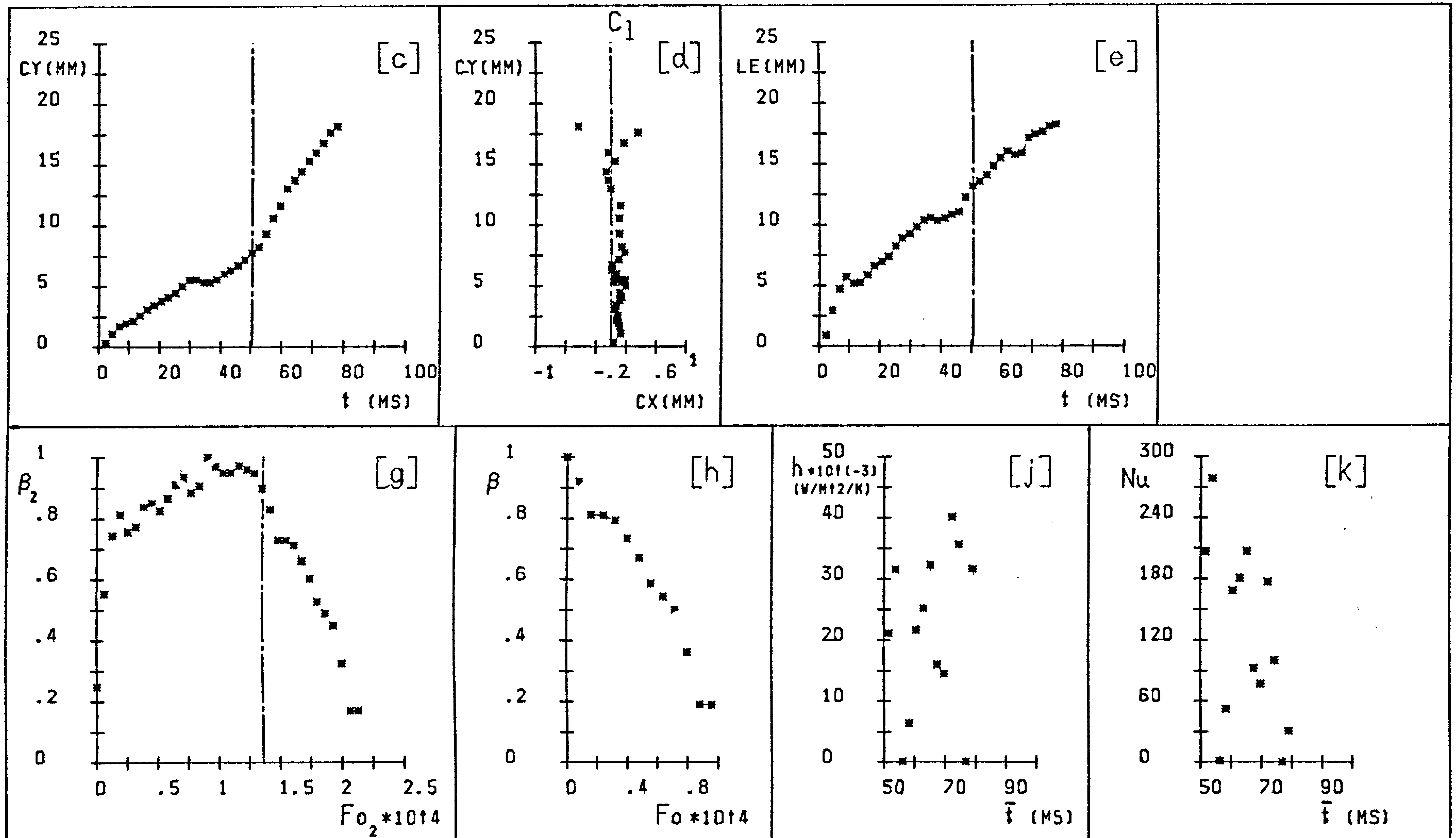

TEST NO : (1.1).3   FILM NO : 34-2/5

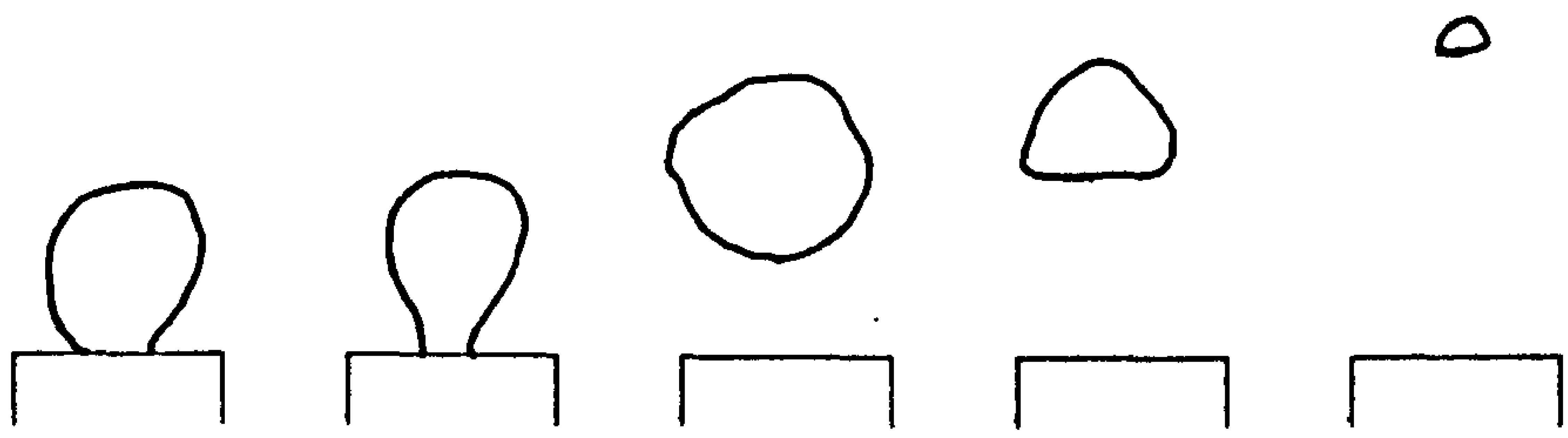

FRAME NUMBERS : 1 -6 7 -13 14-15 16-17 18-19

EXPERIMENTAL PARAMETERS :

d	2	Z	40	F	19
$\dot{m}_s$	.5	P	.991	Ja	30
(V_s	13935)	Δt	2.31	T_p	165
ΔT	10	(CS	433)		

EXPERIMENTAL RESULTS :

t_g	32.33	h_c	17905	Pe_o	12080
t_c	8.25	Nu_c	65		
t_t	40.58	Z_d	4.92		
f_s	33	Z_c	9.24		
R_m	2.82	U	437		
R_o	2.3	Fo_c	6.49E-05		

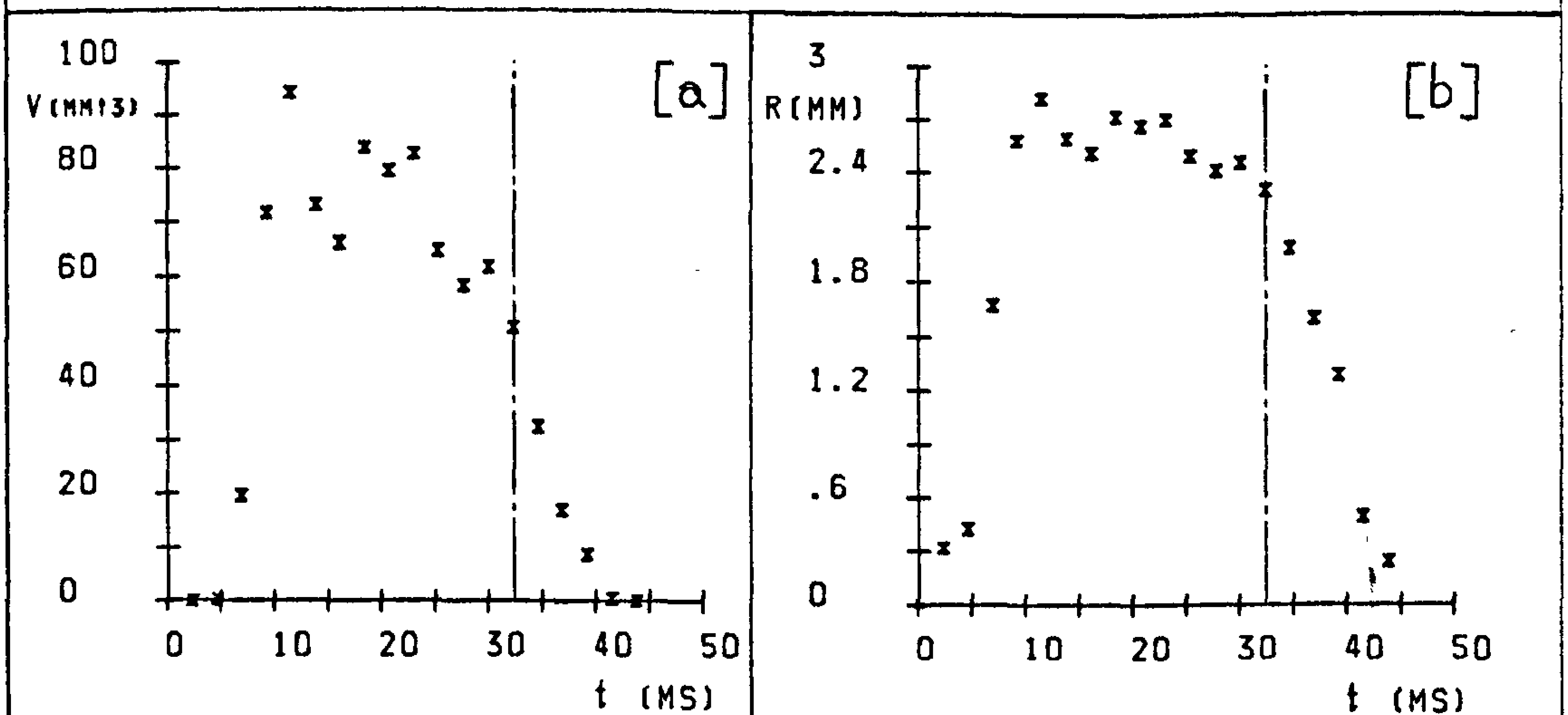

TEST NO : (1.2).1 FILM NO : 34-3/6

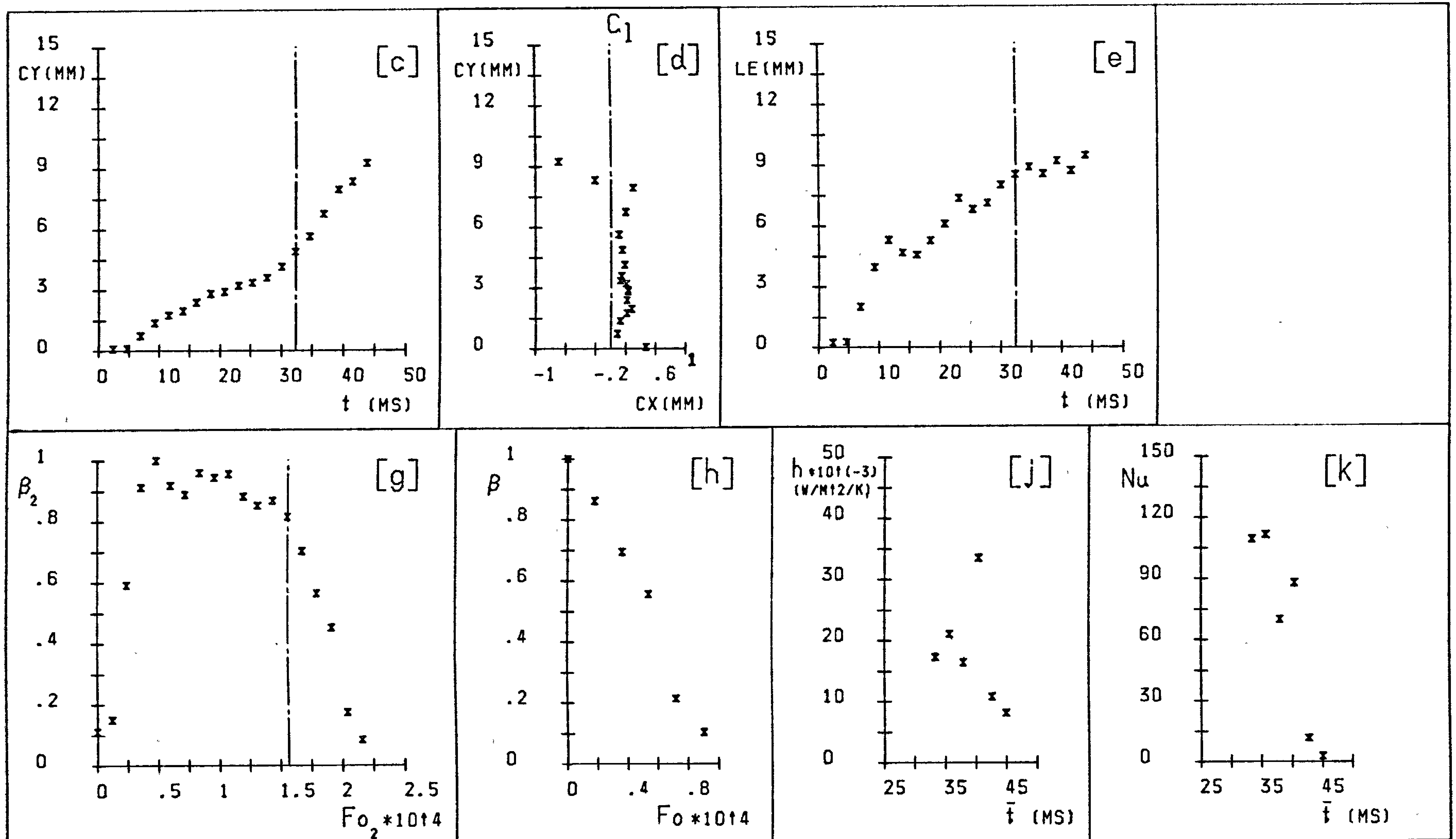

TEST NØ : (1.2).1 FILM NØ : 34-3/6

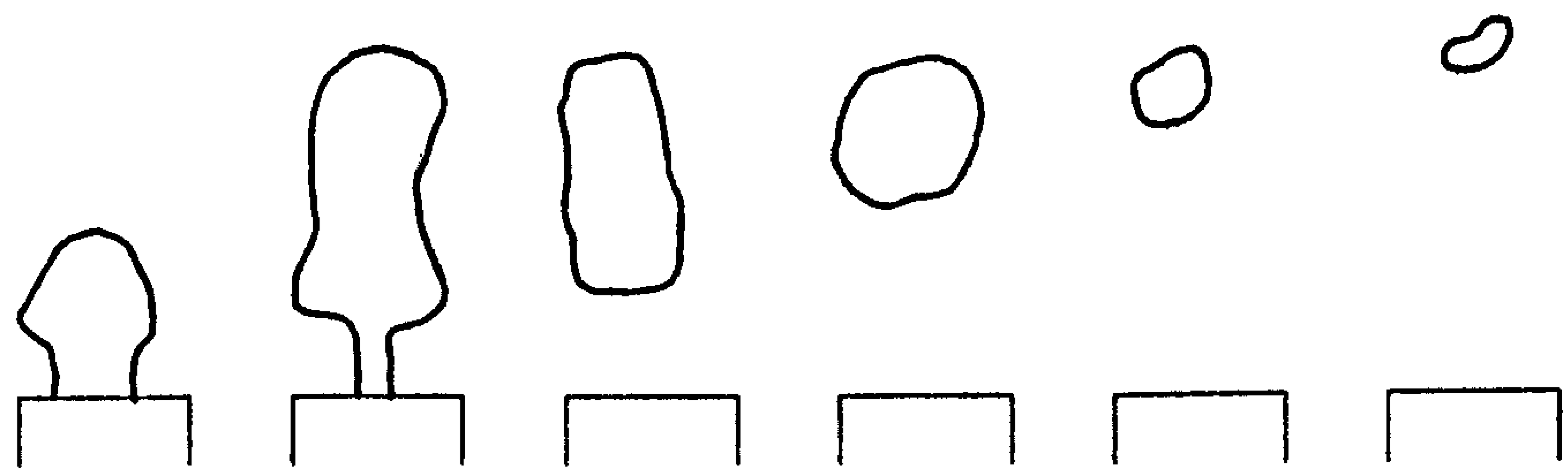

FRAME NUMBERS : 1 -6 7 -16 17-19 20-23 24-26 27-30

EXPERIMENTAL PARAMETERS :

d	2
$\dot{m}_s$	1
(V_s	27871)
ΔT	5

Z	40
P	.995
Δt	2.37
(CS	422)

F	30
Ja	15
T_p	165

EXPERIMENTAL RESULTS :

t_g	37.92
t_c	35
t_t	72.92
f_s	28
R_m	4.68
R_o	4.49

h_c	26596
Nu_c	195
Z_d	13.71
Z_c	30.54
U	524
Fo_c	7.26E-05

Pe_o	28110

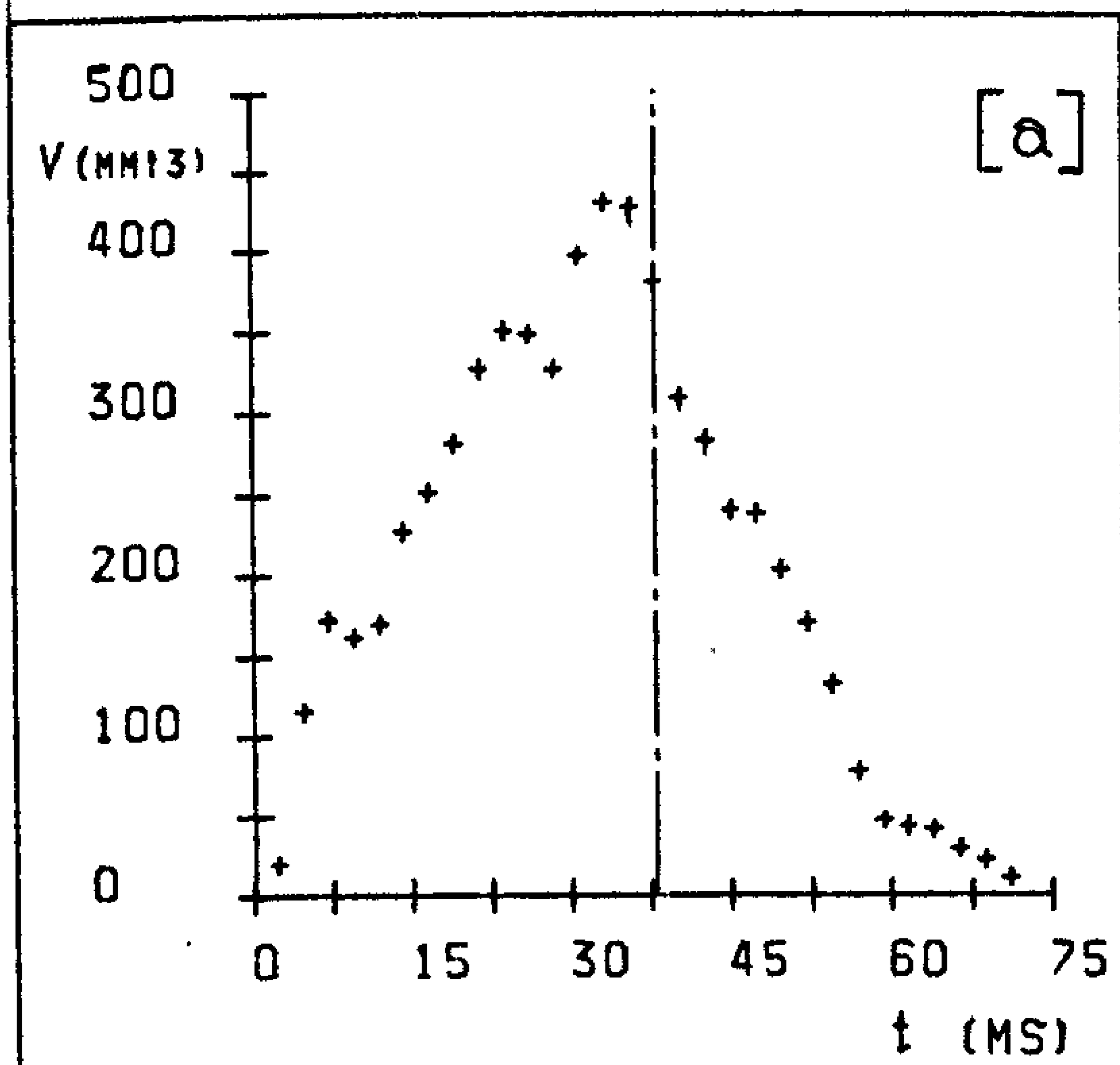

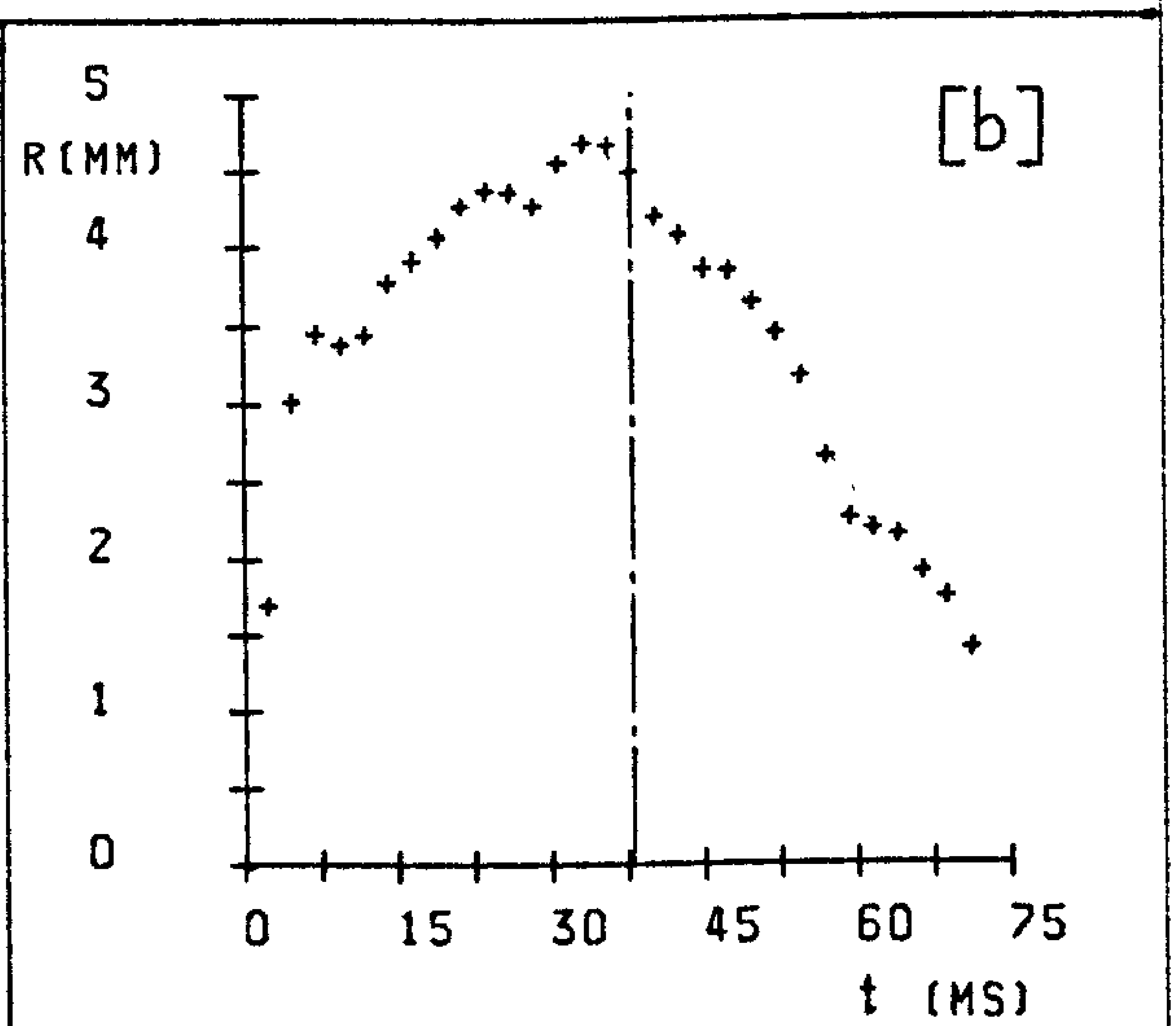

TEST NO : (2.1).2 FILM NO : 38-1/2

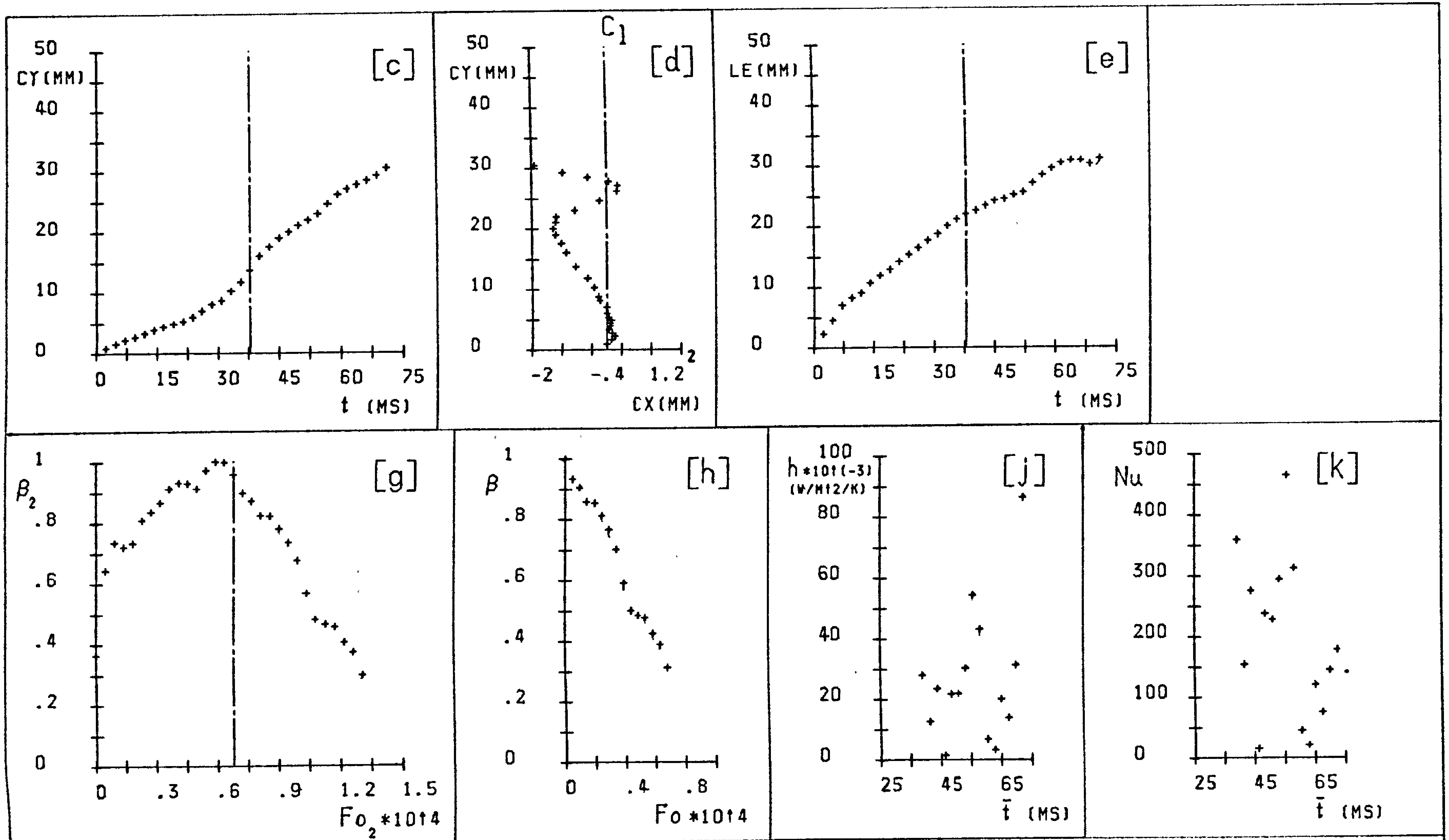

TEST NØ : (2.1).2 FILM NØ : 38-1/2

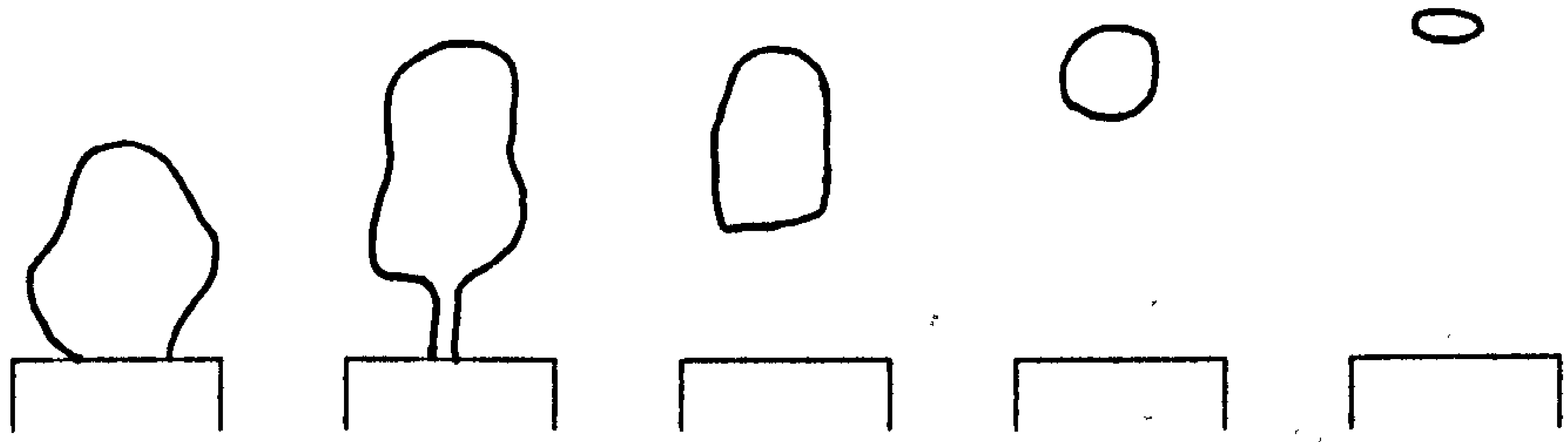

FRAME NUMBERS : 1 -12 13-22 23-31 32-33 34-36

EXPERIMENTAL PARAMETERS :

d	2
$\dot{m}_s$	1
(V_s	27871)
ΔT	10

Z	40
P	.995
Δt	1.14
(CS	875)

F	36
Ja	30
T_p	165

EXPERIMENTAL RESULTS :

t_g	26.39
t_c	15
t_t	41.39
f_s	40
R_m	3.9
R_o	3.8

h_c	26206
Nu_c	159
Z_d	9.27
Z_c	18.42
U	520
Fo_c	4.32E-05

Pe_o	23750

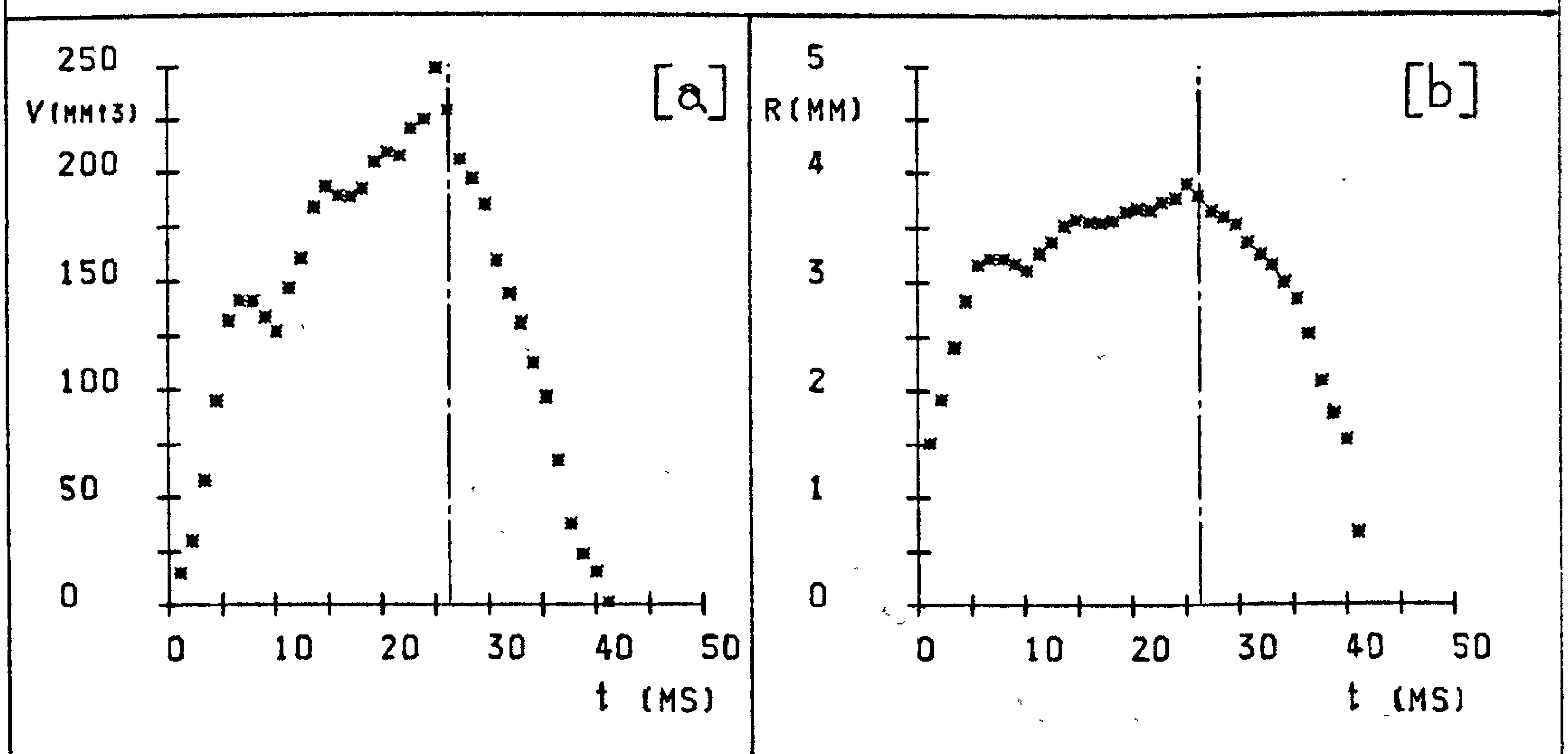

TEST NO : (2.2).3 FILM NO : 38-2/3

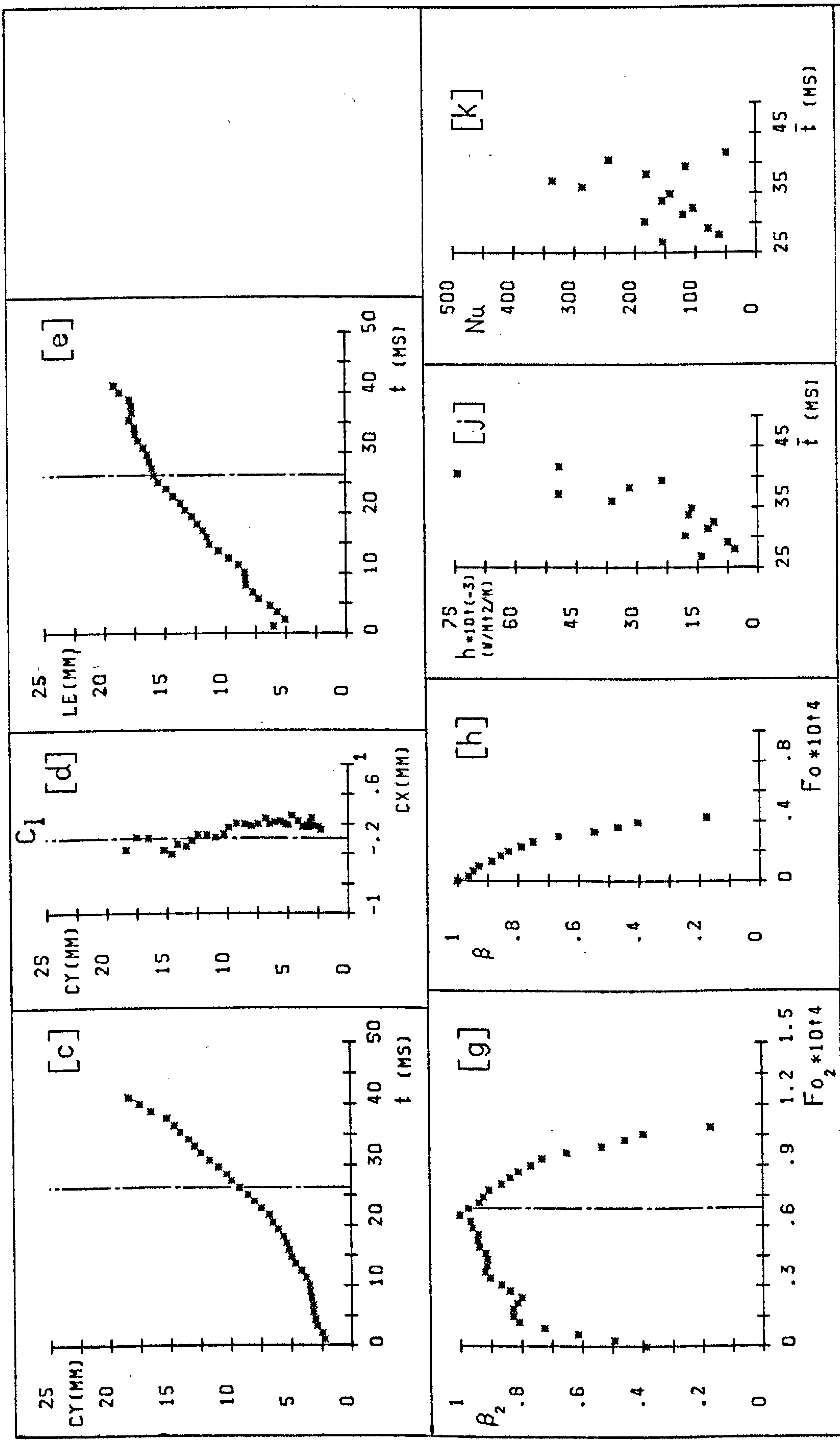

TEST NO : (2.2).3 FILM NO : 38-2/3

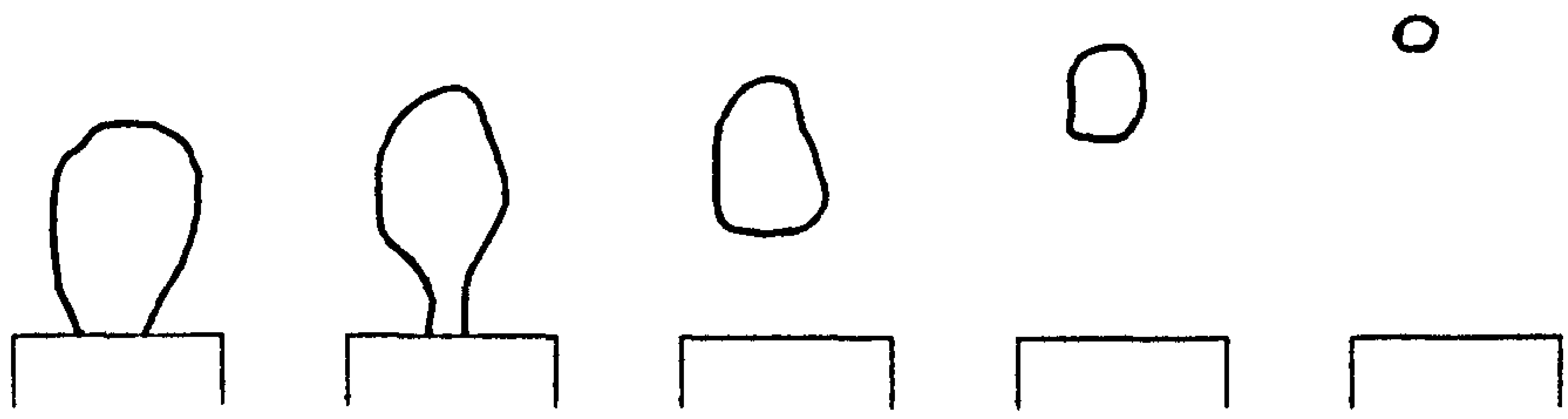

FRAME NUMBERS :	1 -7	8 -10	11-12	13-14	15

EXPERIMENTAL PARAMETERS :

d	2	Z	40	F	15
$\dot{m}_s$	1	P	.995	Ja	45
(V_s	27871)	Δt	1.13	T_p	165
ΔT	15	(CS	885)		

EXPERIMENTAL RESULTS :

t_g	12.43	h_c	26367	Pe_o	20170
t_c	4.5	Nu_c	91		
t_t	16.93	Z_d	4.85		
f_s	88	Z_c	8.14		
R_m	2.43	U	775		
R_o	2.15	Fo_c	4.02E-05		

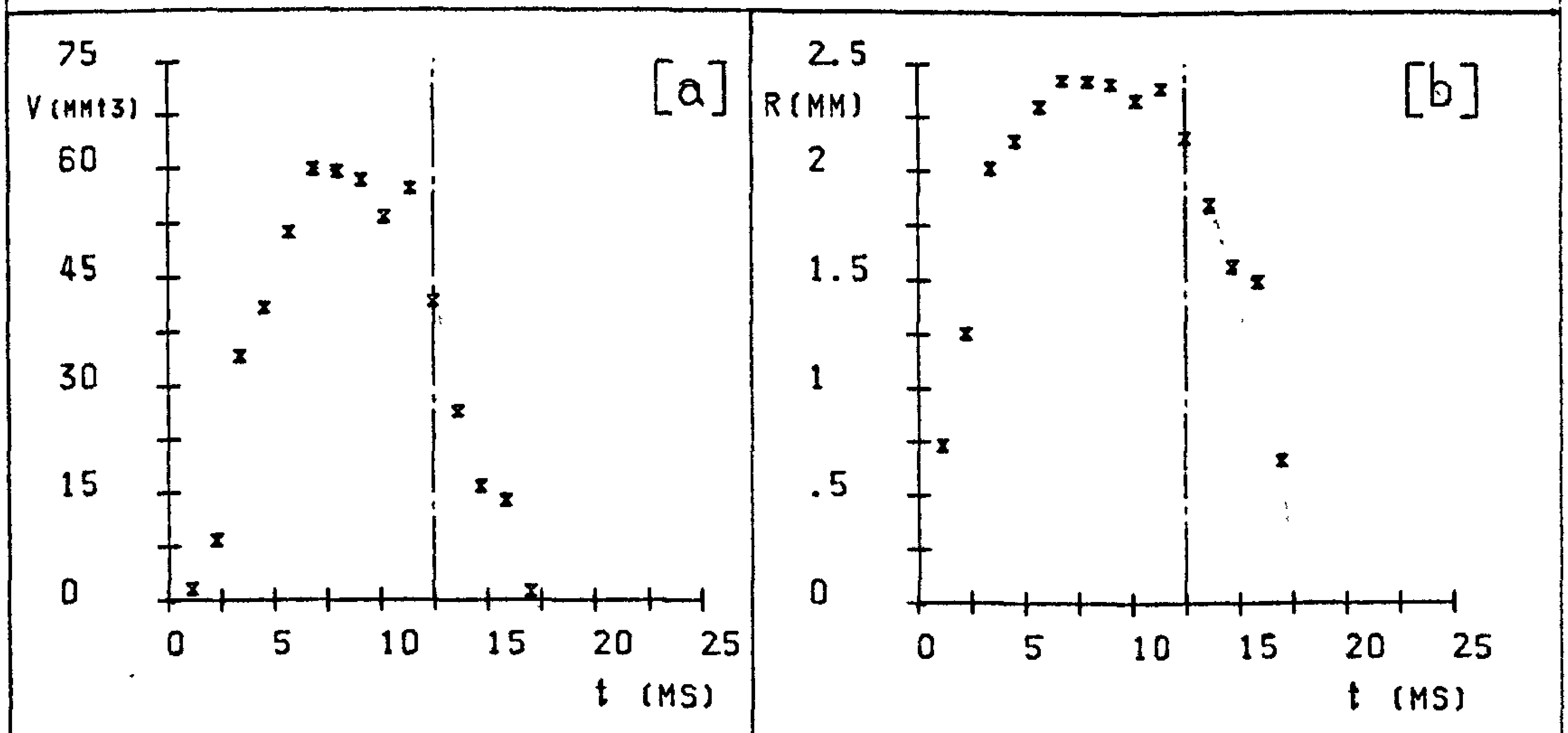

TEST NO : (2.3).1 FILM NO : 38-3/1

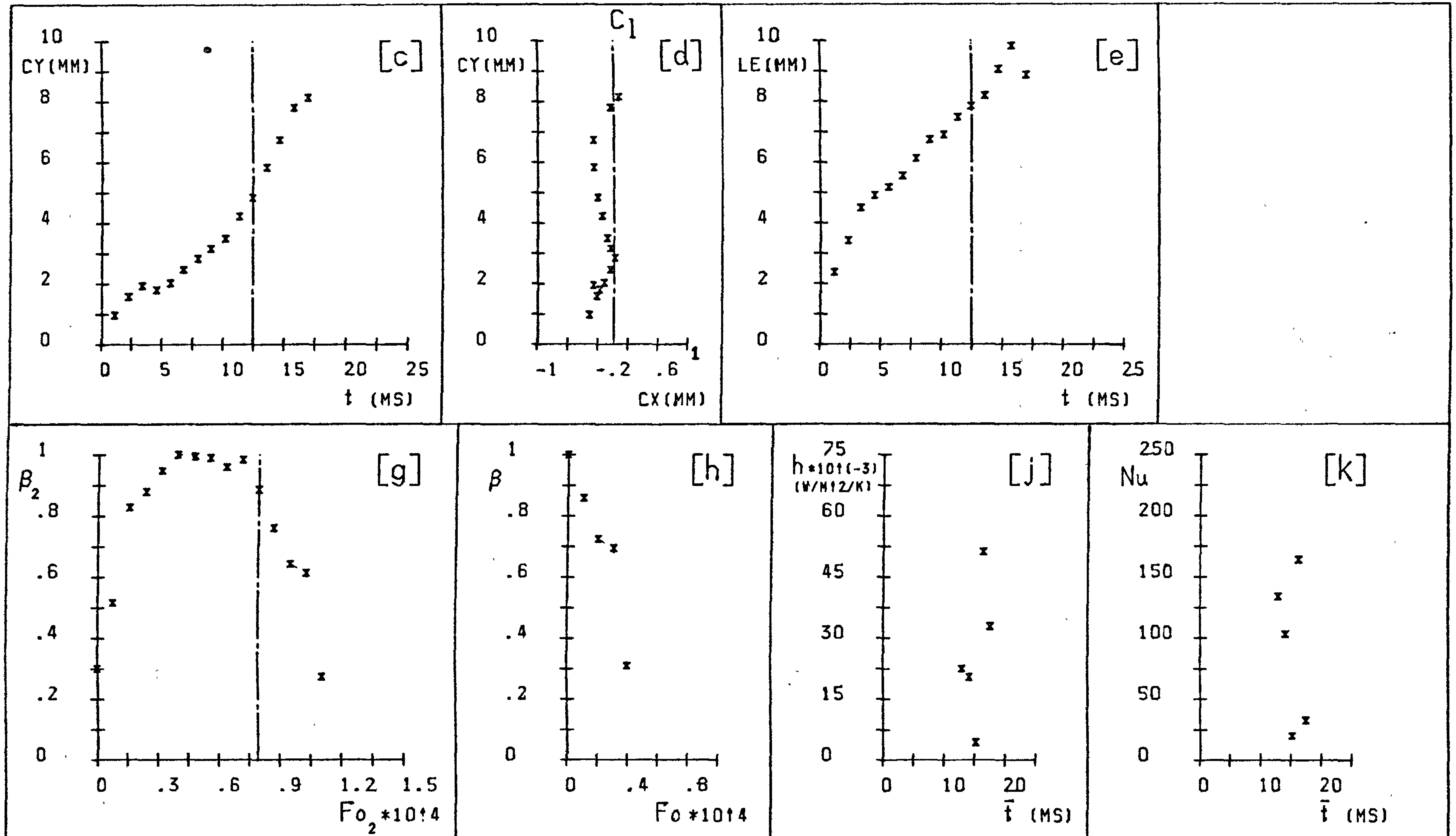

TEST NO : (2.3).1 FILM NO : 38-3/1

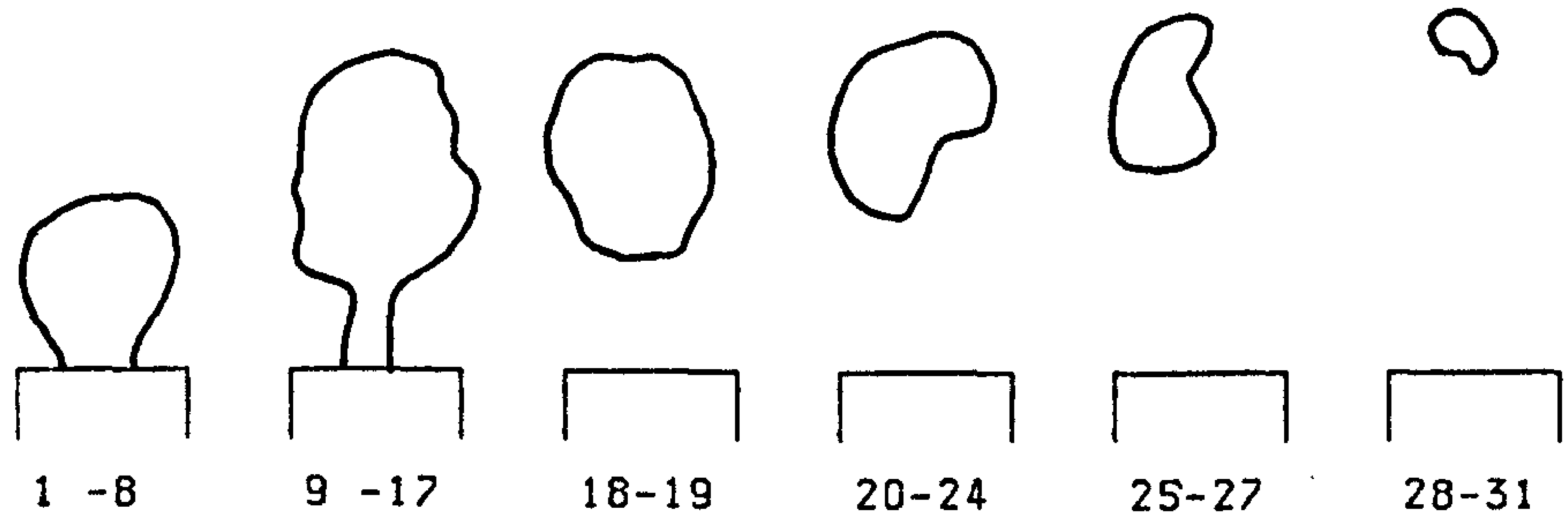

EXPERIMENTAL PARAMETERS :

d	2	Z	40	F	31
$\dot{m}_s$	1.5	P	.995	Ja	15
(V_s	41806)	Δt	2.18	T_p	165
ΔT	5	(CS	458)		

EXPERIMENTAL RESULTS :

t_g	37.11	h_c	33643	Pe_o	40330
t_c	35.6	Nu_c	281		
t_t	72.71	Z_d	13.86		
f_s	29	Z_c	30.25		
R_m	5.4	U	643		
R_o	5.25	Fo_c	5.41E-05		

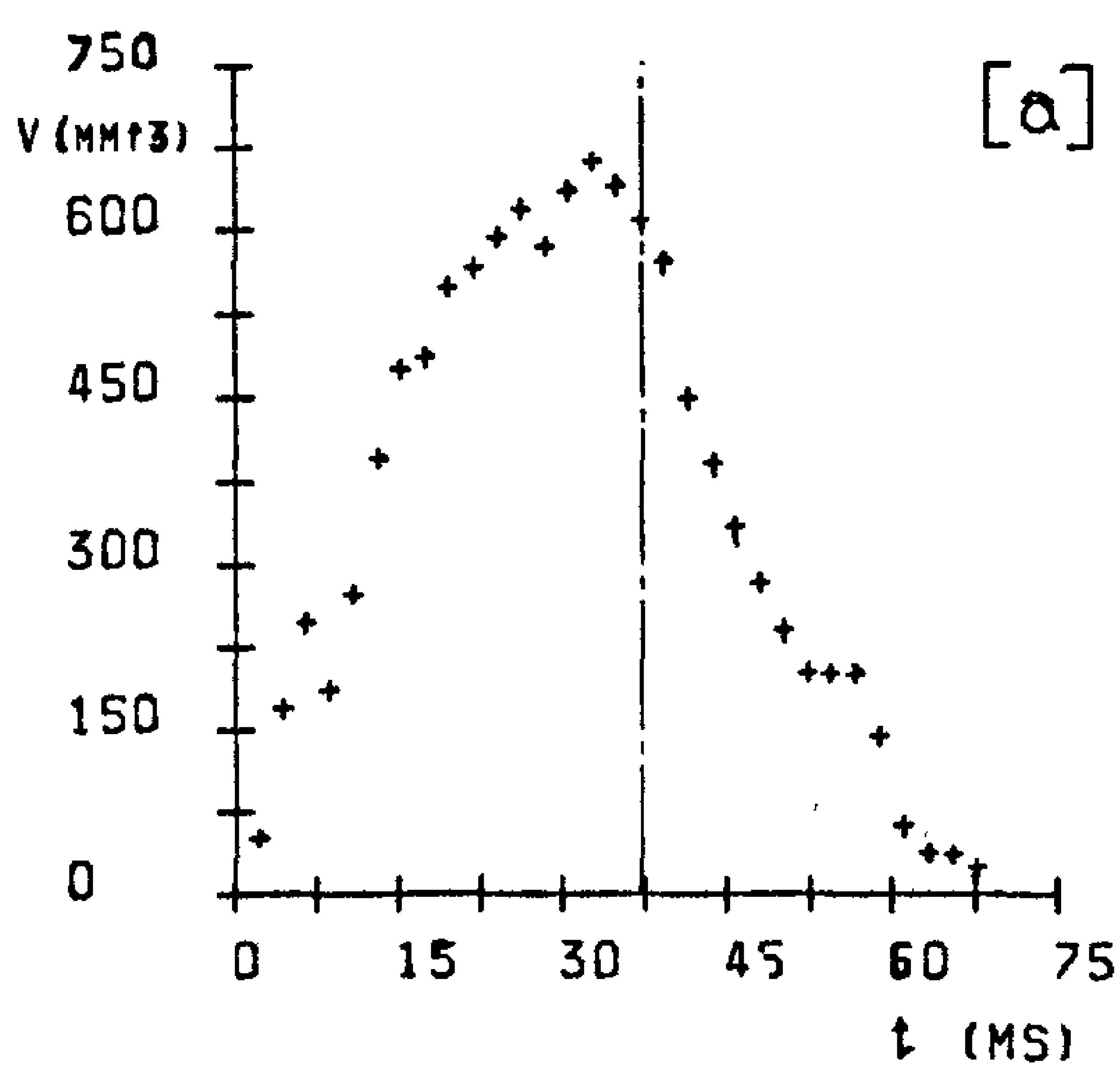

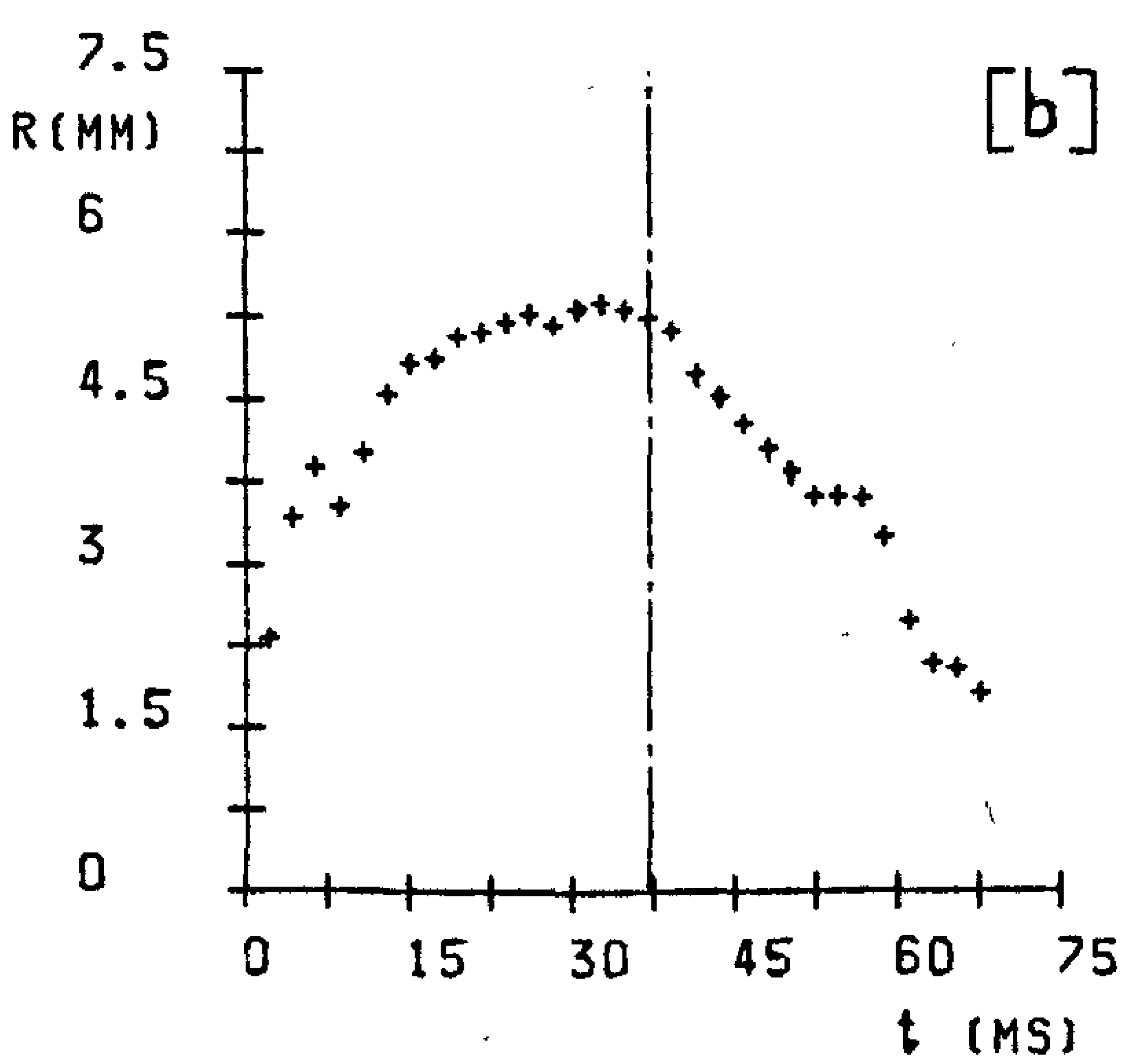

TEST NO : (3.1).2 FILM NO : 35-3/2

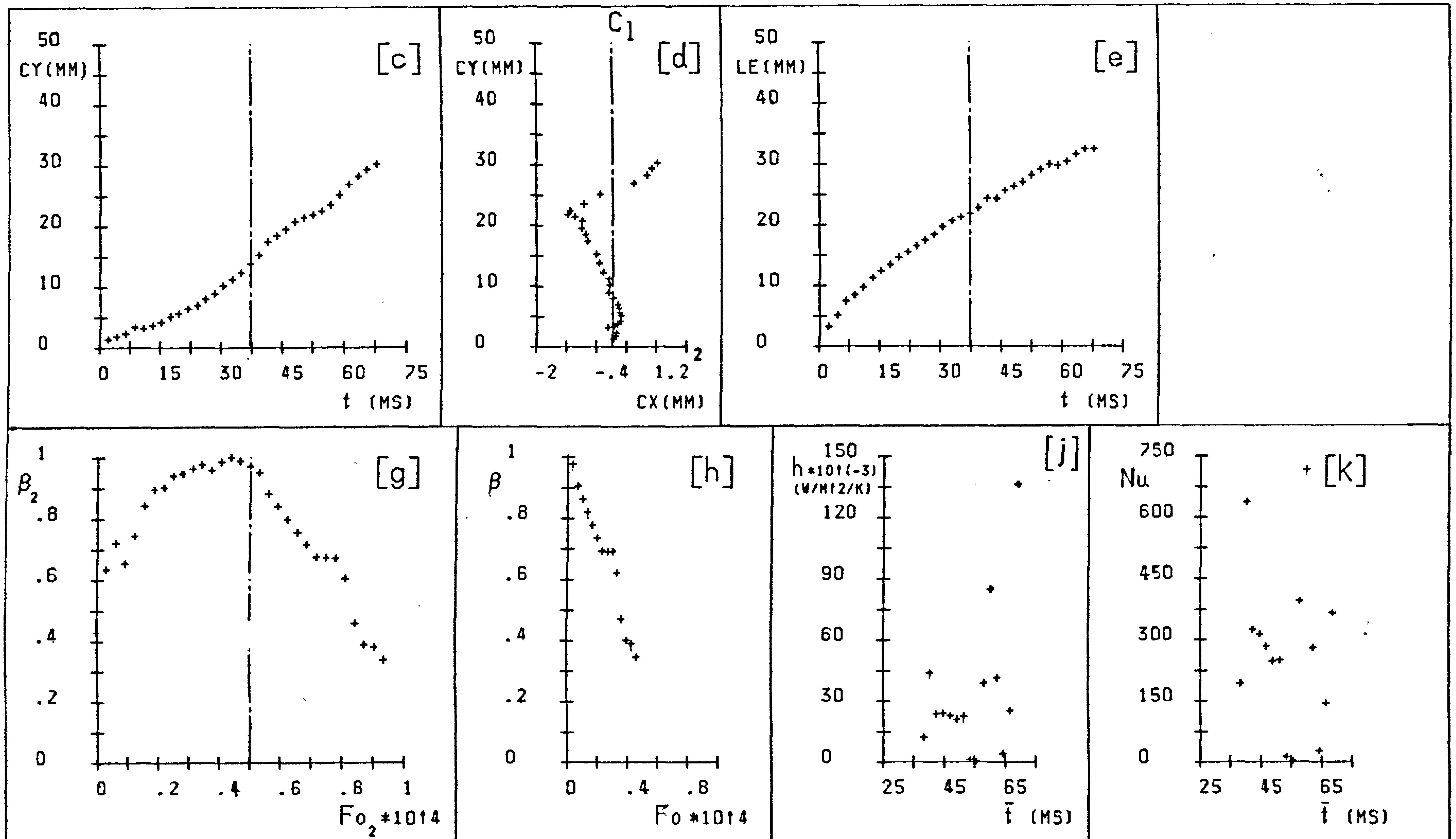

TEST NO : (3.1).2 FILM NO : 35-3/2

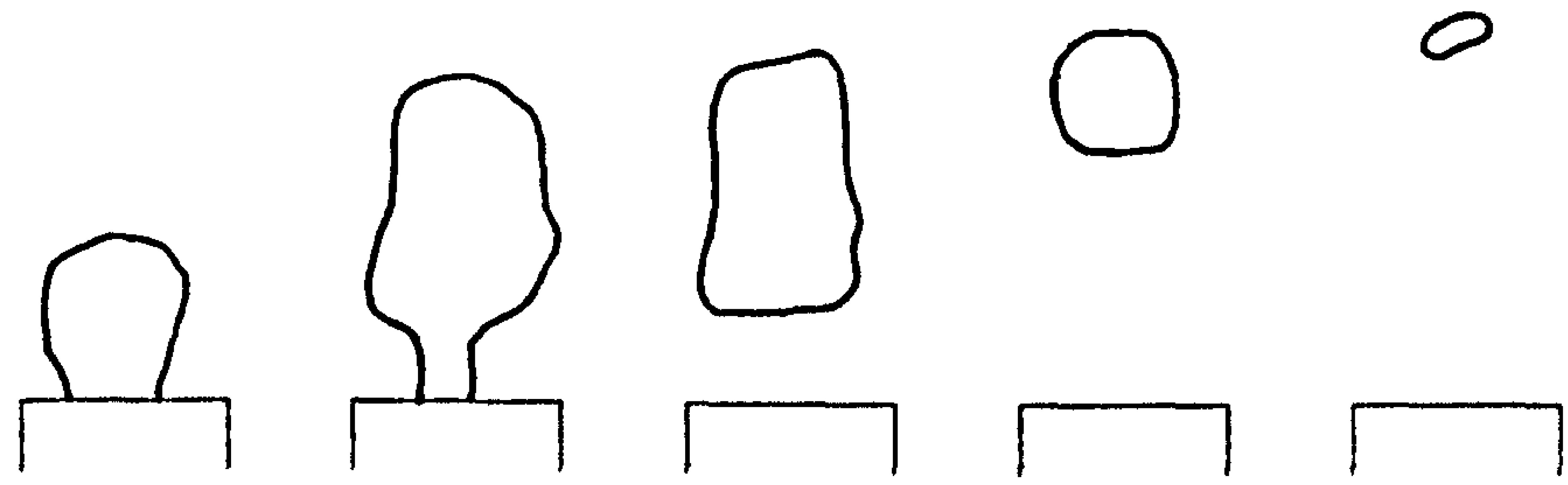

FRAME NUMBERS : 1 -14 15-22 23-30 31-34 35-38

EXPERIMENTAL PARAMETERS :

d	2	Z	40	F	38
$\dot{m}_s$	1.5	P	.995	Ja	30
(V_s	41806)	Δt	1.37	T_p	165
ΔT	10	(CS	730)		

EXPERIMENTAL RESULTS :

t_g	31.51	h_c	24055	Pe_o	32830
t_c	19	Nu_c	179		
t_t	50.51	Z_d	10.63		
f_s	33	Z_c	21.88		
R_m	4.87	U	590		
R_o	4.63	Fo_c	3.69E-05		

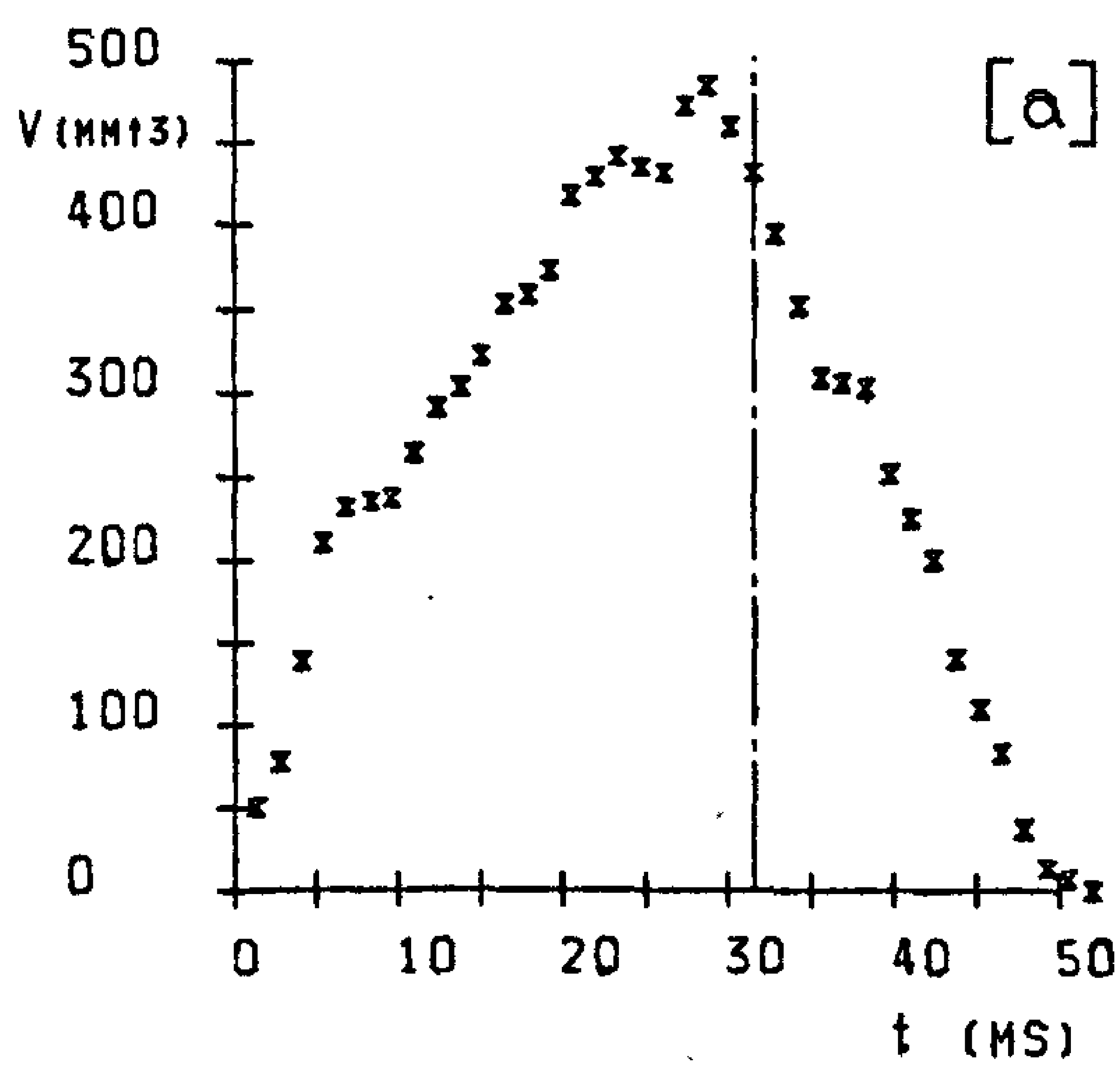

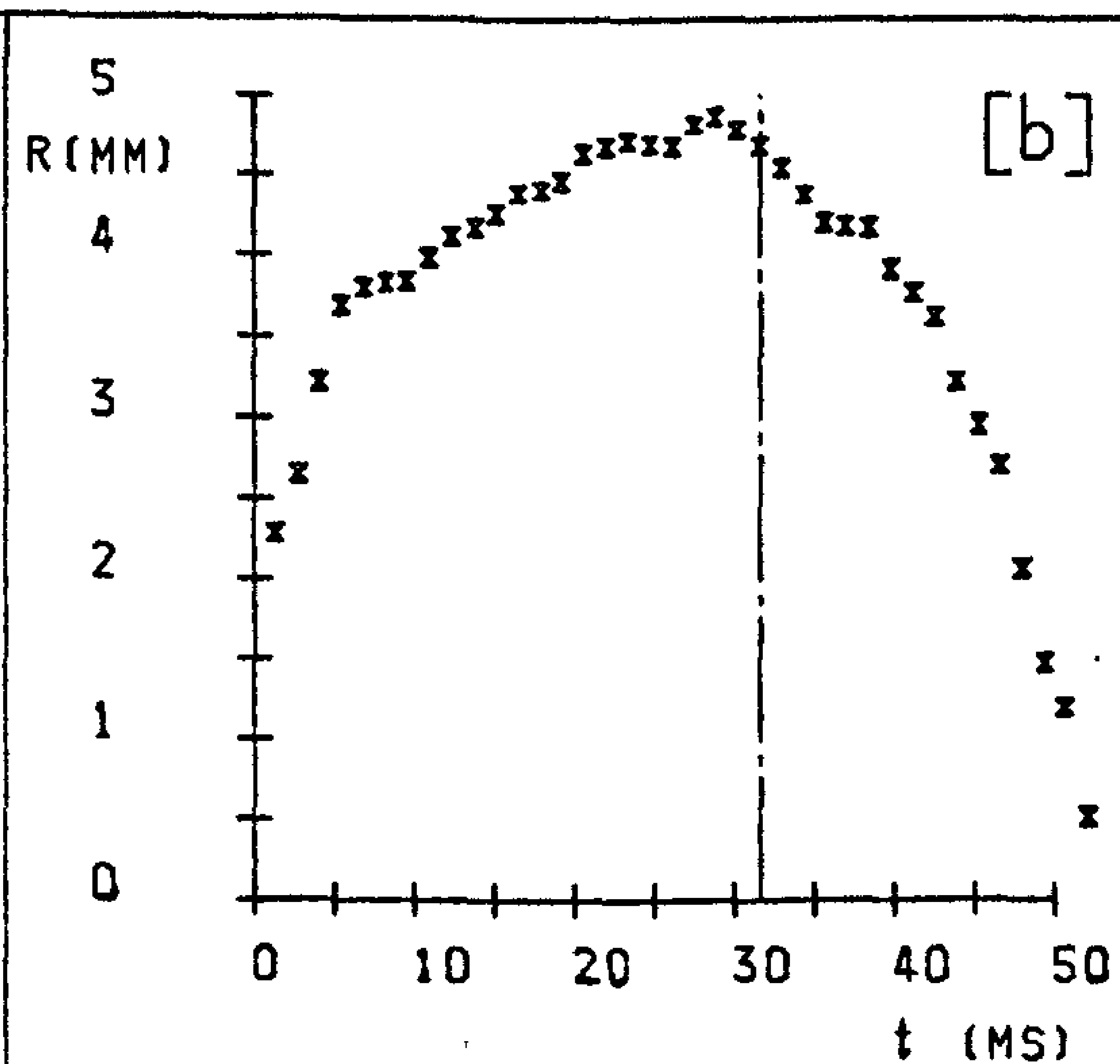

TEST NO : (3.2).1 FILM NO : 36-1/1

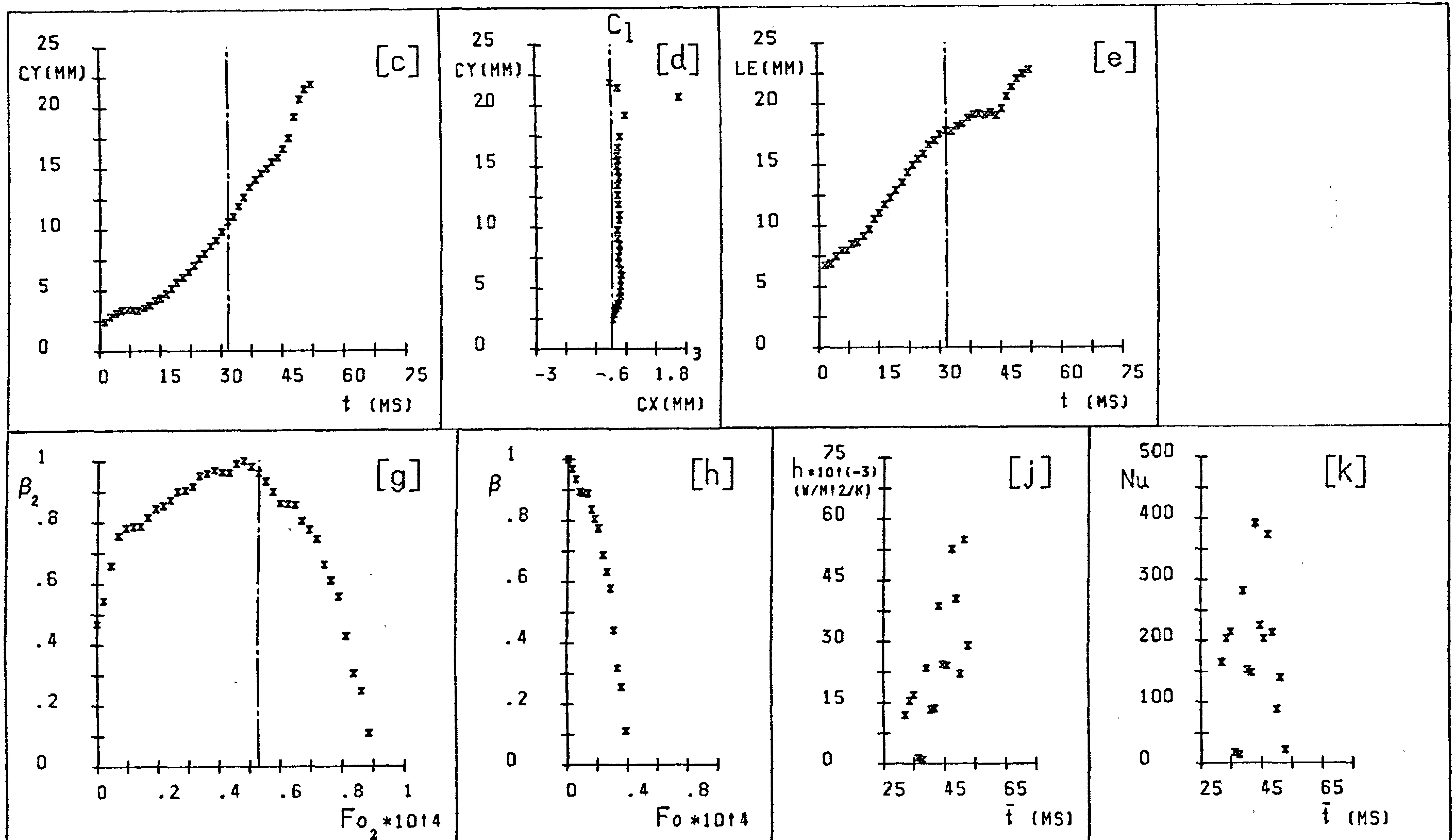

TEST NØ : (3.2).1 FILM NØ : 36-1/1

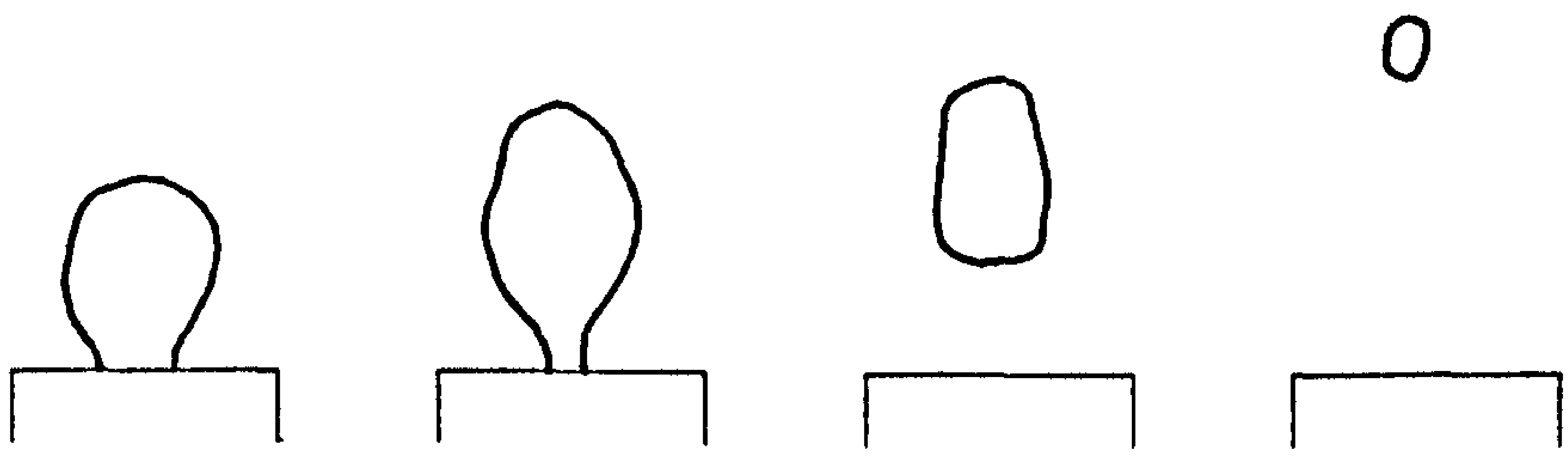

FRAME NUMBERS : 1 -14 15-16 17-23 24-25

EXPERIMENTAL PARAMETERS :

d	2	Z	40	F	25
$\dot{m}_s$	1.5	P	.995	Ja	45
(V_s	41806)	Δt	1.11	T_p	165
ΔT	15	(CS	905)		

EXPERIMENTAL RESULTS :

t_g	18.79	h_c	24719	Pe_o	34380
t_c	8.3	Nu_c	141		
t_t	27.09	Z_d	7.26		
f_s	57	Z_c	16.34		
R_m	4.01	U	800		
R_o	3.55	Fo_c	2.72E-05		

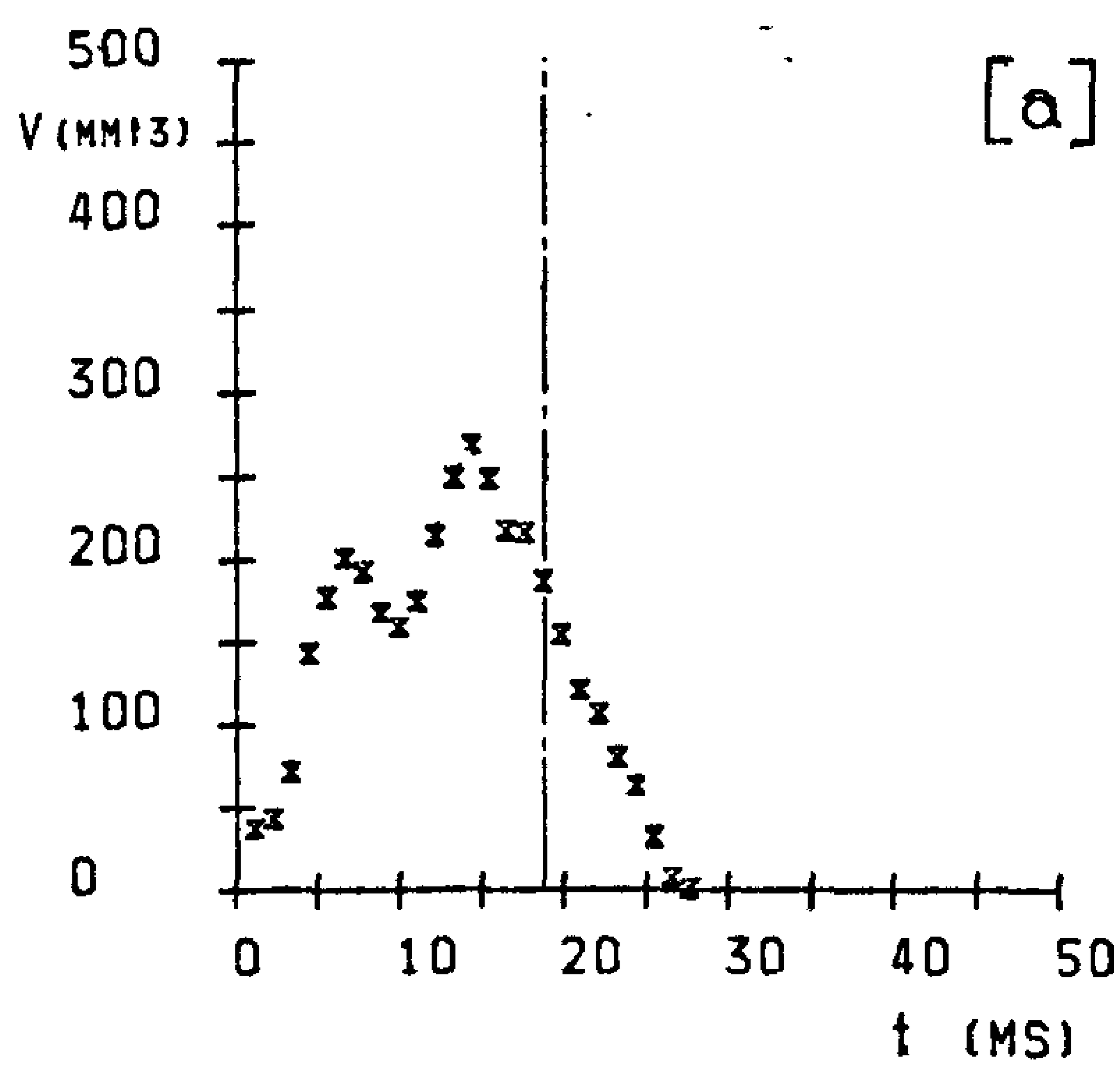

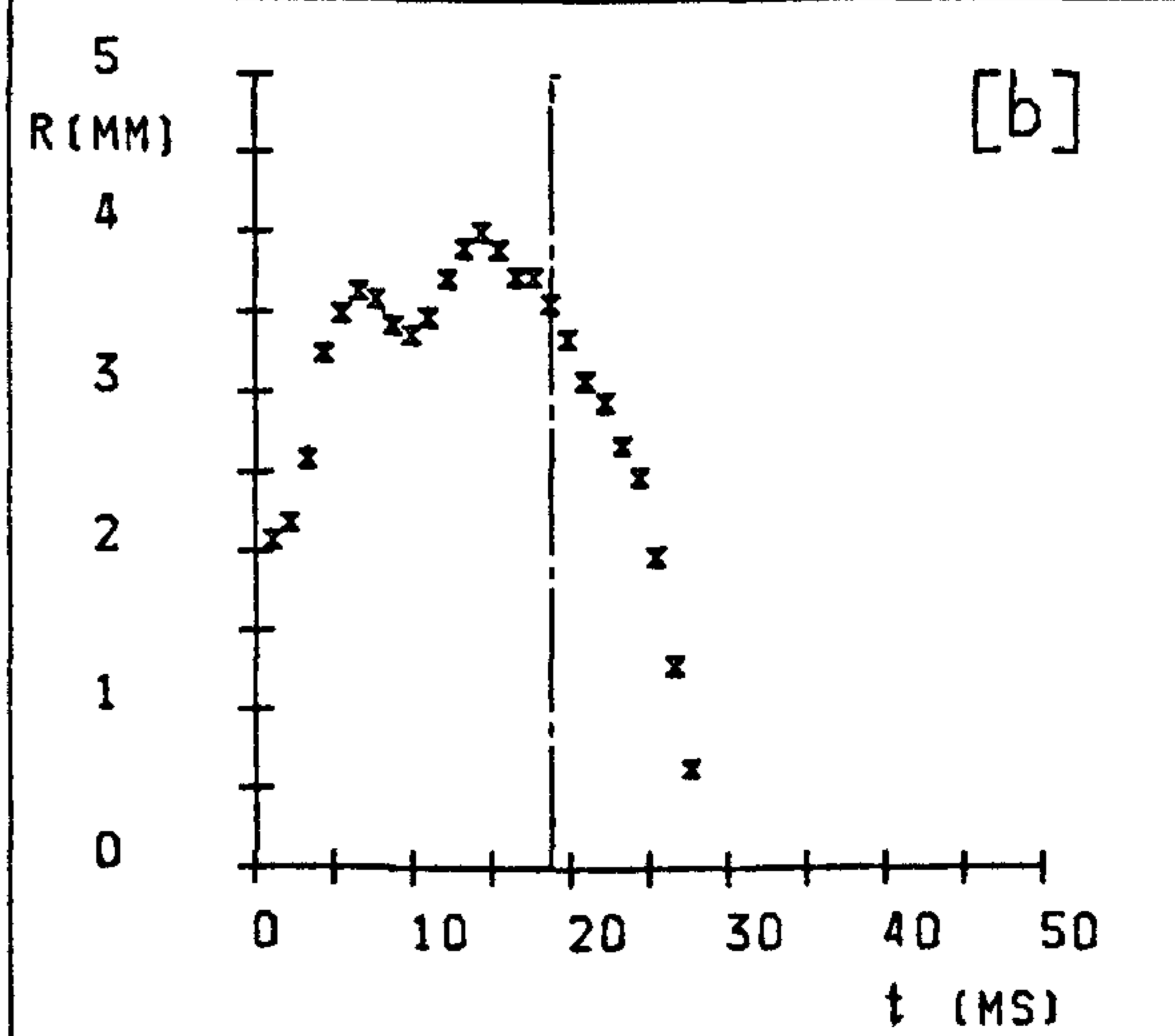

TEST NO : (3.3).1 FILM NO : 36-2/1

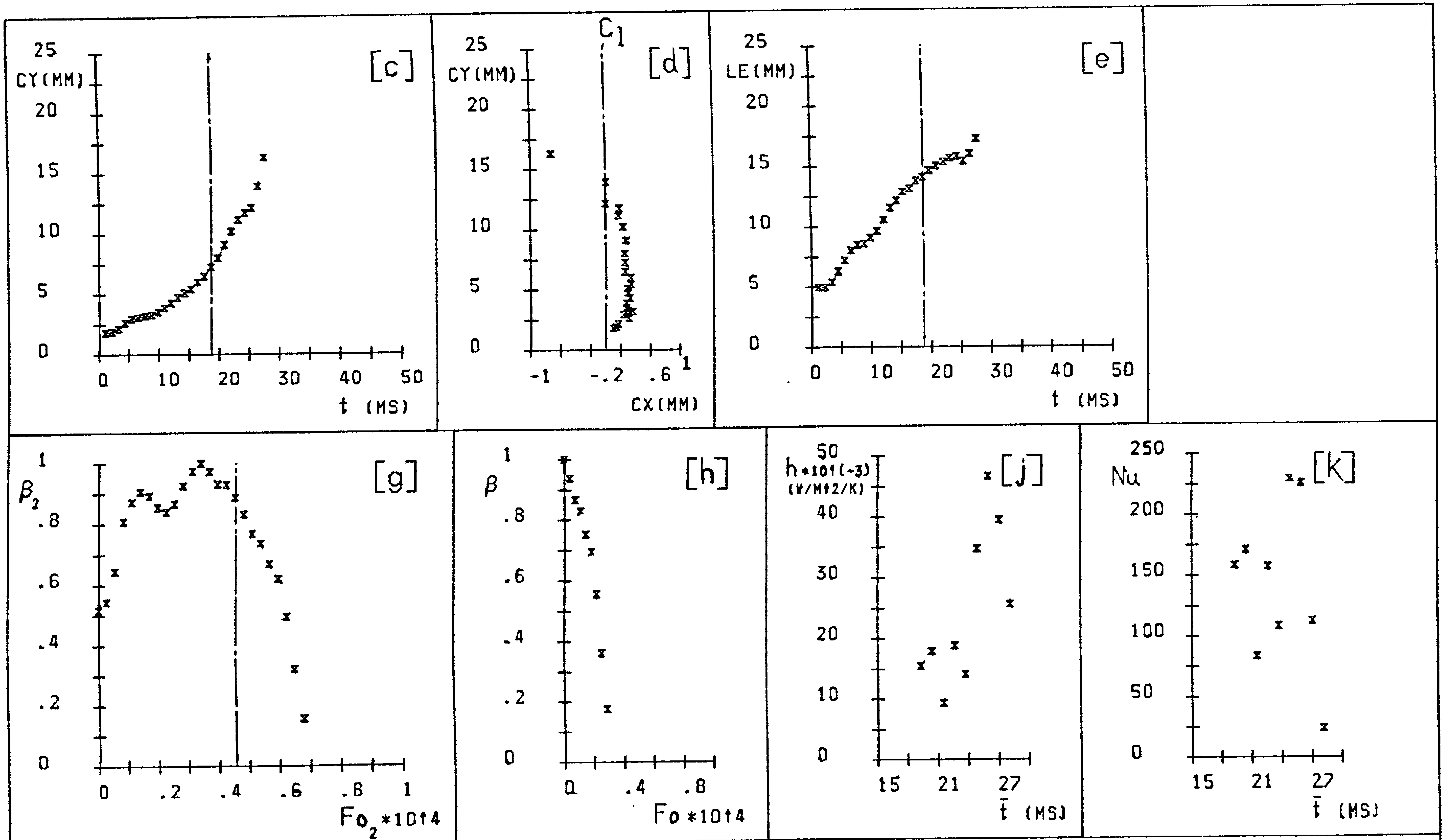

TEST NØ : (3.3).1 FILM NØ : 36-2/1

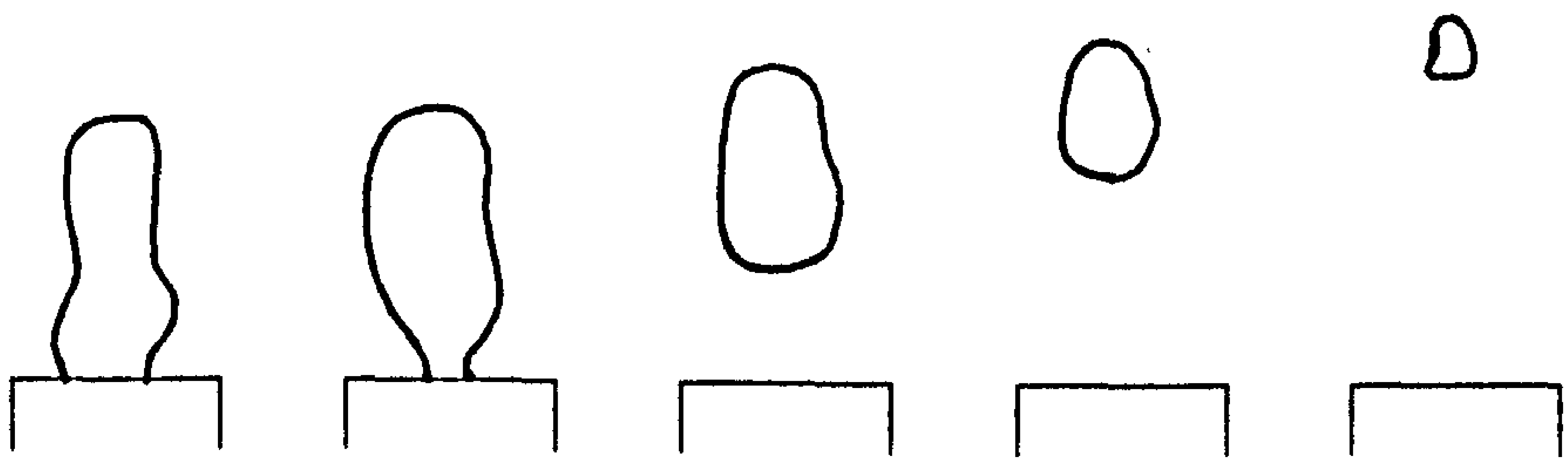

FRAME NUMBERS : 1 -16 17-20 21-24 25-26 27-28

EXPERIMENTAL PARAMETERS :

d	2	Z	40	F	28
$\dot{m}_s$	1.5	P	.995	Ja	60
(V_s	41806)	Δt	.8	T_p	165
ΔT	20	(CS	1256)		

EXPERIMENTAL RESULTS :

t_g	16.72	h_c	24967	Pe_o	30390
t_c	5.5	Nu_c	125		
t_t	22.22	Z_d	6.27		
f_s	63	Z_c	10.43		
R_m	3.33	U	810		
R_o	3.08	Fo_c	2.38E-05		

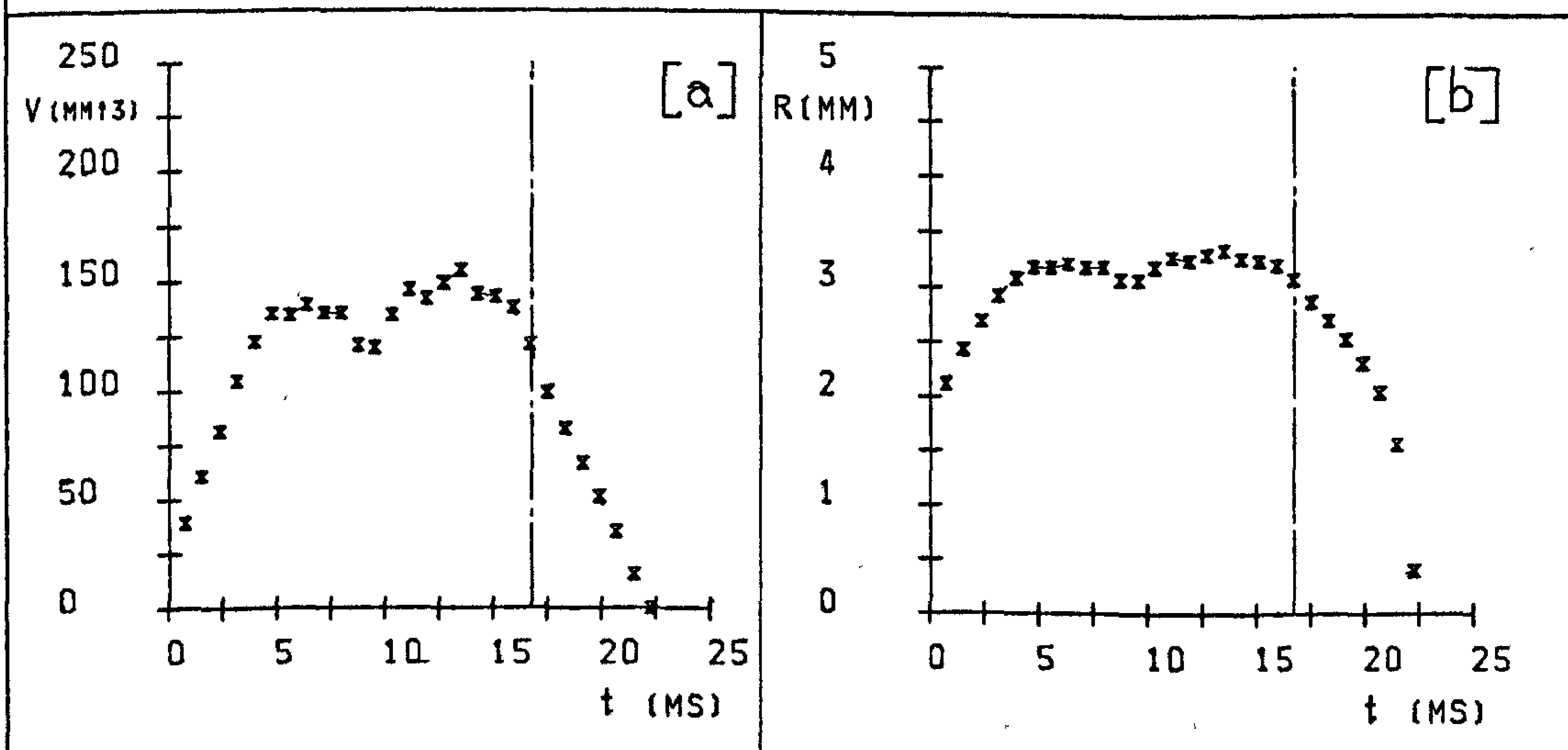

TEST NO : (3.4).1 FILM NO : 37-1/2

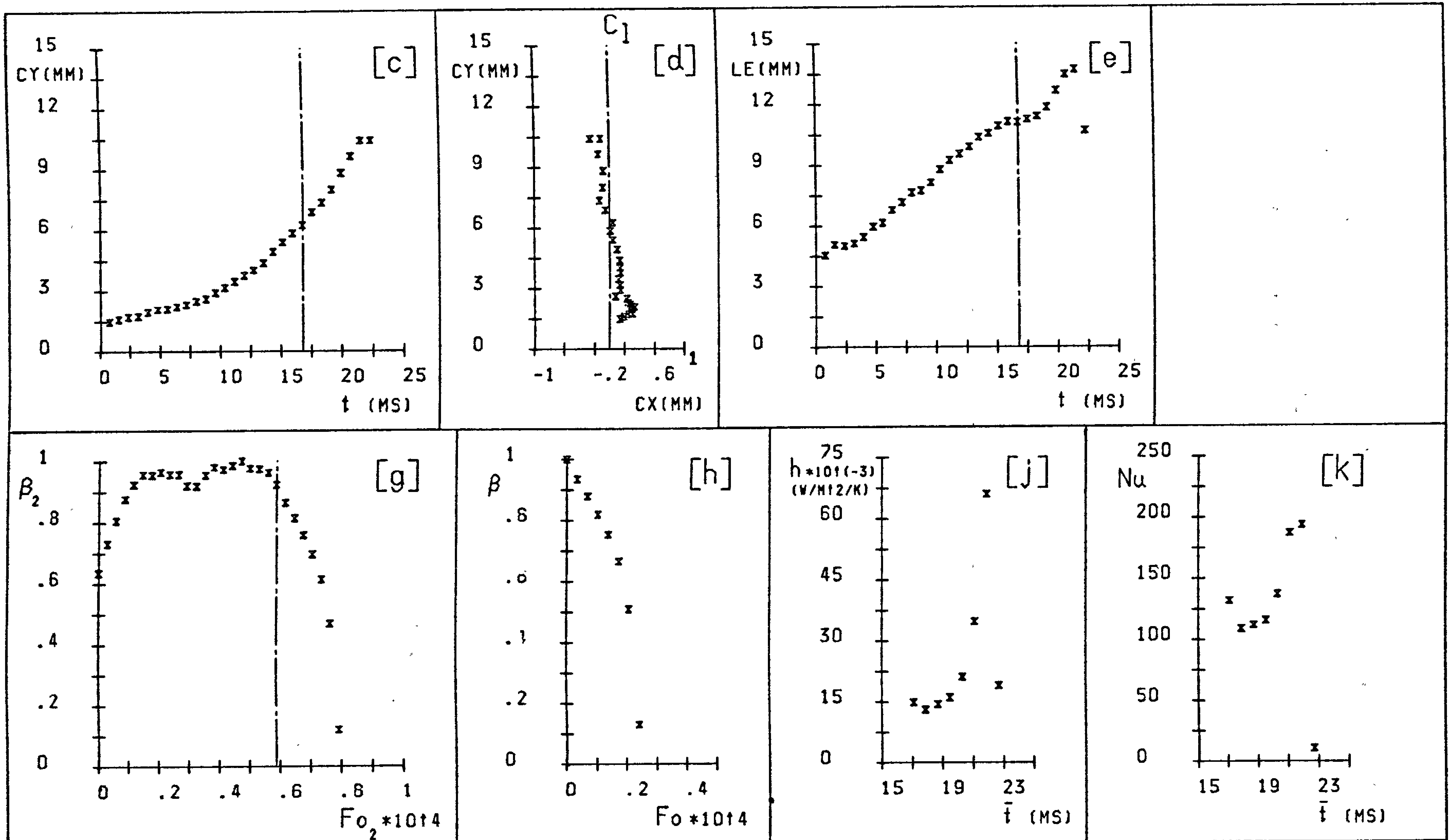

TEST NØ : (3.4).1 FILM NØ : 37-1/2

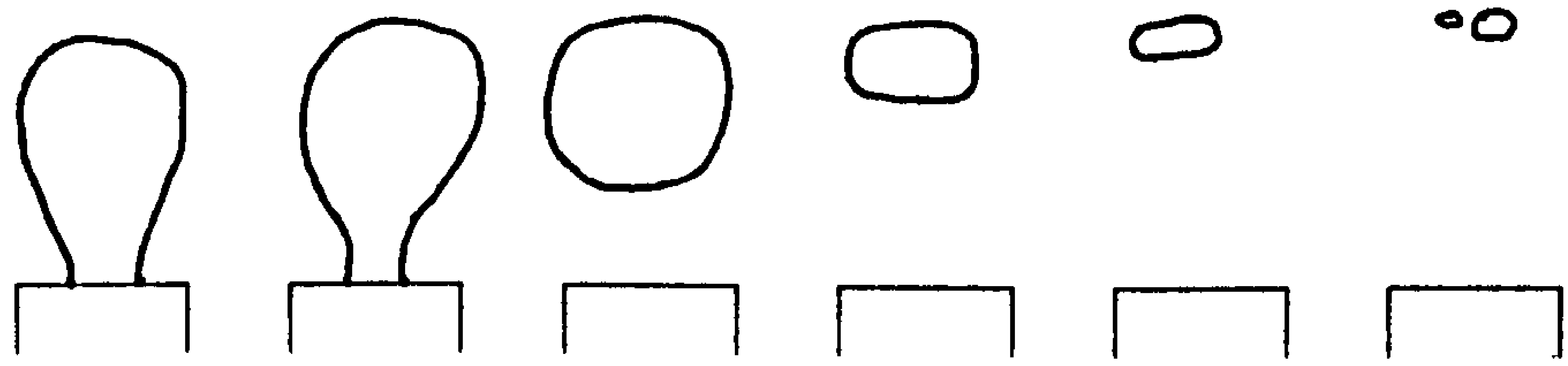

FRAME NUMBERS : 1 -14 15-16 17-19 20-22 23-24 25

EXPERIMENTAL PARAMETERS :

d	2	Z	40	F	25
$\dot{m}_s$	.45	P	2.005	Ja	30
(V_s	6643)	Δt	1.51	T_p	165
ΔT	18.5	(CS	663)		

EXPERIMENTAL RESULTS :

t_g	25.64	h_c	16723	Pe_o	6360
t_c	12	Nu_c	58		
t_t	37.64	Z_d	3.58		
f_s	41	Z_c	6.87		
R_m	2.16	U	249		
R_o	2.16	Fo_c	1.087E-04		

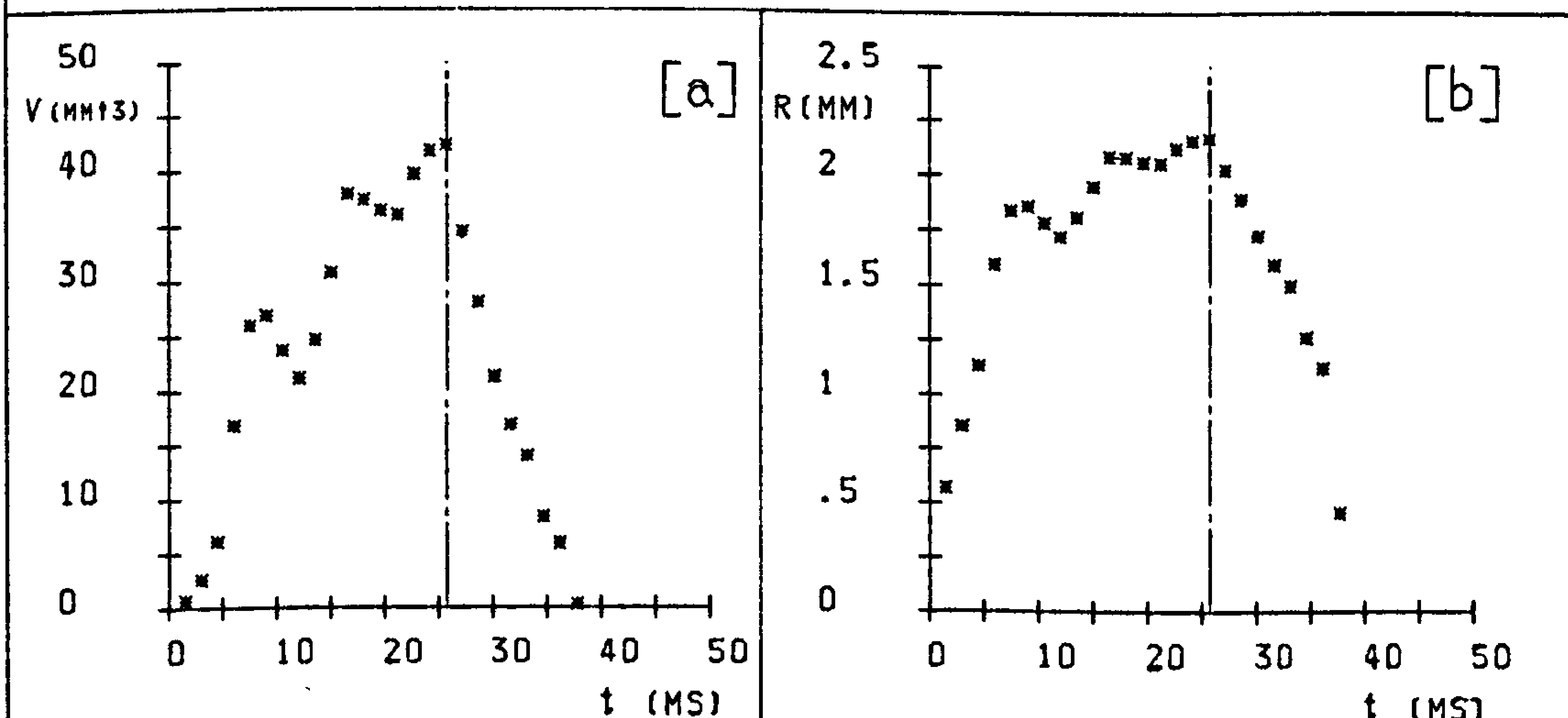

TEST NO : (4.2).3 FILM NO : 45-1/4

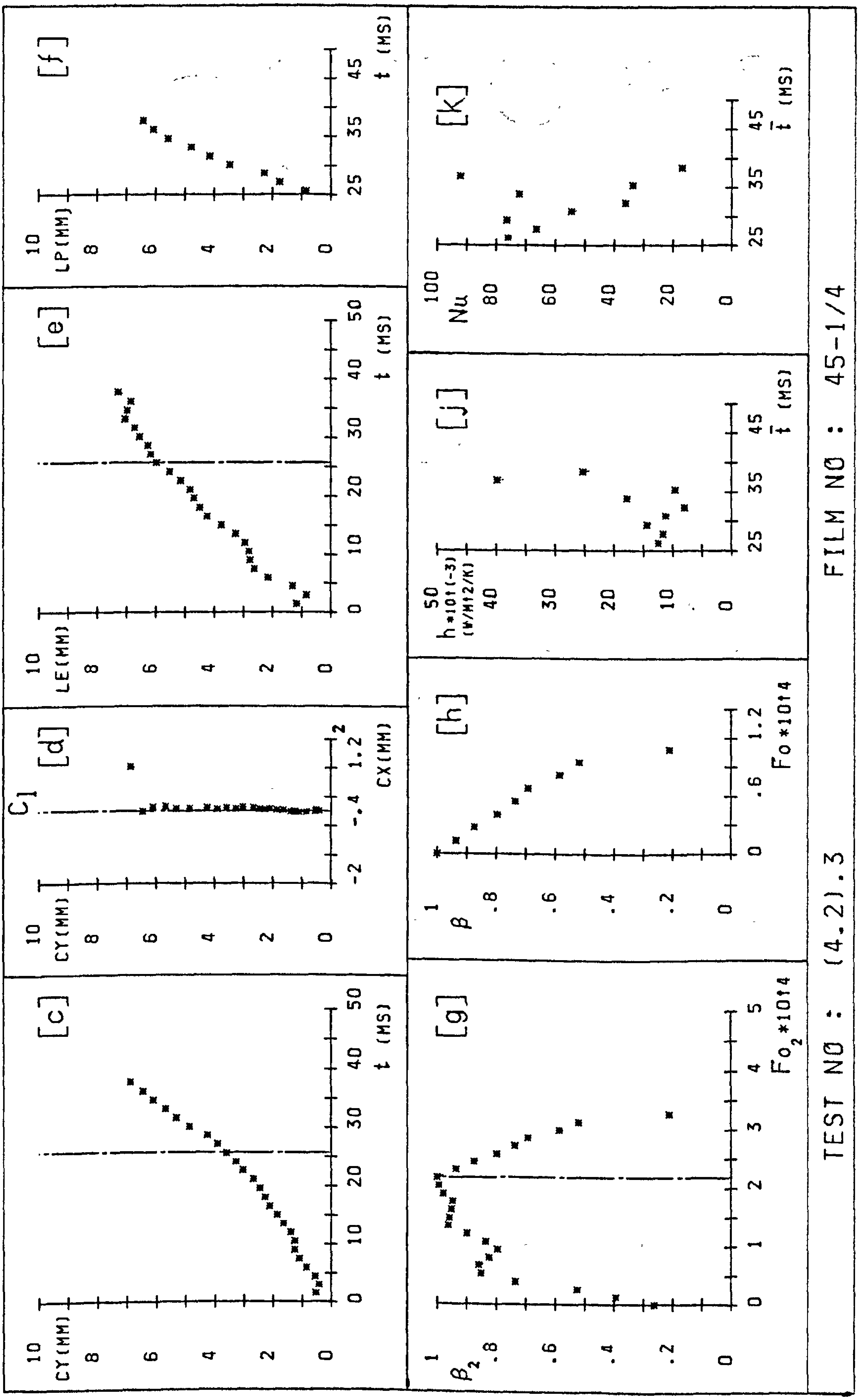
[c]
CY(MM)
t (MS)
[d]
C_1
CY(MM)
CX(MM)
[e]
LE(MM)
t (MS)
[f]
LP(MM)
t (MS)
[g]
β_2
Fo_2*10↑4
[h]
β
Fo*10↑4
[j]
h*10↑(-3)
(W/M↑2/K)
$\bar{t}$ (MS)
[k]
Nu
$\bar{t}$ (MS)
TEST NO : (4.2).3
FILM NO : 45-1/4

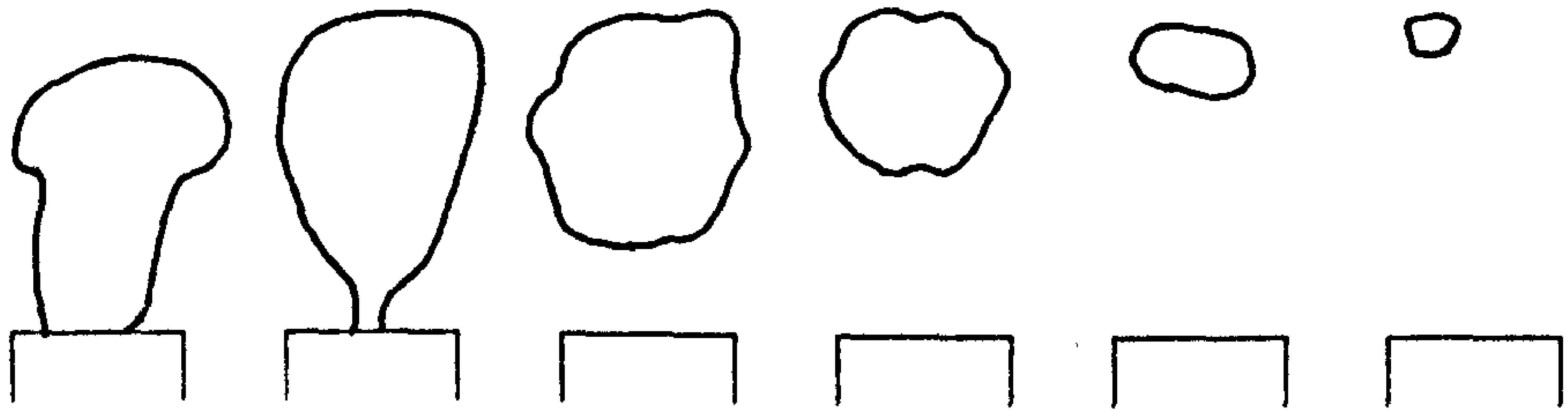

FRAME NUMBERS : 1 -8 | 9 -10 | 11-12 | 13-16 | 17-20 | 21-27

EXPERIMENTAL PARAMETERS :

d	2
$\dot{m}_s$	.92
(V_s	13560)
ΔT	9.3

Z	40
P	2.011
Δt	2.23
(CS	449)

F	27
Ja	15
T_p	165

EXPERIMENTAL RESULTS :

t_g	22.26
t_c	30
t_t	52.26
f_s	50
R_m	3.5
R_o	3.42

h_c	20042
Nu_c	104
Z_d	6.25
Z_c	17.78
U	338
Fo_c	1.09E-04

Pe_o	13600

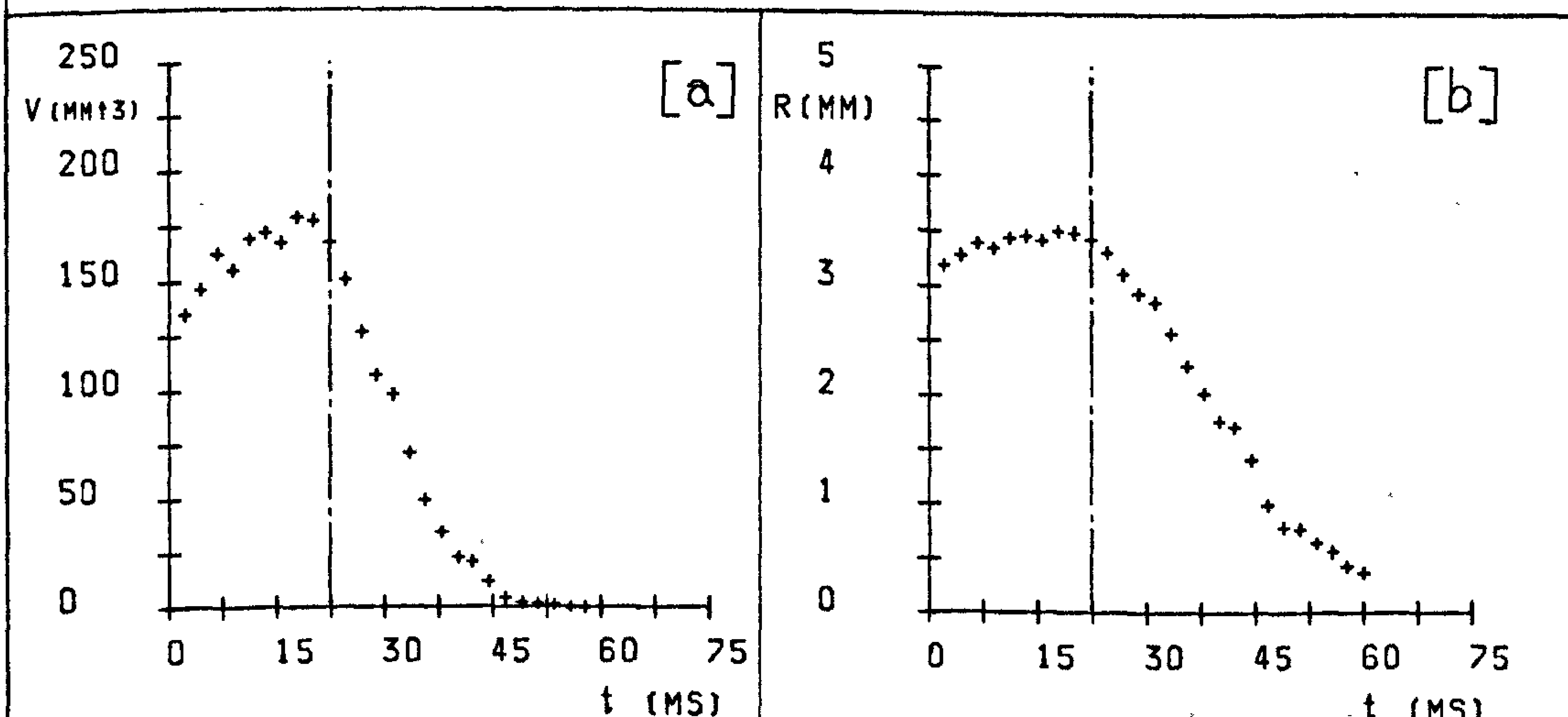

TEST NØ : (5.1).2 FILM NØ : 51-1/6

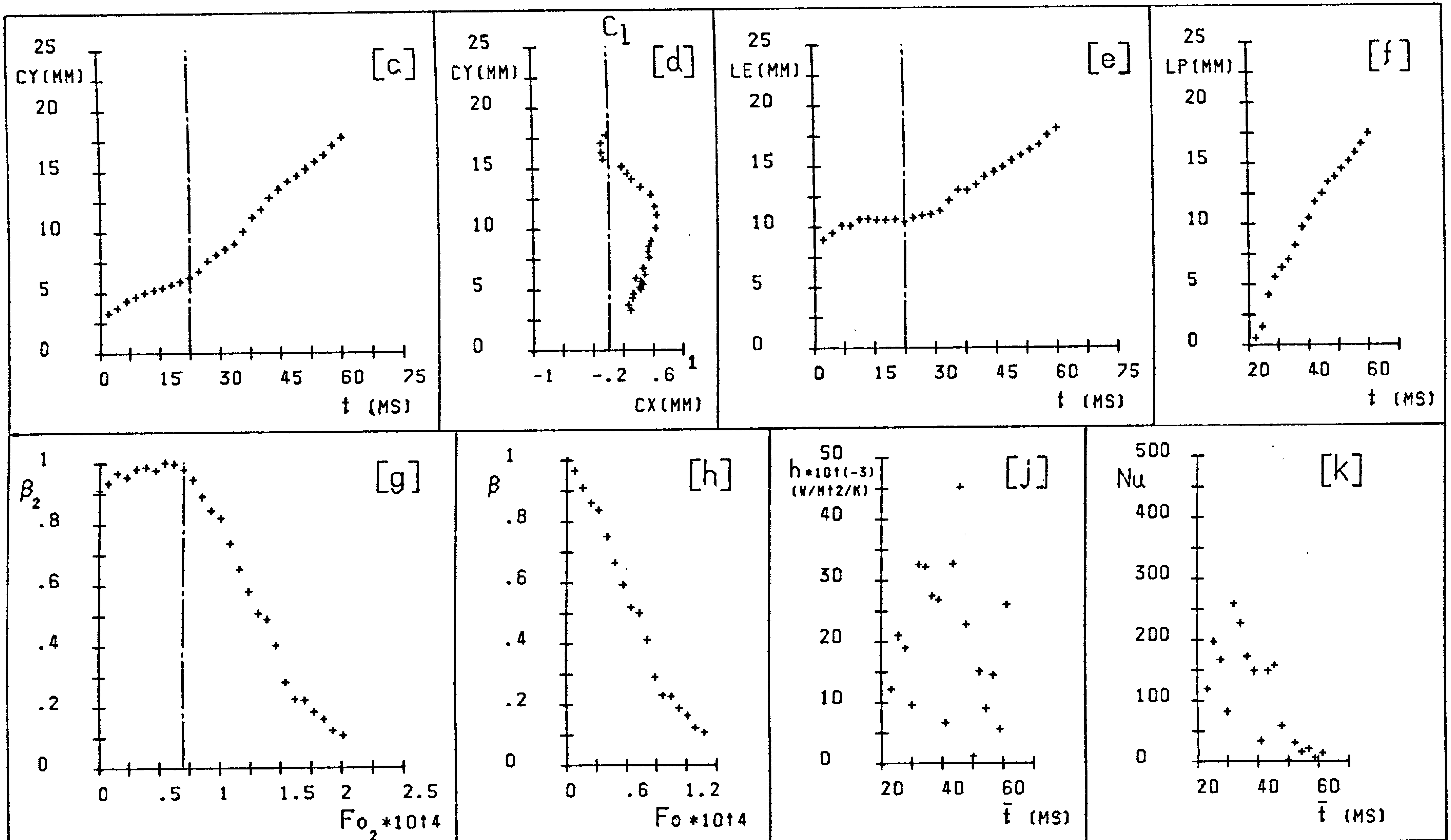

TEST NØ : (5.1).2   FILM NØ : 51-1/6

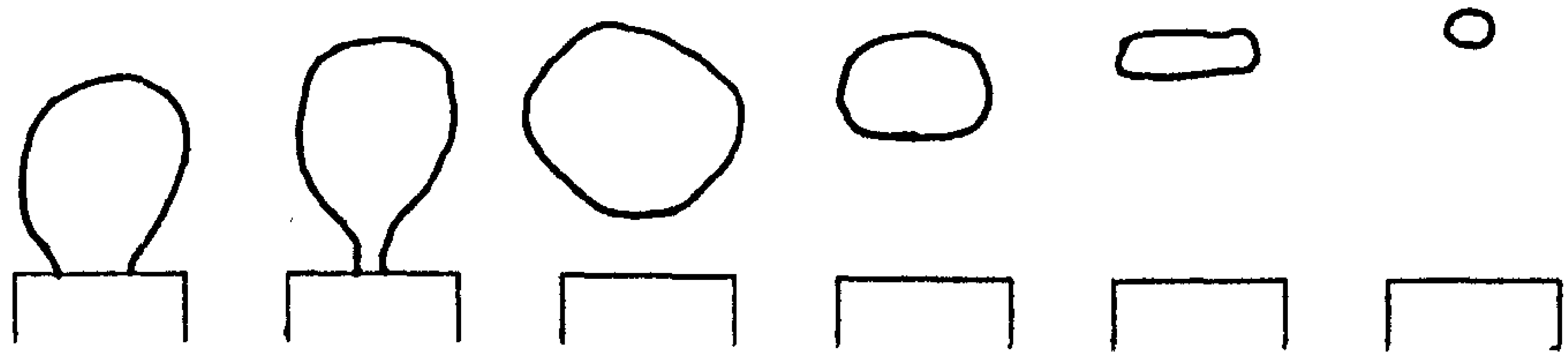

FRAME NUMBERS : 1 -13 | 14-15 | 16-17 | 18-20 | 21 -24 | 25 -26'

EXPERIMENTAL PARAMETERS :

d	2		Z	40		F	26
$\dot{m}_s$	.92		P	2.008		Ja	30
(V_s	13560)		Δt	1.58		T_p	165
ΔT	18.5		(CS	633)			

EXPERIMENTAL RESULTS :

t_g	25.25		h_c	15874		Pe_o	10380
t_c	14.2		Nu_c	70			
t_t	39.48		Z_d	4.06			
f_s	42		Z_c	7.32			
R_m	2.58		U	320			
R_o	2.74		Fo_c	7.99E-05			

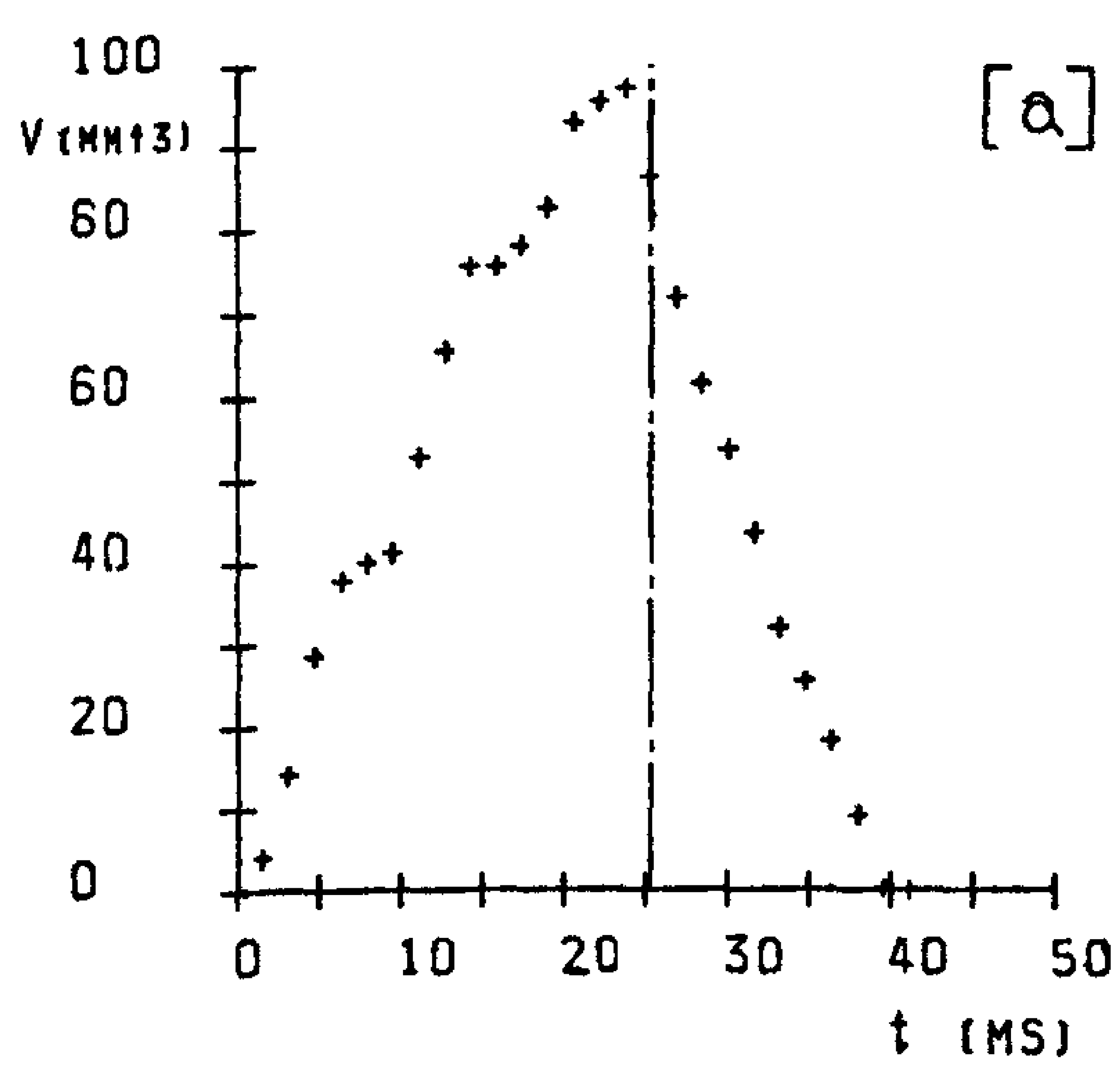

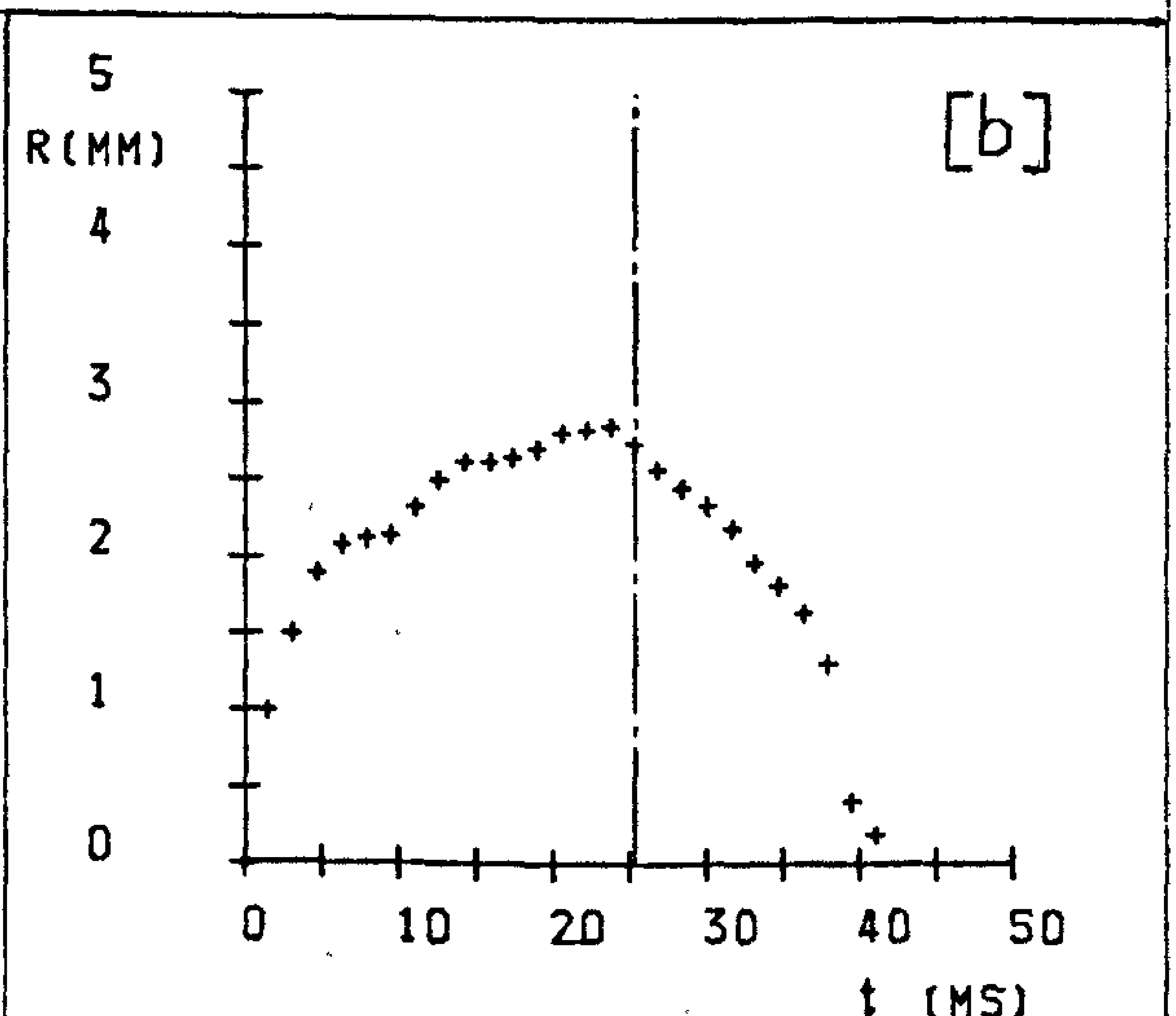

TEST NO : (5.2).2 FILM NO : 42-2/3

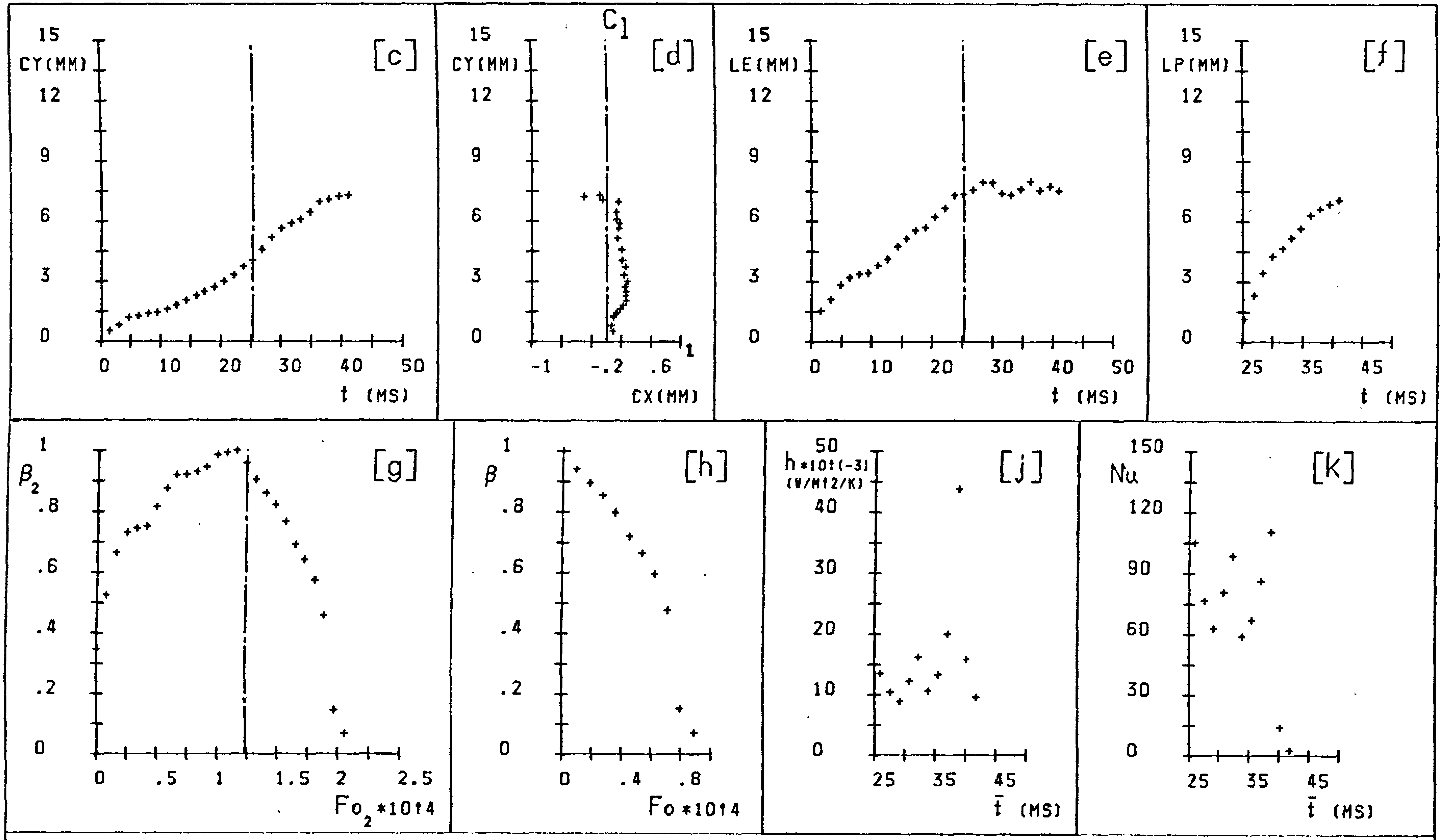

TEST NØ : (5.2).2 FILM NØ : 42-2/3

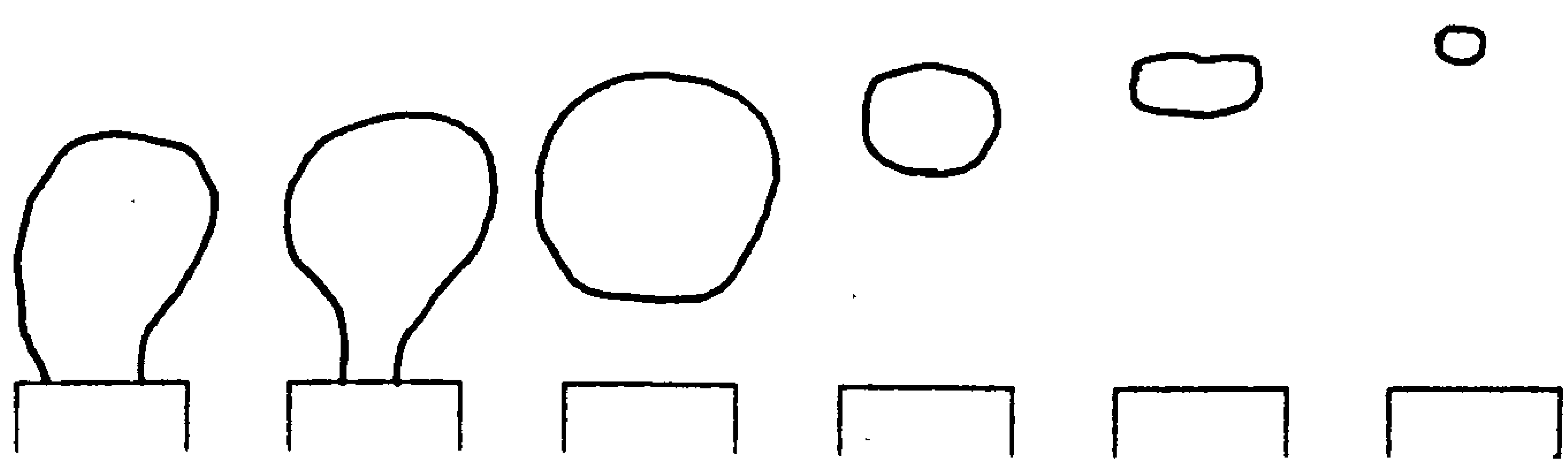

FRAME NUMBERS : 1 -25 26-27 28-33 34-35 36-38 39-40

EXPERIMENTAL PARAMETERS :

d	2
$\dot{m}_s$	.92
(V_s	13560)
ΔT	27.6

Z	40
P	2.008
Δt	.77
(CS	1298)

F	40
Ja	45
T_p	165

EXPERIMENTAL RESULTS :

t_g	21.56
t_c	8.7
t_t	30.26
f_s	48
R_m	2.49
R_o	2.29

h_c	16664
Nu_c	61
Z_d	3.91
Z_c	6.36
U	247
Fo_c	6.93E-05

Pe_o	6770

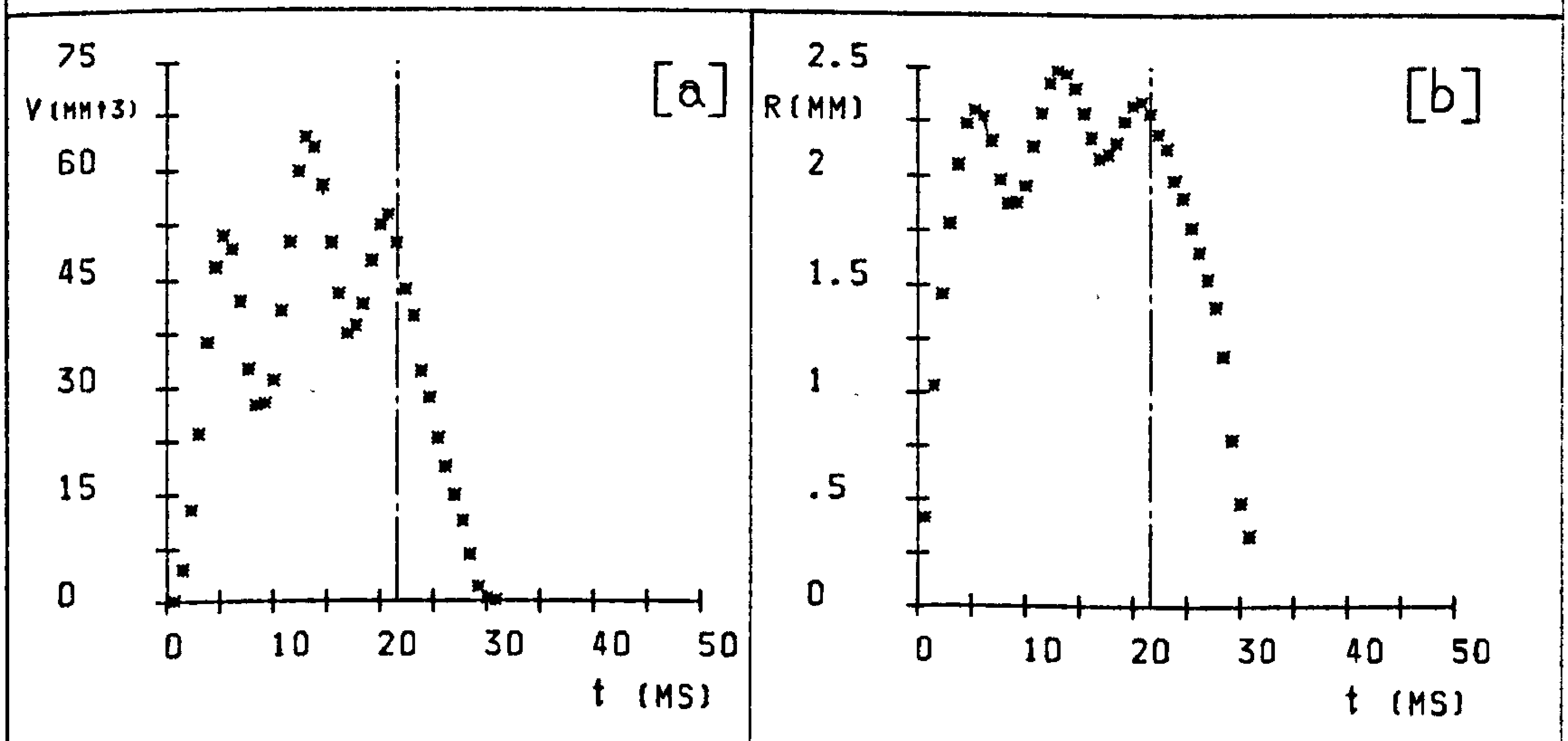

TEST NO : (5.3).3 FILM NO : 43-1/3

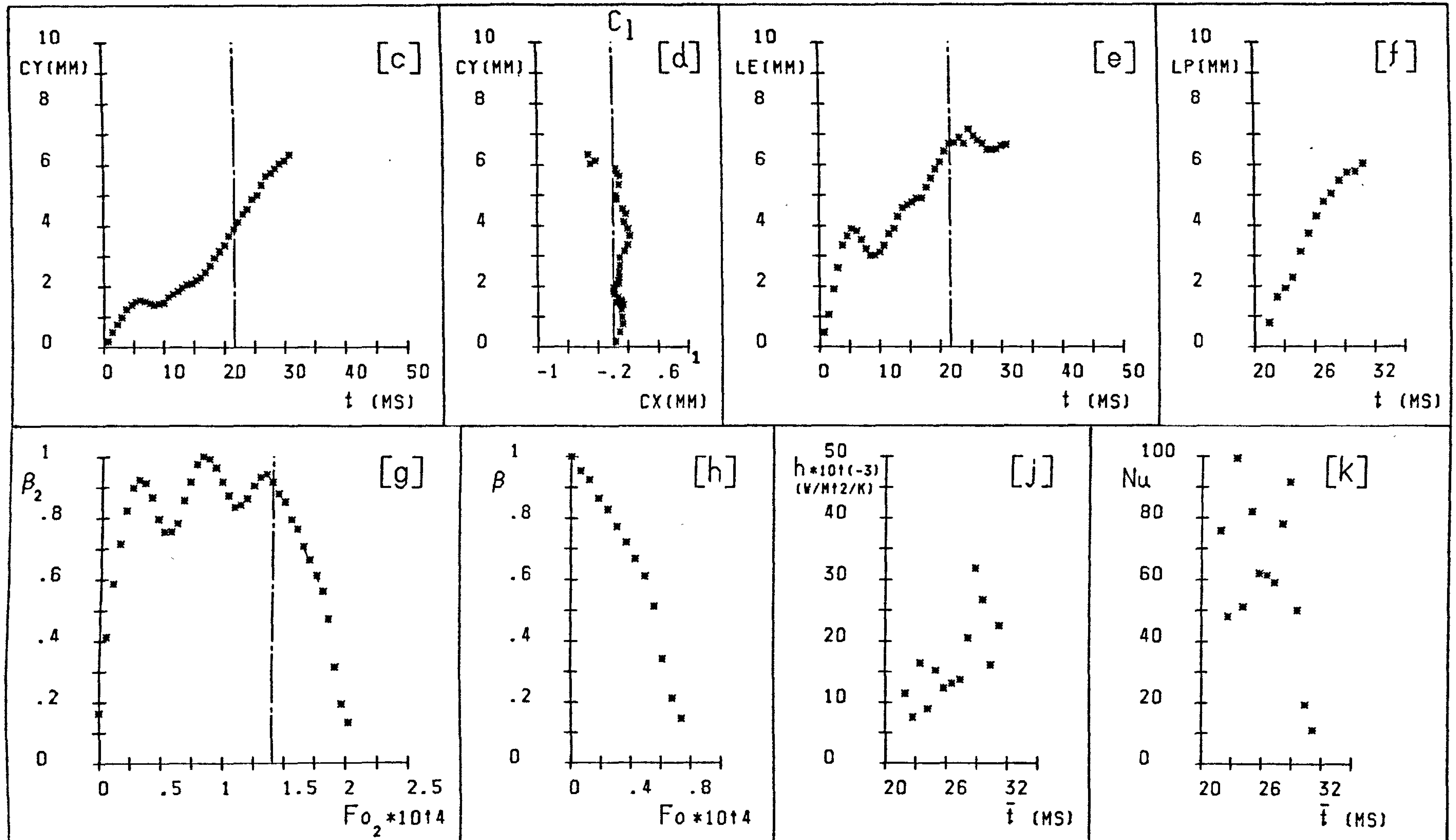

TEST NØ : (5.3).3 FILM NØ : 43-1/3

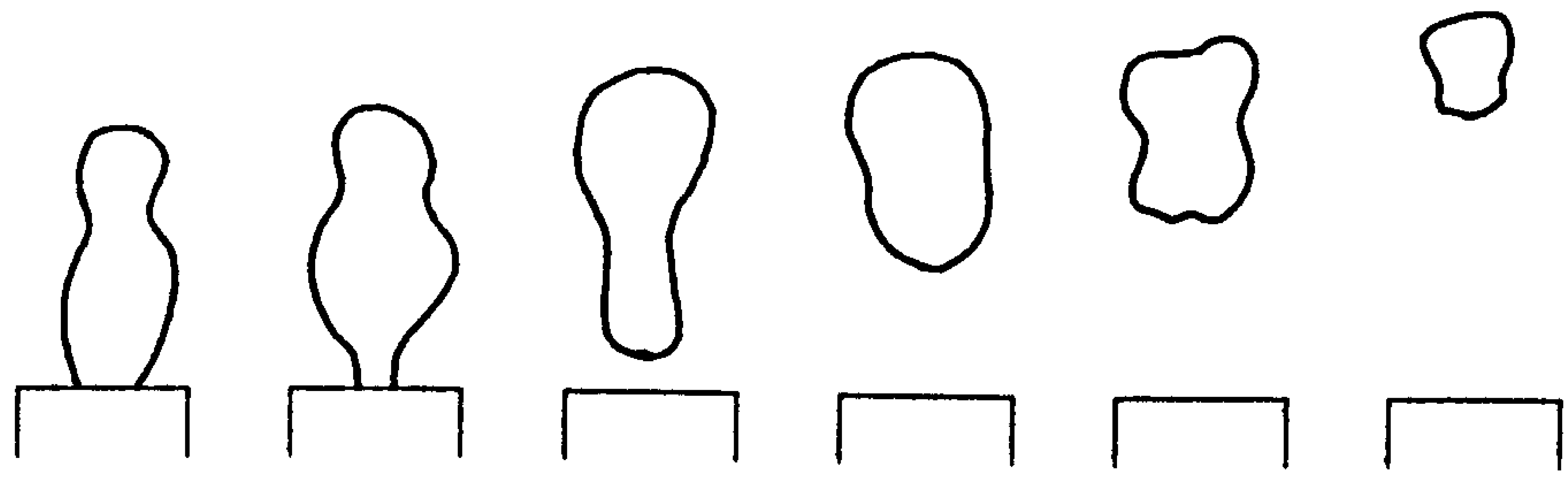

FRAME NUMBERS : 1 -16 | 17-18 | 19-21 | 22-25 | 26-29 | 30-41

EXPERIMENTAL PARAMETERS :

d	2
$\dot{m}_s$	1.42
(V_s	20963)
ΔT	9.3

Z	40
P	2.011
Δt	1.12
(CS	896)

F	41
Ja	15
T_p	165

EXPERIMENTAL RESULTS :

t_g	21.21
t_c	23
t_t	44.21
f_s	50
R_m	3.7
R_o	3.37

h_c	28956
Nu_c	148
Z_d	9.34
Z_c	22.58
U	589
Fo_c	8.61E-05

Pe_o	23350

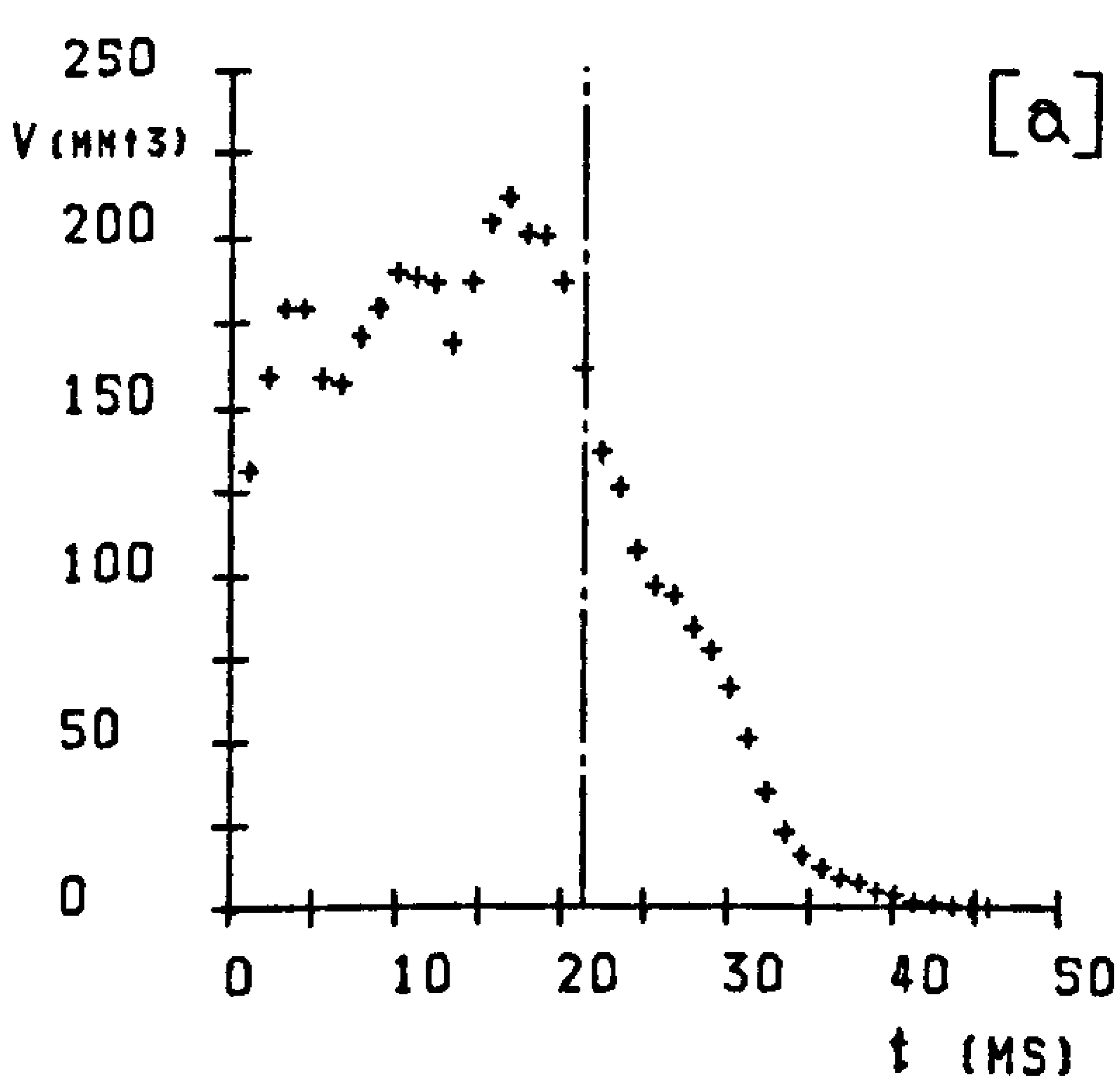

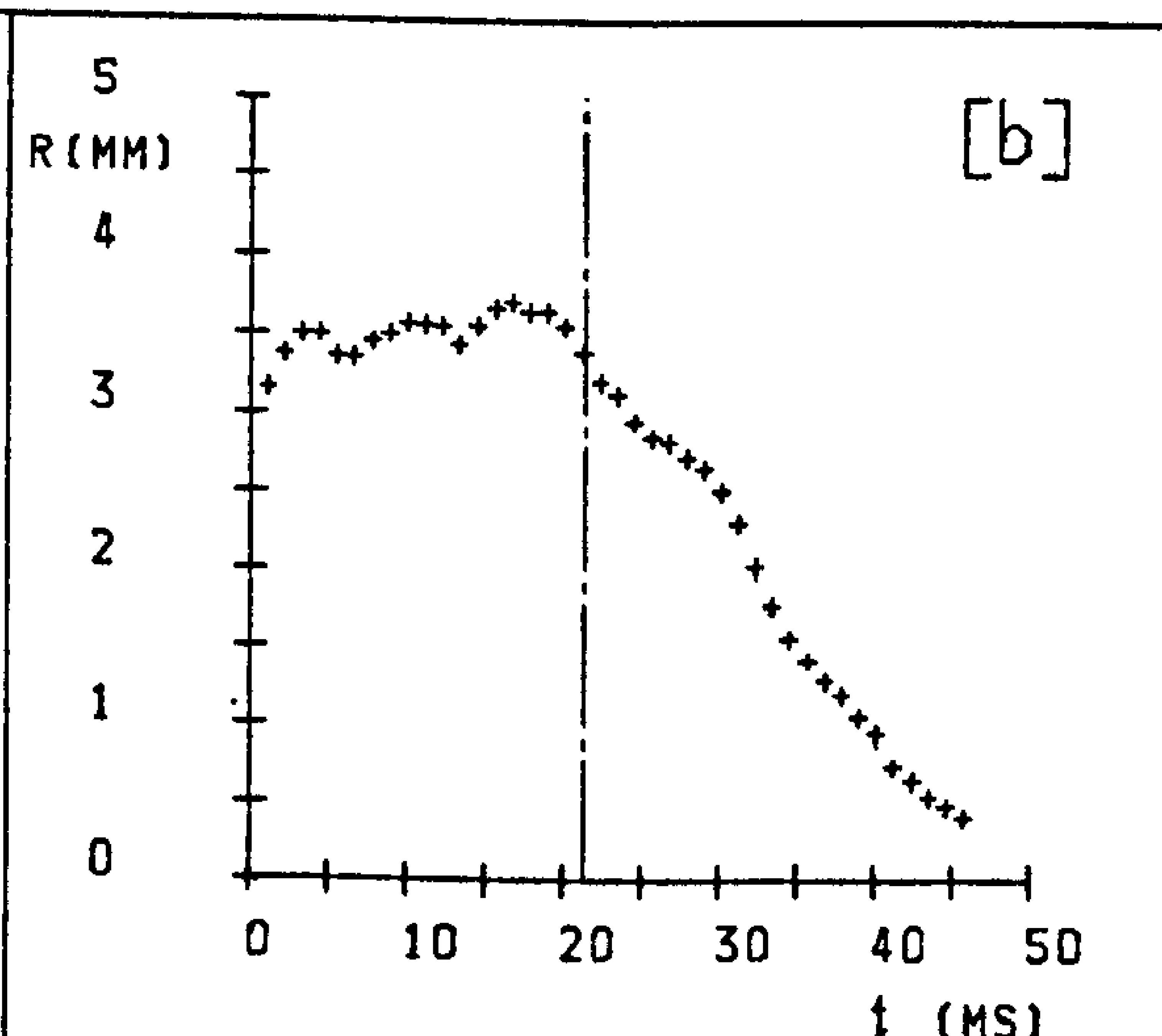

TEST NO : (6.1).2 FILM NO : 52-1/2

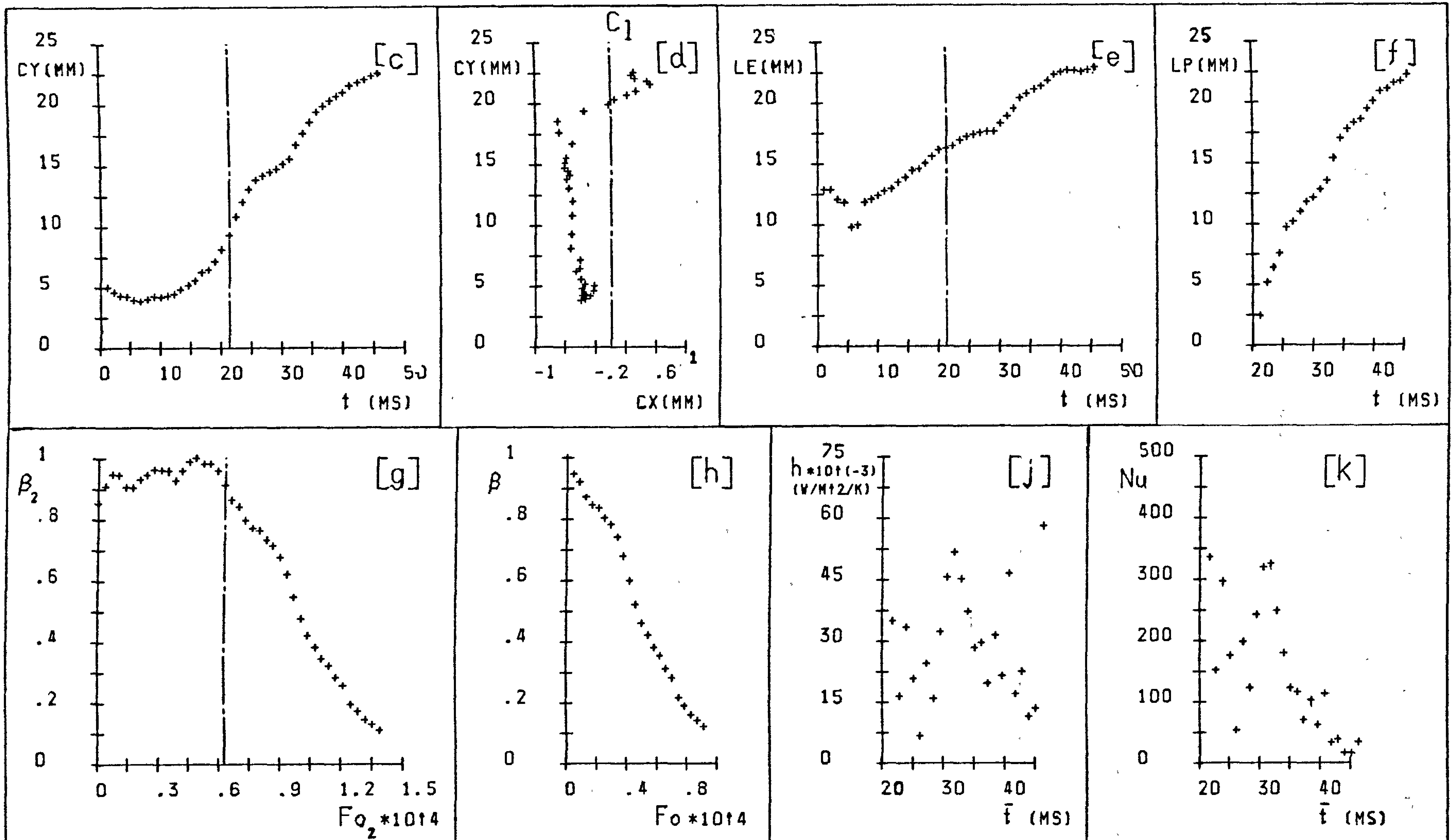

TEST NØ : (6.1).2 FILM NØ : 52-1/2

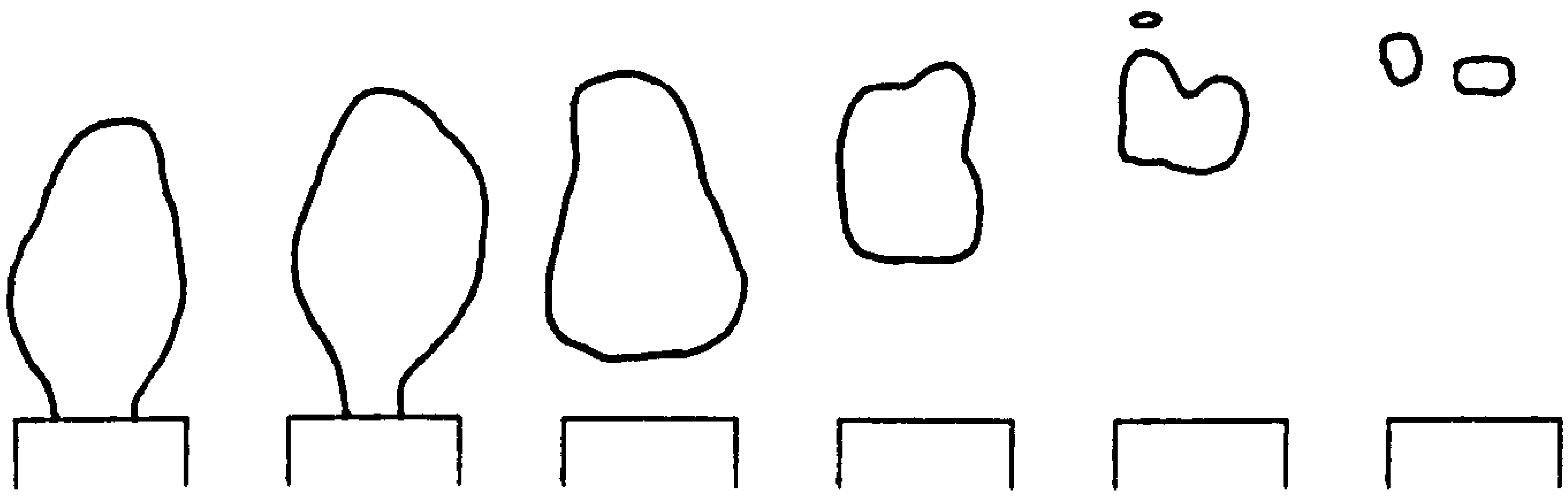

FRAME NUMBERS : 1 -11 | 12-13 | 14-22 | 23-24 | 25-27 | 28-30

EXPERIMENTAL PARAMETERS :

d	2
$\dot{m}_s$	1.42
(V_s	20963)
ΔT	18.5

Z	40
P	2.011
Δt	.81
(CS	1228)

F	30
Ja	30
T_p	165

EXPERIMENTAL RESULTS :

t_g	11.39
t_c	12.5
t_t	23.89
f_s	95
R_m	3.13
R_o	3.04

h_c	22580
Nu_c	109
Z_d	5.06
Z_c	11.54
U	495
Fo_c	5.71E-05

Pe_o	17810

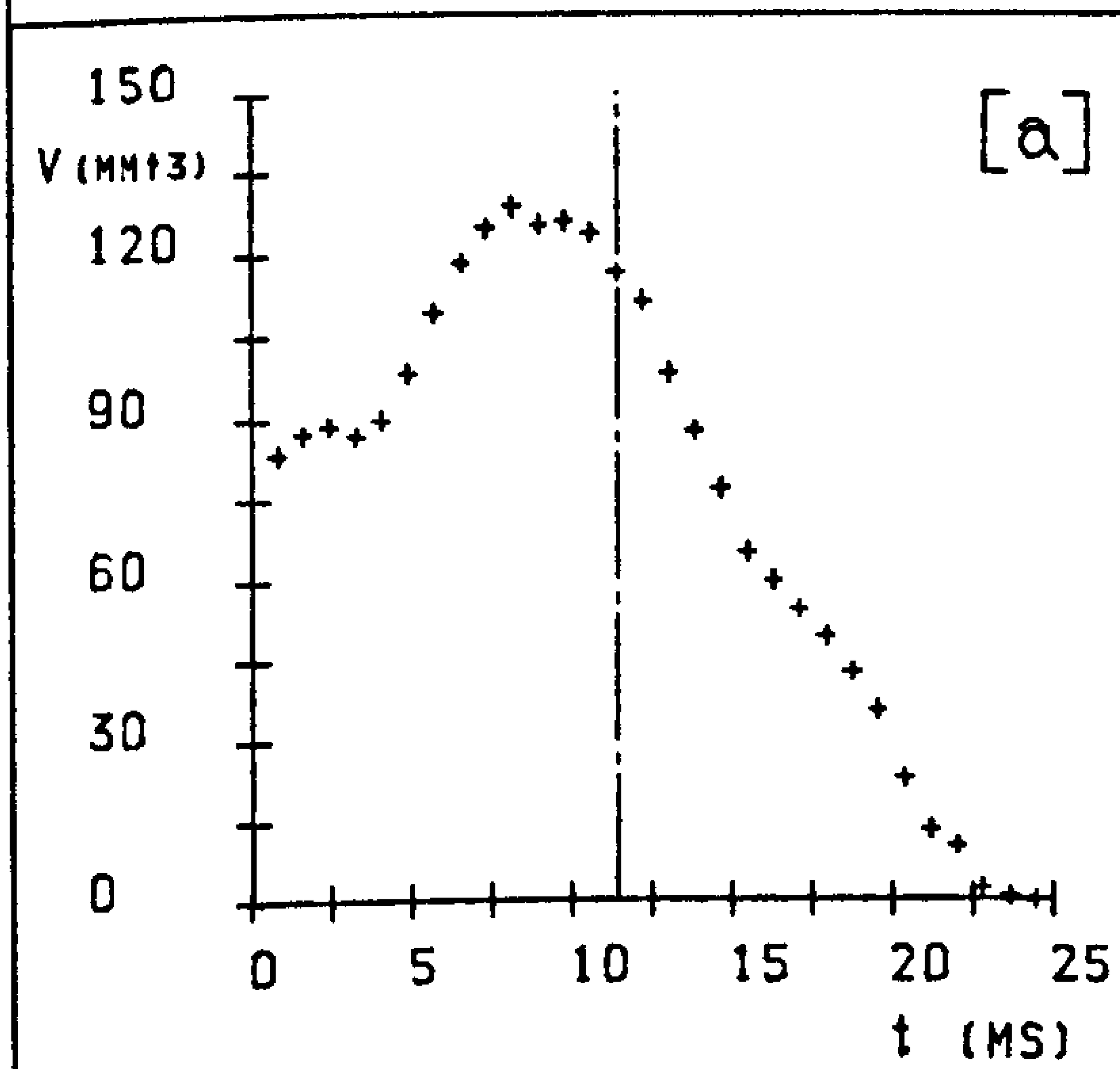

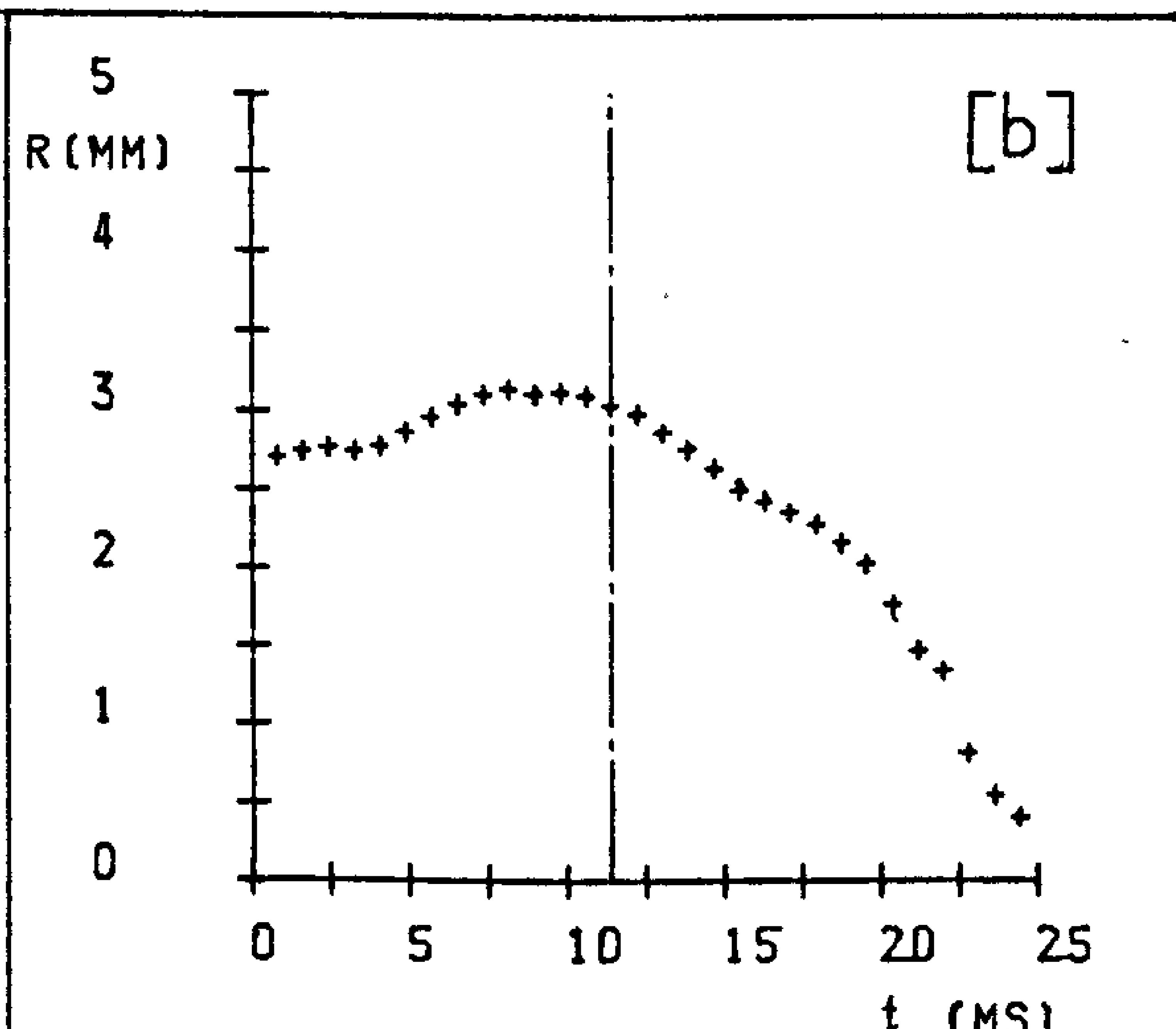

TEST NO : (6.2).2 FILM NO : 48-2/3

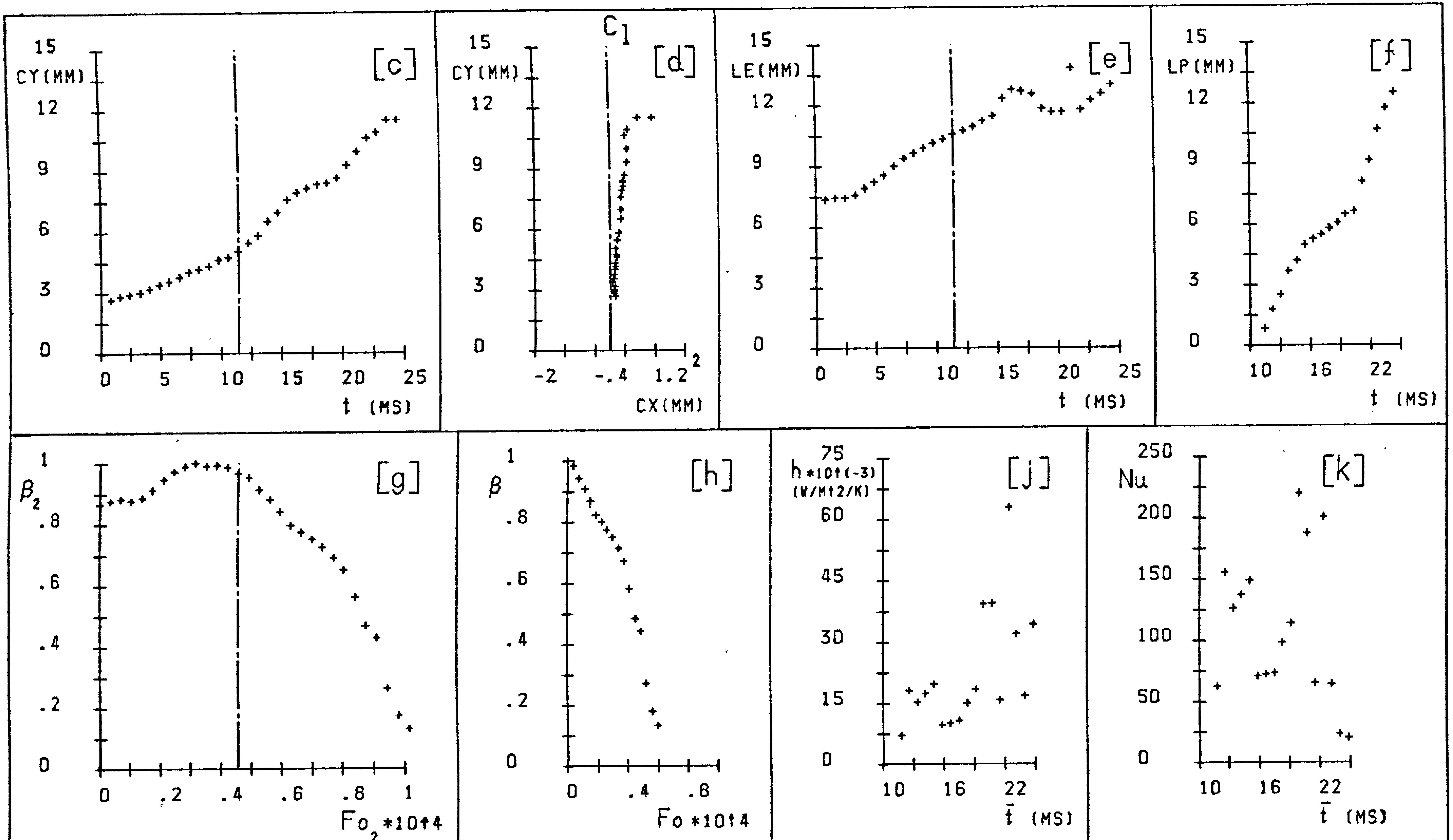

TEST NØ : (6.2).2 FILM NØ : 48-2/3

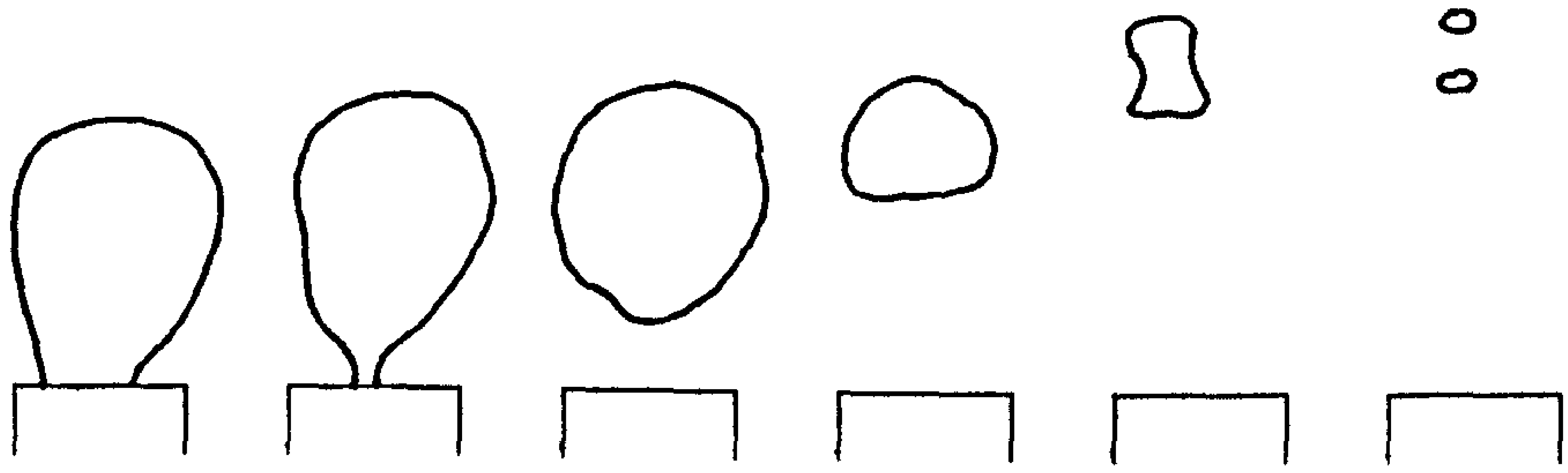

FRAME NUMBERS : 1 -16 | 17 | 18-21 | 22-25 | 26 | 27

EXPERIMENTAL PARAMETERS :

d	2	Z	40	F	27
$\dot{m}_s$	1.42	P	2.011	Ja	45
(V_s	20963)	Δt	.81	T_p	165
ΔT	27.6	(CS	1233)		

EXPERIMENTAL RESULTS :

t_g	14.6	h_c	23346	Pe_o	14610
t_c	7.5	Nu_c	107		
t_t	22.1	Z_d	4.07		
f_s	73	Z_c	6.85		
R_m	2.9	U	447		
R_o	2.73	Fo_c	4.2E-05		

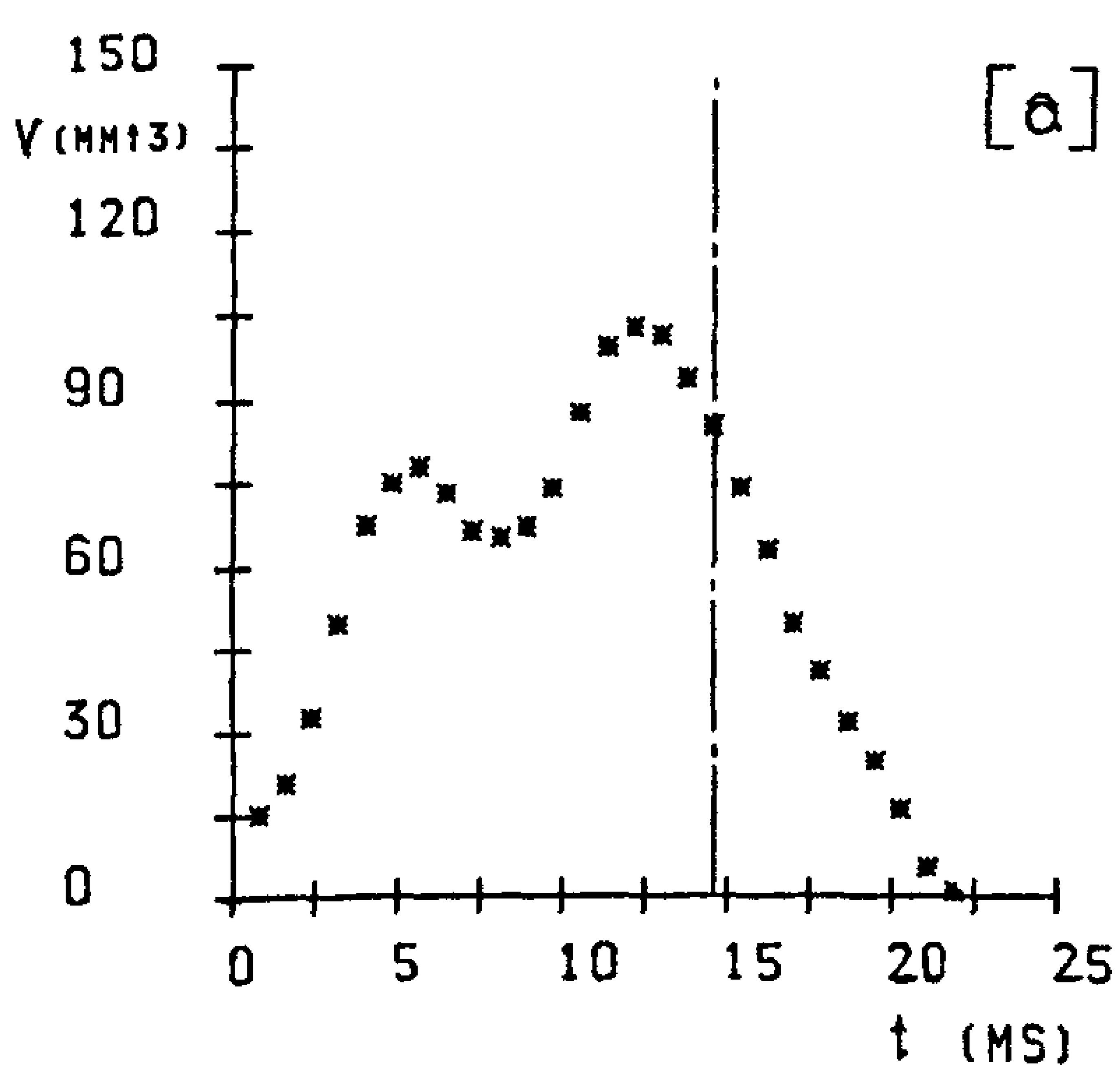

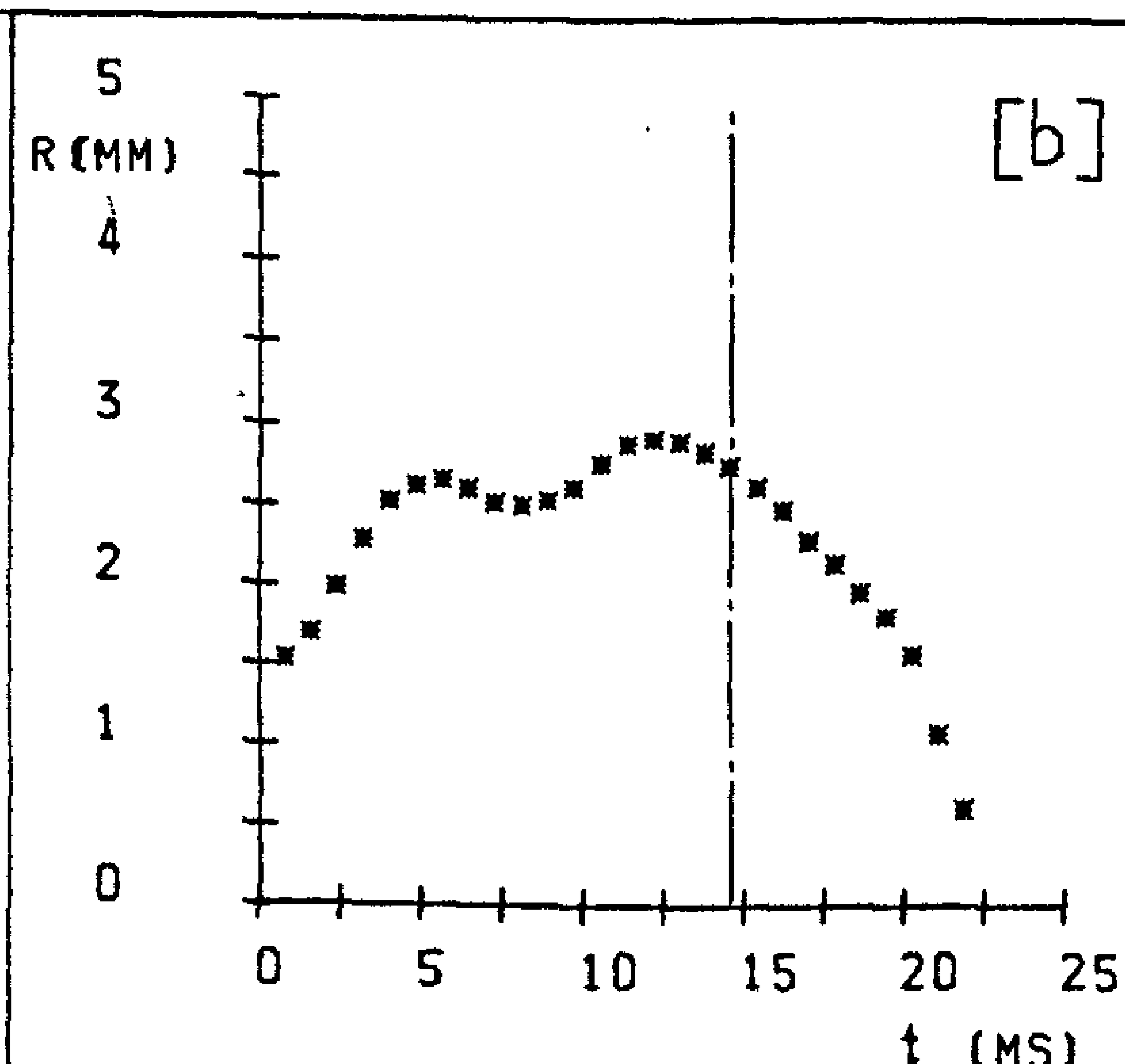

TEST NO : (6.3).3 FILM NO : 49-1/5

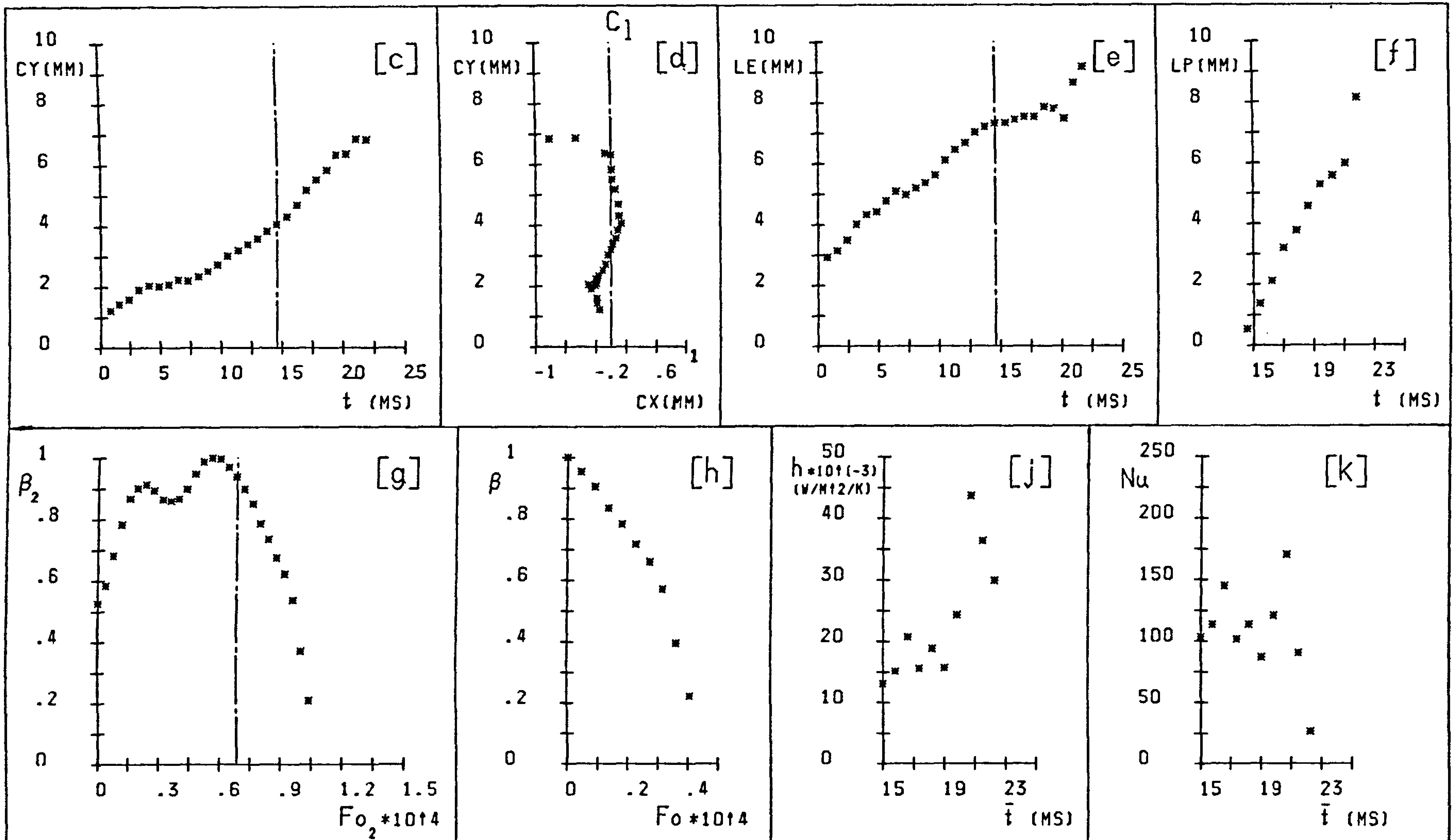

TEST NØ : (6.3).3 FILM NØ : 49-1/5

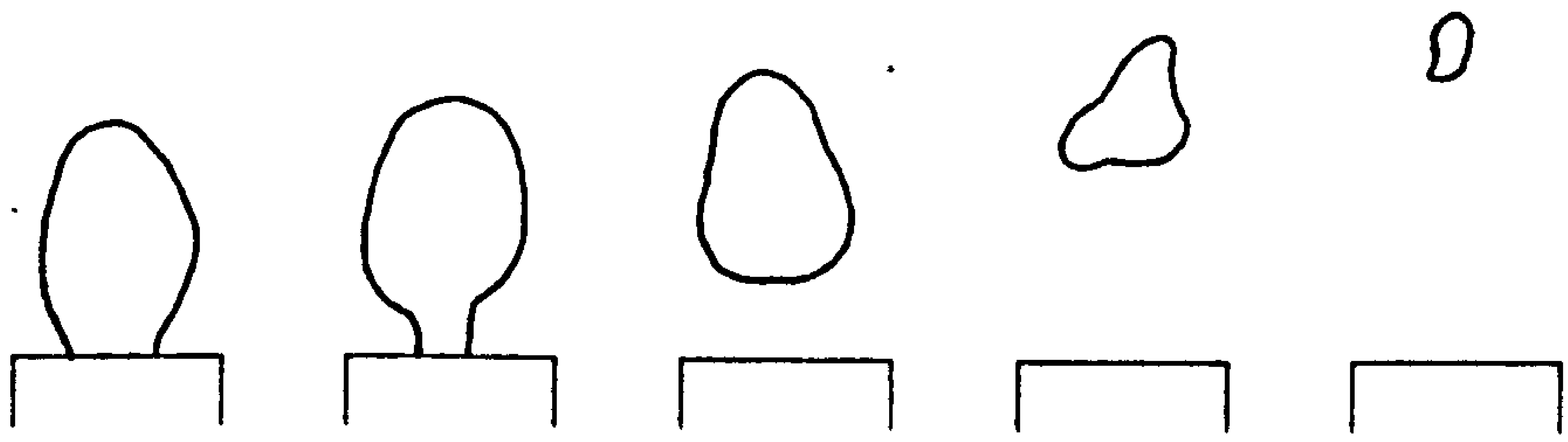

FRAME NUMBERS : 1 -18 19-20 21-23 24-25 26-27

EXPERIMENTAL PARAMETERS :

d	2	Z	40	F	27
$\dot{m}_s$	1.42	P	2.011	Ja	60
(V_s	20963)	Δt	.81	T_p	165
ΔT	36.6	(CS	1233)		

EXPERIMENTAL RESULTS :

t_g	17.03	h_c	21777	Pe_o	12300
t_c	5	Nu_c	79		
t_t	22.03	Z_d	3.65		
f_s	62	Z_c	6.41		
R_m	2.47	U	447		
R_o	2.27	Fo_c	4E-05		

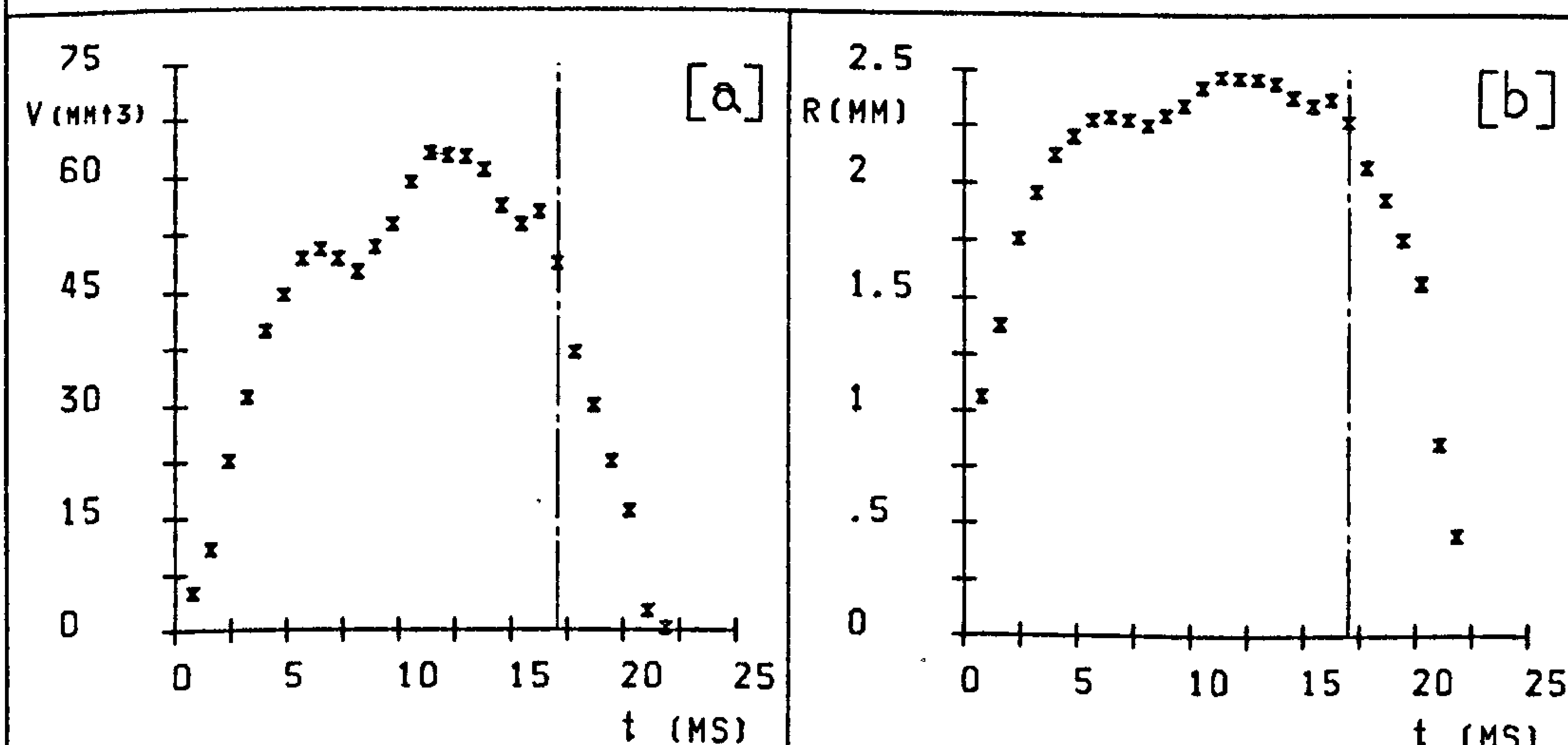

TEST NO : (6.4).1 FILM NO : 50-1/2

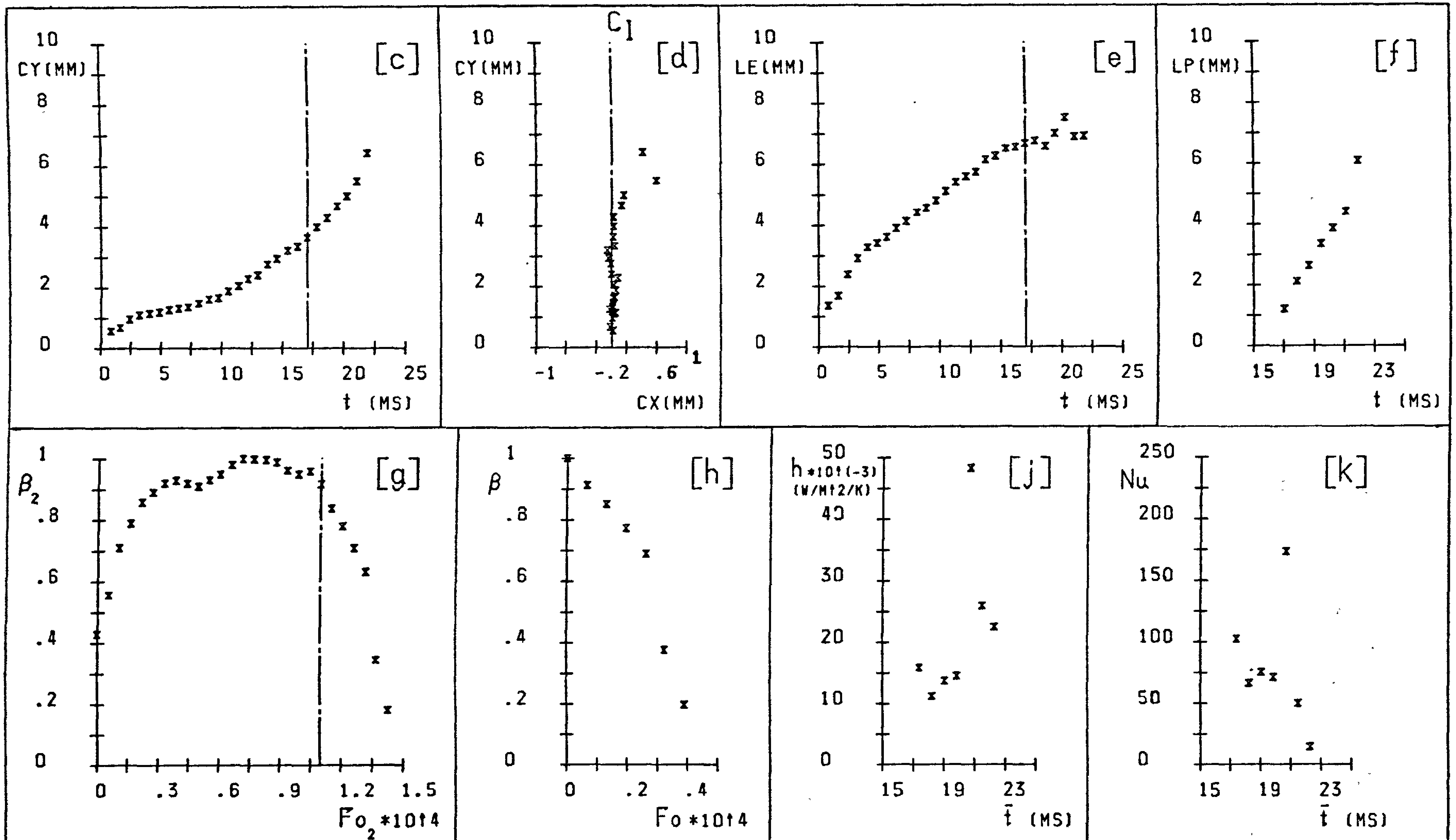

TEST NØ : (6.4).1 FILM NØ : 50-1/2

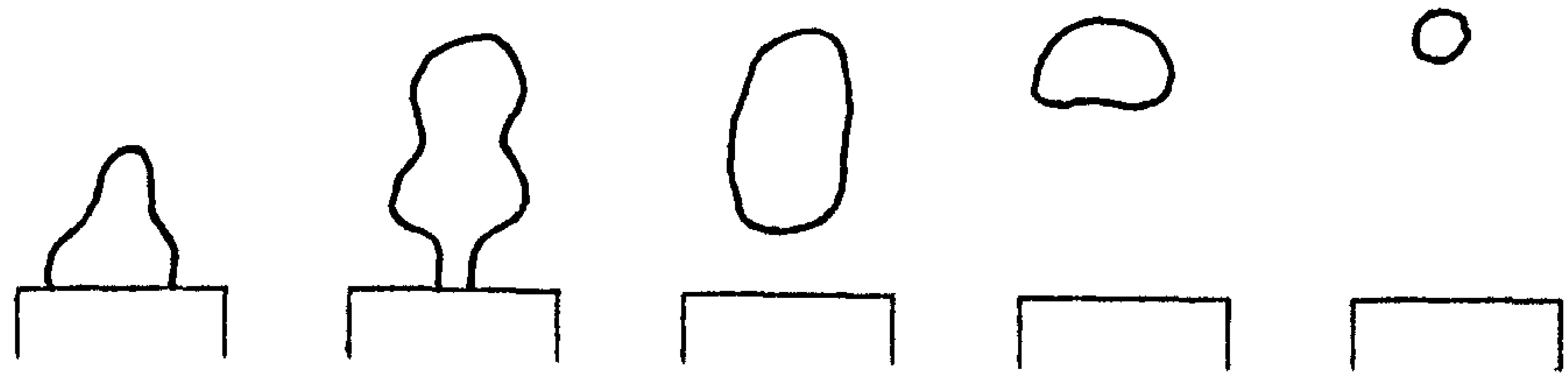

FRAME NUMBERS : 1 -7 | 8 -12 | 13-17 | 18-22 | 23-27

EXPERIMENTAL PARAMETERS :

d	1	Z	40	F	27
$\dot{m}_s$	.42	P	1.02	Ja	15
(V_s	11706)	Δt	2.15	T_p	165
ΔT	5	(CS	466)		

EXPERIMENTAL RESULTS :

t_g	27.98	h_c	26777	Pe_o	22340
t_c	29	Nu_c	153		
t_t	56.93	Z_d	9.13		
f_s	39	Z_c	22.55		
R_m	3.73	U	500		
R_o	3.73	Fo_c	8.7E-05		

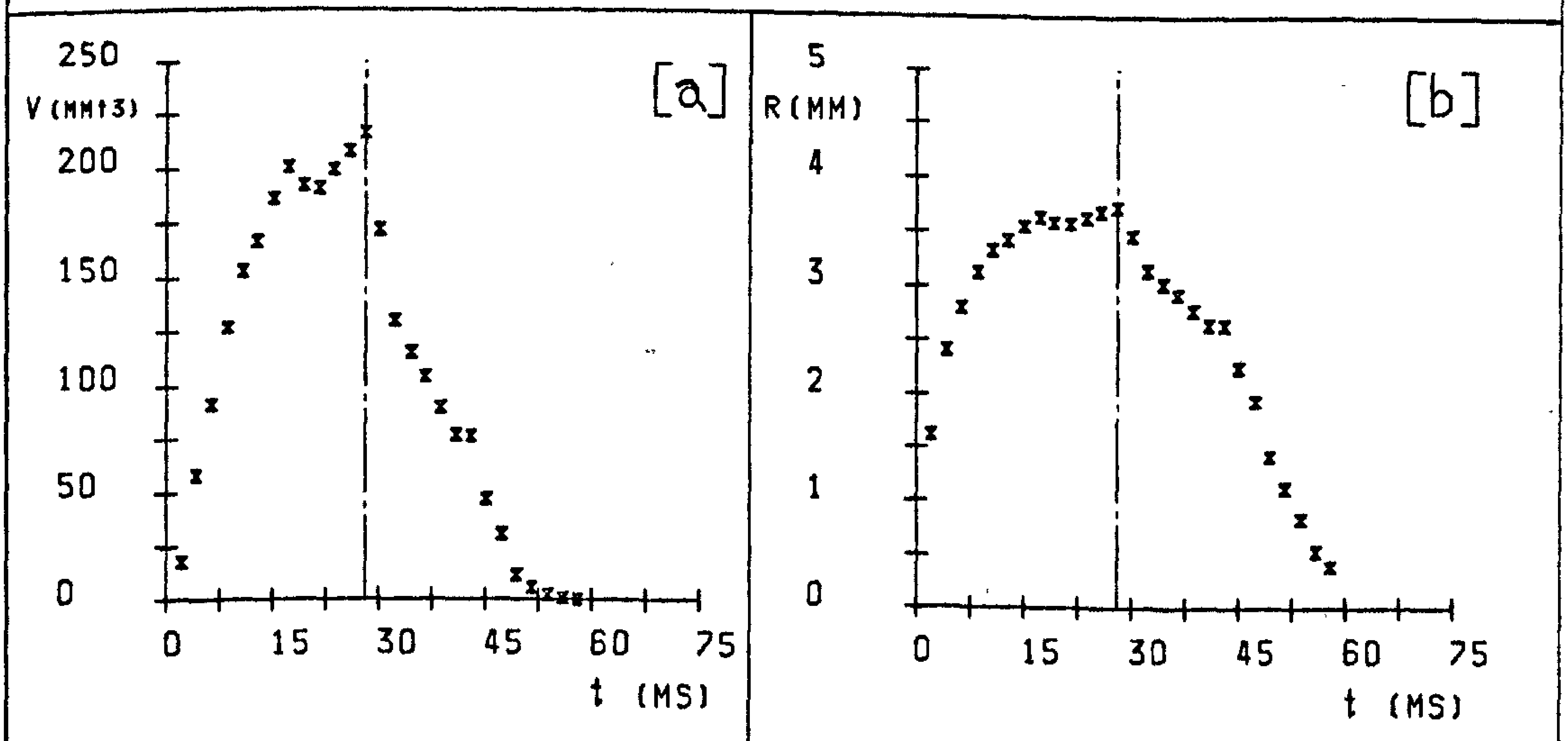

TEST NO : (7.1).1 FILM NO : 53-2/1

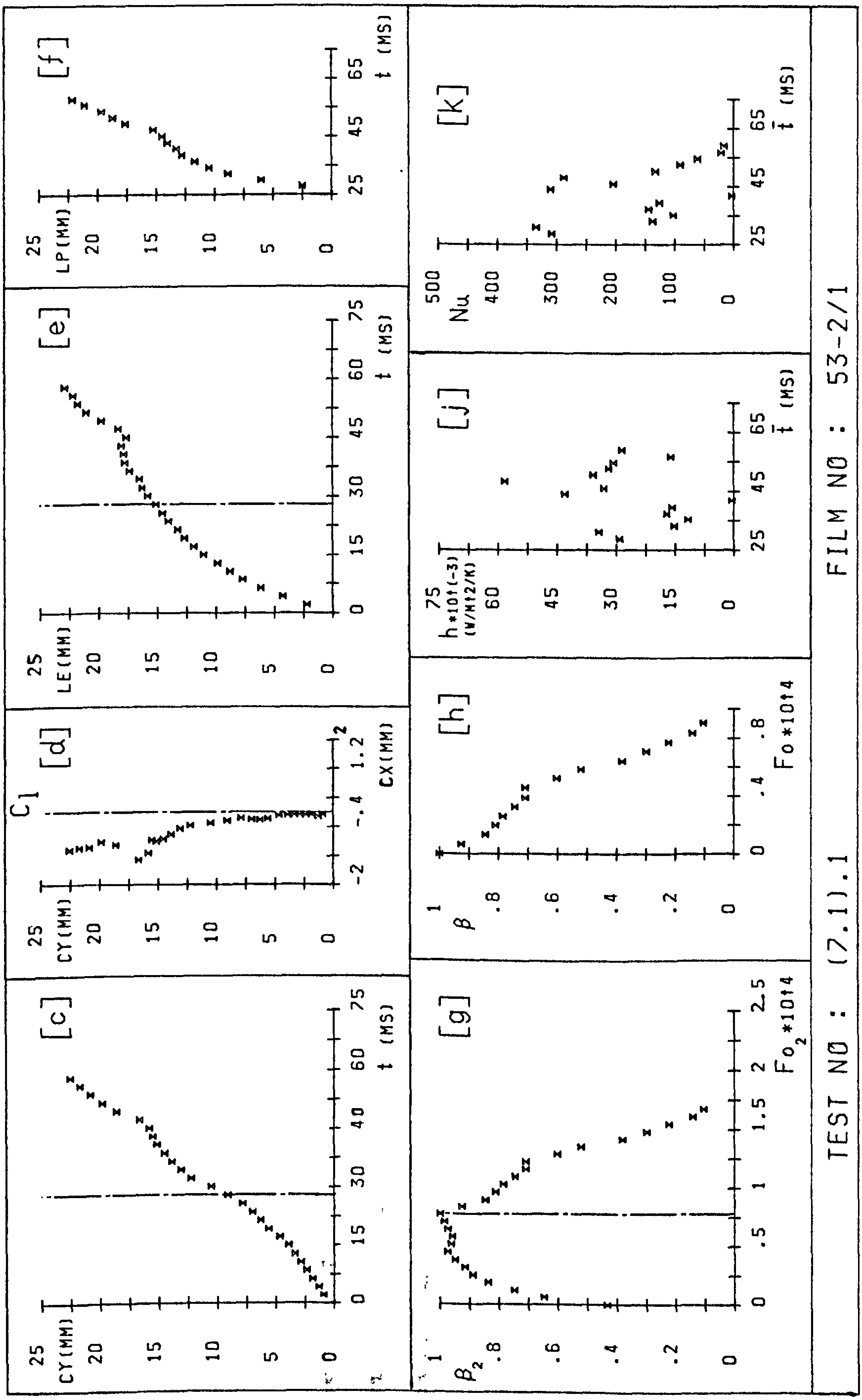
[c]
CY(MM)
t (MS)
[d]
C_1
CY(MM)
CX(MM)
[e]
LE(MM)
t (MS)
[f]
LP(MM)
t (MS)
[g]
B_2
Fo_2 *10↑4
[h]
β
Fo *10↑4
[j]
h *10↑(-3) (W/M↑2/K)
$\bar{t}$ (MS)
[k]
Nu
$\bar{t}$ (MS)
TEST NO : (7.1).1
FILM NO : 53-2/1

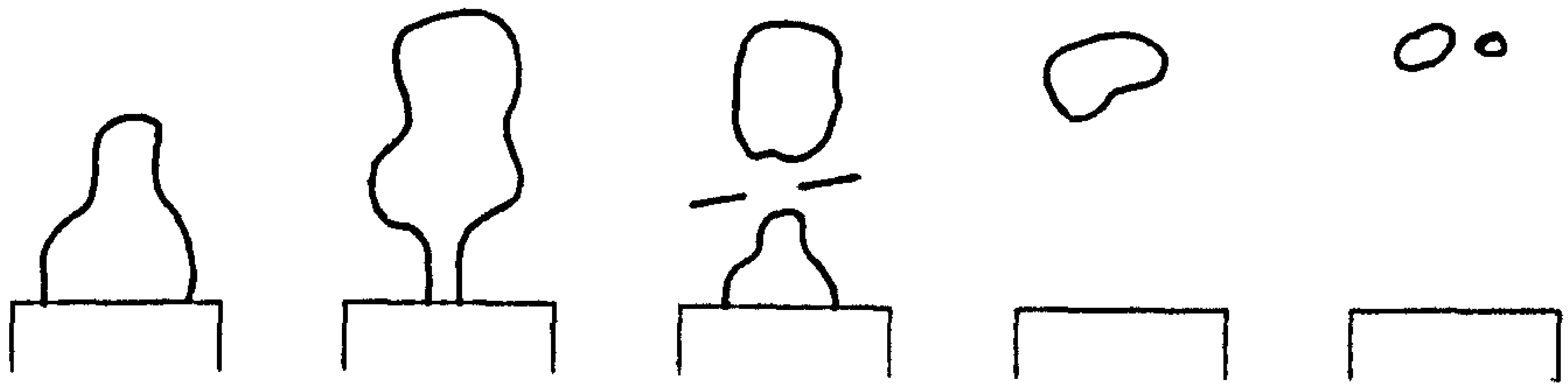

FRAME NUMBERS : 1 -12 | 13-21 | 22-26 | 27-29 | 30-33

EXPERIMENTAL PARAMETERS :

d	1	Z	40	F	33
$\dot{m}_s$	.42	P	1.02	Ja	30
(V_s	11706)	Δt	1.03	T_p	165
ΔT	10	(CS	967)		

EXPERIMENTAL RESULTS :

t_g	22.74	h_c	23402	Pe_o	16320
t_c	10.5	Nu_c	97		
t_t	33.24	Z_d	7.89		
f_s	46	Z_c	12.21		
R_m	2.96	U	515		
R_o	2.63	Fo_c	6.3E-05		

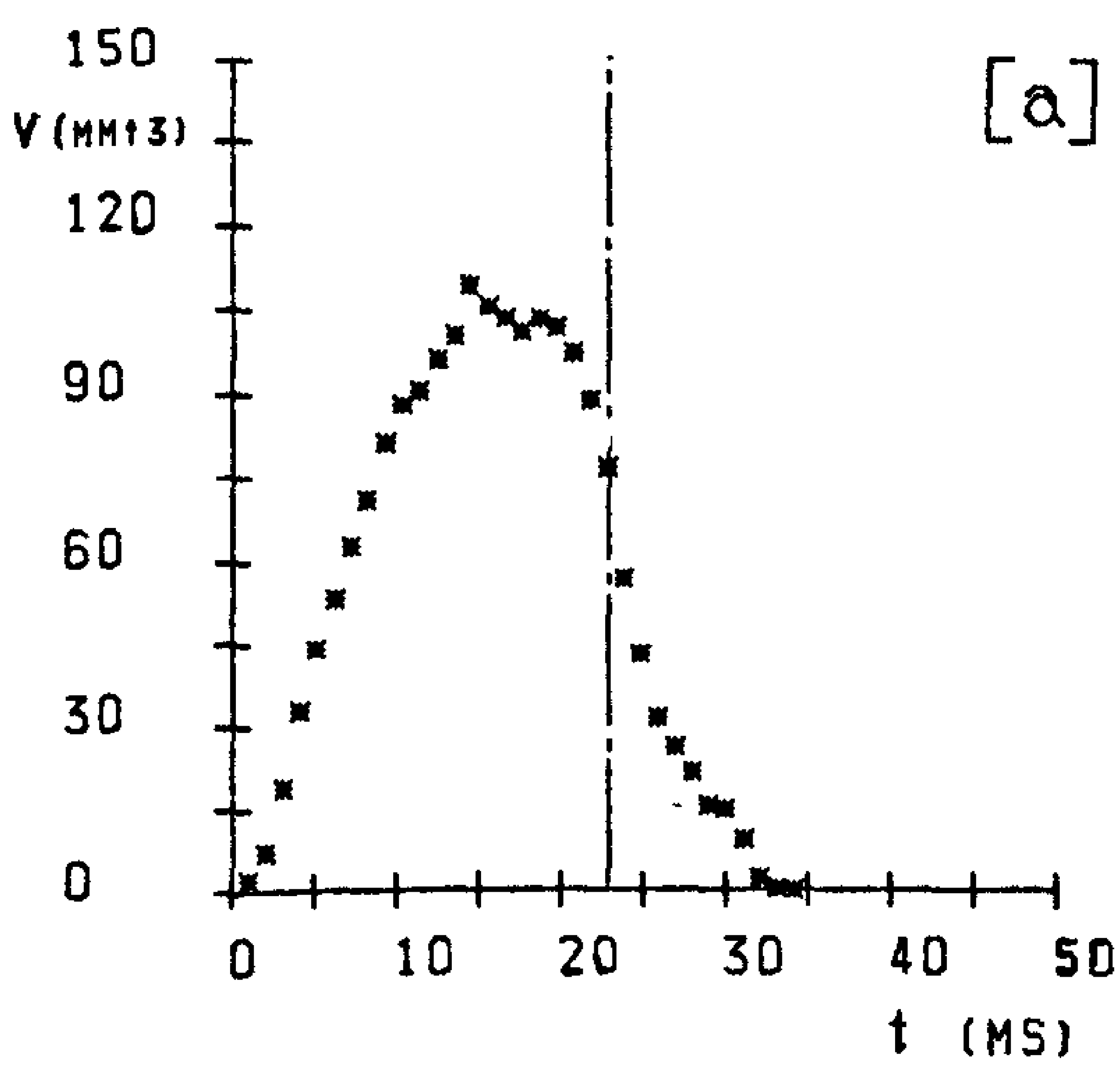

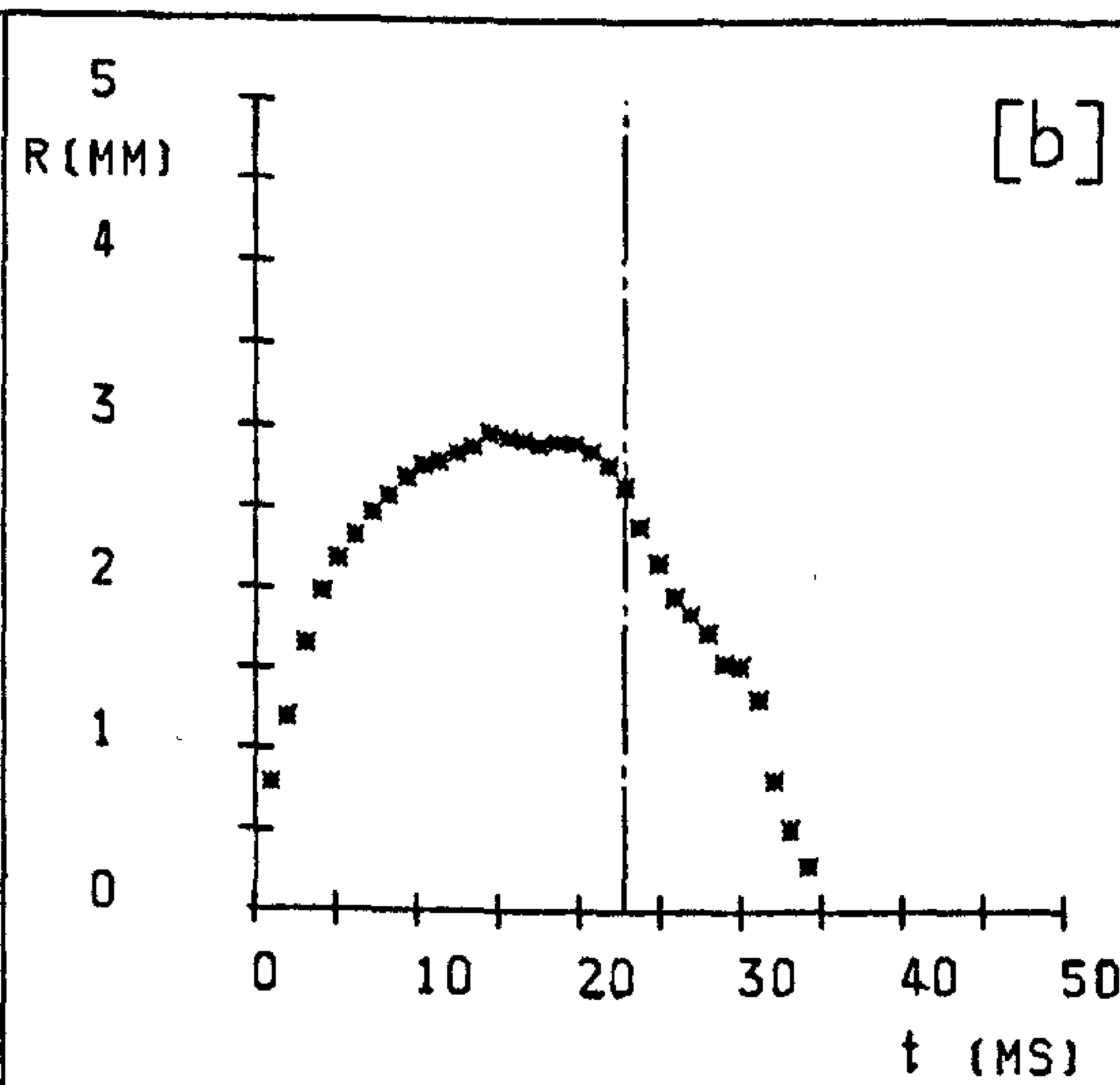

TEST NØ : (7.2).3 FILM NØ : 54-1/3

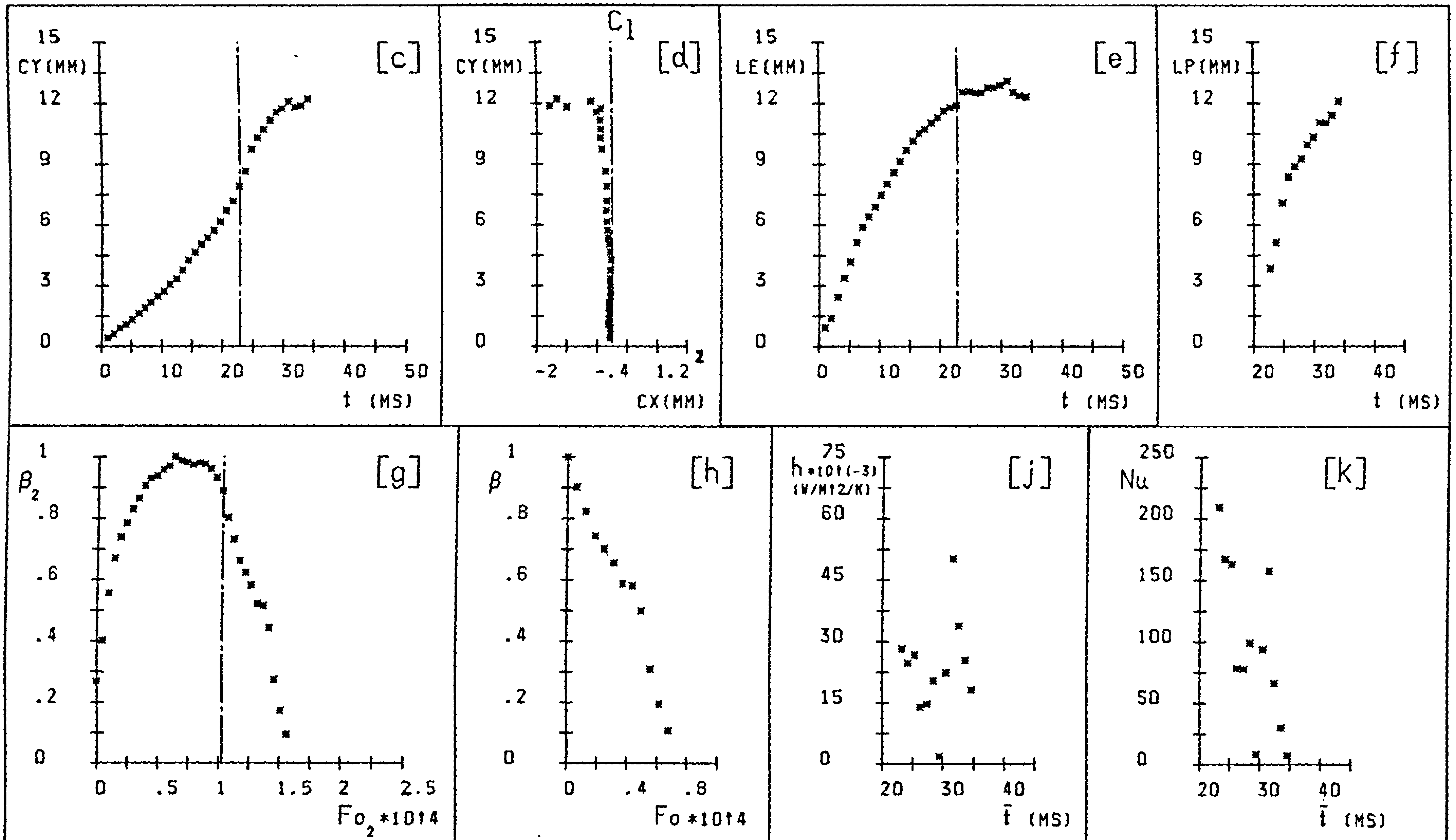

TEST NØ : (7.2).3 FILM NO : 54-1/3

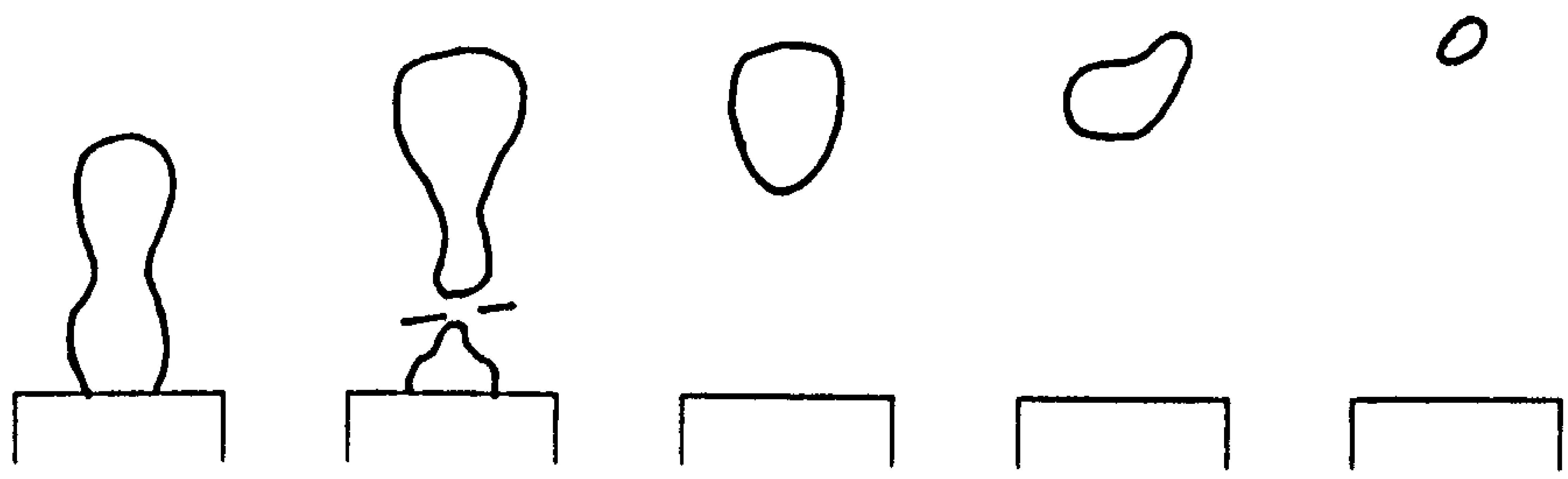

FRAME NUMBERS :	1 -11	12	13-14	15-16	17

EXPERIMENTAL PARAMETERS :

d	1	Z	40	F	17
$\dot{m}_s$	.42	P	1.02	Ja	45
(V_s	11706)	Δt	.78	T_p	165
ΔT	15	(CS	1289)		

EXPERIMENTAL RESULTS :

t_g	9.32	h_c	27982	Pe_o	11950
t_c	4	Nu_c	84		
t_t	13.32	Z_d	7.33		
f_s	117	Z_c	9.59		
R_m	2.13	U	533		
R_o	1.85	Fo_c	4.77E-05		

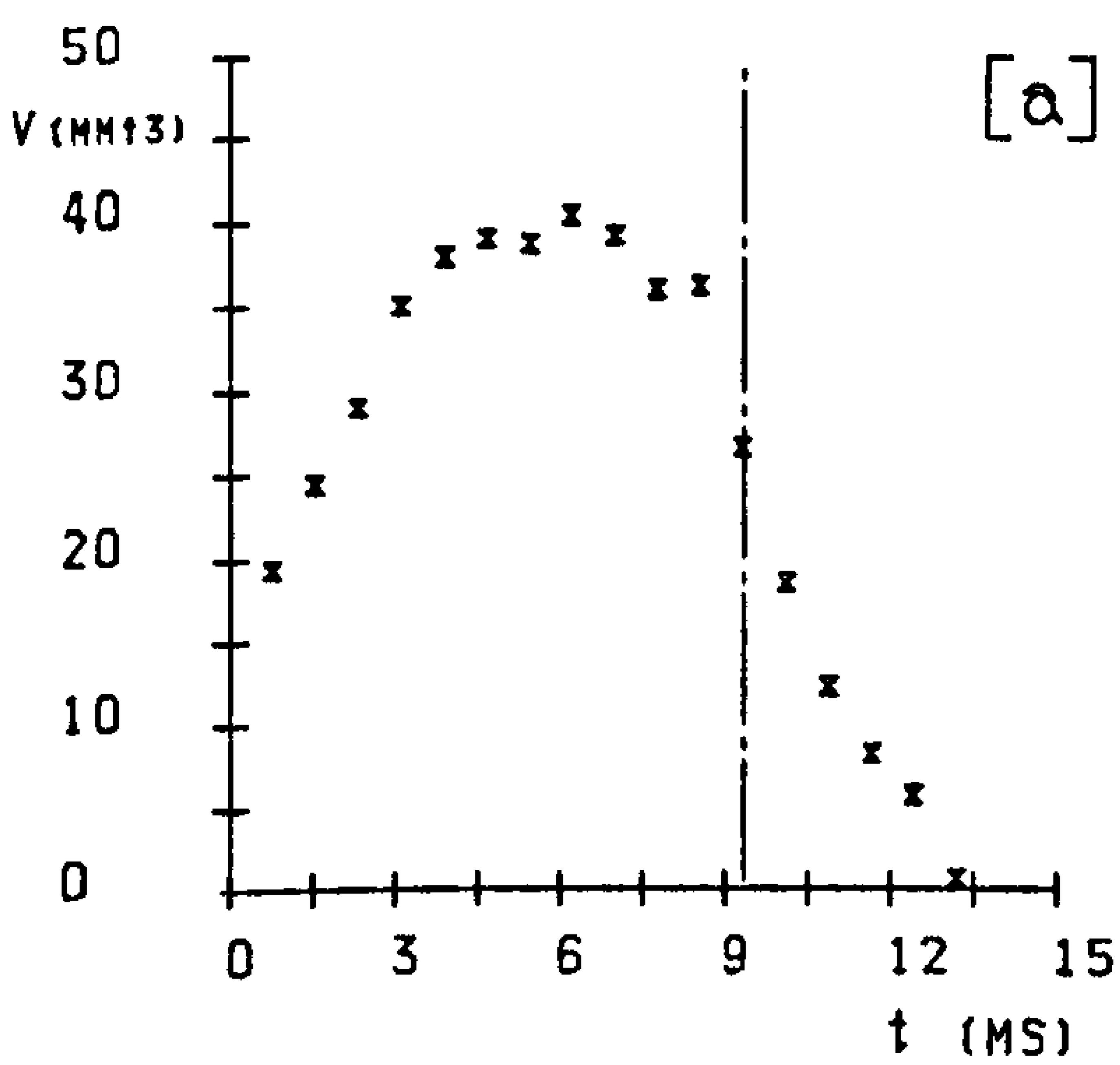

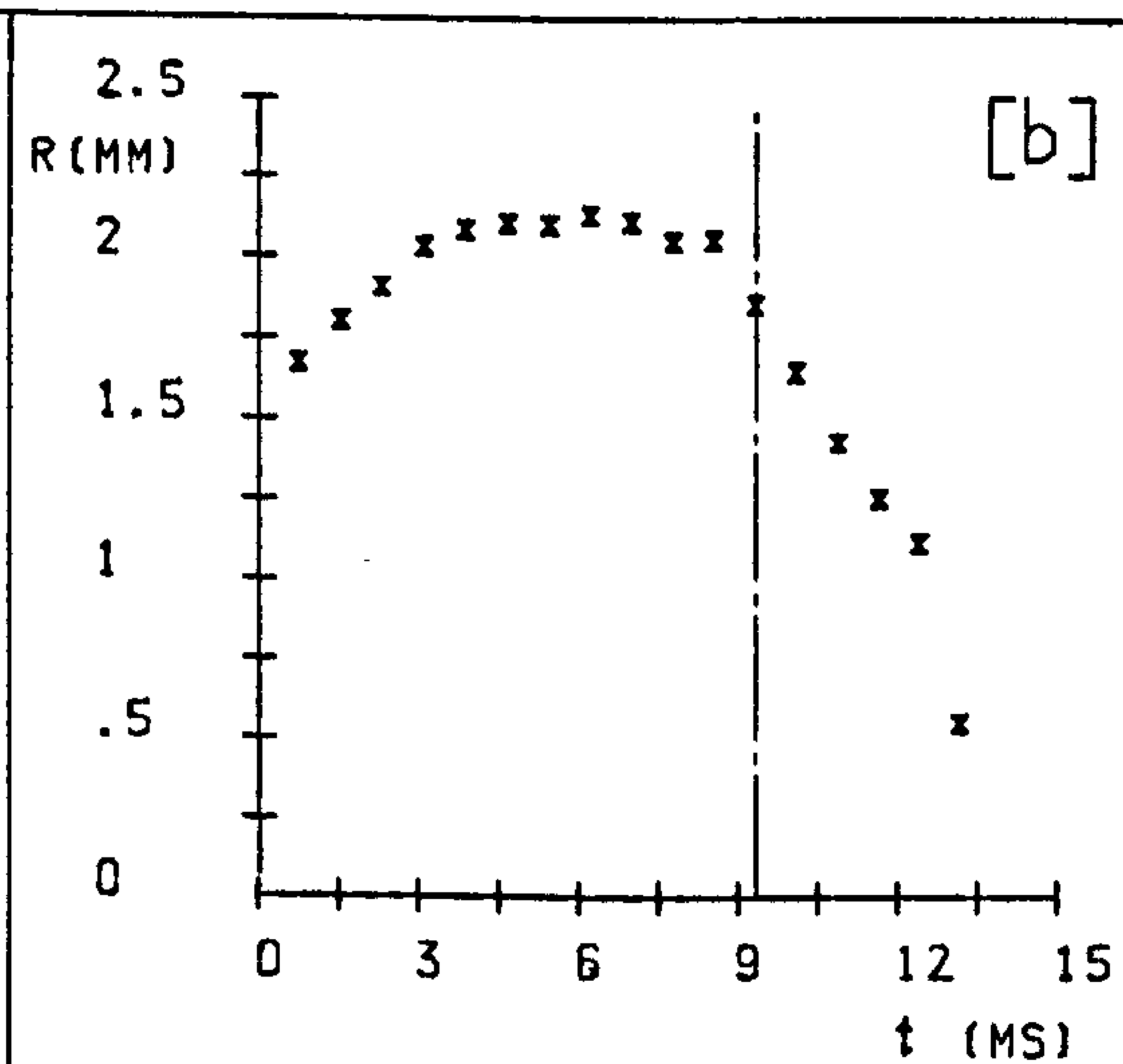

TEST NO : (7.3).1 FILM NO : 54-2/2

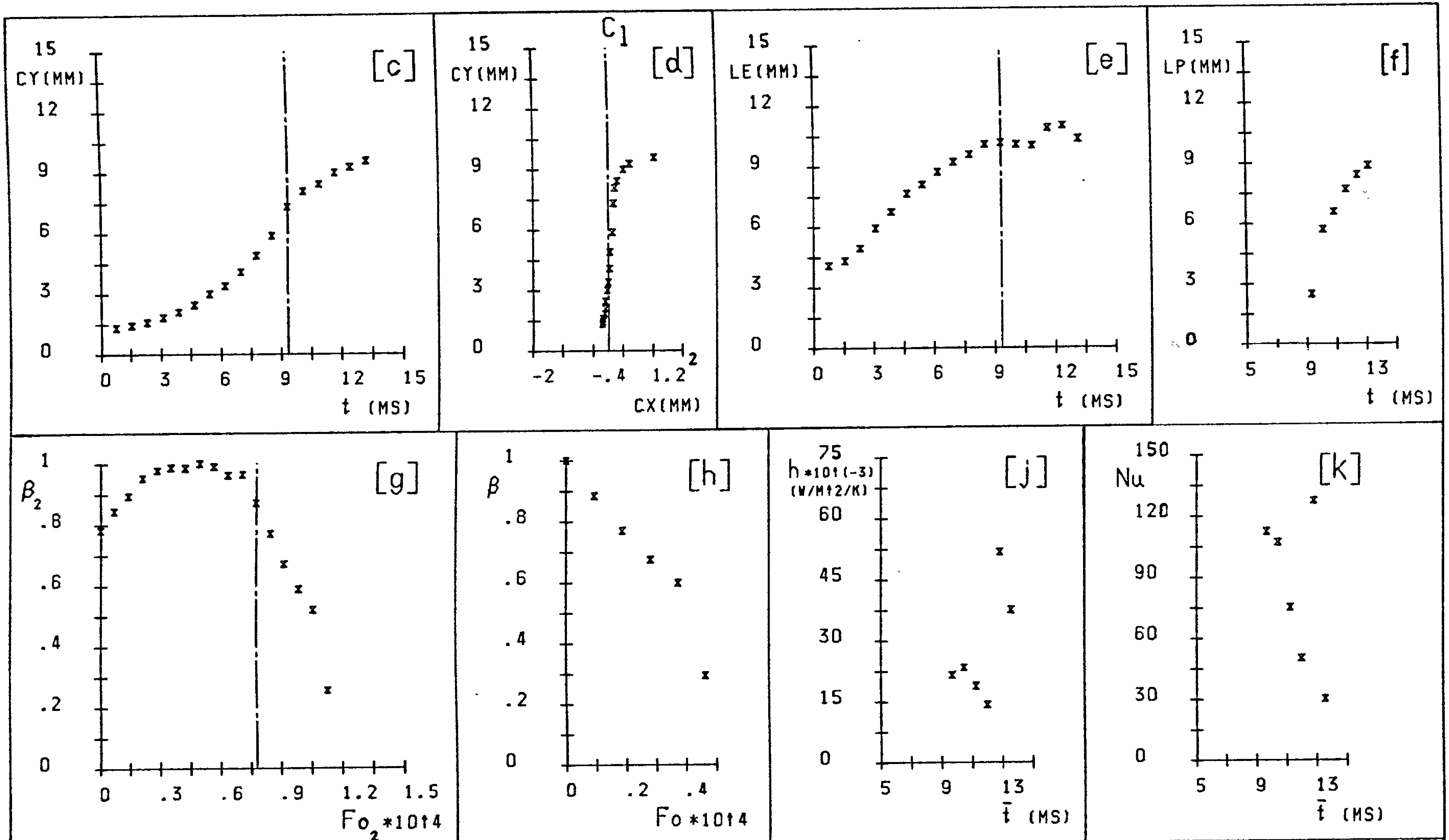

TEST NØ : (7.3).1 FILM NØ : 54-2/2

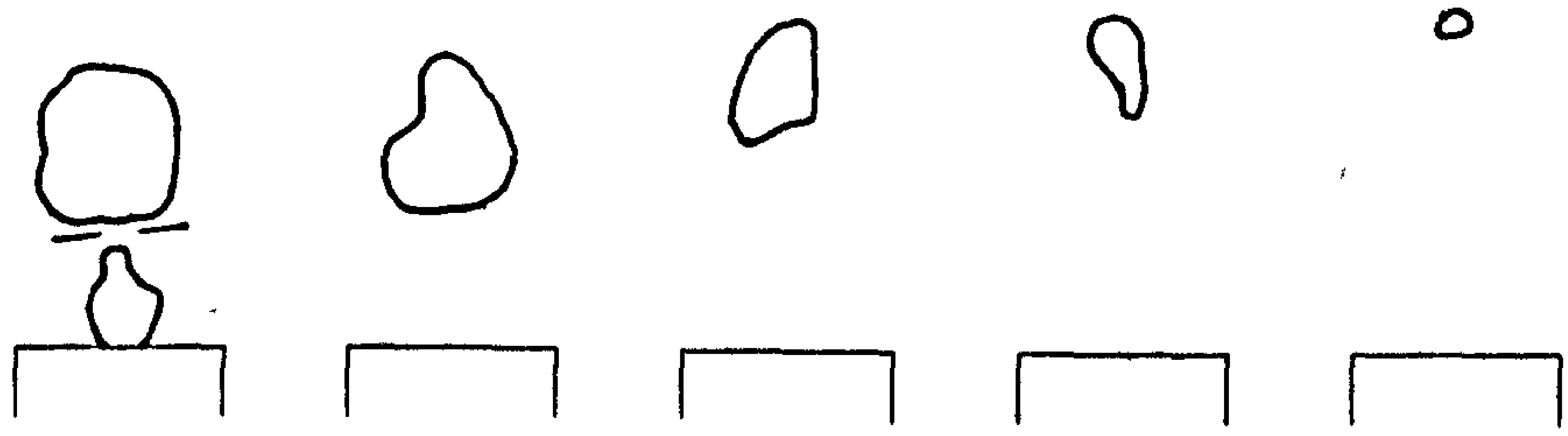

FRAME NUMBERS : 1 | 2 -3 | 4 -5 | 6 -7 | 8 -10

EXPERIMENTAL PARAMETERS :

d	1
$\dot{m}_s$	1
(V_s	27871)
ΔT	5

Z	40
P	1.017
Δt	2.25
(CS	444)

F	10
Ja	15
T_p	165

EXPERIMENTAL RESULTS :

t_g	-
t_c	18.8
t_t	—
f_s	-
R_m	3.44
R_o	3.44

h_c	33435
Nu_c	177
Z_d	12.57
Z_c	24.4
U	680
Fo_c	6.63E-05

Pe_o	28010

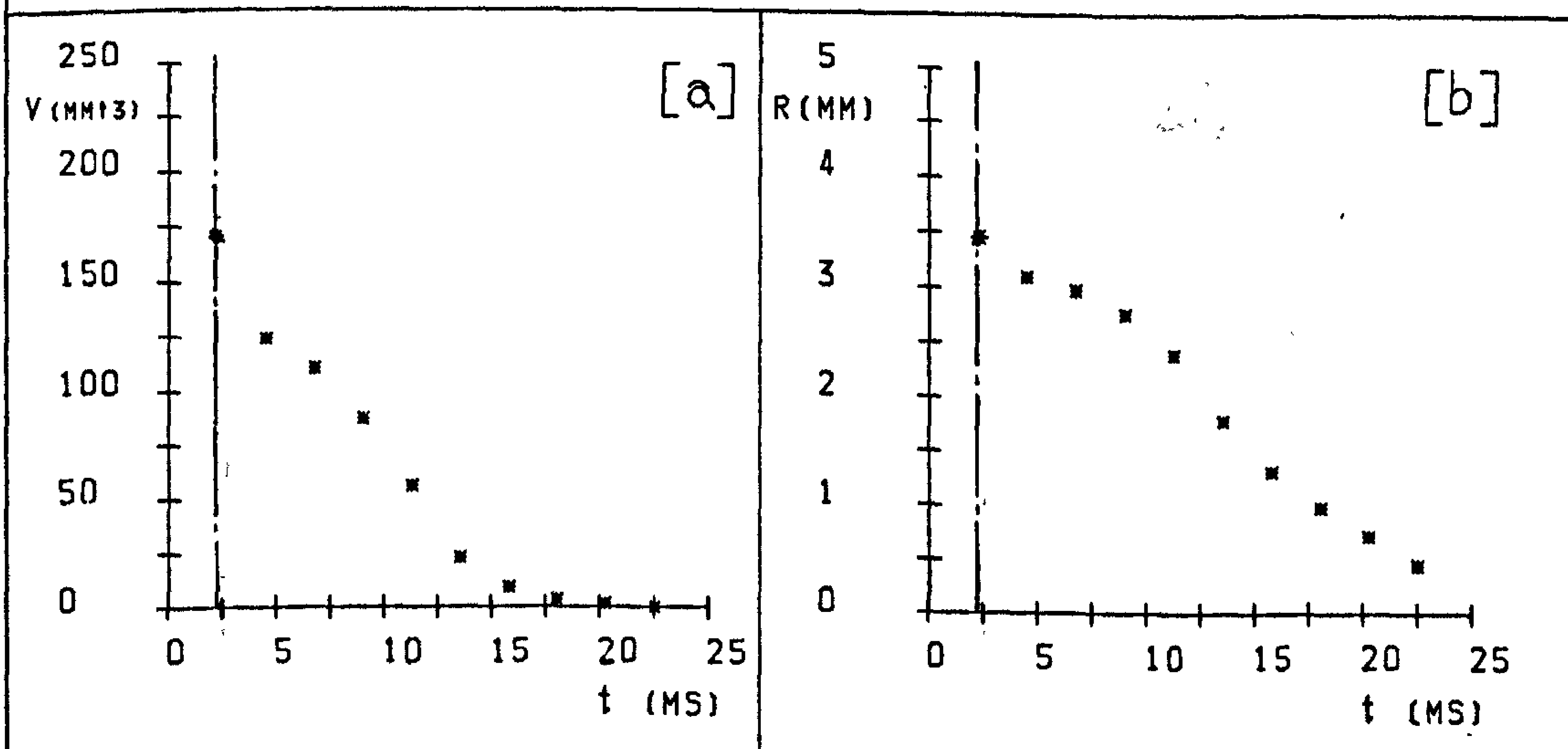

TEST NØ : (8.1).3 FILM NØ : 55-2/5

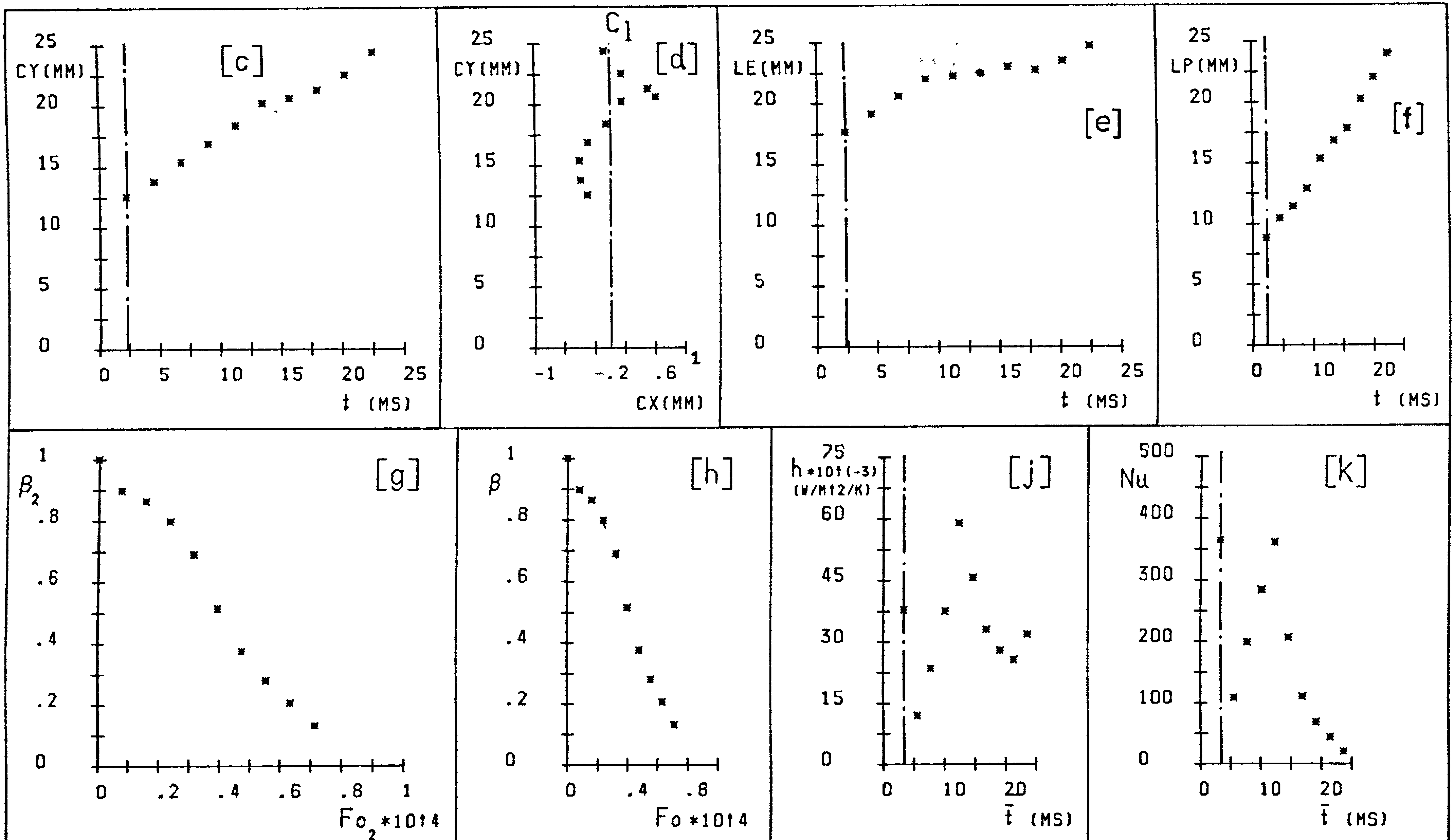

TEST NØ : (8.1).3 FILM NØ : 55-2/5

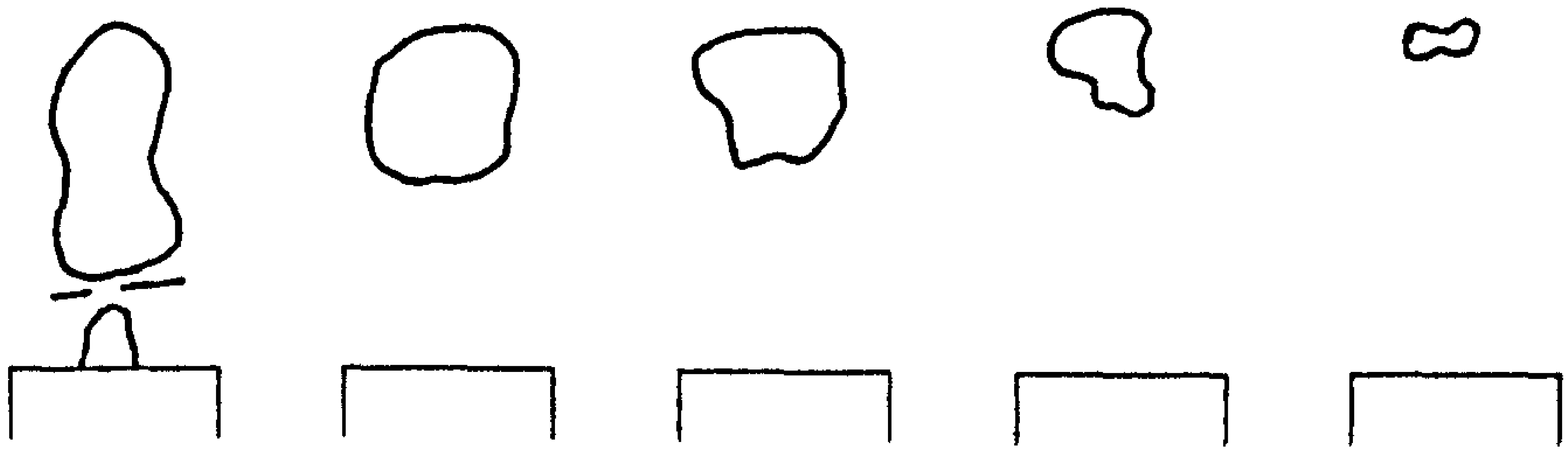

FRAME NUMBERS : 1 -3 4 -6 7 -8 9 10-11

EXPERIMENTAL PARAMETERS :

d	1
$\dot{m}_s$	1
(V_s	27871)
ΔT	10

Z	40
P	1.017
Δt	1.07
(CS	934)

F	11
Ja	30
T_p	165

EXPERIMENTAL RESULTS :

t_g	-
t_c	10.9
t_t	-
f_s	-
R_m	3.17
R_o	3.13

h_c	29081
Nu_c	149
Z_d	8.25
Z_c	16.26
U	593
Fo_c	4.62E-05

Pe_o	22360

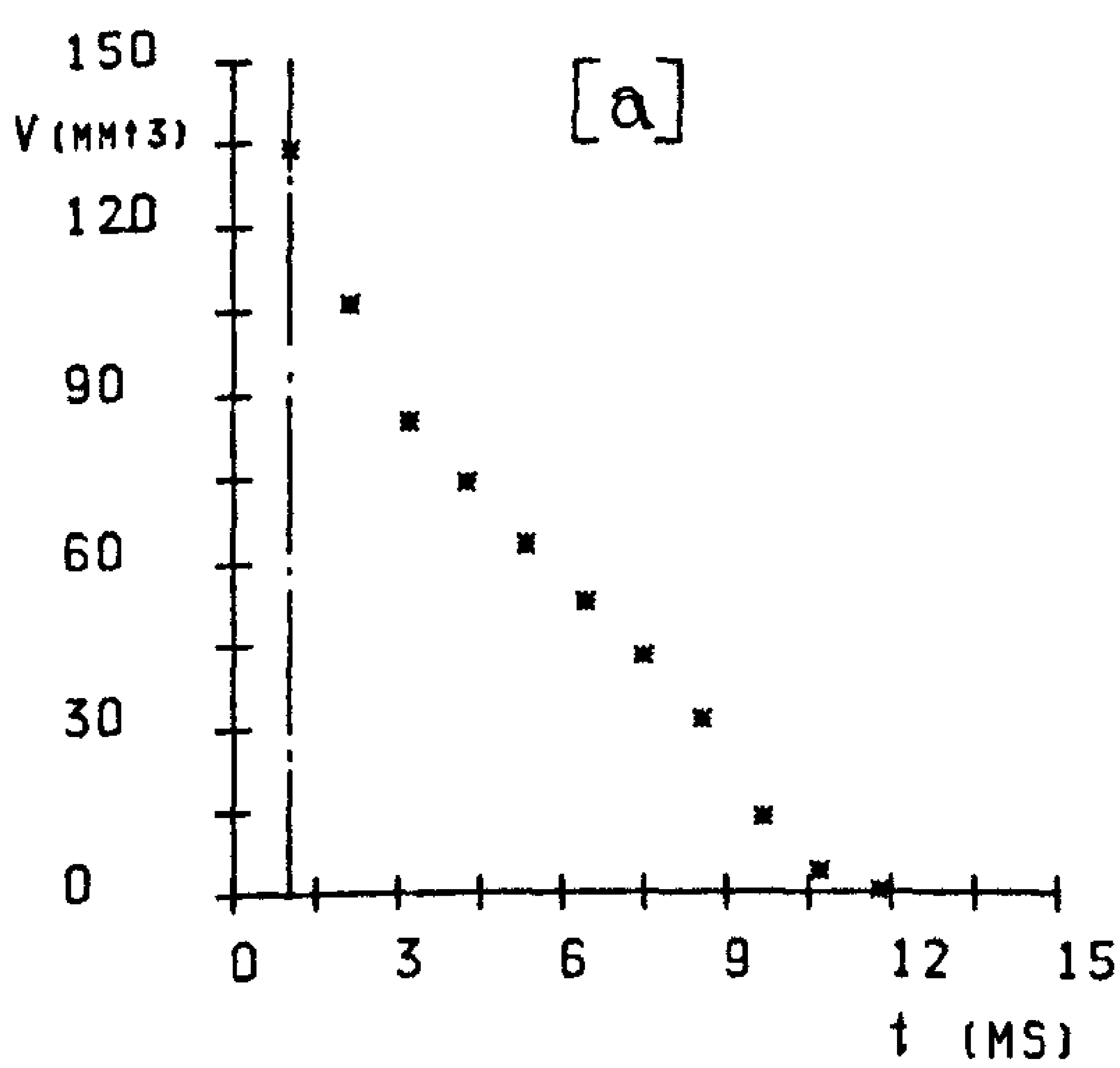

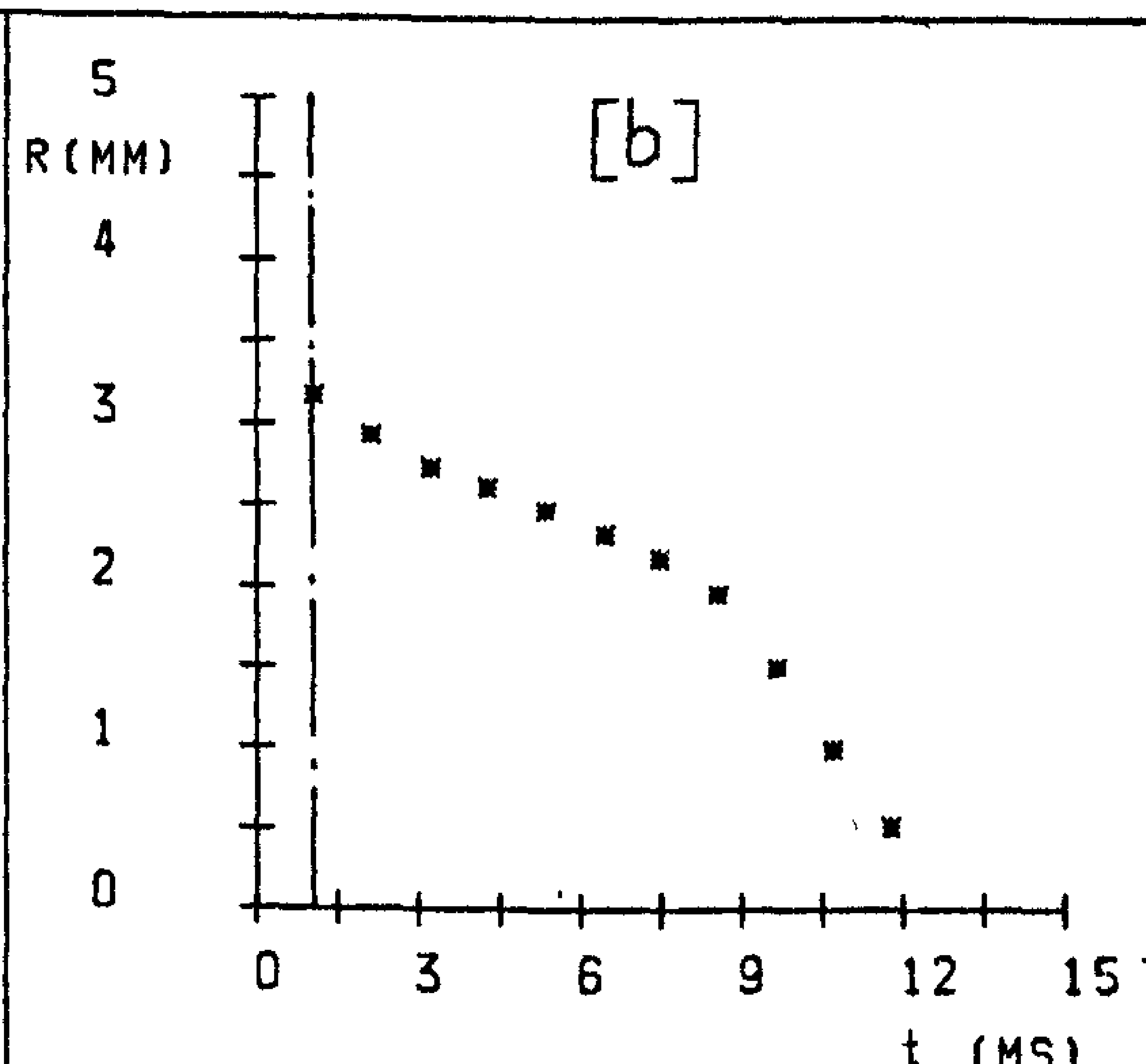

TEST NO : (8.2).3 FILM NO : 56-1/3

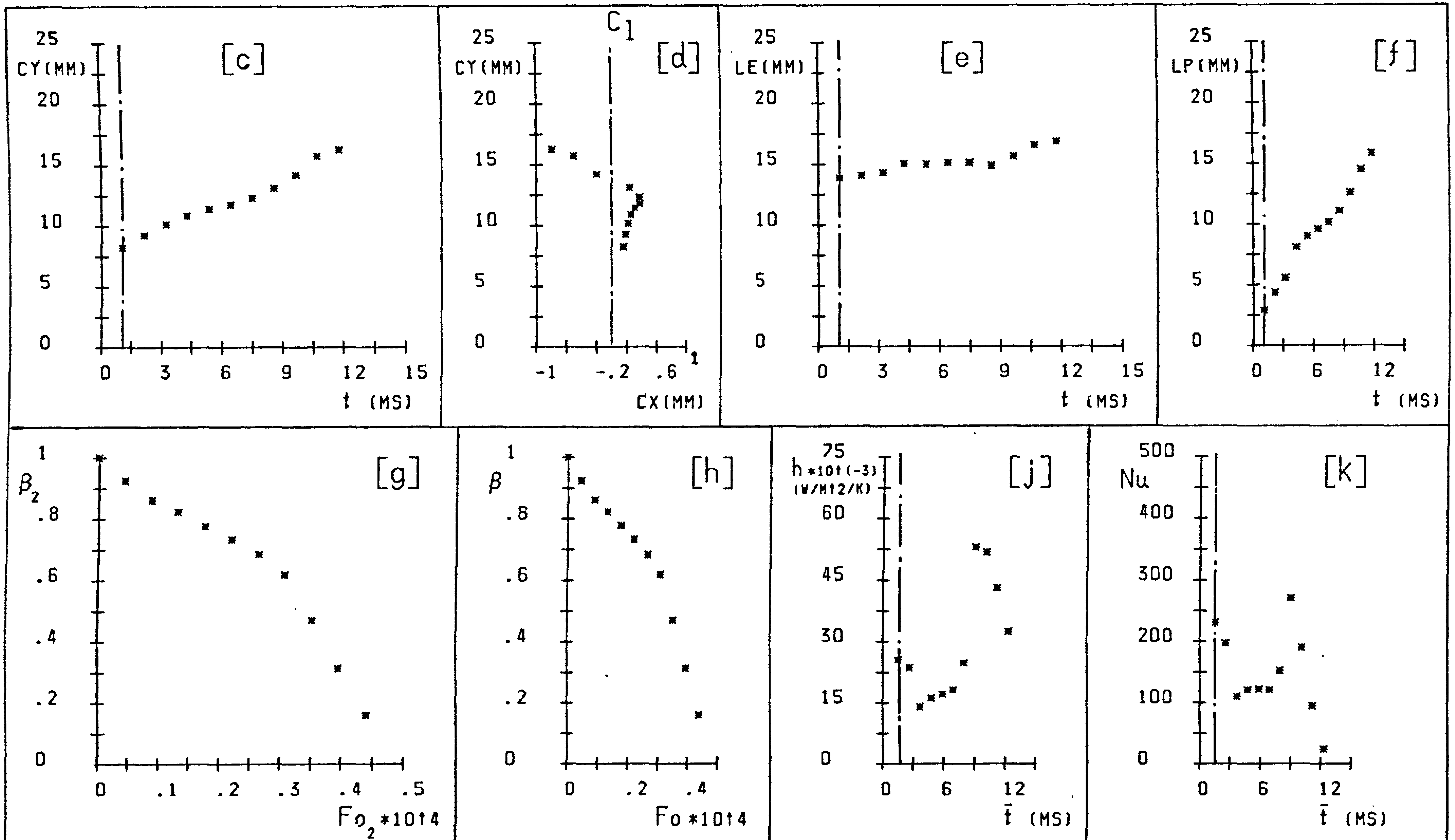

TEST NØ : (8.2).3 FILM NO : 56-1/3

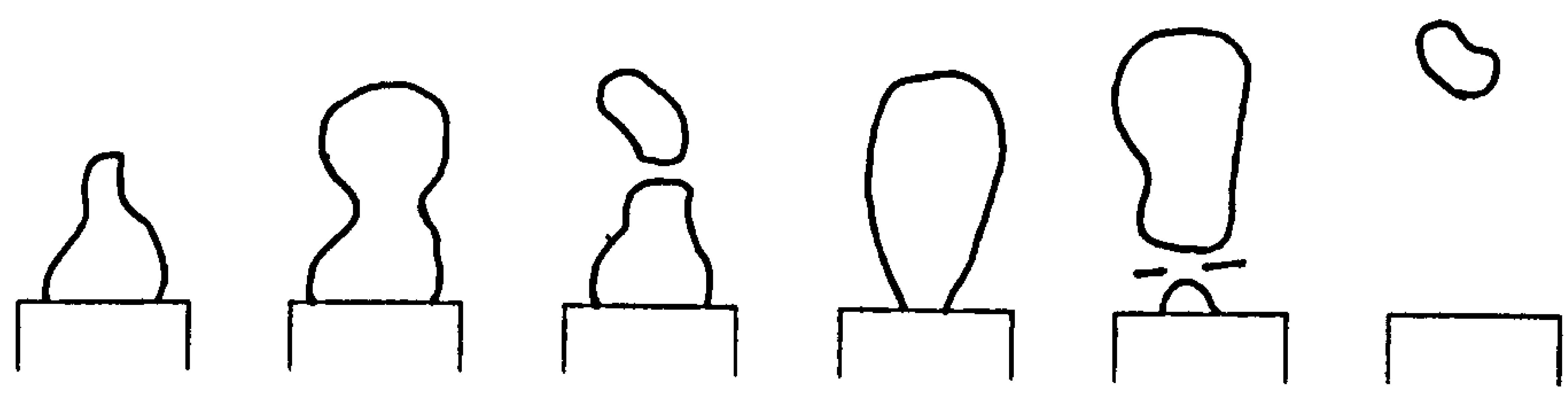

FRAME NUMBERS : 1 -3 | 4 -6 | 7 -8 | 9 -20 | 21-25 | 26-27

EXPERIMENTAL PARAMETERS :

d	1	Z	40	F	27
$\dot{m}_s$	1	P	1.017	Ja	45
(V_s	27871)	Δt	.79	T_p	165
ΔT	15	(CS	1272)		

EXPERIMENTAL RESULTS :

t_g	16.51	h_c	34227	Pe_o	21510
t_c	5.5	Nu_c	155		
t_t	22.01	Z_d	6.58		
f_s	64	Z_c	11.51		
R_m	2.84	U	650		
R_o	2.73	Fo_c	3.05E-05		

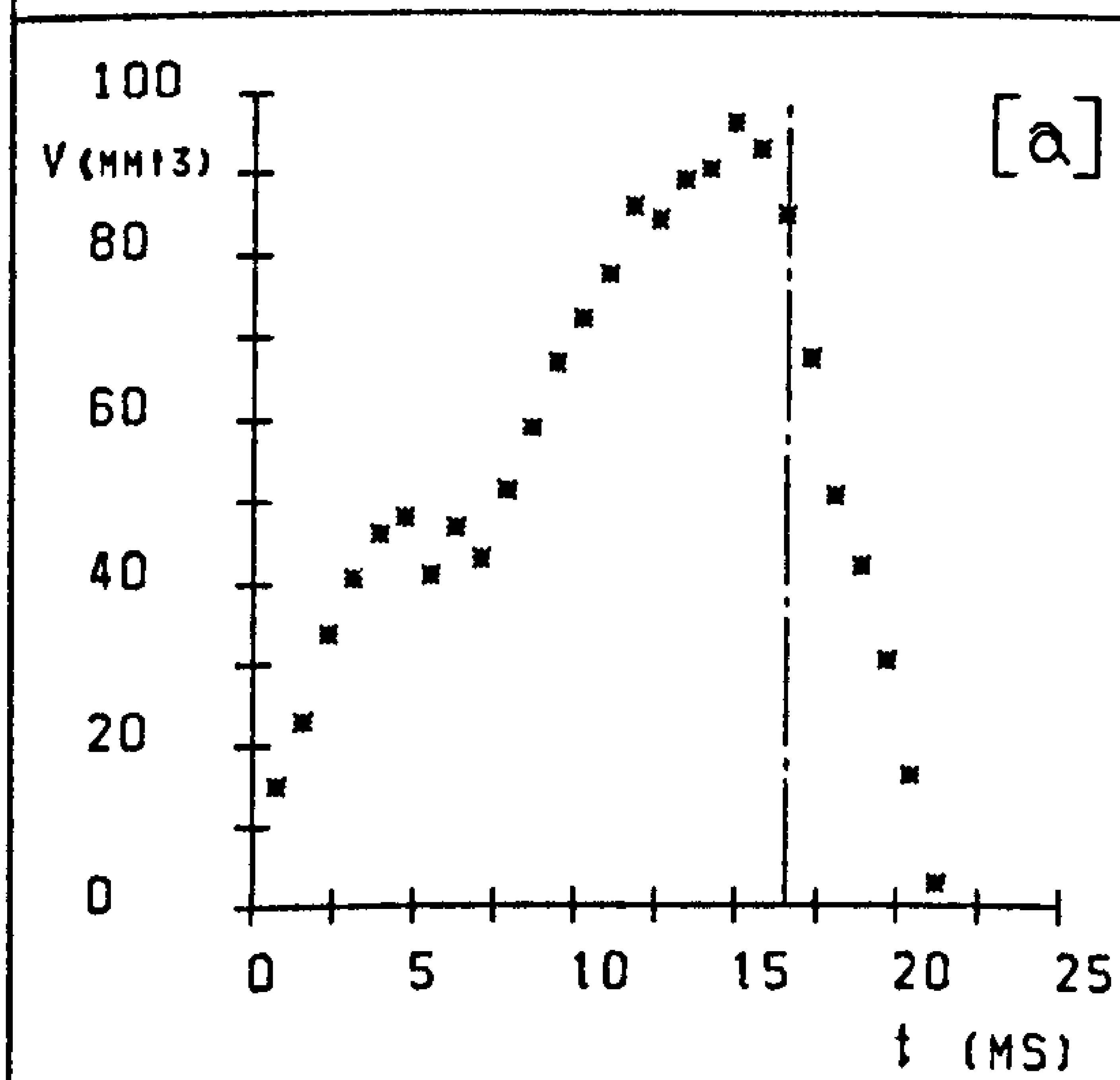

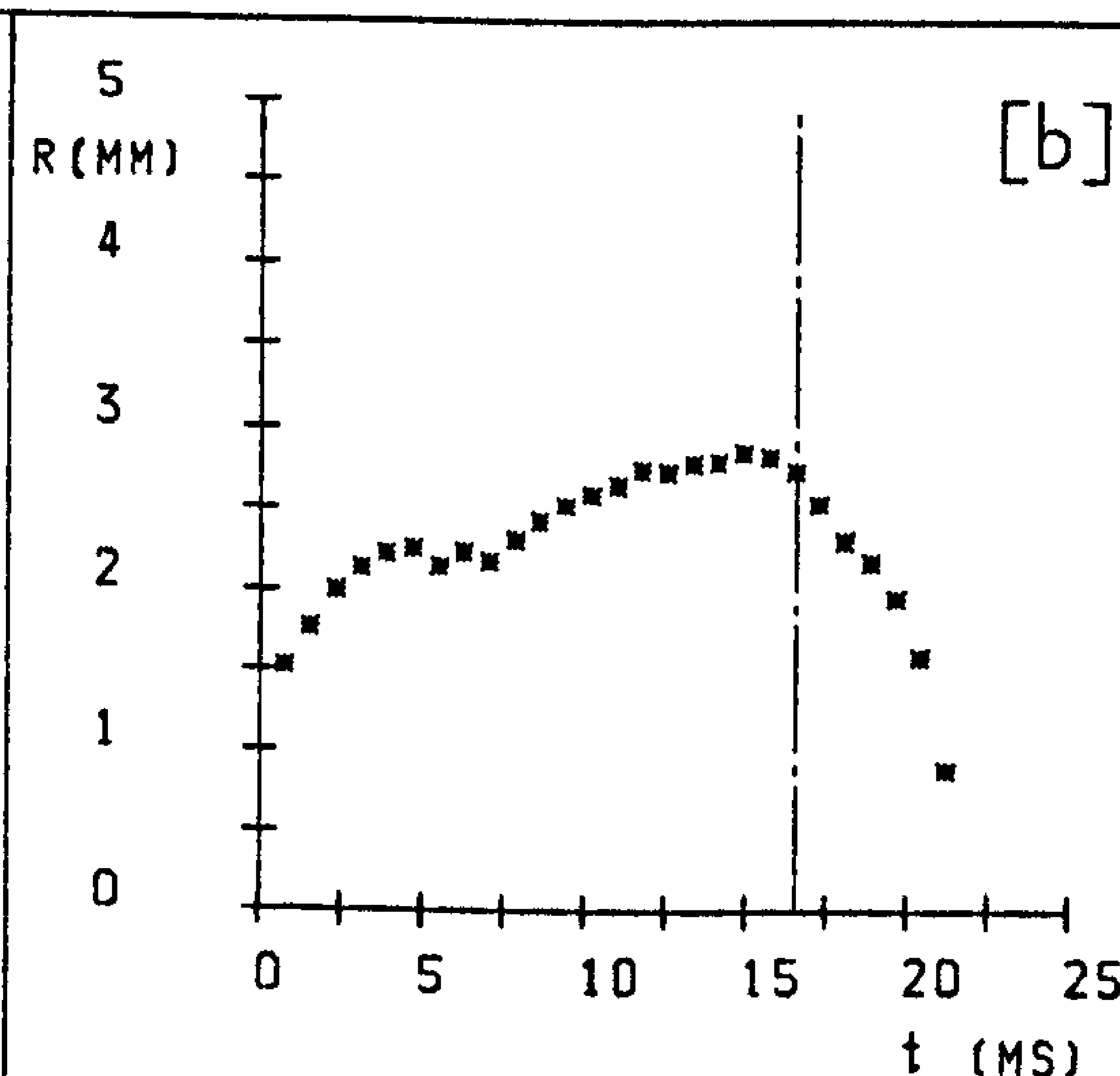

TEST NO : (8.3).3 FILM NO : 56-2/4

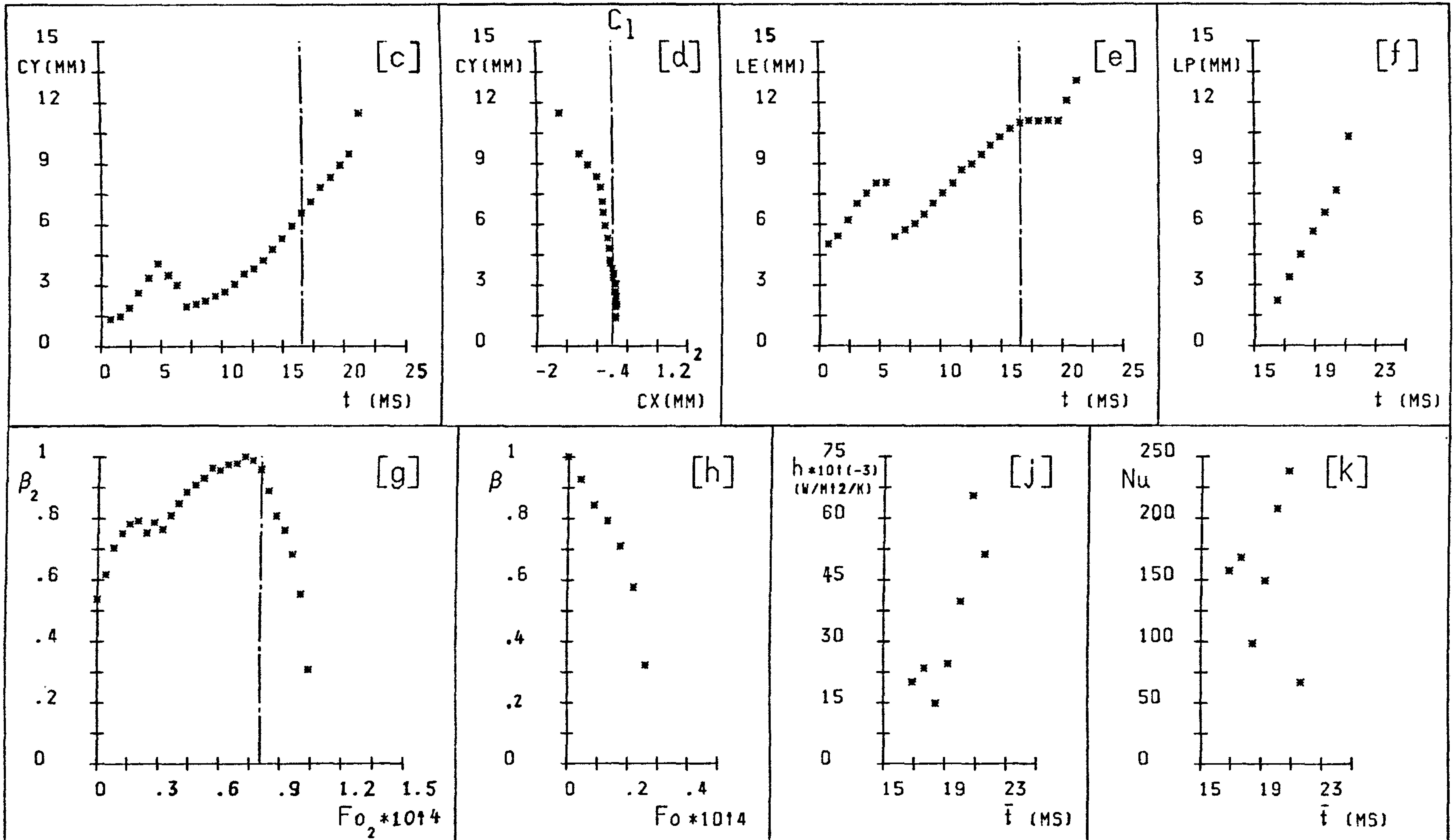

TEST NØ : (8.3).3 FILM NØ : 56-2/4

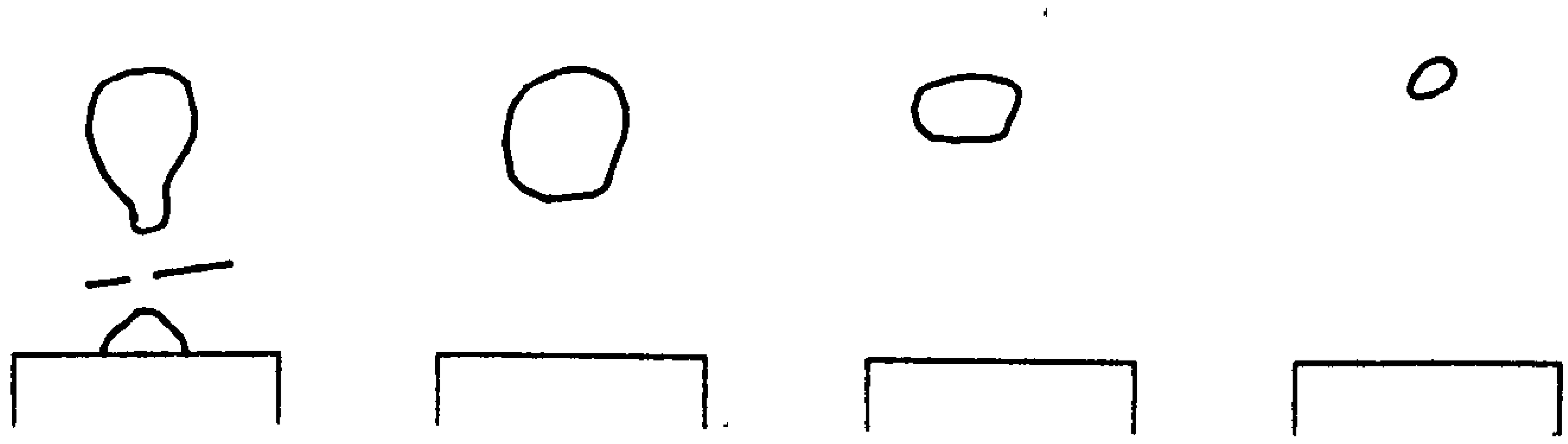

FRAME NUMBERS : 1   2 -3   4 -5   6 -8

EXPERIMENTAL PARAMETERS :

d	1	Z	40	F	8
$\dot{m}_s$	1	P	1.017	Ja	60
(V_s	27871)	Δt	.58	T_p	165
ΔT	20	(CS	1718)		

EXPERIMENTAL RESULTS :

t_g	-	h_c	25525	Pe_o	13740
t_c	3.6	Nu_c	84		
t_t	-	Z_d	6.18		
f_s	-	Z_c	9.29		
R_m	2.06	U	547		
R_o	2.06	Fo_c	3.47E-05		

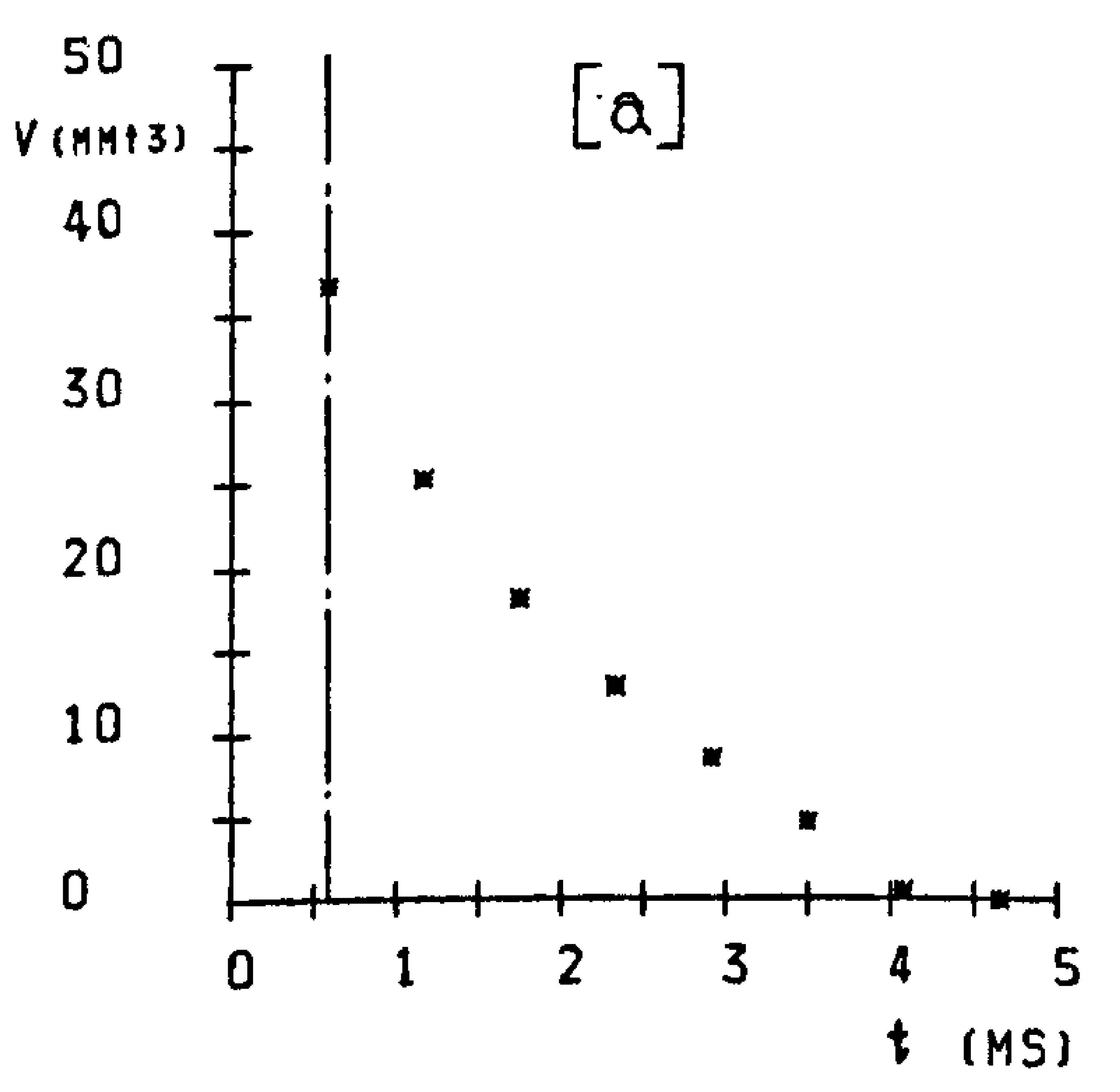

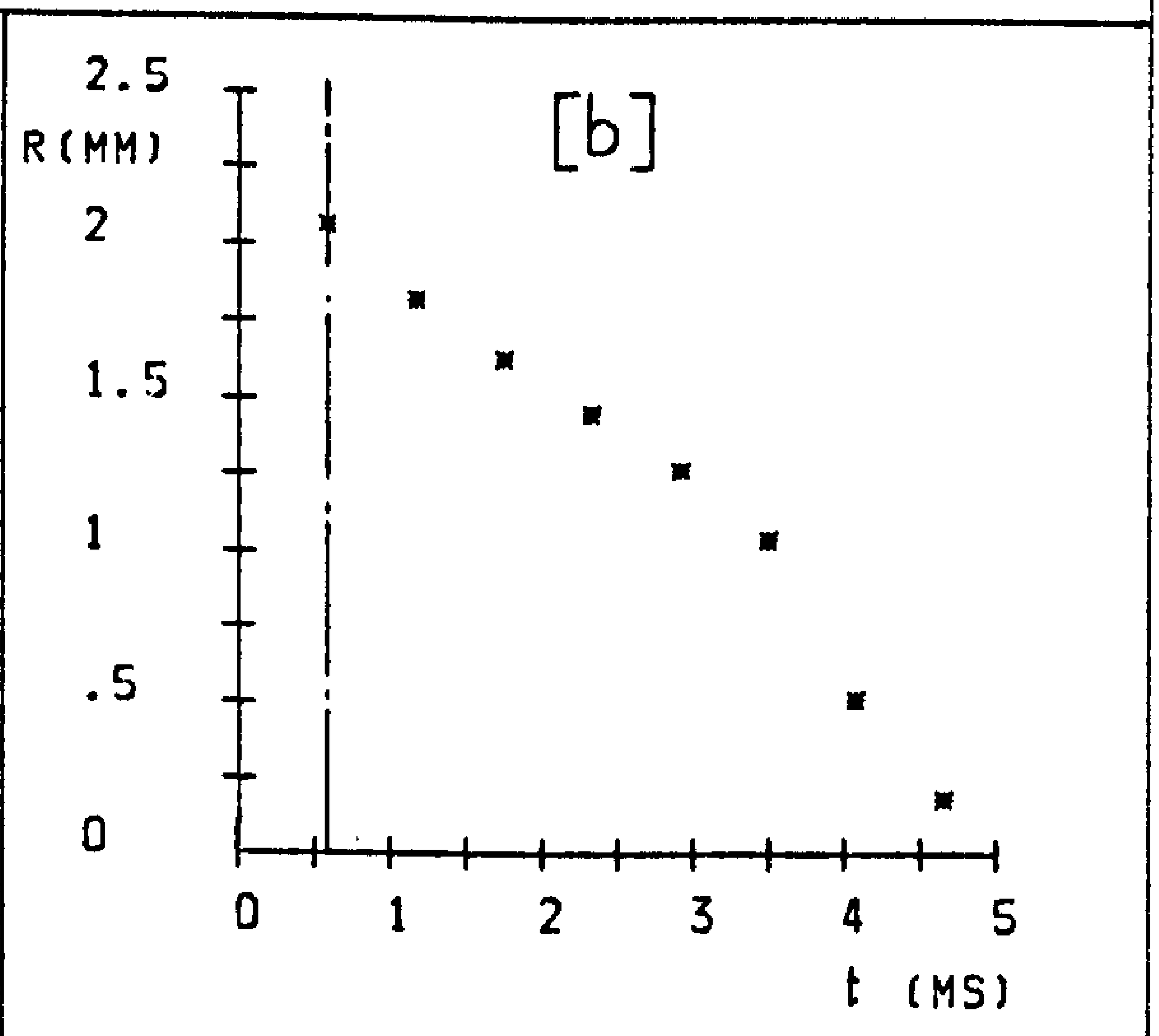

TEST NO : (8.4).3   FILM NO : 57-1/4

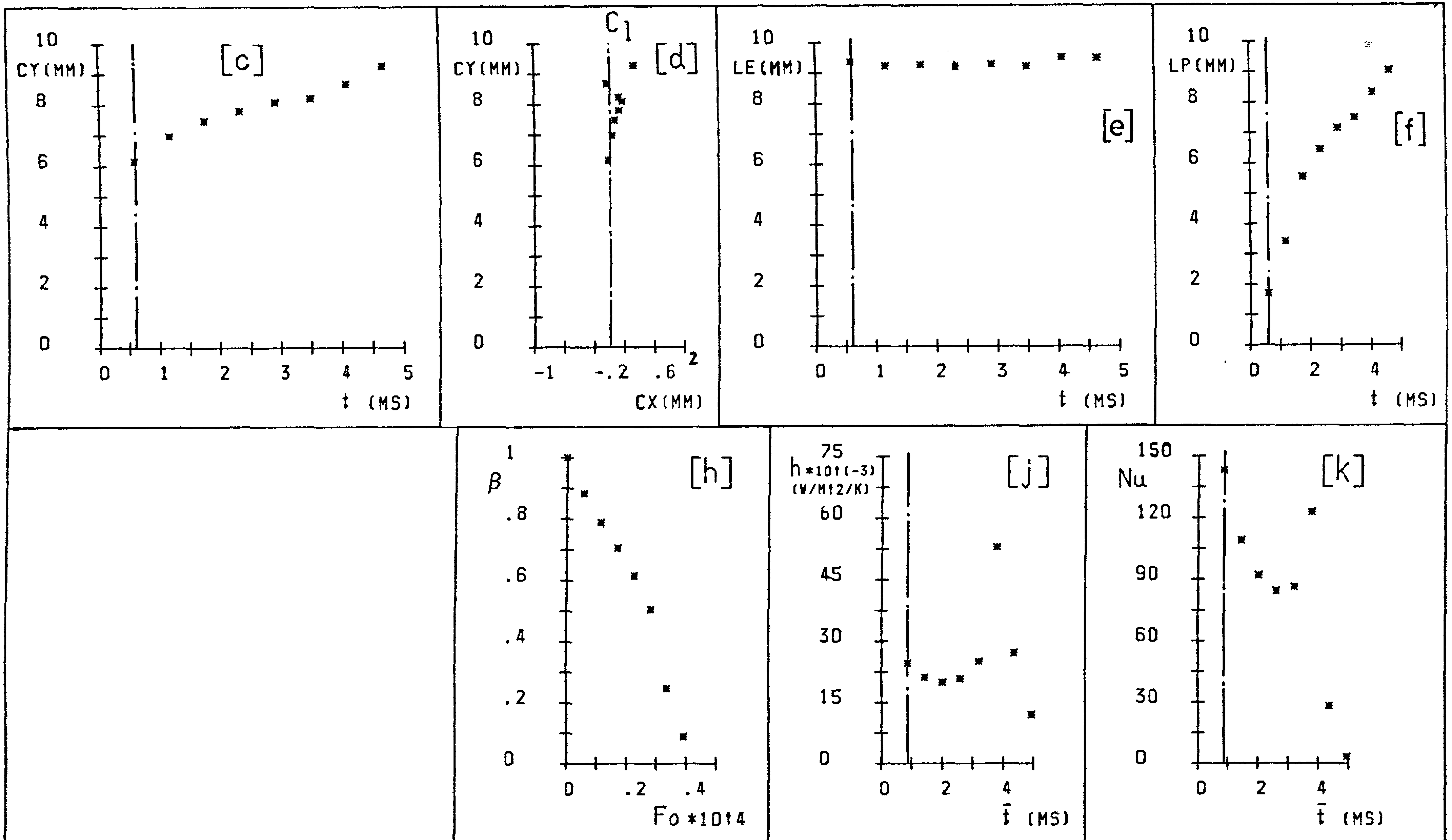

TEST NØ : (8.4).3 FILM NO : 57-1/4

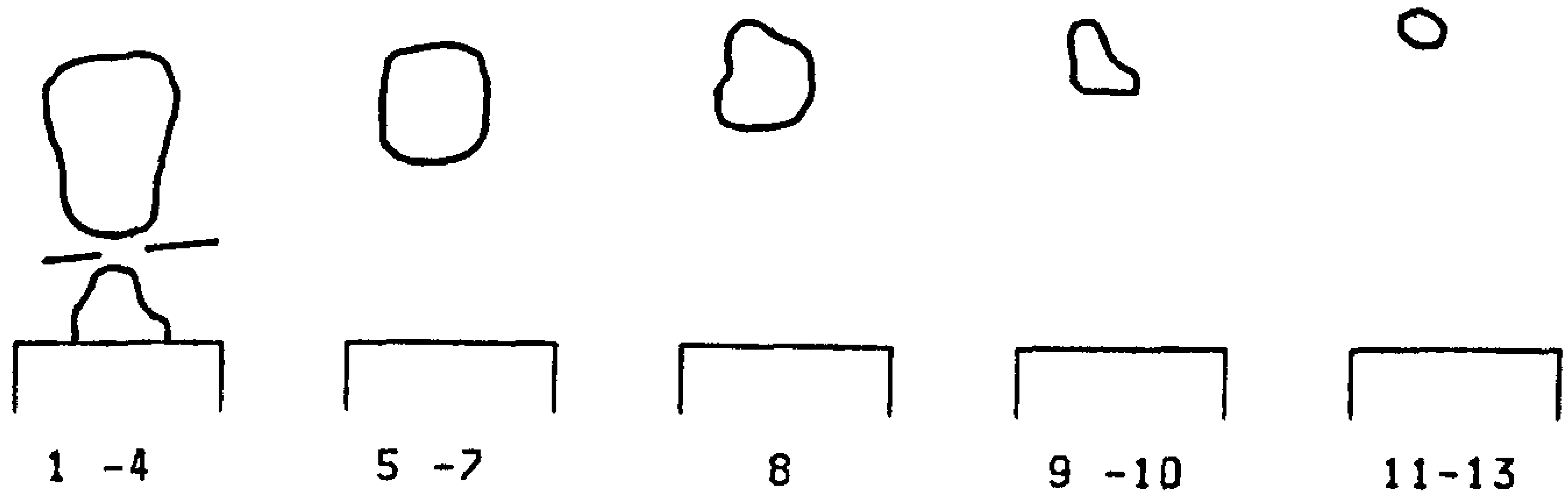

EXPERIMENTAL PARAMETERS :

d	1	Z	40	F	13
$\dot{m}_s$	1.42	P	1.003	Ja	30
(V_s	39576)	Δt	1.02	T_p	165
ΔT	10	(CS	980)		

EXPERIMENTAL RESULTS :

t_g	-	h_c	29663	Pe_o	26520
t_c	12	Nu_c	167		
t_t	-	Z_d	10.95		
f_s	-	Z_c	18.26		
R_m	3.51	U	627		
R_o	3.51	Fo_c	4.04E-05		

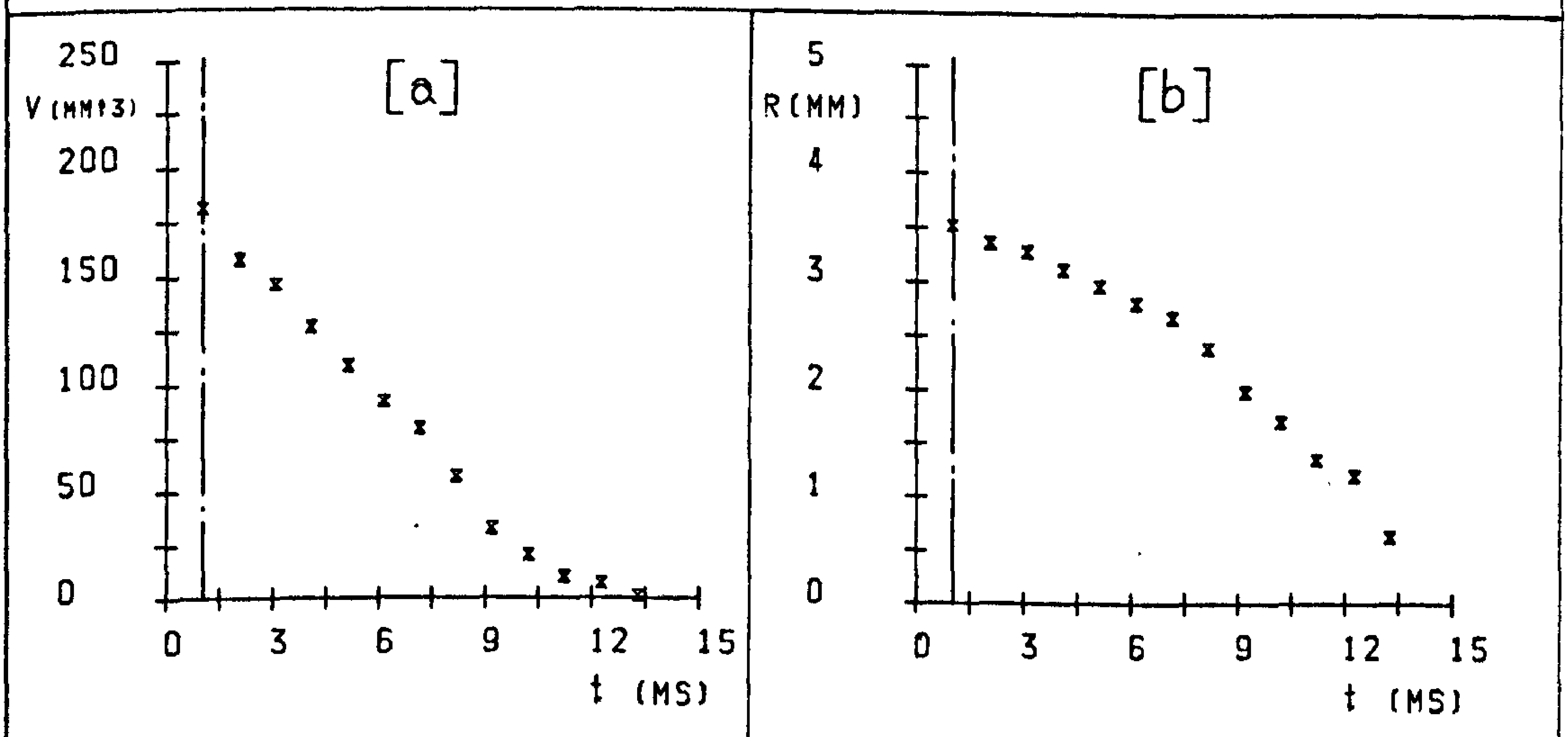

TEST NO : (9.2).1 FILM NO : 58-2/1

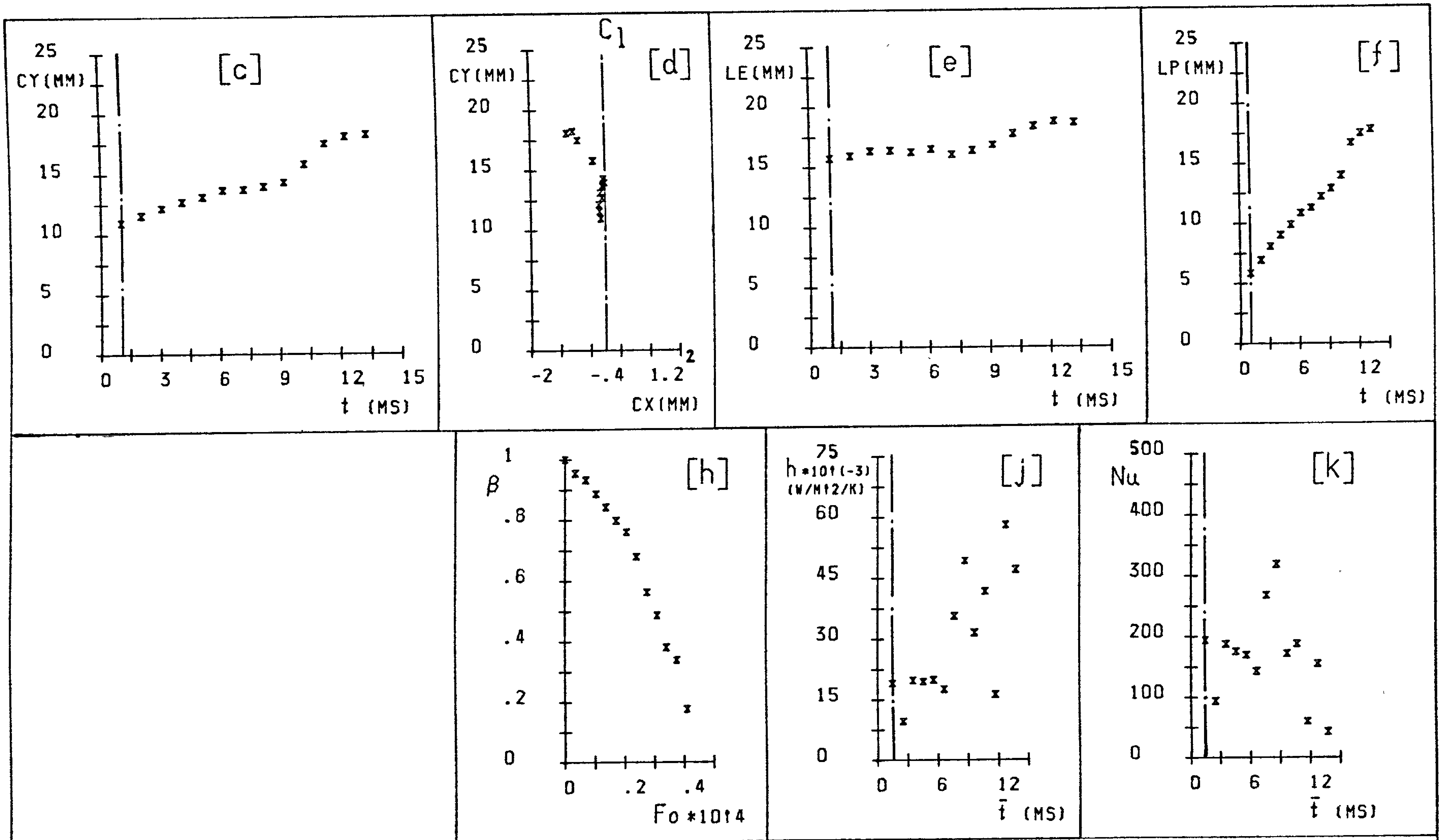

TEST NØ : (9.2).1 FILM NØ : 58-2/1

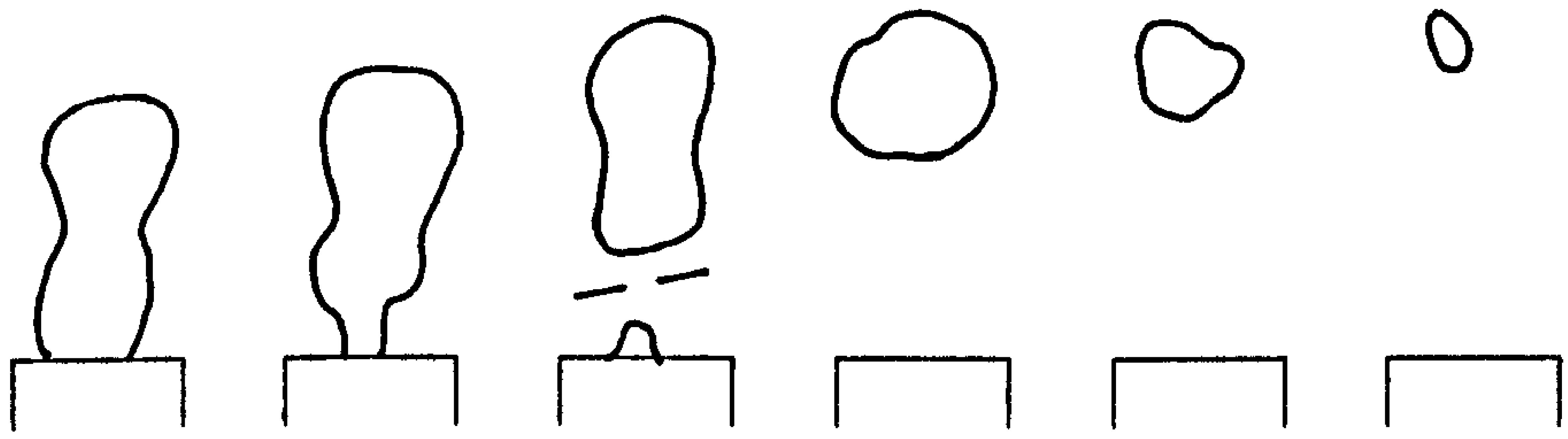

FRAME NUMBERS : 1 -15 16-19 20-21 22-25 26 27-28

EXPERIMENTAL PARAMETERS :

d	1	Z	40	F	28
$\dot{m}_s$	1.42	P	1.003	Ja	45
(V_s	39576)	Δt	.79	T_p	165
ΔT	15	(CS	1272)		

EXPERIMENTAL RESULTS :

t_g	15.72	h_c	29261	Pe_o	20360
t_c	6.6	Nu_c	132		
t_t	22.32	Z_d	7.2		
f_s	67	Z_c	11.91		
R_m	3.02	U	600		
R_o	2.8	Fo_c	3.47E-05		

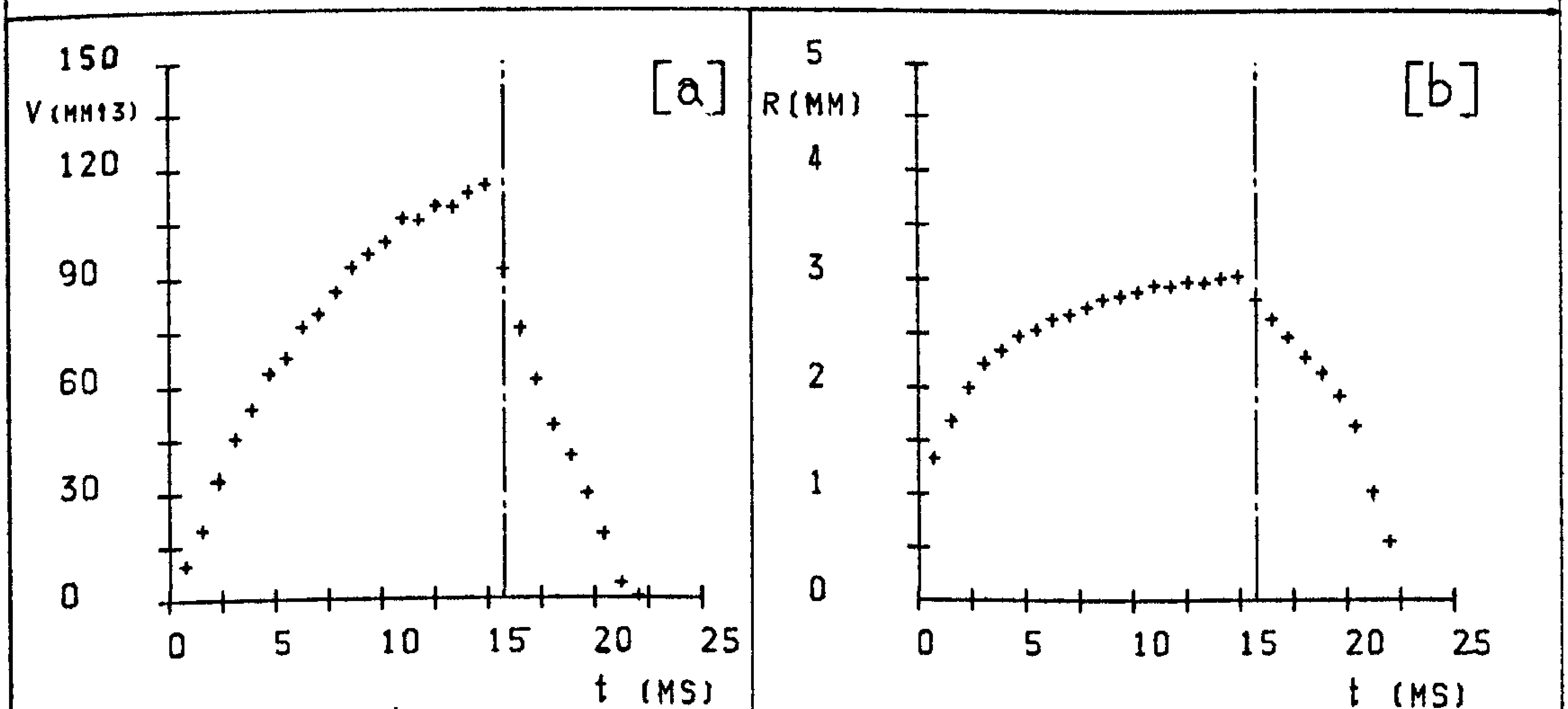

TEST NO : (9.3).2 FILM NO : 59-1/2

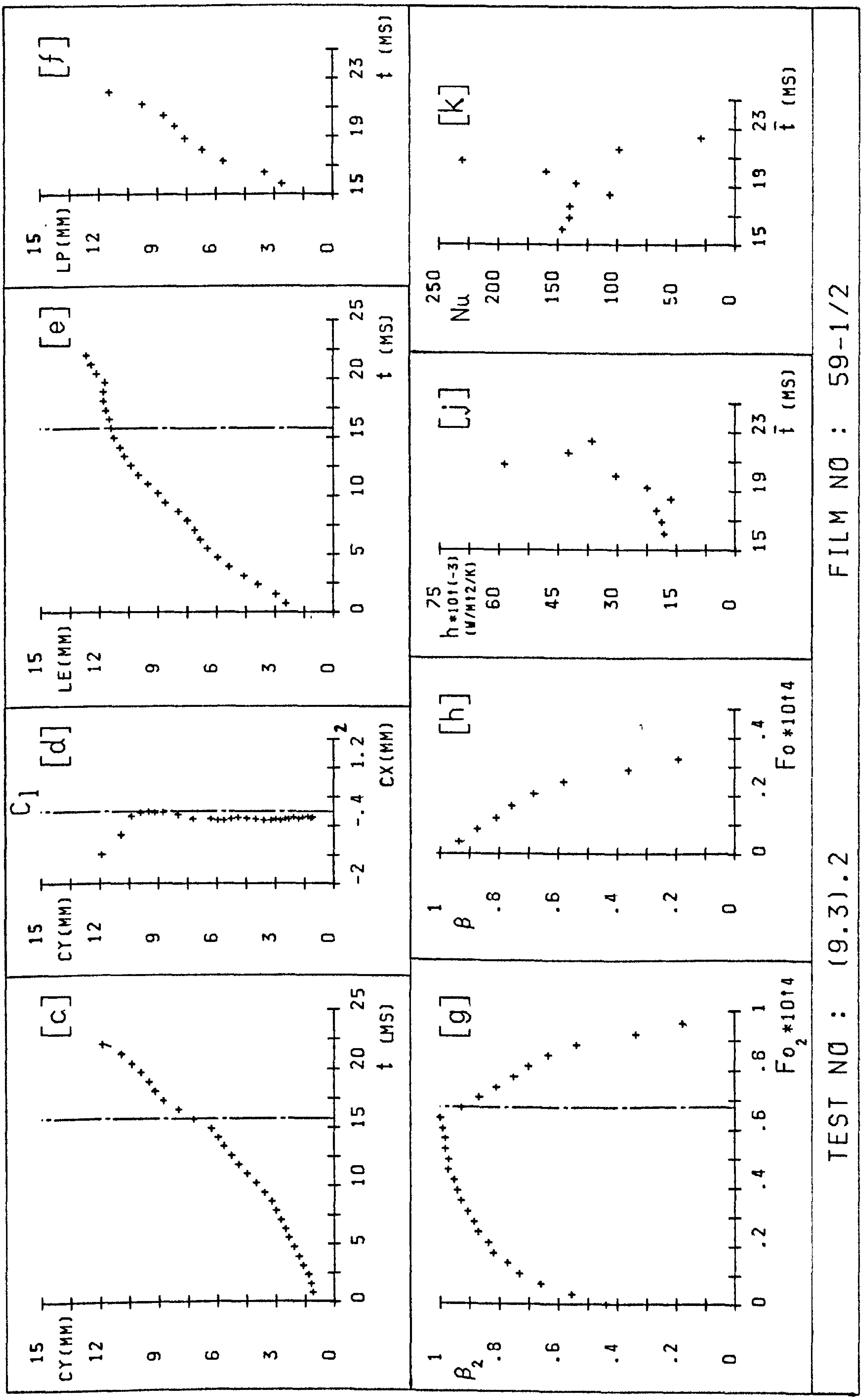
[c]
[d]
[e]
[f]
[g]
[h]
[j]
[k]
CY(MM)
CX(MM)
LE(MM)
LP(MM)
t (MS)
C1
β_2
β
Fo_2*10↑4
Fo*10↑4
h*10↑(-3)
(W/M↑2/K)
Nu
$\bar{t}$ (MS)
TEST NO : (9.3).2
FILM NO : 59-1/2

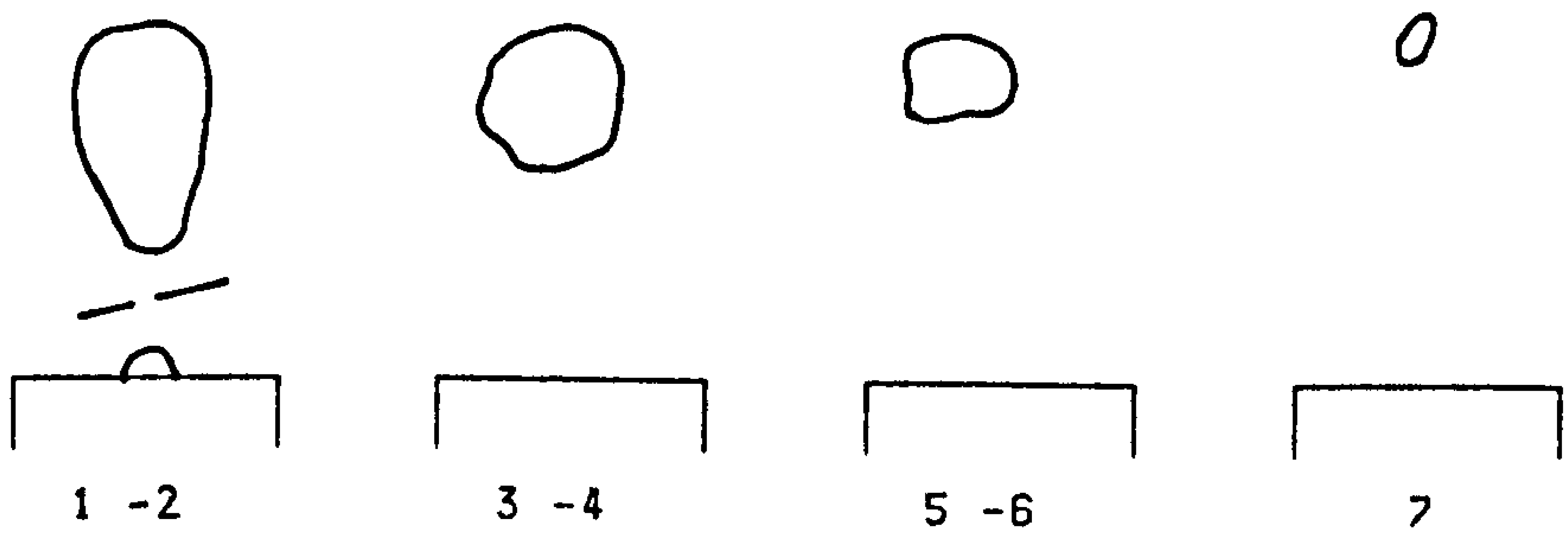

FRAME NUMBERS :

EXPERIMENTAL PARAMETERS :

d	1	Z	40	F	7
$\dot{m}_s$	1.42	P	1.003	Ja	60
(V_s	39576)	Δt	.58	T_p	165
ΔT	20	(CS	1738)		

EXPERIMENTAL RESULTS :

t_g	-	h_c	29328	Pe_o	14960
t_c	3.5	Nu_c	99		
t_t	-	Z_d	6.72		
f_s	-	Z_c	9.03		
R_m	2.09	U	587		
R_o	2.09	Fo_c	3.29E-05		

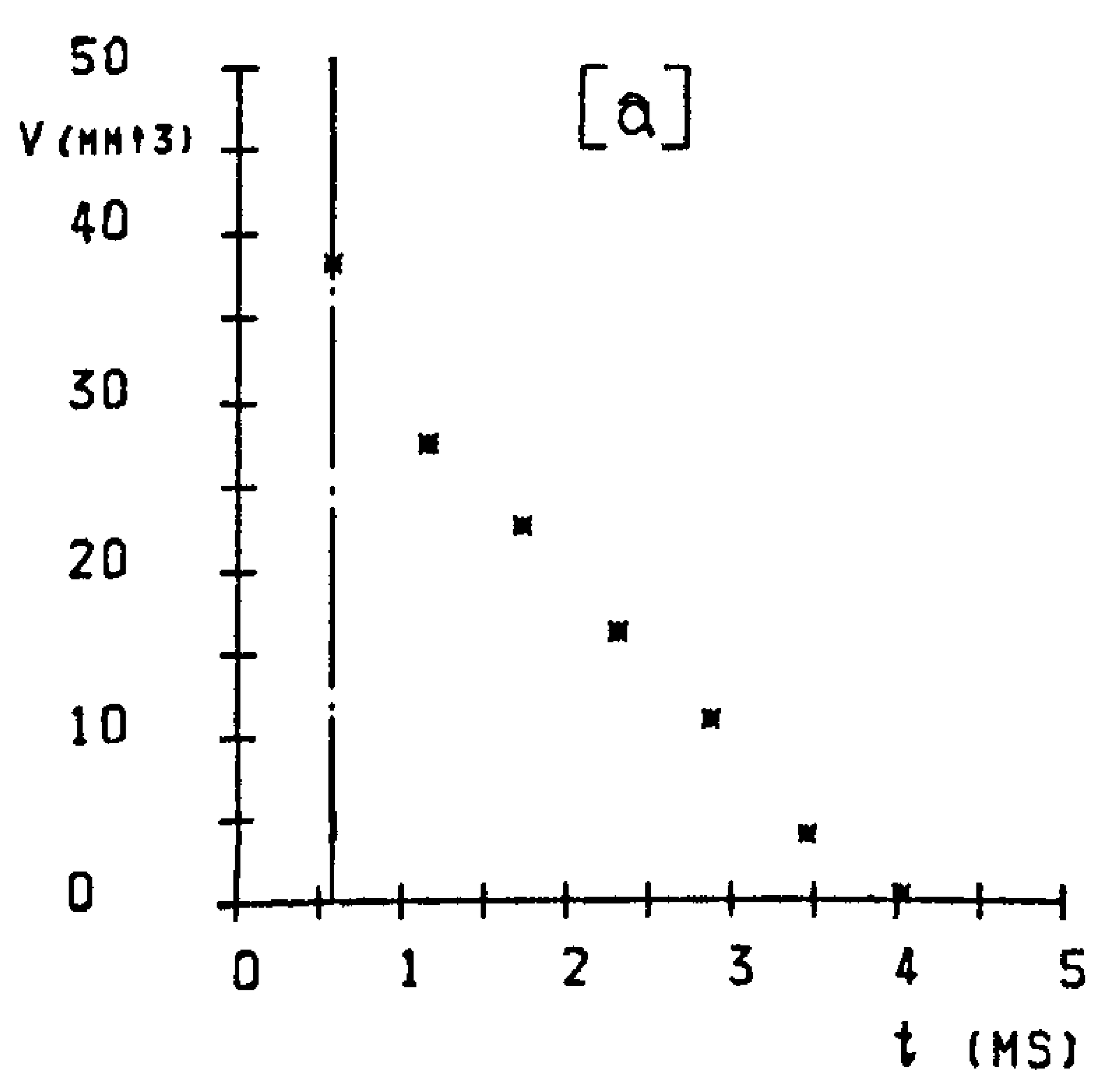

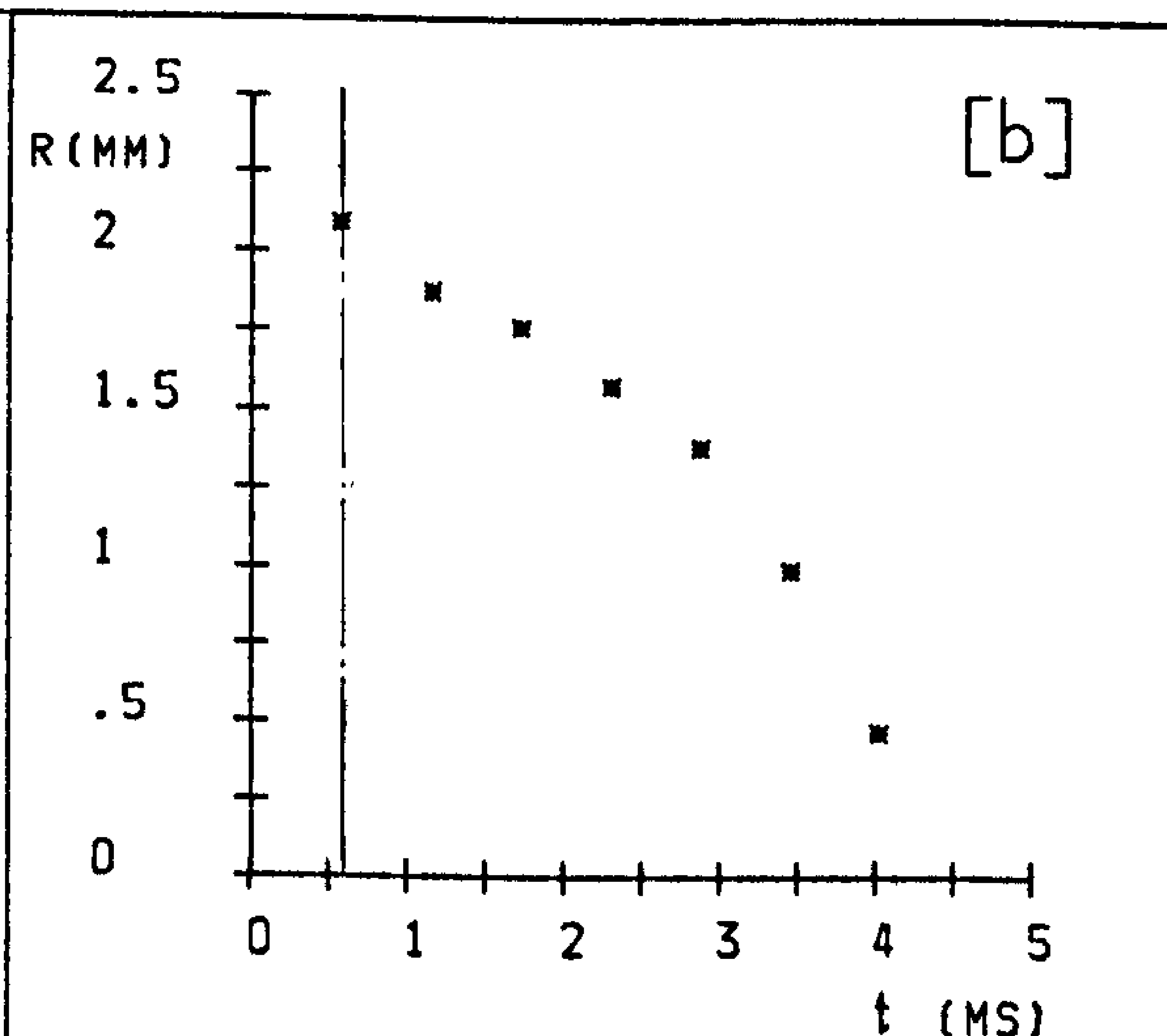

TEST NO : (9.4).3 FILM NO : 60-1/4

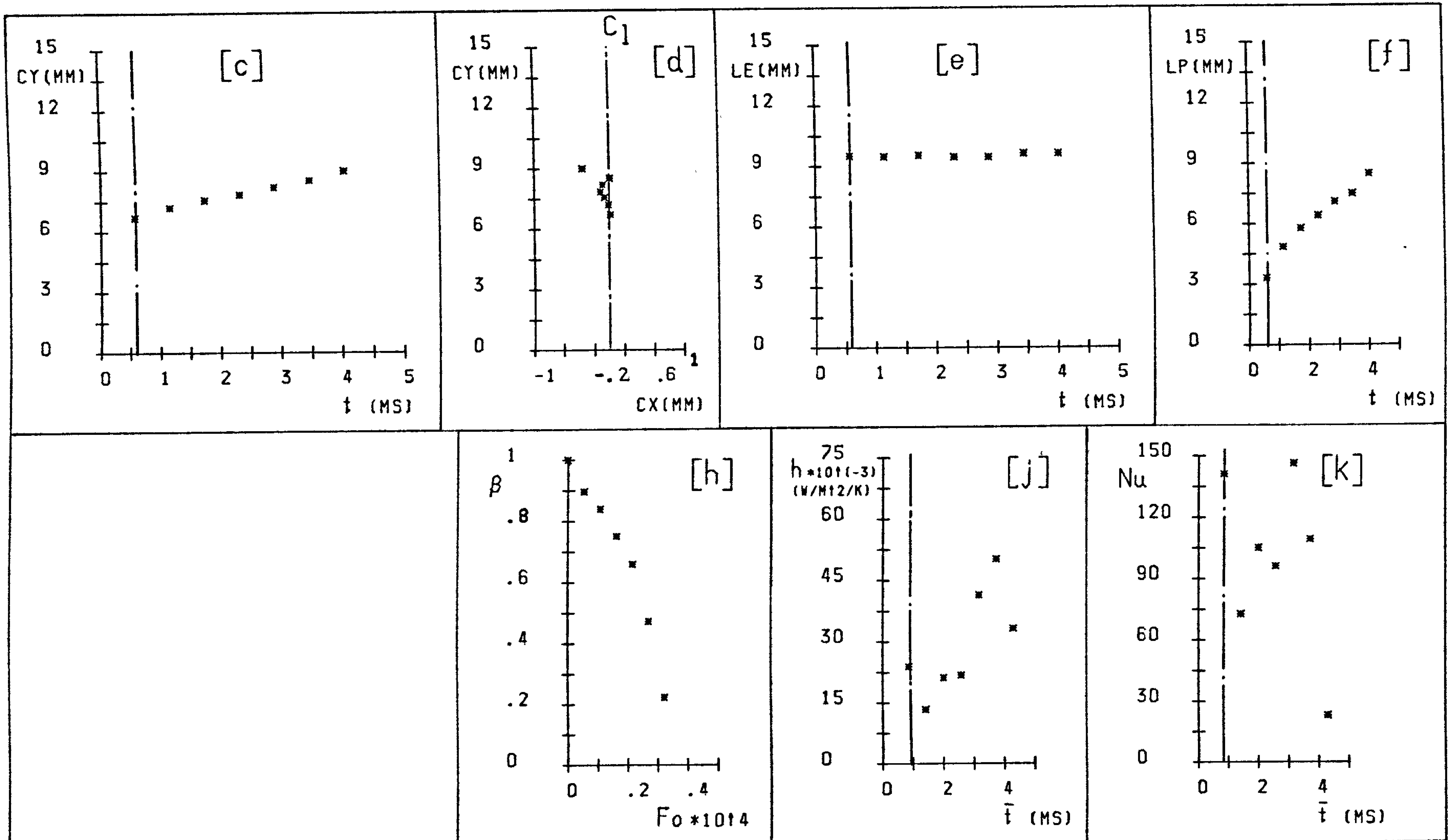

TEST NØ : (9.4).3 FILM NO : 60-1/4

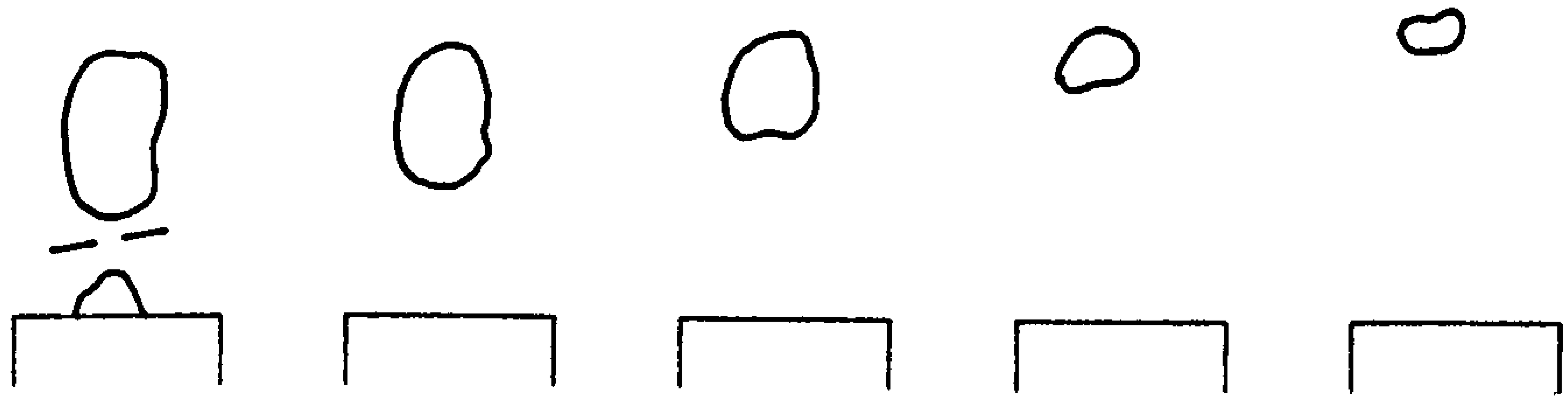

FRAME NUMBERS : 1 2 3 4 5

EXPERIMENTAL PARAMETERS :

d	1
$\dot{m}_s$	1.42
(V_s	39576)
ΔT	25

Z	40
P	1.003
Δt	.46
(CS	2177)

F	5
Ja	75
T_p	165

EXPERIMENTAL RESULTS :

t_g	-
t_c	2.1
t_t	-
f_s	-
R_m	1.65
R_o	1.69

h_c	29127
Nu_c	82
Z_d	5.62
Z_c	6.96
U	640
Fo_c	3E-05

Pe_o	13270

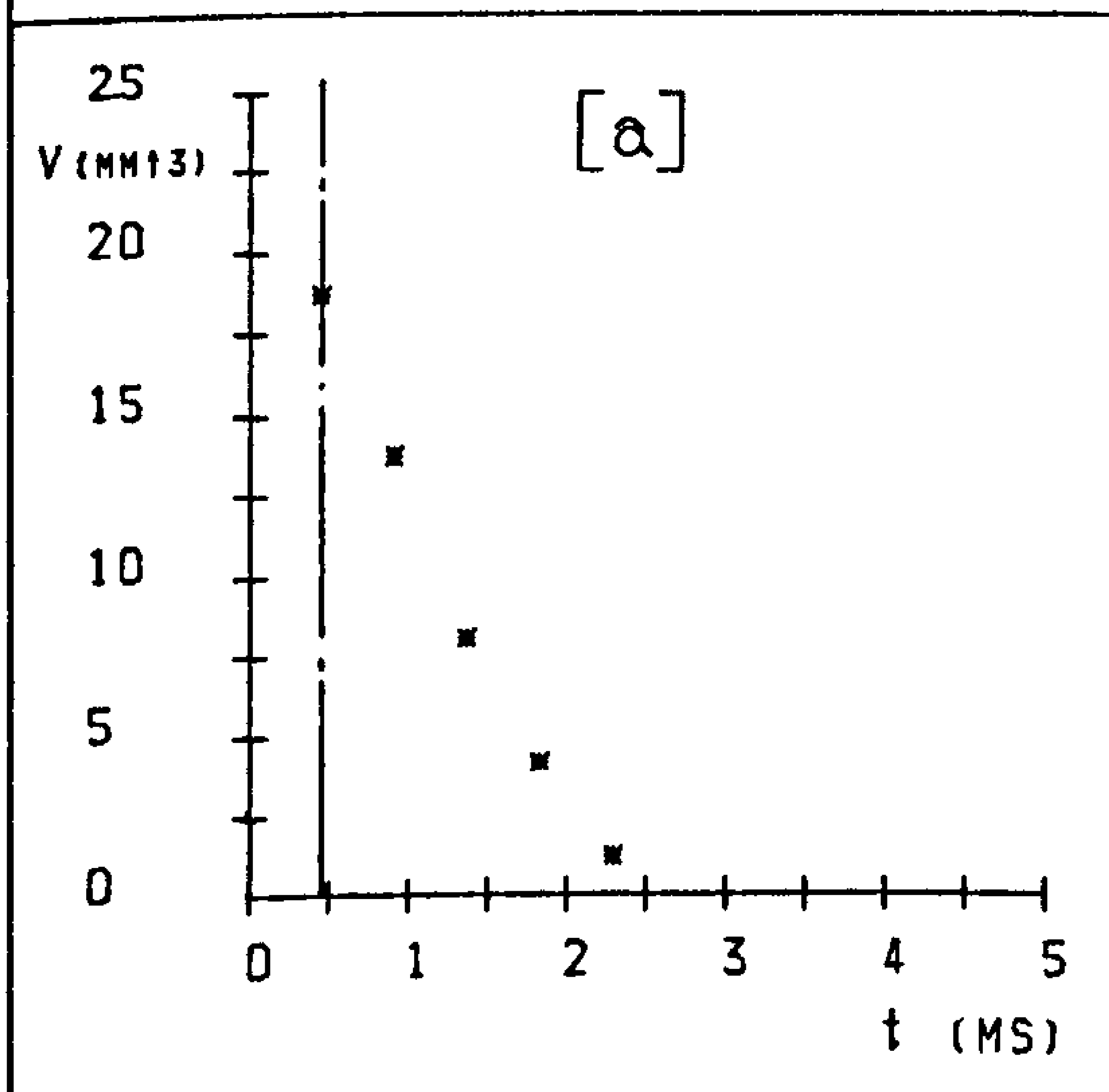

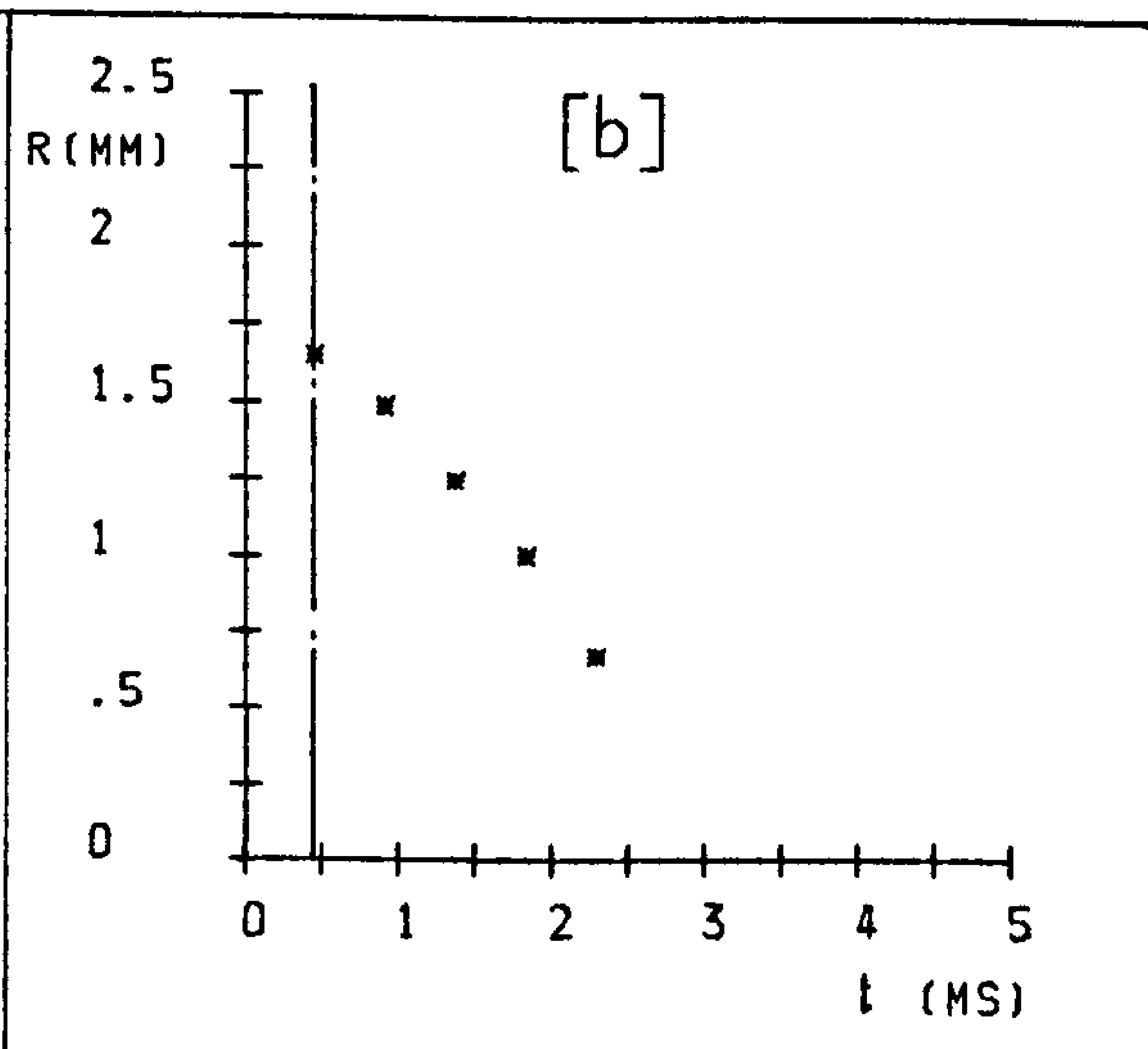

TEST NO : (9.5).3 FILM NO : 61-1/6

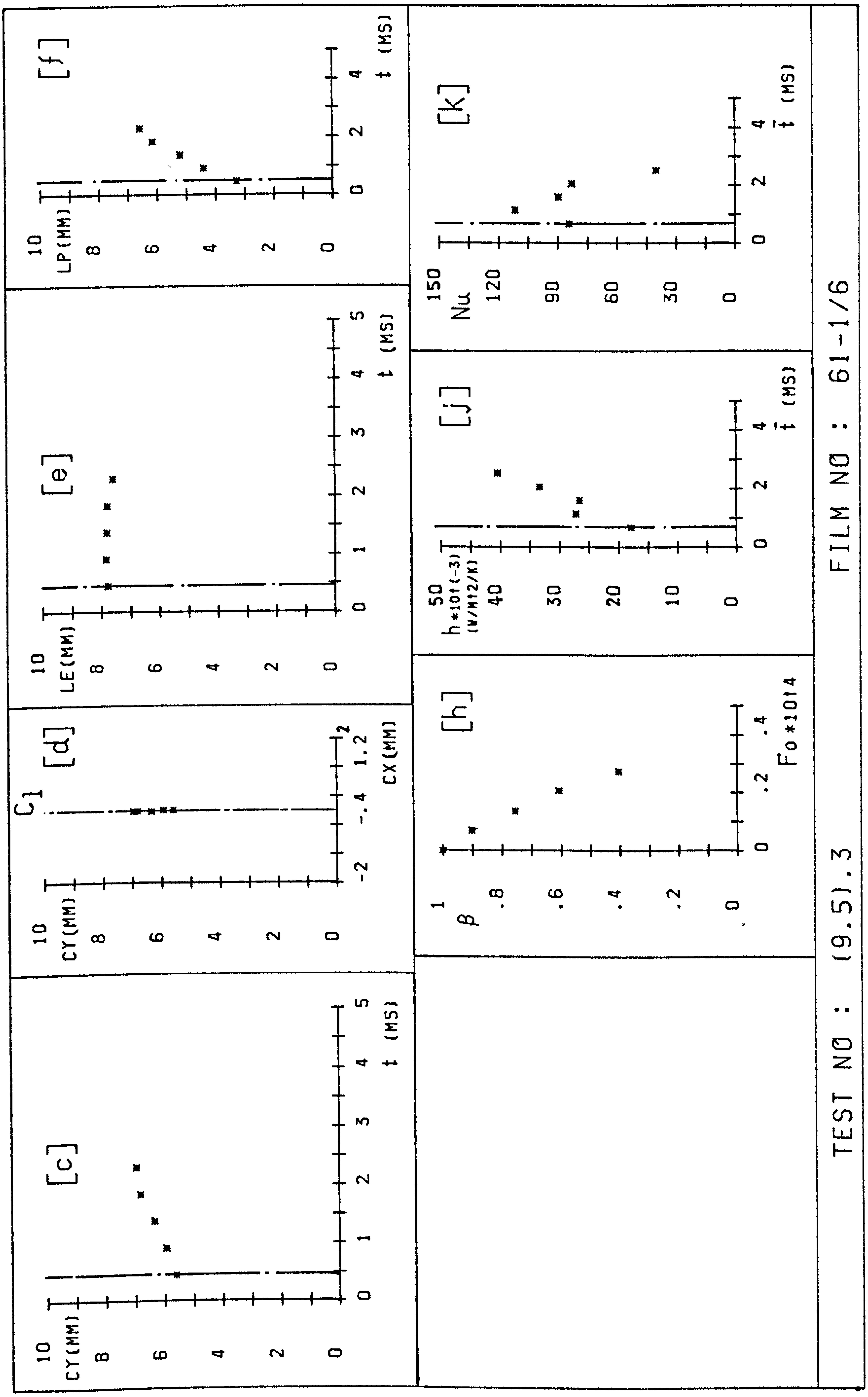
TEST NØ : (9.5).3
FILM NØ : 61-1/6
[c]
CY(MM)
t (MS)
[d]
C_l
CY(MM)
CX(MM)
[e]
LE(MM)
t (MS)
[f]
LP(MM)
t (MS)
[h]
β
Fo*10↑4
[j]
h*10↑(-3)
(W/M↑2/K)
$\bar{t}$ (MS)
[k]
Nu
$\bar{t}$ (MS)

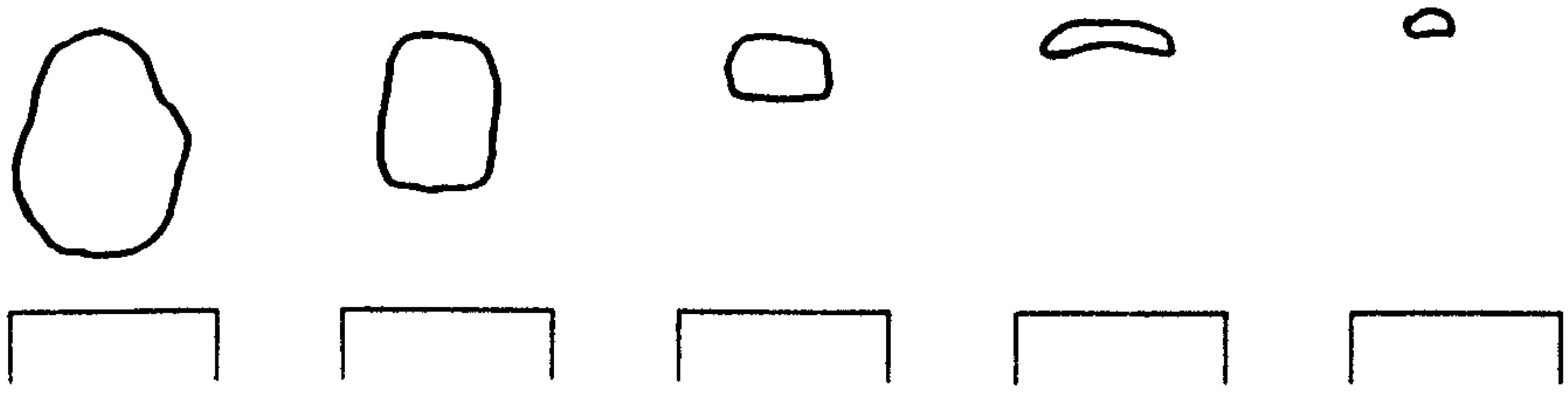

FRAME NUMBERS : 1 -2 3 -5 6 -8 9 -10 11-17

EXPERIMENTAL PARAMETERS :

d	1
$\dot{m}_s$	.45
(V_s	6643)
ΔT	9.3

Z	40
P	2.011
Δt	1.99
(CS	503)

F	17
Ja	15
T_p	165

EXPERIMENTAL RESULTS :

t_g	–
t_c	29.3
t_t	–
f_s	–
R_m	2.63
R_o	2.63

h_c	16913
Nu_c	68
Z_d	4.82
Z_c	12.96
U	258
Fo_c	1.8E-04

Pe_o	7980

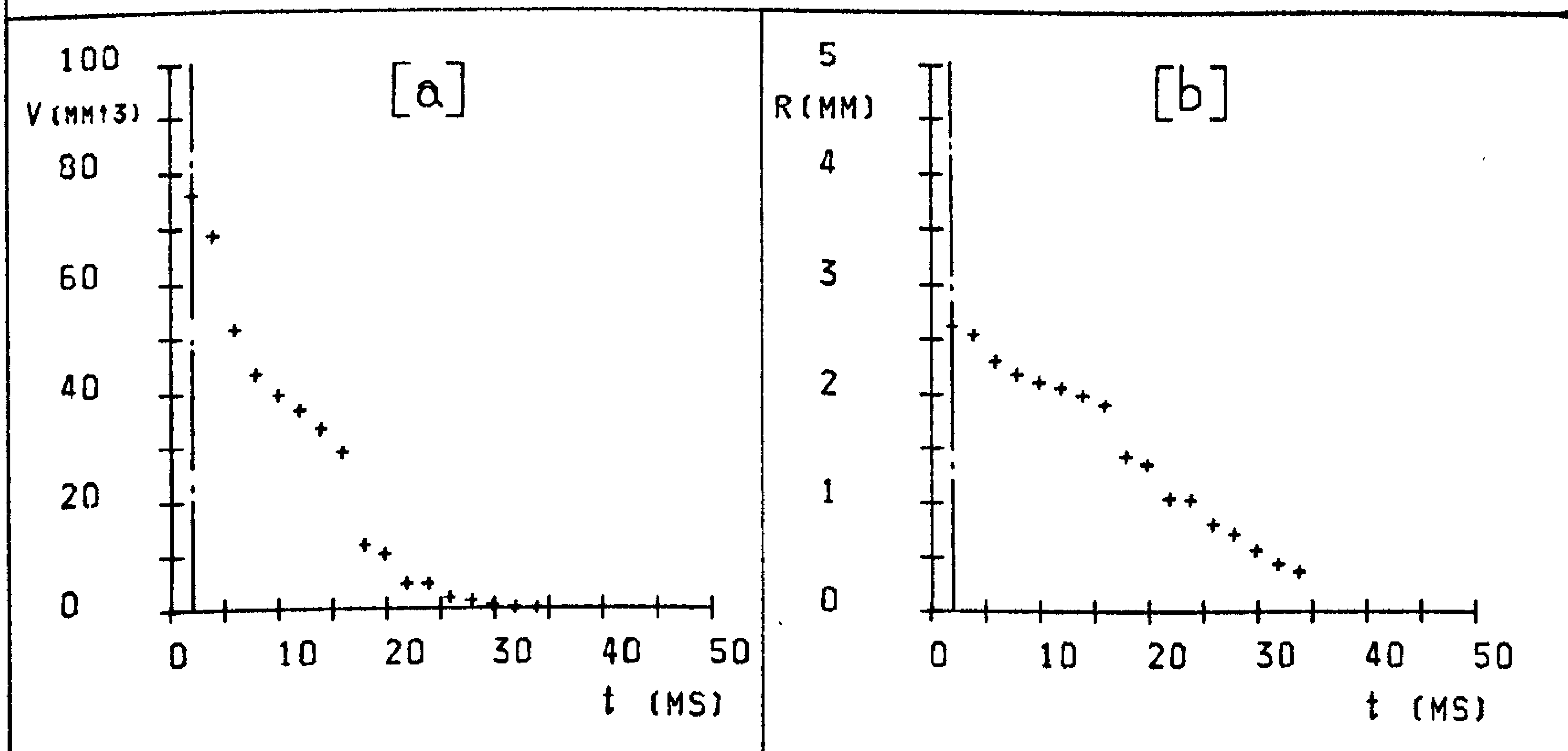

TEST NO : (10.1).2 FILM NO : 65-1/7

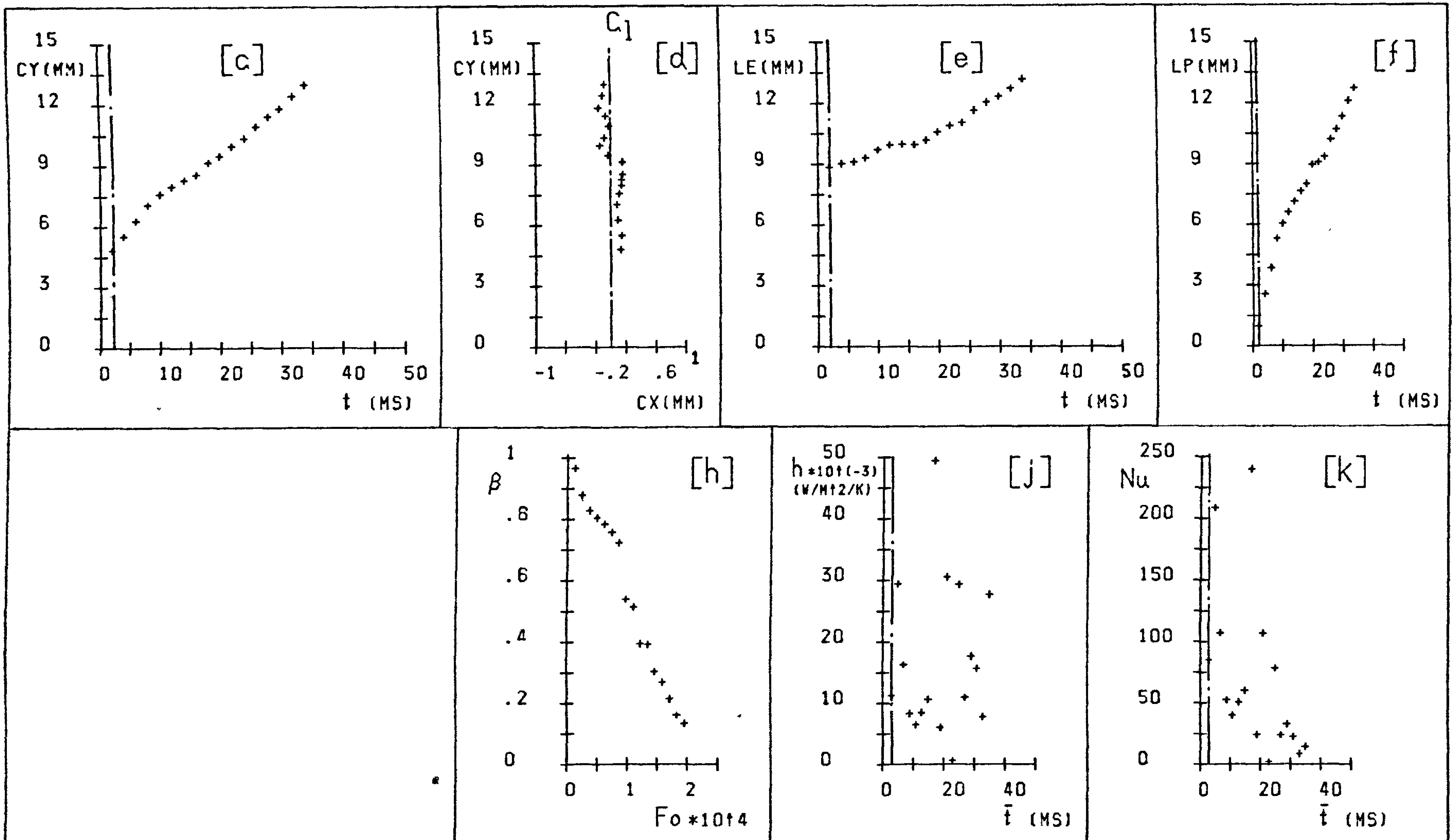

TEST NO : (10.1).2 FILM NØ : 65-1/7

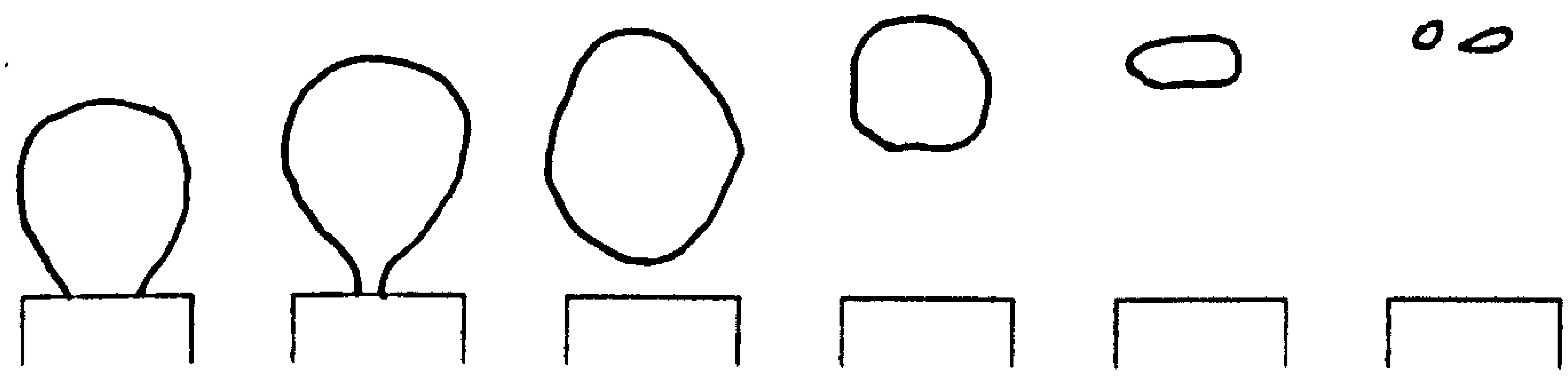

FRAME NUMBERS :

EXPERIMENTAL PARAMETERS :

d	1
$\dot{m}_s$	.45
(V_s	6643)
ΔT	18.5

Z	40
P	2.011
Δt	.82
(CS	1220)

F	34
Ja	30
T_p	165

EXPERIMENTAL RESULTS :

t_g	18.04
t_c	9.3
t_t	27.34
f_s	58
R_m	1.94
R_o	1.93

h_c	18618
Nu_c	58
Z_d	3.06
Z_c	5.98
U	285
Fo_c	1.055E-04

Pe_o	6510

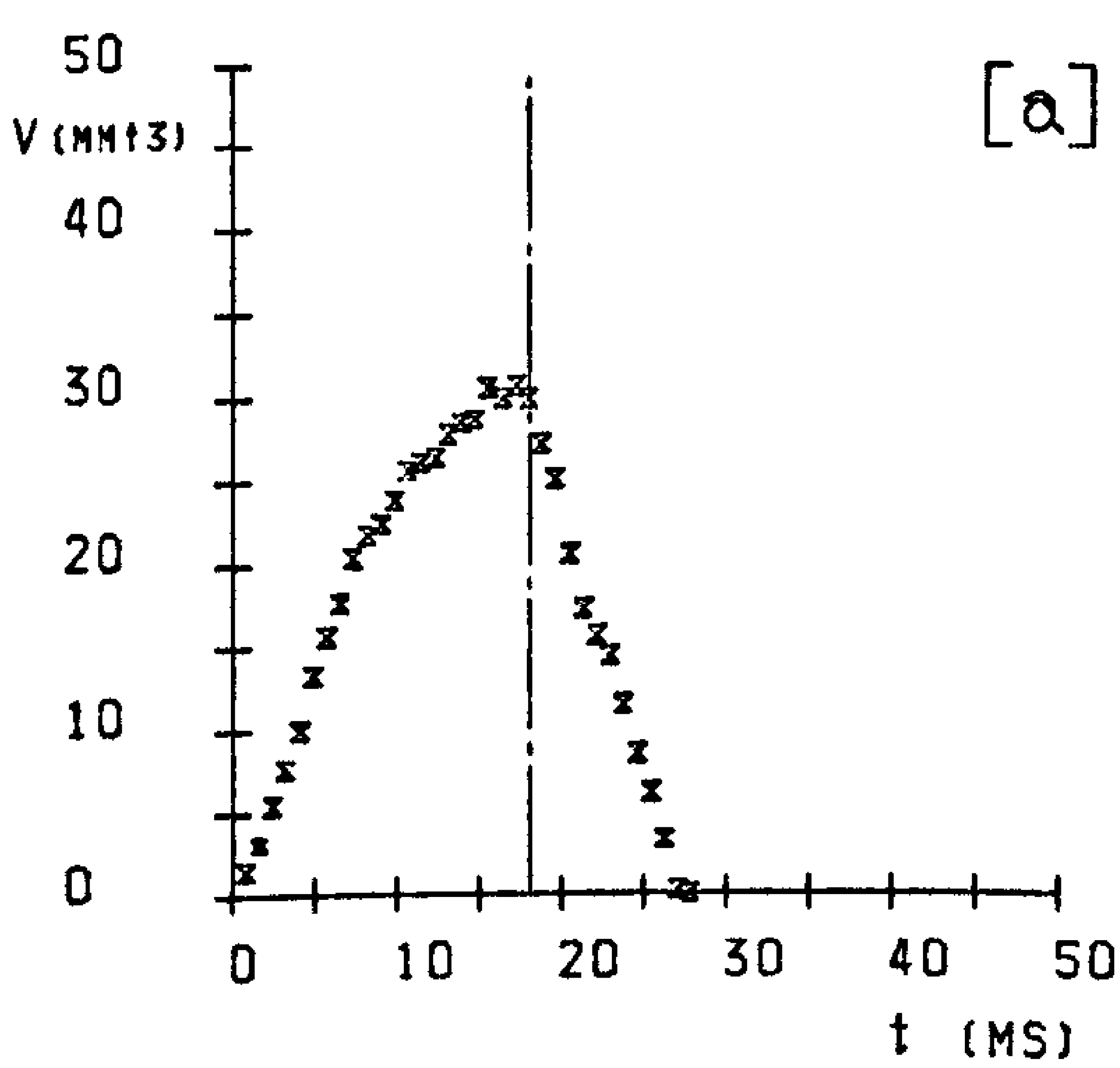

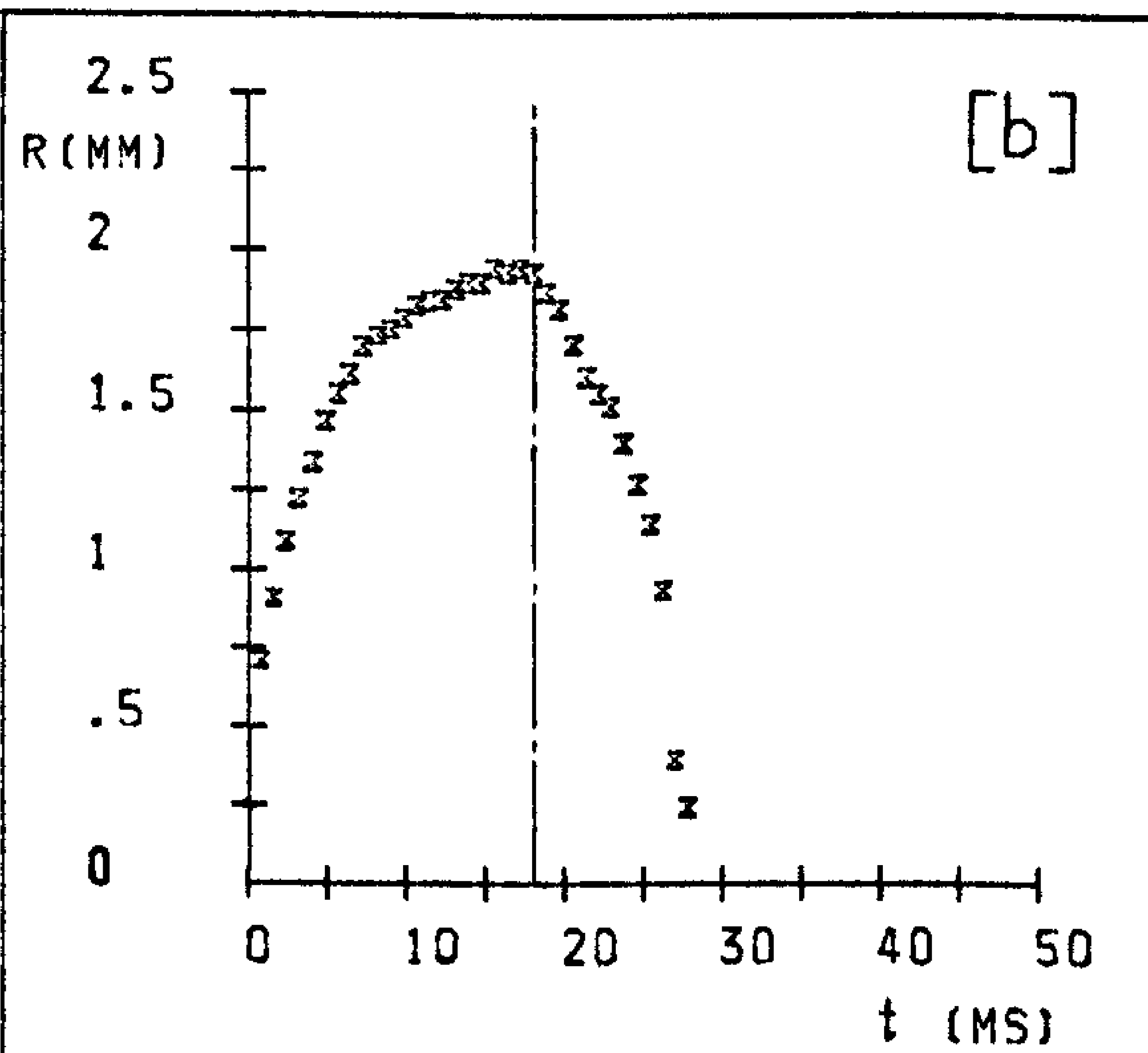

TEST NO : (10.2).1 FILM NO : 65-2/1

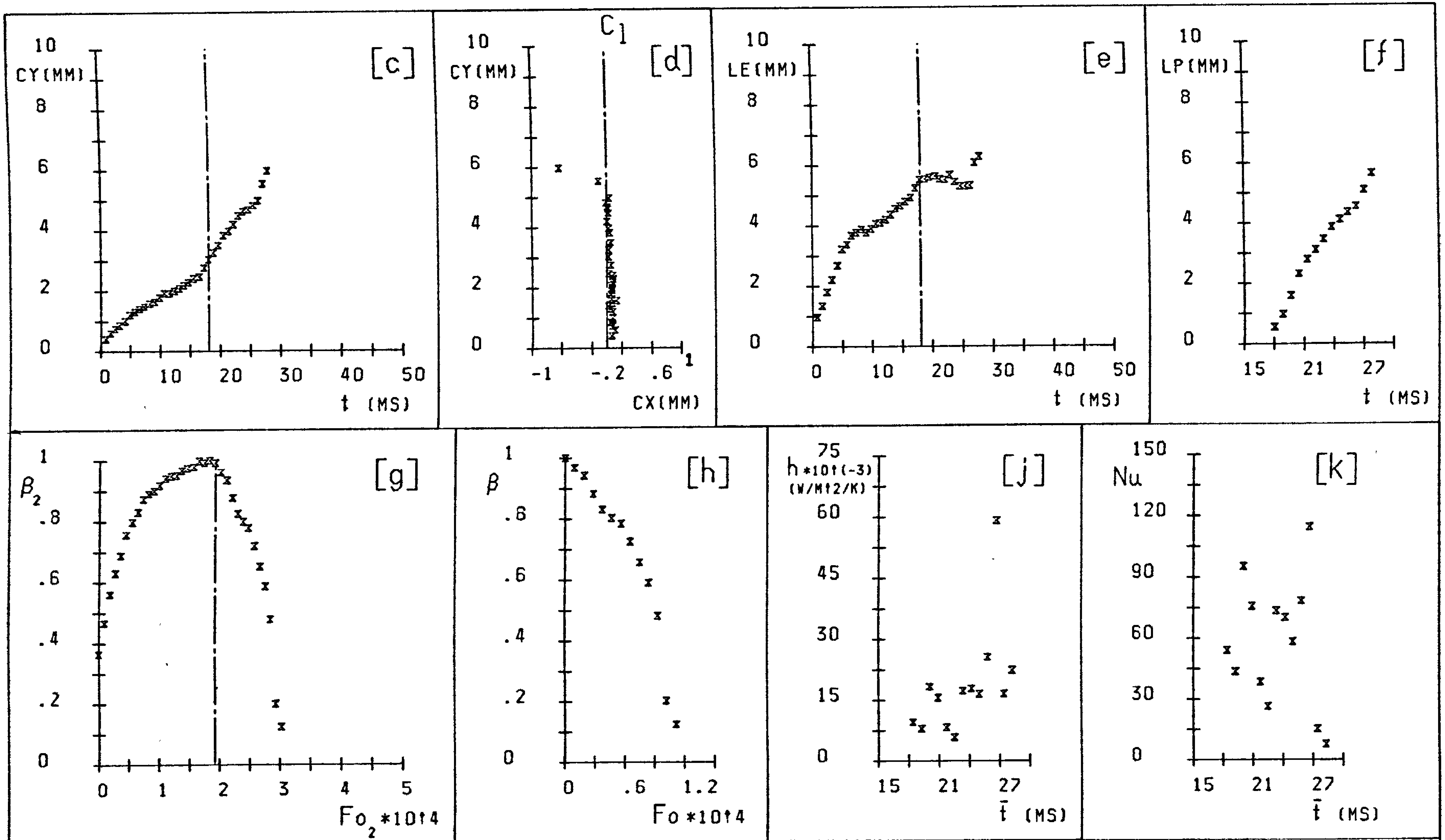

TEST NØ : (10.2).1 FILM NØ : 65-2/1

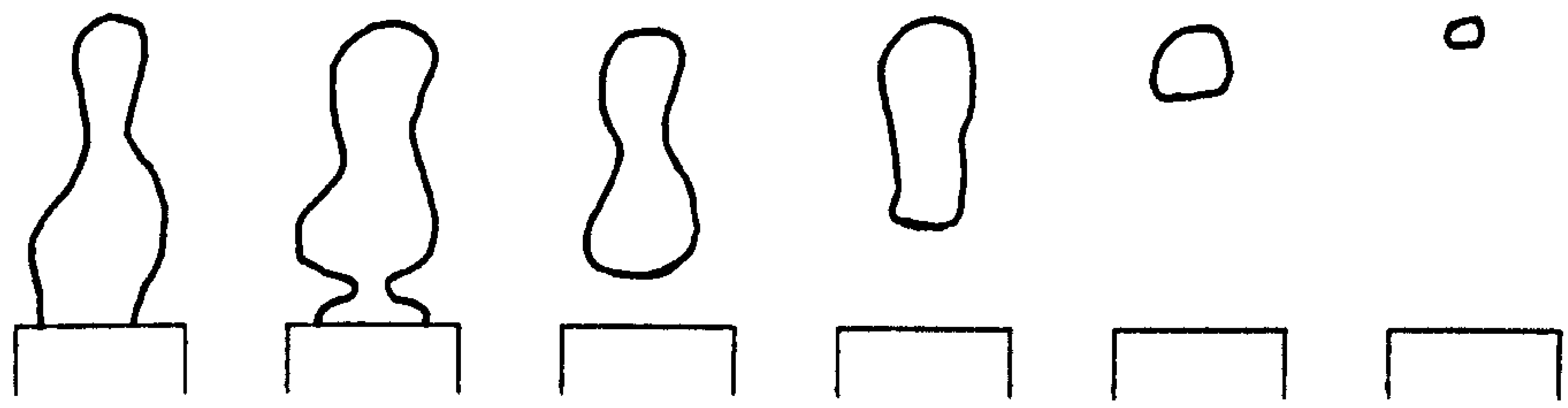

FRAME NUMBERS :	1 -4	5	6 -7	8 -10	11-12	13-16

EXPERIMENTAL PARAMETERS :

d	1	Z	40	F	16
$\dot{m}_s$	.82	P	2.011	Ja	15
(V_s	12105)	Δt	1.74	T_p	165
ΔT	9.3	(CS	575)		

EXPERIMENTAL RESULTS :

t_g	10.44	h_c	26177	Pe_o	12140
t_c	18	Nu_c	94		
t_t	28.44	Z_d	5.69		
f_s	115	Z_c	13.99		
R_m	2.38	U	443		
R_o	2.33	Fo_c	1.409E-04		

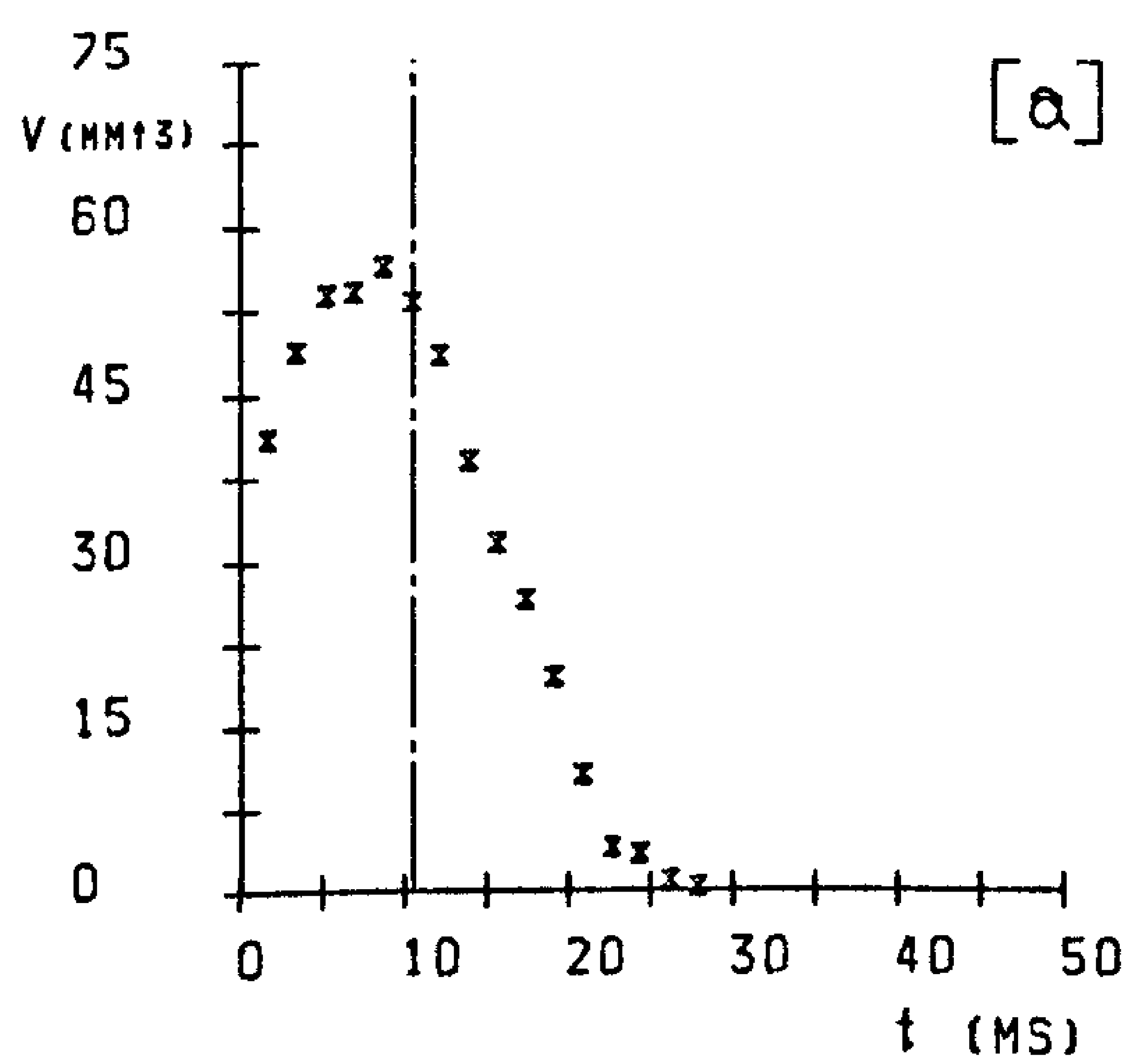

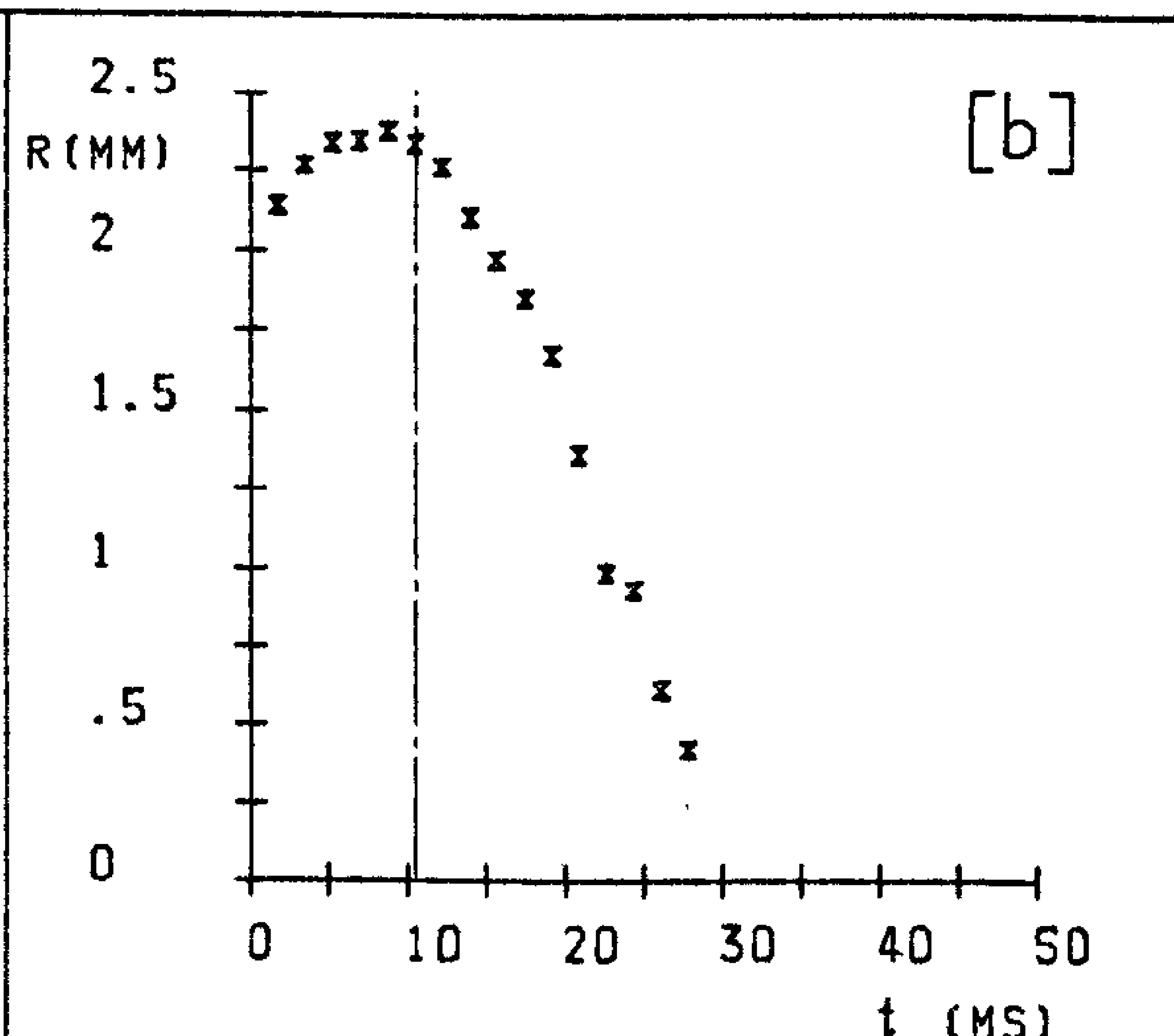

TEST NO : (11.1).1 FILM NO : 62-2/2

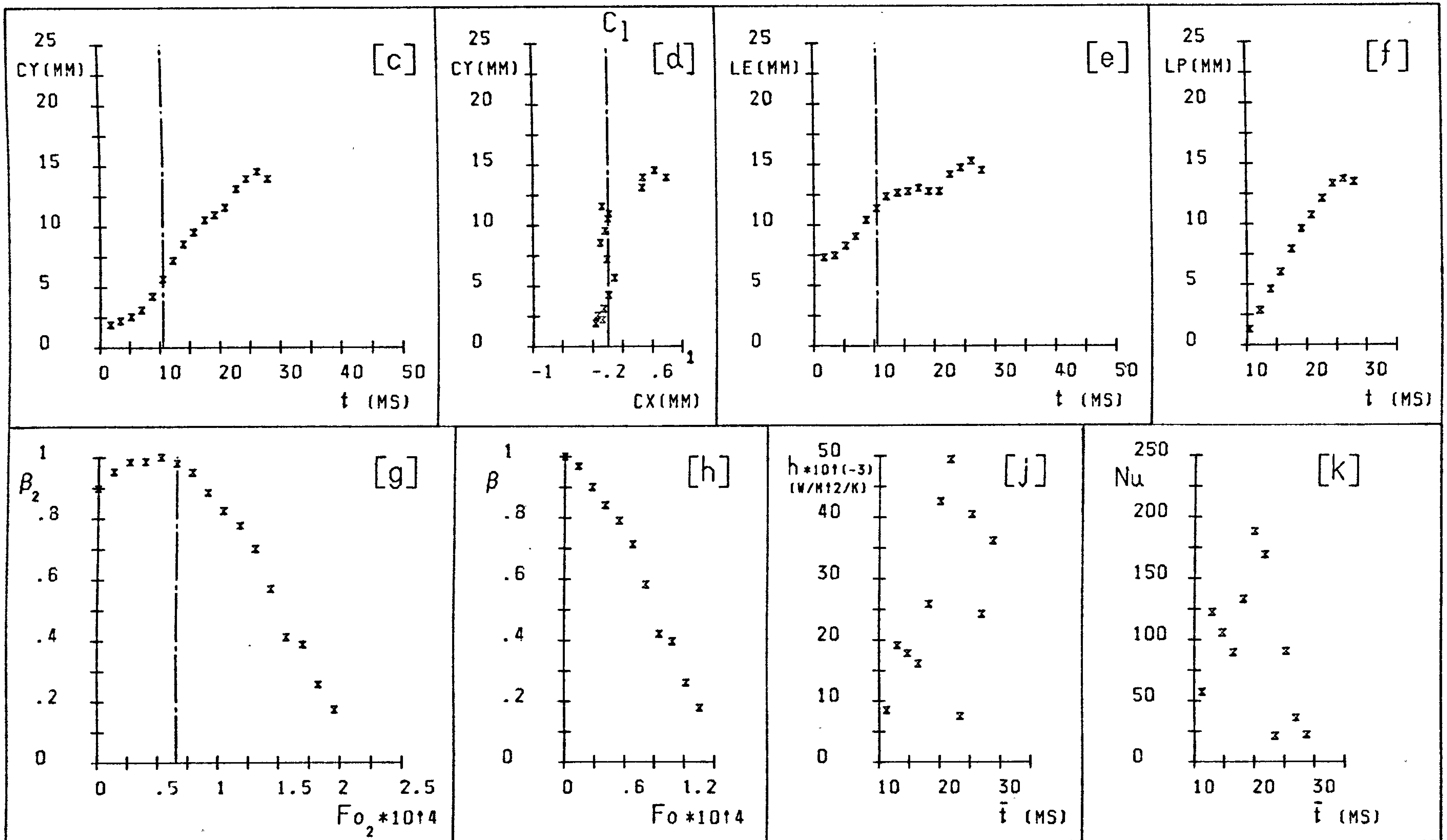

TEST NO : (11.1).1 FILM NO : 62-2/2

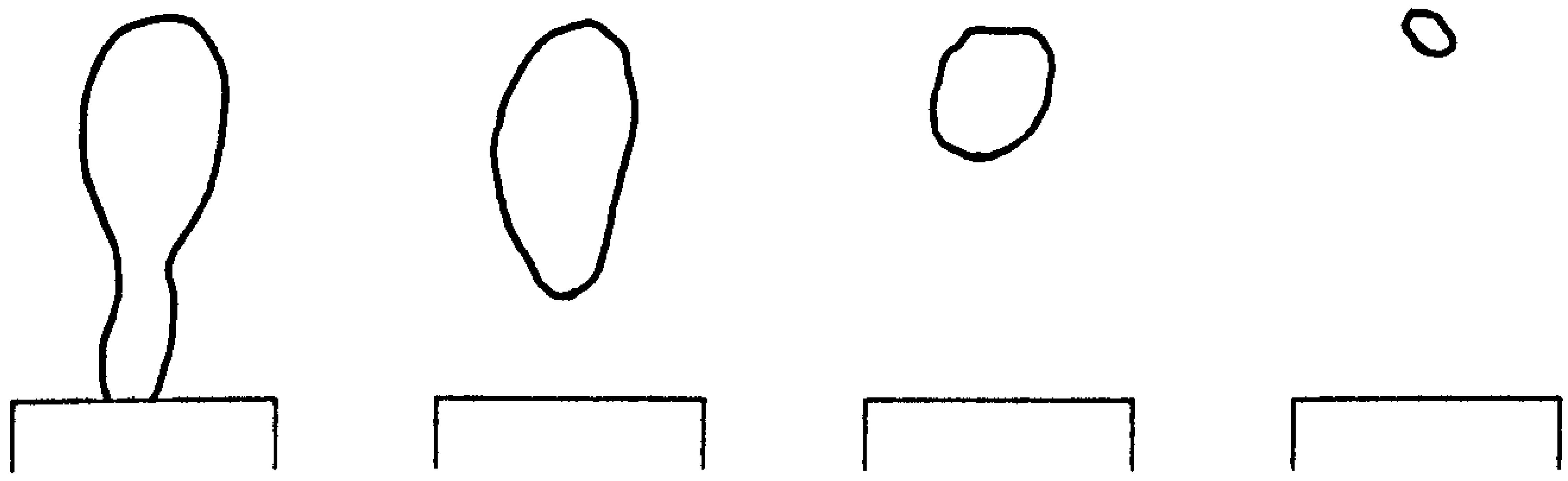

FRAME NUMBERS : 1 -16 17-19 20-23 24-26

EXPERIMENTAL PARAMETERS :

d	1	Z	40	F	26
$\dot{m}_s$	.82	P	2.011	Ja	30
(V_s	12105)	Δt	.95	T_p	165
ΔT	18.5	(CS	1056)		

EXPERIMENTAL RESULTS :

t_g	16.1	h_c	23149	Pe_o	9190
t_c	8	Nu_c	68		
t_t	24.1	Z_d	5.71		
f_s	66	Z_c	9.27		
R_m	2.1	U	413		
R_o	1.88	Fo_c	9.56E-05		

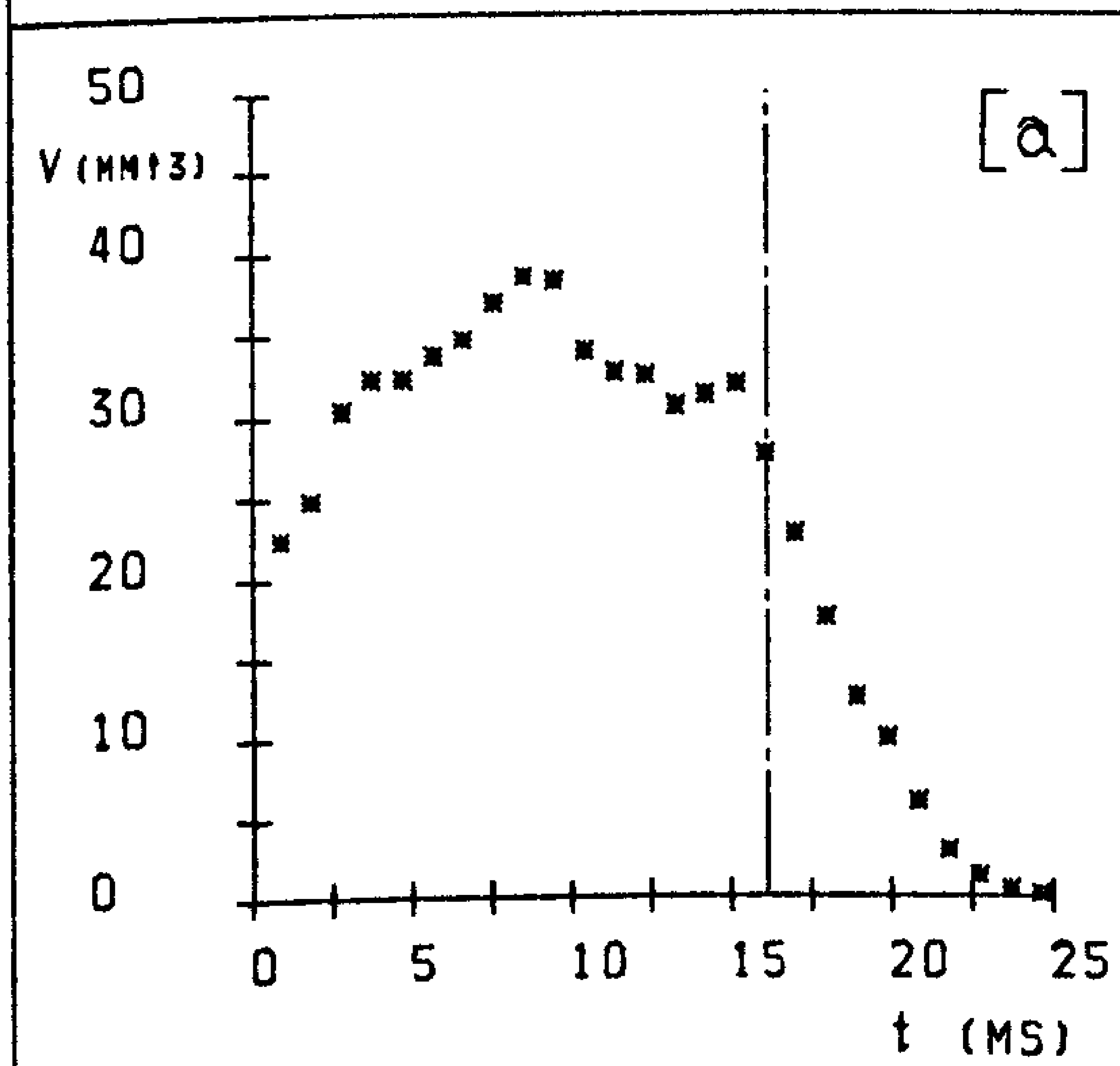

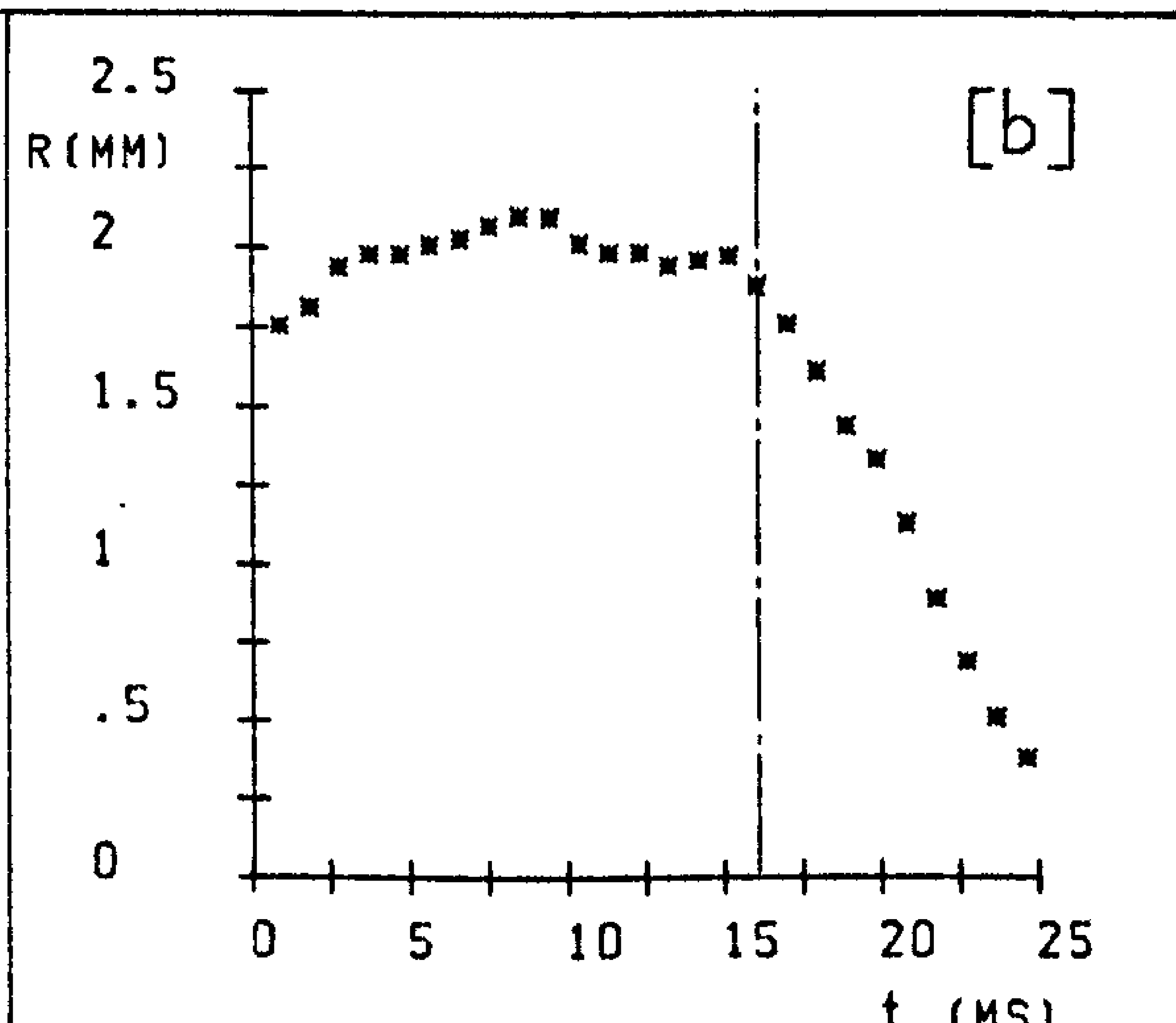

TEST NO : (11.2).3 FILM NØ : 63-1/4

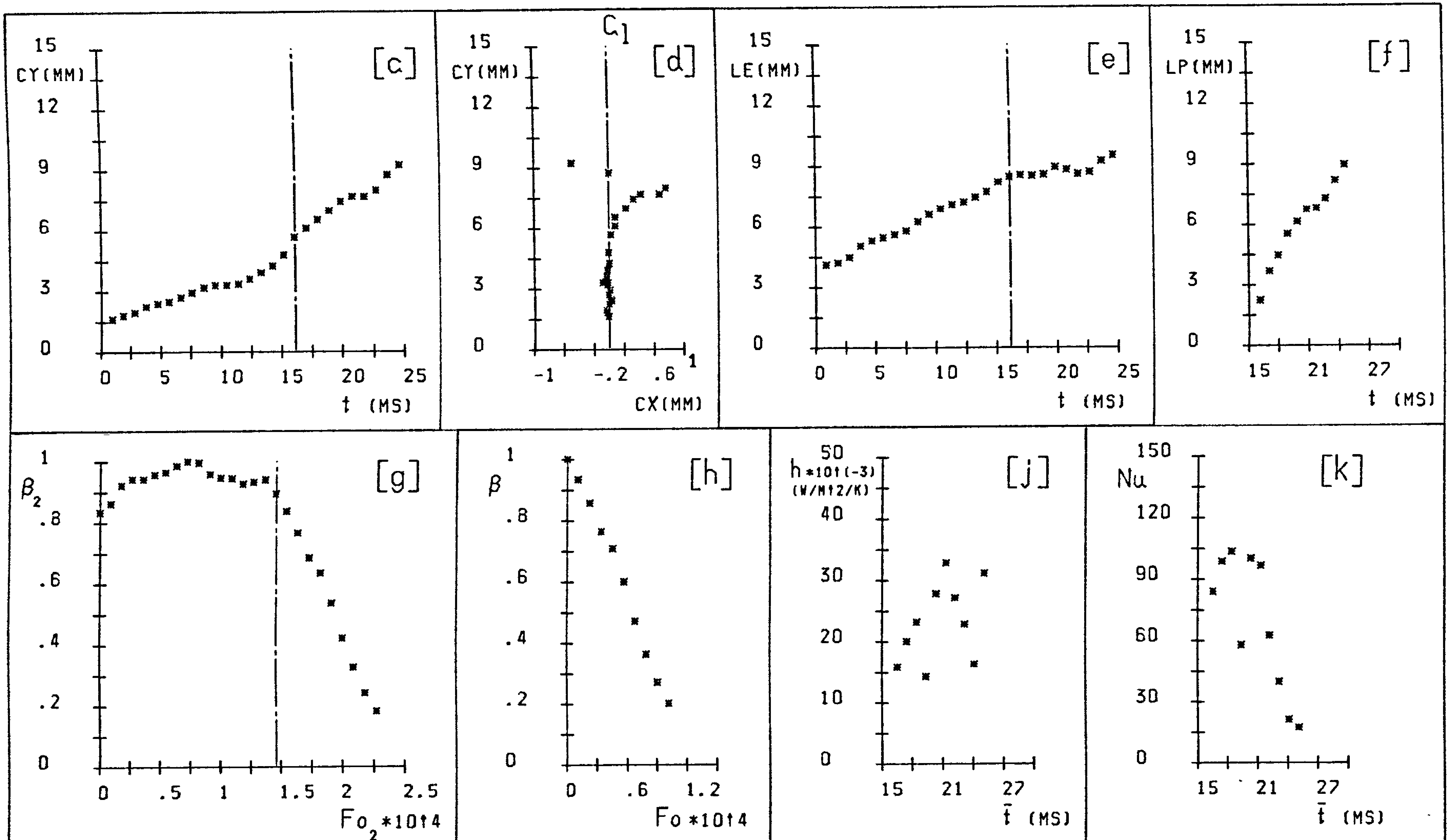

TEST NØ : (11.2).3 FILM NØ : 63-1/4

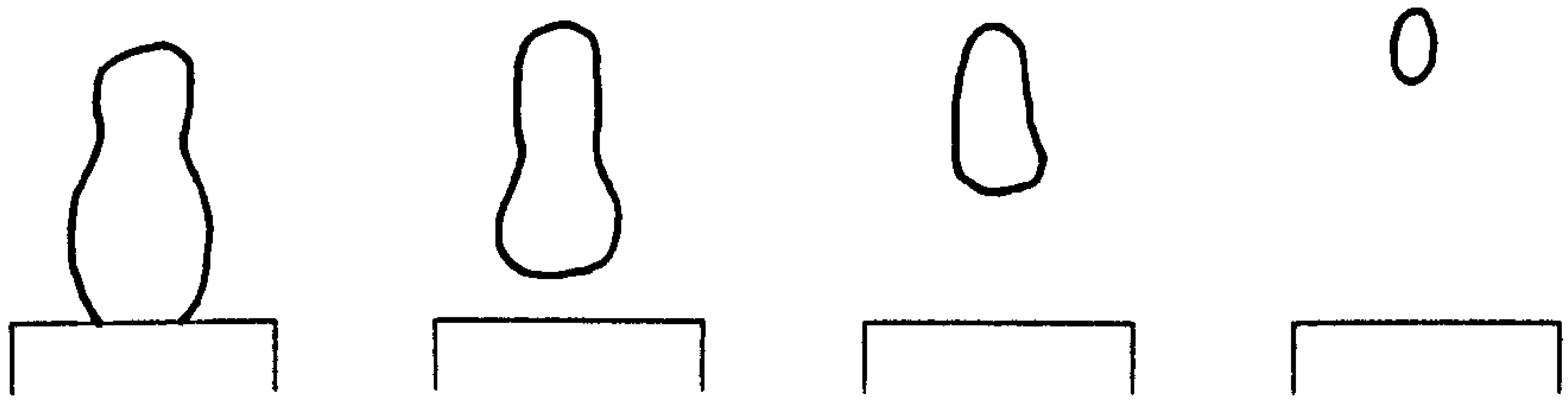

FRAME NUMBERS :	1 -14	15-17	18-19	20-21

EXPERIMENTAL PARAMETERS :

d	1	Z	40	F	21
$\dot{m}_s$	.82	P	2.011	Ja	45
(V_s	12105)	Δt	.74	T_p	165
ΔT	27.6	(CS	1351)		

EXPERIMENTAL RESULTS :

t_g	11.1	h_c	22474	Pe_o	8500
t_c	4.6	Nu_c	60		
t_t	15.7	Z_d	3.25		
f_s	97	Z_c	5.9		
R_m	1.83	U	420		
R_o	1.69	Fo_c	6.72E-05		

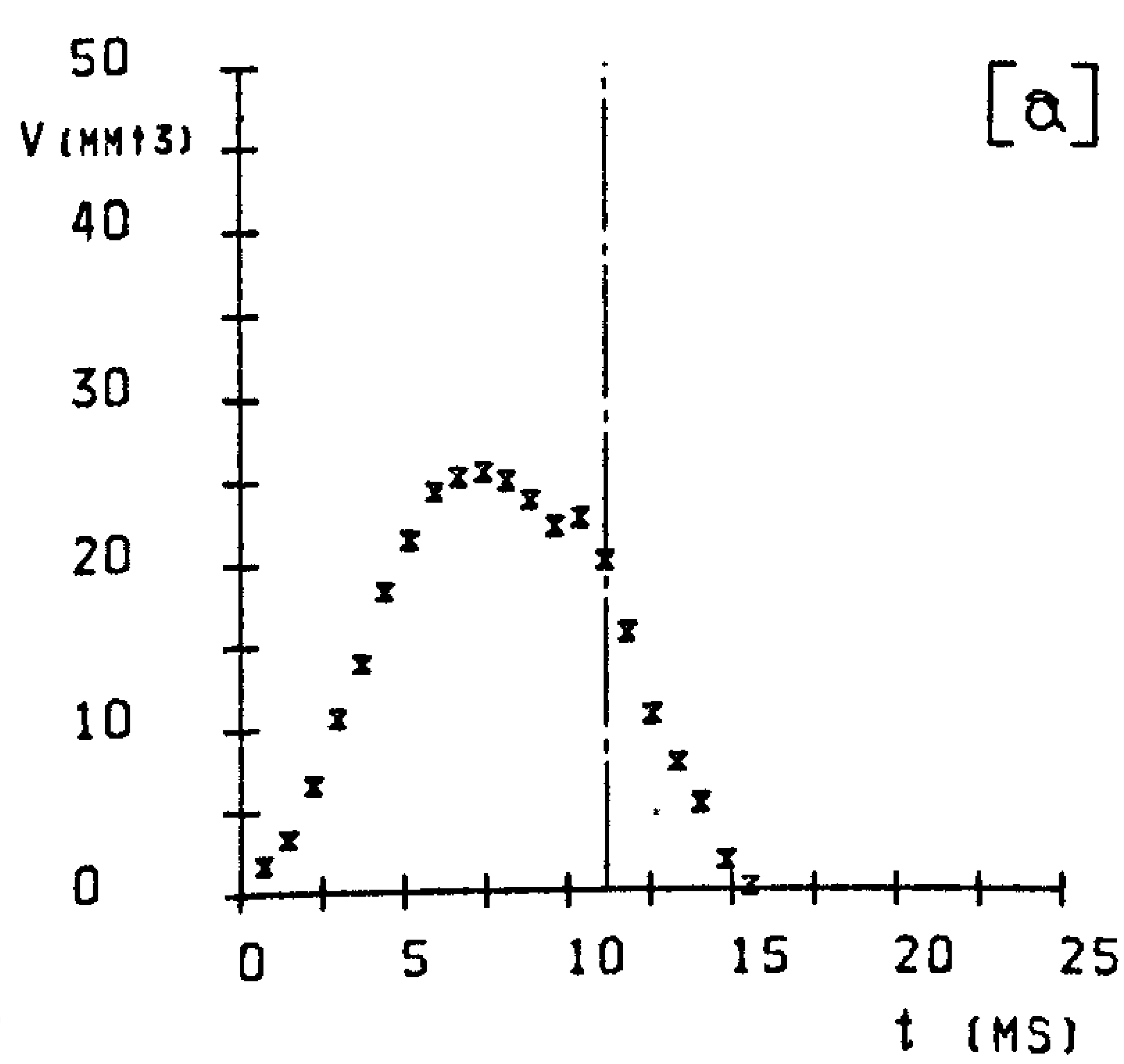

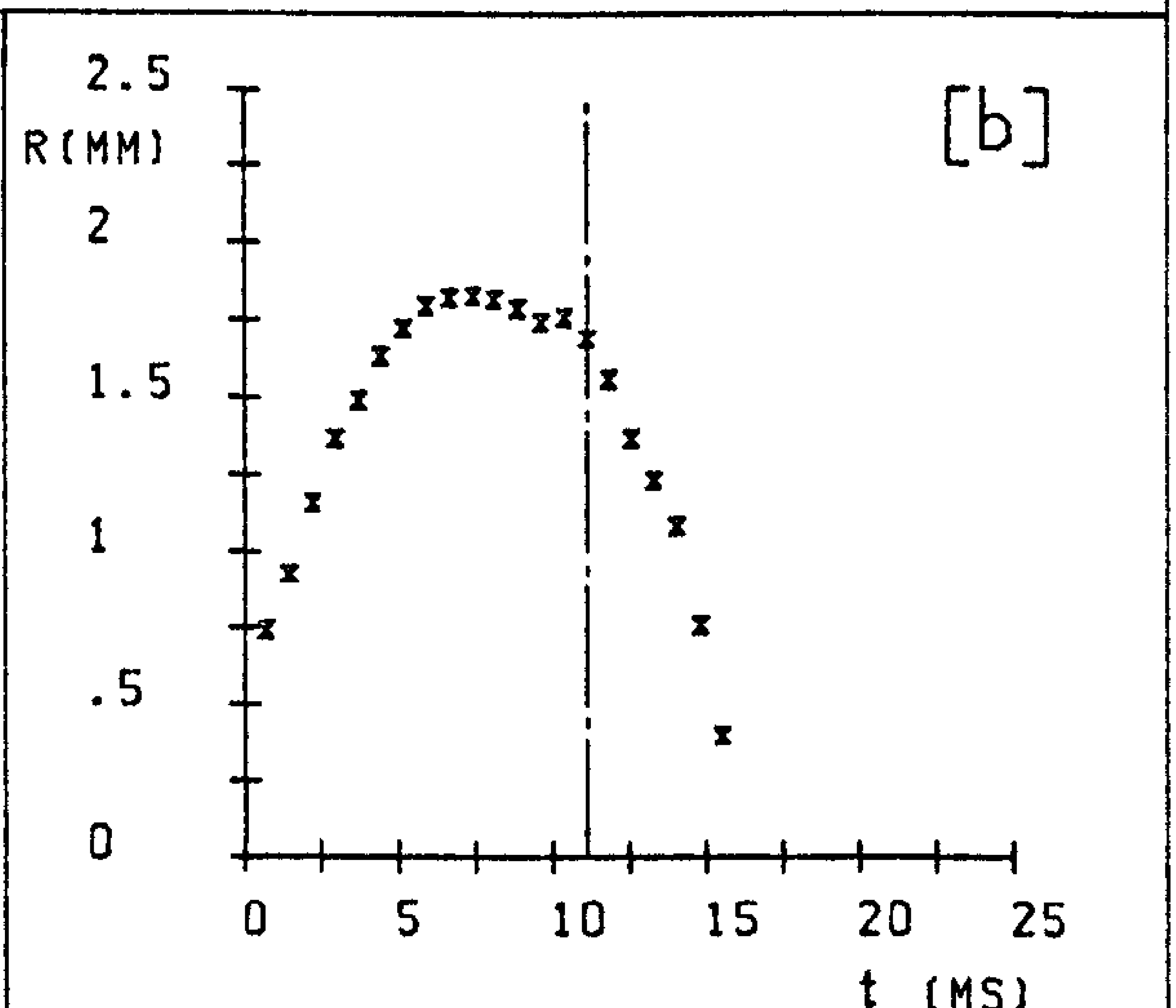

TEST NO : (11.3).1 FILM NO : 63-2/1

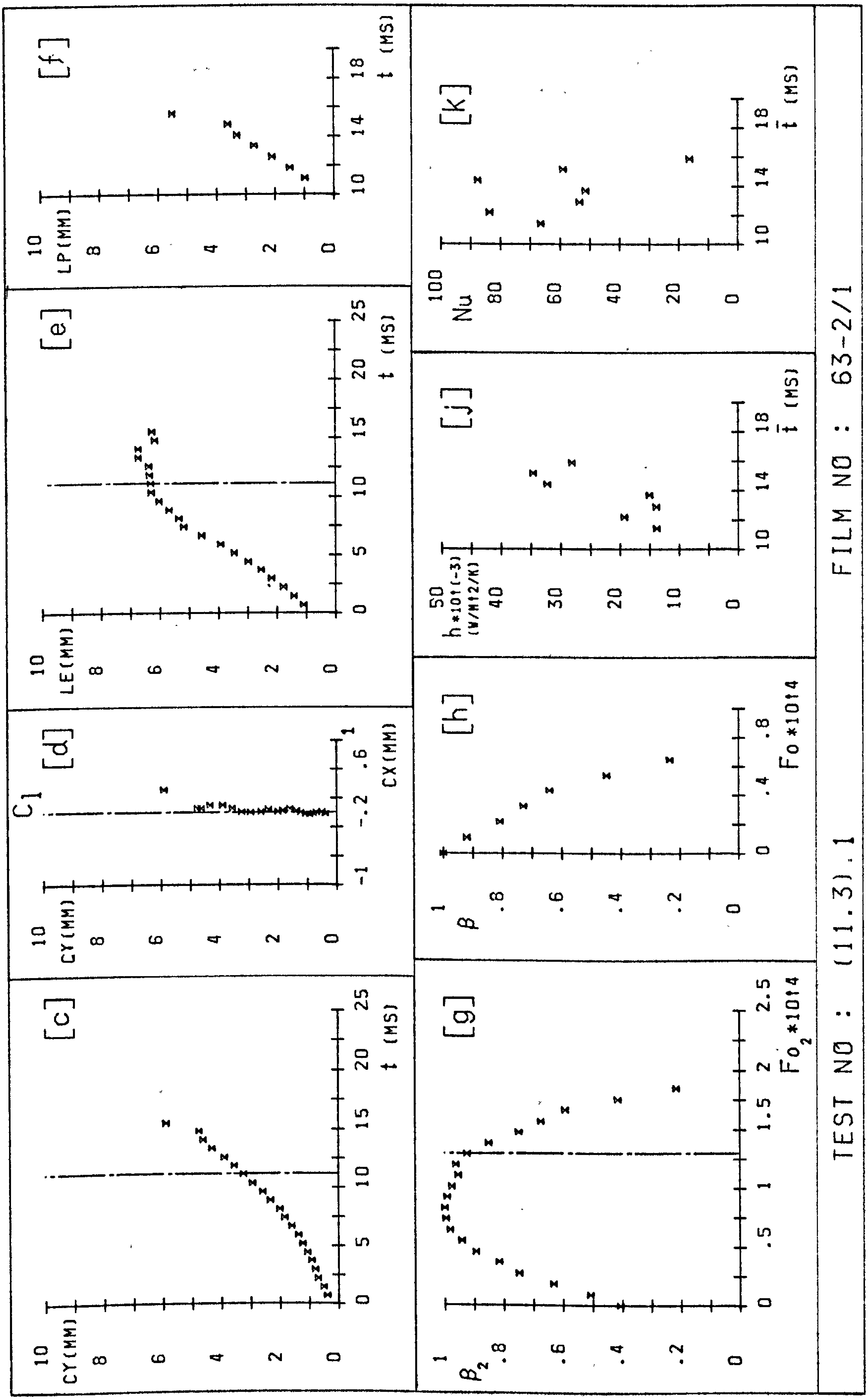
[c]
CY(MM)
t (MS)
[d]
C1
CY(MM)
CX(MM)
[e]
LE(MM)
t (MS)
[f]
LP(MM)
t (MS)
[g]
β2
Fo2*10↑4
[h]
β
Fo*10↑4
[j]
h*10↑(-3)
(W/M↑2/K)
t̄ (MS)
[k]
Nu
t̄ (MS)
TEST NØ : (11.3).1
FILM NØ : 63-2/1

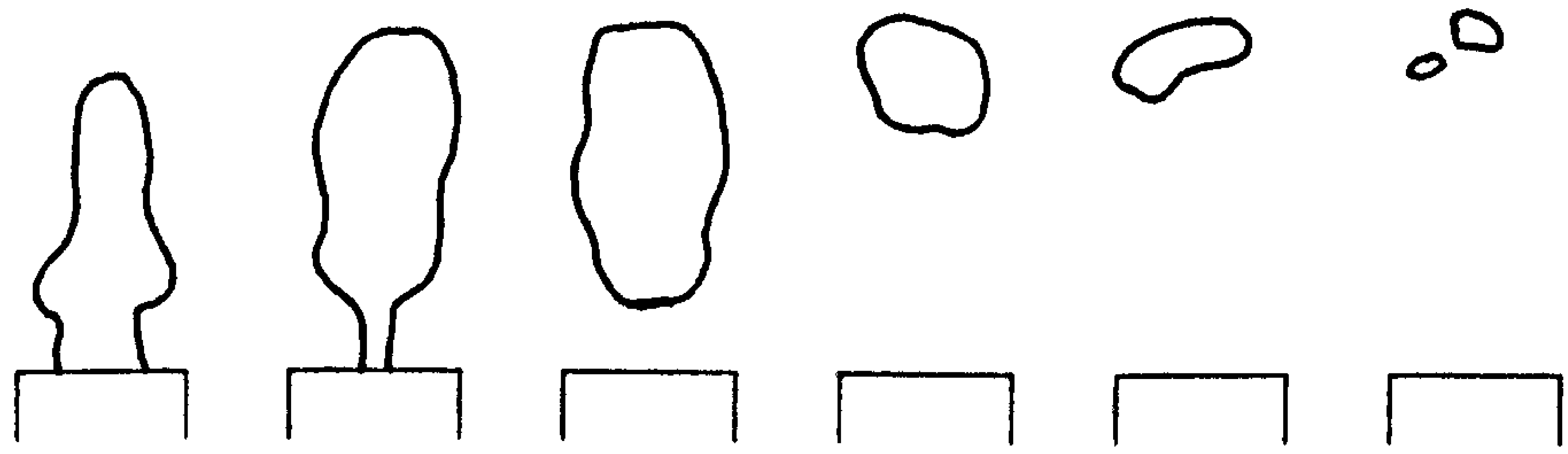

FRAME NUMBERS : 1 - 8 | 9 - 12 | 13-17 | 18-20 | 21-22 | 23-28

EXPERIMENTAL PARAMETERS :

d	1	Z	40	F	28
$\dot{m}_s$	1.39	P	2.011	Ja	15
(V_s	20520)	Δt	2.13	T_p	165
ΔT	9.3	(CS	470)		

EXPERIMENTAL RESULTS :

t_g	27.69	h_c	20883	Pe_o	18230
t_c	28	Nu_c	107		
t_t	55.69	Z_d	10.39		
f_s	39	Z_c	24.4		
R_m	3.45	U	471		
R_o	3.29	Fo_c	1.099E-04		

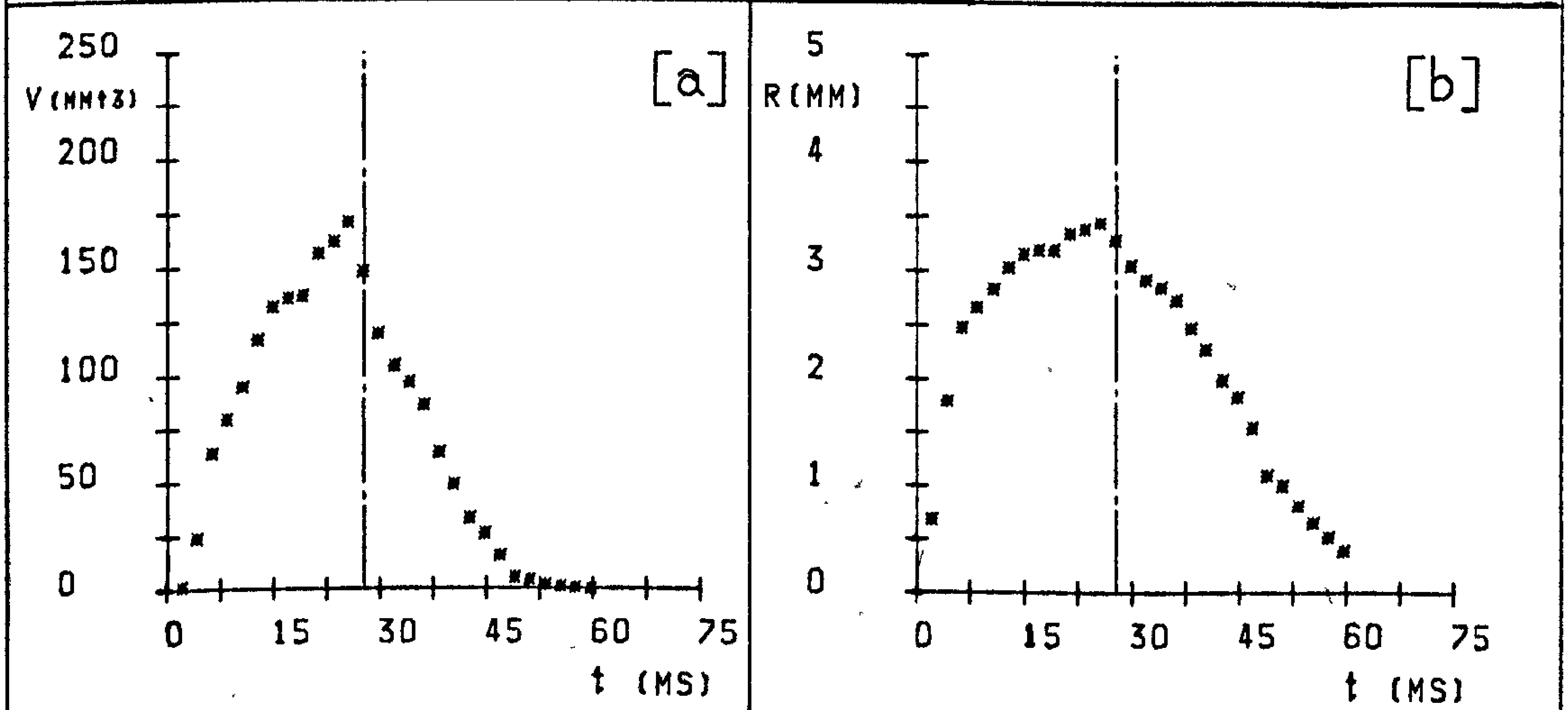

TEST NO : (12.1).3 FILM NO : 66-2/3

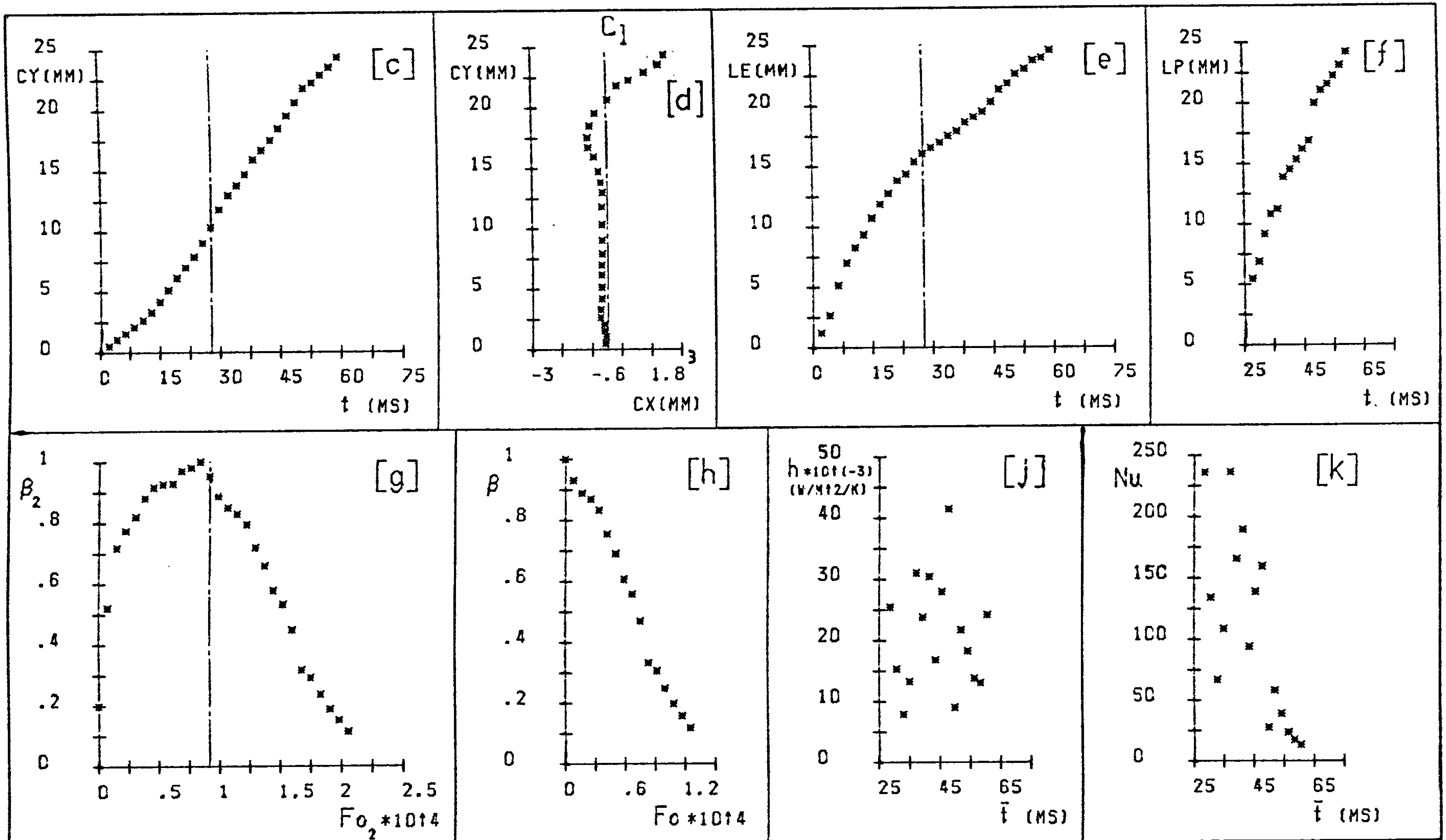

TEST NØ : (12.1).3 FILM NØ : 66-2/3

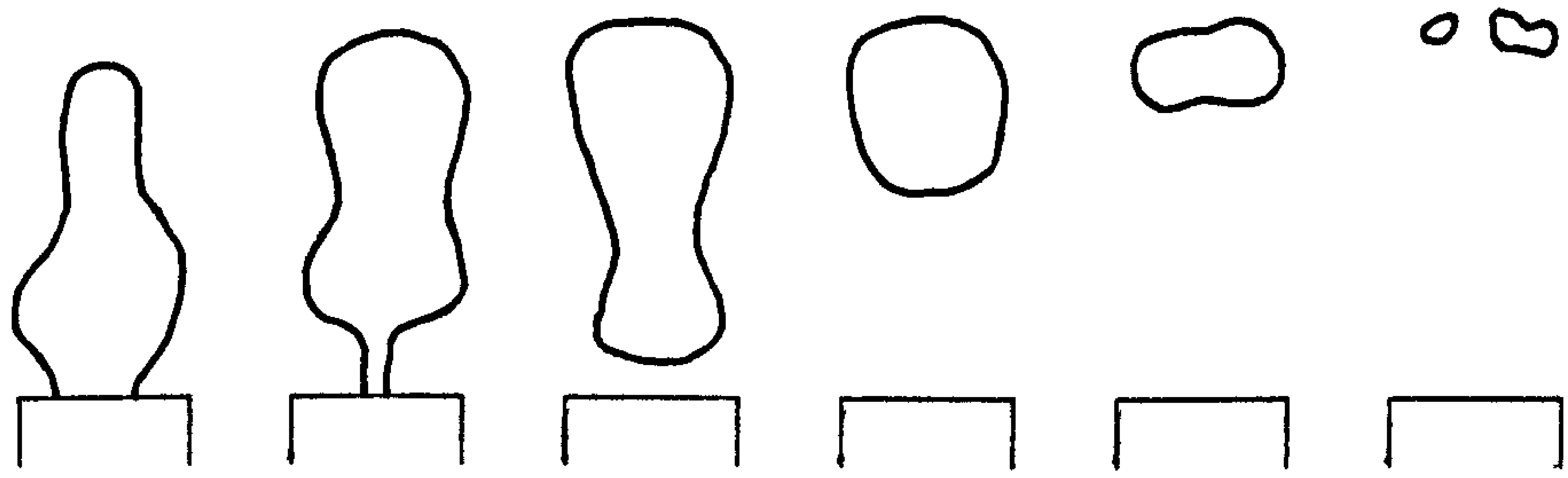

EXPERIMENTAL PARAMETERS :

d	1	Z	40	F	22
$\dot{m}_s$	1.39	P	2.011	Ja	30
(V_s	20520)	Δt	1.17	T_p	165
ΔT	18.5	(CS	857)		

EXPERIMENTAL RESULTS :

t_g	15.17	h_c	22186	Pe_o	12750
t_c	9.5	Nu_c	85		
t_t	24.67	Z_d	6.08		
f_s	71	Z_c	10.36		
R_m	2.55	U	447		
R_o	2.41	Fo_c	6.91E-05		

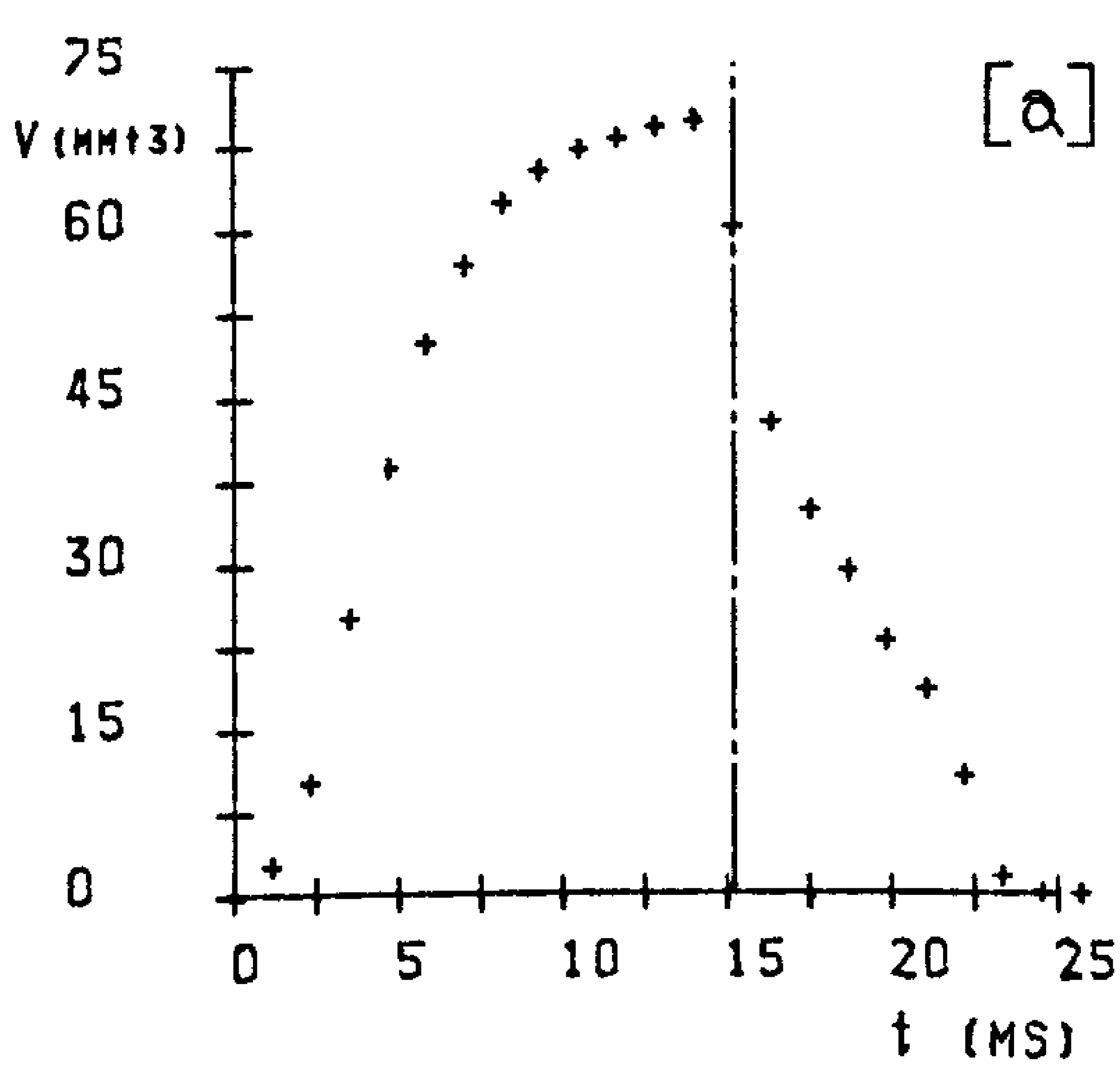

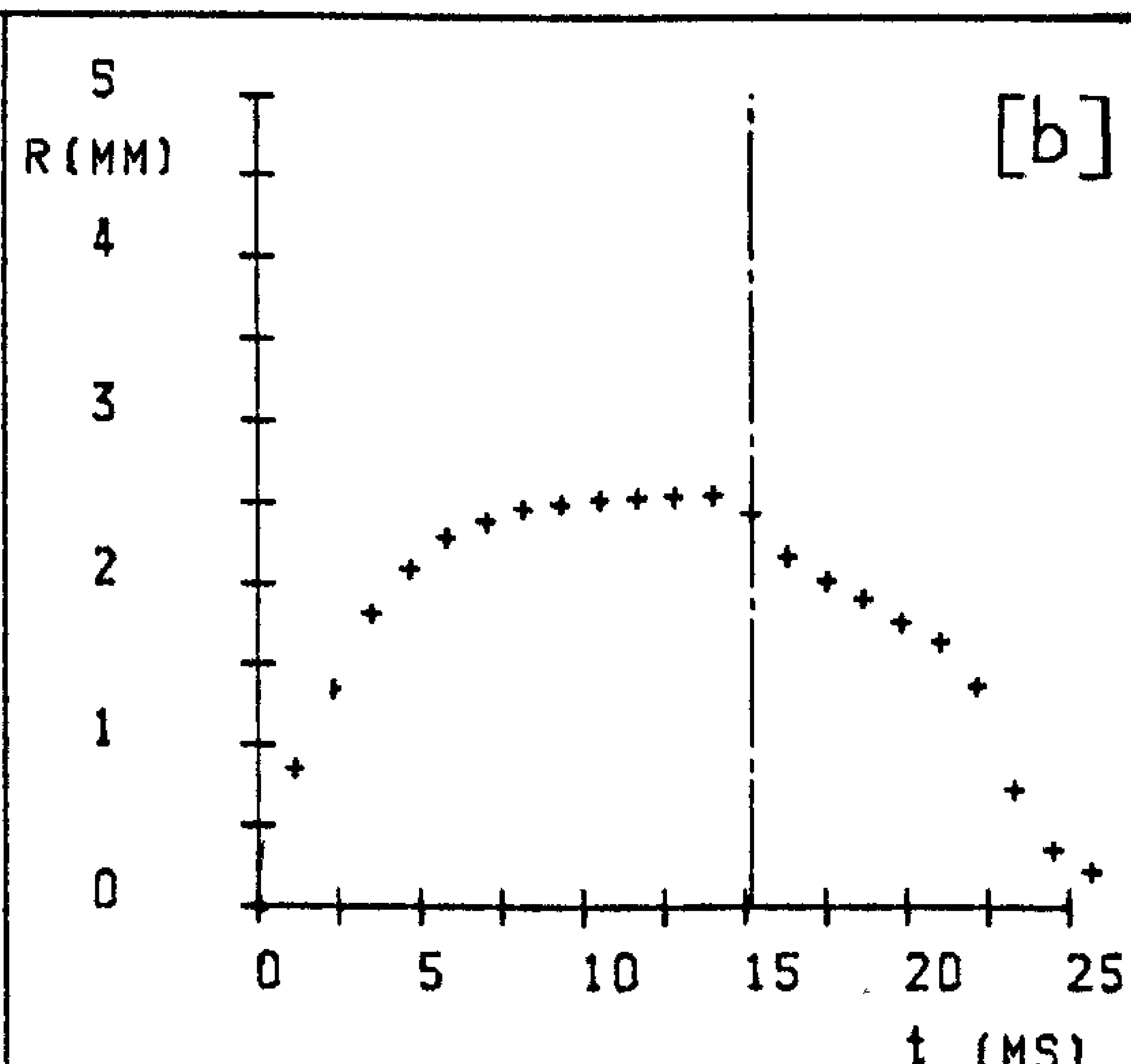

TEST NO : (12.2).2 FILM NO : 67-1/2

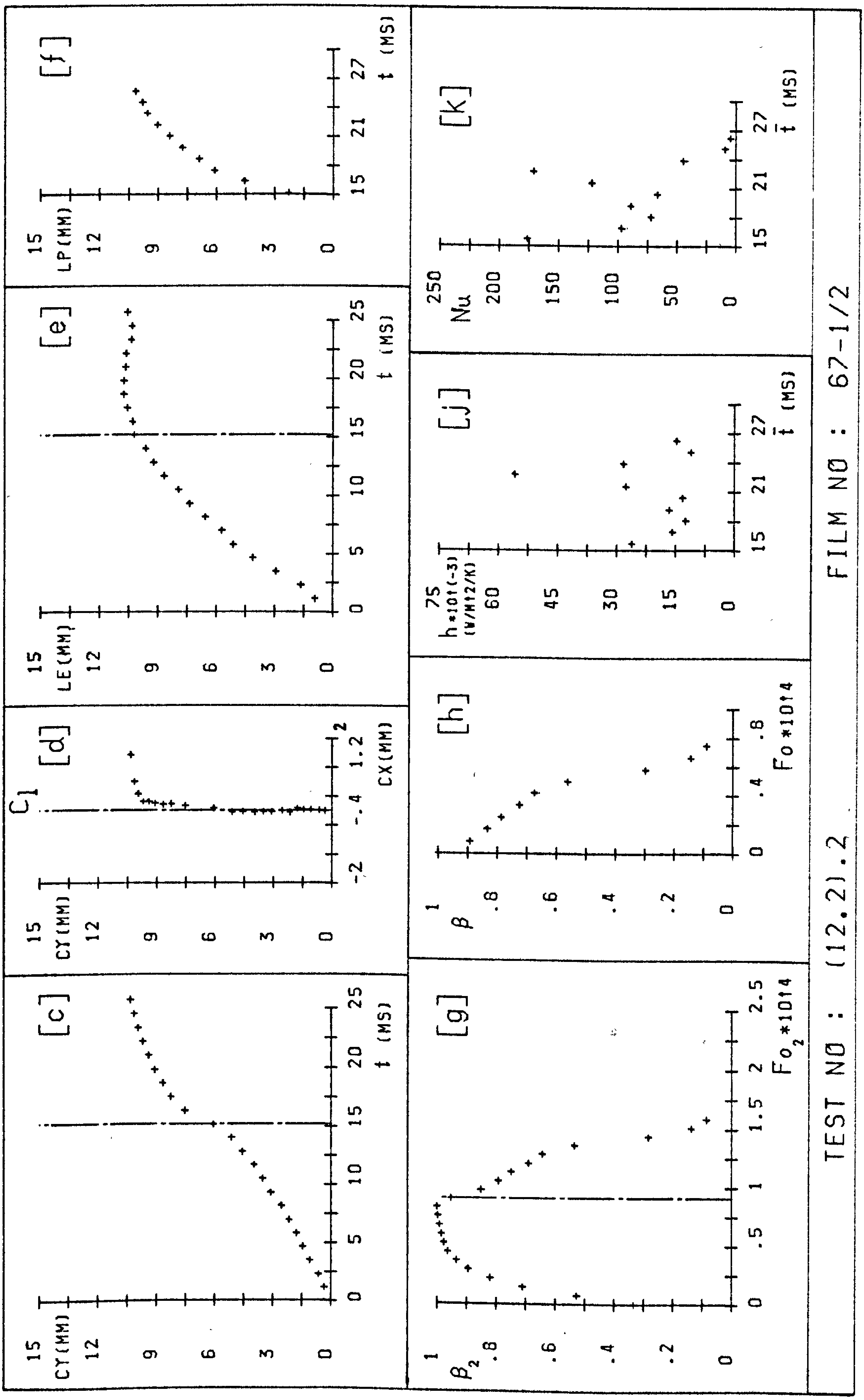
[c]
CY(MM)
t (MS)
[d]
C_1
CY(MM)
CX(MM)
[e]
LE(MM)
t (MS)
[f]
LP(MM)
t (MS)
[g]
β_2
Fo_2*10↑4
[h]
β
Fo*10↑4
[j]
h*10↑(-3) (W/M↑2/K)
$\bar{t}$ (MS)
[k]
Nu
$\bar{t}$ (MS)
TEST NØ : (12.2).2
FILM NØ : 67-1/2

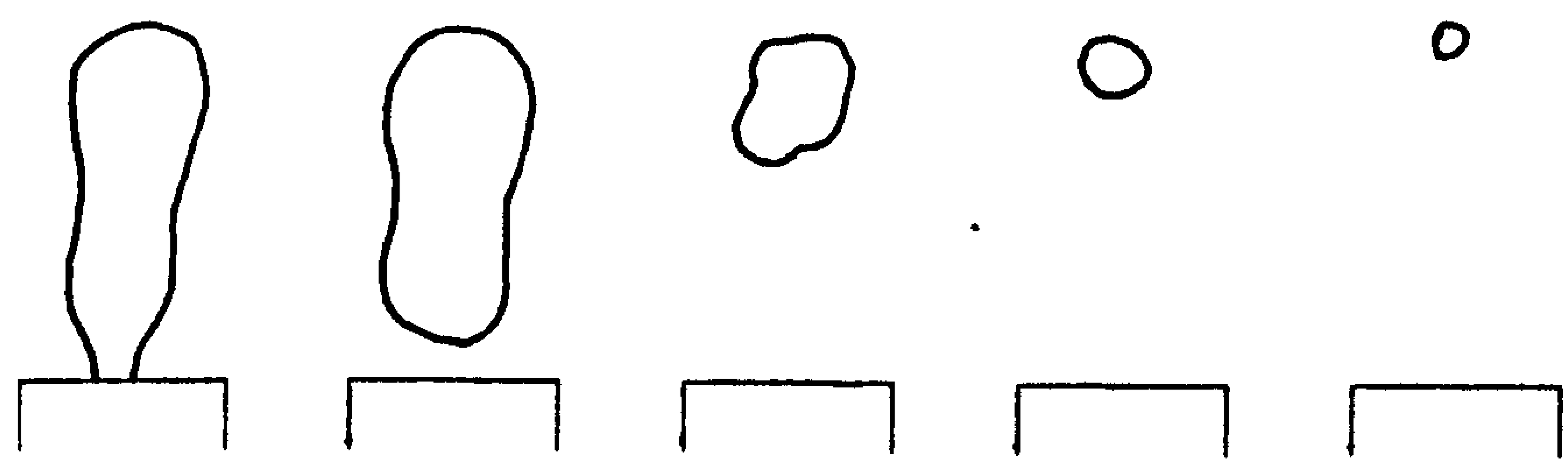

FRAME NUMBERS : 1 -10   11-14   15   16   17

EXPERIMENTAL PARAMETERS :

d	1	Z	40	F	17
$\dot{m}_s$	1.39	P	2.011	Ja	45
(V_s	20520)	Δt	.77	T_p	165
ΔT	27.6	(CS	1295)		

EXPERIMENTAL RESULTS :

t_g	8.49	h_c	27144	Pe_o	11310
t_c	4.8	Nu_c	89		
t_t	13.29	Z_d	4.32		
f_s	130	Z_c	7.41		
R_m	2.16	U	463		
R_o	2.04	Fo_c	4.82E-05		

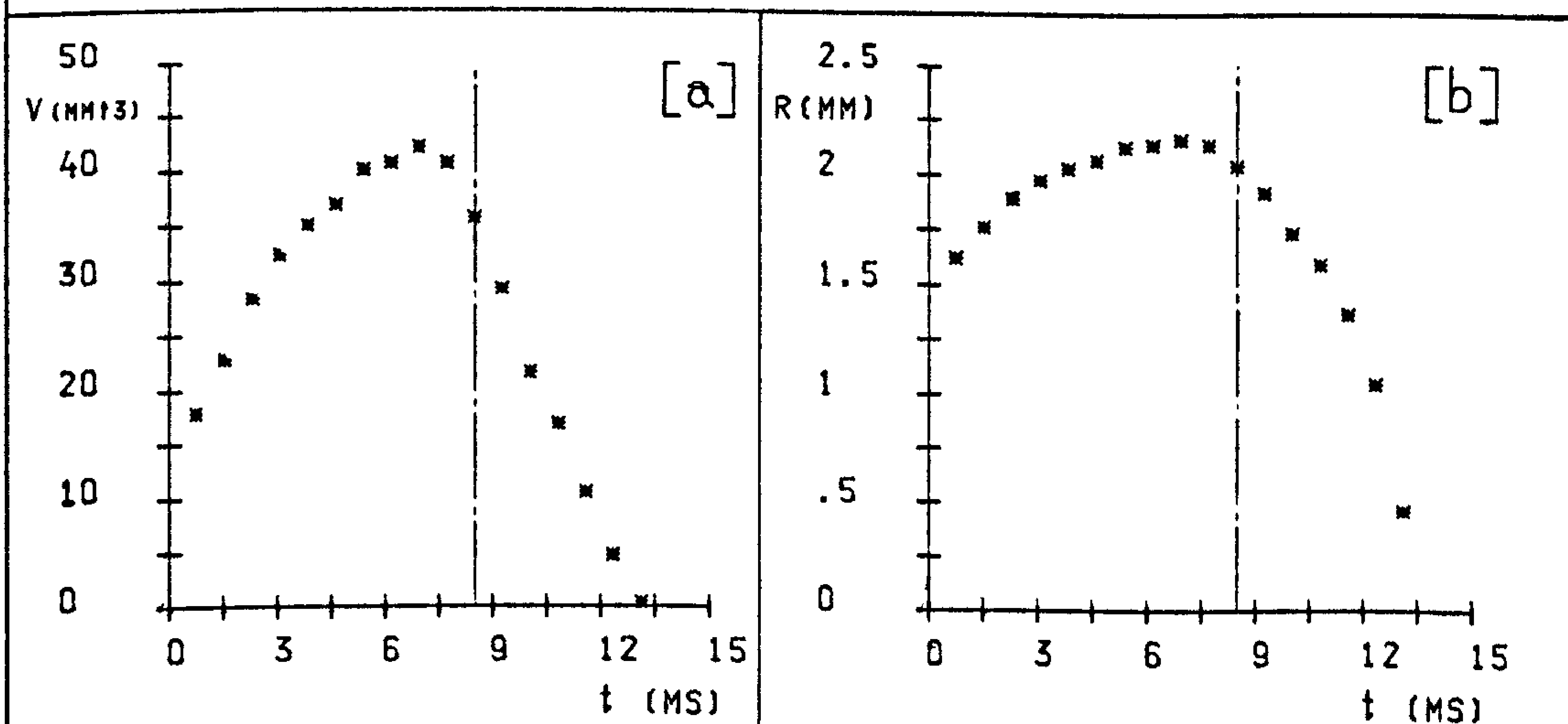

TEST NO : (12.3).3   FILM NO : 67-2/5

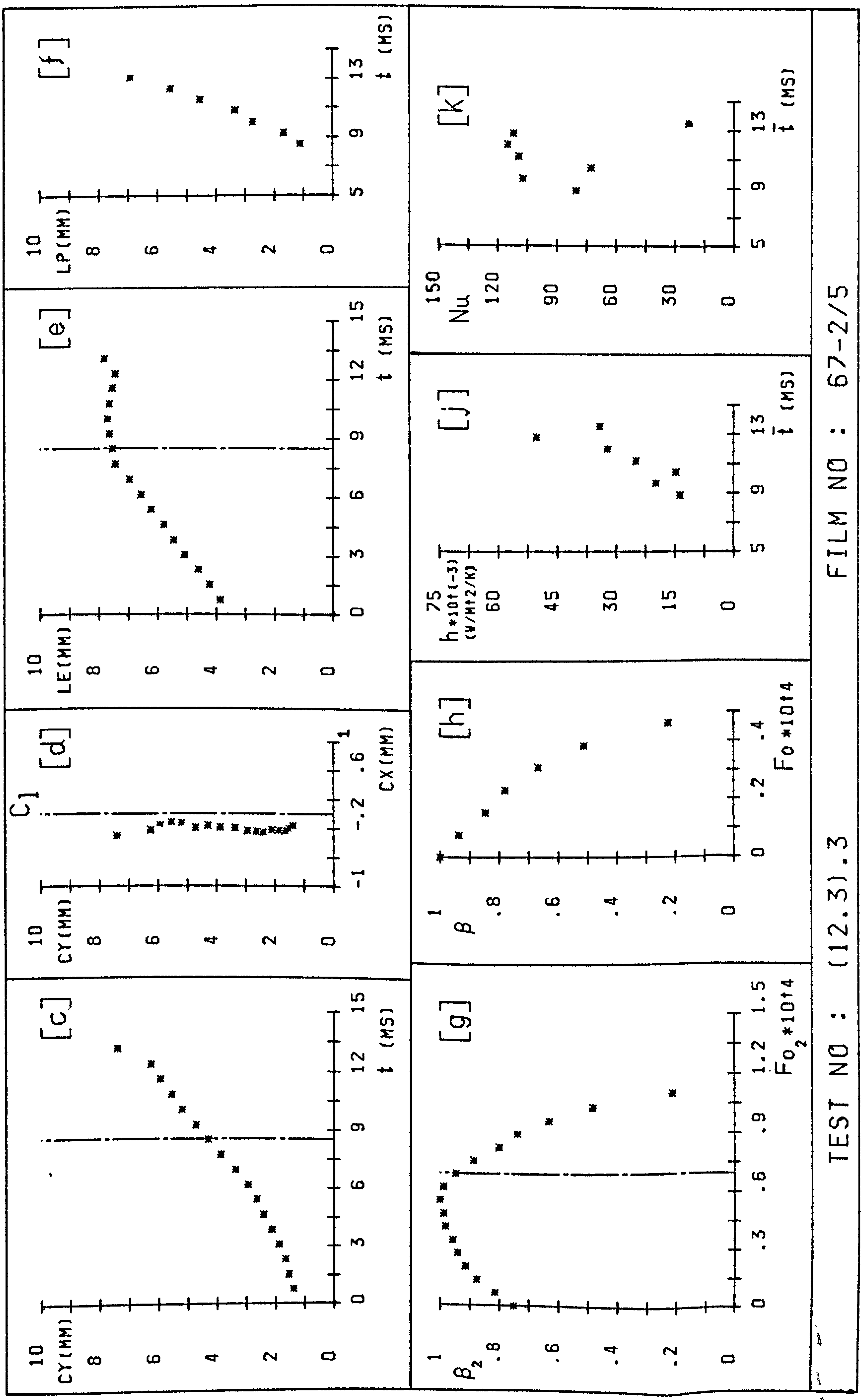
[c]
CY(MM)
t (MS)
[d]
C1
CY(MM)
CX(MM)
[e]
LE(MM)
t (MS)
[f]
LP(MM)
t (MS)
[g]
β_2
Fo_2 *10↑4
[h]
β
Fo *10↑4
[j]
h*10↑(-3) (W/M↑2/K)
t̄ (MS)
[k]
Nu
t̄ (MS)
TEST NO : (12.3).3
FILM NO : 67-2/5

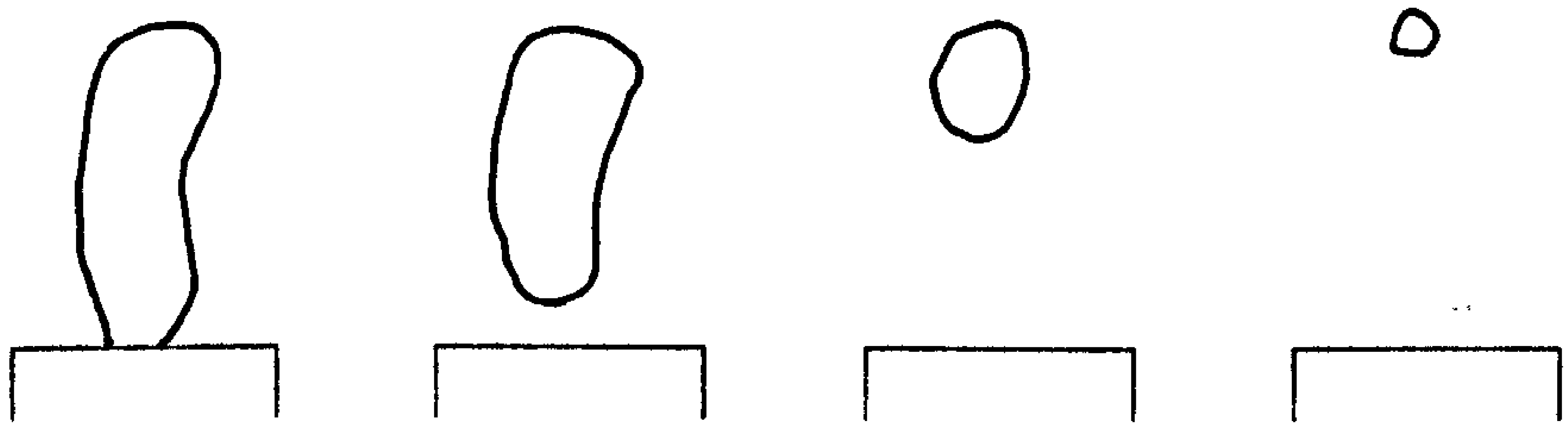

FRAME NUMBERS : 1 -11 12-13 14-15 16-18

EXPERIMENTAL PARAMETERS :

d	1	Z	40	F	18
$\dot{m}_s$	1.39	P	2.011	Ja	60
(V_s	20520)	Δt	.56	T_p	165
ΔT	36.6	(CS	1800)		

EXPERIMENTAL RESULTS :

t_g	6.68	h_c	25544	Pe_o	8200
t_c	3	Nu_c	72		
t_t	9.68	Z_d	4.16		
f_s	164	Z_c	6.14		
R_m	1.91	U	380		
R_o	1.78	Fo_c	3.91E-05		

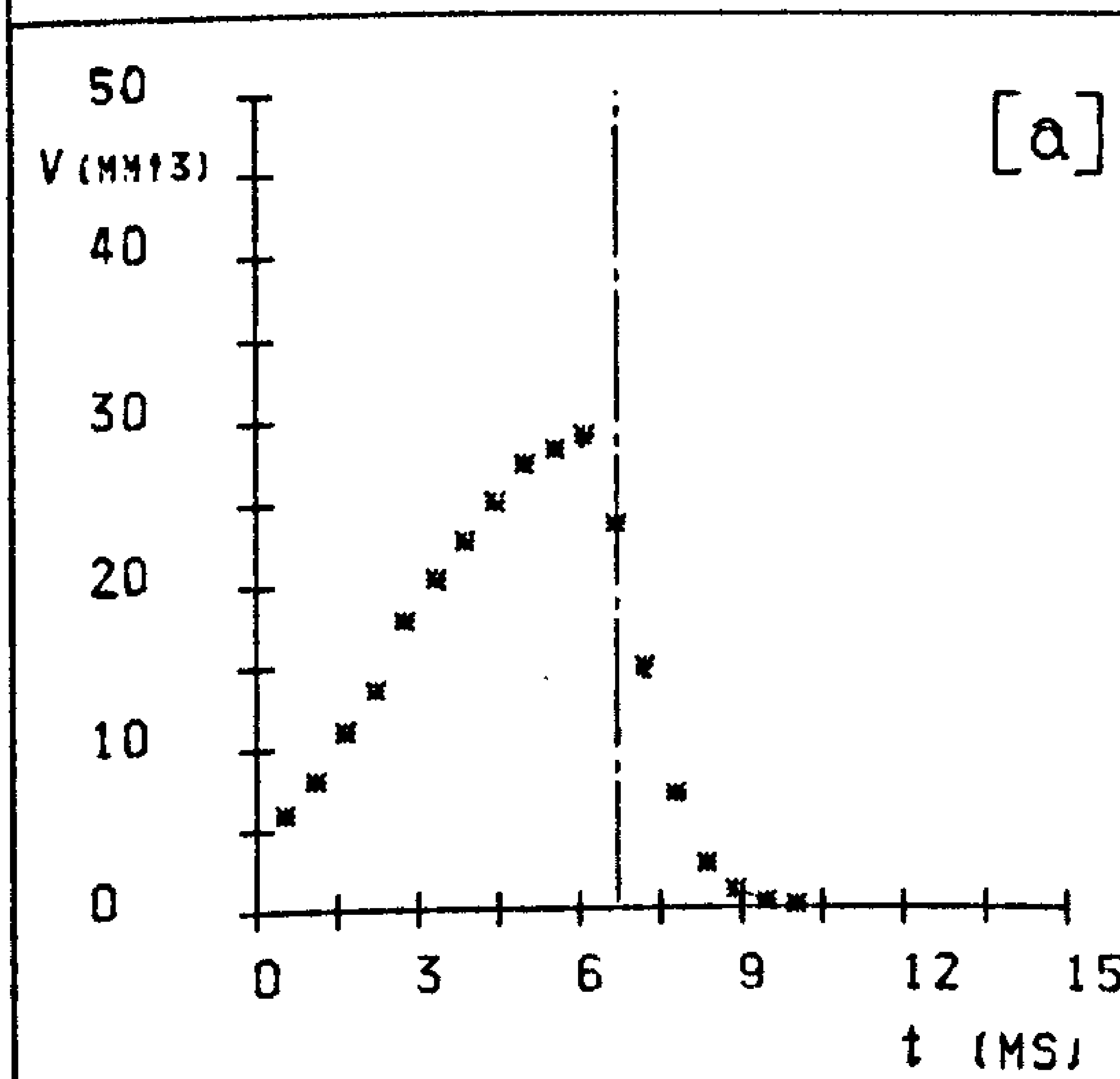

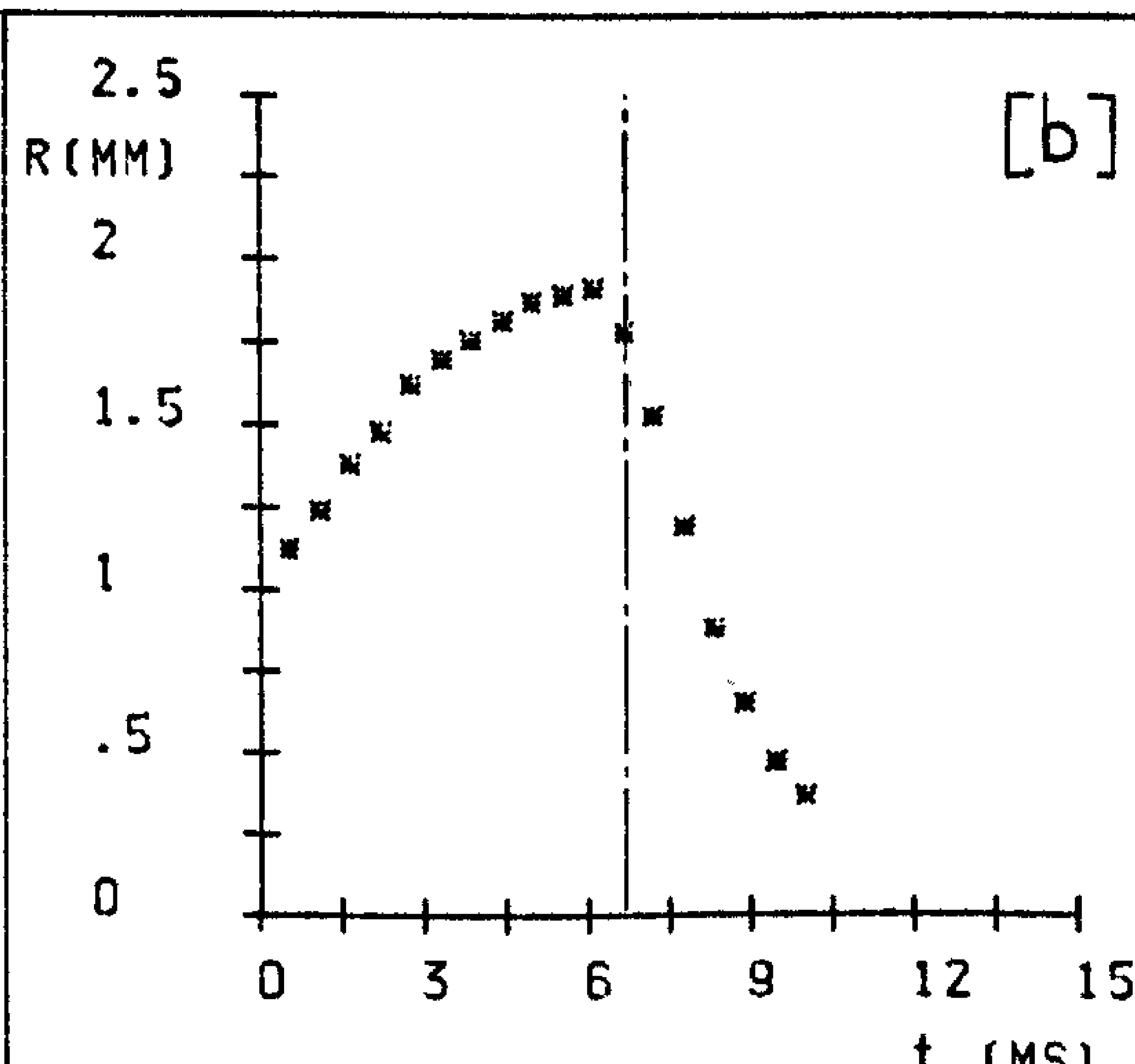

TEST NO : (12.4).3 FILM NO : 68-1/3

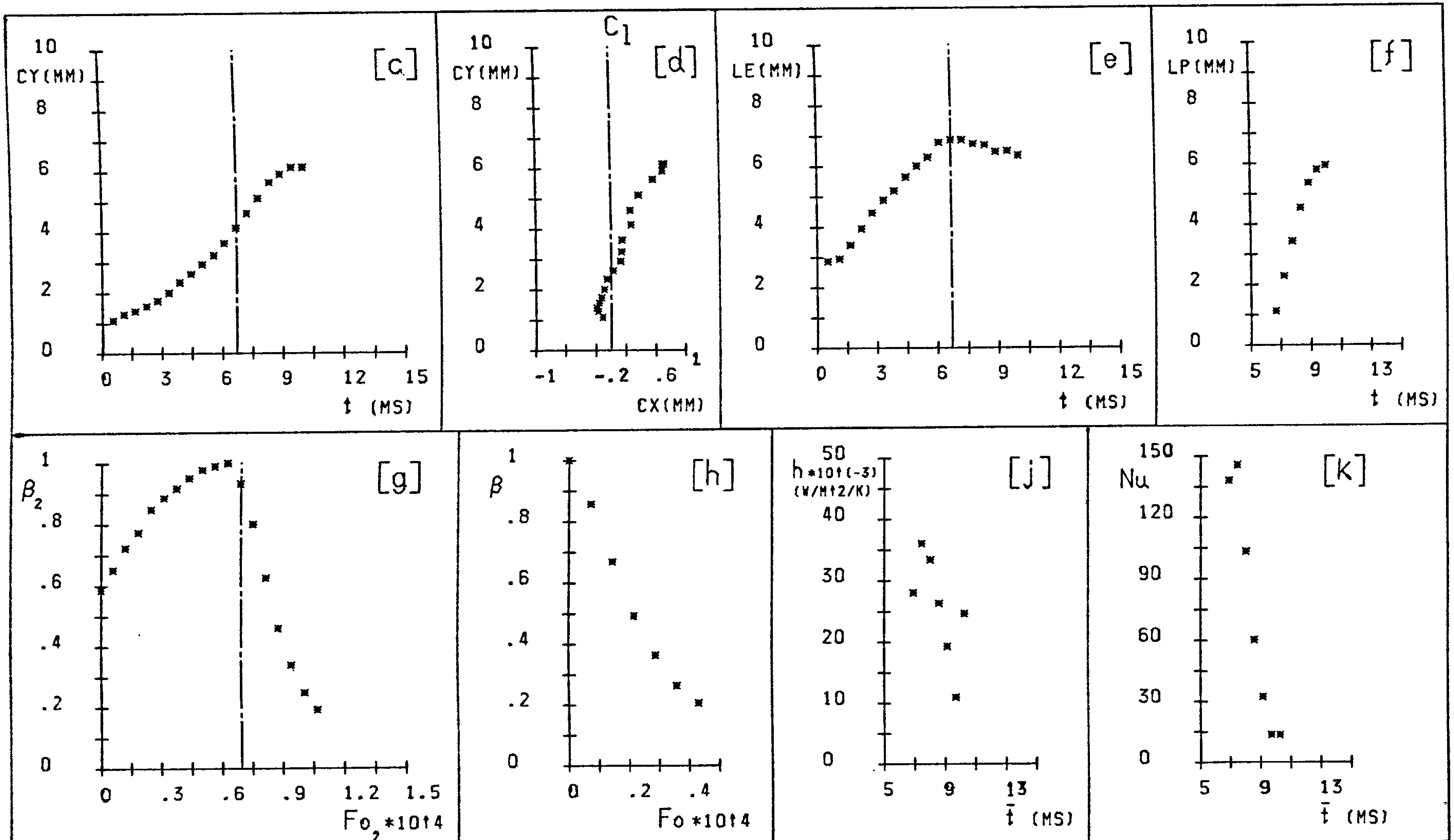

TEST NØ : (12.4).3 FILM NØ : 68-1/3

especially at low subcoolings. Values of R_o, t_c and U for each bubble are given in Table 4.2. These values, together with the thermal diffusivity of water as given in Appendix 1, were used to determine the collapse Fourier numbers $\left(Fo_c = \frac{\alpha t_c}{4R_o^2}\right)$ and the Peclet numbers $\left(Pe_o = \frac{2UR_o}{\alpha}\right)$, and these are also shown in Table 4.2.

The experimental values of Fo_c and Pe_o are plotted as shown in Figs. 4.3 to 4.10 (as functions of Jakob number and steam mass flow rate), and the resulting smoothed values for each experimental condition, as shown in Table 4.3, are used in the comparison between the experimental data and the theoretical analysis.

4.6 The bubble rise velocity

The curves of 'CY and t' shown in section 4.4 suggested that the velocity of bubble rise after detachment was generally constant, despite the effects of bubble collapse, oscillations, and distortion from the spherical shape. Thus a comparison was made of the measured rise velocities with various correlations in the literature for large bubbles. A popular one is the combination of the Peebles and Garber [46] expression $U = \left(\frac{\sigma}{R\rho_f}\right)^{\frac{1}{2}}$ with the Davies and Taylor [47] expression

Test No.	Bubble symbol	R_o (mm)	t_c (ms)	U (mm/s)	$Fo_c.10^4$	Pe_o
1.1	x	3.54	27.0	476	0.902	20130
	+	3.57	27.5	465	0.903	19830
	*	3.46	26.0	480	0.909	19840
1.2	x	2.30	8.25	437	0.649	12080
	+	2.31	8.0	580	0.624	16100
	*	2.01	7.0	560	0.721	13530
2.1	x	4.70	34.7	522	0.657	29310
	+	4.49	35.0	524	0.726	28110
	*	4.39	32.0	514	0.695	26960
2.2	x	3.34	13.0	605	0.485	24290
	+	3.58	13.5	502	0.438	21600
	*	3.80	15.0	520	0.432	23750
2.3	x	2.15	4.5	775	0.402	20170
	+	2.29	4.5	533	0.354	14780
	*	2.27	4.0	533	0.321	14650
3.1	x	4.92	31.0	714	0.536	41970
	+	5.25	35.6	643	0.541	40330
	*	3.87	20.0	802	0.559	37080
3.2	x	4.63	19.0	590	0.369	32830
	+	4.39	17.0	600	0.367	31660
	*	4.58	18.0	590	0.357	32480
3.3	x	3.55	8.3	800	0.272	34380
	+	3.13	6.1	830	0.257	31450
	*	3.39	6.7	800	0.241	32830

Table 4.2 Values of R_o, t_c, U, Fo_c and Pe_o for each bubble

Test No.	Bubble symbol	R_o (mm)	t_c (ms)	U (mm/s)	$Fo_c.10^4$	Pe_o
	x	3.08	5.5	810	0.238	30390
3.4	+	2.75	4.65	940	0.252	31490
	*	3.13	5.4	740	0.226	28210
	x	2.43	23.7	250	1.706	7150
4.1	+	2.45	24.7	250	1.749	7210
	*	2.52	25.3	250	1.693	7410
	x	2.12	11.5	311	1.081	7800
4.2	+	2.16	12.0	249	1.087	6360
	*	2.16	12.0	249	1.087	6360
	x	3.43	27.0	346	0.975	13960
5.1	+	3.42	30.0	338	1.090	13600
	*	3.37	30.0	350	1.123	13880
	x	2.68	13.5	338	0.794	10720
5.2	+	2.74	14.2	320	0.799	10380
	*	2.72	13.0	325	0.742	10460
	x	2.02	7.3	340	0.747	8230
5.3	+	2.29	8.7	293	0.693	8040
	*	2.29	8.7	247	0.693	6770
	x	3.31	25.0	520	0.970	20250
6.1	+	3.37	23.0	589	0.861	23350
	*	3.08	22.0	575	0.986	20840
	x	3.16	12.5	390	0.529	14580
6.2	+	3.04	12.5	495	0.571	17810
	*	3.07	12.5	555	0.560	20160

Table 4.2 (continued)

Test No.	Bubble symbol	R_o (mm)	t_c (ms)	U (mm/s)	$Fo_c.10^4$	Pe_o
	x	2.56	7.5	493	0.478	15115
6.3	+	2.71	8.0	460	0.455	14930
	*	2.73	7.5	447	0.420	14610
	x	2.27	5.0	447	0.400	12300
6.4	+	2.27	5.2	423	0.416	11640
	*	2.40	5.9	427	0.422	12420
	x	3.73	29.0	500	0.870	22340
7.1	+	3.62	27.5	465	0.877	20160
	*	3.65	27.0	495	0.846	21640
	x	3.00	11.5	450	0.530	16270
7.2	+	2.62	10.5	515	0.635	16260
	*	2.63	10.5	515	0.630	16320
	x	1.85	4.0	533	0.477	11950
7.3	+	1.91	4.9	533	0.554	12340
	*	2.00	3.9	733	0.402	17770
	x	4.03	22.5	600	0.578	28960
8.1	+	3.90	25.0	570	0.686	26620
	*	3.44	18.8	680	0.663	28010
	x	2.99	9.6	613	0.446	22080
8.2	+	3.09	10.2	593	0.443	22080
	*	3.13	10.9	593	0.462	22360
	x	2.34	6.2	600	0.467	17020
8.3	+	2.71	6.4	510	0.359	16750
	*	2.73	5.5	650	0.305	21510

Table 4.2 (continued)

Test No.	Bubble symbol	R_o (mm)	t_c (ms)	U (mm/s)	$Fo_c.10^4$	Pe_o
	x	2.02	3.3	740	0.332	18230
8.4	+	2.41	4.1	560	0.289	16460
	*	2.06	3.6	547	0.347	13740
	x	3.51	12.0	627	0.404	26520
9.2	+	3.52	11.0	627	0.368	26590
	*	3.42	11.4	700	0.404	28840
	x	2.73	6.3	650	0.349	21510
9.3	+	2.80	6.6	600	0.347	20360
	*	3.33	8.8	540	0.327	21800
	x	2.06	3.7	587	0.357	14750
9.4	+	2.07	3.7	587	0.354	14820
	*	2.09	3.5	587	0.329	14960
	x	1.60	1.87	840	0.298	16490
9.5	+	1.74	1.90	764	0.256	16310
	*	1.69	2.10	640	0.300	13270
	x	2.66	30.0	258	1.802	8070
10.1	+	2.63	29.3	258	1.800	7980
	*	2.55	28.0	258	1.830	7740
	x	1.93	9.3	285	1.055	6510
10.2	+	1.96	8.8	284	0.968	6590
	*	2.01	10.0	284	1.046	6760
	x	2.33	18.0	443	1.409	12140
11.1	+	2.65	24.7	305	1.495	9510
	*	2.53	23.3	329	1.547	9790

Table 4.2 (continued)

Test No.	Bubble symbol	R_o (mm)	t_c (ms)	U (mm/s)	$Fo_c.10^4$	Pe_o
	x	2.05	8.0	727	0.804	17640
11.2	+	2.00	7.5	633	0.792	14980
	*	1.88	8.0	413	0.956	9190
	x	1.69	4.6	420	0.672	8500
11.3	+	1.60	4.5	560	0.734	10730
	*	1.74	4.7	520	0.648	10840
	x	3.54	30.0	412	1.017	17160
12.1	+	3.15	28.0	471	1.199	17450
	*	3.29	28.0	471	1.099	18230
	x	2.41	9.5	433	0.691	12350
12.2	+	2.41	9.5	447	0.691	12750
	*	2.52	9.5	420	0.632	12530
	x	1.92	5.4	480	0.612	11040
12.3	+	2.01	4.5	540	0.465	13000
	*	2.04	4.8	463	0.482	11310
	x	1.56	2.70	533	0.458	10080
12.4	+	1.71	2.87	760	0.405	15750
	*	1.78	3.00	380	0.391	8200

Table 4.2 (continued)

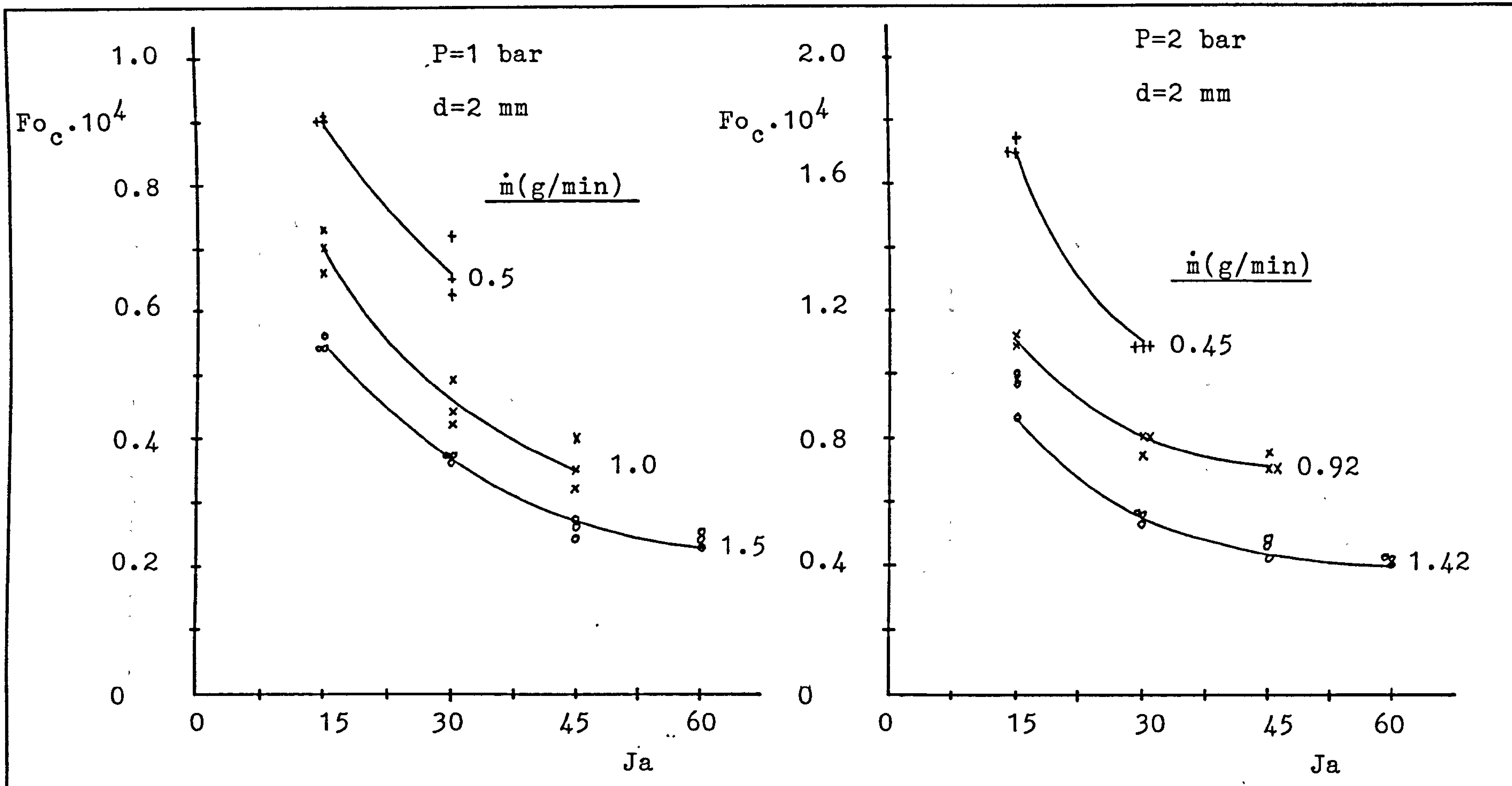

Fig.4.3 Fo_c versus Ja for different $\dot{m}$

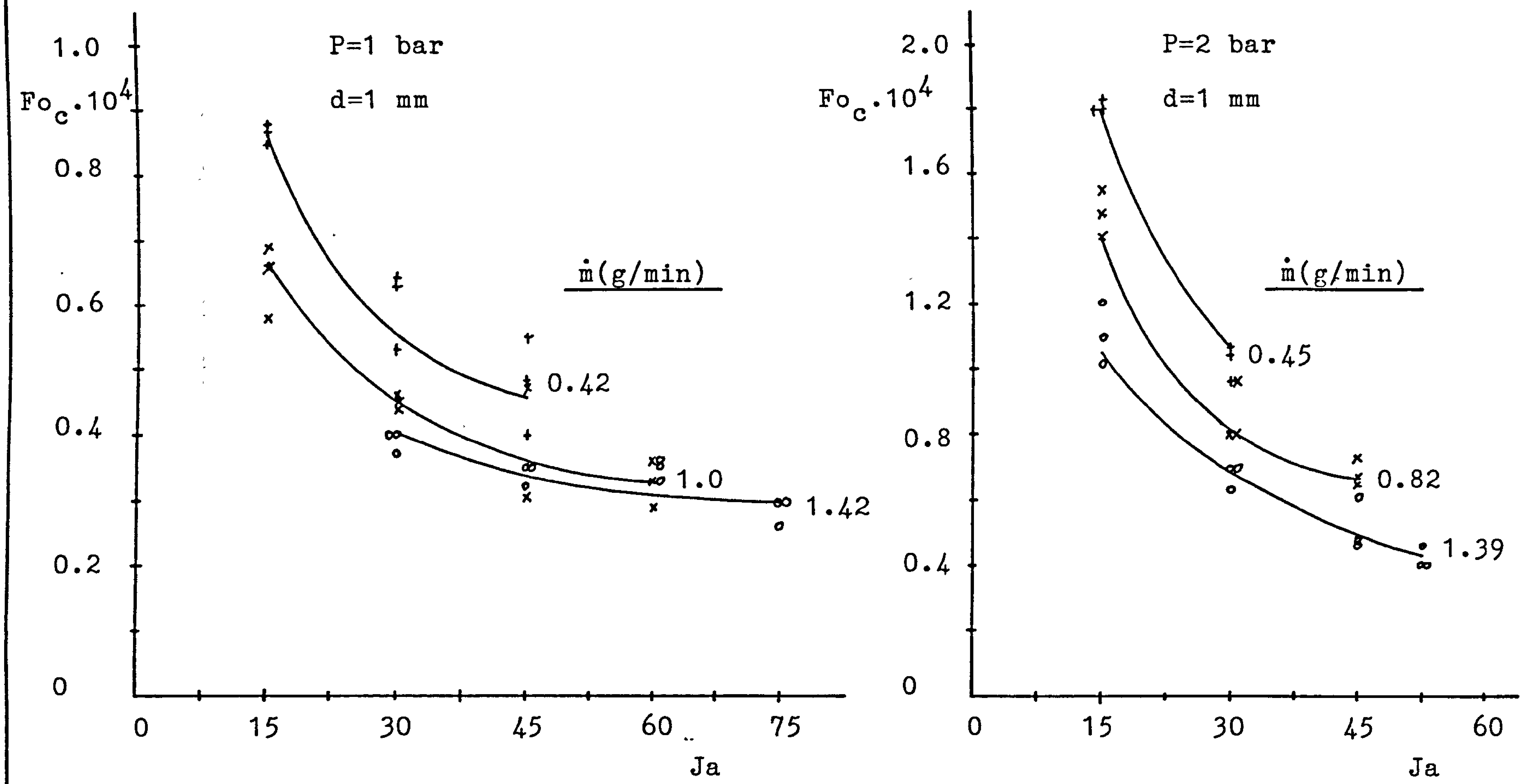

Fig.4.4 Fo_c versus Ja for different $\dot{m}$

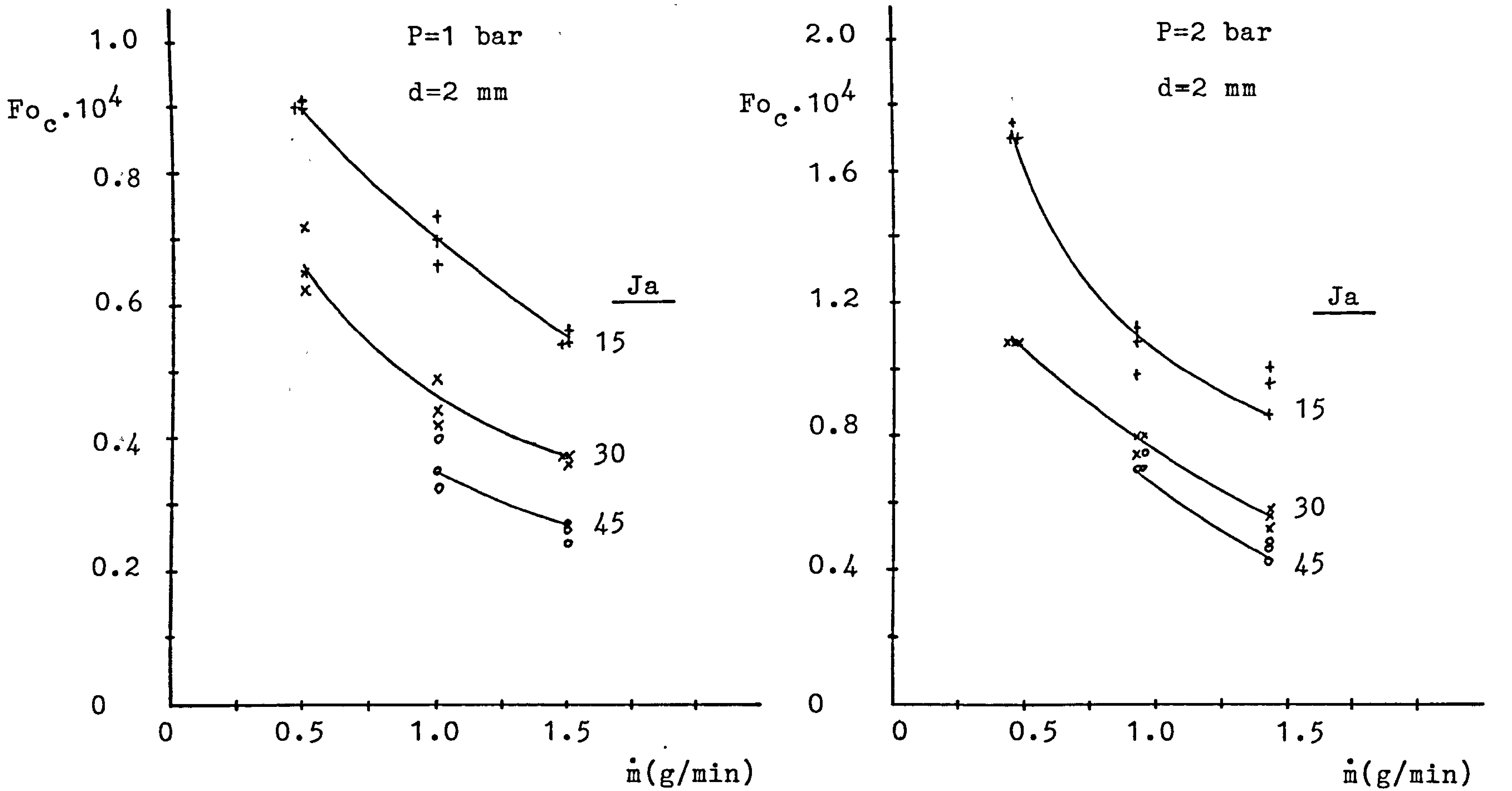

Fig.4.5 Fo_c versus $\dot{m}$ for different Ja

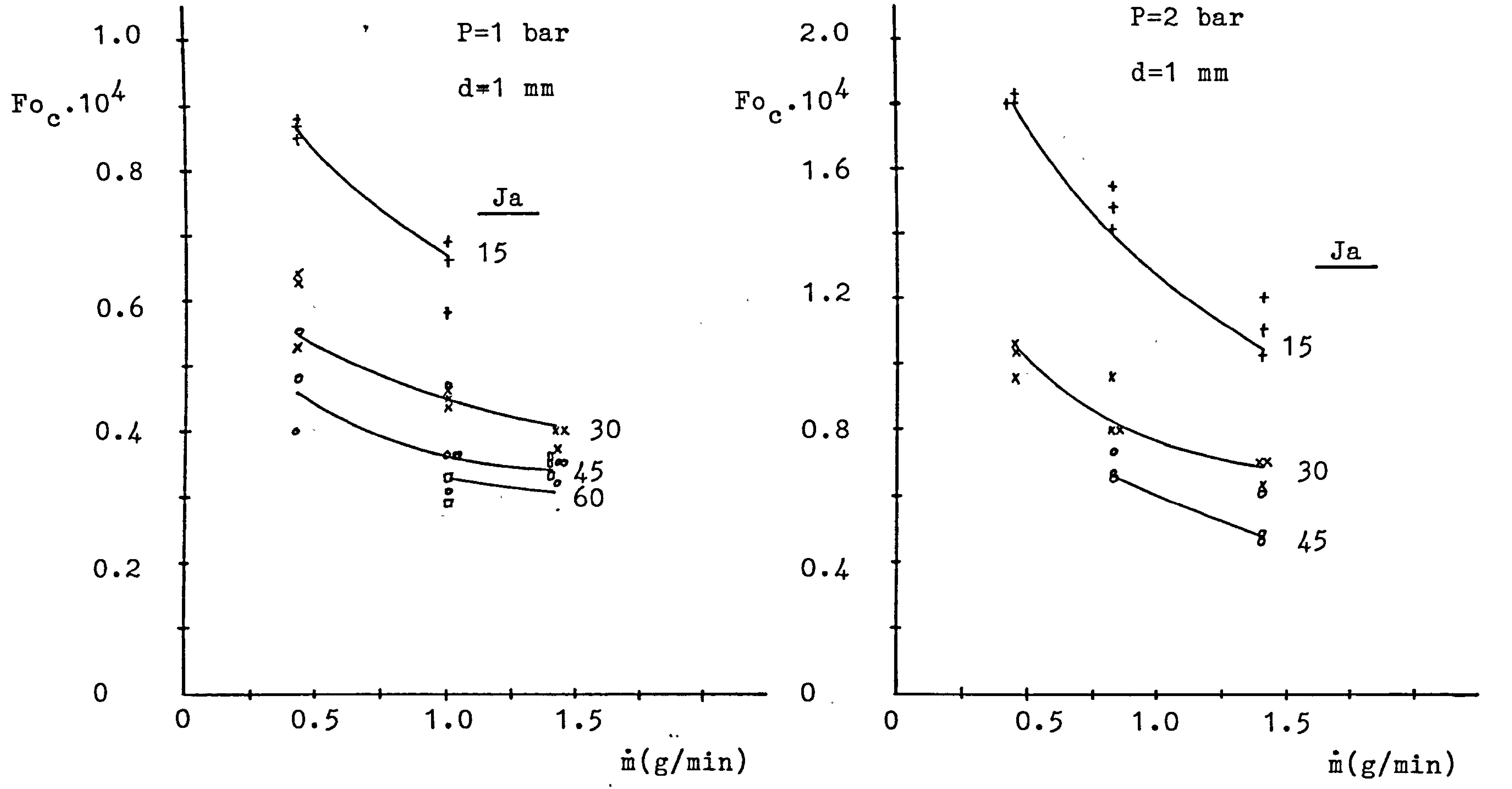

Fig.4.6 Fo_c versus $\dot{m}$ for different Ja

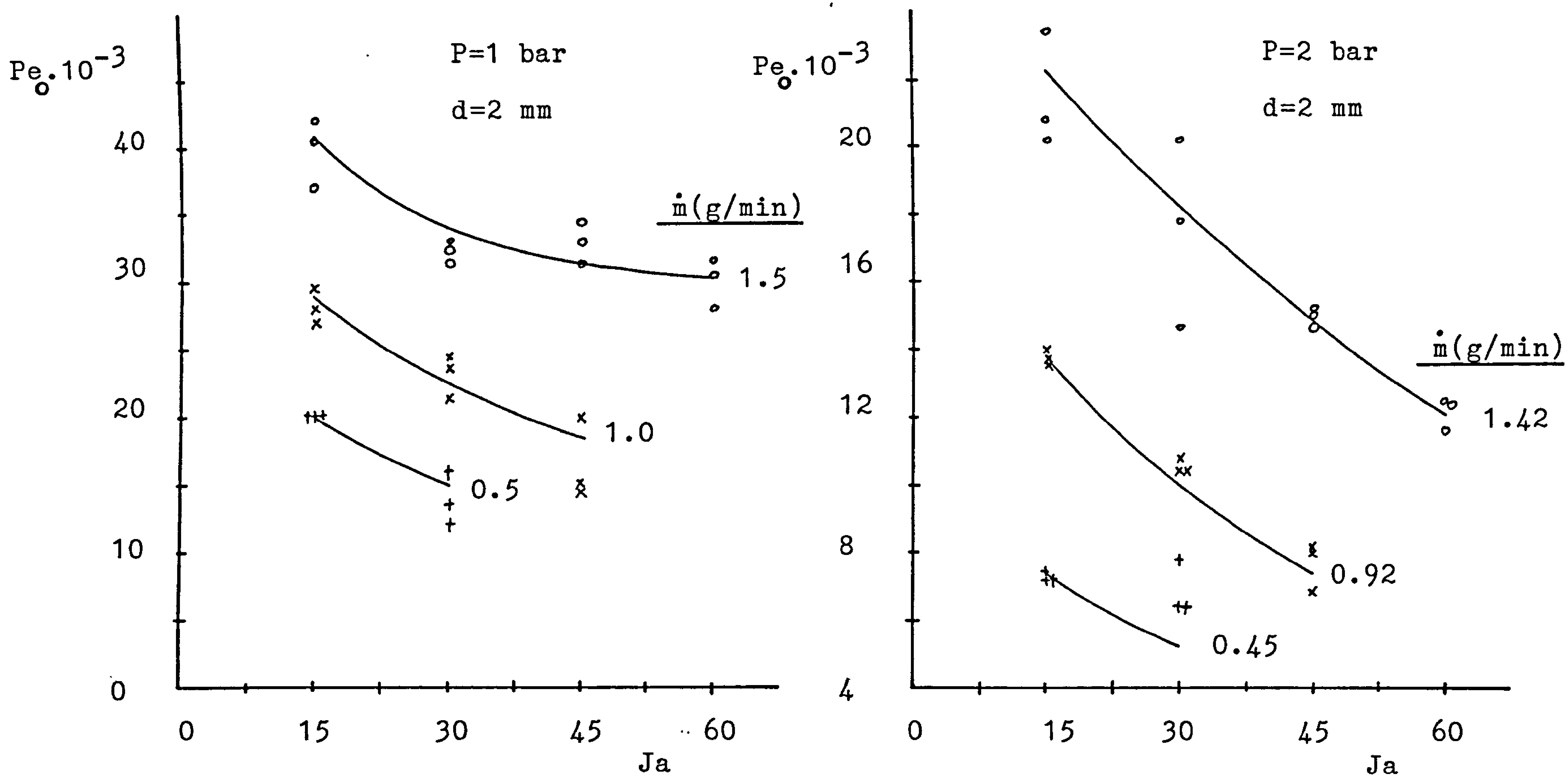

Fig.4.7 Pe_o versus Ja for different $\dot{m}$

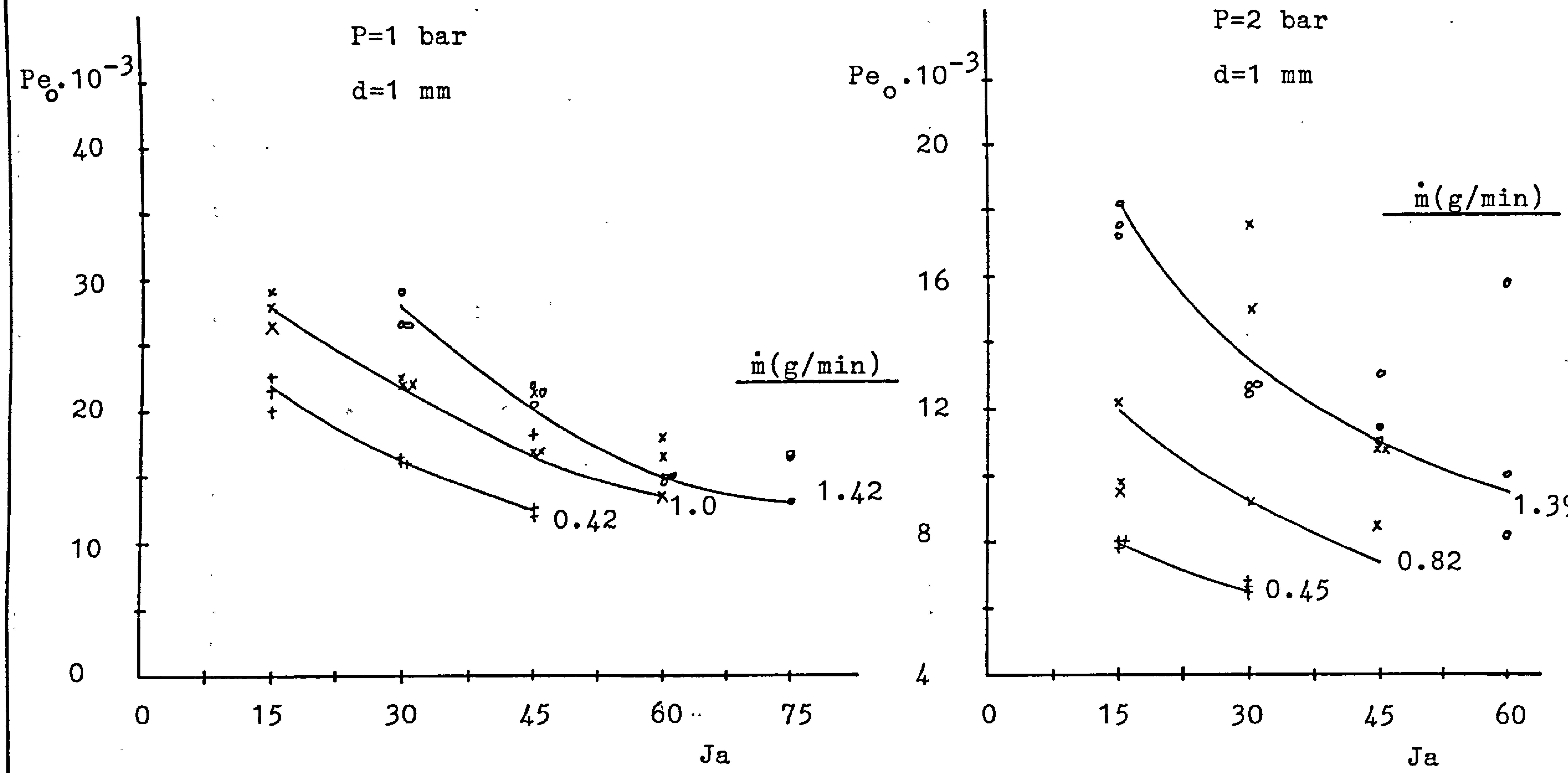

Fig.4.8 Pe_o versus Ja for different $\dot{m}$

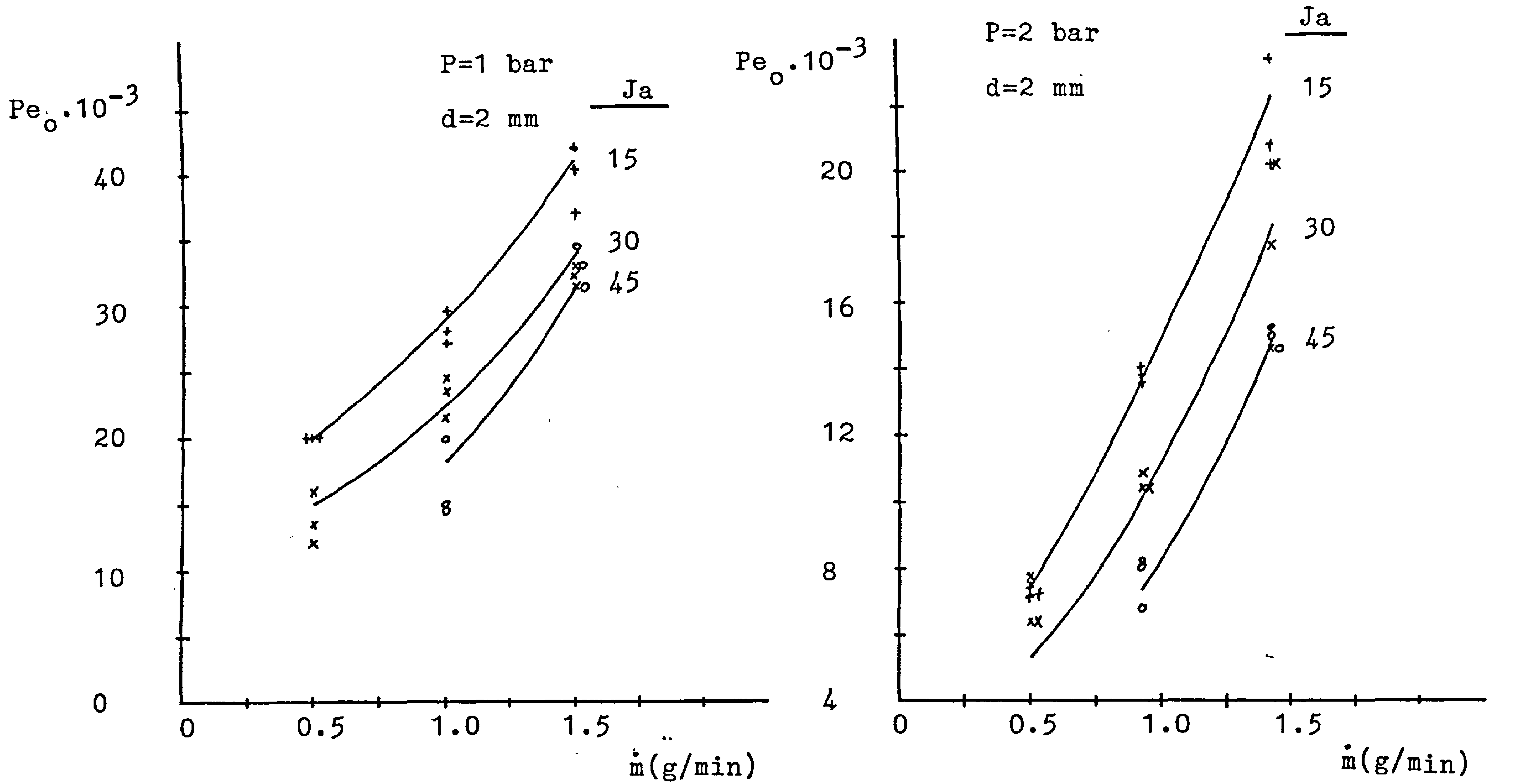

Fig.4.9 Pe_o versus $\dot{m}$ for different Ja

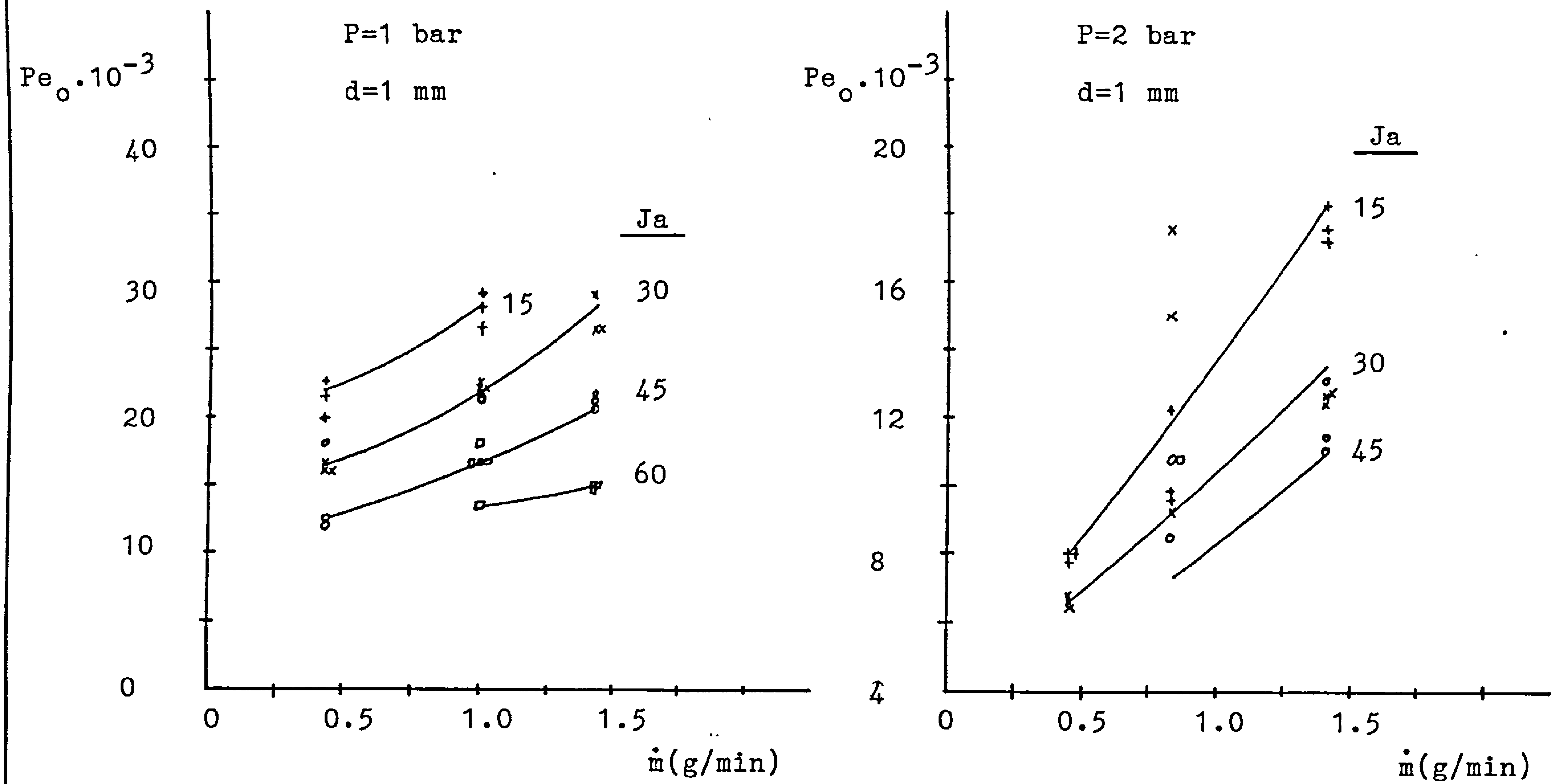

Fig.4.10 Pe_o versus $\dot{m}$ for different Ja

Test No.	$Fo_c.10^4$	Pe_o
1.1	0.90	19800
1.2	0.66	15000
2.1	0.70	29000
2.2	0.46	22300
2.3	0.35	18400
3.1	0.55	41000
3.2	0.37	34000
3.3	0.27	31500
3.4	0.23	30200
4.1	1.72	7400
4.2	1.10	5300
5.1	1.10	13800
5.2	0.79	10000
5.3	0.70	7400
6.1	0.86	22400
6.2	0.55	18300
6.3	0.43	14800
6.4	0.40	12100

Table 4.3 The smoothed values of Fo_c and Pe_o for each experimental condition

Test No.	$Fo_o.10^4$	Pe_o
7.1	0.87	22000
7.2	0.55	16500
7.3	0.46	12500
8.1	0.67	28000
8.2	0.45	22000
8.3	0.36	16600
8.4	0.33	13300
9.2	0.41	28000
9.3	0.34	20500
9.4	0.31	15000
9.5	0.30	13000
10.1	1.80	8000
10.2	1.06	6500
11.1	1.40	12000
11.2	0.82	9200
11.3	0.66	7400
12.1	1.05	18200
12.2	0.68	13500
12.3	0.49	11000
12.4	0.43	9500

Table 4.3 (Continued)

$$U = \left(\frac{\rho_f - \rho_g}{\rho_f} . gR\right)^{1/2}$$ in the form,

$$U_1 = \left(\frac{\sigma}{R\,\rho_f} + \frac{\rho_f - \rho_g}{\rho_f} . gR\right)^{1/2} \qquad (4.4)$$

A justification for this type of expression was given by Mendelson [48]. The average rise velocities, U and the initial radii, R_O for the different Jakob numbers and system pressures are given in table 4.4. Bubble rise velocities, U_1 determined from equation (4.4) using the initial bubble radius are also presented in table 4.4 together with the ratio of the velocities.

A comparison of the velocities according to equation (4.4) with the observed velocities, as shown in Fig. 4.11, indicated that equation (4.4) underpredicted the experimental results by a factor between 1.67 and 3.18, and that in addition U appeared to vary with the collapse rate through the Jakob number and with the pressure relative to a reference pressure, P_O = 1 bar. Consequently, we employed an empirical correlation of the form ,

$$U = 2.148\left(\frac{P_O}{P}\right)^{1/2}(1+6.52.10^{-3}\ Ja)\left(\frac{\sigma}{R_O\,\rho_f} + \frac{\rho_f - \rho_g}{\rho_f} . g . R_O\right)^{1/2} \qquad (4.5)$$

and this was found to describe the experimental data with a percentage deviation of about 2%, as shown in Fig. 4.12.

P = 1 bar				
Ja	U (mm/s)	R_o (mm)	U_1 (mm/s)	$\frac{U}{U_1} \cdot (\frac{P}{P_o})^{\frac{1}{2}}$
15	563	4.04	234	2.41
30	568	3.27	226	2.51
45	641	2.61	223	2.87
60	678	2.41	224	3.03
75	748	1.68	235	3.18

P = 2 bar					
Ja	U (mm/s)	R_o (mm)	U_1 (mm/s)	$\frac{U}{U_1}$	$\frac{U}{U_1} \cdot (\frac{P}{P_o})^{\frac{1}{2}}$
15	371	2.94	222	1.67	2.36
30	398	2.39	221	1.80	2.55
45	434	2.13	224	1.94	2.74
60	495	2.00	227	2.18	3.08

Table 4.4 Measured and calculated bubble rise velocities and the velocity ratio. (P_o = 1 bar)

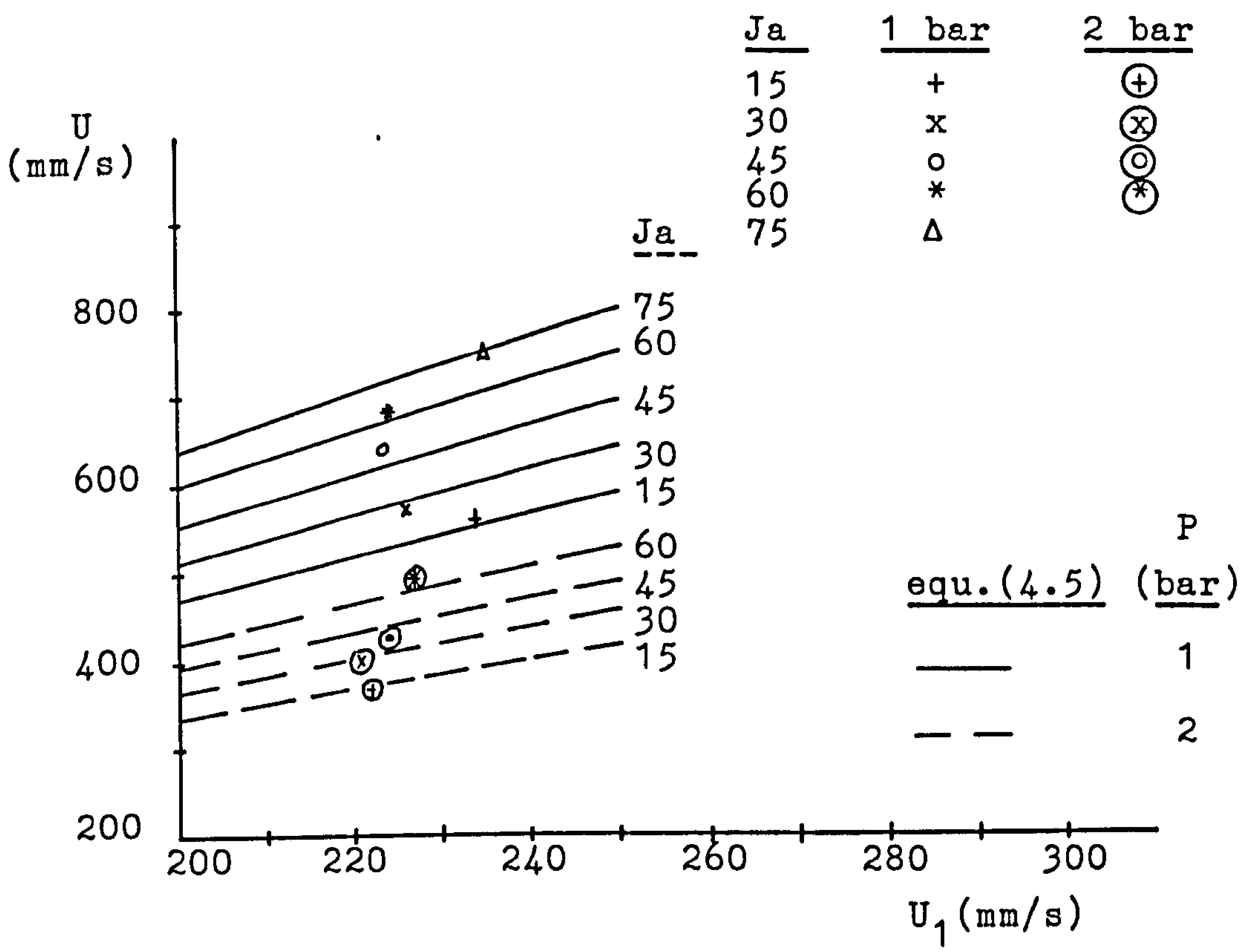

Fig.4.11 Measured bubble rise velocity versus velocity according to equation(4.4).

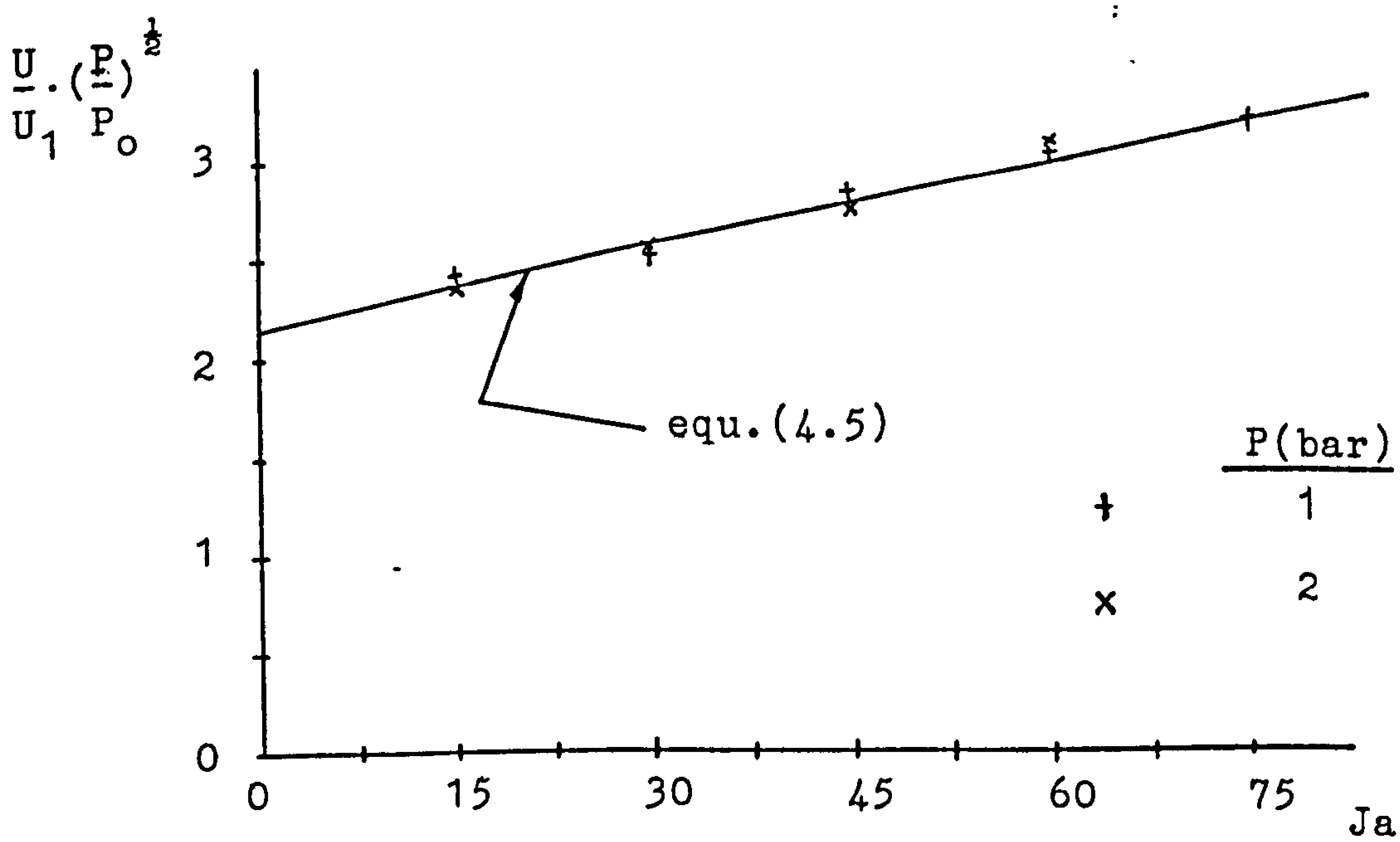

Fig.4.12 Rise velocity ratio versus Jakob number

CHAPTER 5

THEORETICAL ANALYSIS

5.1 Introduction

It has already been pointed out that very little research has been carried out into the condensation of vapour bubbles in subcooled liquids and that the existing quasi-steady state theories did not, in general, take account of radial velocities, despite the fact that, especially at high subcoolings, the radial velocities were comparable with the rise velocity of the bubble.

Ruckenstein and Davis [31] presented a general solution for a growing bubble with allowance made for radial velocity effects, but this solution is not considered to be suitable for ready engineering use.

A simplified approximate solution is presented below, allowing for radial velocities in addition to the velocities due to the vertical motion of the bubbles.

5.2 The Model

The collapsing bubble (illustrated in Fig. 5.1) is assumed to be spherical and rising freely in a vertical path with a constant velocity, U. Alternatively, it can be visualised as being at rest with the continuous medium moving against it with an approach velocity, U.

5.2.1 The energy equation

The convection of heat in the water flowing around a spherical bubble is assumed to be given, in spherical coordinates, by the energy equation as

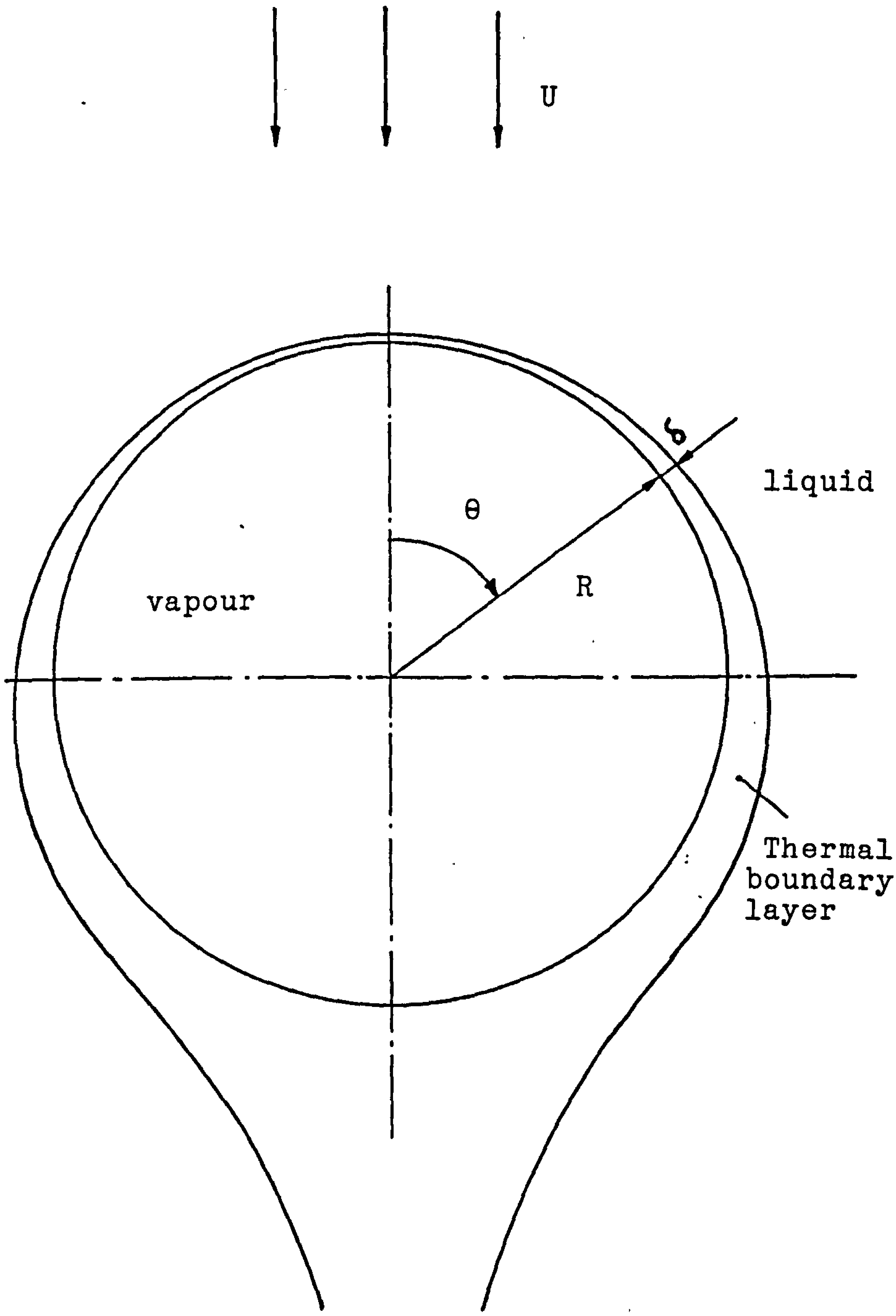

Fig.5.1 Theoretical bubble collapse model

$$\frac{\partial T}{\partial t} + u_r \frac{\partial T}{\partial r} + \frac{u_\theta}{r} \frac{\partial T}{\partial \theta} = \alpha \left(\frac{\partial^2 T}{\partial r^2} + \frac{2}{r}\frac{\partial T}{\partial r}\right) \quad (5.1)$$

where conduction in the tangential direction is assumed to be much smaller than in the radial direction, and hence is neglected. Viscous dissipation is also neglected because flow around the bubble is assumed to be inviscid.

Assuming simplified potential flow around the bubble and that the thickness of the thermal boundary layer is small, the velocities in the radial direction, u_r and in the tangential direction u_θ are given as

$$u_r = -U\left[1-\left(\frac{R}{r}\right)^3\right]\cos\theta + \dot{R}\,\frac{R^2}{r^2} \quad (5.2)$$

$$u_\theta = U\left[1+\frac{1}{2}\left(\frac{R}{r}\right)^3\right]\sin\theta \quad (5.3)$$

Changing the coordinate system to a moving coordinate, $y = r-R$ and neglecting second or higher order terms since

$$\frac{y}{R} << 1$$

$$u_r = -U\left[1-\left(1+\frac{y}{R}\right)^{-3}\right]\cos\theta + \dot{R}\left(1+\frac{y}{R}\right)^{-2}$$

$$\cong -U\left[1-\left(1-3\frac{y}{R}\right)\right]\cos\theta + \dot{R}\left(1-2\frac{y}{R}\right)$$

$$\therefore \quad u_r \cong -3U\frac{y}{R}\cos\theta + \dot{R}\left(1-2\frac{y}{R}\right) \quad (5.4)$$

$$u_\theta = U\left[1+\frac{1}{2}\left(1-3\frac{y}{R}\right)\right]\sin\theta$$

neglecting y/R term,

$$u_\theta \cong \frac{3}{2}U\sin\theta \quad (5.5)$$

Returning to the energy equation (5.1),

$$\frac{\partial^2 T}{\partial r^2} \sim \frac{T}{y^2} \text{ and } \frac{2}{r}\frac{\partial T}{\partial r} \sim \frac{2}{r}\frac{T}{y}$$

Hence $\frac{\partial^2 T}{\partial r^2} >> \frac{2}{r}\frac{\partial T}{\partial r}$, and the term $\frac{2}{r}\frac{\partial T}{\partial r}$

can be neglected.

In the moving coordinate system,

$$\left(\frac{\partial T}{\partial t}\right)_{r,\theta} = \left(\frac{\partial T}{\partial t}\right)_{y,\theta} - \dot{R}\left(\frac{\partial T}{\partial y}\right) \text{ and } \frac{\partial T}{\partial r} = \frac{\partial T}{\partial y}$$

Thus equation (5.1) becomes,

$$\frac{\partial T}{\partial t} - \frac{y}{R}\left[3U\cos\theta + 2\dot{R}\right]\frac{\partial T}{\partial y} + \frac{3}{2}\frac{U}{R}\sin\theta\frac{\partial T}{\partial \theta} = \alpha\frac{\partial^2 T}{\partial y^2} \tag{5.6}$$

which is equation (9) of Ruckenstein and Davis [31].

If it is now further assumed that*

$\frac{\partial T}{\partial t} << \frac{y}{R}\dot{R}\frac{\partial T}{\partial y}$ and if equation (5.6) is integrated across the thermal boundary layer thickness $\delta(\theta)$,

$$\alpha\int_0^\delta \frac{\partial^2 \phi}{\partial y^2}dy = -\left(3\frac{U}{R}\cos\theta + 2\frac{\dot{R}}{R}\right)\int_0^\delta y\frac{\partial \phi}{\partial y}dy + \frac{3}{2}\frac{U}{R}\sin\theta\frac{\partial}{\partial \theta}\int_0^\delta \phi dy \tag{5.7}$$

where ϕ is the dimensionless temperature ratio,

$$\frac{T - T_\infty}{T_1 - T_\infty}$$

Assuming the boundary condition,

$$\frac{\partial \phi}{\partial y} = 0 \text{ at } y = \delta$$

the left hand side of equation (5.7) becomes

* Quasi-steady state assumption

$$\alpha \int_0^{\delta} \frac{\partial^2\phi}{\partial y^2}dy = \alpha\frac{\partial\phi}{\partial y}\Big|_0^{\delta} = -\alpha\left(\frac{\partial\phi}{\partial y}\right)_{y=0} \qquad (5.8)$$

and equation (5.7) is expressed as

$$-\alpha\left(\frac{\partial\phi}{\partial y}\right)_{y=0} = -\left(3\frac{U}{R}\cos\theta+2\frac{\dot{R}}{R}\right)\int_0^{\delta} y\frac{\partial\phi}{\partial y}dy+\frac{3}{2}\,\frac{U}{R}\,\sin\theta\frac{\partial}{\partial\theta}\int_0^{\delta}\phi dy \qquad (5.9)$$

As in boundary layer theory, if ϕ is taken to be a simple power series in y, equation (5.9) can be simplified further. Here a cubic of the form,

$$\phi = \frac{3}{2}\left(1-\frac{y}{\delta}\right)^2 - \frac{1}{2}\left(1-\frac{y}{\delta}\right)^3 \qquad (5.10)$$

is assumed, with boundary conditions

$$\phi = 1 \quad , \quad \frac{\partial^2\phi}{\partial y^2} = 0 \quad \text{at } y = 0$$

$$\text{and } \phi = \frac{\partial\phi}{\partial y} = 0 \quad \text{at } y = \delta$$

As the temperature at the vapour-liquid interface, T_i is constant at all points on the bubble surface,

$$\frac{\partial\phi}{\partial\theta} = 0 \qquad (5.11)$$

Calculating the terms in equation (5.9) by substituting the value of ϕ, given by equation (5.10),

$$\left(\frac{\partial\phi}{\partial y}\right)_{y=0} = \left(-\frac{3}{\delta}\left(1-\frac{y}{\delta}\right) + \frac{3}{2\delta}\left(1-\frac{y}{\delta}\right)^2\right)_{y=0} = -\frac{3}{2\delta} \qquad (5.12)$$

$$\int_0^{\delta} y\frac{\partial\phi}{\partial y}dy = \frac{1}{\delta}\int_0^{\delta} y\left[-3\left(1-\frac{y}{\delta}\right) + \frac{3}{2}\left(1-\frac{y}{\delta}\right)^2\right]dy$$

$$= \frac{1}{\delta}\int_0^\delta y[-3+\frac{3y}{\delta} + \frac{3}{2}(1-\frac{2y}{\delta} + \frac{y^2}{\delta^2})]dy$$

$$= \frac{1}{\delta}\int_0^\delta y\ [-3 + \frac{3}{2} + \frac{3}{2}\frac{y^2}{\delta^2}\ ]dy$$

$$= \frac{3}{2\delta}\int_0^\delta y\ (\frac{y^2}{\delta^2} - 1)dy = \frac{3}{2\delta}\left|\frac{y^4}{4\delta^2} - \frac{y^2}{2}\right|_0^\delta$$

$$= \frac{3}{2\delta}\ (\frac{\delta^2}{4} - \frac{\delta^2}{2})$$

$$\therefore \int_0^\delta y\ \frac{\partial\phi}{\partial y}\ dy = -\ \frac{3}{8}\delta \qquad (5.13)$$

$$\int_0^\delta \phi dy = \frac{3}{2}\int_0^\delta (1-\frac{y}{\delta})^2\ dy - \frac{1}{2}\int_0^\delta (1-\frac{y}{\delta})^3\ dy$$

$$= -\left|\frac{\delta}{2}(1-\frac{y}{\delta})^3\right|_0^\delta + \left|\frac{\delta}{8}\ (1-\frac{y}{\delta})^4\right|_0^\delta = \delta\ (\frac{1}{2} - \frac{1}{8}) = \frac{3}{8}\delta$$

$$\therefore \frac{\partial}{\partial\theta}\int_0^\delta \phi dy = \frac{3}{8}\frac{\partial\delta}{\partial\theta} \qquad (5.14)$$

Substitution of equations (5.12), (5.13) and (5.14) in equation (5.9) gives,

$$\frac{3}{2}\frac{\alpha}{\delta} = (2\frac{\dot{R}}{R} + 3\frac{U}{R}\cos\theta)\frac{3}{8}\delta + \frac{9}{16}\frac{U}{R}\sin\theta\ \frac{\partial\delta}{\partial\theta}$$

$$\therefore \frac{3}{8}\frac{U}{R}\sin\theta\ \frac{\partial\delta}{\partial\theta} = \frac{\alpha}{\delta} - \frac{1}{4}\ (2\frac{\dot{R}}{R} + \frac{3U}{R}\cos\theta)\delta$$

$$\therefore \frac{\partial\delta}{\partial\theta} = \frac{\alpha}{\delta}\ \frac{8\ R}{3\ U\ \sin\theta} - \frac{2\ R}{3\ U\ \sin\theta}\ (2\frac{\dot{R}}{R} + \frac{3U}{R}\cos\theta)\delta$$

$$\therefore \frac{1}{2}\frac{\partial \delta^2}{\partial \theta} = \frac{8}{3}\frac{\alpha\ R}{U\ \sin\theta} - \frac{2}{3\ \sin\theta}\left(\frac{2\dot{R}}{U} + 3\ \cos\theta\right)\delta^2$$

Dividing by R^2 and letting $\varepsilon = \left(\frac{\delta}{R}\right)^2$ and hence $\partial\delta^2 = R^2\partial\varepsilon$,

$$\frac{\partial\varepsilon}{\partial\theta} = \frac{16}{3}\frac{\alpha}{UR\ \sin\theta} - \frac{4}{3\ \sin\theta}\left(\frac{2\dot{R}}{U} + 3\cos\theta\right)\varepsilon$$

$$\therefore \frac{\partial\varepsilon}{\partial\theta} = -\frac{4}{3}\left(\frac{2\dot{R}}{U} + 3\cos\theta\right)\frac{\varepsilon}{\sin\theta} + \frac{16}{3}\left(\frac{\alpha}{UR}\right)\frac{1}{\sin\theta} \qquad (5.15)$$

This is a first order, first degree, linear differential equation in ε, which can be solved as follows:

$$\frac{\partial\varepsilon}{\partial\theta} + P\varepsilon = Q \qquad (5.16)$$

where $P = \frac{4}{3\sin\theta}\left(\frac{2\dot{R}}{U} + 3\cos\theta\right)$ and

$$Q = \frac{16}{3}\left(\frac{\alpha}{UR}\right)\frac{1}{\sin\theta}$$

The solution for the differential equation (5.16) is given as

$$\varepsilon = e^{-\int P d\theta}\left[\int e^{\int P d\theta}.Q d\theta + c\right] \qquad (5.17)$$

Assuming $\varepsilon = 0$ when $\theta = 0$, gives $c = 0$.
Substituting the values of P and Q,

$$\int P d\theta = \frac{4}{3}\int\left(\frac{2\ \dot{R}}{U\ \sin\ \theta} + \frac{3\ \cos\ \theta}{\sin\ \theta}\right)d\theta$$

$$= \frac{4}{3}\left[\frac{2\ \dot{R}}{U}\ \ln\left(\tan\frac{\theta}{2}\right) + 3\ln(\sin\theta)\right]$$

$$= \ln\left[\sin^4\theta.\left(\tan\frac{\theta}{2}\right)^{\frac{8}{3}\frac{\dot{R}}{U}}\right]$$

$$\therefore e^{\int P d\theta} = \sin^4\theta.\left(\tan\ \frac{\theta}{2}\right)^{\frac{8}{3}\frac{\dot{R}}{U}}$$

Hence, equation (5.17) becomes,

$$\varepsilon = \frac{1}{\sin^4\theta.(\tan\frac{\theta}{2})^{\frac{8}{3}\frac{\dot{R}}{U}}} \cdot \left[\frac{16}{3}\left(\frac{\alpha}{UR}\right)\int_0^\theta \sin^3\theta.(\tan\frac{\theta}{2})^{\frac{8}{3}\frac{\dot{R}}{U}}\,d\theta\right] \tag{5.18}$$

$$\therefore \frac{\delta}{R} = \frac{1}{\sin^2\theta.(\tan\frac{\theta}{2})^{\frac{4}{3}\frac{\dot{R}}{U}}} \cdot \frac{4}{\sqrt{3}}\left(\frac{\alpha}{UR}\right)^{1/2}\left[\int_0^\theta \sin^3\theta.(\tan\frac{\theta}{2})^{\frac{8}{3}\frac{\dot{R}}{U}}\,d\theta\right]^{1/2} \tag{5.19}$$

$$\therefore \frac{\delta}{R} = \frac{4}{\sqrt{3}}\left(\frac{\alpha}{UR}\right)^{1/2}\frac{1}{\sqrt{\sin\theta.F(\theta,\frac{\dot{R}}{U})}}\left[\int_0^\theta F(\theta,\frac{\dot{R}}{U})\,d\theta\right]^{1/2} \tag{5.20}$$

$$\text{where } F(\theta,\frac{\dot{R}}{U}) = \left[\sin^3\theta.(\tan\frac{\theta}{2})^{\frac{8}{3}\frac{\dot{R}}{U}}\right] \tag{5.21}$$

The integral can be evaluated further in terms of incomplete beta functions, as follows,

Let $\zeta = \sin^2\frac{\theta}{2}$, $\alpha = -\frac{4}{3}\frac{\dot{R}}{U}$

$d\zeta = \sin\frac{\theta}{2}\cos\frac{\theta}{2}\,d\theta$

$$\therefore \frac{\sin^3\theta d\theta}{(\tan^2\frac{\theta}{2})^\alpha} = \frac{8\sin^3\frac{\theta}{2}.\cos^3\frac{\theta}{2}.(\cos^2\frac{\theta}{2})^\alpha}{(\sin^2\frac{\theta}{2})^\alpha}\,d\theta$$

$$= \frac{8\sin^2\frac{\theta}{2}\cos^2\frac{\theta}{2}\,(\cos^2\frac{\theta}{2})^\alpha}{(\sin^2\frac{\theta}{2})^\alpha}\,d\zeta = 8\zeta^{1-\alpha}\,(1-\zeta)^{1+\alpha}\,d\zeta$$

Hence,

$$\int_0^\theta \frac{\sin^3\theta}{(\tan^2\frac{\theta}{2})^\alpha}\, d\theta = 8 \int_0^\zeta \zeta^{1-\alpha}\,(1-\zeta)^{1+\alpha}\, d\zeta$$

$$= 8 \int_0^\zeta \zeta^{(2-\alpha)-1}\,(1-\zeta)^{(2+\alpha)-1}\, d\zeta = 8B_\zeta\big((2-\alpha),(2+\alpha)\big)$$

where $0 \leq \zeta \leq 1$.

Incomplete beta functions are tabulated in mathematical tables, e.g. Pearson [49].

Substitution of equation (5.20) in (5.10) gives the temperature distribution ϕ.

5.2.2 Total heat transfer from the bubble

The heat flux at an angular position θ on the surface of the bubble is given as

$$q_\theta = -k\left(\frac{\partial T}{\partial y}\right)_{y=0} = -k\left(\frac{\partial \phi}{\partial y}\right)_{y=0} \Delta T = \frac{3}{2}\,\frac{k\ \Delta T}{R}\,\left(\frac{R}{\delta}\right) \tag{5.22}$$

where (δ/R) is given by equation (5.20) and $\Delta T = T_i - T_\infty$ is the liquid subcooling.

For the simple case of $\frac{\dot{R}}{U} = 0$,

equation (5.22) can be calculated as follows:

$$F(\theta,0) = \sin^3\theta,$$

$$\left[\int_0^\theta F(\theta,0)\,d\theta\right]^{1/2} = \left[\int_0^\theta \sin^3\theta\, d\theta\right]^{1/2}$$

$$=\left[\frac{\cos^3\theta}{3} - \cos\theta + \frac{2}{3}\right]^{1/2} \tag{5.23}$$

Substituting the value of $\frac{\delta}{R}$ (with $\frac{\dot{R}}{U} = 0$)

from equation (5.20) in equation (5.22) gives,

$$\therefore q_\theta = \frac{3}{2}\cdot\frac{k.\Delta T}{R}\cdot\frac{\sin^2\theta}{\sqrt{\frac{16}{3}\left(\frac{\alpha}{UR}\right)\left(\frac{2}{3}-\cos\theta+\frac{1}{3}\cos^3\theta\right)}}$$

$$\therefore q_\theta = \frac{\rho_\ell . c_p . \Delta T . \left(\frac{3}{2}\right) \alpha U.R \sin^2\theta}{\sqrt{\frac{16}{3}\alpha UR^3\left(\frac{2}{3}-\cos\theta+\frac{1}{3}\cos^3\theta\right)}} \tag{5.24}$$

which is of the same form as the exact solution of Rückenstein [8] but gives a value 6% lower than his solution.

An energy balance on the steam bubble states that the total heat transferred from the bubble at time t is given as

$$Q = \int_0^\pi 2\pi R^2 \sin\theta q_\theta d\theta = -h_{fg}\rho_v \frac{dV}{dt} \tag{5.25}$$

where $\frac{dV}{dt}$ is the rate of change of volume of the bubble.

5.2.3 Bubble collapse rate

Substitution of the value of $\left(\frac{R}{\delta}\right)$ (where $\frac{\dot{R}}{U} \neq 0$)

from equation (5.20) in (5.22) gives,

$$q_\theta = \frac{3\sqrt{3}}{8}\cdot\frac{k.\Delta T}{R}\left(\frac{UR}{\alpha}\right)^{1/2}\frac{\left[\sin\theta . F\left(\theta,\frac{\dot{R}}{U}\right)\right]^{1/2}}{\left[\int_0^\theta F\left(\theta,\frac{\dot{R}}{U}\right)d\theta\right]^{1/2}} \tag{5.26}$$

This value is then introduced into equation (5.25) to give,

$$-h_{fg}\cdot\rho_v\cdot\frac{dV}{dt}=\frac{3\sqrt{3}}{8}.k.\Delta T.\left(\frac{UR}{\alpha}\right)^{1/2}.\ 2\pi R\int_0^{\pi}\frac{\left[\sin^3\theta.F(\theta,\frac{\dot{R}}{U})\right]^{1/2}}{\left[\int_0^{\theta}F(\theta,\frac{\dot{R}}{U})d\theta\right]^{1/2}}d\theta$$

$$\therefore -\frac{dV}{dt}=\frac{3\sqrt{6}}{8}.\left(\frac{c_p.\Delta T.\rho_1}{h_{fg}.\rho_v}\right).\left(\frac{2UR}{\alpha}\right)^{1/2}\pi R\alpha\int_0^{\pi}\frac{\left[\sin^3\theta.F(\theta,\frac{\dot{R}}{U})\right]^{1/2}}{\left[\int_0^{\theta}F(\theta,\frac{\dot{R}}{U})d\theta\right]^{1/2}}d\theta \quad (5.27)$$

The rate of change of bubble volume is expressed as

$$-\frac{dV}{dt}=-\frac{d}{dt}\left(\frac{4}{3}\pi R^3\right)=-4\pi R^2\dot{R}=-4\pi R_o^3\dot{\beta}\ \beta^2 \quad (5.28)$$

where the dimensionless radius, $\beta=\frac{R}{R_o}$.

Introducing the Fourier number, $Fo=\frac{\alpha t}{4R_o^2}$ and

substituting $\frac{d\beta}{dt}=\frac{d\beta}{dFo}\cdot\frac{\alpha}{4R_o^2}$ in equation (5.28) gives,

$$-\frac{dV}{dt}=-\pi R_o\beta^2\alpha\frac{d\beta}{dFo} \quad (5.29)$$

Thus equation (5.27) can be rearranged to give,

$$-\pi R_o\beta^2\alpha.\frac{d\beta}{dFo}=\frac{3\sqrt{6}}{8}.Ja\left(\frac{2UR}{\alpha}\right)^{1/2}\pi R\alpha.\int_0^{\pi}\frac{\left[\sin^3\theta.F(\theta,\frac{\dot{R}}{U})\right]^{1/2}}{\left[\int_0^{\theta}F(\theta,\frac{\dot{R}}{U})d\theta\right]^{1/2}}d\theta$$

$$\therefore \beta\frac{d\beta}{dFo}=-\frac{9}{4\sqrt{6}}.Ja\left(\frac{2UR_o}{\alpha}\right)^{1/2}\beta^{1/2}\int_0^{\pi}\frac{\left[\sin^3\theta.F(\theta,\frac{\dot{R}}{U})\right]^{1/2}}{\left[\int_0^{\theta}F(\theta,\frac{\dot{R}}{U})d\theta\right]^{1/2}}d\theta$$

Thus the equation for the rate of collapse of the bubble is obtained as

$$\beta^{1/2}\frac{d\beta}{dFo} = -\frac{9}{4\sqrt{6}} Ja\ Pe_o^{1/2} \int_0^{\pi} \frac{[\sin^3\theta . F(\theta.\frac{\dot{R}}{U})]^{1/2}}{[\int_0^{\theta} F(\theta,\frac{\dot{R}}{U})d\theta]^{1/2}} d\theta \tag{5.30}$$

Also,

$$\frac{\dot{R}}{U} = \frac{R_o}{U}.\frac{d\beta}{dt} = \frac{R_o}{U}\ \frac{\alpha}{4R_o^2}\ \frac{d\beta}{dFo} = \frac{1}{2}\ (\frac{\alpha}{2UR_o}).\frac{d\beta}{dFo}$$

$$\therefore \frac{\dot{R}}{U} = \frac{1}{2\ Pe_o}\ \frac{d\beta}{dFo} \tag{5.31}$$

Equations (5.30) and (5.31) can be combined to give β in terms of $\frac{\dot{R}}{U}$ with Ja and Pe_o as parameters, viz.,

$$\beta = [\ -\frac{9}{8\sqrt{6}} (\frac{Ja}{Pe_o^{1/2}})(\frac{1}{\dot{R}/U}) \int_0^{\pi} \frac{[\sin^3\theta . F(\theta,\frac{\dot{R}}{U})]^{1/2}}{[\int_0^{\theta} F(\theta,\frac{\dot{R}}{U})d\theta]^{1/2}} d\theta]^2 \tag{5.32}$$

A typical plot of $(-\frac{U}{\dot{R}})$ versus β is shown in Figure (5.2) for Ja = 15 and $Pe_o = 10^4$.

Equation (5.31) can be rewritten as

$$Fo_i = \frac{1}{2Pe_o} \int_{\beta_i}^{1} (-\frac{U}{\dot{R}})\ d\beta \tag{5.33}$$

Thus, when the curve in Figure 5.2 is integrated the corresponding values of Fo_i and β_i can be found, and plotted as shown in Figure 5.3 . Details of the calculation of these curves by a simulation program, TUTSIM are given in Appendix 3.

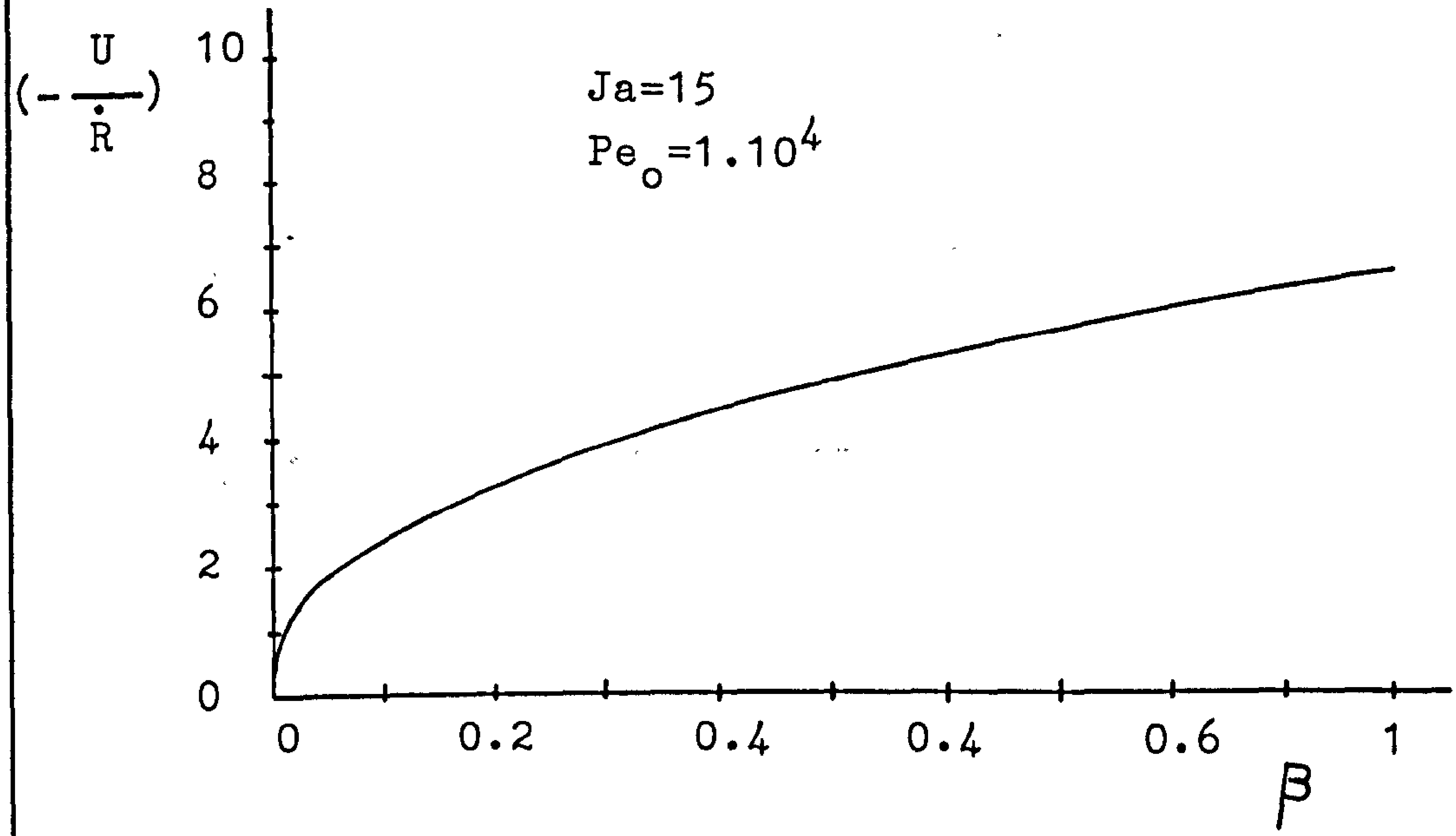

Fig.5.2 A typical plot of $\left(-\frac{U}{\dot{R}}\right)$ versus β according to equation(5.32).

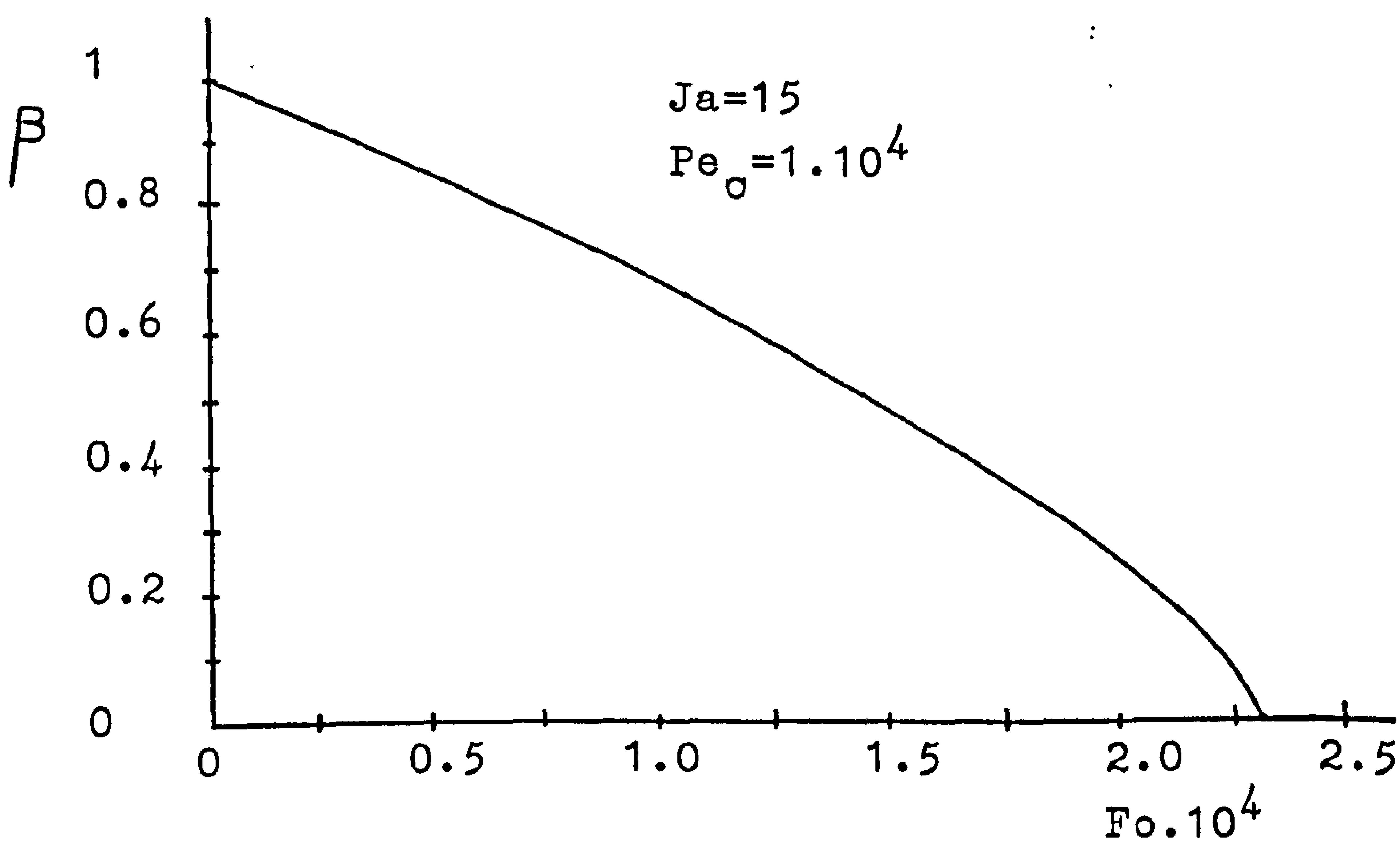

Fig.5.3 β versus Fo according to equation(5.33)

5.2.4 Negligible bubble wall velocity ($\dot{R} = 0$)

When $\frac{\dot{R}}{U} = 0, F(\theta, \frac{\dot{R}}{U})_{\dot{R}=0} = \sin^3\theta$, and equation (5.30) becomes,

$$\beta^{1/2}\frac{d\beta}{dFo} = -\frac{9}{4\sqrt{6}} \cdot Ja\, Pe_o^{1/2} \int_0^{\pi} \frac{[\sin^6\theta]^{1/2}}{[\int_0^{\theta} \sin^3\theta d\theta]^{1/2}} d\theta \tag{5.34}$$

Substituting $Z = \int_0^{\theta} \sin^3\theta d\theta = (\frac{\cos^3\theta}{3} - \cos\theta + \frac{2}{3})$,

$dZ = \sin^3\theta d\theta$, the integral can be calculated as

$$\int_0^{\pi} \frac{\sin^3\theta d\theta}{[\int_0^{\theta} \sin^3\theta d\theta]^{1/2}} = \int_0^{4/3} \frac{dZ}{Z^{1/2}} = 2Z^{1/2} \Big|_0^{4/3} = \frac{4}{\sqrt{3}} \tag{5.35}$$

Therefore equation (5.34) becomes

$$\beta^{1/2} \frac{d\beta}{dFo} = -\frac{3}{\sqrt{2}} Ja\, Pe_o^{1/2} \tag{5.36}$$

Hence

$$\frac{2}{3} \frac{d\beta^{3/2}}{dFo} = -\frac{3}{\sqrt{2}} Ja\, Pe_o^{1/2} \tag{5.37}$$

Integrating,

$$\beta^{3/2} \Big|_1^{\beta} = -\frac{9}{2\sqrt{2}} Ja\, Pe_o^{1/2}\, Fo \Big|_0^{Fo} \tag{5.38}$$

or

$$\beta^{3/2} - 1 = -\frac{9}{2\sqrt{2}} Ja\, Pe_o^{1/2}\, Fo$$

$$\therefore \beta = (1 - 3.182\, Ja\, Pe_o^{1/2}\, Fo)^{2/3} \tag{5.39}$$

It should be noted that Isenberg et al.[23] obtained a very similar equation by employing Ruckenstein's [8] exact heat transfer solution for bubbles rising with negligible radial velocity as

$$\beta = (1-3.385\ Ja.Pe_o^{0.5}\ .\ Fo)^{2/3} \tag{5.40}$$

5.3 Simplification of the theory

Equation (5.30) can be written as

$$\beta^{1/2}\frac{d\beta}{dFo} = -\frac{9}{4\sqrt{6}} Ja\ Pe_o^{1/2}\ F_1\left(\frac{\dot{R}}{U}\right) \tag{5.41}$$

where

$$F_1\left(\frac{\dot{R}}{U}\right) = \int_0^{\pi} \frac{\left[\sin^3\theta\ F\left(\theta,\frac{\dot{R}}{U}\right)\right]^{1/2}}{\left[\int_0^{\theta} F\left(\theta,\frac{\dot{R}}{U}\right)d\theta\right]^{1/2}} d\theta \tag{5.42}$$

An evaluation of $F_1\left(\frac{\dot{R}}{U}\right)$ versus $\left(-\frac{\dot{R}}{U}\right)$ presented in Fig. 5.4, gives the relationship as

$$F_1 \simeq 2.31 - 1.33\left(-\frac{\dot{R}}{U}\right) \tag{5.43}$$

for $0 \leq -\frac{\dot{R}}{U} \leq 1.4$

Hence, equation (5.41) becomes

$$\frac{2}{3}\frac{d\beta^{3/2}}{dFo} = -\frac{9}{4\sqrt{6}} Ja\ Pe_o^{1/2}\ \left(2.31 + 1.33\left(\frac{\dot{R}}{U}\right)\right) \tag{5.44}$$

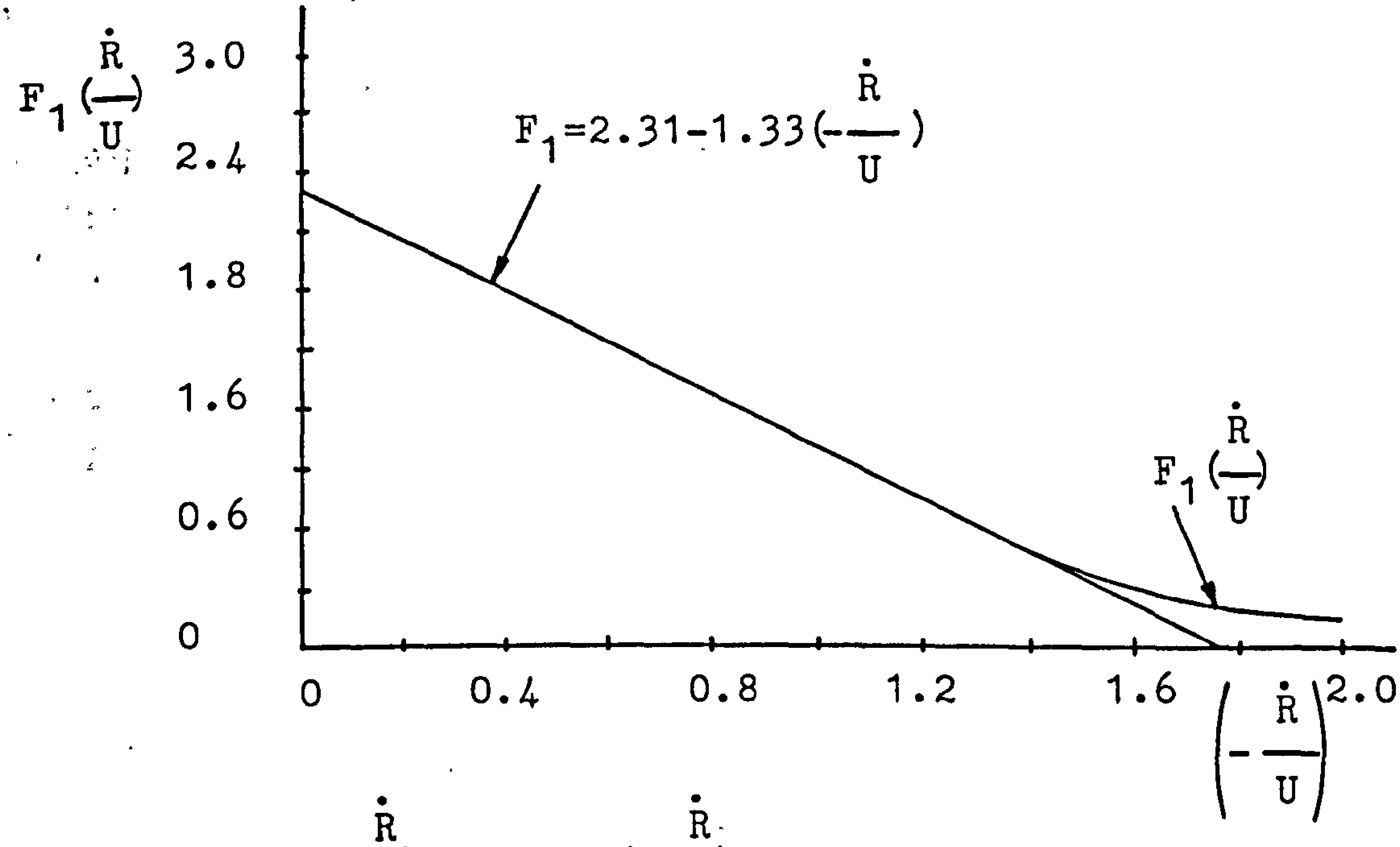

Fig.5.4 $F_1(\frac{\dot{R}}{U})$ versus $(-\frac{\dot{R}}{U})$

Substituting $\frac{\dot{R}}{U} = \frac{1}{2Pe_o}\frac{d\beta}{dFo}$ from equation (5.31)

$$\frac{2}{3}\frac{d\beta^{3/2}}{dFo} = -\frac{9}{4\sqrt{6}} Ja\ Pe_o^{1/2}\ (2.31 + \frac{1.33}{2\ Pe_o}\frac{d\beta}{dFo}) \qquad (5.45)$$

and integrating,

$$\beta^{3/2}\Big|_1^{\beta} = -\frac{27}{8\sqrt{6}} Ja\ Pe_o^{1/2}\ [2.31\ Fo\Big|_0^{Fo} + \frac{1.33}{2Pe_o}\cdot\beta\Big|_1^{\beta}] \qquad (5.46)$$

$$\therefore (1-\beta^{3/2}) = 3.182\ Ja\ Pe_o^{1/2}[Fo - \frac{0.288}{Pe_o}(1-\beta)] \qquad (5.47)$$

Hence, the simplified form of equation (5.32) can be expressed as

$$\beta = [1 - 3.182\ Ja\ Pe_o^{1/2}[Fo - \frac{0.288}{Pe_o}(1-\beta)]\ ]^{2/3} \qquad (5.48)$$

A comparison of the curve according to the complete equations (5.32) and (5.33) calculated by a computer simulation program, TUTSIM with the curve according to the simplified equation (5.48) is given in Fig. 5.5 for $Ja = 15$ and $Pe_o = 10^4$. The collapse Fourier number according to the simplified equation is about 2.5% higher than that from equations (5.32) and (5.33).

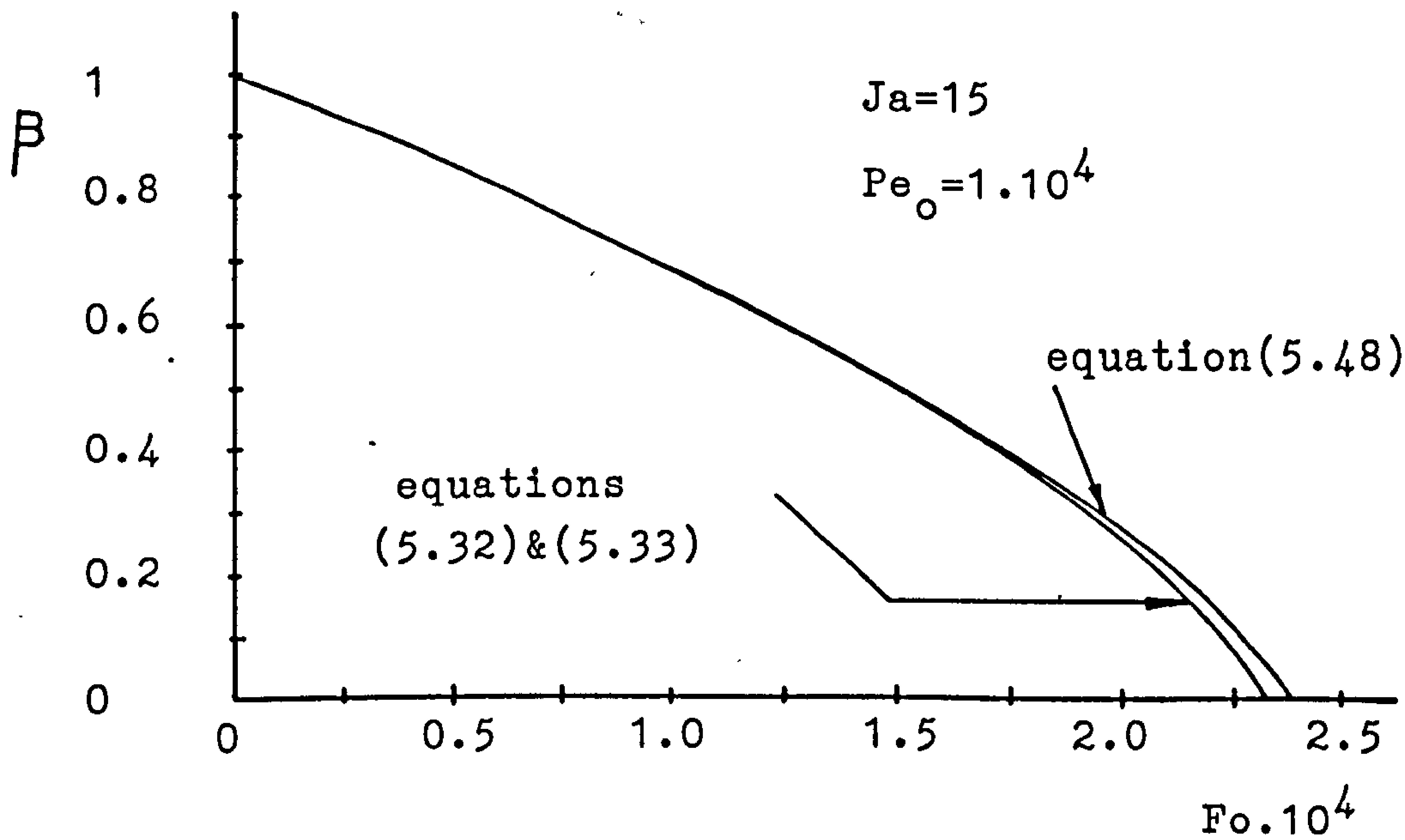

Fig.5.5 Comparison of complete and simplified solutions

The collapse Fourier number for the simplified theory in equation (5.48) is given by

$$Fo_c = \frac{1}{3.182\ Ja\ Pe_o^{1/2}} + \frac{0.288}{Pe_o} \qquad (5.49)$$

When $\dot{R} = 0$ the term $\frac{0.288}{Pe_o}$ vanishes and equation (5.48) reduces to equation (5.39).

5.4 Effect of bubble distortion and heating of liquid near the injection orifice

As can be seen from the impressions of bubble shapes (section 4.2.1), the bubbles were generally far from spherical and indeed changed in shape, sometimes in an oscillating manner, after detachment.

In section 3.4, the equivalent bubble radius, R was calculated as the radius of a sphere of volume equal to the measured bubble volume V_B. This radius was used in the heat transfer calculations in equation (5.25).

To account for the non-spherical shape of the bubble a shape factor, ψ defined as

$$\psi = \frac{\text{measured bubble surface area}}{4.\pi.R^2} \qquad (5.50)$$

was included in equation (5.25) to give

$$Q = [\int_0^\pi 2\pi R^2 \sin\theta \; q_\theta].\psi.d\theta \qquad (5.51)$$

Assuming $\psi = \psi(\beta)$, the simplified equation for the bubble collapse rate is now obtained from equation (5.41) as

$$\beta^{\frac{1}{2}}\frac{d\beta}{dFo} = - \frac{9}{4\sqrt{6}} Ja\ Pe_o^{\frac{1}{2}}\ \psi(\beta).F_1(\frac{\dot{R}}{U}) \qquad (5.52)$$

Substituting the approximate expression, given in equation (5.43), for

$F_1(\frac{\dot{R}}{U})$ together with the value of $(\frac{\dot{R}}{U})$ in equation (5.31), equation (5.52) can be written as

$$\beta^{\frac{1}{2}}\frac{d\beta}{dFo} = -\frac{9}{4\sqrt{6}} Ja\ Pe_o^{\frac{1}{2}}\psi(\beta)[2.31 + \frac{1.33}{2Pe_o}\frac{d\beta}{dFo}] \qquad (5.53)$$

Hence,

$$\int_1^{\beta}\frac{\beta^{\frac{1}{2}}d\beta}{\psi(\beta)} = -2.122\ Ja\ Pe_o^{\frac{1}{2}}[Fo\Big|_o^{Fo} + \frac{0.288}{Pe_o}\beta\Big|_1^{\beta}] \qquad (5.54)$$

$$\therefore \int_1^{\beta}\frac{\beta^{\frac{1}{2}}}{\psi(\beta)}d\beta = -2.122\ Ja\ Pe_o^{\frac{1}{2}}[Fo - \frac{0.288}{Pe_o}(1-\beta)] \qquad (5.55)$$

In the case of $\psi(\beta)$ = constant, equation (5.55) gives

$$\beta = [1 - 3.182\ Ja\ Pe_o^{\frac{1}{2}}\ \psi\ [Fo - \frac{0.288}{Pe_o}(1-\beta)]]^{2/3} \qquad (5.56)$$

Examination of the bubble volume and equivalent radius versus time curves (section 4.4) showed that there was significant condensation of the bubble before detachment from the orifice. Therefore, it was assumed that the condensation of the predetached bubble heated the liquid close to the orifice, so that after detachment the bubble rose through liquid where the temperature difference, $\Delta T'$ between the steam and the surrounding water rose from zero to ΔT, the nominal value, according to the simple expression,

$$\frac{\Delta T'}{\Delta T} = \frac{Ja'}{Ja} = (\frac{Z}{Z_c})^n = (\frac{Fo}{Fo_c})^n \qquad (5.57)$$

where Z_c and Fo_c are the collapse height and collapse Fourier number respectively. It is expected that the index n will be between zero (no heating) and 1 (plane heating) and can be used as an adjustable parameter.

In the case of ψ = const. and negligible bubble wall velocity ($\dot{R}=0$), the simplified equation (5.53) for the bubble collapse rate can now be written as

$$\frac{2}{3}\frac{d\beta^{3/2}}{dFo} = -2.122\ \psi\ Ja'\ Pe_o^{1/2} \tag{5.58}$$

Substituting $Ja' = Ja\left(\frac{Fo}{Fo_c}\right)^n$ from equation (5.57) and integrating,

$$\beta^{3/2}\Big|_1^{\beta} = \frac{-3.182\ \psi\ Ja\ Pe_o^{1/2}}{Fo_c^{\,n}}\ \frac{Fo^{n+1}}{n+1}\Big|_o^{Fo} \tag{5.59}$$

$$\therefore\ 1-\beta^{3/2} = \frac{3.182\ \psi\ Ja\ Pe_o^{1/2}}{n+1}\ \frac{Fo^{n+1}}{Fo_c^{\,n}} \tag{5.60}$$

The collapse Fourier number, Fo_c = Fo at $\beta = 0$, is

$$Fo_c = \frac{n+1}{3.182\ \psi\ Ja\ Pe_o^{1/2}} \tag{5.61}$$

Thus, equation (5.60) can be written as

$$(1-\beta^{3/2}) = \left(\frac{3.182\ \psi}{n+1}\right)^{n+1} Ja^{n+1}\ Pe_o^{\frac{n+1}{2}}\ Fo^{n+1} \tag{5.62}$$

where a value of n can be chosen to suit the experimental conditions.

In our case, as can be seen later in chapter 6, the experimental conditions suggest a value of n=0.1 .

5.5 Collapse of spherical-cap bubbles

In some cases it was observed that when a near spherical bubble detached from the orifice, it became slightly flattened at the rear of the bubble, passing through hemispherical to spherical-cap shape as represented in the impressions of bubble shape given for tests 4.1, 4.2, 3.2 and 7.1 in section 4.4 and illustrated in the collapse pattern shown in Fig. 5.6.

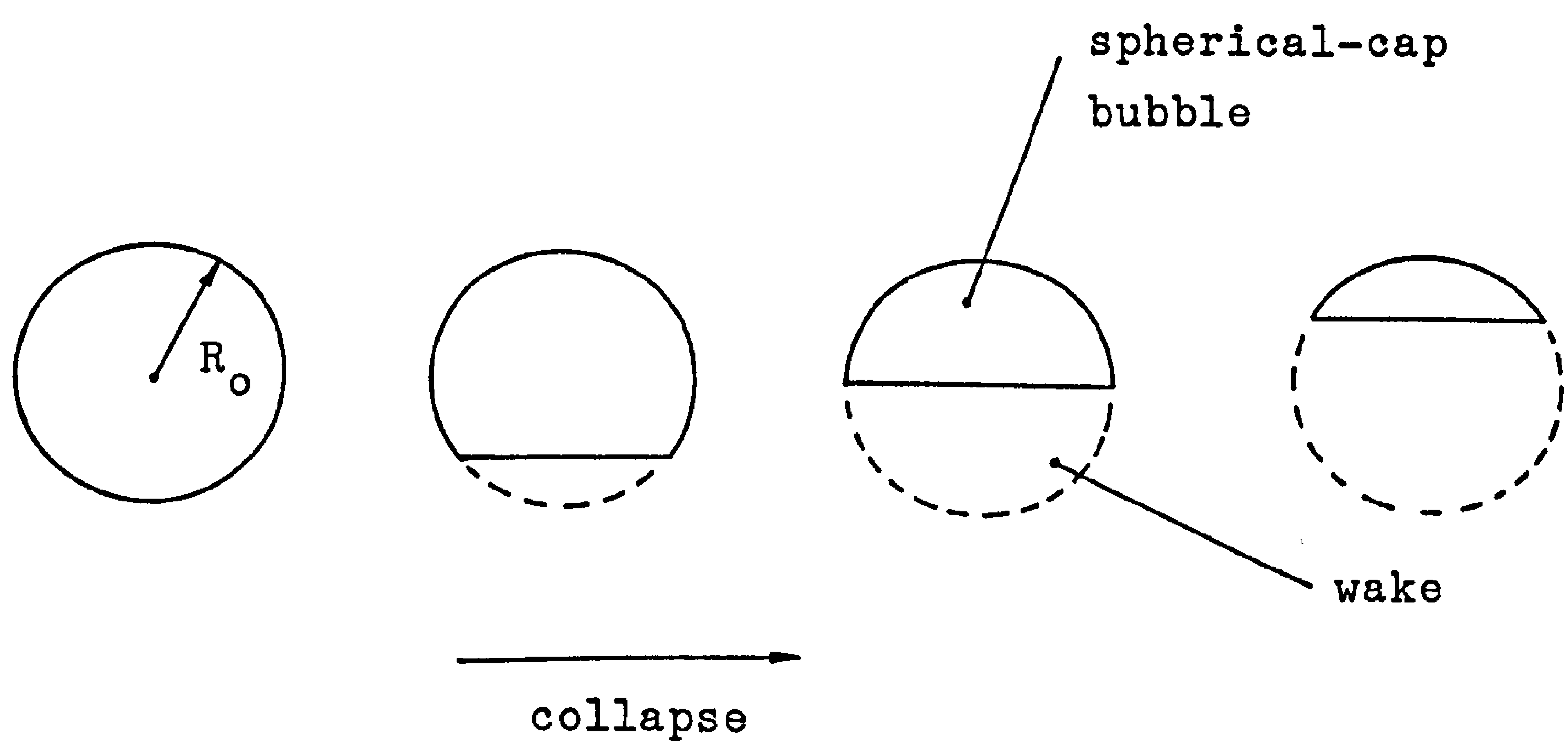

Fig.5.6 Impressions of collapse pattern of spherical-cap bubbles

The effect of conduction into the wake at the rear of such bubbles may be a significant factor in the total amount of heat transferred from the bubble and hence on the rate of collapse of the bubble.

In Appendix 6, the heat transfer into the wake is derived by applying a heat transfer analogy to a mass transfer approach suggested by Coppus [50]. When this is combined with the heat transfer over the front spherical surface, the bubble collapse is expressed by the equations

$$Fo = \frac{-3}{16 Ja Pe_o^{1/2}} \cdot \int_{\pi}^{\gamma} \frac{\sin^3\gamma . d\gamma}{\frac{3}{2} \cdot \frac{\sqrt{3}}{\pi} \cdot C_1^{1/2} + \left(\frac{3}{4} \cdot C_b \cdot Re_o^{1/4}\right) \cdot \left(\frac{3}{4}\right)^{1/4} \frac{\sin^2\gamma . C_1^{1/4}}{\left(1 - \frac{3}{4} C_1\right)^{1/4}}} \tag{5.63}$$

and

$$\beta = \left(\frac{3}{4} C_1\right)^{1/3} \tag{5.64}$$

where $C_1 = \frac{2}{3} - \cos\gamma + \frac{\cos^3\gamma}{3}$ and

$$C_b = 0.30 \left(\frac{gR}{8U^2}\right)^{0.25}$$

The experimental data is compared with these equations in chapter 6.

CHAPTER 6

DISCUSSION

6.1 Comparison of theory with experimental data

Preliminary study of the radius ratio versus Fourier number curves in Section 4.4 suggested that the shape curve could well be followed if n = 0.1 in equation (5.62), thus reducing that equation to the form,

$$\left(1-\beta^{3/2}\right)=\left(\frac{3.182.\psi}{1.1}\right)^{1.1} Ja^{1.1} . Pe_o^{0.55} . Fo^{1.1} \tag{6.1}$$

A plot of all the experimental data in the form of $\beta^{3/2}$ versus $Ja^{1.1}Pe_o^{0.55}Fo^{1.1}$ is shown in Fig. 6.1. The equation,

$$\left(1-\beta^{3/2}\right) = 4.35\ Ja^{1.1} . Pe^{0.55} . Fo^{1.10} \tag{6.2}$$

fits the 1134 experimental points with a percentage standard deviation, S_1 of 27.5% of the X coordinate calculated as

$$S_1 = \sqrt{\frac{\sum_{i=1}^{N} \left[(F-X)/F\right]^2}{N}} \times 100\% \tag{6.3}$$

where X is the data point given by ($Ja^{1.1}\ Pe^{0.55}\ Fo^{1.1}$) for any particular value of $\beta^{3/2}$ and F is the corresponding parameter determined by equation (6.2).

The standard deviation defined as

$$S_2 = \sqrt{\frac{\sum_{i=1}^{N} (F-X)^2}{N}} \tag{6.4}$$

is calculated to be 0.0285.

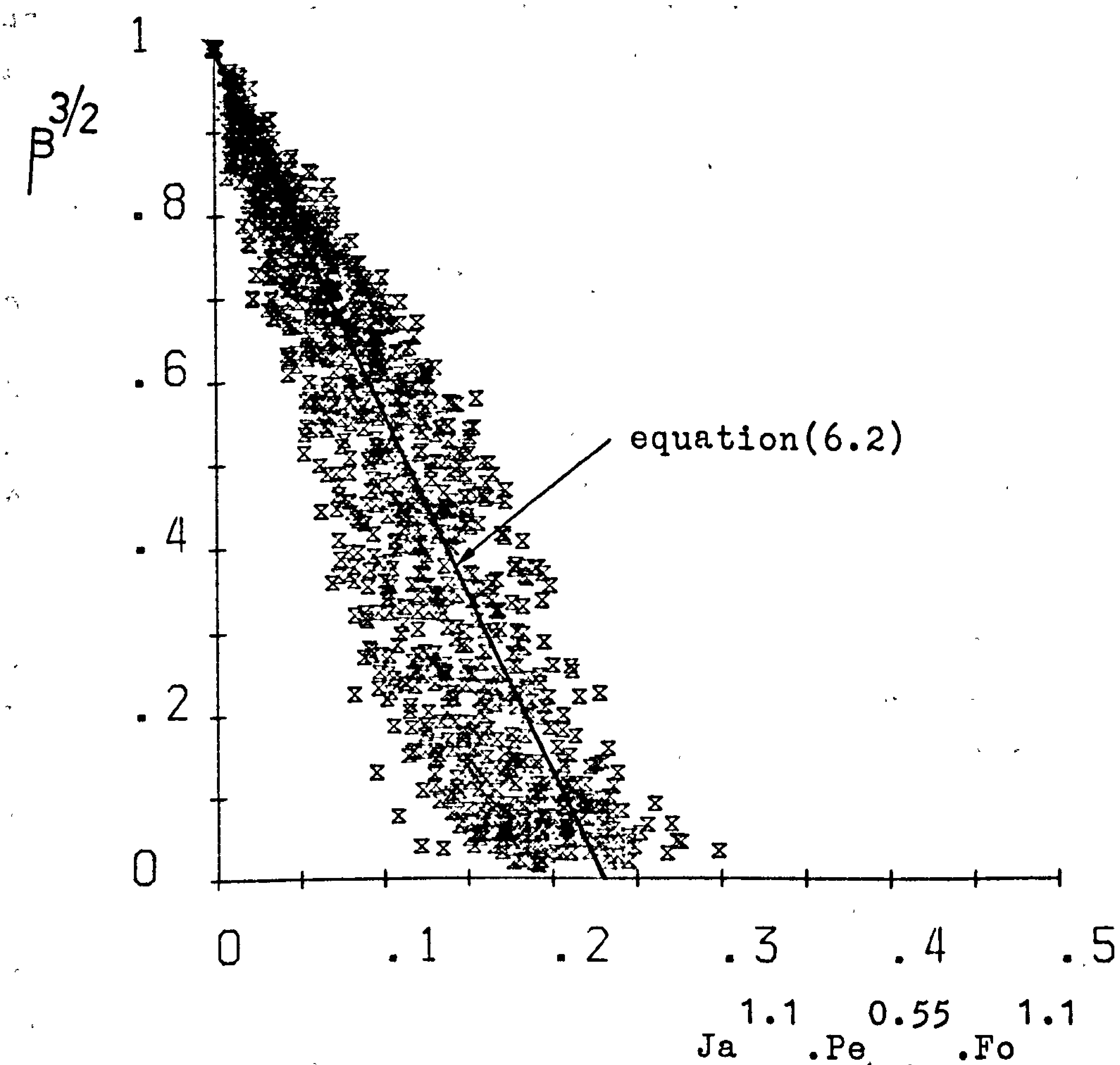

Fig.6.1 Plot of all the experimental data

From equation (6.2), the value of X at the end of bubble collapse is given as

$$X_o = Ja^{1.1}\, Pe^{0.55}\, Fo_c^{1.1} = \frac{1}{4.35} \cong 0.23 \qquad (6.5)$$

Thus, a percentage standard deviation related to the collapse Fourier number is found as

$$\frac{S_2}{X_o}.100 = 12.4\% \qquad (6.6)$$

Since $4.35 = \left(\frac{3.182\ \psi}{1.1}\right)^{1.1}$, the coefficient 4.35 implies a shape factor, ψ of 1.316, about 16% higher than the average of the shape factors (ψ_a = 1.134) presented in Table A 5.1 in Appendix 5.

In general, as is implied by equation (6.2) the bubbles condensed more slowly at low values of Jakob number and even in a few cases, at a pressure of 1 bar, reached the surface of the water without collapsing completely.

In Figures 6.2, the experimental data plotted individually for each test as radius ratio (β) versus Fourier number (Fo) are compared with equation (6.2). The plots indicate that in most cases equation (6.2) gives a fairly accurate prediction of the collapse time. However, the form of the collapse curve for tests carried out at the lowest value of Jakob number (Ja = 15) differs from the form at higher Jakob numbers, in that the curve is very nearly linear with a collapse time shorter than that predicted by equation (6.2). For these low Jakob number tests the collapse time as predicted by equation (6.2) is up to 70% greater than the experimental collapse time. Exceptions to this early collapse time are noted for tests 10.1, 11.1 and 12.1, which are all at 2 bar with

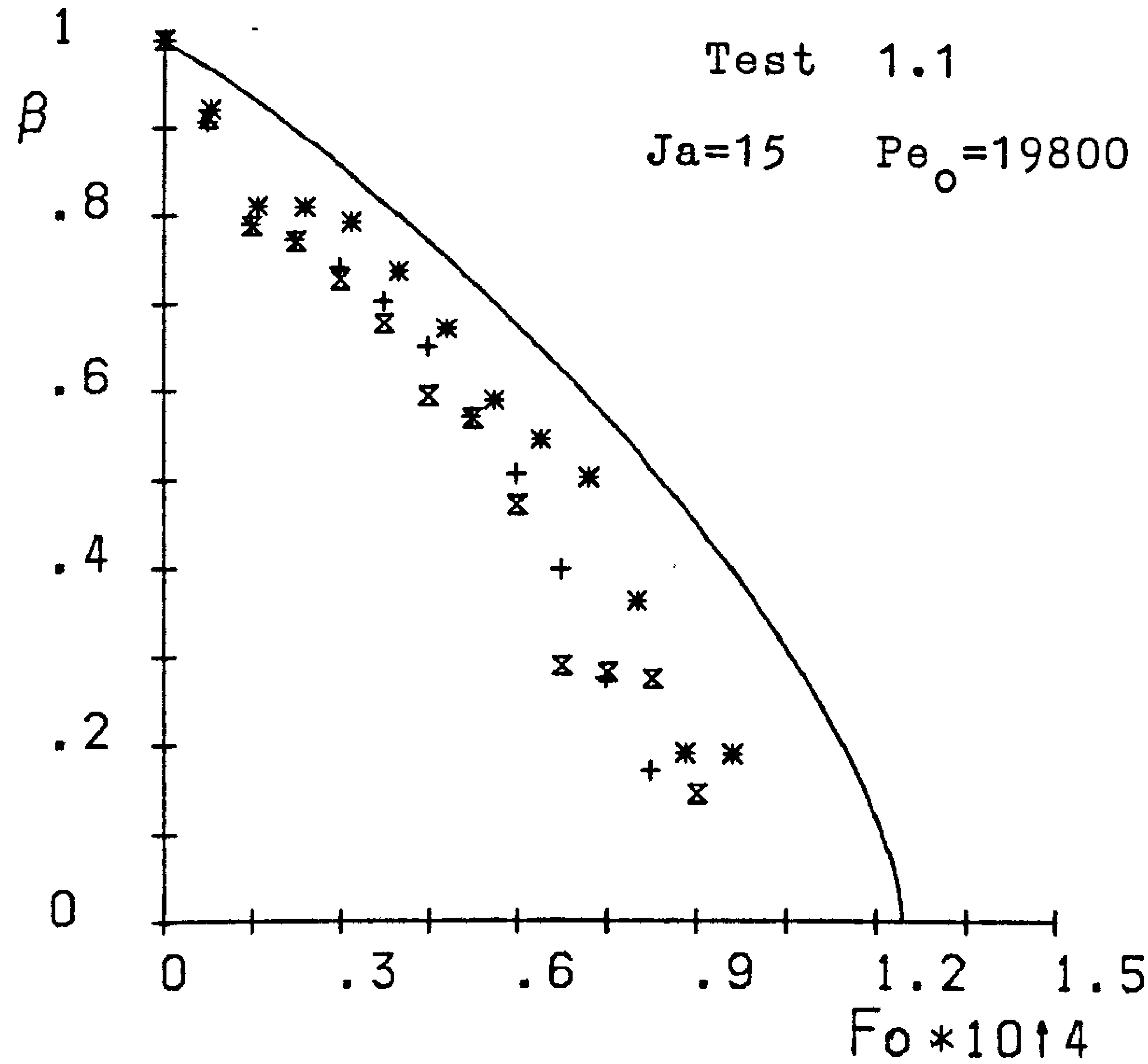

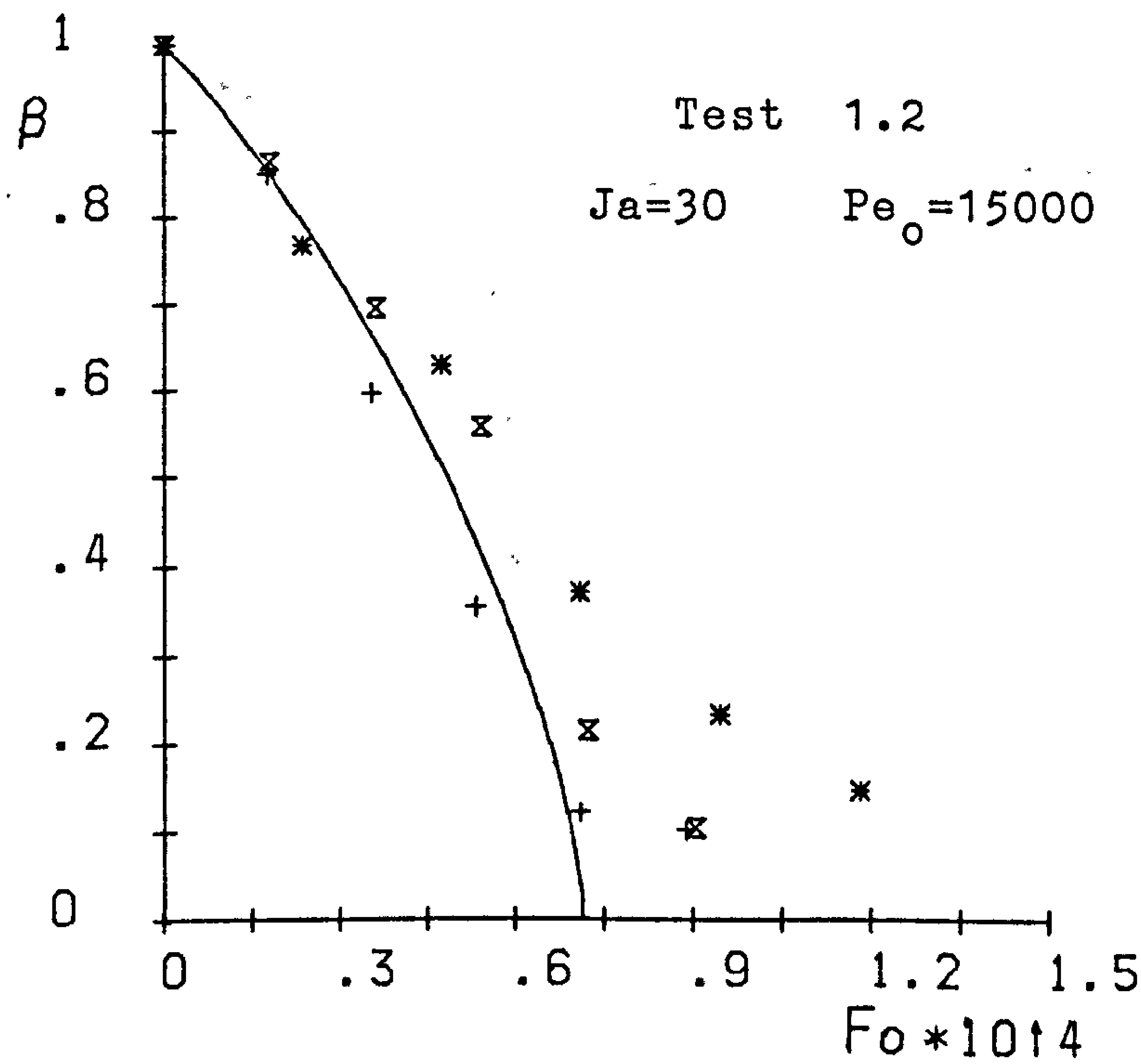

Fig.6.2 Radius ratio (β) versus Fourier number (Fo)

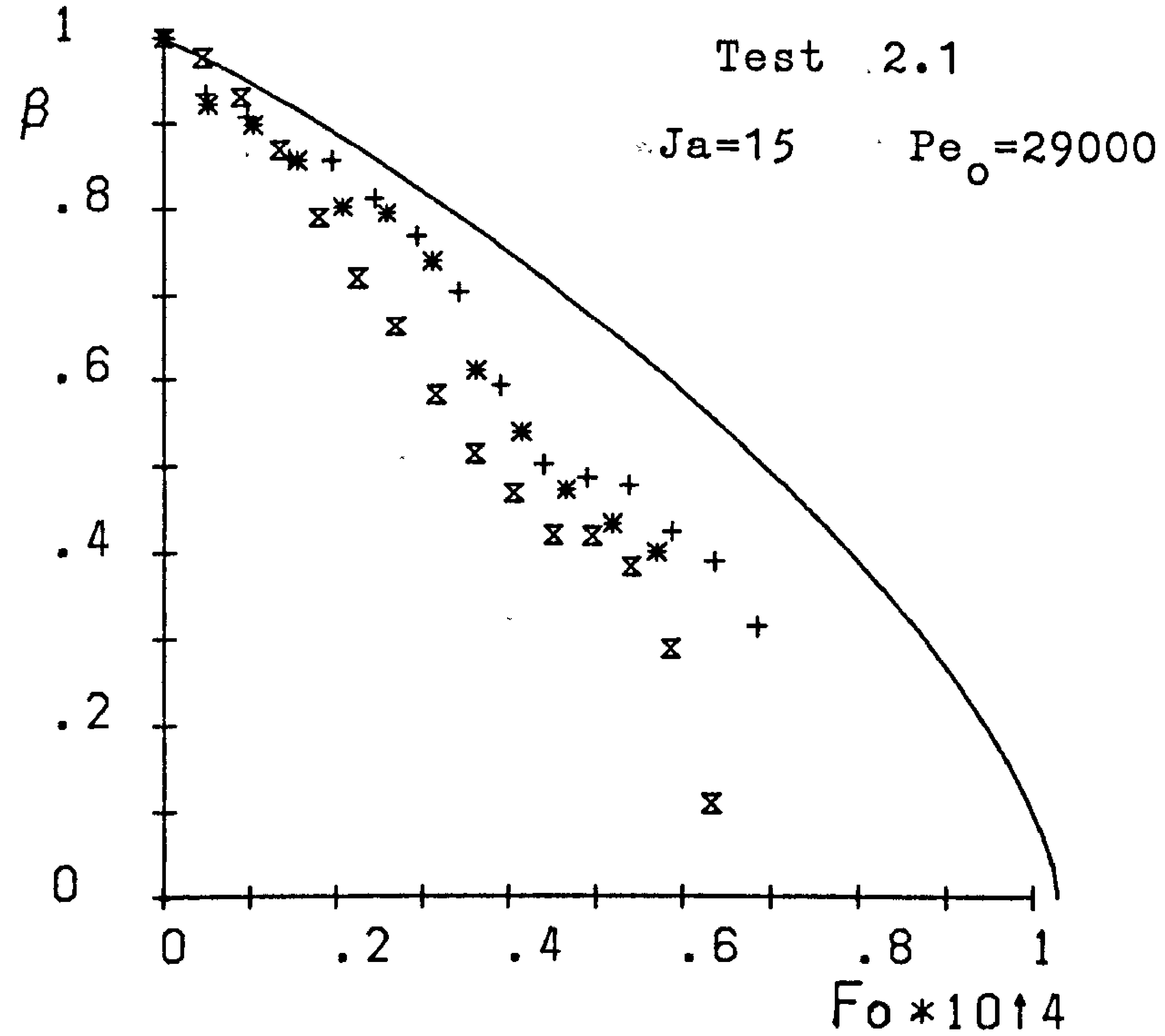

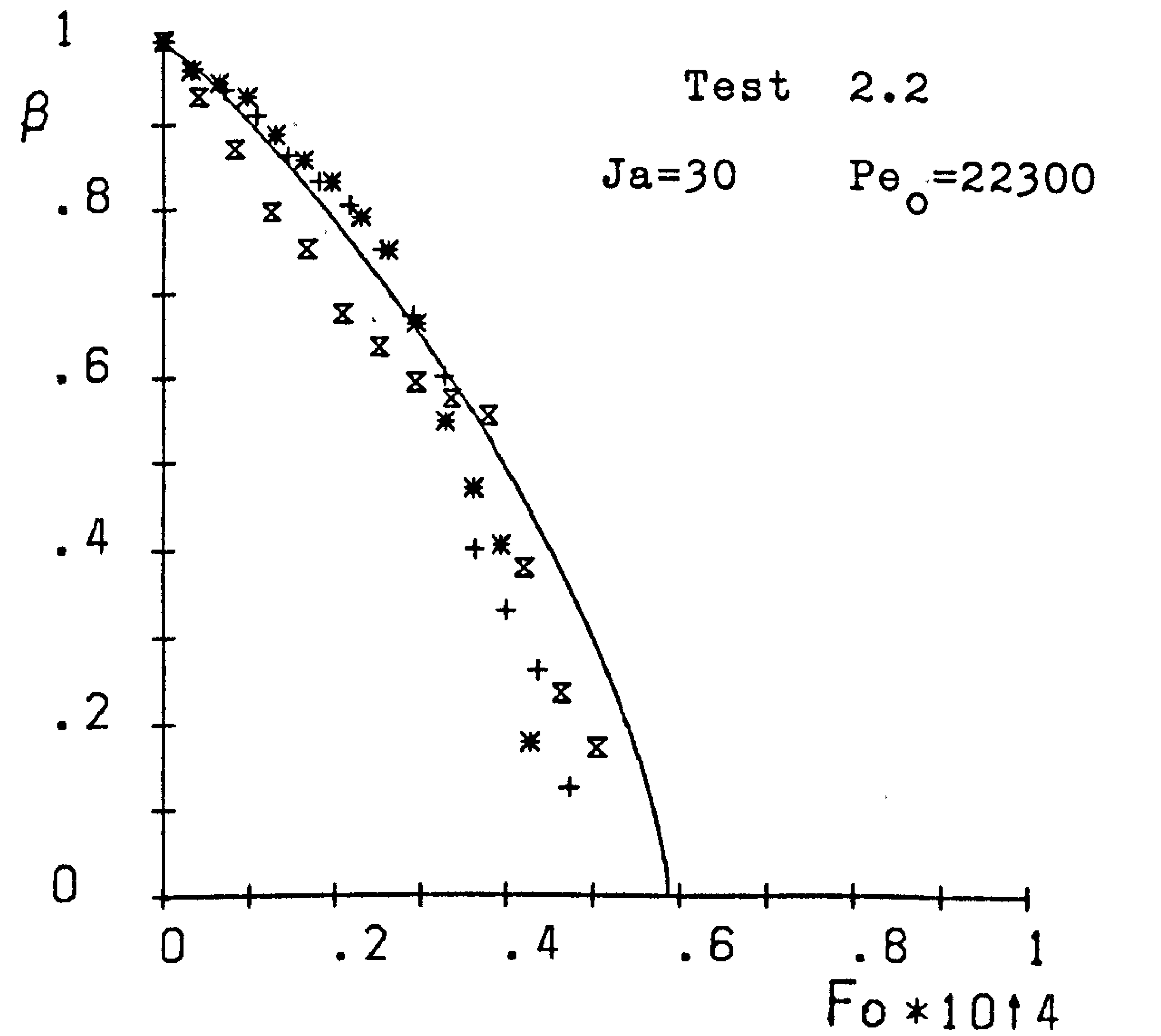

Fig.6.2 Radius ratio (β) versus Fourier number (Fo)

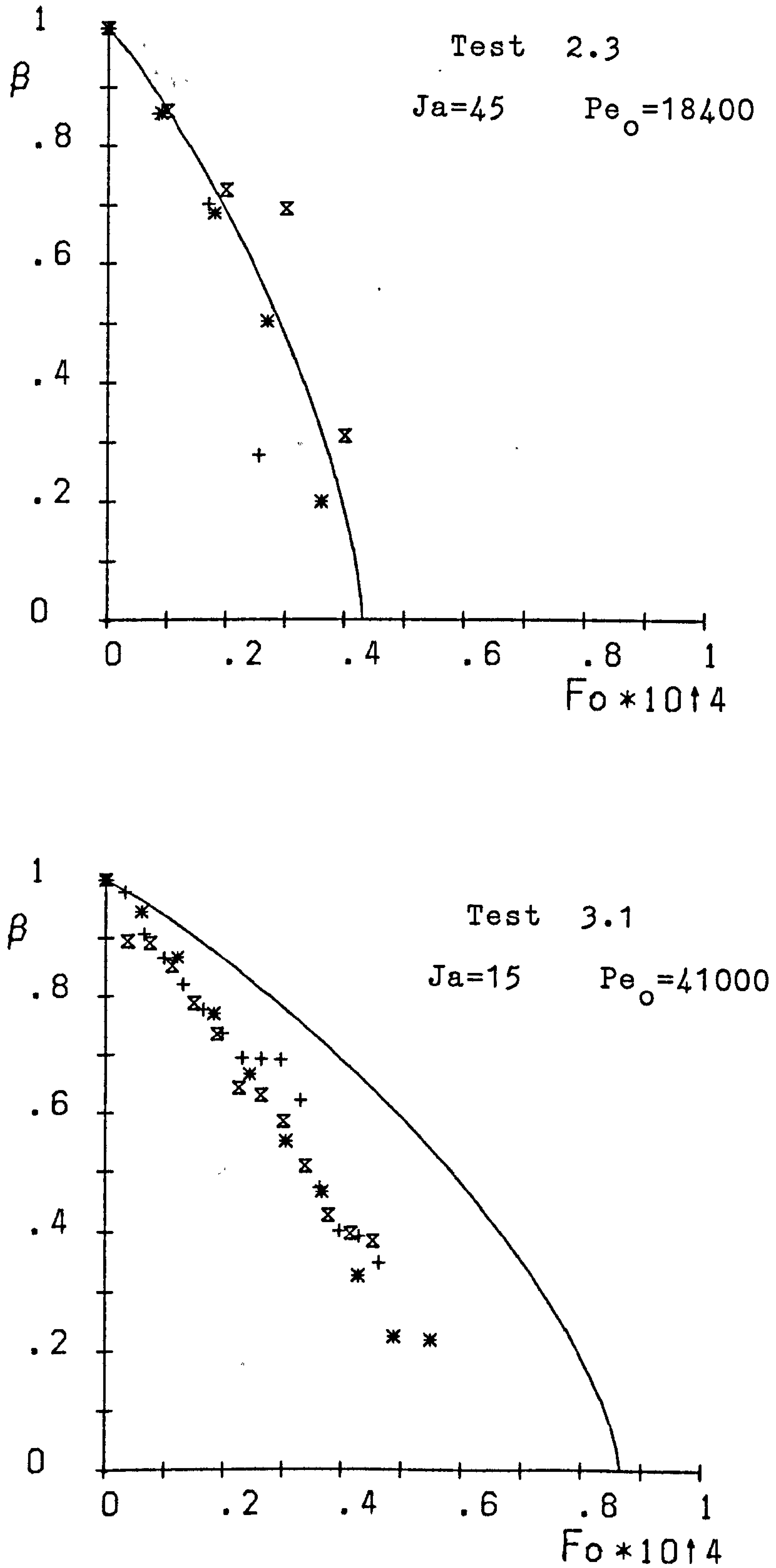

Fig.6.2 Radius ratio (β) versus Fourier number (Fo)

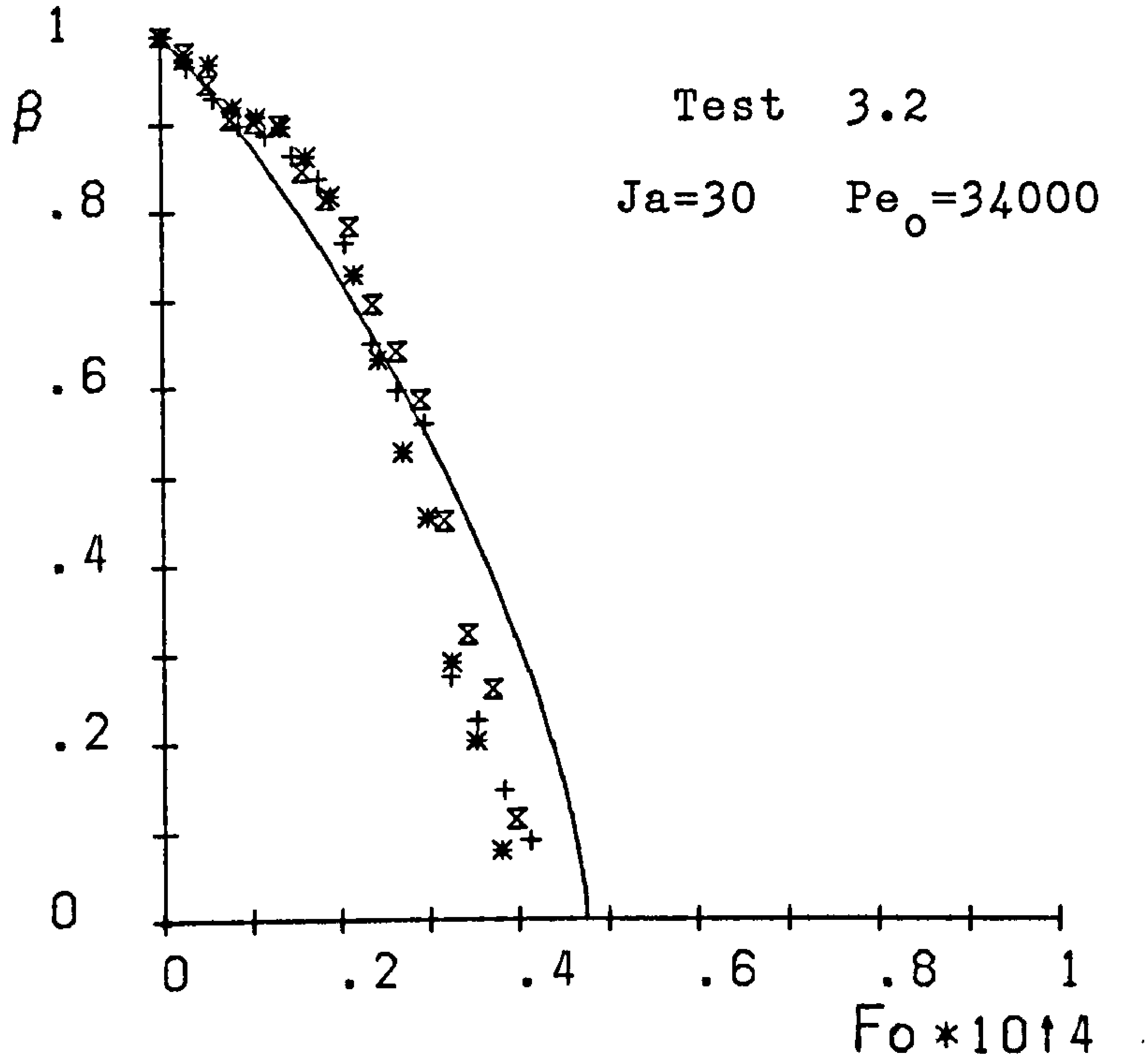

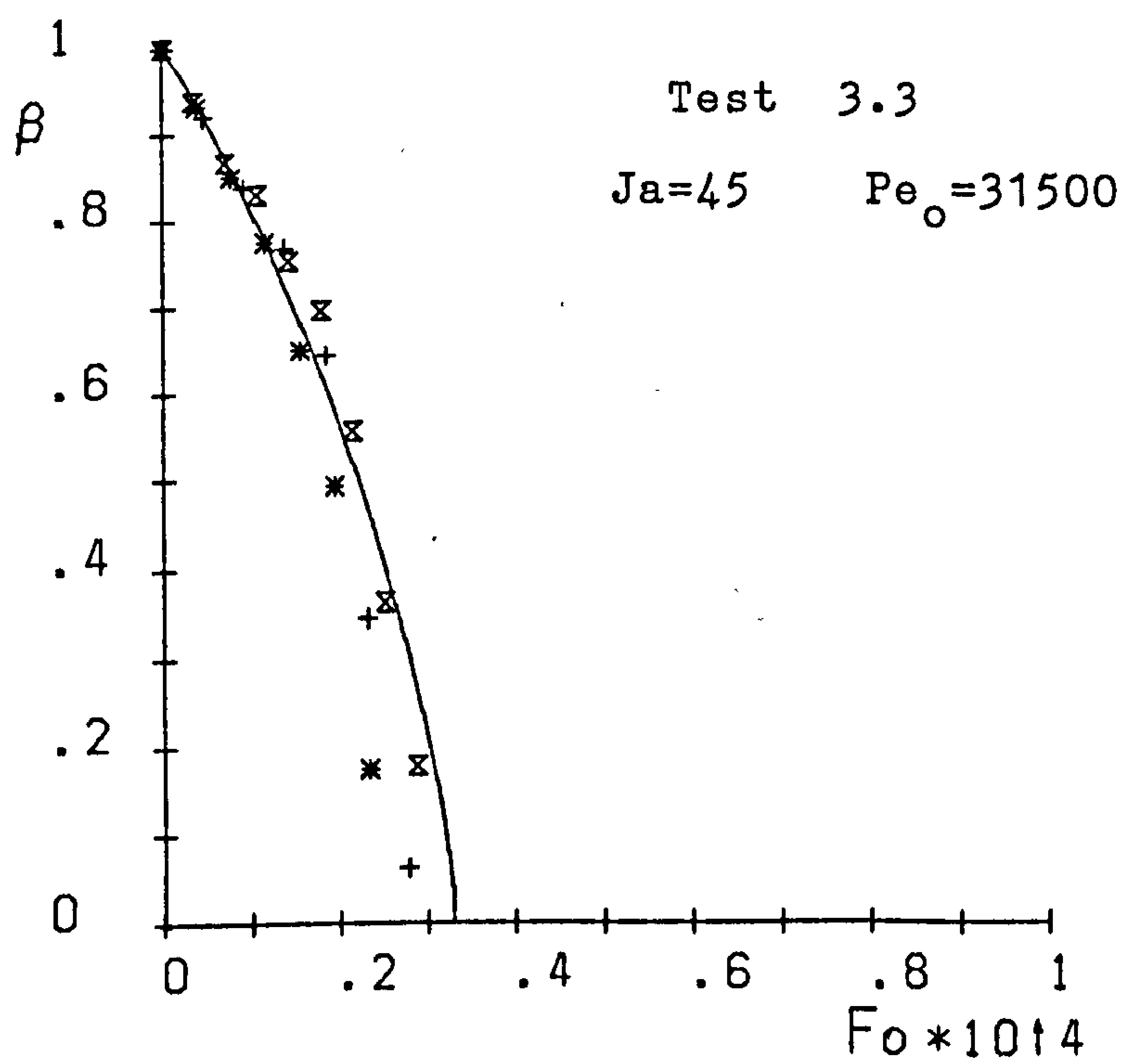

Fig.6.2 Radius ratio (β) versus Fourier number(Fo)

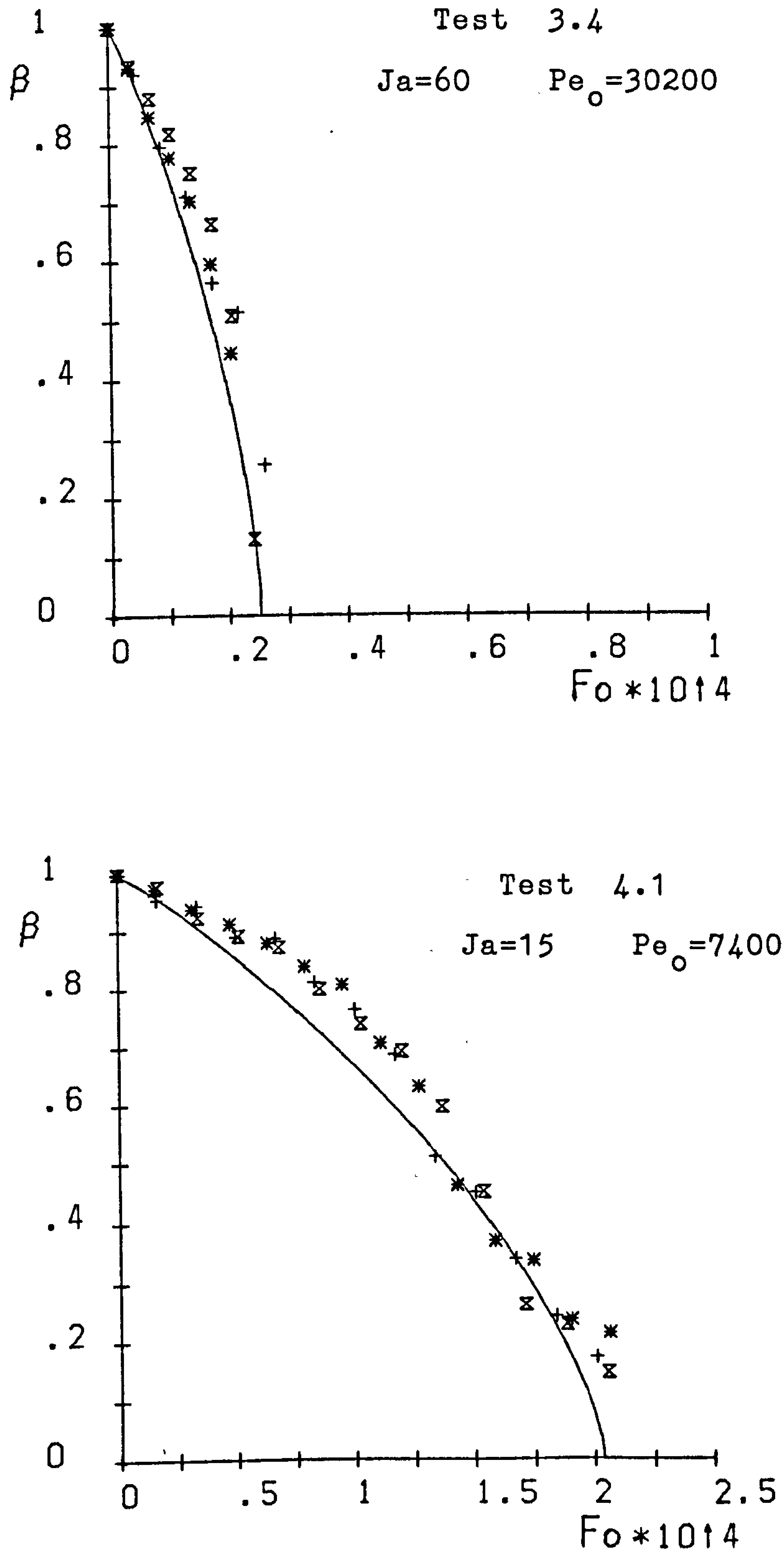

Fig.6.2 Radius ratio (β) versus Fourier number (Fo)

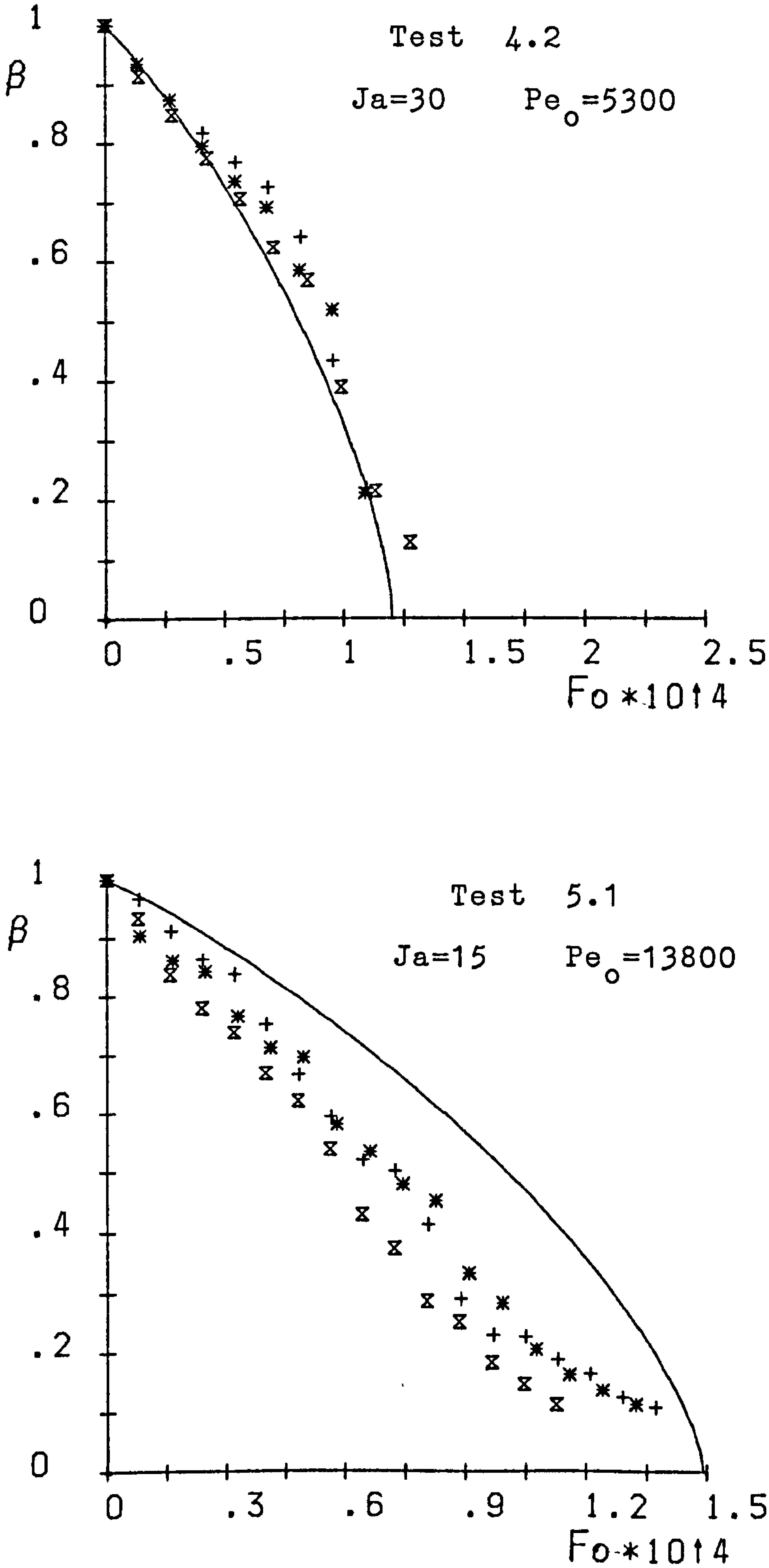

Fig.6.2 Radius ratio (β) versus Fourier number (Fo)

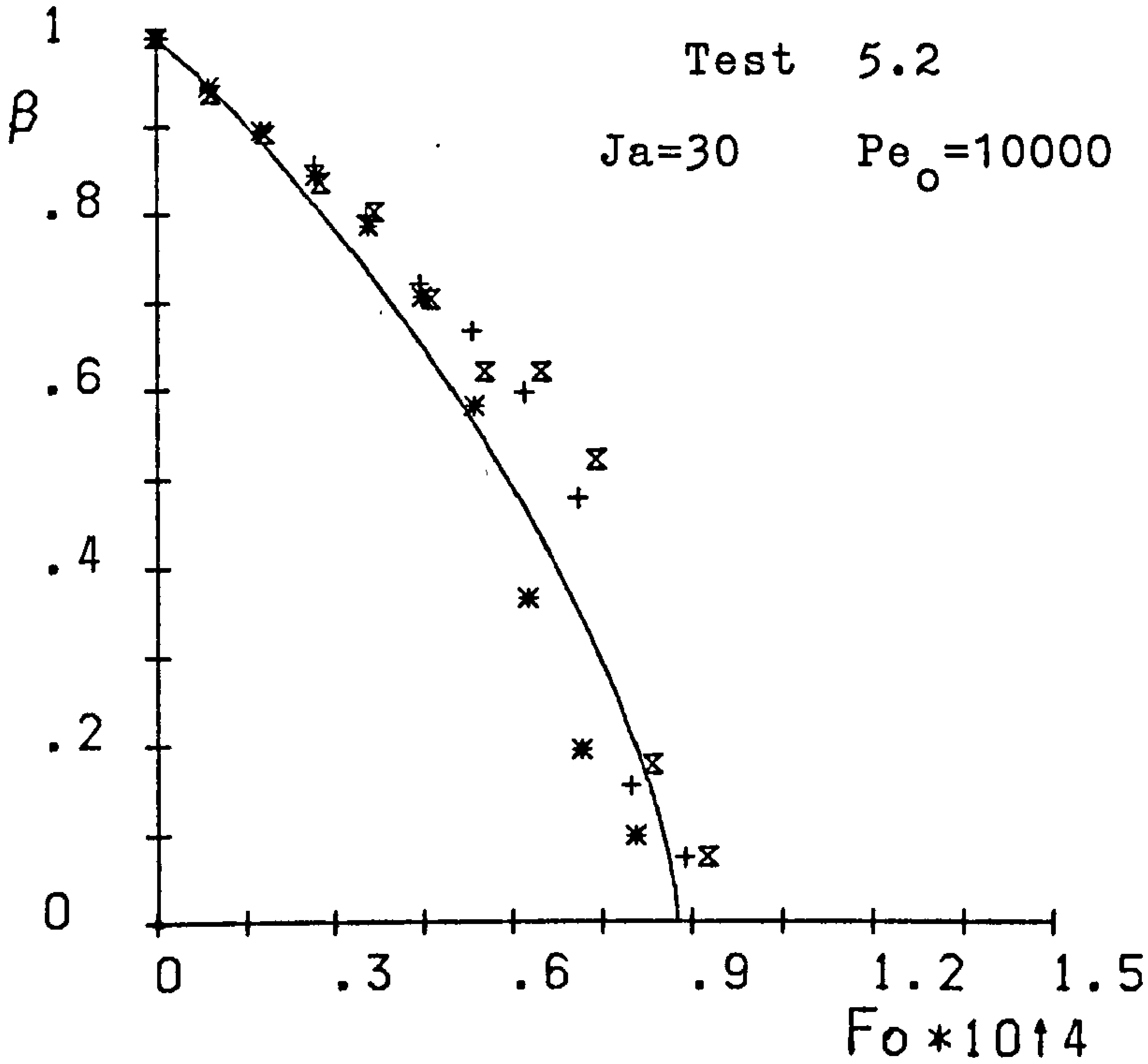

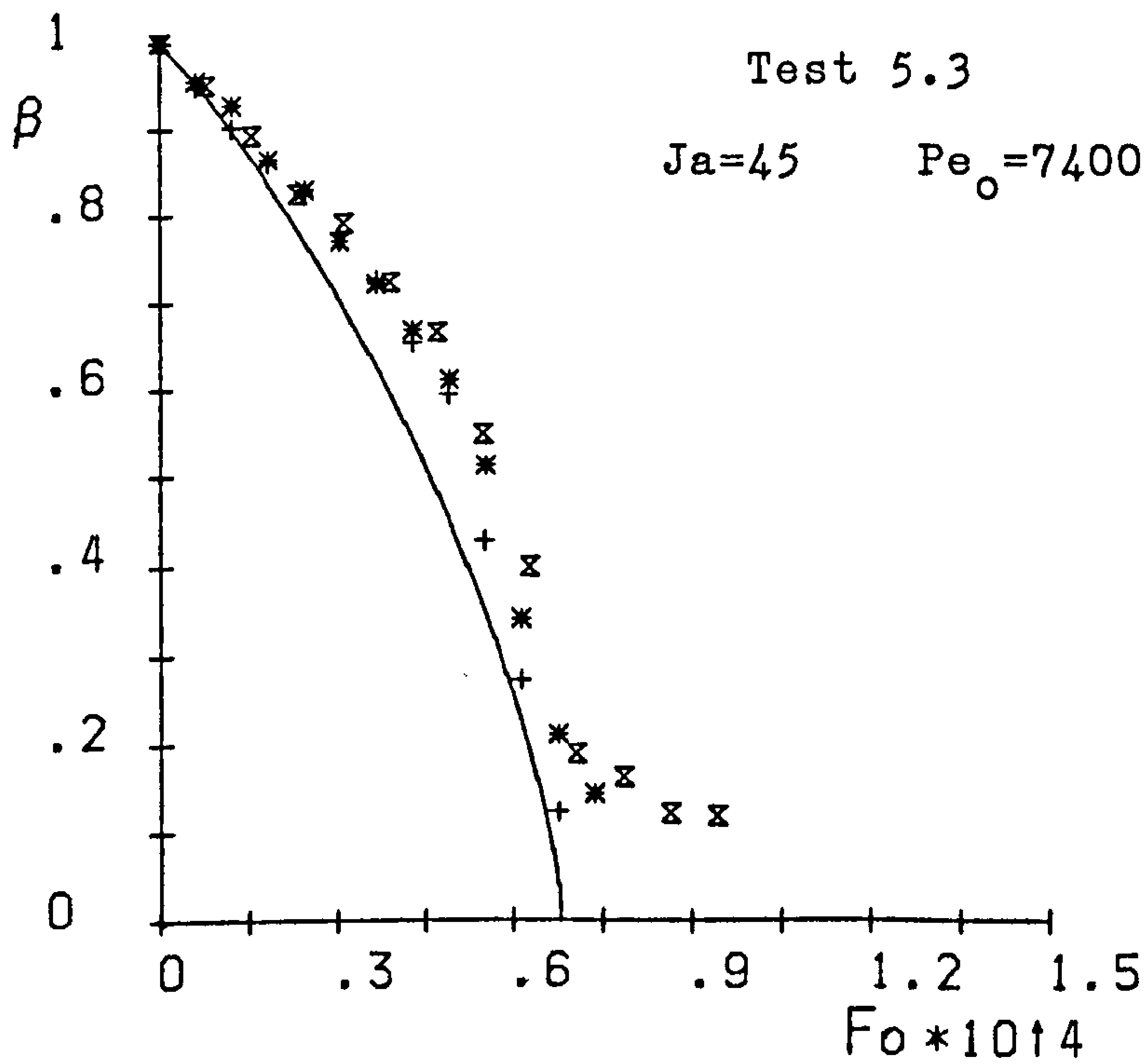

Fig.6.2 Radius ratio (β) versus Fourier number (Fo)

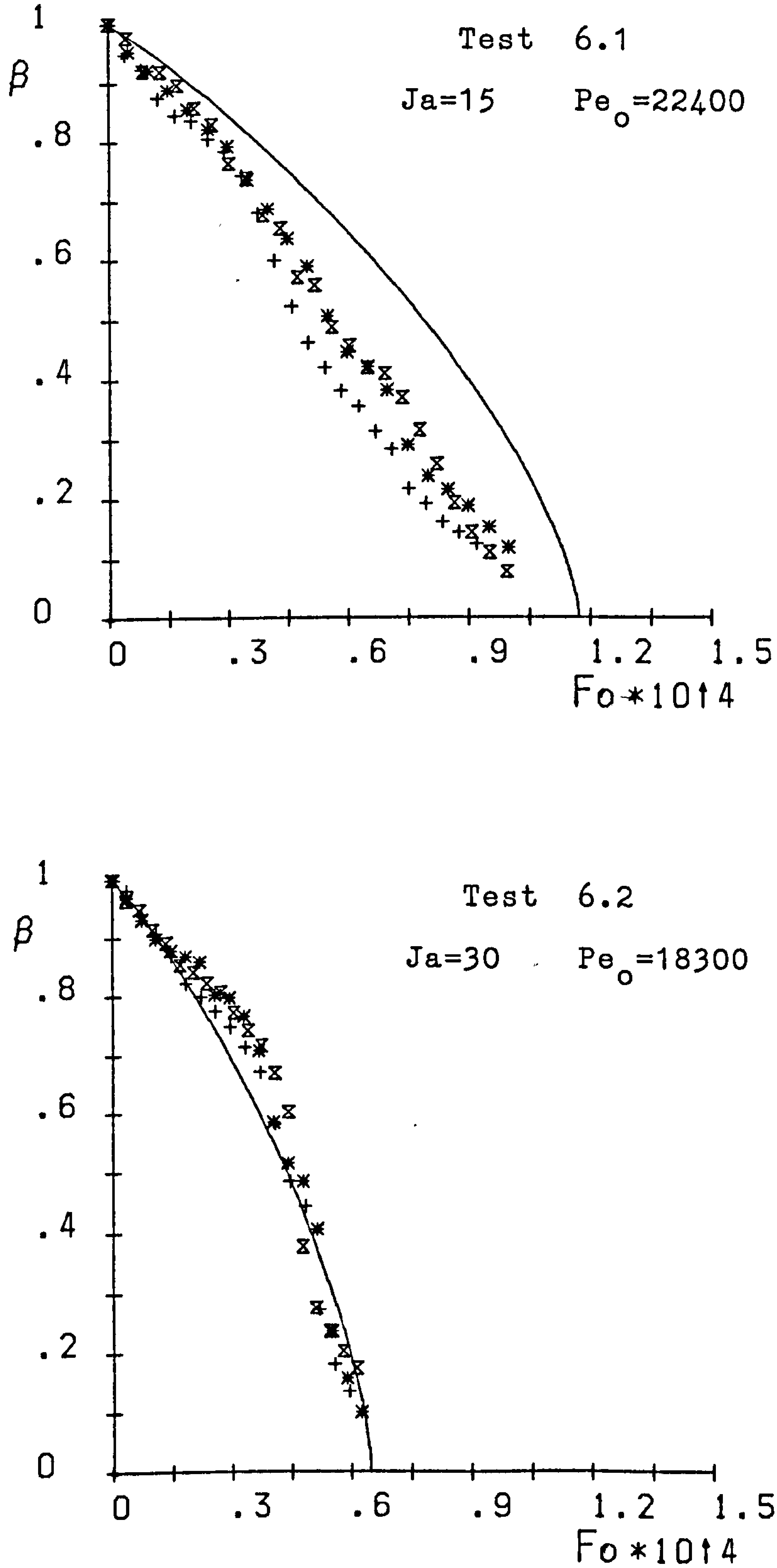

Fig.6.2 Radius ratio (β) versus Fourier number (Fo)

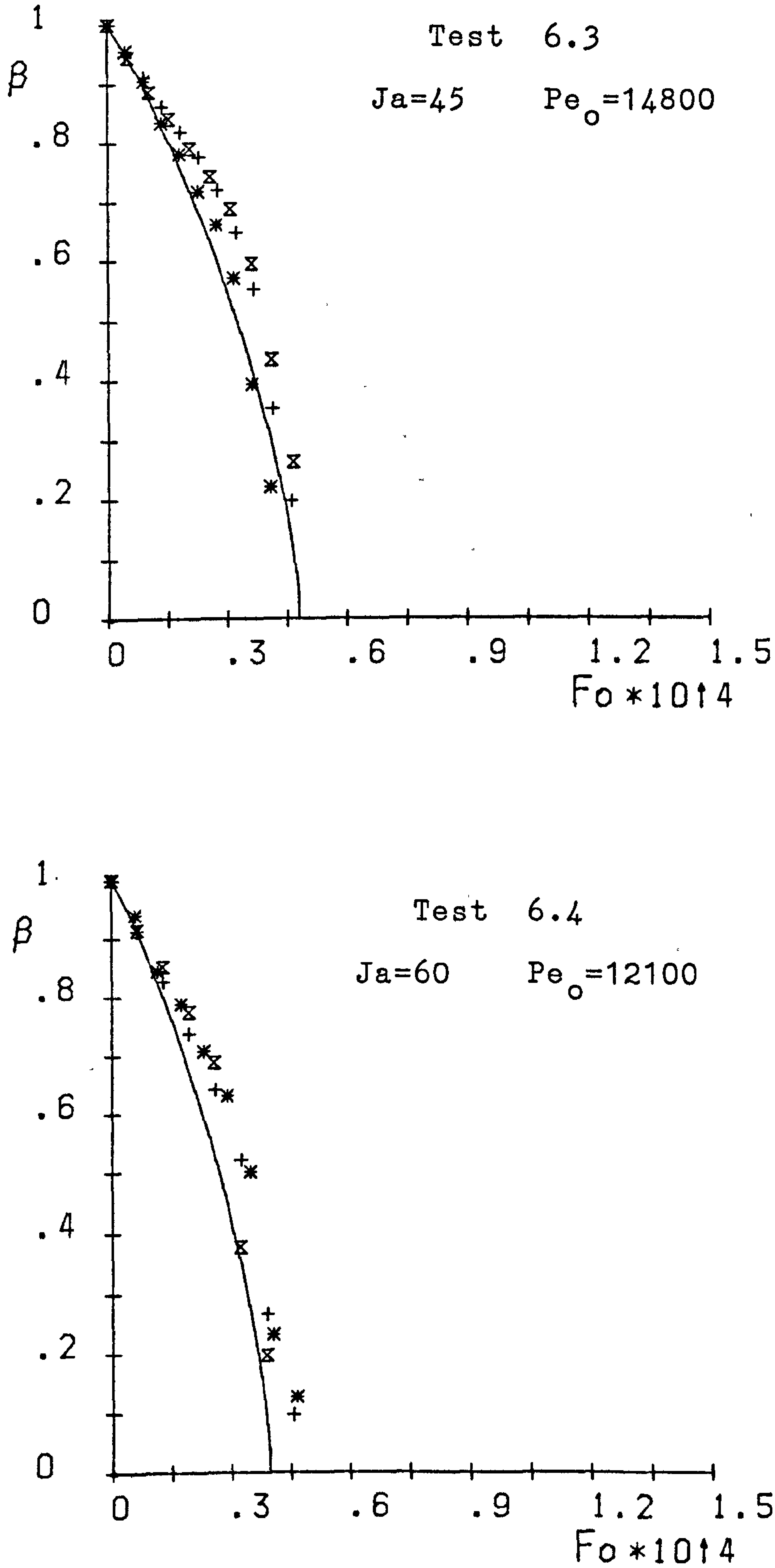

Fig.6.2 Radius ratio (β) versus Fourier number (Fo)

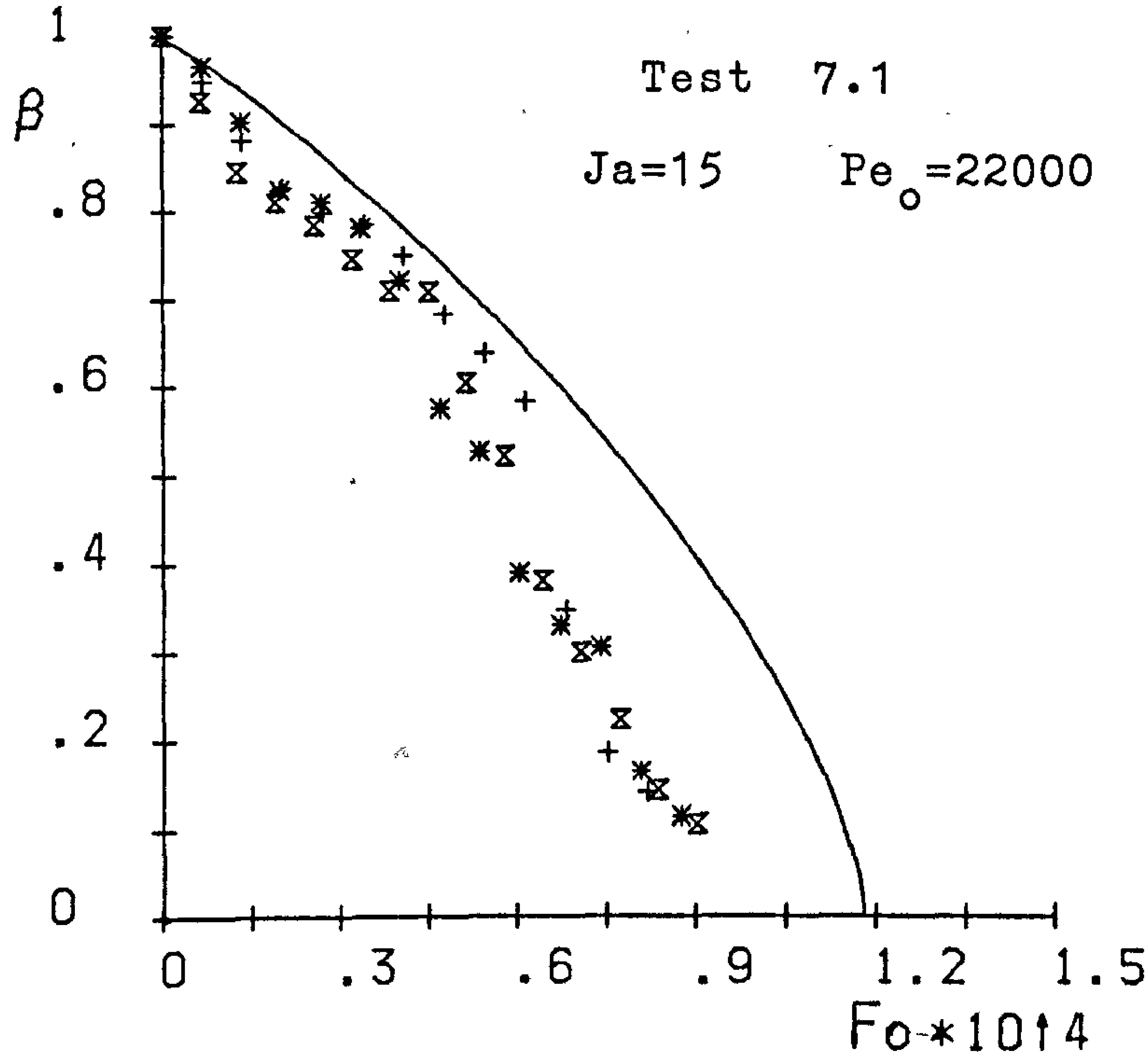

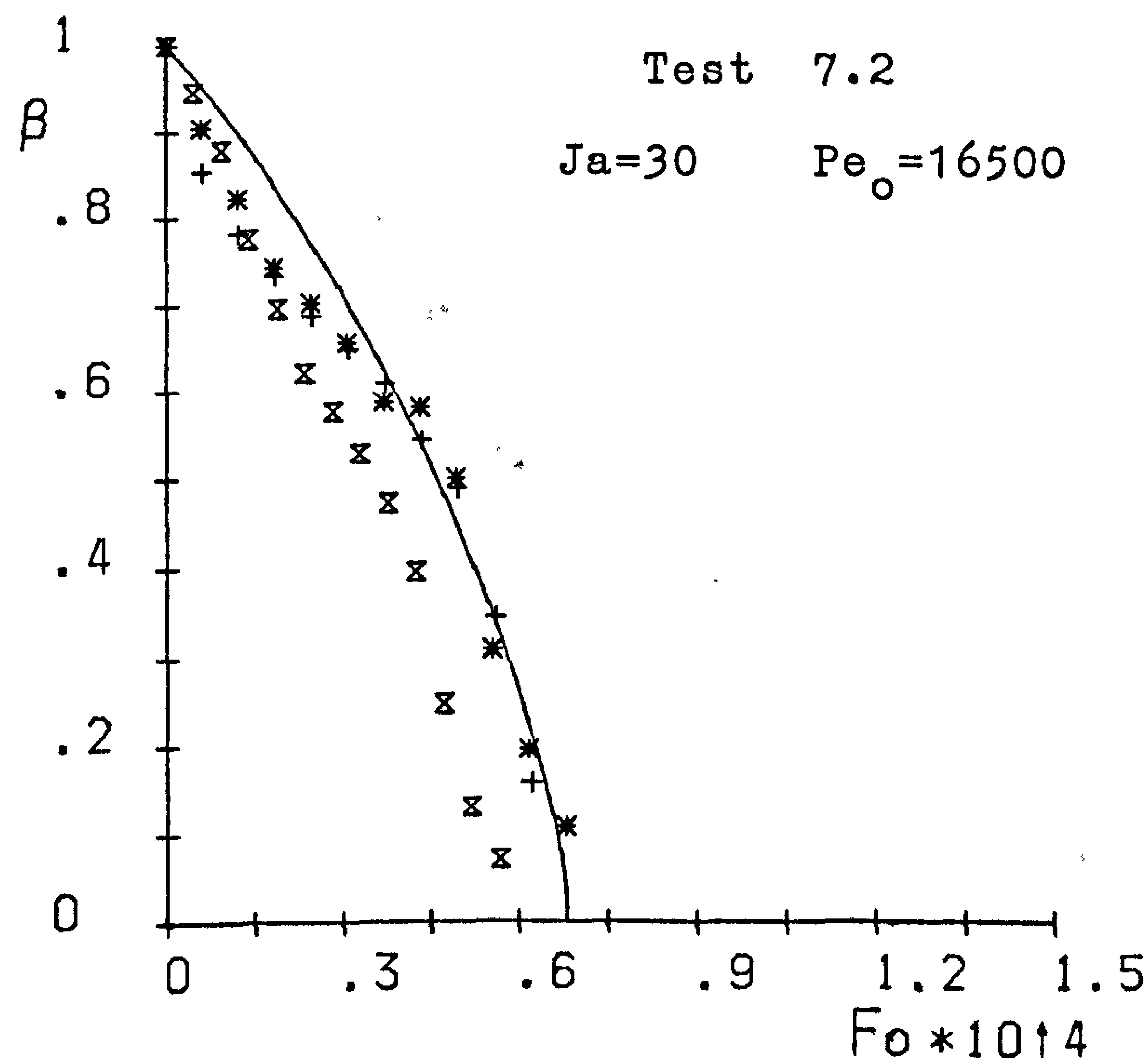

Fig.6.2 Radius ratio (β) versus Fourier number (Fo)

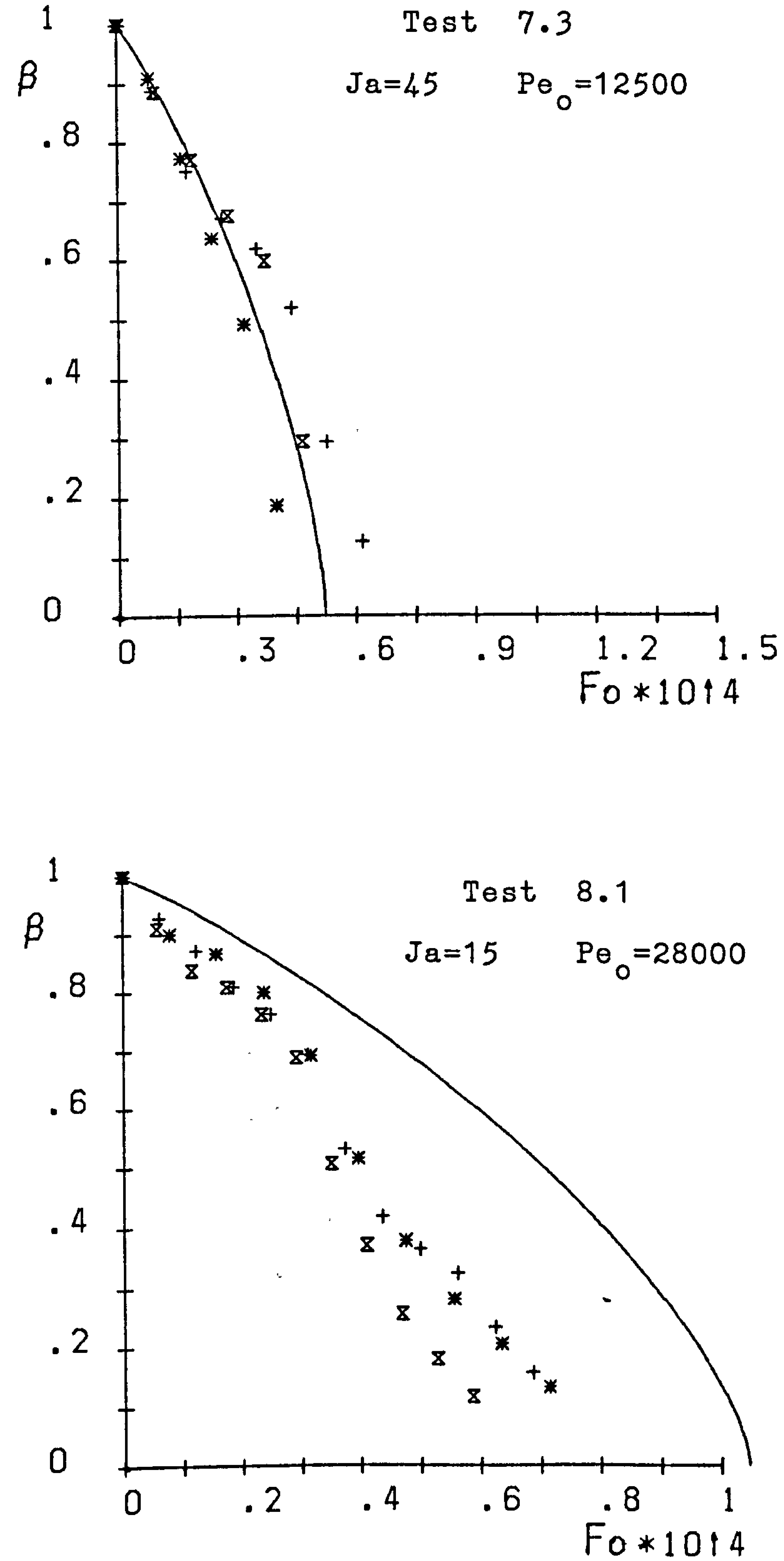

Fig.6.2 Radius ratio (β) versus Fourier number (Fo)

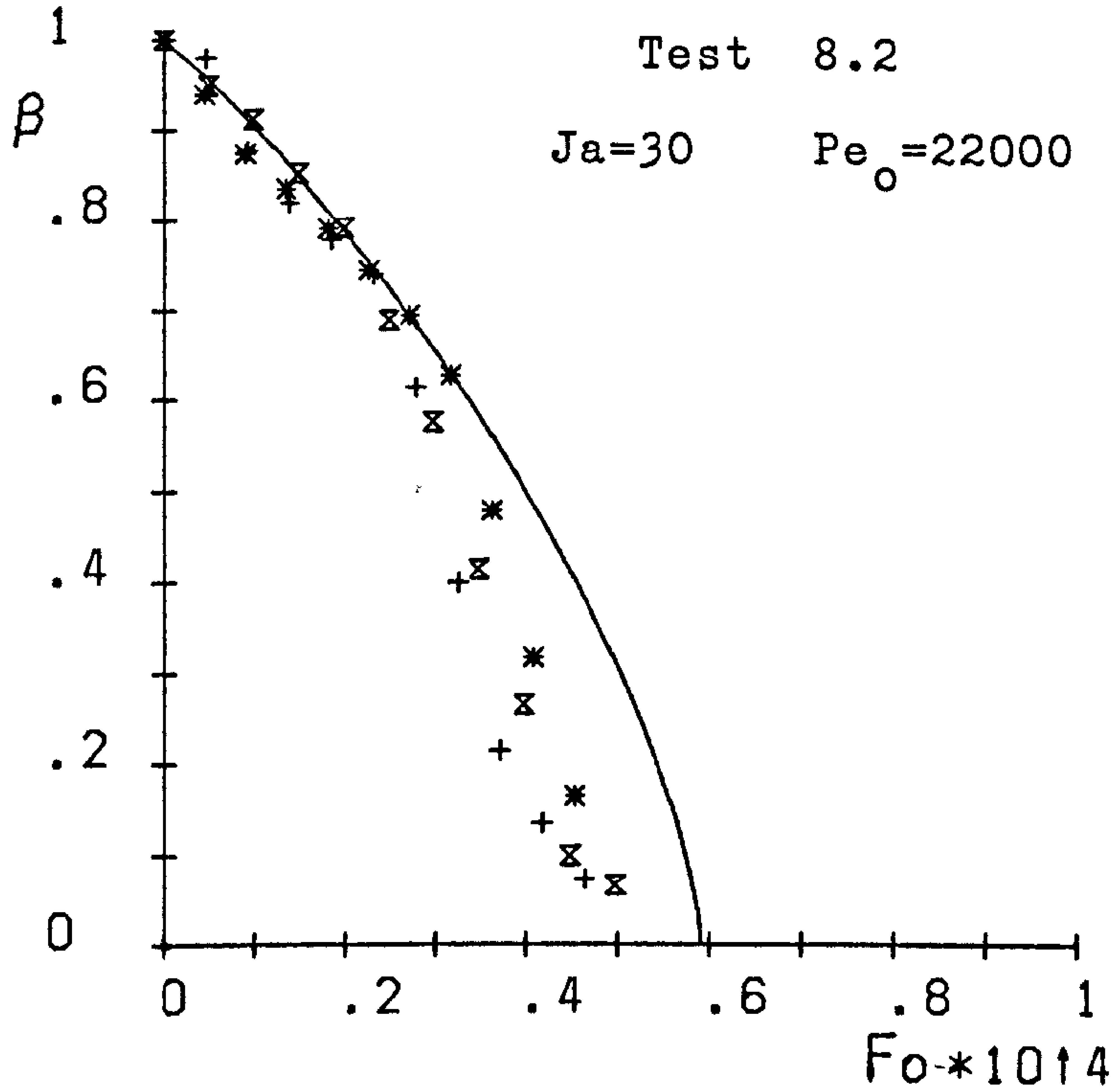

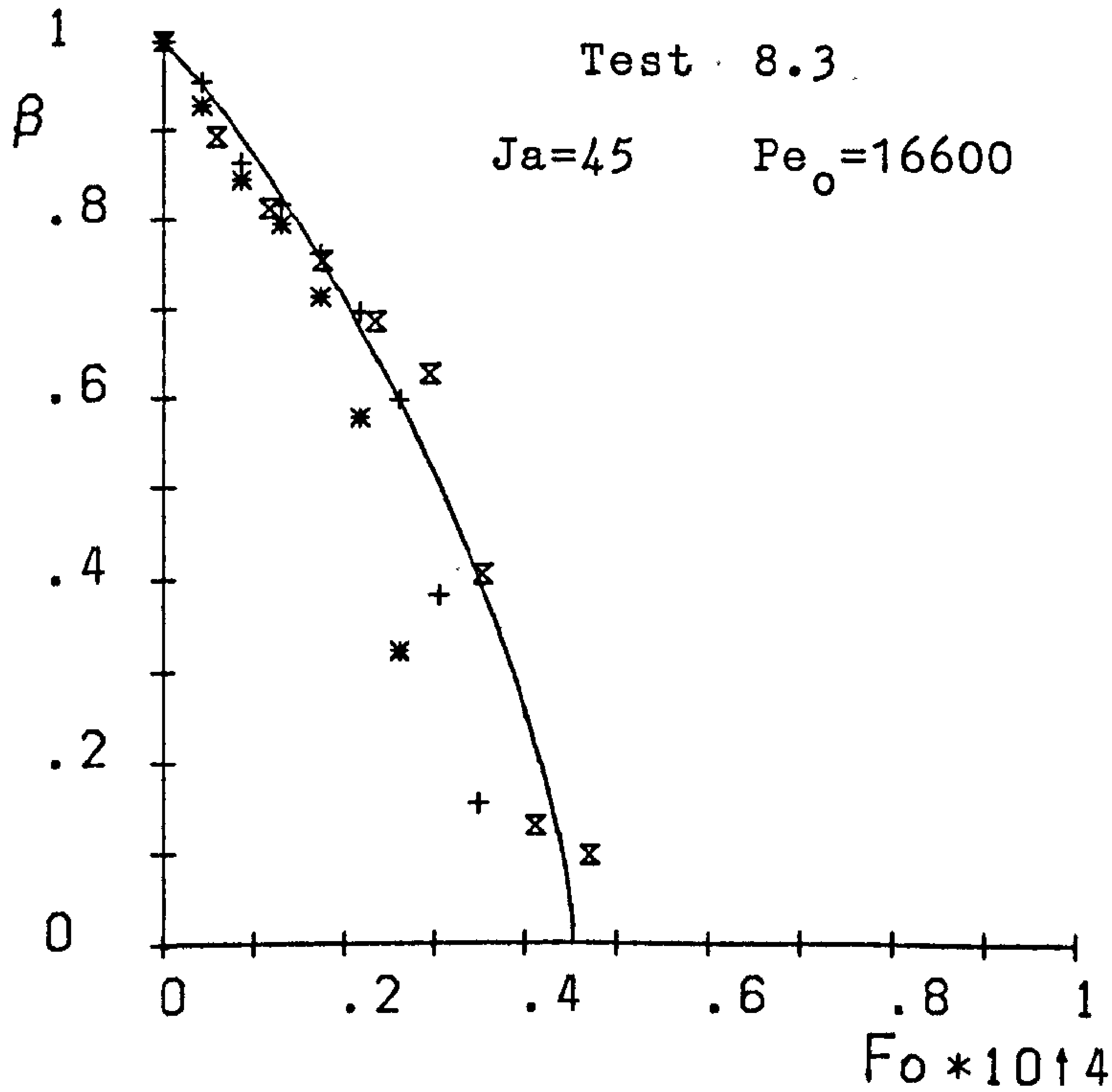

Fig.6.2 Radius ratio (β) versus Fourier number (Fo)

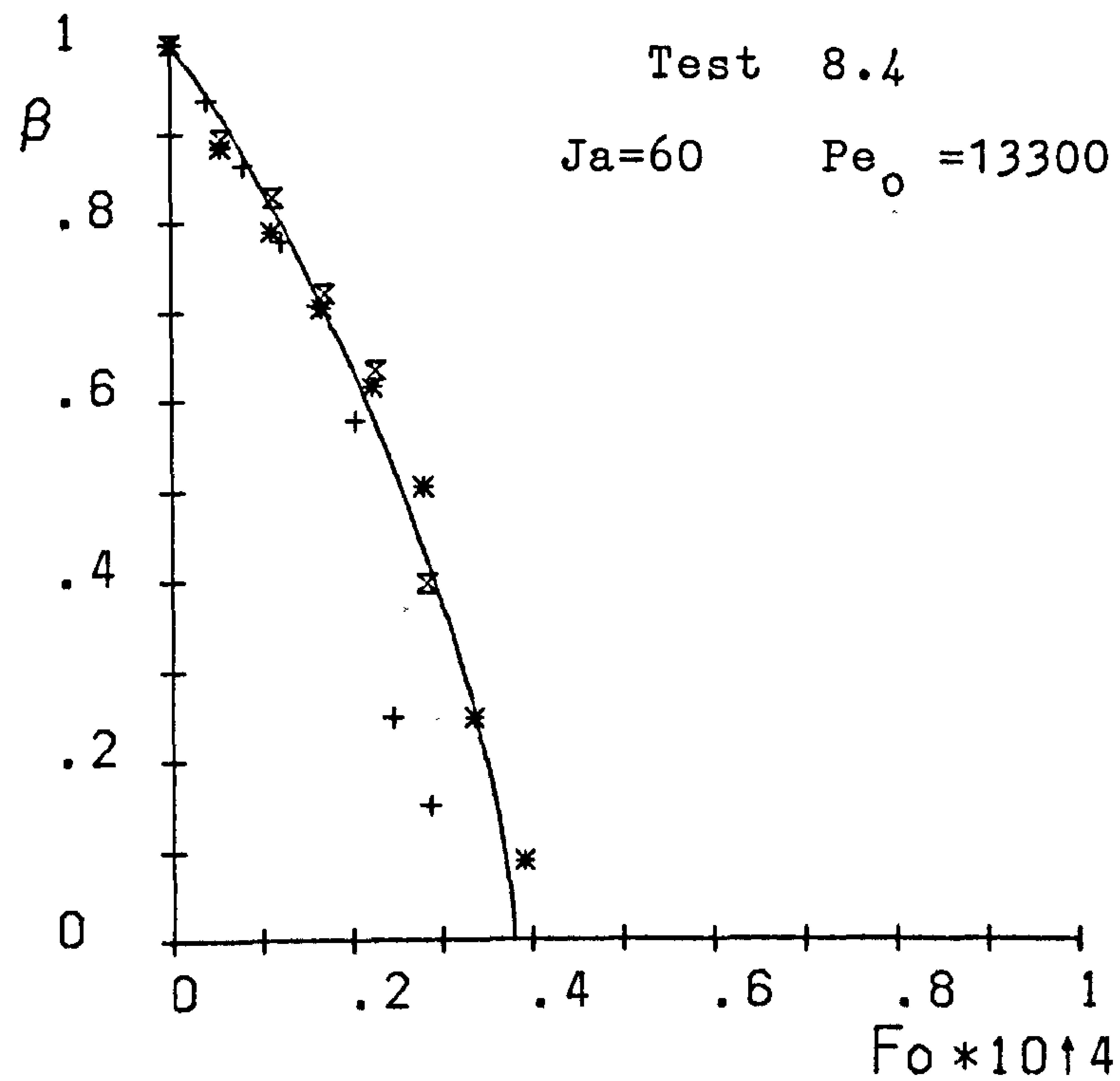

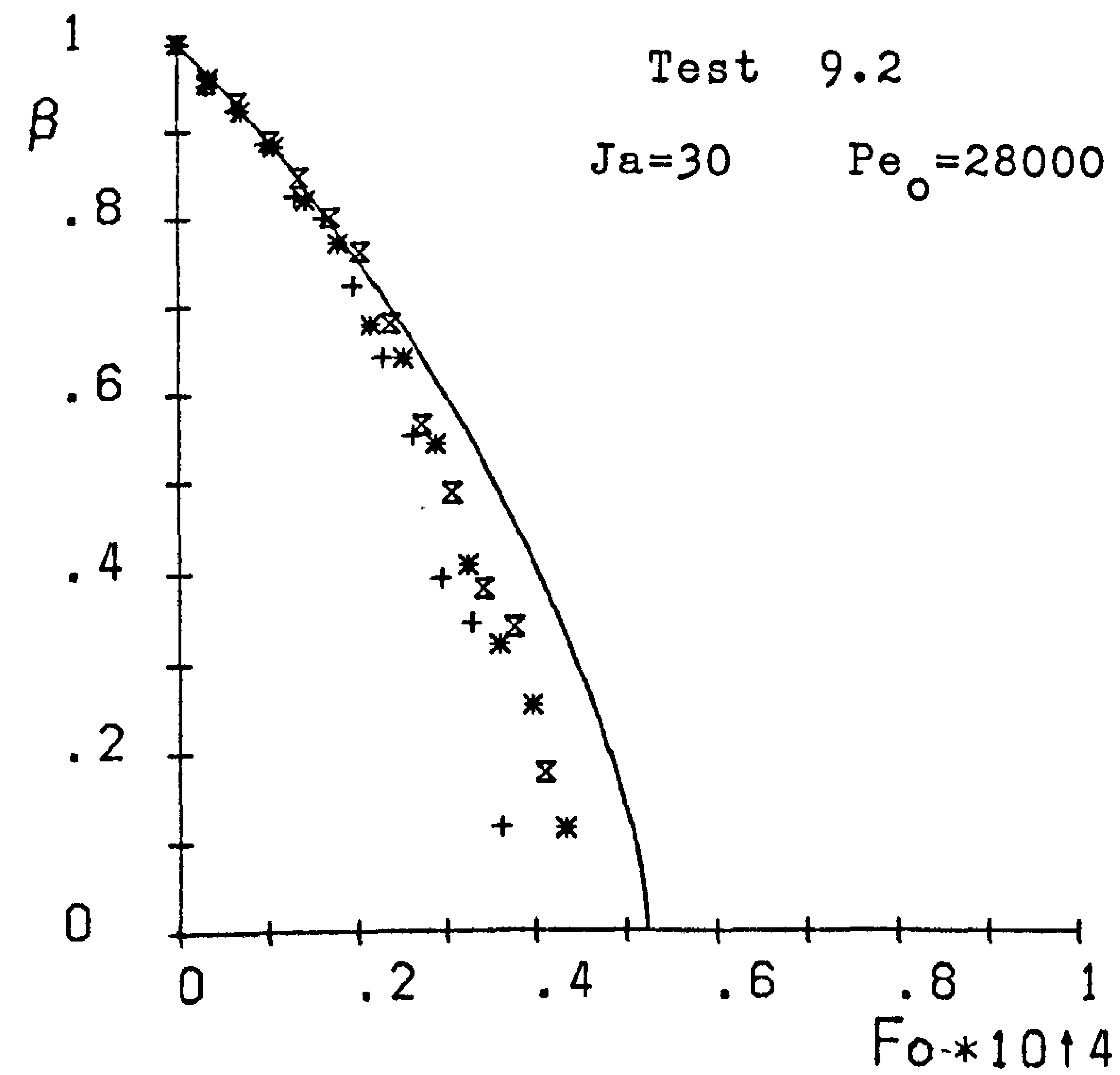

Fig.6.2 Radius ratio (β) versus Fourier number (Fo)

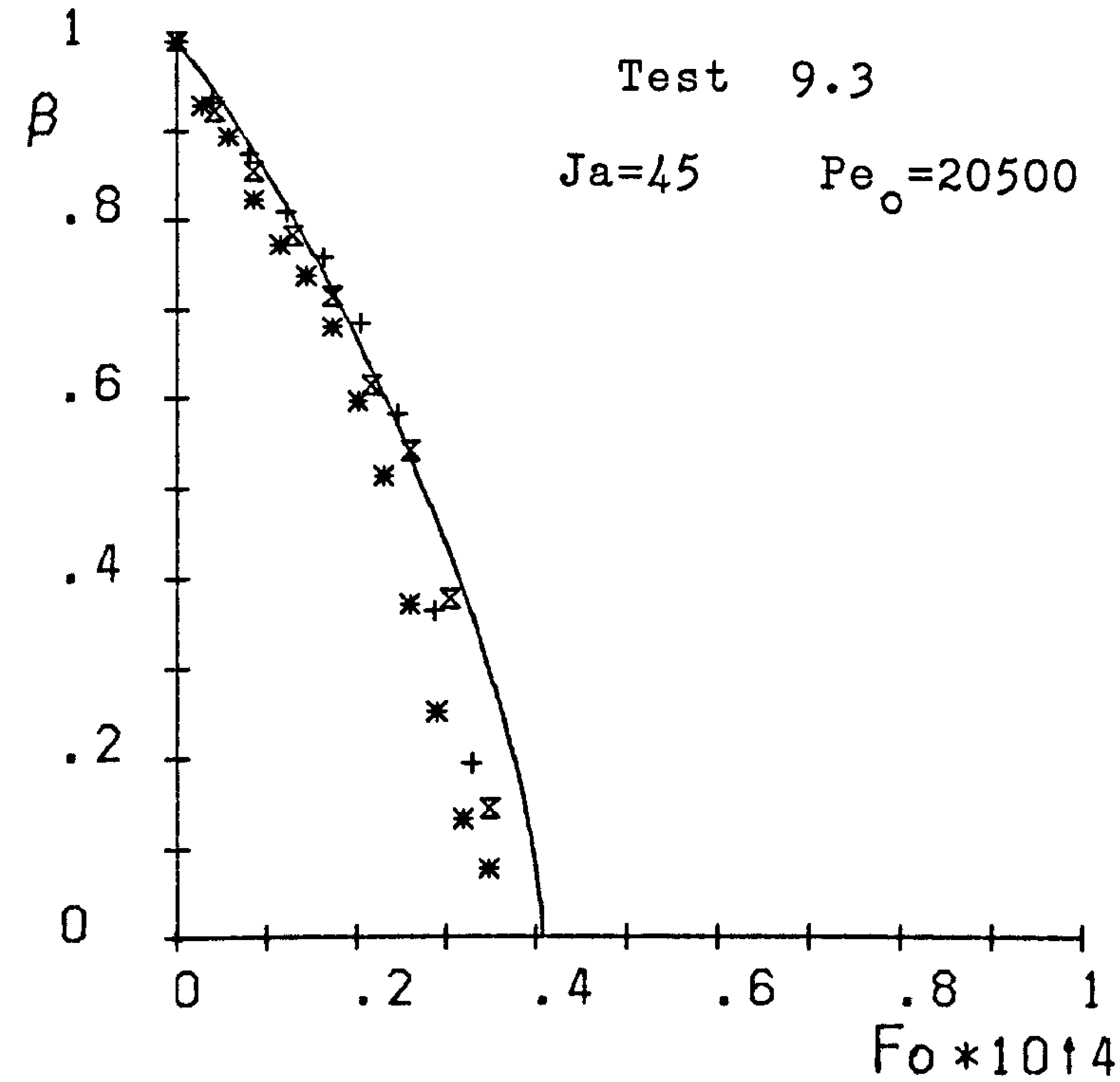

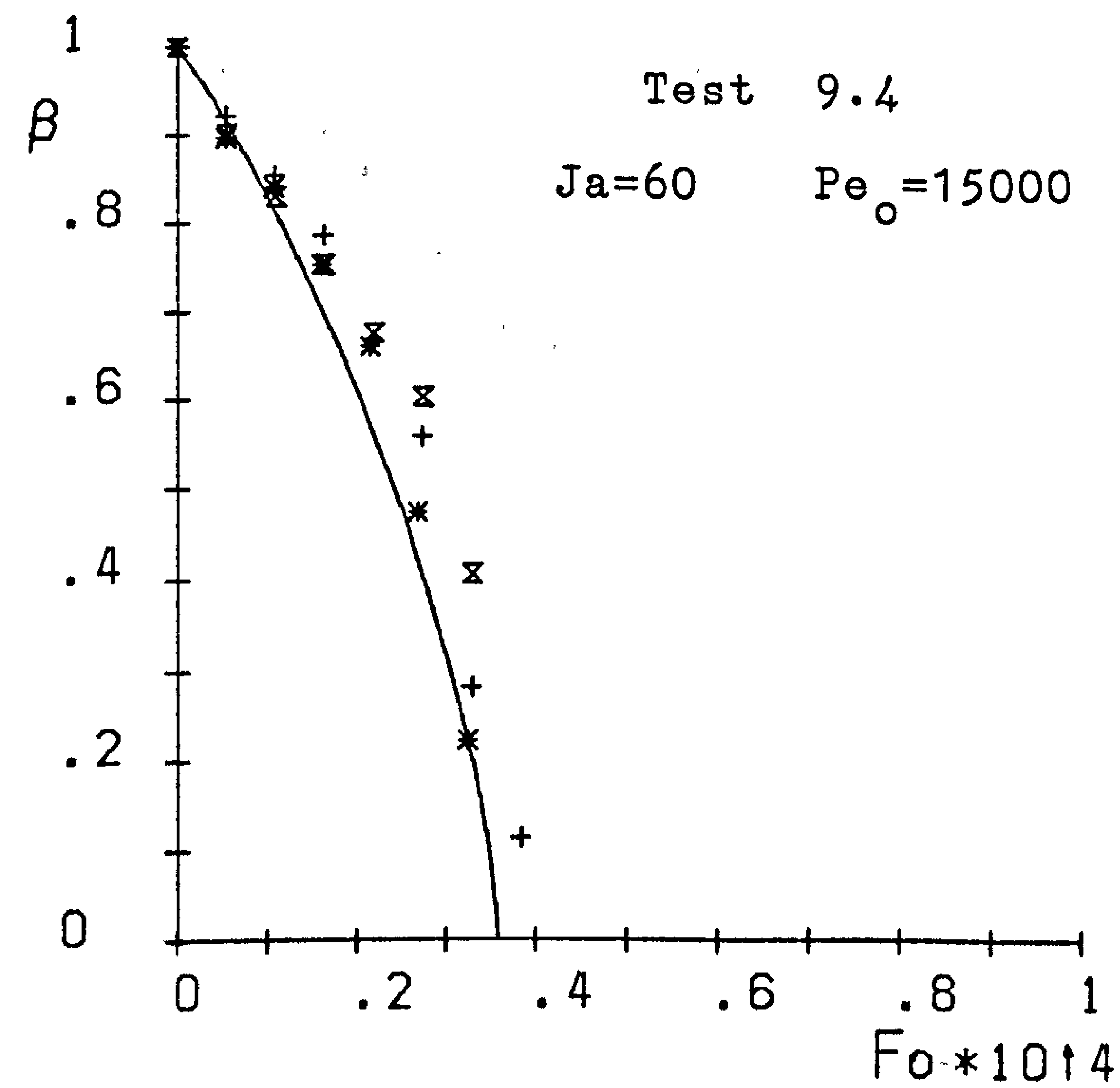

Fig.6.2 Radius ratio (β) versus Fourier number (Fo)

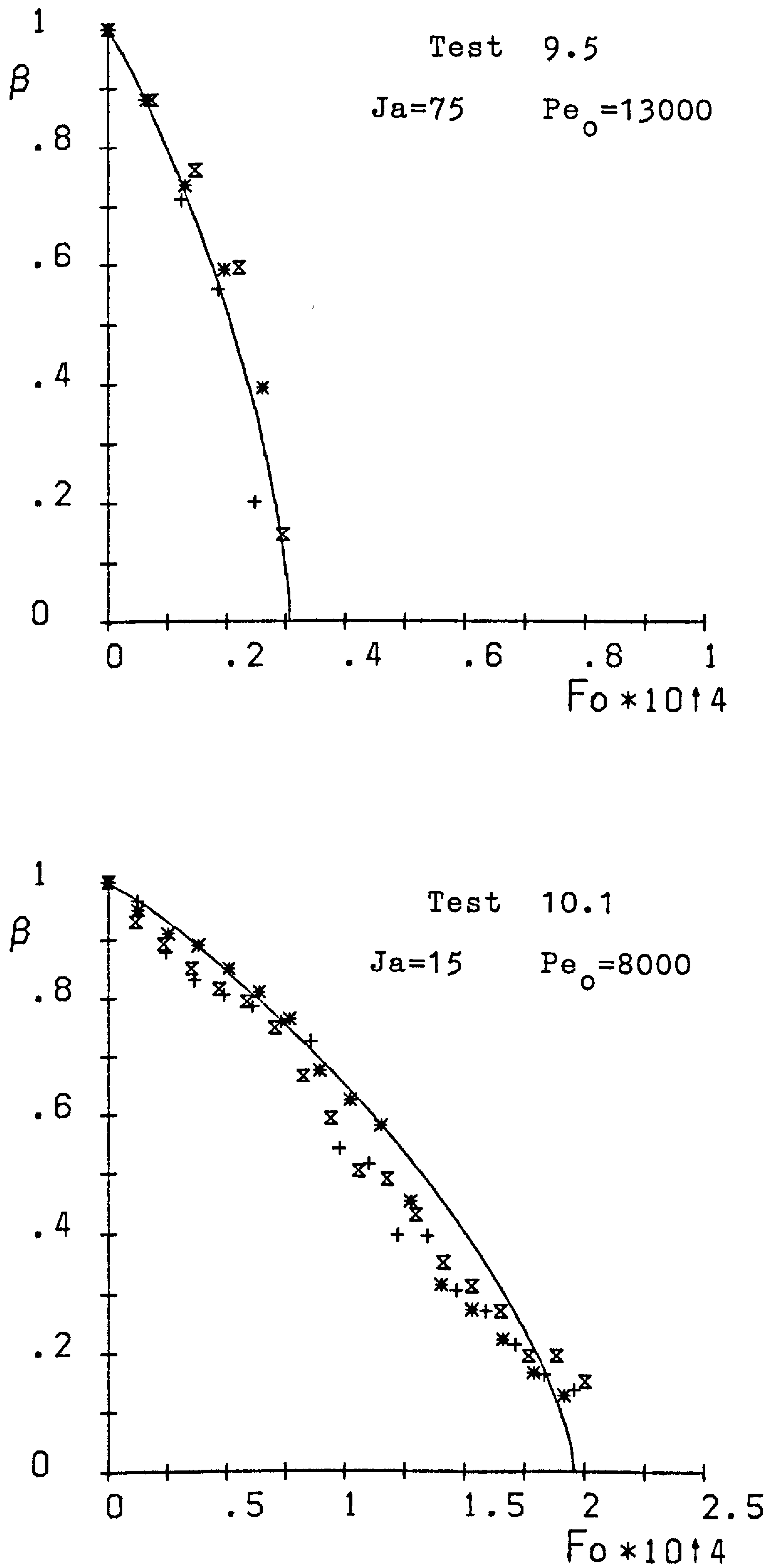

Fig.6.2 Radius ratio (β) versus Fourier number (Fo)

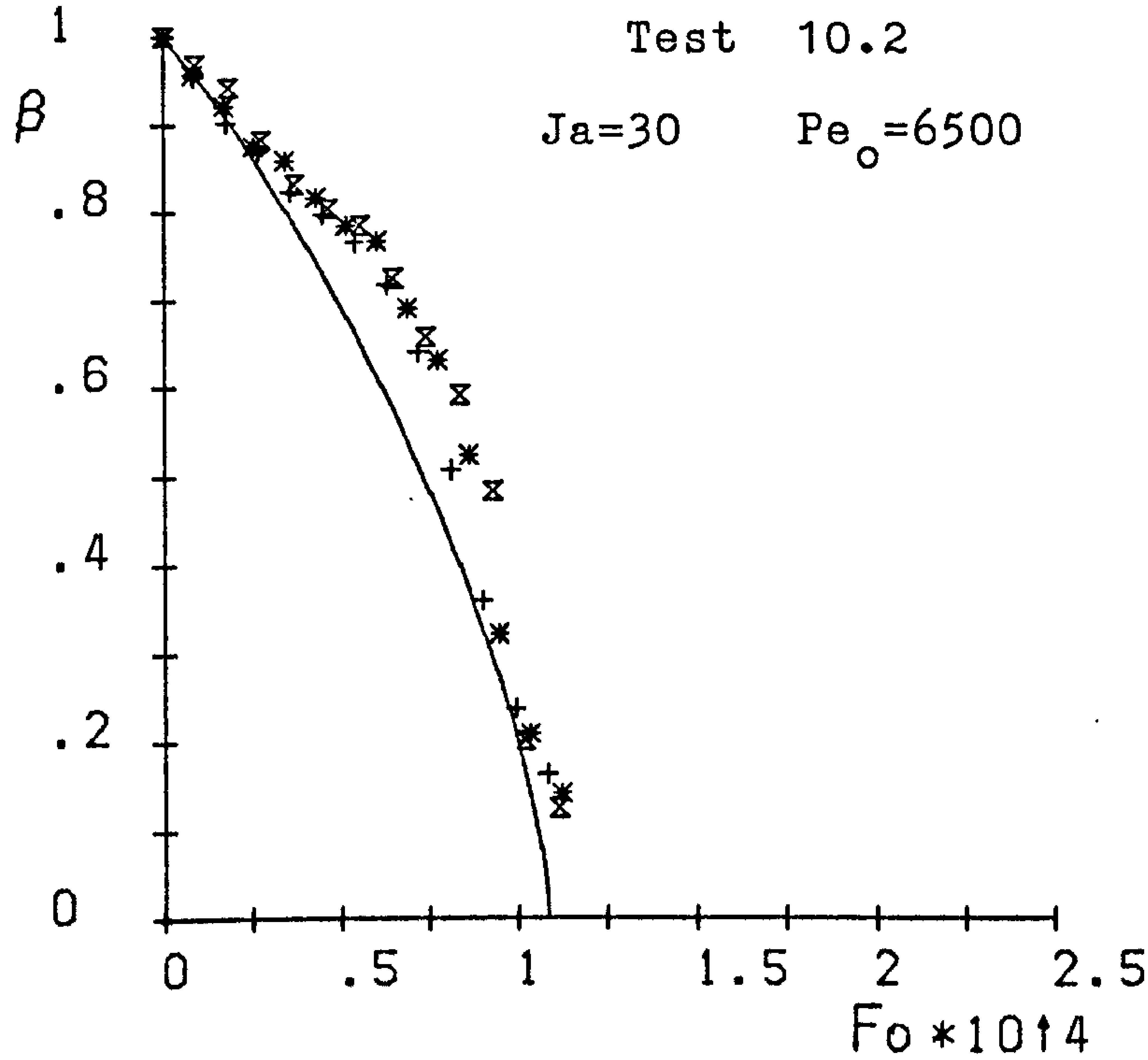

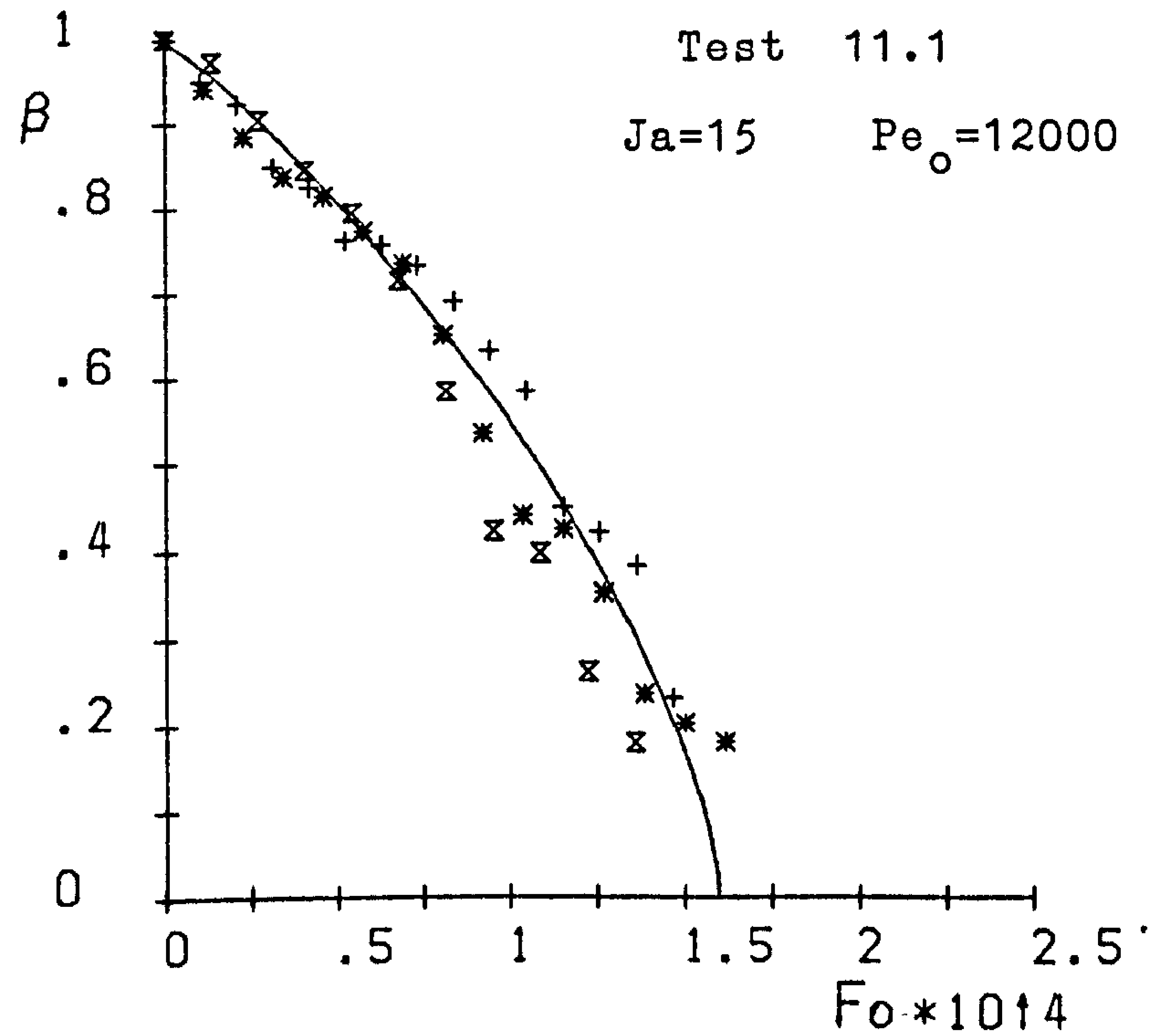

Fig.6.2 Radius ratio (β) versus Fourier number (Fo)

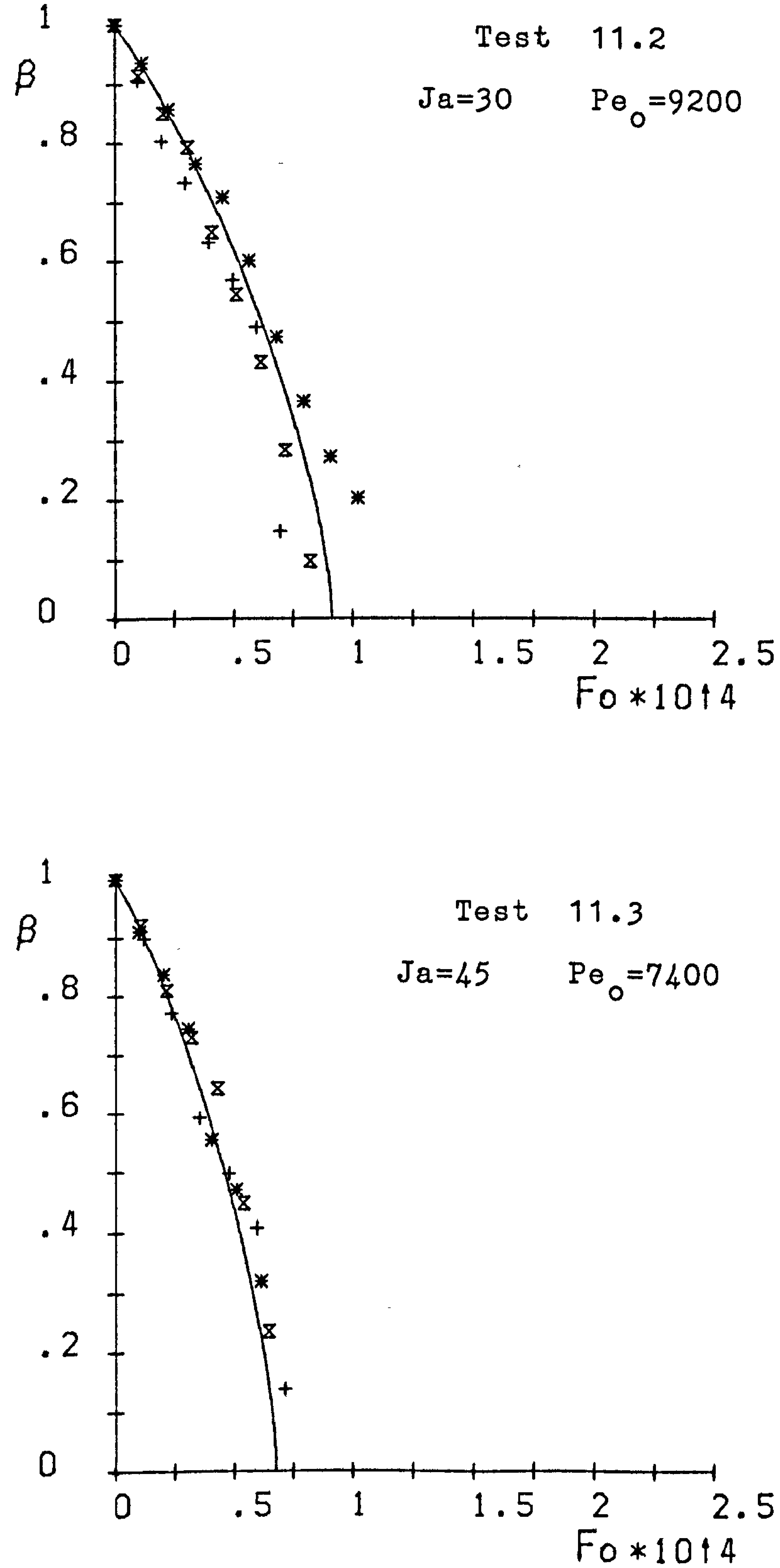

Fig.6.2 Radius ratio (β) versus Fourier number (Fo)

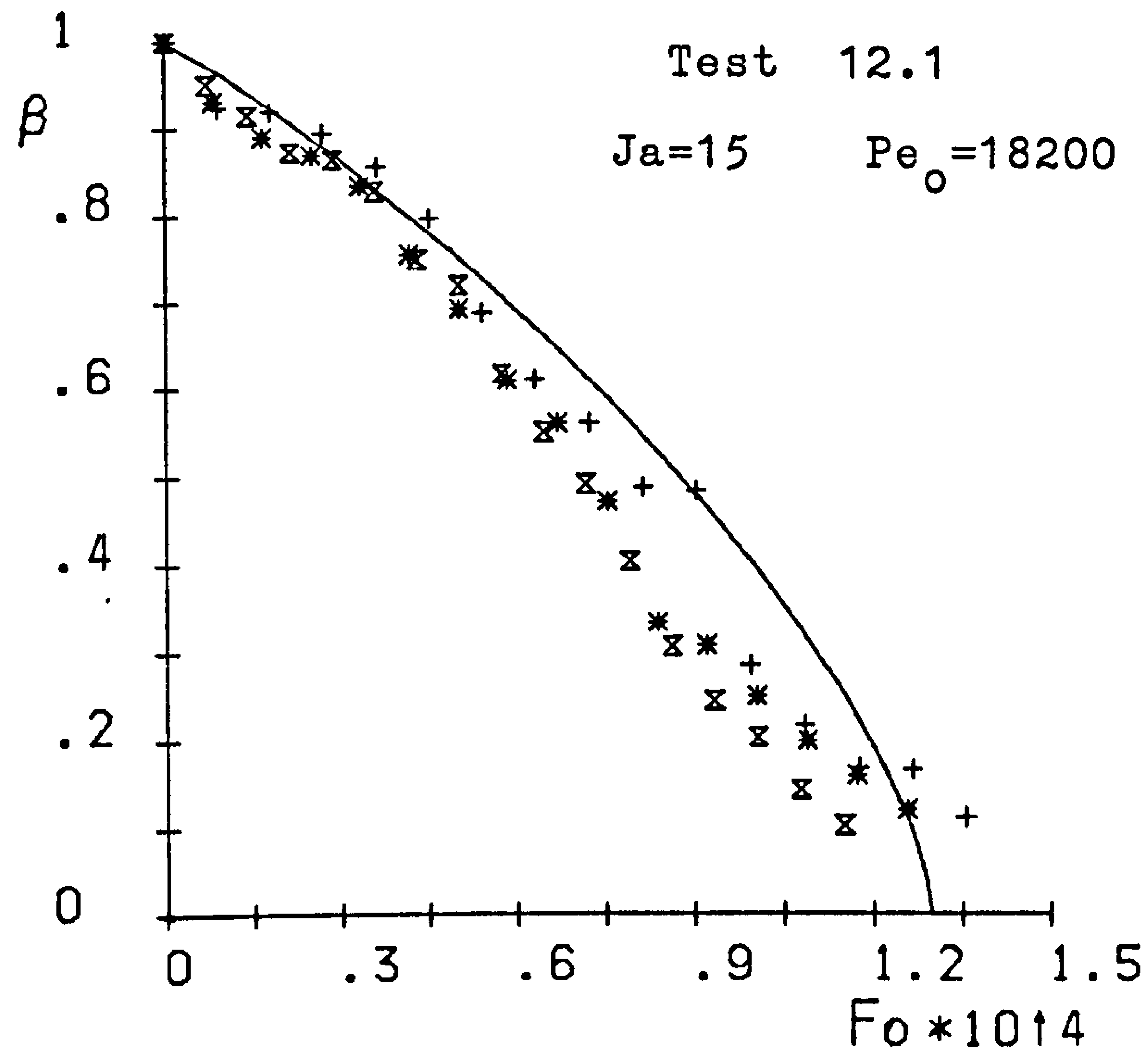

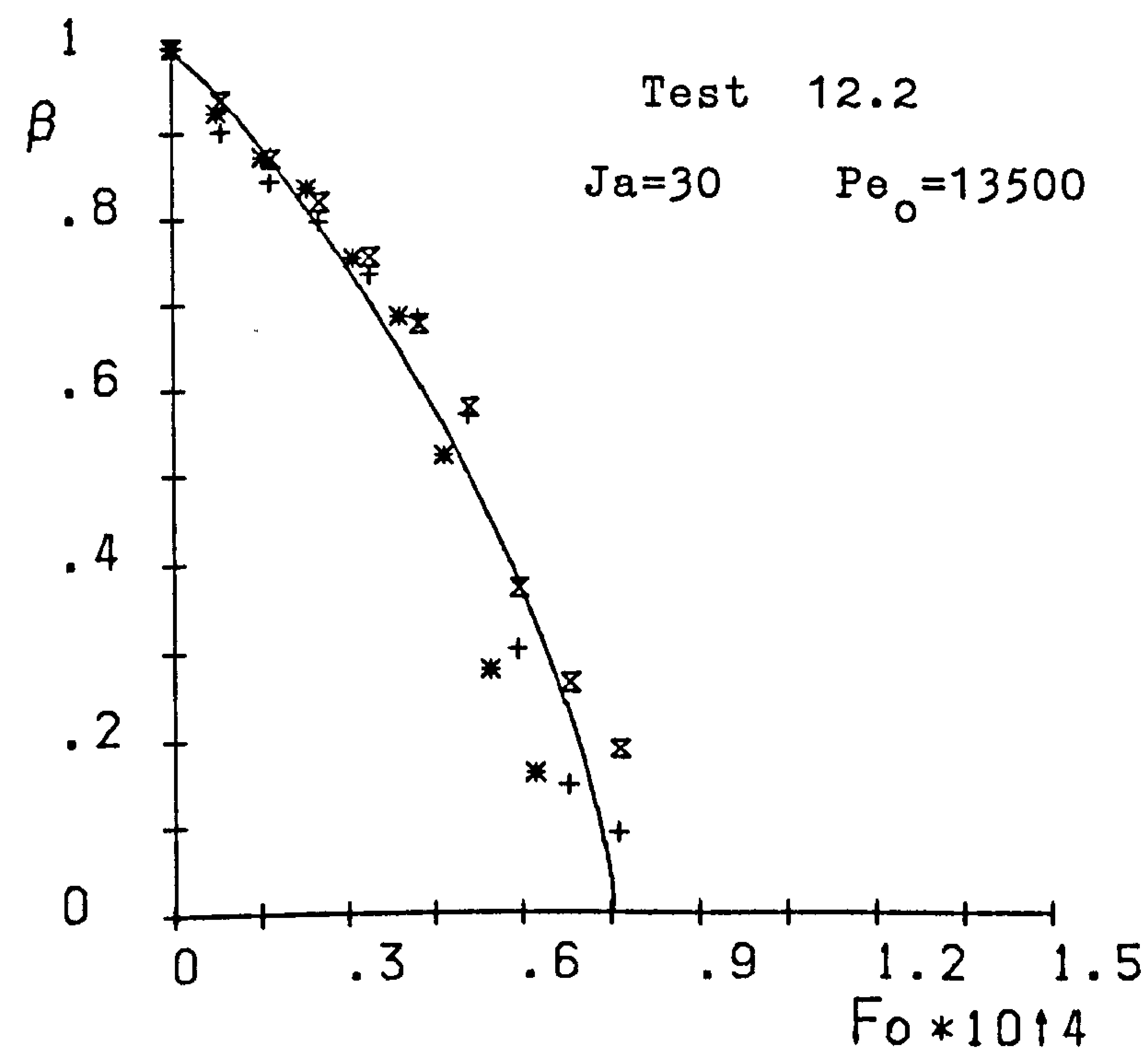

Fig.6.2 Radius ratio (β) versus Fourier number (Fo)

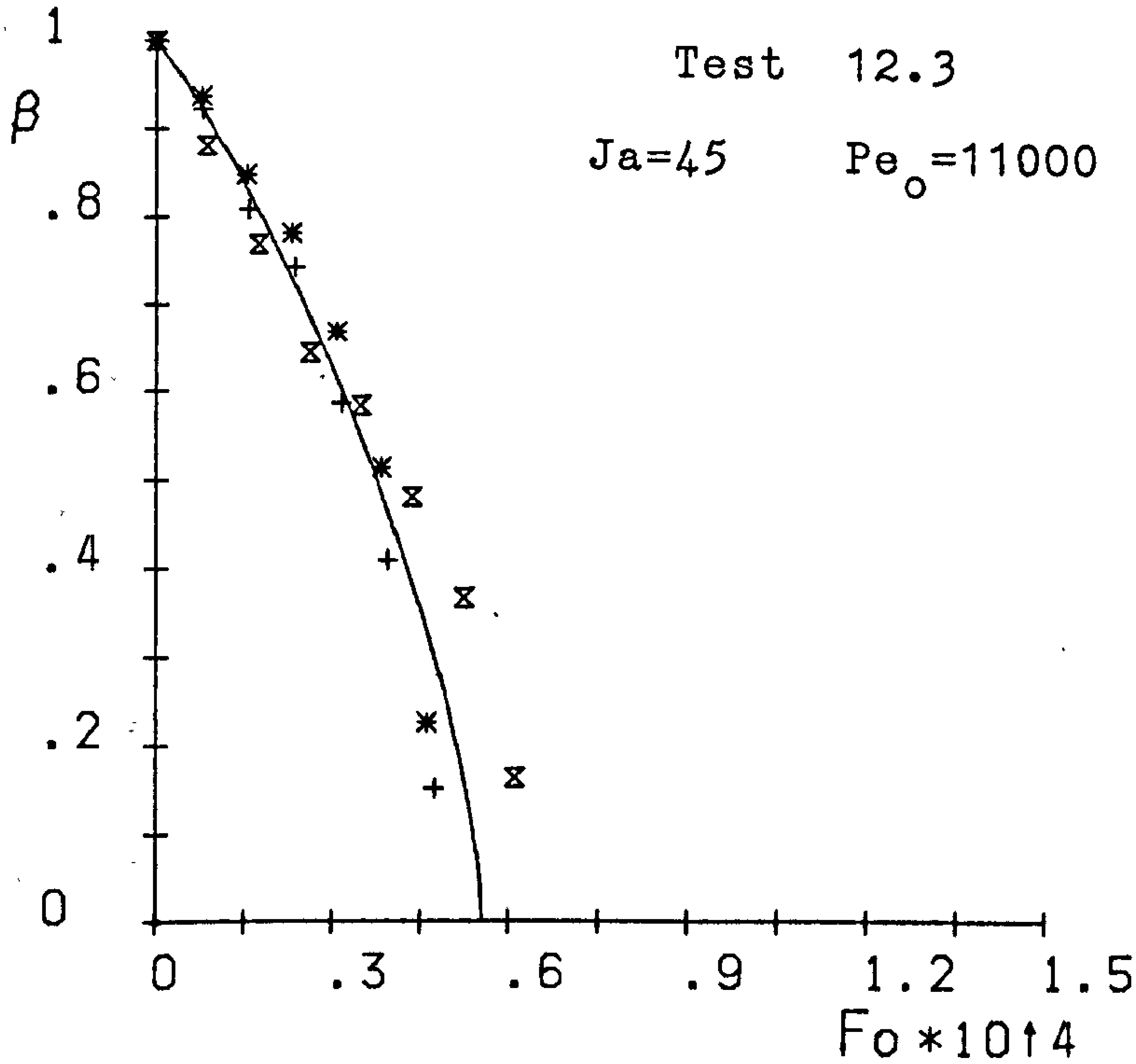

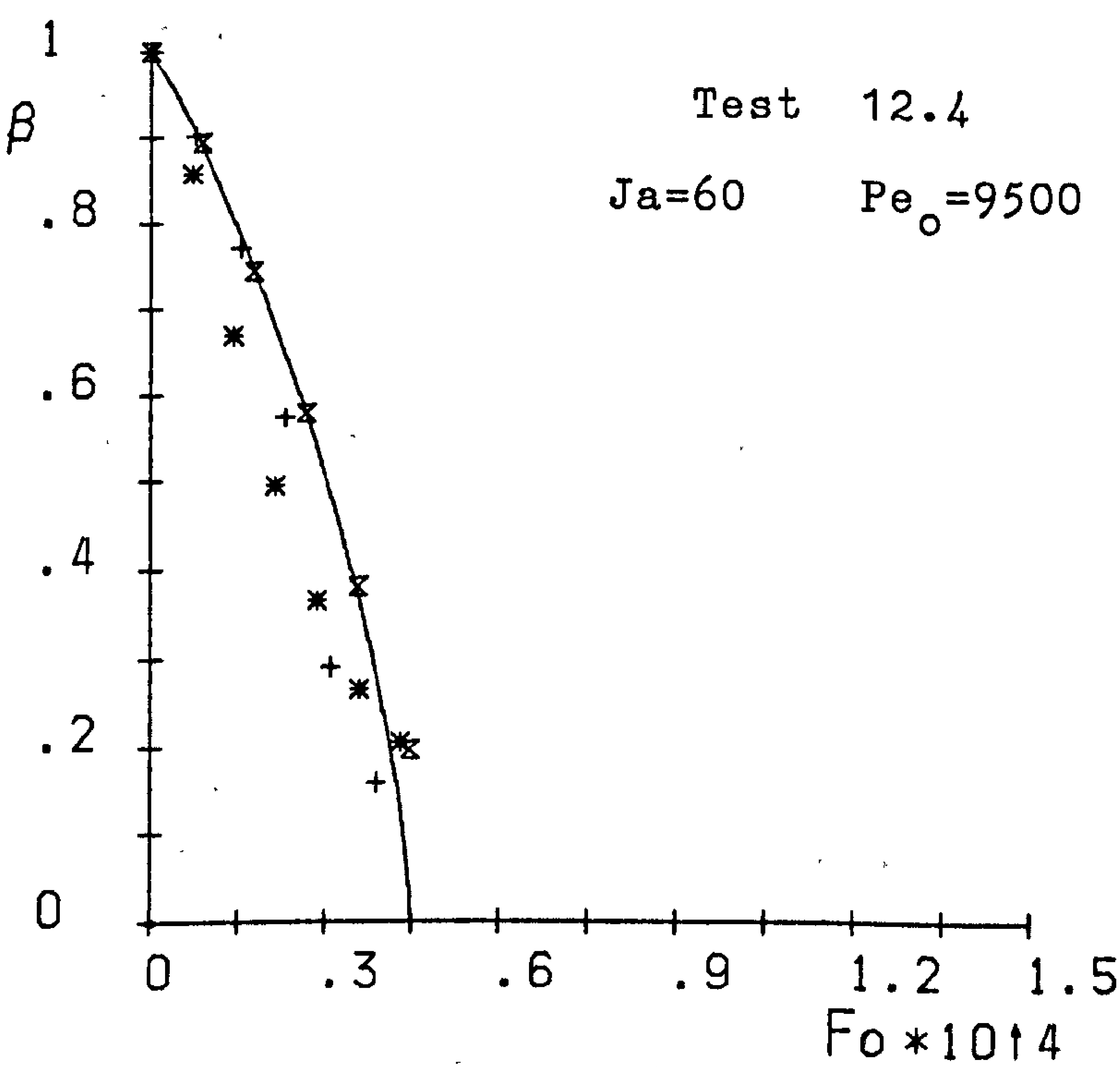

Fig.6.2 Radius ratio (β) versus Fourier number (Fo)

the smaller orifice of 1 mm, and show reasonable agreement with equation (6.2). In addition the form of the collapse curve for test 4.1 is much more curved and closer to the form indicated for higher values of Jakob number.

It was noted during both testing and the subsequent analysis of the cine films that, at 1 bar and Ja=15, the bubbles were larger, elongated and more distorted and the water in the chamber was more agitated than for the other tests. This may have been because there was less pre-detachment condensation at the lowest value of Jakob number. This is illustrated in Fig. 6.3, in a typical set of photographs, taken from test 2.1, showing the bubble growth at the orifice and the collapse after detachment. At 2 bar and Ja = 15, because of the greater steam density, the bubbles were smaller for the same steam flow rate. This meant that both water agitation and bubble distortion were lower than for a pressure of 1 bar. Thus it would appear that the faster collapse of the bubbles for Ja = 15 and 1 bar could be attributed to the effects of large bubble size giving oscillation, greater distortion and increased water agitation.

In many of the tests, especially at higher Jakob numbers, the collapse rate is slower, during the early stages of collapse, than the predicted collapse rate, but later on the rate of collapse increases so that the final collapse time shows reasonable agreement with that predicted, and in a few cases gives a faster collapse than the predicted rate. This type of collapse is illustrated in Fig. 6.4, in a typical set of photographs taken from test 5.2.

This collapse pattern may be due to the effect of the bubble condensation giving some heating of the water near the orifice and so reducing the effective driving

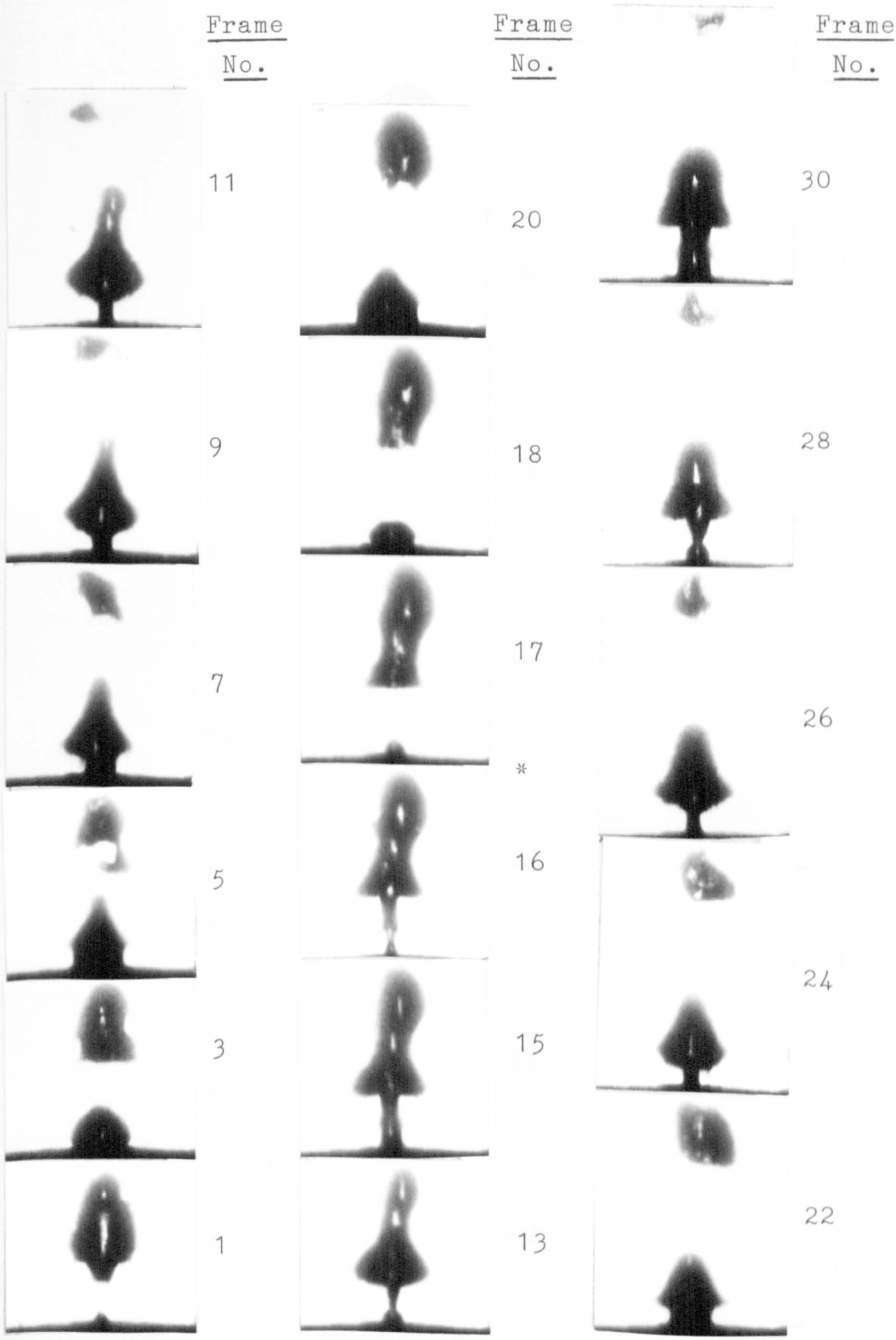

Fig.6.3 Photographs of bubble growth and collapse
Test 2.1 , Δt/Frame=2.37 ms
* Detachment point

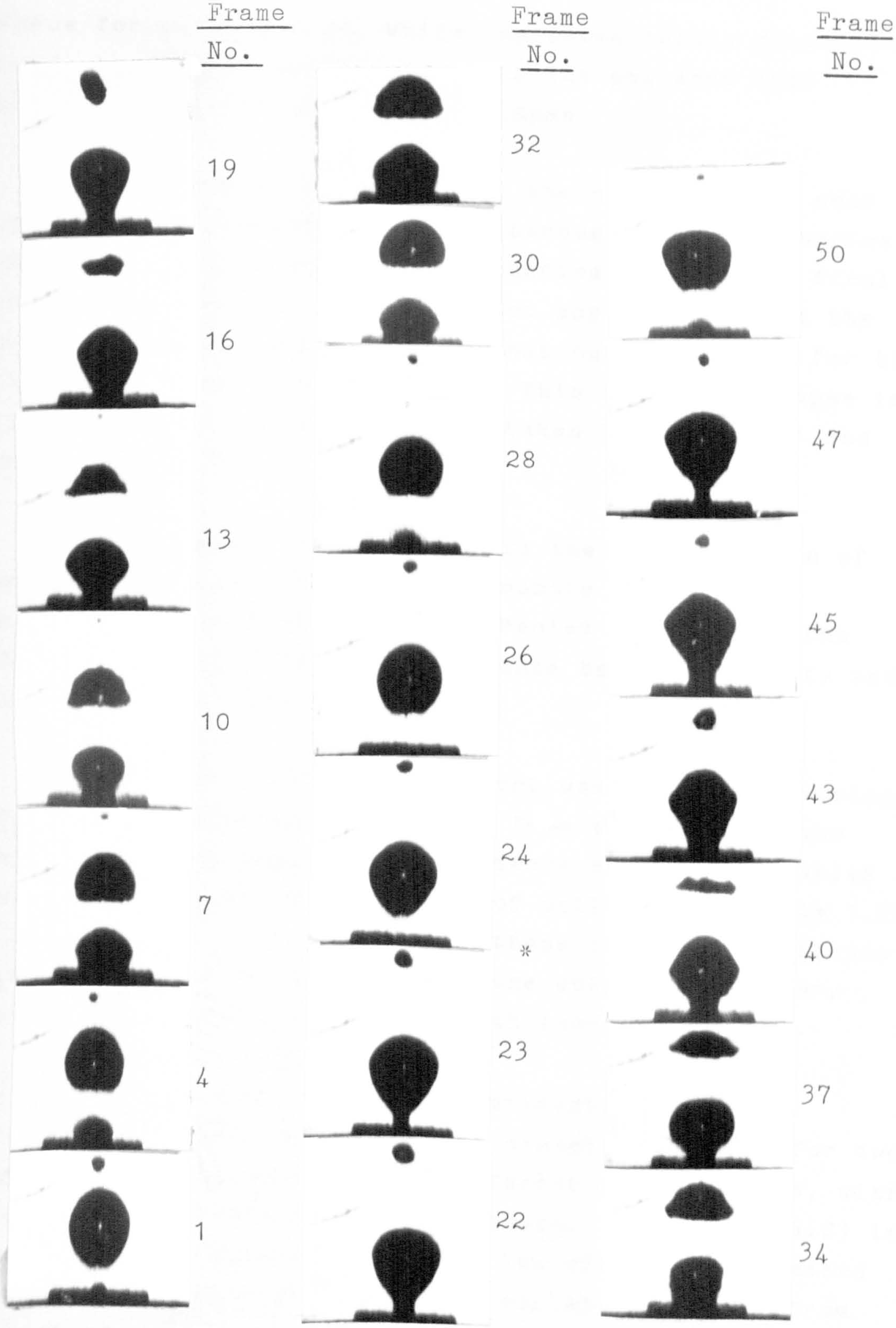

Fig.6.4 Photographs of bubble growth and collapse
Test 5.2 , Δt/Frame=0.79 ms
* Detachment point

force for condensation, while increased bubble distortion leads to a more rapid increase in the collapse rate towards the later stages of collapse.

In a number of the tests, the bubble, while near spherical at detachment, passes through a short spherical cap phase before reverting to spherical before the final collapse. However, this does not appear to affect the collapse pattern which follows that outlined above for the tests at higher Jakob numbers. This type of collapse is illustrated in the photographs, taken from test 4.1 and shown in Fig. 6.5.

Considering the accuracy in the determination of bubble rise velocities for each bubble and later in deciding the smoothed values of Peclet numbers for the different conditions, the agreements between the data and the curves are good.

Although considerable effort was spent in removing air from the apparatus and hence from the bubbles, the data still show signs of the presence of noncondensables especially in the latest stages of collapse for tests 1.2, 4.1, 5.1, 5.3, 10.1, 12.1. In these tests, the collapse rate tends to slow down late in the collapse with very little change in radius ratio with increase in time.

In Fig. 6.6 (a to d), experimental data are presented for the larger orifice diameter of 2 mm, for two different pressures and four different Jakob numbers, with a nominal mass flow rate of 1.5 g/min. Equation (6.2) is also shown for each condition. The effect of increased Jakob number leading to a faster collapse is clear from the plots. For the same Jakob number, the bubbles have a smaller value of Peclet number at a pressure of 2 bar and

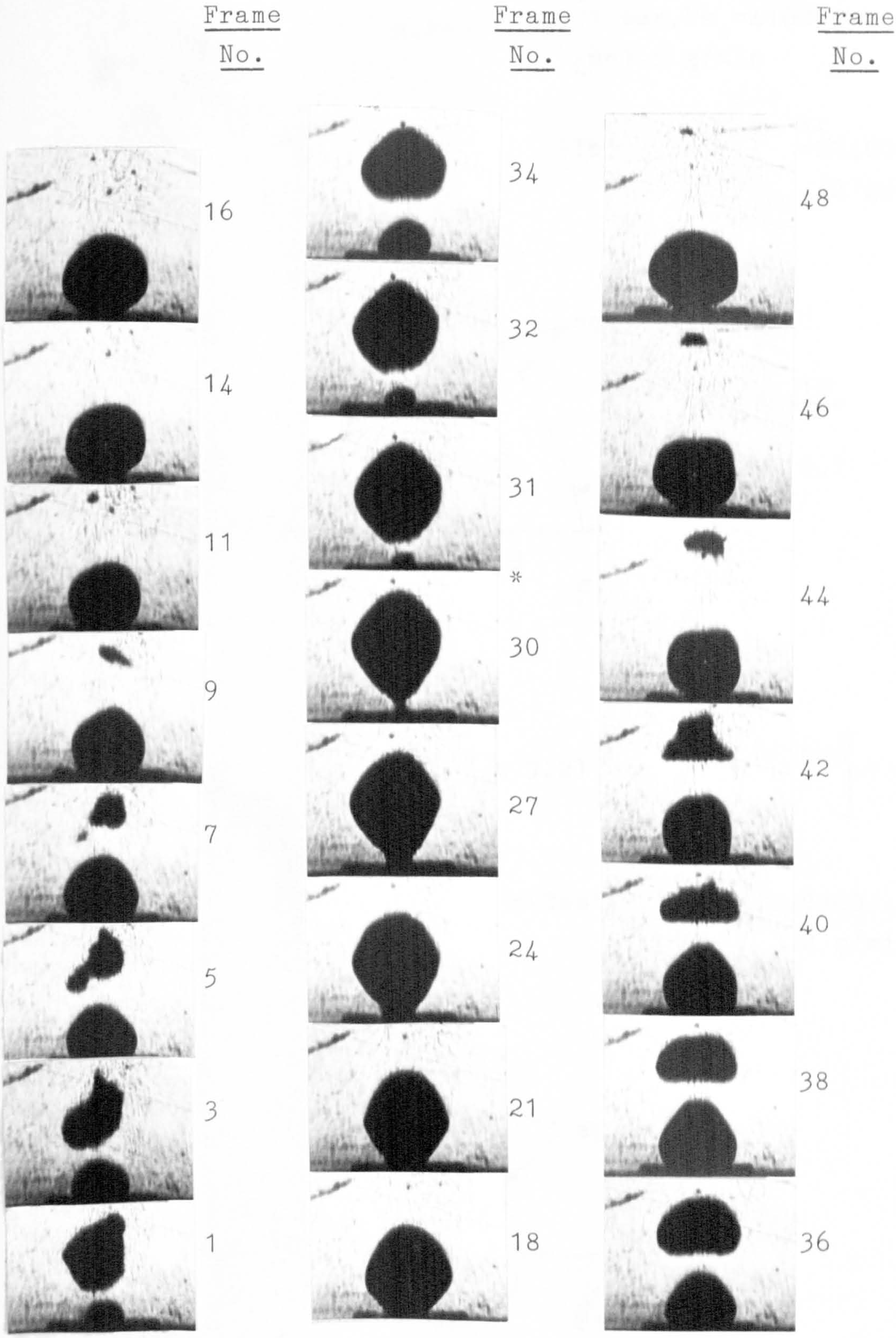

Fig.6.5 Photographs of bubble growth and collapse
Test 4.1 , Δt/Frame=1.186 ms
* Detachment point

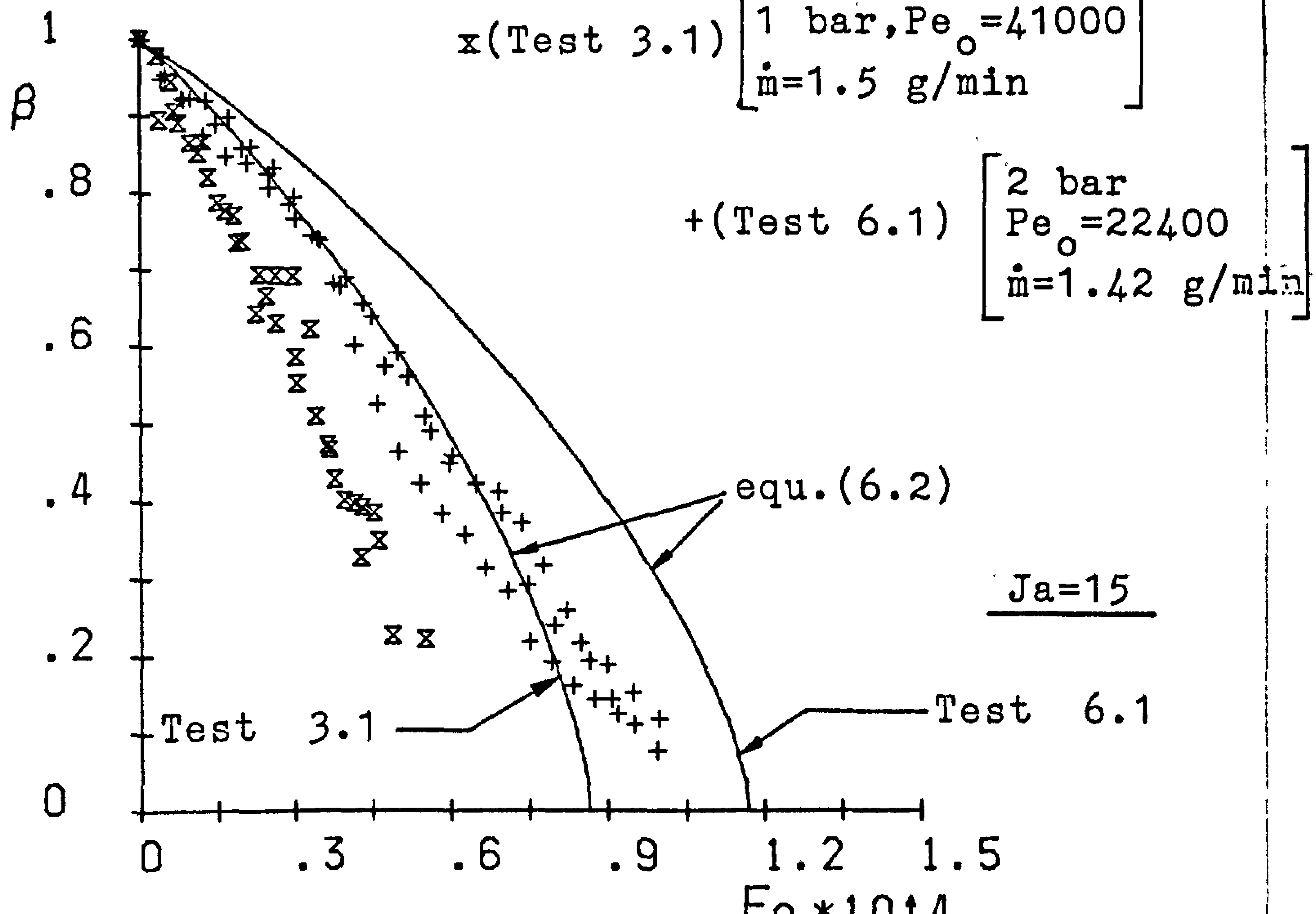

(a)

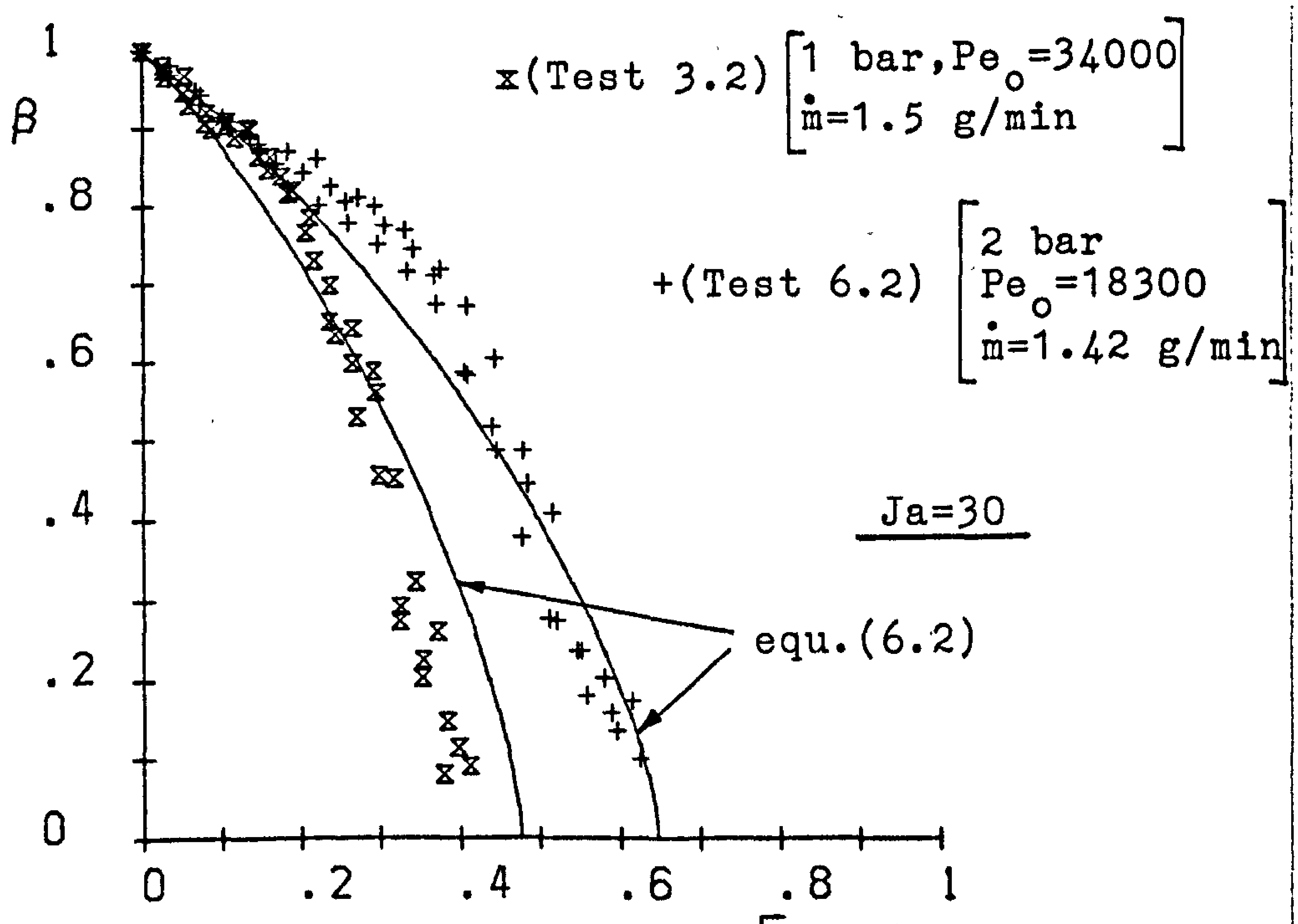

(b)

Fig.6.6 Radius ratio versus Fourier number with pressure and Jakob number as parameters

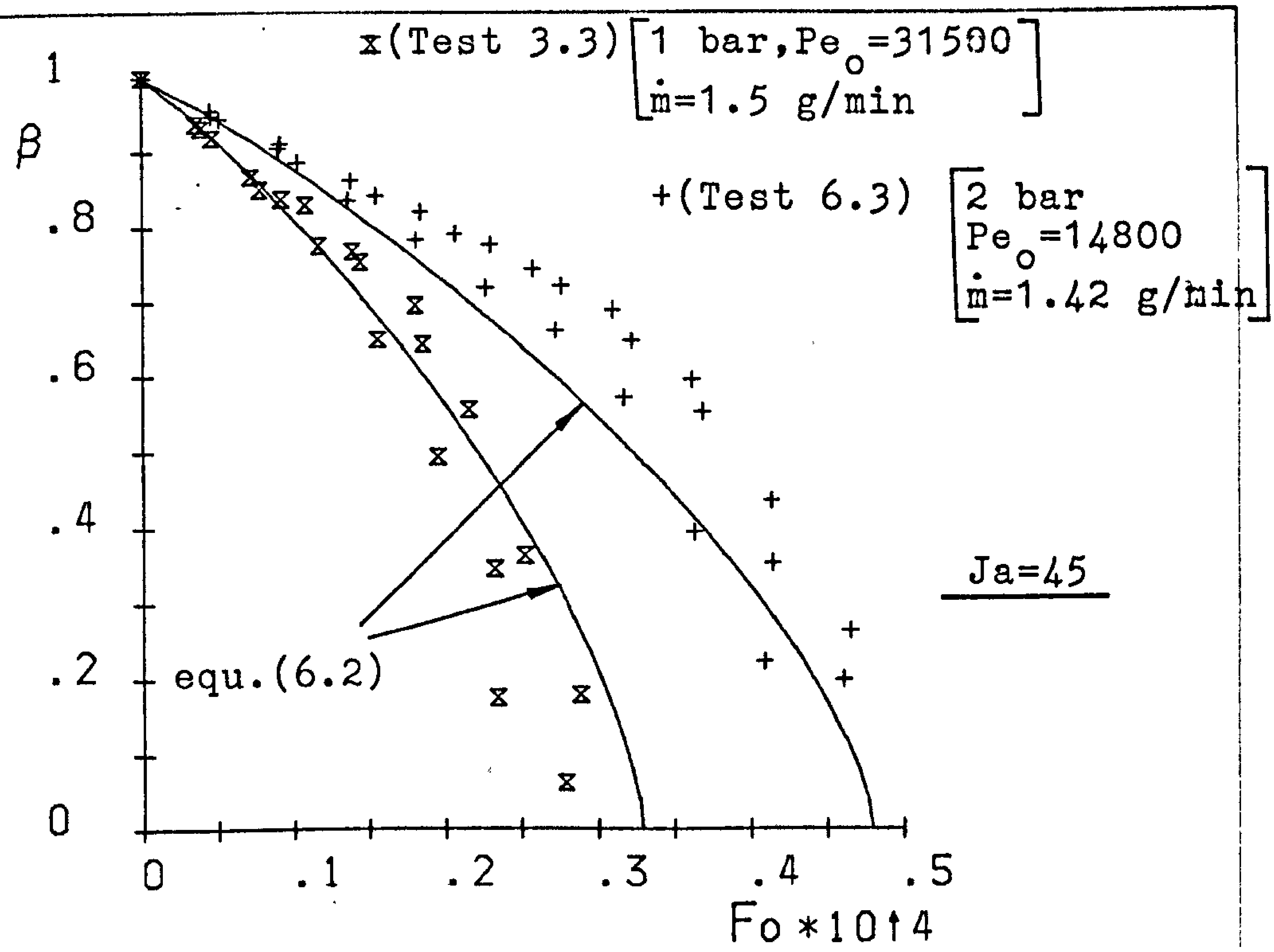

(c)

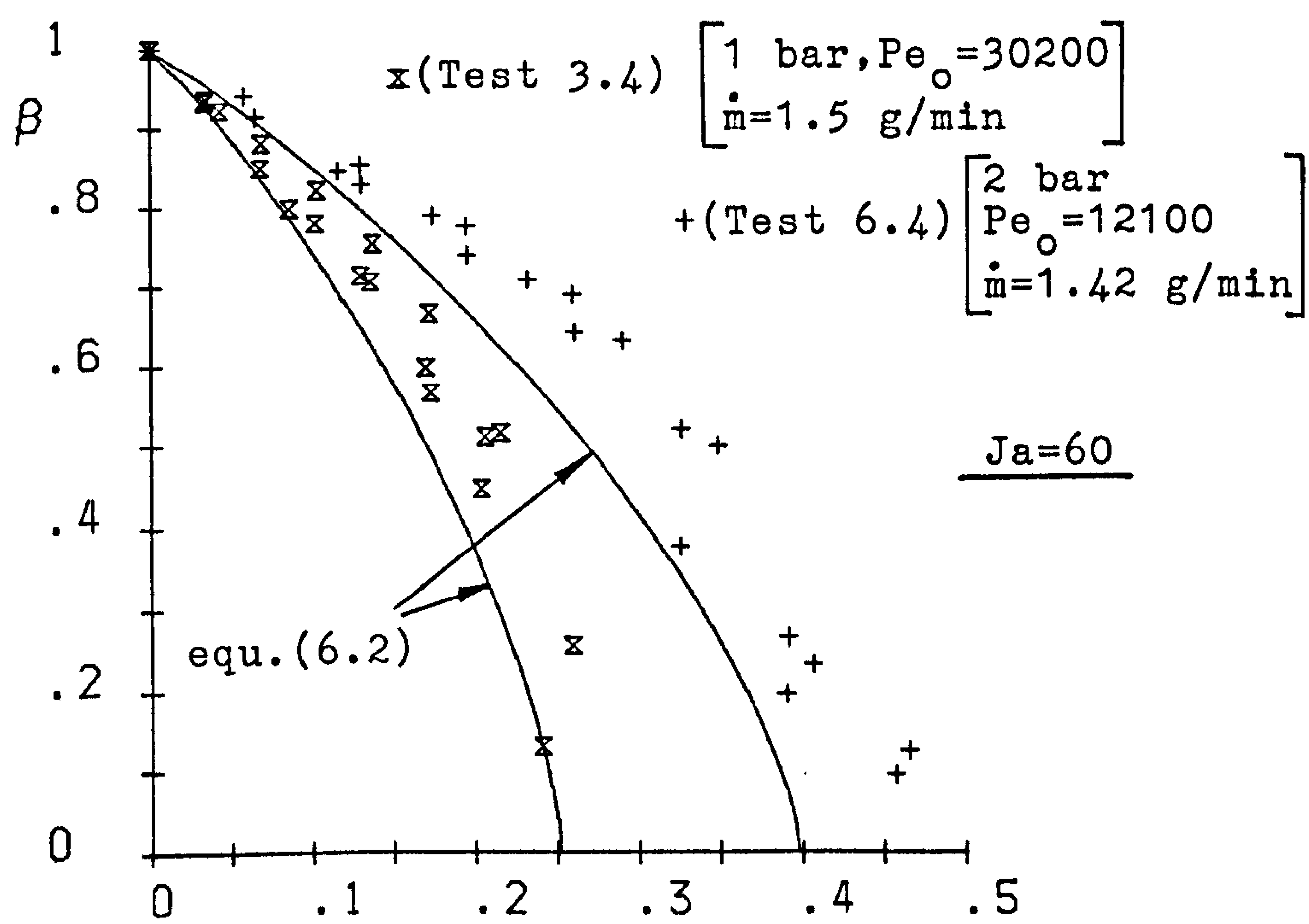

(d)

Fig 6.6 Radius ratio versus Fourier number with pressure and Jakob number as parameters consequently collapse at a slower rate than those at a pressure of 1 bar.

In Fig. 6.7 (a to c), the data are presented, for a Jakob number of 30 and a pressure of 2 bar, for different steam flow rates and different orifice diameters. With increase in steam flow rate the Peclet number increases, and consequently the collapse rate also increases, but there is little indication of any effect from change in orifice diameter.

The effect of Jakob number is explicitly allowed for in the theory but the effects of orifice diameter, steam flow rate and pressure are only taken into account indirectly through the properties of steam and water, the initial bubble radius and the rise velocity of the bubble.

The collapse Fourier number (Fo_c) according to equation (6.2) is given, when $\beta = 0$, as

$$Fo_c = \left(\frac{1}{4.35}\right)^{\frac{1}{1.10}} \cdot \frac{1}{Ja.Pe^{0.5}} = \frac{0.263}{Ja.Pe^{0.5}} \qquad (6.7)$$

The collapse height, Z_c is given as

$$Z_c = t_c.U = Fo_c.\frac{4\ R_o^2}{\alpha}.U \qquad (6.8)$$

Substituting the value of bubble rise velocity, U from equation (4.5), in this equation, gives

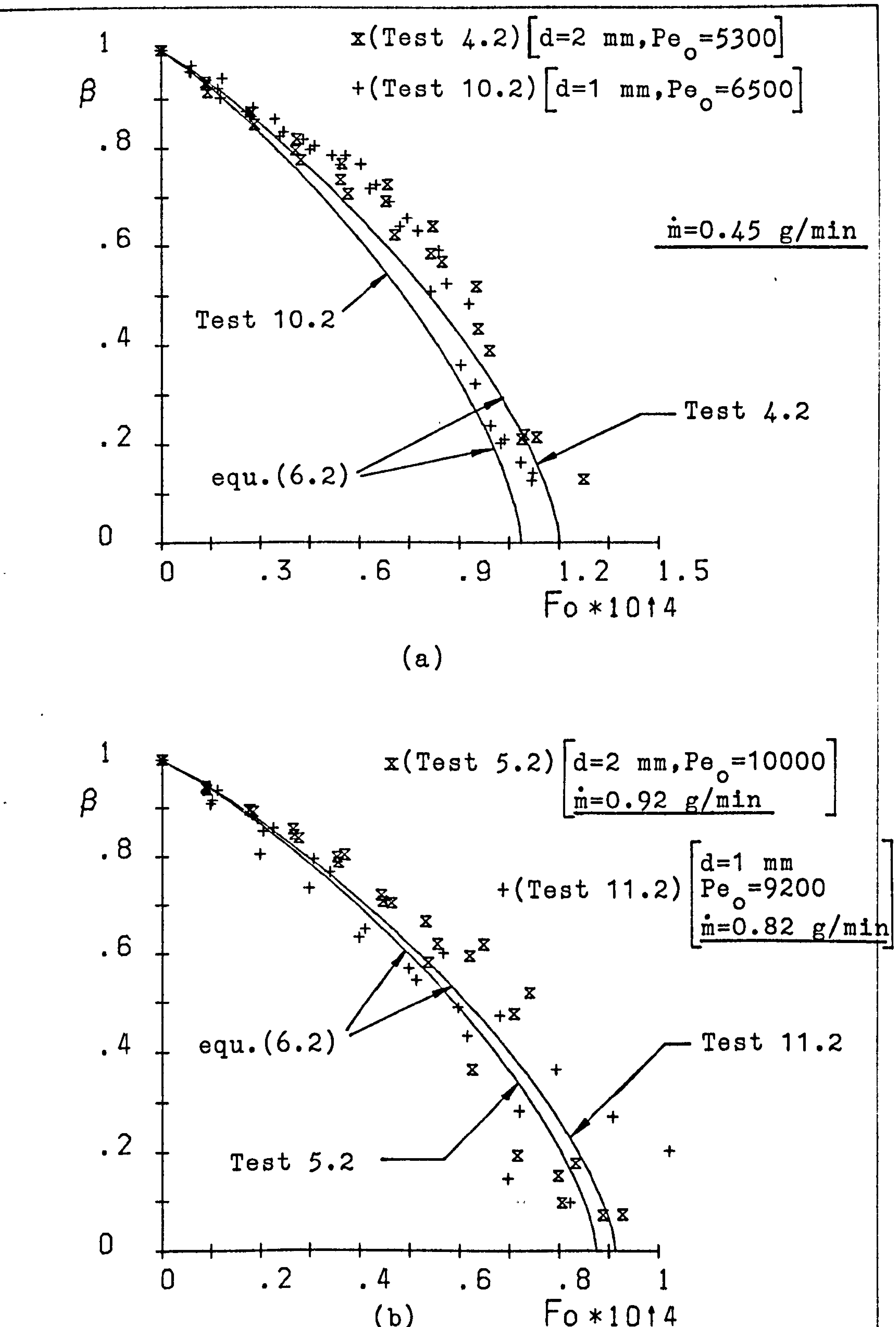

Fig.6.7 Radius ratio versus Fourier number with orifice diameter and steam flow rate as parameters. Ja=30 , P=2 bar

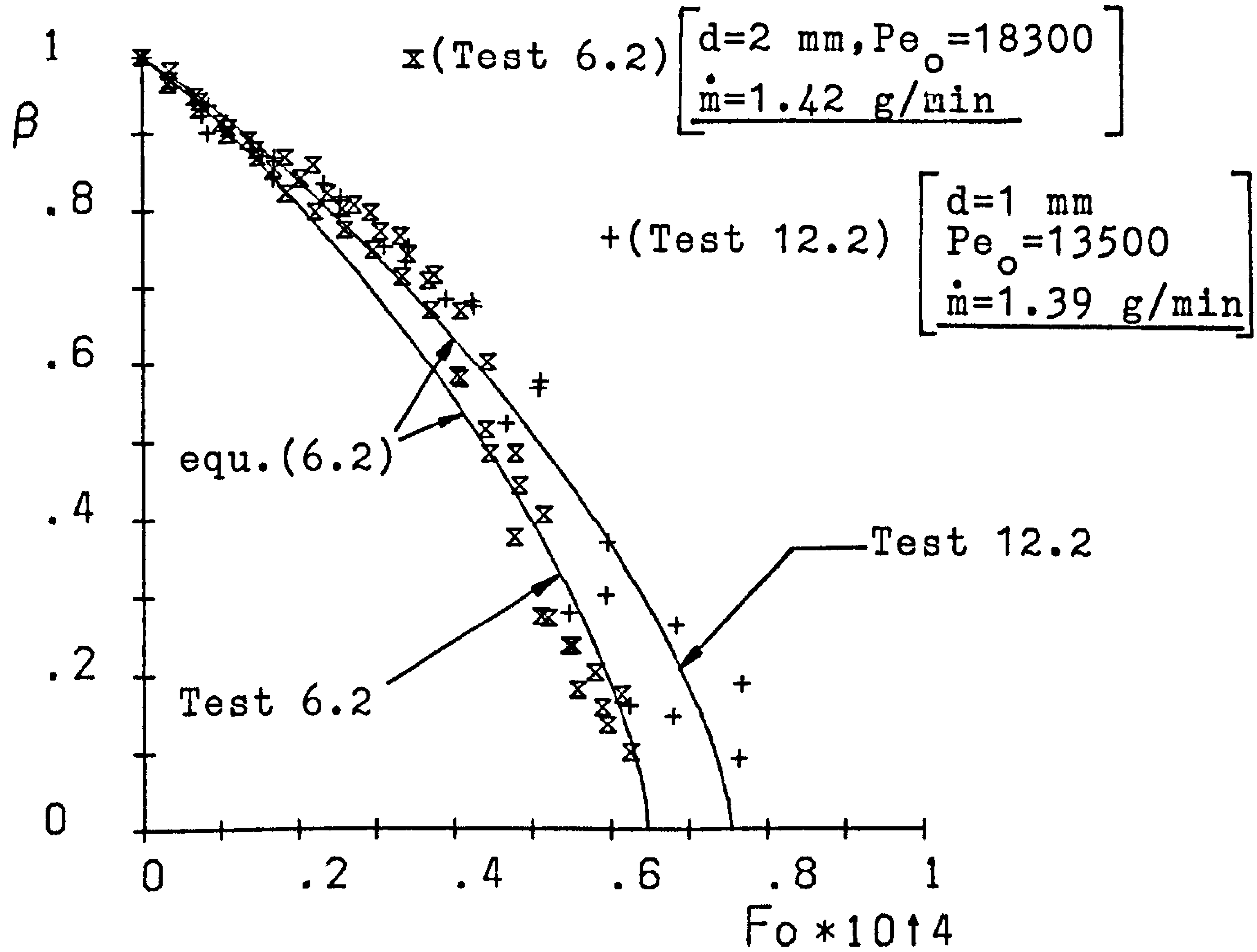

(c)

Fig.6.7 Radius ratio versus Fourier number with orifice diameter and steam flow rate as parameters. Ja=30 , P=2 bar

*

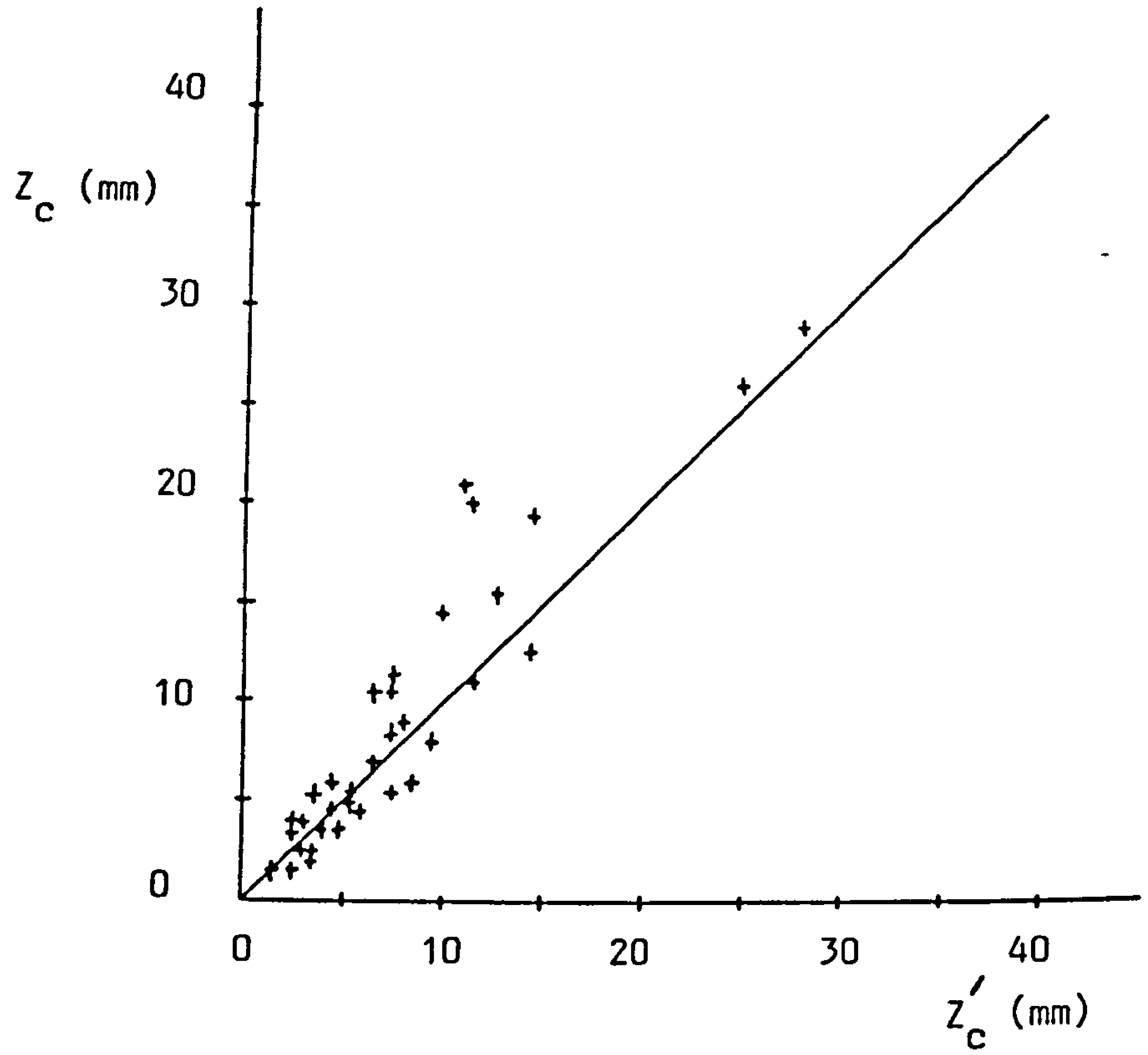

Fig. 6.11 Theoretical distance to collapse Z_c versus experimental distance to collapse Z_c' .

The theoretical distance to collapse Z_c is calculated according to equ.(6.9) .
The experimental distance to collapse Z_c' is the experimental height at collapse minus the experimental height at detachment .As can be seen from Fig. 6.11 , approximately 80 percent of the experimental data indicate experimental distances to collapse within ±30% of the predicted values .

$$Z_c = \frac{\dfrac{0.263}{Ja\ Pe^{0.5}} \cdot \dfrac{4\ R_o^2}{\alpha}\ 2.148\ \left(\dfrac{P_o}{P}\right)^{1/2} (1+6.52.10^{-3}\ Ja)}{\left(\dfrac{\sigma}{R_o \rho_f} + \dfrac{\rho_f - \rho_g}{\rho_f} gR_o\right)^{-1/2}}$$

$$\therefore \frac{Z_c}{R_o} = \frac{2.26.(1+6.52.10^{-3} Ja)\left(\dfrac{\sigma}{R_o \rho_f} + \left(\dfrac{\rho_f - \rho_g}{\rho_f}\right) g.R_o\right)^{1/2} \left(\dfrac{R_o}{\alpha}\right)}{\left(\dfrac{P}{P_o}\right)^{1/2} .\ Ja.\ Pe^{0.5}} \qquad (6.9)$$

If it is assumed that there is unlikely to be entrainment of water by the rising steam bubble, provided the liquid height is greater than that given by equation (6.9), then this equation should prove useful in determining the likelihood of entrainment for the range of Jakob number and Peclet number considered in this work.*

The complete solutions (equations (5.32) and (5.33)) or the simplified solution (equation (5.48)), which does not consider bubble distortion or heating of the water around the bubbles, both overpredict the collapse time as shown for test 4.2 in Fig. 6.8.

The theoretical model for a spherical-cap bubble derived in Appendix 6 leads to the bubble collapse being expressed in equations (5.63) and (5.64). This theory is compared with the data for tests 4.1 and 3.2 in Fig. 6.9 (a and b) which indicates that the theory greatly underpredicts the collapse time.

There may be several reasons to account for the underprediction of the collapse time by this theory.

Firstly, Coppus [50] stated that the value of the proportionality constant used for the average mass transfer coefficient would vary between 0.2 and 0.4 for

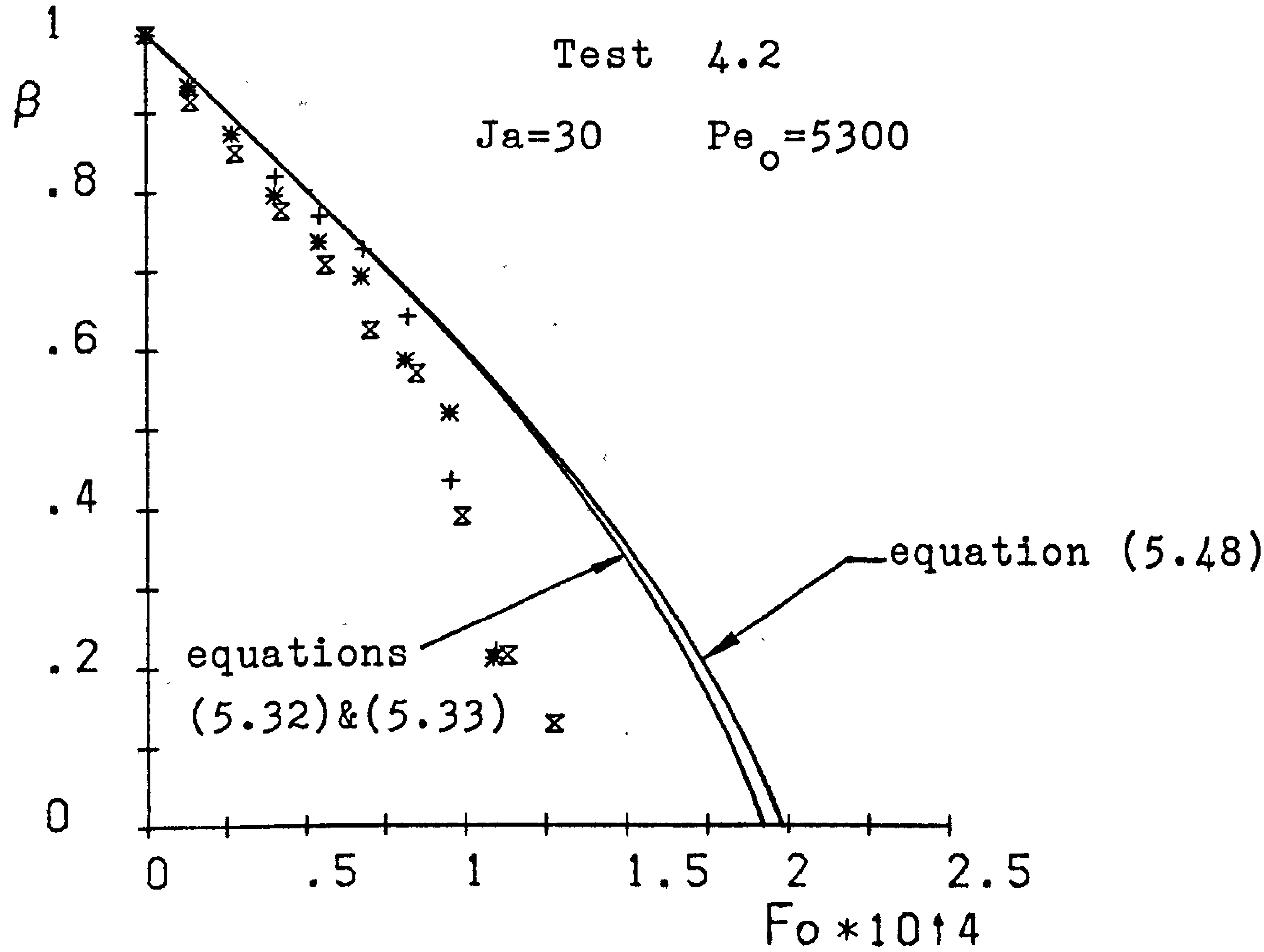

Fig.6.8 Comparison of collapse data (Test 4.2) with both complete and simplified solutions

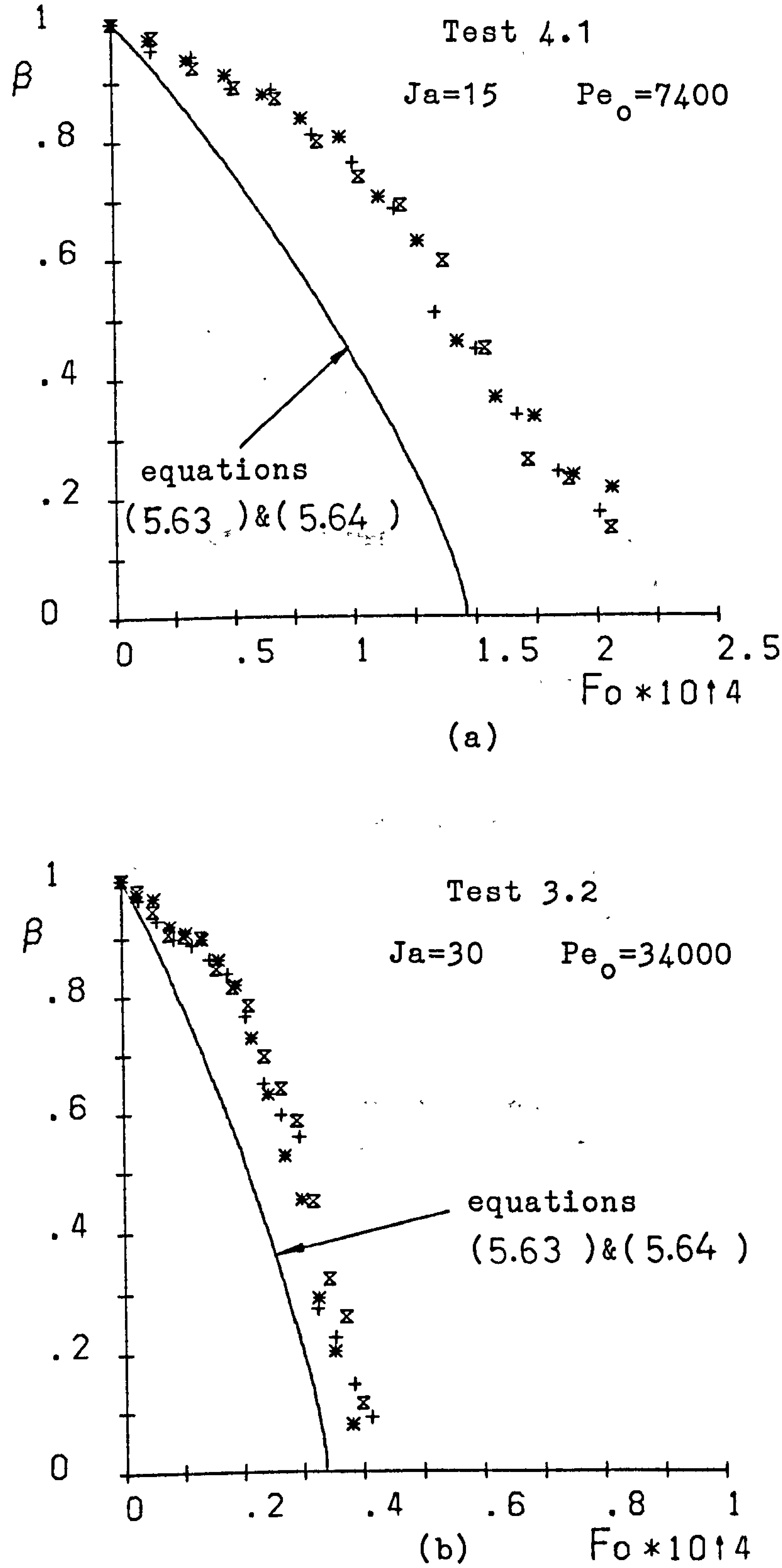

Fig.6.9 Comparison of collapse data (Tests 4.1 & 3.2) with solution for spherical-cap bubble

open channel flow or film flow. As there is no information available about the value of this constant in the wake of a bubble we have chosen a value of 0.3 which led to the relationship

$$C_b = 0.30 \left(\frac{gR}{8U}\right)^{0.25} .$$

A lower value of constant would result in a lower value of C_b in equation (5.63), this leading to an increase in the predicted collapse time.

Secondly, the calculation of wake volume in equation (A 6.17) assumes that the closed wake occupies the remaining portion of the sphere behind the bubble. This assumption may not be valid, especially when γ is smaller than 90 degrees.

Thirdly, we have assumed turbulent flow in the wake, which implies a relatively quick collapse. However, as we have no real information on whether the wake is fully turbulent or not it is not possible to evaluate the collapse rate with any degree of certainty.

Because of the uncertainties associated with these effects, the theoretical model for the spherical-cap bubble collapse has not been pursued further.

6.2 Comparison with other theories.

The experimental data for test 11.1 is compared in Fig. 6.10 with equation (6.2) and also with five other theoretical relationships. It is clear from the figure that equation (6.2) gives a much closer agreement with the experimental data than any of the other theories and should be much more useful in predicting the collapse

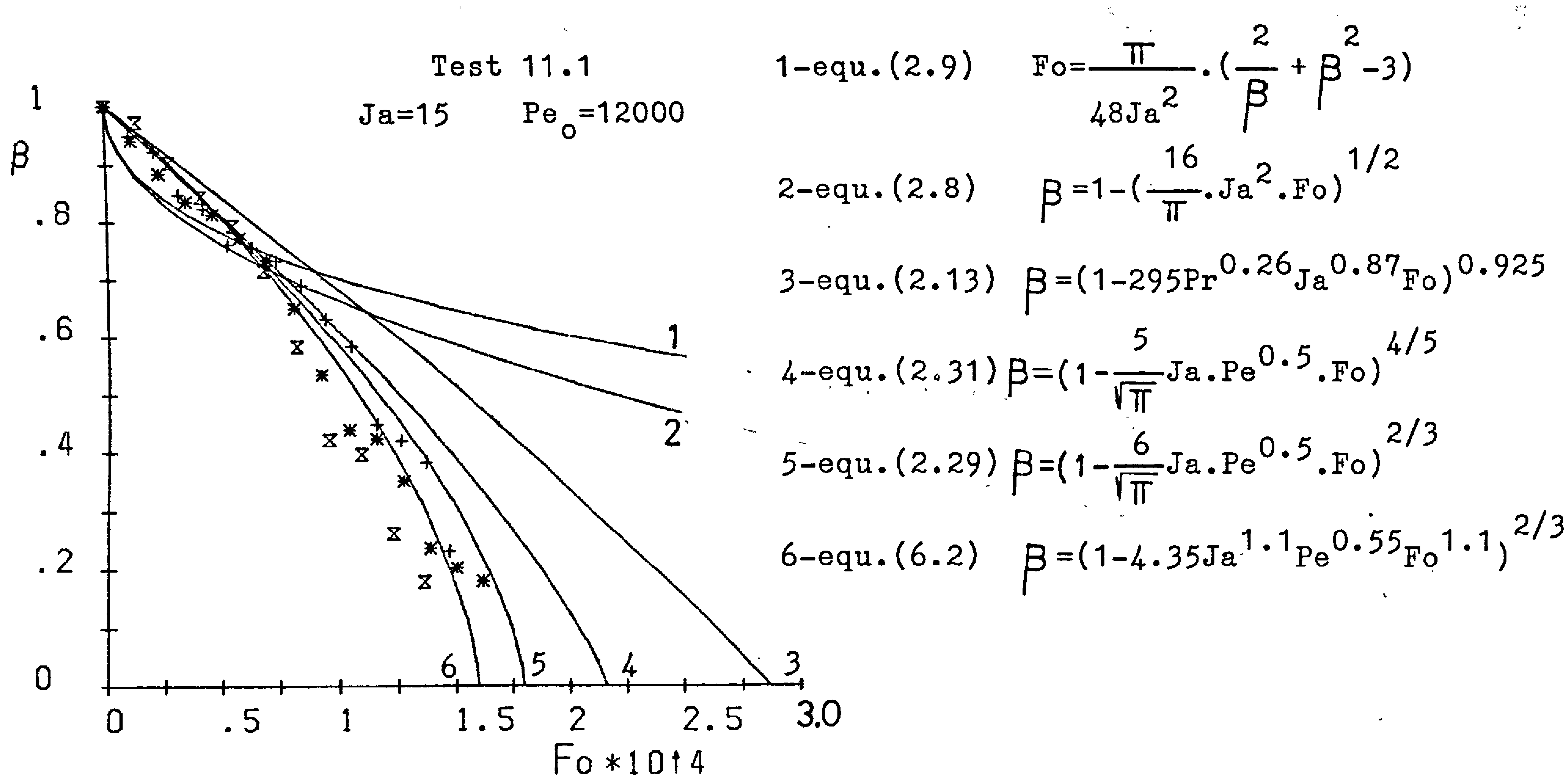

Fig.6.10 Comparison of equation(6.2) with other theories

Fourier number. Of the other theories the heat transfer controlled relationships developed by Florschuetz and Chao [10] (i.e. equations (2.8) and (2.9)) clearly indicate a different collapse pattern from all other theories. These two relationships show initially a rapid rate of collapse, which decreases rapidly as collapse proceeds. With equation (2.9) complete collapse cannot occur while with equation (2.8) the collapse time will be very large (e.g. for the condition in Fig. 6.10, t_c = 0.128 seconds). Thus, neither of these relationships appears to be much value in establishing the collapse rate of bubbles under the specified conditions.

Equation (2.13) developed by Nordmann [13] for $0 < Ja < 100$, which agreed with his data, also indicated a much slower collapse rate than the other theories,apart from the above two heat transfer controlled relationships. It should be noted that he used a stainless steel orifice, which, because of its relatively high thermal conductivity, probably heated the water around the orifice so producing a slower collapse rate. In contrast, in this work, the heating around the orifice was minimized by the use of a low thermal conductivity polycarbonate fitted to the base of the chamber, and a PTFE orifice was used. Although it is clear that the Peclet number would have a significant effect on the collapse rate, no Peclet number term appears in Nordmann's relationship.

Equation (2.31) by Moalem and Sideman [26], for small bubbles (R_0 < 1 mm) with the translational velocity $U \propto \sqrt{R}$, is closer to the present data but still predicts a significantly slower collapse rate than equation (6.2).

The relationship leading to equation (2.29) by Isenberg et al [23], derived for low Jakob number conditions, is closer to equation (6.2) than any of the others but,in this case,still predicts a final collapse time which is about 12% slower than that predicted by equation (6.2).

CHAPTER 7

CONCLUSIONS

A number of observations have been made during this study, and these can be summarised as follows:

The condensation process of steam bubbles injected through an orifice is quite complicated, since all bubbles are distorted to some extent, although the distortion is greater for the larger bubbles corresponding to the lowest value of Jakob number (Ja = 15). Also the heating of the water, close to the orifice, caused by the condensing bubbles, introduces changes in the experimental conditions around the emerging and condensing bubbles.

As has been observed in a few cases, that the presence of air in the bubble has no significant effect on the collapse except towards the latest stages of collapse.

The experimental results show that bubbles generally rise at a more or less constant velocity, but at higher values than the velocities predicted by existing correlations for gas bubbles. A correlation, for the velocity of steam bubbles condensing in subcooled water is proposed in this work, to describe the experimentally obtained values of the velocity.

It has been observed that, for the limited range considered, the orifice diameter has no significant influence on the collapse rate, but an increase in the steam flow rate increases the Peclet number and hence the bubble collapse rate. However, an increase in pressure decreases the Peclet number and also the collapse rate.

Within the range of the experimental parameters considered in this work, average values of heat transfer coefficient around the collapsing bubbles have been determined to be between $0.15.10^5$ - $0.35.10^5$ W/m^2K.

The semi-empirical equation (6.2), which considers both bubble distortion and the heating of the liquid around the condensing bubble, correlates the experimental data reasonably well. Within the range of Jakob numbers and Peclet numbers considered, equation (6.9) gives a method for determining the bubble height to collapse. This should prove useful in determining whether entrainment of water by steam bubbles is likely to occur or not.

APPENDICES

APPENDIX 1.

Physical Properties

The properties of steam and water, except for the surface tension, are given by Mayhew and Rogers [45]. The values of surface tension of saturated water are given by Parker et al.[52]. These, together with the corresponding Jakob numbers at the two pressures used, are as follows:

T(°C)	$\alpha_f \cdot 10^7$ (m^2/s)	k_f (W/mK)	C_{pf} (kJ/kgK)	$\sigma_f \cdot 10^4$ (N/m)	Ja (at 2 bar)
110.9	1.70	0.684	4.234	567	15
101.7	1.69	0.682	4.221	585	30
92.6	1.67	0.677	4.221	602	45
83.6	1.65	0.672	4.202	619	60

T(°C)	ρ_f (kg/m^3)	$\mu_f \cdot 10^6$ (kg/ms)	$\nu_f \cdot 10^7$ (m^2/s)	Pr_f
110.9	950	250	2.63	1.55
101.7	957	274	2.86	1.70
92.6	963	302	3.14	1.88
83.6	970	336	3.46	2.10

T(°C)	$\alpha_f \cdot 10^7$ (m^2/s)	k_f (W/mK)	C_{pf} (kJ/kgK)	$\sigma_f \cdot 10^4$ (N/m)	Ja (at 1 bar)
95	1.67	0.678	4.213	597	15
90	1.66	0.676	4.208	607	30
85.1	1.65	0.673	4.203	616	45
80.2	1.64	0.670	4.198	625	60
75.3	1.63	0.666	4.194	634	75

T(°C)	ρ_f (kg/m^3)	$\mu_f \cdot 10^6$ (kg/ms)	$\nu_f \cdot 10^7$ (m^2/s)	Pr_f
95	962	294	3.06	1.83
90	965	311	3.22	1.94
85.1	969	330	3.41	2.06
80.2	972	351	3.61	2.20
75.3	975	374	3.84	2.36

Density of steam, saturation temperature and specific enthalpy of evaporation at the two pressures are :

ρ_s (kg/m³)	T_s (°C)	h_{fg} (kJ/kg)	P (bar)
0.590	99.6	2258	1
1.129	120.2	2202	2

APPENDIX 2.

Computer Program for analysis of cine films

A 2.1 Introduction

The computer program, written in APPLESOFT II BASIC language, requires the following input data : test number(TITLE),date , F, Δt (DT in the program), α_w (ALFAF), ρ_s (DES), h_{fg} (HFG), ΔT (TEMD), $\dot{m}_s$ (MS), V_s (VS), k_w (KF), Ja (JA).

Then, N - the number of pairs of points whose coordinates are required to be recorded; the first pair of points for the reference length taken as the diameter of the orifice tip, the rest for frustums of cones. For example, in Fig. 3.7, the number of frustums of cones forming the bubble is n = 16, therefore N = 1 + 16 + 1 = 18.

Afterwards, the computer is connected to the digitiser and the coordinates of the N pair of points are sent to the computer by placing the cursor of the digitiser on each point in turn and pushing the cursor button in.

The program then calculates bubble volume, bubble surface area and bubble position as described in Chapter 3 (section 3.4), and some other parameters, such as dimensionless radius, Fourier number, as described in Chapter 4 (section 4.2.4). The results are later printed, and stored in a diskette for future use.

A.2.2 Sample input

Below is the input data for the bubble for which data plots and other information are presented in Fig. 4.1 and Fig. 4.2.

```
]RUN
WHAT TITLE?          (4.1).2
DATE?           12  MAY  1984

TYPE F:NUMBER OF FRAMES TO BE ANALYSED                      24

TYPE DT:TIME BETWEEN THE FRAMES AS SEC.                 2.372E-3

TYPE ALFAF:THERMAL DIFFUSIVITY OF WATER AS M^2/SEC.
 1.70E-7

TYPE DES:DENSITY OF STEAM AS KG/M^3                     1.129

TYPE HFG:LATENT HEAT OF EVAPORATION AS KJ/KG          2202

TYPE TEMD:SUBCOOLING OF WATER AS DEGREE CENTIGRADE     9.3

TYPE MS:(MASS) STEAM FLOW RATE AS G/MIN.                0.45

TYPE VS:VOLUMETRIC STEAM FLOW RATE AS MM^3/SEC.          6643

TYPE KF:THERMAL CONDUCTIVITY OF WATER AS W/(M*K)       0.684

TYPE JA:JACOB NUMBER           15

F=24             DT=2.372E-03
ALFAF=1.7E-07    DES=1.129
HFG=2202         TEMD=9.3
VS=6643          KF=.684         JA=15
PRESS RETURN TO CONTINUE
ATTENTION ! THIS PROGRAM  IS SET FOR FRAME NUMBERS SMALLER THAN 70

PRESS RETURN TO CONTINUE
NOW TYPE N
?15
```

A 2.3 Program Listing

A listing of the computer program is given in Fig. A 2.1.

```
5  REM    PROG. MOD. ON 13TH APRIL
10 D$ =  CHR$ (4)
20  PRINT D$;"BLOADATAB"
25  INPUT "WHAT TITLE?";TITLE$
30  INPUT "DATE?";DA$: PRINT
32  INPUT "TYPE F:NUMBER OF FRAMES TO BE ANALYSED  ";F: PRINT
34  INPUT "TYPE DT:TIME BETWEEN THE FRAMES AS SEC.  ";DT: PRINT
36  INPUT "TYPE ALFAF:THERMAL DIFFUSIVITY OF WATER AS M^2/SEC.  ";ALFAF: PRINT

38  INPUT "TYPE DES:DENSITY OF STEAM AS KG/M^3  ";DES: PRINT
40  INPUT "TYPE HFG:LATENT HEAT OF EVAPORATION AS KJ/KG  ";HFG: PRINT
42  INPUT "TYPE TEMD:SUBCOOLING OF WATER AS DEGREE CENTIGRADE  ";TEMD: PRINT

43  INPUT "TYPE MS:(MASS) STEAM FLOW RATE AS G/MIN.  ";MS: PRINT
44  INPUT "TYPE VS:VOLUMETRIC STEAM FLOW RATE AS MM^3/SEC.  ";VS: PRINT
46  INPUT "TYPE KF:THERMAL CONDUCTIVITY OF WATER AS W/(M*K)  ";KF: PRINT
48  INPUT "TYPE JA:JACOB NUMBER  ";JA: PRINT
70  PRINT "F="F,"DT="DT,"ALFAF="ALFAF,"DES="DES,"HFG="HFG,"TEMD="TEMD,"VS=
     "VS,"KF="KF,"JA="JA
71  INPUT "PRESS RETURN TO CONTINUE  ";Q$
72  HOME : PRINT "ATTENTION ! THIS PROGRAM  IS SET FOR FRAME NUMBERS SMALL
     ER THAN 70  ": PRINT : PRINT : INPUT "PRESS RETURN TO CONTINUE  ";Q$
75  DIM CO(70,4),V1(70),A1(70),VB(70),AB(70),BETA(70),TIME(70),NU(70),FO(7
     0),HTIME(70),HC(70),LP(70)
80  DIM RE(70),VD(70),G3(70),G4(70),GX(70),GY(70),C1(70),C2(70),CX(70),CY(
     70),RD(70),LE(70),VY(70)
90  DEF  FN P(Z) = 4 *  ATN (1)
100  FOR I = 1 TO F
102  INPUT "TYPE THE NUMBER OF VOLUMES TO CALCULATE IN THIS FRAME --V2 ";V
     2
104  FOR S = 1 TO V2
110  PRINT "NOW TYPE N"
120  INPUT N
130  GOSUB 1050
```

Fig.A2.1 The listing of the computer program for the analysis of cine films

```
135 R1 = CO(1,3) - CO(1,1):A2 =  FN P(Z) * (CO(2,3) - CO(2,1)) ^ 2 / 4:A3 =
     FN P(Z) * (CO(N,3) - CO(N,1)) ^ 2 / 4
140 VT = 0:AS = 0:G1 = 0:G2 = 0
150  FOR M = 2 TO N - 1
155 V0 =  FN P(Z) / 12 * (CO(M + 1,2) - CO(M,2)) * ((CO(M,3) - CO(M,1)) ^
    2 + (CO(M + 1,3) - CO(M + 1,1)) ^ 2 + (CO(M,3) - CO(M,1)) * (CO(M + 1
    ,3) - CO(M + 1,1)))
160 AR =  FN P(Z) / 4 * (CO(M,3) - CO(M,1) + CO(M + 1,3) - CO(M + 1,1)) *
     SQR (4 * (CO(M + 1,2) - CO(M,2)) ^ 2 + ((CO(M,3) - CO(M,1)) - (CO(M +
    1,3) - CO(M + 1,1))) ^ 2)
161 K8 = CO(M,3) - CO(M,1): IF K8 = 0 THEN 163
162 K1 =  ABS (CO(M + 1,3) - CO(M + 1,1)) /  ABS (CO(M,3) - CO(M,1)): GOTO
    164
163 K1 =  ABS (CO(M + 1,3) - CO(M + 1,1)) / (1E - 10)
164 K2 =  SQR ((CO(M + 1,2) - CO(M,2)) ^ 2 + ((CO(M + 1,1) + CO(M + 1,3)) /
    2 - (CO(M,1) + CO(M,3)) / 2) ^ 2)
166 K3 = (K2 / 4) * (1 + 2 * K1 + 3 * K1 ^ 2) / (1 + K1 + K1 ^ 2)
167  IF (CO(M + 1,1) + CO(M + 1,3)) - (CO(M,1) + CO(M,3)) = 0 THEN 182
168 T1 =  ATN ((CO(M + 1,2) - CO(M,2)) / ((CO(M + 1,1) + CO(M + 1,3)) / 2 -
    (CO(M,1) + CO(M,3)) / 2))
170  IF T1 < 0 THEN 178
174 K4 = K3 *  COS (T1):K5 = K3 *  SIN (T1)
176 K6 = (CO(M,1) + CO(M,3)) / 2 + K4:K7 = CO(M,2) + K5: GOTO 184
178 T1 =  ABS (T1):K4 = K3 *  COS (T1):K5 = K3 *  SIN (T1)
180 K6 = (CO(M,1) + CO(M,3)) / 2 - K4:K7 = CO(M,2) + K5: GOTO 184
182 K4 = 0:K5 = K3:K6 = (CO(M,1) + CO(M,3)) / 2:K7 = CO(M,2) + K5
184 VT = VT + V0:AS = AS + AR:G1 = G1 + V0 * K6:G2 = G2 + V0 * K7
200  NEXT M
201  IF V2 = 1 THEN 205
202  INPUT "DO YOU WISH TO SUBTRACT THE AREA OF THE BASE(A2) FROM THE TOTA
     L AREA (A2(S))  ?";A$: IF  LEFT$ (A$,1) = "Y" THEN A2 =  - A2: PRINT

204  INPUT "DO YOU WISH TO SUBTRACT THE AREA OF THE TOP SURFACE(A3) FROM T
     HE TOTAL AREA(A2(S))  ?";B$: IF  LEFT$ (B$,1) = "Y" THEN A3 =  - A3: PRINT
```

Fig.A2.1 (continued)

```
205 V2(S) = VT:A2(S) = AS + A2 + A3:G1(S) = G1:G2(S) = G2: NEXT S
207 V1(I) = 0:A1(I) = 0:G3 = 0:G4 = 0
210  FOR S = 1 TO V2:V1(I) = V1(I) + V2(S):A1(I) = A1(I) + A2(S):G3 = G3 +
      G1(S):G4 = G4 + G2(S): NEXT S
215 G3(I) = G3 / V1(I):G4(I) = G4 / V1(I):C1(I) = CO(1,2):C2(I) = (CO(1,3)
      + CO(1,1)) / 2:LE(I) = CO(N,2):LP(I) = CO(2,2)
217  INPUT "DO YOU WISH TO REPEAT THE WHOLE FRAME  ?";Q$: IF  LEFT$ (Q$,1)
      = "Y" THEN 102
220  NEXT I
222  INPUT "TYPE GT:THE FRAME NUMBER WHERE BUBBLE DETACHES   ";GT
230  FOR J = 1 TO F
240 VB(J) = V1(J) * (7 / R1) ^ 3
250 AB(J) = A1(J) * (7 / R1) ^ 2
260 RE(J) = (3 * VB(J) / (4 *  FN P(Z))) ^ (1 / 3)
265 GX(J) = G3(J) * (7 / R1):GY(J) = G4(J) * (7 / R1)
270 TIME(J) = DT * J:C1(J) = C1(J) * (7 / R1):C2(J) = C2(J) * (7 / R1)
275 HTIME(J) = DT * (J + 0.5):LE(J) = LE(J) * (7 / R1):LP(J) = LP(J) * (7 /
      R1)
280  NEXT J
282  FOR I = 1 TO F - 1
284 VD(I) = VB(I + 1) - VB(I)
285 RD(I) = RE(I + 1) - RE(I)
286  NEXT I
290 TT = TIME(F) - TIME(1)
298  IF TEMD = 0 THEN 2000
300 RM = 0
310  FOR K = 1 TO F
320  IF RE(K) < RM THEN  GOTO 350
330 RM = RE(K)
340 TM = TIME(K) - TIME(1):MT = K
350  NEXT K
355 TG = TIME(GT) - TIME(1)
360 TC = TT - TG
302  IF TG <  > 0 THEN FS = 1 / TG
```

Fig.A2.1 (continued)

```
400 VB(F + 1) = 0:AB(F + 1) = 0
410  FOR I = 1 TO F
420  IF I >  = GT THEN  GOTO 440
430 HC(I) = ((VS - (VB(I + 1) - VB(I)) / DT) * DES * HFG) / (TEMD * (AB(I +
      1) + AB(I)) / 2): GOTO 445
440 HC(I) = ((VB(I) - VB(I + 1)) * DES * HFG) / (DT * TEMD * (AB(I) + AB(I
      + 1)) / 2)
445 CY(I) = GY(I) - C1(I):CX(I) = GX(I) - C2(I):LE(I) = LE(I) - C1(I):LP(I
      ) = LP(I) - C1(I)
450  NEXT I
455 R0 = RE(GT)
470  FOR J = 1 TO F
480 BETA(J) = RE(J) / RM
490 FO(J) = (ALFAF * TIME(J)) / ((2E - 3) * RM) ^ 2
500 NU(J) = HC(J) * (1E - 3) * (RE(J + 1) + RE(J)) / KF
510  NEXT J
520  FOR I = 1 TO F - 1:VY(I) = (CY(I + 1) - CY(I)) / DT: NEXT I
600 ZD = CY(GT):ZC = CY(F)
610 H1 = 0:N1 = 0
620  FOR I = GT TO F:H1 = H1 + HC(I):N1 = N1 + NU(I): NEXT I
625 HC = H1 / (F - GT + 1):NC = N1 / (F - GT + 1)
630 UC = (CY(F) - CY(GT)) / (DT * (F - GT)):UA = (CY(F) - CY(1)) / (DT * (
      F - 1))
640 H2 = 0:N2 = 0
645  FOR I = 1 TO F:H2 = H2 + HC(I):N2 = N2 + NU(I): NEXT I
650 HA = H2 / F:NA = N2 / F
662  IF GT = 1 THEN 680
665 H3 = 0:N3 = 0:UG = (CY(GT) - CY(1)) / (DT * (GT - 1))
670  FOR I = 1 TO GT - 1:H3 = H3 + HC(I):N3 = N3 + NU(I): NEXT I
675 HG = H3 / (GT - 1):NG = N3 / (GT - 1)
677 VR = VS * TG:CN = (VR - VB(GT)) / VR * 100
680 FC = ALFAF * TC / ((2E - 3) * R0) ^ 2
830  GOTO 2000
1030  FOR K = 1 TO 3 STEP 2
```

Fig.A2.1 (continued)

```
1060  FOR J = 1 TO N
1070  PRINT "ABOUT TO CALL 775","  ";"I="I;"  ";"N="N;"  ";"S="S;"  ";"V2=
     "V2
1080  CALL 775
1090  PRINT "775 CALLED"
1100 X =  PEEK ( - 16384)
1110  IF X > 127 THEN 1200
1120 CO(J,K) = ( PEEK (769) * 256 +  PEEK (770)) / 10
1130 CO(J,K + 1) = ( PEEK (772) * 256 +  PEEK (773)) / 10
1140  PRINT CO(J,K),CO(J,K + 1),"GOING BACK"
1145  PRINT "N="J,"K="K
1150  NEXT J,K
1155  HOME
1160  FOR L = 1 TO N
1170  PRINT CO(L,1);"   ";CO(L,2),CO(L,3);"   ";CO(L,4);"   "CO(L,2) - CO(
     L,4)
1175  IF L = 15 THEN 1178
1177  GOTO 1180
1178  INPUT "PRESS RETURN TO CONTINUE  ";Q$: HOME
1180  NEXT L
1188  PRINT "F="I,"S="S
1189  INPUT "DO YOU WISH TO REPEAT?";Q$
1190  IF  LEFT$ (Q$,1) = "Y" THEN 1050
1200  RETURN
2000  HOME
2005  PRINT D$;"MONIO"
2010  INPUT "DO YOU WISH TO STORE THE   DATA ? ";Q$
2020  IF  LEFT$ (Q$,1) = "Y" THEN 2050
2030  GOTO 2170
2050 F$ = TITLE$
2060  PRINT D$;"OPEN";F$
2070  PRINT D$;"WRITE";F$
2080  PRINT TITLE$: PRINT DA$
2090  FOR I = 1 TO F
```

Fig.A2.1 (continued)

```
2100  PRINT UB(I): PRINT AB(I): PRINT CX(I): PRINT CY(I): PRINT LE(I): PRINT
     LP(I)
2110  NEXT I
2115  PRINT DT: PRINT ALFAF: PRINT DES: PRINT HFG: PRINT TEMD: PRINT VS: PRINT
     KF: PRINT GT
2150  PRINT D$;"CLOSE";F$
2151  PRINT TITLE$,DA$
2170  INPUT "DO YOU WISH TO PRINT THE DATA ON THE SCREEN?";Q$
2175  IF  LEFT$ (Q$,1) = "Y" THEN 2196
2180  INPUT "DO YOU WISH TO PRINT THE DATA?";Q$
2185  IF  LEFT$ (Q$,1) = "Y" THEN 2190
2186  END
2190 D$ =  CHR$ (4): REM  CTRL-D
2193  PRINT D$;"PR#1"
2196  PRINT TITLE$: PRINT DA$: PRINT
2200  PRINT "F","TIME","VB","AB","RE"
2210  PRINT "-","----","--","--","--"
2220  FOR I = 1 TO F
2230  PRINT I,TIME(I),VB(I),AB(I),RE(I)
2232  IF I = GT - 1 THEN  GOSUB 4000
2240  NEXT I
2241  GOSUB 4020: PRINT
2250  IF TEMD = 0 THEN 2355
2255  PRINT "F+1/2","HTIME","HC","NU","LE"
2260  PRINT "-----","-----","--","--","--"
2270  FOR I = 1 TO F
2280  PRINT I + 1 / 2,HTIME(I),HC(I),NU(I),LE(I)
2282  IF I = GT - 1 THEN  GOSUB 4000
2290  NEXT I
2291  GOSUB 4020: PRINT
2300  PRINT "F","BETA","FO","CX","CY"
2305  PRINT "-","----","--","--","--"
2310  FOR I = 1 TO F
2315  PRINT I,BETA(I),FO(I),CX(I),CY(I)
2317  IF I = GT - 1 THEN  GOSUB 4000
```

Fig.A2.1 (continued)

```
2320  NEXT I
2325  GOSUB 4020: PRINT
2330  PRINT "EXPERIMENTAL PARAMETERS :"
2332  PRINT "-------------------------"
2333  PRINT "F="F,"DT="DT,"ALFAF="ALFAF,"DES="DES,"HFG="HFG: PRINT
2334  PRINT "TEMD="TEMD,"MS="MS,"VS="VS,"KF="KF,"JA="JA: PRINT
2336  PRINT "EXPERIMENTAL RESULTS :"
2338  PRINT "---------------------"
2340  PRINT "TG="TG,"GT="GT,"HG="HG,"NG="NG: PRINT : PRINT "TC="TC,"FS="FS
     ,"HC="HC,"NC="NC: PRINT
2342  PRINT "TT="TT,"TM="TM,"HA="HA,"NA="NA: PRINT : PRINT "MT="MT,"RM="RM
     ,"R0="R0,"UG="UG,"UA="UA: PRINT
2344  PRINT "ZD="ZD,"ZC="ZC,"FC="FC,"UC="UC: PRINT
2346  PRINT "CN="CN: PRINT
2351  GOSUB 4020: PRINT
2352  GOTO 2380
2355  PRINT "F","TIME","CX","CY","LE"
2360  PRINT "-","----","--","--","--"
2365  FOR I = 1 TO F
2370  PRINT I,TIME(I),CX(I),CY(I),LE(I)
2372  IF I = GT - 1 THEN  GOSUB 4000
2375  NEXT I
2377  GOSUB 4020: PRINT
2380  PRINT "F+1/2","RD","VD","UY","LP"
2385  PRINT "-----","--","--","--","--"
2390  FOR I = 1 TO F
2392  IF I = F THEN G$ = "GO ON": PRINT I + 1 / 2,"-----","-----","-----",
     LP(I): GOTO 2400
2395  PRINT I + 1 / 2,RD(I),VD(I),UY(I),LP(I)
2397  IF I = GT - 1 THEN  GOSUB 4000
2400  NEXT I
2405  PRINT
3000  PRINT D$;"PR#0"
3010  GOTO 2180
```

Fig.A2.1 (continued)

```
4000  REM  SUB. FOR DRAWING LINE ACROSS THE PAGE
4002  FOR J = 1 TO 75: PRINT "-";: NEXT J
4005  PRINT " ": RETURN
4020  REM   SUB. FOR DRAWING LINE              ACROSS THE PAGE

4022  FOR I = 1 TO 80: PRINT "-";: NEXT I
4025  RETURN
```

Fig.A2.1 (continued)

APPENDIX 3

Computer program for calculation of bubble collapse history

A.3.1 Introduction

The computer package used for calculation of bubble collapse history was "TUTSIM V8201" (copyright Twente University, The Netherlands). This is a simulation program in BASIC language to be used in an APPLE II computer, to calculate models of continuous dynamic systems defined as block diagrams or block graphs. When simulation data are put into the computer, the results are shown directly in a graphical way on a display screen. Simulation model data can be stored on floppy disk, and model listings and numerical or graphical results can be printed.

A simulation with TUTSIM is performed by means of calculations by the computer. A block diagram of the model is drawn for solving differential equations or calculating integrals in an equation.

A.3.2 Computer program for calculation of bubble collapse history according to equations (5.32) and (5.33) (the complete solution)

For a given experimental condition both Jakob number and Peclet number are known and the value of $\beta = 1$, is obtained for a particular value of

$\left(-\frac{U}{R}\right)$ (positive) according to equation (5.32).

This $\left(-\frac{U}{R}\right)$value is found by trial and error and fed into the program as an input. The program changes

$(-\frac{U}{R})$ values between this maximum value and a value very near to zero in 80 steps and, as shown in Fig. 5.2, calculates corresponding β values according to equation (5.32). At the same time the integral in equation (5.33) is calculated and the β versus Fourier number relationship is drawn as shown in Fig. 5.3.

The block diagram for these calculations is presented in Fig. A 3.1 (a and b) in the attached portfolio. The Listing of the model is given in table A 3.1.

```
TIMING
 0.30000E-01  0.13000E+02

OUTPUTBLOCKS AND RANGES
X1:    78      0.00000E+00   0.10000E+01
Y1:    85      0.00000E+00   0.15000E-03
Y2:    87      0.00000E+00   0.15000E-03
Y3:     1      0.00000E+00   0.10000E-04
Y4:     1      0.00000E+00   0.10000E-04

MODEL
                         1 TIM
                         2 SIN   60
                         3 MUL    2     2     2
 0.50000E+00             4 GAI   60
                         5 SIN    4
                         6 COS    4
                         7 DIV    5     6
                         8 MUL    7     7
                         9 LOG   24
                        10 MUL   13     9
 0.31416E+01            11 CON
 0.66667E+00            12 GAI   61
 0.20000E+01            13 GAI   12
                        14 EXP   10
                        15 MUL   12     9
                        16 EXP   15
                        17 DIV    3    14
 0.00000E+00            18 INT   17
                        19 SQT   56
                        20 DIV    3    16
                        21 DIV   20    26
 0.00000E+00            22 INT   21
 0.34446E+00            23 GAI   55
 0.00000E+00            24 REL    8    25     8     8
 0.10000E+02            25 CON
 0.00000E+00            26 REL   19    27    19    19
 0.10000E+01            27 CON
 0.15000E+02            28 CON
                        29 MUL   28    40
                        30 MUL   29    31
                        31 SQT   32
 0.19800E+05            32 CON
                        33 MUL   36    36
                        34 MUL   31    61    35
```

Table A3.1 The listing of the model for the complete solution

0.75000E+00	35	CON				
	36	DIV	29	34		
0.15000E+01	37	PWR	78			
	38	SUM	27	-37		
	39	DIV	38	30		
-0.00000E+00	40	REL	23	27	23	23
0.31831E+00	41	GAI	1			
	42	FIX	41			
0.31416E+01	43	GAI	-42	41		
0.10300E+00	44	GAI	42			
	45	SUM	-44	46		
0.82400E+01	46	CON				
	47	SUM	-60	11		
	48	DIV	38	49		
	49	MUL	28	31	51	
0.60000E-01	50	REL	27	33	33	47
0.84628E+00	51	CON				
0.31416E+01	52	SPL	18	-81		
	53	SUM	18	-52		
0.31416E+01	54	SPL	22	-83		
	55	SUM	22	-54		
0.35000E-01	56	REL	53	27	27	60
0.35000E-01	57	ATT	1			
	58	SUM	27	57		
0.31416E+01	59	SPL	43			
	60	SUM	43	-59		
	61	DIV	27	45		
0.10000E+01	62	ADL	50			
	63	SUM	-62	27		
0.31416E+01	64	SPL	63			
0.00000E+00	65	ADL	64			
	66	SUM	63	-65		
0.10000E+01	67	ADL	62			
	68	SUM	45	-69		
0.51500E-01	69	CON				
0.00000E+00	70	ADL	68			
0.00000E+00	71	REL	76	70	70	60
	72	MUL	66	71		
0.30000E-01	73	ATT	72			
0.00000E+00	74	EUL	73			
0.20000E+01	75	GAI	74			
0.00000E+00	76	CON				
	77	DIV	75	32		
0.10000E-01	78	REL	67	27	27	60
0.10000E-01	79	REL	77	76	76	60
0.00000E+00	80	ADL	17			
0.15000E-01	81	GAI	80			
0.00000E+00	82	ADL	21			
0.15000E-01	83	GAI	82			
0.31416E+01	84	SPL	62			
0.40000E+01	85	ATT	48			
0.40000E-01	86	REL	76	79	79	60
0.40000E+01	87	ATT	86			

Table A3.1 (continued)

APPENDIX 4.

Experimental Data

TEST NO : (1.1).3 FILM NO : 34-2/5

FR	TIME	VOLUME	AREA	RADIUS
1	2.29	3.69	15.07	.96
2	4.59	40.72	64.08	2.13
3	6.88	98.52	115.22	2.87
4	9.18	127.6	135.28	3.12
5	11.47	103.02	118.03	2.91
6	13.76	110.15	122.63	2.97
7	16.06	140.72	141.86	3.23
8	18.35	146.65	146.54	3.27
9	20.65	133.21	139.83	3.17
10	22.94	155.14	156.29	3.33
11	25.23	180.46	169.28	3.51
12	27.53	195.21	171.03	3.6
13	29.82	164.67	162.71	3.4
14	32.12	177.93	203.79	3.49
15	34.41	237.92	244.73	3.84
16	36.7	217.23	232.12	3.73
17	39	204.32	228.03	3.65
18	41.29	205.27	231.73	3.66
19	43.59	219.29	238.14	3.74
20	45.88	211.45	233.53	3.7
21	48.17	202.94	231.09	3.65
22	50.47	173.01	215.26	3.46
23	52.76	135.06	207.6	3.18
24	55.06	92.11	112.65	2.8
25	57.35	91.94	111.45	2.8
26	59.64	86.09	103.11	2.74
27	61.94	68.75	84.94	2.54
28	64.23	52.2	69.42	2.32
29	66.53	35.12	54.92	2.03
30	68.82	27.86	51.38	1.88
31	71.11	21.88	46.2	1.74
32	73.41	8.3	33.41	1.26
33	75.7	1.2	13.38	.66
34	78	1.19	8.8	.66

FR	CY	CX	LE	LP
1	.39	.03	.91	—
2	1.12	.13	2.98	—
3	1.7	.12	4.74	—
4	1.99	.1	5.72	—

CONT.-

FR	CY	CX	LE	LP
5	2.15	.07	5.2	—
6	2.61	.09	5.23	—
7	3.12	.06	5.85	—
8	3.47	.07	6.62	—
9	3.84	.12	6.98	—
10	4.11	.14	7.4	—
11	4.49	.12	8.28	—
12	5.04	.19	8.93	—
13	5.54	.19	9.3	—
14	5.58	.15	9.81	—
15	5.32	.14	10.38	—
16	5.33	.04	10.56	—
17	5.55	.05	10.33	—
18	6.02	.07	10.52	—
19	6.33	.01	10.81	—
20	6.71	.01	11	—
21	7.15	.1	12.23	—
22	7.76	.18	13.19	—
23	8.23	.14	13.57	—
24	9.31	.11	14.1	—
25	10.58	.11	14.83	—
26	11.6	.12	15.45	—
27	13.01	0	16.01	—
28	13.73	-.04	15.74	—
29	14.41	-.07	15.88	—
30	15.28	.05	17.13	—
31	15.96	-.05	17.43	—
32	16.75	.17	17.62	—
33	17.61	.36	18.05	—
34	18.12	-.43	18.23	—

EXPERIMENTAL PARAMETERS :

$d = 2$ $\dot{m}_s = .5$ $V_s = 13935$ $P = .991$

$Ja = 15$ $\Delta T = 5$ $\Delta t = 2.29$ $CS = 436$

$F = 34$ $Z = 40$ $T_p = 165$

EXPERIMENTAL RESULTS :

$t_g = 50.46$ $t_c = 26$ $t_t = 76.46$ $f_s = 20$

$R_o = 3.46$ $U = 480$ $h_c = 21285$

$R_m = 3.84$ $Pe_o^* = 19840$ $Nu_c = 121$

$Z_d = 7.76$ $Z_c = 18.12$ $Fo_c = 9.09E-05$

(1.1).3

TEST NØ : (1.2).1 FILM NØ : 34-3/6

FR	TIME	VØLUME	AREA	RADIUS
1	2.31	.14	1.97	.32
2	4.62	.33	5.13	.43
3	6.93	19.76	41.4	1.68
4	9.24	71.71	93.29	2.58
5	11.54	94.36	110.61	2.82
6	13.85	73.05	88.45	2.59
7	16.16	66.38	83.22	2.51
8	18.47	83.98	101.21	2.72
9	20.78	79.49	102.9	2.67
10	23.09	82.61	108.08	2.7
11	25.4	64.99	83.84	2.49
12	27.71	58.53	80.12	2.41
13	30.02	61.85	85.25	2.45
14	32.33	50.94	70.39	2.3
15	34.63	32.73	52.53	1.98
16	36.94	17.07	34.24	1.6
17	39.25	8.78	24.73	1.28
18	41.56	.51	4.06	.5
19	43.87	.06	.84	.24

FR	CY	CX	LE	LP
1	.11	.46	.26	–
2	.11	.48	.28	–
3	.78	.08	2.02	–
4	1.4	.12	3.97	–
5	1.78	.21	5.32	–
6	1.99	.28	4.69	–
7	2.4	.21	4.57	–
8	2.84	.23	5.29	–
9	2.94	.22	6.11	–
10	3.23	.21	7.38	–
11	3.39	.13	6.84	–
12	3.63	.14	7.11	–
13	4.16	.18	8.03	–
14	4.92	.15	8.55	–
15	5.66	.11	8.88	–
16	6.77	.2	8.56	–
17	7.97	.3	9.18	–
18	8.36	-.21	8.72	–

CØNT.-

FR	CY	CX	LE	LP
19	9.24	-.69	9.45	–

EXPERIMENTAL PARAMETERS :

$d = 2$	$\dot{m}_s = .5$	$V_s = 13935$	$P = .991$
$Ja = 30$	$\Delta T = 10$	$\Delta t = 2.31$	$CS = 433$
$F = 19$	$Z = 40$	$T_p = 165$	

EXPERIMENTAL RESULTS :

$t_g = 32.33$	$t_c = 8.25$	$t_t = 40.58$	$f_s = 33$
$R_o = 2.3$	$U = 437$	$h_c = 17905$	
$R_m = 2.82$	$Pe_o = 12080$	$Nu_c = 65$	
$Z_d = 4.92$	$Z_c = 9.24$	$Fo_c = 6.49E-05$	

TEST NO : (2.1).2 FILM NO : 38-1/2

FR	TIME	VOLUME	AREA	RADIUS
1	2.37	20.75	40.96	1.7
2	4.74	115.15	127.97	3.02
3	7.11	172.22	170.05	3.45
4	9.48	162.39	170.02	3.38
5	11.85	170.85	182.91	3.44
6	14.22	227.67	218.87	3.79
7	16.59	251.69	226.22	3.92
8	18.96	281.03	244.47	4.06
9	21.33	328	276.35	4.28
10	23.7	350.41	293.89	4.37
11	26.07	348.18	298.08	4.36
12	28.44	327.86	307.88	4.28
13	30.81	396.51	370.2	4.56
14	33.18	430.16	386.87	4.68
15	35.55	427.74	379.37	4.67
16	37.92	380.08	323.32	4.49
17	40.29	309.82	247.77	4.2
18	42.66	283.59	222.67	4.08
19	45.03	240.61	193.16	3.86
20	47.4	238.25	190.73	3.85
21	49.77	203.66	173.71	3.65
22	52.14	171.45	161.7	3.45
23	54.51	132.47	132.14	3.16
24	56.88	78.66	93.72	2.66
25	59.25	47.81	69.02	2.25
26	61.62	43.42	75.52	2.18
27	63.99	41.2	75.28	2.14
28	66.36	29.1	61.39	1.91
29	68.73	22.39	47.82	1.75
30	71.1	11.6	30.59	1.4

FR	CY	CX	LE	LP
1	.99	0	2.28	-
2	1.63	.13	4.52	-
3	2.29	.22	7.04	-
4	2.71	.14	8.3	-
5	3.37	.05	9.09	-
6	3.93	.11	10.76	-
7	4.5	.08	11.93	-
8	4.93	.12	12.91	-

CONT.-

FR	CY	CX	LE	LP
9	5.38	.04	14.28	-
10	6.09	0	15.47	-
11	7.1	-.01	16.6	-
12	8.17	-.19	17.76	-
13	8.72	-.23	18.78	-
14	10.34	-.35	20.17	-
15	11.9	-.53	21.26	-
16	13.71	-.83	22.09	-
17	16.12	-1.1	22.69	-
18	17.68	-1.23	23.48	-
19	19.08	-1.37	24.22	-
20	20.03	-1.44	24.52	-
21	21.16	-1.36	25.23	-
22	22.07	-1.35	25.65	-
23	23.05	-.85	27.12	-
24	24.68	-.19	28.49	-
25	26.24	.28	29.52	-
26	27.12	.29	30.41	-
27	27.85	.06	30.86	-
28	28.52	-.51	30.86	-
29	29.39	-1.18	30.22	-
30	30.54	-1.92	31.2	-

EXPERIMENTAL PARAMETERS :

$d = 2$	$\dot{m}_s = 1$	$V_s = 27871$	$P = .995$
$Ja = 15$	$\Delta T = 5$	$\Delta t = 2.37$	$CS = 422$
$F = 30$	$Z = 40$	$T_p = 165$	

EXPERIMENTAL RESULTS :

$t_g = 37.92$	$t_c = 35$	$t_t = 72.92$	$f_s = 28$
$R_o = 4.49$	$U = 524$	$h_c = 26596$	
$R_m = 4.68$	$Pe_o = 28110$	$Nu_c = 195$	
$Z_d = 13.71$	$Z_c = 30.54$	$Fo_c = 7.26E-05$	

TEST NØ : (2.2).3 FILM NØ : 38-2/3

FR	TIME	VØLUME	AREA	RADIUS
1	1.14	14.57	35.08	1.52
2	2.29	30.11	52.75	1.93
3	3.43	58.15	80.04	2.4
4	4.57	95.29	107.22	2.83
5	5.72	132.27	132.98	3.16
6	6.86	141.02	139.28	3.23
7	8	140.93	143.03	3.23
8	9.14	133.6	139.87	3.17
9	10.29	127.09	137.32	3.12
10	11.43	146.53	151.84	3.27
11	12.57	160.86	165.59	3.37
12	13.72	183.87	181.43	3.53
13	14.86	193.22	189.24	3.59
14	16	189.44	186.41	3.56
15	17.15	188.52	185.04	3.56
16	18.29	192.14	188.82	3.58
17	19.43	204.84	195.29	3.66
18	20.57	209.05	199.46	3.68
19	21.72	207.54	201.64	3.67
20	22.86	220.32	213.25	3.75
21	24	224.77	217.17	3.77
22	25.15	249.22	229.75	3.9
23	26.29	229.26	205.98	3.8
24	27.43	205.64	191.45	3.66
25	28.58	196.52	183.13	3.61
26	29.72	185.15	174.2	3.54
27	30.86	159.85	155.83	3.37
28	32	144.1	143.65	3.25
29	33.15	131.15	134.34	3.15
30	34.29	112.79	119.22	3
31	35.43	96.89	108.66	2.85
32	36.58	67.23	84.72	2.52
33	37.72	37.77	56.19	2.08
34	38.86	23.91	46.86	1.79
35	40.01	15.34	38.4	1.54
36	41.15	1.29	6.22	.68

FR	CY	CX	LE	LP
1	2.3	.12	6	-
2	2.46	.17	5.08	-

CONT.-

FR	CY	CX	LE	LP
3	2.86	.18	5.7	-
4	3.04	.28	6.34	-
5	3.18	.22	7.28	-
6	3.19	.18	7.72	-
7	3.31	.16	8.32	-
8	3.42	.18	8.35	-
9	3.48	.15	8.45	-
10	3.76	.17	8.9	-
11	4.19	.24	9.73	-
12	4.65	.31	10.59	-
13	4.96	.19	11.31	-
14	5.15	.19	11.55	-
15	5.36	.21	11.85	-
16	5.6	.24	12.33	-
17	6.06	.22	12.78	-
18	6.51	.2	13.32	-
19	6.83	.26	13.72	-
20	7.45	.19	14.34	-
21	8.04	.17	14.87	-
22	8.59	.19	15.51	-
23	9.27	.21	15.86	-
24	9.91	.15	16.01	-
25	10.35	.06	16.26	-
26	10.96	.02	16.43	-
27	11.72	.05	16.77	-
28	12.5	.06	17.2	-
29	12.98	-.02	17.41	-
30	13.42	-.09	17.46	-
31	14.19	-.07	17.88	-
32	14.65	-.2	17.69	-
33	15.29	-.15	17.71	-
34	16.6	.01	17.9	-
35	17.54	.02	18.7	-
36	18.42	-.15	19.19	-

EXPERIMENTAL PARAMETERS :

$d = 2$ $\dot{m}_s = 1$ $V_s = 27871$ $P = .995$

$Ja = 30$ $\Delta T = 10$ $\Delta t = 1.14$ $CS = 875$

$F = 36$ $Z = 40$ $T_p = 165$

EXPERIMENTAL RESULTS :

$t_g = 26.39$ $t_c = 15$ $t_t = 41.39$ $f_s = 40$

CONT.-

(2.2).3

$R_o = 3.8$ $U = 520$ $h_c = 26206$
$R_m = 3.9$ $Pe_o = 23750$ $Nu_c = 159$
$Z_d = 9.27$ $Z_c = 18.42$ $Fo_c = 4.32E-05$

TEST NO : (2.3).1 FILM NO : 38-3/1

FR	TIME	VOLUME	AREA	RADIUS
1	1.13	1.64	8.05	.73
2	2.26	8.33	22.96	1.26
3	3.39	34.11	56.21	2.01
4	4.52	40.93	62.13	2.14
5	5.65	51.17	71.64	2.3
6	6.78	59.96	80.67	2.43
7	7.91	59.57	79.39	2.42
8	9.04	58.42	77.98	2.41
9	10.17	53.26	74.13	2.33
10	11.3	57.17	78.38	2.39
11	12.43	41.79	61.72	2.15
12	13.56	26.47	46.07	1.85
13	14.69	15.95	35.82	1.56
14	15.82	14	33.53	1.5
15	16.95	1.25	6.04	.67

FR	CY	CX	LE	LP
1	.98	-.31	2.4	-
2	1.6	-.21	3.44	-
3	1.95	-.27	4.51	-
4	1.81	-.18	4.9	-
5	2.03	-.13	5.19	-
6	2.46	-.04	5.57	-
7	2.85	.02	6.13	-
8	3.16	-.03	6.75	-
9	3.51	-.09	6.9	-
10	4.22	-.15	7.49	-
11	4.85	-.2	7.86	-
12	5.86	-.26	8.19	-
13	6.76	-.27	9.07	-
14	7.8	-.03	9.82	-
15	8.14	.07	8.87	-

CONT.-

EXPERIMENTAL PARAMETERS :

$d = 2$	$\dot{m}_s = 1$	$V_s = 27871$	$P = .995$
$Ja = 45$	$\Delta T = 15$	$\Delta t = 1.13$	$CS = 885$
$F = 15$	$Z = 40$	$T_p = 165$	

EXPERIMENTAL RESULTS :

$t_g = 12.43$	$t_c = 4.5$	$t_t = 16.93$	$f_s = 88$
$R_o = 2.15$	$U = 775$	$h_c = 26367$	
$R_m = 2.43$	$Pe_o = 20170$	$Nu_c = 91$	
$Z_d = 4.85$	$Z_c = 8.14$	$Fo_c = 4.02E-05$	

(2.3).1

TEST NØ : (3.1).2 FILM NØ : 35-3/2

FR	TIME	VØLUME	AREA	RADIUS
1	2.18	52.12	80.33	2.32
2	4.37	168.09	171.06	3.42
3	6.55	246.89	219.5	3.89
4	8.73	185.2	196.84	3.54
5	10.92	273.09	232.83	4.02
6	13.1	395.36	296.19	4.55
7	15.28	474.52	333.04	4.84
8	17.46	485.57	354.53	4.88
9	19.65	548.06	381.55	5.08
10	21.83	564.53	396.14	5.13
11	24.01	592.21	402.3	5.21
12	26.2	617.84	425.78	5.28
13	28.38	584.28	427.37	5.19
14	30.56	632.59	461.48	5.33
15	32.74	659.41	460.84	5.4
16	34.93	637.22	447.62	5.34
17	37.11	606.84	396.56	5.25
18	39.29	568.54	359.32	5.14
19	41.48	449.8	310.3	4.75
20	43.66	391.14	297.72	4.54
21	45.84	334.39	283.97	4.31
22	48.03	283.6	261.16	4.08
23	50.21	241.47	230.4	3.86
24	52.39	202.46	193.54	3.64
25	54.57	200.55	193.59	3.63
26	56.76	200.09	189.95	3.63
27	58.94	145.47	156.56	3.26
28	61.12	63.57	81.54	2.48
29	63.31	38.84	65.32	2.1
30	65.49	36.55	61.49	2.06
31	67.67	25.49	46.26	1.83

FR	CY	CX	LE	LP
1	1.34	.05	3.2	-
2	1.83	.1	5.11	-
3	2.4	.12	7.49	-
4	3.42	.05	8.46	-
5	3.23	-.1	9.77	-
6	3.71	.14	11.34	-
7	4.3	.22	12.47	-

CONT.-

FR	CY	CX	LE	LP
8	5.14	.25	13.44	-
9	5.64	.19	14.64	-
10	6.41	.18	15.59	-
11	7.02	.15	16.51	-
12	8.03	.02	17.54	-
13	8.96	-.08	18.47	-
14	10.24	-.06	19.61	-
15	11.23	-.1	20.61	-
16	12.34	-.25	21.26	-
17	13.86	-.35	21.84	-
18	15.27	-.42	22.8	-
19	17.44	-.66	24.39	-
20	18.53	-.71	24.39	-
21	19.51	-.83	25.64	-
22	20.77	-.8	26.32	-
23	21.42	-1	27.03	-
24	21.86	-1.18	28.13	-
25	22.46	-1.1	29.07	-
26	23.59	-.76	29.93	-
27	25.19	-.31	29.78	-
28	26.95	.59	30.36	-
29	28.23	.93	31.54	-
30	29.31	1.06	32.49	-
31	30.25	1.2	32.45	-

EXPERIMENTAL PARAMETERS :

$d = 2$	$\dot{m}_s = 1.5$	$V_s = 41806$	$P = .995$
$Ja = 15$	$\Delta T = 5$	$\Delta t = 2.18$	$CS = 458$
$F = 31$	$Z = 40$	$T_p = 165$	

EXPERIMENTAL RESULTS :

$t_g = 37.11$	$t_c = 35.6$	$t_t = 72.71$	$f_s = 29$
$R_o = 5.25$	$U = 643$	$h_c = 33643$	
$R_m = 5.4$	$Pe_o = 40330$	$Nu_c = 281$	
$Z_d = 13.86$	$Z_c = 30.25$	$Fo_c = 5.41E-05$	

TEST NO : (3.2).1 FILM NO : 36-1/1

FR	TIME	VOLUME	AREA	RADIUS
1	1.37	50.11	75.33	2.29
2	2.74	78.26	101.91	2.65
3	4.11	139.05	147.75	3.21
4	5.48	210.24	179.05	3.69
5	6.85	231.57	192.63	3.81
6	8.22	235.65	197.59	3.83
7	9.59	237.84	199.1	3.84
8	10.96	264.23	215.88	3.98
9	12.33	291.68	230.9	4.11
10	13.7	303.6	237.98	4.17
11	15.07	321.06	247.84	4.25
12	16.44	352.94	268.59	4.38
13	17.81	358.13	271.44	4.41
14	19.18	372.43	282.8	4.46
15	20.55	416.19	302.03	4.63
16	21.92	427.77	306.93	4.67
17	23.29	440.38	315.79	4.72
18	24.66	433.14	309.48	4.69
19	26.03	430.49	321.69	4.68
20	27.4	471.86	351.76	4.83
21	28.77	484.11	355.77	4.87
22	30.14	458.51	342.15	4.78
23	31.51	430.48	311.62	4.68
24	32.88	393.92	283.49	4.55
25	34.25	351.37	258.71	4.38
26	35.62	308.82	234.36	4.19
27	36.99	305.21	230.62	4.18
28	38.36	302.44	227.99	4.16
29	39.73	251.01	200.46	3.91
30	41.1	224.64	185.32	3.77
31	42.47	200.06	170.92	3.63
32	43.84	140.09	134.37	3.22
33	45.21	109.18	113.28	2.96
34	46.58	83.6	95.14	2.71
35	47.95	37.66	76.62	2.08
36	49.32	13.85	38.97	1.49
37	50.69	7.25	19.57	1.2
38	52.06	.62	4.2	.53

FR	CY	CX	LE	LP
1	2.4	.07	6.76	-

CONT.-

FR	CY	CX	LE	LP
2	2.84	.1	6.91	-
3	3.15	.1	7.51	-
4	3.34	.15	8.03	-
5	3.45	.12	8.01	-
6	3.42	.15	8.52	-
7	3.34	.17	8.68	-
8	3.56	.27	9.17	-
9	3.79	.22	9.71	-
10	4.16	.26	10.56	-
11	4.37	.34	11.06	-
12	4.74	.33	11.79	-
13	5.16	.36	12.32	-
14	5.66	.35	12.93	-
15	6.06	.4	13.64	-
16	6.5	.35	14.45	-
17	7.1	.28	15.05	-
18	7.62	.29	15.53	-
19	8.04	.3	15.95	-
20	8.6	.29	16.7	-
21	9.11	.24	17.03	-
22	9.82	.22	17.54	-
23	10.63	.29	17.84	-
24	11.01	.33	17.78	-
25	11.94	.28	18.16	-
26	12.68	.24	18.36	-
27	13.5	.24	18.87	-
28	14.14	.3	19.11	-
29	14.61	.25	19.24	-
30	15.01	.24	19.15	-
31	15.51	.27	19.32	-
32	15.87	.21	19.05	-
33	16.56	.26	19.63	-
34	17.45	.35	20.61	-
35	19.23	.57	21.36	-
36	20.69	2.72	22.07	-
37	21.49	.25	22.5	-
38	21.88	-.03	22.78	-

CONT.-

EXPERIMENTAL PARAMETERS :

$d = 2$	$\dot{m}_s = 1.5$	$V_s = 41806$	$P = .995$
$Ja = 30$	$\Delta T = 10$	$\Delta t = 1.37$	$CS = 730$
$F = 38$	$Z = 40$	$T_p = 165$	

EXPERIMENTAL RESULTS :

$t_g = 31.51$	$t_c = 19$	$t_t = 50.51$	$f_s = 33$
$R_o = 4.63$	$U = 590$	$h_c = 24055$	
$R_m = 4.87$	$Pe_o = 32830$	$Nu_c = 179$	
$Z_d = 10.63$	$Z_c = 21.88$	$Fo_c = 3.69E-05$	

(3.2).1

TEST NO : (3.3).1 FILM NO : 36-2/1

FR	TIME	VOLUME	AREA	RADIUS
1	1.11	37.32	58.31	2.07
2	2.21	43.52	63.84	2.18
3	3.32	72.04	87.82	2.58
4	4.42	143.07	136.51	3.24
5	5.53	178.72	160.17	3.49
6	6.63	201.48	174.06	3.64
7	7.74	193.37	171.41	3.59
8	8.84	168.53	158.25	3.43
9	9.95	159.76	155	3.37
10	11.05	175.57	165.07	3.47
11	12.16	214.46	188	3.71
12	13.26	249.94	210.16	3.91
13	14.37	269.51	221.31	4.01
14	15.47	248.41	211.8	3.9
15	16.58	217.21	197.29	3.73
16	17.68	216.66	198.08	3.73
17	18.79	187.6	180.82	3.55
18	19.89	154.97	161.1	3.33
19	21	121.99	137.85	3.08
20	22.1	106.9	125.06	2.94
21	23.21	80.22	105.16	2.68
22	24.31	63.22	89.83	2.47
23	25.42	32.25	55.22	1.97
24	26.52	8.96	25.98	1.29
25	27.63	1.05	6.67	.63

FR	CY	CX	LE	LP
1	1.82	.11	4.99	-
2	1.91	.15	4.97	-
3	2.2	.17	5.44	-
4	2.69	.31	6.3	-
5	2.97	.25	7.21	-
6	3.12	.31	8.09	-
7	3.24	.36	8.51	-
8	3.32	.3	8.61	-
9	3.58	.28	9.11	-
10	3.92	.28	9.69	-
11	4.31	.32	10.57	-
12	4.75	.3	11.65	-
13	5.11	.3	12.18	-

CONT.-

FR	CY	CX	LE	LP
14	5.44	.34	12.92	-
15	6.02	.33	13.19	-
16	6.54	.26	13.82	-
17	7.26	.26	14.14	-
18	8.02	.25	14.66	-
19	9.12	.28	15	-
20	10.21	.23	15.38	-
21	11.17	.18	15.68	-
22	11.78	.19	15.82	-
23	12.18	0	15.43	-
24	13.97	.01	16.02	-
25	16.34	-.72	17.29	-

EXPERIMENTAL PARAMETERS :

$d = 2$ $\dot{m}_s = 1.5$ $V_s = 41806$ $P = .995$

$Ja = 45$ $\Delta T = 15$ $\Delta t = 1.11$ $CS = 905$

$F = 25$ $Z = 40$ $T_p = 165$

EXPERIMENTAL RESULTS :

$t_g = 18.79$ $t_c = 8.3$ $t_t = 27.09$ $f_s = 57$

$R_o = 3.55$ $U = 800$ $h_c = 24719$

$R_m = 4.01$ $Pe_o = 34380$ $Nu_c = 141$

$Z_d = 7.26$ $Z_c = 16.34$ $Fo_c = 2.72E-05$

TEST NO : (3.4).1 FILM NO : 37-1/2

FR	TIME	VOLUME	AREA	RADIUS
1	.8	39.79	61.6	2.12
2	1.59	60.6	81.56	2.44
3	2.39	81.64	99.51	2.69
4	3.18	104.86	117.86	2.93
5	3.98	122.54	130.8	3.08
6	4.78	135.85	143.93	3.19
7	5.57	135.46	144.19	3.19
8	6.37	139.56	146.45	3.22
9	7.16	135.75	144.58	3.19
10	7.96	135.95	147.32	3.19
11	8.76	121.09	134.82	3.07
12	9.55	120.15	138.66	3.06
13	10.35	135.14	145.7	3.18
14	11.14	146.8	154.08	3.27
15	11.94	142.91	151.78	3.24
16	12.74	149.54	154.56	3.29
17	13.53	155.06	158.1	3.33
18	14.33	144.55	149.79	3.26
19	15.12	143.73	152.1	3.25
20	15.92	138.52	149.32	3.21
21	16.72	121.84	133	3.08
22	17.51	99.85	117.18	2.88
23	18.31	83.02	100.7	2.71
24	19.1	67.04	87.35	2.52
25	19.9	51.89	72.28	2.31
26	20.7	35.71	57.33	2.04
27	21.49	16.07	38.09	1.57
28	22.29	.27	2.42	.4

FR	CY	CX	LE	LP
1	1.49	.14	4.53	-
2	1.61	.19	5.1	-
3	1.73	.25	5.01	-
4	1.75	.31	5.15	-
5	1.96	.3	5.47	-
6	2.08	.33	5.98	-
7	2.13	.29	6.15	-
8	2.23	.28	6.79	-
9	2.33	.25	7.18	-
10	2.5	.23	7.67	-

CONT.-

FR	CY	CX	LE	LP
11	2.63	.07	7.75	-
12	2.91	.14	8.15	-
13	3.15	.14	8.8	-
14	3.46	.12	9.25	-
15	3.77	.14	9.56	-
16	4.05	.13	9.91	-
17	4.4	.13	10.39	-
18	4.92	.1	10.57	-
19	5.43	.04	10.93	-
20	5.88	.01	11.16	-
21	6.27	.05	11.12	-
22	6.89	-.05	11.27	-
23	7.38	-.13	11.42	-
24	8	-.08	11.85	-
25	8.83	-.08	12.66	-
26	9.65	-.14	13.5	-
27	10.43	-.12	13.72	-
28	10.43	-.25	10.69	-

EXPERIMENTAL PARAMETERS :

$d = 2$ $\dot{m}_s = 1.5$ $V_s = 41806$ $P = .995$

$Ja = 60$ $\Delta T = 20$ $\Delta t = .8$ $CS = 1256$

$F = 28$ $Z = 40$ $T_p = 165$

EXPERIMENTAL RESULTS :

$t_g = 16.72$ $t_c = 5.5$ $t_t = 22.22$ $f_s = 63$

$R_o = 3.08$ $U = 810$ $h_c = 24967$

$R_m = 3.33$ $Pe_o = 30390$ $Nu_c = 125$

$Z_d = 6.27$ $Z_c = 10.43$ $Fo_c = 2.38E-05$

TEST NO : (4.1).2 FILM NO : 44-2/4

FR	TIME	VOLUME	AREA	RADIUS
1	2.37	4.56	16.3	1.03
2	4.74	24.28	44.45	1.8
3	7.12	30.8	50.77	1.94
4	9.49	28.35	46.63	1.89
5	11.86	34.72	52.46	2.02
6	14.23	47.58	66.1	2.25
7	16.6	48.91	67.28	2.27
8	18.98	47.54	67.02	2.25
9	21.35	57.82	75.88	2.4
10	23.72	62.45	79.9	2.46
11	26.09	66.01	82.57	2.51
12	28.46	61.86	76.92	2.45
13	30.84	53.78	70.56	2.34
14	33.21	51.8	69.82	2.31
15	35.58	43.44	64.46	2.18
16	37.95	43.15	66.17	2.18
17	40.32	32.95	58.51	1.99
18	42.7	27.46	57.49	1.87
19	45.07	19.96	46.27	1.68
20	47.44	8.16	27.11	1.25
21	49.81	5.63	16.76	1.1
22	52.18	2.41	9.66	.83
23	54.56	.89	5.22	.6
24	56.93	.33	2.45	.43

FR	CY	CX	LE	LP
1	.48	.03	1.32	0
2	1.05	.07	2.65	0
3	1.24	.06	3.1	0
4	1.46	.15	3.19	0
5	1.79	.09	3.63	0
6	2.19	.17	4.46	0
7	2.31	.19	4.76	0
8	2.59	.2	5.17	0
9	2.96	.2	5.29	0
10	3.28	.25	5.65	0
11	3.69	.2	6.28	0
12	4.22	.23	7.06	1.56
13	4.81	.24	7.51	2.69

CONT.-

FR	CY	CX	LE	LP
14	5.66	.3	8.07	3.9
15	6.08	.18	8.3	4.62
16	6.42	.29	8.49	5.11
17	7.12	.22	8.99	6.06
18	7.62	.24	9.14	6.77
19	8.18	.41	9.78	7.44
20	8.89	.27	9.56	8.31
21	9.5	.44	10.27	8.45
22	9.68	.57	10.93	8.61
23	10.57	.5	11.35	9.76
24	11.36	.58	11.76	10.85

EXPERIMENTAL PARAMETERS :

$d = 2$	$\dot{m}_s = .45$	$V_s = 6643$	$P = 2.005$
$Ja = 15$	$\Delta T = 9.3$	$\Delta t = 2.37$	$CS = 422$
$F = 24$	$Z = 40$	$T_p = 165$	

EXPERIMENTAL RESULTS :

$t_g = 28.46$	$t_c = 24.7$	$t_t = 53.16$	$f_s = 38$
$R_o = 2.45$	$U = 250$	$h_c = 17086$	
$R_m = 2.51$	$Pe_o = 7210$	$Nu_c = 63$	
$Z_d = 4.22$	$Z_c = 11.36$	$Fo_c = 1.749E-04$	

TEST NO : (4.2).3   FILM NO : 45-1/4

FR	TIME	VOLUME	AREA	RADIUS
1	1.51	.76	4.82	.57
2	3.02	2.61	11.33	.85
3	4.52	6.12	19.74	1.13
4	6.03	16.84	35.04	1.59
5	7.54	26.08	45.77	1.84
6	9.05	26.91	46.28	1.86
7	10.56	23.77	41.82	1.78
8	12.06	21.28	38.07	1.72
9	13.57	24.73	42.43	1.81
10	15.08	30.86	49.34	1.95
11	16.59	37.93	56.57	2.08
12	18.1	37.45	56.84	2.08
13	19.6	36.47	56.12	2.06
14	21.11	36.1	56.42	2.05
15	22.62	39.76	60.43	2.12
16	24.13	41.83	62.5	2.15
17	25.64	42.4	59.84	2.16
18	27.14	34.57	52.59	2.02
19	28.65	28.18	45.64	1.89
20	30.16	21.38	38.21	1.72
21	31.67	16.88	32.97	1.59
22	33.18	14.03	30.37	1.5
23	34.68	8.46	25.15	1.26
24	36.19	5.91	21.86	1.12
25	37.7	.4	2.78	.46

FR	CY	CX	LE	LP
1	.51	.06	1.17	0
2	.4	.03	.86	0
3	.55	.02	1.3	0
4	.84	-.01	2.16	0
5	1.11	0	2.63	0
6	1.25	.01	2.79	0
7	1.25	.01	2.8	0
8	1.39	-.01	2.95	0
9	1.65	.04	3.27	0
10	1.87	.04	3.78	0
11	2.11	.06	4.24	0
12	2.27	.05	4.49	0
13	2.46	.07	4.7	0

CONT.-

FR	CY	CX	LE	LP
14	2.67	.1	4.83	0
15	3.03	.12	5.16	0
16	3.28	.07	5.52	0
17	3.58	.1	5.97	.85
18	3.91	.07	6.18	1.75
19	4.26	.1	6.27	2.28
20	4.86	.09	6.54	3.46
21	5.31	.09	6.71	4.15
22	5.66	.13	7.04	4.79
23	6.11	.12	6.97	5.57
24	6.46	.01	6.85	6.07
25	6.87	1.25	7.28	6.4

EXPERIMENTAL PARAMETERS :

$d = 2$ $\dot{m}_s = .45$ $V_s = 6643$ $P = 2.005$

$Ja = 30$ $\Delta T = 18.5$ $\Delta t = 1.51$ $CS = 663$

$F = 25$ $Z = 40$ $T_p = 165$

EXPERIMENTAL RESULTS :

$t_g = 25.64$ $t_c = 12$ $t_t = 37.64$ $f_s = 41$

$R_o = 2.16$ $U = 249$ $h_c = 16723$

$R_m = 2.16$ $Pe_o = 6360$ $Nu_c = 58$

$Z_d = 3.58$ $Z_c = 6.87$ $Fo_c = 1.087E-04$

TEST NO : (5.1).2 FILM NO : 51-1/6

FR	TIME	VOLUME	AREA	RADIUS
1	2.23	135.35	136.74	3.19
2	4.45	146.55	144.44	3.27
3	6.68	162.22	154.92	3.38
4	8.9	155.44	158.22	3.34
5	11.13	169.48	175.02	3.43
6	13.36	172.3	177.98	3.45
7	15.58	167.01	172	3.42
8	17.81	179.15	181.03	3.5
9	20.03	177.77	180.14	3.49
10	22.26	167.73	163.35	3.42
11	24.49	151.42	156.53	3.31
12	26.71	126.51	127.78	3.11
13	28.94	107.36	113.87	2.95
14	31.16	98.45	107.71	2.86
15	33.39	71.12	93.15	2.57
16	35.62	49.42	68.64	2.28
17	37.84	34.93	57.53	2.03
18	40.07	23.43	44.95	1.78
19	42.29	21.04	40.16	1.71
20	44.52	11.78	27.71	1.41
21	46.75	4.09	13.11	.99
22	48.97	2.07	8.11	.79
23	51.2	1.99	8.05	.78
24	53.42	1.13	5.56	.65
25	55.65	.76	4.27	.57
26	57.88	.33	2.7	.43
27	60.1	.22	2.06	.38

FR	CY	CX	LE	LP
1	3.33	.29	8.97	0
2	3.79	.26	9.52	0
3	4.31	.32	10.13	0
4	4.66	.32	10.13	0
5	5.02	.42	10.62	0
6	5.23	.41	10.7	0
7	5.42	.45	10.57	0
8	5.7	.42	10.56	0
9	5.91	.36	10.63	0
10	6.25	.47	10.41	.6

CONT.-

FR	CY	CX	LE	LP
11	6.76	.45	10.73	1.55
12	7.65	.53	10.91	4.18
13	8.14	.52	11.01	5.6
14	8.56	.53	11.34	6.4
15	9.01	.57	12.18	7.09
16	10.09	.64	13.05	8.29
17	11.16	.65	13.02	9.8
18	11.89	.62	13.47	10.46
19	12.83	.56	14.12	11.82
20	13.49	.43	14.54	12.53
21	14.16	.31	14.94	13.48
22	14.64	.25	15.45	13.93
23	15.16	.18	15.87	14.59
24	15.78	-.07	16.32	15.15
25	16.35	-.09	16.8	15.89
26	17.12	-.09	17.6	16.64
27	17.78	-.03	18.05	17.46

EXPERIMENTAL PARAMETERS :

$d = 2$ $\dot{m}_s = .92$ $V_s = 13560$ $P = 2.011$

$Ja = 15$ $\Delta T = 9.3$ $\Delta t = 2.23$ $CS = 449$

$F = 27$ $Z = 40$ $T_p = 165$

EXPERIMENTAL RESULTS :

$t_g = 22.26$ $t_c = 30$ $t_t = 52.26$ $f_s = 50$

$R_o = 3.42$ $U = 338$ $h_c = 20042$

$R_m = 3.5$ $Pe_o = 13600$ $Nu_c = 104$

$Z_d = 6.25$ $Z_c = 17.78$ $Fo_c = 1.09E-04$

(S.1).2

TEST NO : (5.2).2 FILM NO : 42-2/3

FR	TIME	VOLUME	AREA	RADIUS
1	1.58	4.13	15.03	1
2	3.16	14.01	31.23	1.5
3	4.74	28.42	48.94	1.89
4	6.32	37.8	58.27	2.08
5	7.9	40.09	59.48	2.12
6	9.48	41.27	60.11	2.14
7	11.06	52.69	69.94	2.33
8	12.64	65.56	80.65	2.5
9	14.22	75.64	88.12	2.62
10	15.8	75.63	87.87	2.62
11	17.38	78.17	89.79	2.65
12	18.96	82.69	93.18	2.7
13	20.54	93.15	101.3	2.81
14	22.12	95.6	103.52	2.84
15	23.7	97.08	105.11	2.85
16	25.28	86.22	96.1	2.74
17	26.86	71.82	85.26	2.58
18	28.44	61.76	78.81	2.45
19	30.02	53.72	73.88	2.34
20	31.6	43.7	65.43	2.19
21	33.18	32.08	56.44	1.97
22	34.76	25.46	49.61	1.82
23	36.34	18.25	42.55	1.63
24	37.92	9.36	32.76	1.31
25	39.5	.31	2.38	.42
26	41.08	.03	.58	.2

FR	CY	CX	LE	LP
1	.53	.09	1.53	0
2	.83	.06	2.13	0
3	1.2	.09	2.84	0
4	1.29	.09	3.19	0
5	1.39	.13	3.36	0
6	1.47	.14	3.4	0
7	1.64	.19	3.81	0
8	1.8	.22	4.11	0
9	2.06	.26	4.77	0
10	2.29	.25	5.19	0
11	2.5	.26	5.56	0
12	2.73	.24	5.7	0

CONT.-

FR	CY	CX	LE	LP
13	3.03	.28	6.23	0
14	3.31	.24	6.69	0
15	3.75	.25	7.29	0
16	4.06	.21	7.36	1.17
17	4.59	.2	7.58	2.34
18	5.18	.15	7.97	3.42
19	5.66	.16	7.97	4.28
20	5.91	.18	7.41	4.68
21	6.09	.13	7.29	5.18
22	6.46	.12	7.61	5.65
23	6.96	.17	7.98	6.33
24	7.08	-.05	7.52	6.64
25	7.24	-.31	7.71	6.88
26	7.32	-.1	7.51	7.07

EXPERIMENTAL PARAMETERS :

$d = 2$ $\dot{m}_s = .92$ $V_s = 13560$ $P = 2.008$
$Ja = 30$ $\Delta T = 18.5$ $\Delta t = 1.58$ $CS = 633$
$F = 26$ $Z = 40$ $T_p = 165$

EXPERIMENTAL RESULTS :

$t_g = 25.25$ $t_c = 14.2$ $t_t = 39.48$ $f_s = 42$
$R_o = 2.74$ $U = 320$ $h_c = 15874$
$R_m = 2.85$ $Pe_o = 10380$ $Nu_c = 70$
$Z_d = 4.06$ $Z_c = 7.32$ $Fo_c = 7.99E-05$

TEST NO : (5.3).3 FILM NO : 43-1/3

FR	TIME	VOLUME	AREA	RADIUS
1	.77	.29	2.71	.41
2	1.54	4.58	15.75	1.03
3	2.31	13.02	30.02	1.46
4	3.08	23.7	44.7	1.78
5	3.85	36.31	58.07	2.05
6	4.62	46.9	68.12	2.24
7	5.39	51.11	71.39	2.3
8	6.16	49.31	69.39	2.27
9	6.93	42.07	62.43	2.16
10	7.7	32.61	53.23	1.98
11	8.47	27.47	48.77	1.87
12	9.24	27.8	47.21	1.88
13	10.01	31.06	50.77	1.95
14	10.78	40.72	59.26	2.13
15	11.55	50.15	67.59	2.29
16	12.32	59.86	75.67	2.43
17	13.09	64.53	79.04	2.49
18	13.86	63.29	78.21	2.47
19	14.63	57.92	74.27	2.4
20	15.4	49.99	67.59	2.29
21	16.17	43.05	62.44	2.17
22	16.94	37.55	58.37	2.08
23	17.71	38.66	63.05	2.1
24	18.48	41.59	66.06	2.15
25	19.25	47.7	72.77	2.25
26	20.02	52.53	75.79	2.32
27	20.79	53.96	75.43	2.34
28	21.56	50.1	67.82	2.29
29	22.33	43.75	61.31	2.19
30	23.1	39.91	57.65	2.12
31	23.87	32.32	50.44	1.98
32	24.64	28.6	46.57	1.9
33	25.41	22.9	40.97	1.76
34	26.18	18.8	36.86	1.65
35	26.95	14.92	32.49	1.53
36	27.72	11.38	27.99	1.4
37	28.49	6.74	24.77	1.17
38	29.26	2	10.11	.78
39	30.03	.48	3.17	.49
40	30.8	.15	1.58	.33

CONT.—

FR	CY	CX	LE	LP
1	.19	.03	.47	0
2	.48	.09	1.07	0
3	.75	.13	1.9	0
4	.98	.12	2.6	0
5	1.25	.11	3.37	0
6	1.39	.11	3.68	0
7	1.49	.12	3.91	0
8	1.54	.1	3.83	0
9	1.52	.1	3.54	0
10	1.46	.11	3.26	0
11	1.4	.14	3.03	0
12	1.44	.09	3.03	0
13	1.47	.06	3.14	0
14	1.64	.07	3.34	0
15	1.74	.01	3.74	0
16	1.85	0	3.91	0
17	1.97	0	4.31	0
18	2.06	.05	4.6	0
19	2.11	.07	4.69	0
20	2.21	.07	4.77	0
21	2.31	.09	4.9	0
22	2.46	.08	4.91	0
23	2.69	.09	5.27	0
24	2.94	.1	5.57	0
25	3.16	.16	5.85	0
26	3.36	.2	6.09	0
27	3.66	.23	6.44	0
28	3.91	.2	6.69	.78
29	4.14	.15	6.72	1.63
30	4.38	.18	6.69	1.92
31	4.55	.14	6.7	2.29
32	4.86	.06	7.17	3.15
33	5	.05	6.94	3.74
34	5.35	.08	6.61	4.33
35	5.63	.09	6.71	4.79
36	5.72	.06	6.5	5.04
37	5.89	.03	6.52	5.49
38	6.04	-.29	6.53	5.74
39	6.16	-.22	6.63	5.78
40	6.36	-.33	6.67	6.05

CONT.-

EXPERIMENTAL PARAMETERS :

$d = 2$	$\dot{m}_s = .92$	$V_s = 13560$	$P = 2.008$
$Ja = 45$	$\Delta T = 27.6$	$\Delta t = .77$	$CS = 1298$
$F = 40$	$Z = 40$	$T_p = 165$	

EXPERIMENTAL RESULTS :

$t_g = 21.56$	$t_c = 8.7$	$t_t = 30.26$	$f_s = 48$
$R_o = 2.29$	$U = 247$	$h_c = 16664$	
$R_m = 2.49$	$Pe_o = 6770$	$Nu_c = 61$	
$Z_d = 3.91$	$Z_c = 6.36$	$Fo_c = 6.93E-05$	

TEST NØ : (6.1).2 FILM NØ : 52-1/2

FR	TIME	VØLUME	AREA	RADIUS
1	1.12	131.09	172.08	3.15
2	2.23	159.49	188.47	3.36
3	3.35	179.44	194.67	3.5
4	4.46	179.12	194.87	3.5
5	5.58	158.65	185.62	3.36
6	6.7	157.22	177.32	3.35
7	7.81	170.66	197.39	3.44
8	8.93	179.17	200.23	3.5
9	10.04	189.85	207.16	3.57
10	11.16	188.43	200.13	3.56
11	12.28	186.64	202.22	3.55
12	13.39	168.7	190.14	3.43
13	14.51	186.61	198.73	3.54
14	15.62	204.52	214.36	3.65
15	16.74	211.94	217.16	3.7
16	17.86	201.38	213.03	3.64
17	18.97	200.96	209.25	3.63
18	20.09	186.71	203.92	3.55
19	21.2	161.17	178.1	3.38
20	22.32	136.66	157.33	3.2
21	23.44	126.11	147.65	3.11
22	24.55	107.02	124.86	2.95
23	25.67	96.9	107.55	2.85
24	26.78	93.92	104.08	2.82
25	27.9	83.64	95.56	2.71
26	29.02	77.46	89.89	2.64
27	30.13	65.79	83.05	2.5
28	31.25	50.54	76.83	2.29
29	32.36	34.61	70.48	2.02
30	33.48	22.9	53.73	1.76
31	34.6	15.85	36.94	1.56
32	35.71	11.98	28.35	1.42
33	36.83	8.89	21.64	1.28
34	37.94	7.2	19.28	1.2
35	39.06	4.91	15.54	1.05
36	40.18	3.65	12.71	.95
37	41.29	1.63	8.03	.73
38	42.41	1.14	5.68	.65
39	43.52	.66	4.46	.54
40	44.64	.47	3.38	.48
41	45.76	.3	2.51	.42

CONT.-

FR	CY	CX	LE	LP
1	5.03	-.23	12.9	0
2	4.63	-.23	12.87	0
3	4.31	-.33	12.14	0
4	4.28	-.37	11.86	0
5	3.98	-.34	9.82	0
6	3.87	-.39	10.01	0
7	4.02	-.34	11.88	0
8	4.26	-.34	12.14	0
9	4.22	-.28	12.43	0
10	4.34	-.33	12.77	0
11	4.48	-.35	13	0
12	4.81	-.38	13.55	0
13	5.2	-.35	13.9	0
14	5.58	-.4	14.49	0
15	6.24	-.46	14.63	0
16	6.48	-.41	15.07	0
17	7.16	-.4	15.64	0
18	8.11	-.53	16.12	0
19	9.34	-.51	16.25	2.41
20	10.83	-.51	16.54	5.19
21	12.04	-.5	16.98	6.45
22	13.08	-.55	17.27	7.6
23	13.82	-.58	17.44	9.71
24	14.16	-.54	17.56	10.24
25	14.54	-.57	17.68	11.02
26	14.77	-.61	17.66	11.84
27	15.15	-.6	18.31	12.19
28	15.58	-.58	18.93	12.8
29	16.73	-.5	19.59	13.59
30	17.68	-.69	20.42	15.38
31	18.6	-.7	20.77	17.03
32	19.41	-.35	21.11	17.78
33	19.92	-.02	21.39	18.33
34	20.35	.06	21.83	18.63
35	20.73	.22	22.34	19.46
36	21.02	.35	22.51	20.08
37	21.57	.53	22.67	20.89
38	21.82	.49	22.67	21.06
39	22.05	.33	22.56	21.58
40	22.35	.29	22.72	21.73
41	22.58	.32	22.91	22.22

CONT.-

[6.1].2

EXPERIMENTAL PARAMETERS :

$d = 2$	$\dot{m}_s = 1.42$	$V_s = 20963$	$P = 2.011$
$Ja = 15$	$\Delta T = 9.3$	$\Delta t = 1.12$	$CS = 896$
$F = 41$	$Z = 40$	$T_p = 165$	

EXPERIMENTAL RESULTS :

$t_g = 21.21$	$t_c = 23$	$t_t = 44.21$	$f_s = 50$
$R_o = 3.37$	$U = 589$	$h_c = 28956$	
$R_m = 3.7$	$Pe_o = 23350$	$Nu_c = 148$	
$Z_d = 9.34$	$Z_c = 22.58$	$Fo_c = 8.61E-05$	

TEST NO : (6.2).2 FILM NO : 48-2/3

FR	TIME	VOLUME	AREA	RADIUS
1	.81	83.33	101.13	2.71
2	1.63	87.08	104.41	2.75
3	2.44	88.52	105.11	2.76
4	3.26	86.72	103.37	2.75
5	4.07	89.97	106.38	2.78
6	4.88	98.28	112.21	2.86
7	5.7	109.29	119.86	2.97
8	6.51	118.75	127.13	3.05
9	7.33	124.83	131.28	3.1
10	8.14	128.93	134.54	3.13
11	8.95	125.52	133.47	3.11
12	9.77	126.01	134.69	3.11
13	10.58	124.18	134.15	3.09
14	11.4	116.83	127.93	3.03
15	12.21	111.38	124.02	2.98
16	13.02	98.24	114.53	2.86
17	13.84	87.86	108.43	2.76
18	14.65	76.86	100.36	2.64
19	15.47	65.26	93.09	2.5
20	16.28	59.85	87.64	2.43
21	17.09	54.54	81.71	2.35
22	17.91	49.33	76.3	2.28
23	18.72	42.72	67.74	2.17
24	19.54	35.56	59.76	2.04
25	20.35	23.05	44.97	1.77
26	21.16	13.33	36.09	1.47
27	21.98	10.22	28.74	1.35
28	22.79	2.39	12.29	.83
29	23.61	.7	5.16	.55
30	24.42	.29	2.8	.41

FR	CY	CX	LE	LP
1	2.68	.15	7.38	0
2	2.84	.11	7.47	0
3	2.93	.11	7.47	0
4	3.01	.12	7.56	0
5	3.21	.13	7.91	0
6	3.4	.07	8.23	0
7	3.57	.11	8.55	0
8	3.76	.13	9.01	0

CONT.-

FR	CY	CX	LE	LP
9	4.03	.14	9.38	0
10	4.19	.15	9.64	0
11	4.34	.14	9.88	0
12	4.65	.18	10.13	0
13	4.74	.17	10.33	0
14	5.06	.16	10.58	.87
15	5.48	.2	10.74	1.82
16	5.82	.25	10.93	2.54
17	6.51	.29	11.24	3.71
18	6.99	.29	11.46	4.21
19	7.6	.3	12.34	5
20	7.95	.33	12.75	5.31
21	8.14	.36	12.67	5.51
22	8.36	.35	12.55	5.81
23	8.43	.36	11.83	6.08
24	8.67	.4	11.66	6.5
25	9.33	.47	11.69	6.63
26	9.98	.47	13.83	8.13
27	10.67	.41	11.78	9.15
28	10.95	.49	12.26	10.66
29	11.53	.76	12.57	11.74
30	11.54	1.15	13	12.49

EXPERIMENTAL PARAMETERS :

$d = 2$	$\dot{m}_s = 1.42$	$V_s = 20963$	$P = 2.011$
$Ja = 30$	$\Delta T = 18.5$	$\Delta t = .81$	$CS = 1228$
$F = 30$	$Z = 40$	$T_p = 165$	

EXPERIMENTAL RESULTS :

$t_g = 11.39$	$t_c = 12.5$	$t_t = 23.89$	$f_s = 95$
$R_o = 3.04$	$U = 495$	$h_c = 22580$	
$R_m = 3.13$	$Pe_o = 17810$	$Nu_c = 109$	
$Z_d = 5.06$	$Z_c = 11.54$	$Fo_c = 5.71E-05$	

TEST NO : (6.3).3 FILM NO : 49-1/5

FR	TIME	VOLUME	AREA	RADIUS
1	.81	15.02	30.68	1.53
2	1.62	20.45	37.1	1.7
3	2.43	32.58	50.22	1.98
4	3.24	49.52	66.6	2.28
5	4.06	67.52	82.15	2.53
6	4.87	75.11	88.31	2.62
7	5.68	77.96	90.65	2.65
8	6.49	73.38	86.87	2.6
9	7.3	66.49	82.43	2.51
10	8.11	65.26	82	2.5
11	8.92	67.13	83.44	2.52
12	9.73	74.37	89.73	2.61
13	10.54	87.69	100.6	2.76
14	11.35	99.41	108.8	2.87
15	12.17	102.67	110.43	2.9
16	12.98	101.58	109.64	2.89
17	13.79	94.14	103.16	2.82
18	14.6	85.25	95.93	2.73
19	15.41	74.4	87.72	2.61
20	16.22	63.11	77.98	2.47
21	17.03	49.62	66.6	2.28
22	17.84	40.82	58.7	2.14
23	18.65	31.52	51.17	1.96
24	19.46	24.7	45.12	1.81
25	20.28	15.91	34.99	1.56
26	21.09	5.24	19.3	1.08
27	21.9	.94	6.95	.61

FR	CY	CX	LE	LP
1	1.24	-.15	2.93	0
2	1.45	-.18	3.15	0
3	1.62	-.19	3.5	0
4	1.9	-.26	4.01	0
5	2.04	-.3	4.33	0
6	2.03	-.21	4.42	0
7	2.08	-.19	4.79	0
8	2.22	-.21	5.09	0
9	2.21	-.19	5	0
10	2.35	-.17	5.2	0
11	2.54	-.1	5.4	0

CONT.-

FR	CY	CX	LE	LP
12	2.74	-.07	5.63	0
13	3.04	-.03	6.1	0
14	3.21	0	6.47	0
15	3.41	.03	6.7	0
16	3.6	.07	7.03	0
17	3.84	.09	7.22	0
18	4.07	.14	7.34	.52
19	4.31	.11	7.36	1.4
20	4.68	.1	7.44	2.13
21	5.18	.06	7.54	3.24
22	5.53	.02	7.55	3.78
23	5.86	.01	7.87	4.58
24	6.34	0	7.8	5.31
25	6.36	-.07	7.49	5.58
26	6.87	-.46	8.68	5.99
27	6.85	-.82	9.19	8.15

EXPERIMENTAL PARAMETERS :

$d = 2$ $\quad \dot{m}_s = 1.42$ $\quad V_s = 20963$ $\quad P = 2.011$

$Ja = 45$ $\quad \Delta T = 27.6$ $\quad \Delta t = .81$ $\quad CS = 1233$

$F = 27$ $\quad Z = 40$ $\quad T_p = 165$

EXPERIMENTAL RESULTS :

$t_g = 14.6$ $\quad t_c = 7.5$ $\quad t_t = 22.1$ $\quad f_s = 73$

$R_o = 2.73$ $\quad U = 447$ $\quad h_c = 23346$

$R_m = 2.9$ $\quad Pe_o = 14610$ $\quad Nu_c = 107$

$Z_d = 4.07$ $\quad Z_c = 6.85$ $\quad Fo_c = 4.2E-05$

TEST NO : (6.4).1 FILM NO : 50-1/2

FR	TIME	VOLUME	AREA	RADIUS
1	.81	5.01	19.14	1.06
2	1.62	10.94	28.59	1.38
3	2.43	22.75	44.04	1.76
4	3.24	31.3	53.93	1.96
5	4.06	39.94	63.01	2.12
6	4.87	44.79	69.63	2.2
7	5.68	49.4	74.04	2.28
8	6.49	50.63	75.14	2.29
9	7.3	49.4	73.17	2.28
10	8.11	47.72	69.84	2.25
11	8.92	50.9	72.56	2.3
12	9.73	53.96	74.45	2.34
13	10.54	59.5	78.57	2.42
14	11.35	63.16	81.28	2.47
15	12.17	63	80.34	2.47
16	12.98	62.71	79.71	2.46
17	13.79	61.19	78.42	2.44
18	14.6	56.29	74.69	2.38
19	15.41	54	73.44	2.34
20	16.22	55.54	74.67	2.37
21	17.03	48.76	66.31	2.27
22	17.84	37.14	55.84	2.07
23	18.65	30.07	49.48	1.93
24	19.46	22.56	41.71	1.75
25	20.28	15.93	34.44	1.56
26	21.09	2.61	11.65	.85
27	21.9	.37	2.78	.45

FR	CY	CX	LE	LP
1	.56	.03	1.36	0
2	.68	-.01	1.68	0
3	.97	.02	2.39	0
4	1.12	.05	2.94	0
5	1.16	.06	3.29	0
6	1.19	.01	3.44	0
7	1.27	-.02	3.64	0
8	1.31	.02	3.9	0
9	1.37	.02	4.15	0
10	1.49	.02	4.44	0
11	1.64	.03	4.57	0

CONT.-

FR	CY	CX	LE	LP
12	1.68	.05	4.82	0
13	1.88	.06	5.11	0
14	2.08	.03	5.41	0
15	2.29	.09	5.62	0
16	2.42	0	5.74	0
17	2.78	-.01	6.15	0
18	2.95	-.03	6.27	0
19	3.22	-.05	6.5	0
20	3.35	.05	6.57	0
21	3.65	.03	6.68	1.23
22	3.98	.03	6.78	2.13
23	4.28	.03	6.59	2.65
24	4.66	.13	7	3.39
25	5.01	.17	7.54	3.88
26	5.49	.6	6.9	4.43
27	6.41	.41	6.94	6.09

EXPERIMENTAL PARAMETERS :

$d = 2$ $\dot{m}_s = 1.42$ $V_s = 20963$ $P = 2.011$

$Ja = 60$ $\Delta T = 36.6$ $\Delta t = .81$ $CS = 1233$

$F = 27$ $Z = 40$ $T_p = 165$

EXPERIMENTAL RESULTS :

$t_g = 17.03$ $t_c = 5$ $t_t = 22.03$ $f_s = 62$

$R_o = 2.27$ $U = 447$ $h_c = 21777$

$R_m = 2.47$ $Pe_o = 12300$ $Nu_c = 79$

$Z_d = 3.65$ $Z_c = 6.41$ $Fo_c = 4E-05$

TEST NO : (7.1).1 FILM NO : 53-2/1

FR	TIME	VOLUME	AREA	RADIUS
1	2.15	17.58	36.71	1.61
2	4.3	58.44	111.59	2.41
3	6.44	91.22	132.52	2.79
4	8.59	127.26	163.97	3.12
5	10.74	153.72	192.41	3.32
6	12.89	166.76	219.36	3.41
7	15.04	186.84	244.56	3.55
8	17.18	201.22	267.59	3.64
9	19.33	192.92	191.57	3.58
10	21.48	191.07	204.33	3.57
11	23.63	200.35	214.45	3.63
12	25.78	208.91	218.01	3.68
13	27.92	216.69	213.12	3.73
14	30.07	172.19	170.82	3.45
15	32.22	130.81	130.77	3.15
16	34.37	115.63	119.6	3.02
17	36.52	104.69	113.13	2.92
18	38.66	89.89	103.1	2.78
19	40.81	77.3	97.05	2.64
20	42.96	76.93	95.87	2.64
21	45.11	47.5	75.57	2.25
22	47.26	30.51	53.3	1.94
23	49.4	11.91	26.85	1.42
24	51.55	5.81	16.09	1.12
25	53.7	2.42	10.65	.83
26	55.85	.64	3.9	.54
27	58	.25	2.21	.39

FR	CY	CX	LE	LP
1	.91	-.06	2.23	0
2	1.33	-.12	4.26	0
3	1.88	-.07	6.19	0
4	2.39	-.08	7.7	0
5	2.89	-.07	8.83	0
6	3.4	-.07	9.85	0
7	3.93	-.09	11.07	0
8	4.66	-.09	11.94	0
9	5.64	-.19	12.66	0
10	6.3	-.22	13.27	0
11	7.01	-.2	14.08	0

CONT.-

FR	CY	CX	LE	LP
12	7.86	-.16	14.59	0
13	9.13	-.24	15.12	2.54
14	10.54	-.32	15.8	6.09
15	12.28	-.38	16.3	8.91
16	13.13	-.46	16.54	10.52
17	13.95	-.61	17.4	11.77
18	14.6	-.75	17.76	12.8
19	15.19	-.8	17.86	13.31
20	15.54	-.78	18.05	14.06
21	15.82	-1.13	17.7	14.51
22	16.67	-1.31	18.31	15.26
23	18.6	-.9	19.79	17.7
24	19.86	-.83	21.1	18.78
25	20.86	-.98	21.63	19.74
26	21.73	-.98	22.24	21.19
27	22.55	-1.02	22.93	22.2

EXPERIMENTAL PARAMETERS :

$d = 1$	$\dot{m}_s = .42$	$V_s = 11706$	$P = 1.02$
$Ja = 15$	$\Delta T = 5$	$\Delta t = 2.15$	$CS = 466$
$F = 27$	$Z = 40$	$T_p = 165$	

EXPERIMENTAL RESULTS :

$t_g = 27.98$	$t_c = 29$	$t_t = 56.93$	$f_s = 39$
$R_o = 3.73$	$U = 500$	$h_c = 26777$	
$R_m = 3.73$	$Pe_o = 22340$	$Nu_c = 153$	
$Z_d = 9.13$	$Z_c = 22.55$	$Fo_c = 8.7E-05$	

TEST NO : (7.2).3 FILM NO : 54-1/3

FR	TIME	VOLUME	AREA	RADIUS
1	1.03	2.1	9.32	.79
2	2.07	7.11	21.3	1.19
3	3.1	18.89	37.56	1.65
4	4.14	32.99	56.16	1.99
5	5.17	43.97	68.15	2.19
6	6.2	52.89	78.54	2.33
7	7.24	62.47	86.66	2.46
8	8.27	70.84	93.85	2.57
9	9.31	81.2	101.63	2.69
10	10.34	87.96	106.77	2.76
11	11.37	90.31	109.39	2.78
12	12.41	95.75	114.19	2.84
13	13.44	99.96	119.27	2.88
14	14.48	109.13	127.58	2.96
15	15.51	105.5	129.57	2.93
16	16.54	103.36	132.22	2.91
17	17.58	100.97	132.87	2.89
18	18.61	103.11	136.41	2.91
19	19.65	101.63	135.9	2.9
20	20.68	96.91	131.97	2.85
21	21.71	88.73	124.4	2.77
22	22.75	76.53	102.05	2.63
23	23.78	56.51	82.98	2.38
24	24.82	42.75	61.61	2.17
25	25.85	31.38	49.51	1.96
26	26.88	26.39	43.7	1.85
27	27.92	21.59	41.17	1.73
28	28.95	15.51	36.49	1.55
29	29.99	14.99	35.95	1.53
30	31.02	9.5	27.96	1.31
31	32.05	2.28	9.68	.82
32	33.09	.57	3.5	.51
33	34.12	.1	1.37	.28

FR	CY	CX	LE	LP
1	.41	-.06	.94	0
2	.6	-.05	1.38	0
3	.9	-.04	2.45	0
4	1.09	-.1	3.38	0
5	1.33	-.09	4.19	0

CONT.-

FR	CY	CX	LE	LP
6	1.62	-.08	5.14	0
7	1.91	-.09	5.9	0
8	2.19	-.09	6.41	0
9	2.5	-.04	6.87	0
10	2.76	-.05	7.49	0
11	3.07	-.06	8.02	0
12	3.35	-.06	8.6	0
13	3.75	-.04	9.13	0
14	4.27	-.03	9.66	0
15	4.68	-.06	10.17	0
16	5.05	-.08	10.52	0
17	5.37	-.1	10.71	0
18	5.73	-.12	11.04	0
19	6.15	-.13	11.28	0
20	6.7	-.16	11.64	0
21	7.18	-.13	11.81	0
22	7.89	-.14	11.91	3.87
23	8.64	-.18	12.56	5.15
24	9.73	-.28	12.57	7.1
25	10.32	-.3	12.51	8.37
26	10.72	-.3	12.54	8.9
27	11.18	-.32	12.77	9.27
28	11.56	-.41	12.75	9.97
29	11.75	-.29	12.87	10.33
30	12.09	-.56	13.09	11.06
31	11.84	-1.19	12.52	11.06
32	11.9	-1.64	12.37	11.42
33	12.21	-1.45	12.33	12.1

EXPERIMENTAL PARAMETERS :

$d = 1$	$\dot{m}_s = .42$	$V_s = 11706$	$P = 1.02$
$Ja = 30$	$\Delta T = 10$	$\Delta t = 1.03$	$CS = 967$
$F = 33$	$Z = 40$	$T_p = 165$	

EXPERIMENTAL RESULTS :

$t_g = 22.74$	$t_c = 10.5$	$t_t = 33.24$	$f_s = 46$
$R_o = 2.63$	$U = 515$	$h_c = 23402$	
$R_m = 2.96$	$Pe_o = 16320$	$Nu_c = 97$	
$Z_d = 7.89$	$Z_c = 12.21$	$Fo_c = 6.3E-05$	

TEST NO : (7.3).1 FILM NO : 54-2/2

FR	TIME	VOLUME	AREA	RADIUS
1	.78	19.37	38.29	1.67
2	1.55	24.44	44.55	1.8
3	2.33	29.07	51.17	1.91
4	3.1	35.06	59.83	2.03
5	3.88	37.93	65.93	2.08
6	4.66	39.02	68.55	2.1
7	5.43	38.76	70.96	2.1
8	6.21	40.43	73.86	2.13
9	6.98	39.3	73.78	2.11
10	7.76	36.03	69.87	2.05
11	8.54	36.29	69.37	2.05
12	9.31	26.69	51.81	1.85
13	10.09	18.54	35.31	1.64
14	10.86	12.24	26.88	1.43
15	11.64	8.24	22.12	1.25
16	12.42	5.73	18.35	1.11
17	13.19	.68	4.21	.55

FR	CY	CX	LE	LP
1	1.35	-.15	4.1	0
2	1.45	-.14	4.34	0
3	1.62	-.14	4.96	0
4	1.83	-.09	5.96	0
5	2.12	-.07	6.77	0
6	2.46	-.07	7.66	0
7	3.01	-.02	8.1	0
8	3.39	.01	8.76	0
9	4.09	.04	9.23	0
10	4.92	.05	9.58	0
11	5.91	.12	10.11	0
12	7.33	.15	10.17	2.51
13	8.08	.19	10.11	5.72
14	8.45	.25	10.02	6.59
15	9	.42	10.89	7.7
16	9.28	.58	11.01	8.4
17	9.59	1.25	10.35	8.86

CONT.-

EXPERIMENTAL PARAMETERS :

$d = 1$	$\dot{m}_s = .42$	$V_s = 11706$	$P = 1.02$
$Ja = 45$	$\Delta T = 15$	$\Delta t = .78$	$CS = 1289$
$F = 17$	$Z = 40$	$T_p = 165$	

EXPERIMENTAL RESULTS :

$t_g = 9.32$	$t_c = 4$	$t_t = 13.32$	$f_s = 117$
$R_o = 1.85$	$U = 533$	$h_c = 27982$	
$R_m = 2.13$	$Pe_o = 11950$	$Nu_c = 84$	
$Z_d = 7.33$	$Z_c = 9.59$	$Fo_c = 4.77E-05$	

TEST NO : (8.1).3 FILM NO : 55-2/5

FR	TIME	VOLUME	AREA	RADIUS
1	2.25	171.02	160.19	3.44
2	4.51	124.33	135.55	3.1
3	6.76	110.84	130.98	2.98
4	9.02	87.26	108.64	2.75
5	11.27	56.49	87.43	2.38
6	13.52	23.29	47.29	1.77
7	15.78	9.21	26.55	1.3
8	18.03	3.83	12.46	.97
9	20.29	1.51	7.35	.71
10	22.54	.4	3.01	.46

FR	CY	CX	LE	LP
1	12.57	-.31	17.67	8.88
2	13.85	-.39	19.19	10.46
3	15.43	-.41	20.63	11.46
4	16.91	-.3	22.03	12.93
5	18.41	-.05	22.27	15.38
6	20.26	.15	22.46	16.89
7	20.68	.61	23.04	17.89
8	21.35	.51	22.77	20.28
9	22.58	.16	23.54	22.09
10	24.4	-.06	24.78	24

EXPERIMENTAL PARAMETERS :

$d = 1$ $\dot{m}_s = 1$ $V_s = 27871$ $P = 1.017$

$Ja = 15$ $\Delta T = 5$ $\Delta t = 2.25$ $CS = 444$

$F = 10$ $Z = 40$ $T_P = 165$

EXPERIMENTAL RESULTS :

$t_g = -$ $t_c = 18.8$ $t_t = -$ $f_s = -$

$R_o = 3.44$ $U = 680$ $h_c = 33435$

$R_m = 3.44$ $Pe_o = 28010$ $Nu_c = 177$

$Z_d = 12.57$ $Z_c = 24.4$ $Fo_c = 6.63E-05$

TEST NO : (8.2).3 FILM NO : 56-1/3

FR	TIME	VOLUME	AREA	RADIUS
1	1.07	134.04	149.64	3.17
2	2.14	106.4	123.13	2.94
3	3.21	85.36	101.7	2.73
4	4.28	74.68	90.68	2.61
5	5.35	63.55	83.18	2.48
6	6.42	52.89	73.25	2.33
7	7.49	43.04	63.35	2.17
8	8.56	31.66	52.04	1.96
9	9.63	14.01	31.99	1.5
10	10.7	4.09	16.22	.99
11	11.77	.56	4.4	.51

FR	CY	CX	LE	LP
1	8.25	.16	13.89	2.94
2	9.26	.19	14.05	4.38
3	10.18	.22	14.32	5.58
4	10.85	.26	15.01	8.14
5	11.41	.32	14.98	9.06
6	11.78	.38	15.13	9.64
7	12.34	.38	15.11	10.17
8	13.11	.25	14.89	11.13
9	14.2	-.21	15.69	12.65
10	15.77	-.5	16.58	14.51
11	16.26	-.79	16.88	15.82

EXPERIMENTAL PARAMETERS :

$d = 1$ $\dot{m}_s = 1$ $V_s = 27871$ $P = 1.017$

$Ja = 30$ $\Delta T = 10$ $\Delta t = 1.07$ $CS = 934$

$F = 11$ $Z = 40$ $T_p = 165$

EXPERIMENTAL RESULTS :

$t_g = -$ $t_c = 10.9$ $t_t = -$ $f_s = -$

$R_o = 3.13$ $U = 593$ $h_c = 29081$

$R_m = 3.17$ $Pe_o = 22360$ $Nu_c = 149$

$Z_d = 8.25$ $Z_c = 16.26$ $Fo_c = 4.62E-05$

TEST NO : (8.3).3 FILM NO : 56-2/4

FR	TIME	VOLUME	AREA	RADIUS
1	.79	14.92	36.14	1.53
2	1.57	22.91	48.05	1.76
3	2.36	33.74	65.11	2
4	3.14	40.69	76.55	2.13
5	3.93	46.08	83.54	2.22
6	4.72	48.13	86.09	2.26
7	5.5	41.11	78.89	2.14
8	6.29	46.99	84.08	2.24
9	7.07	43.13	64.74	2.18
10	7.86	51.55	73.23	2.31
11	8.65	59.09	81.16	2.42
12	9.43	66.96	89.14	2.52
13	10.22	72.39	96.55	2.59
14	11	77.72	101.9	2.65
15	11.79	85.95	109.35	2.74
16	12.58	84.4	109.1	2.72
17	13.36	89.19	112.62	2.77
18	14.15	90.57	114.16	2.79
19	14.93	96.35	118.2	2.84
20	15.72	93.06	115.79	2.81
21	16.51	84.81	105.29	2.73
22	17.29	67.48	91.58	2.53
23	18.08	50.87	70.43	2.3
24	18.86	42.33	60.96	2.16
25	19.65	30.58	48.54	1.94
26	20.44	16.22	34.09	1.57
27	21.22	2.84	12.67	.88

FR	CY	CX	LE	LP
1	1.37	.09	5.03	0
2	1.48	.08	5.42	0
3	1.91	.08	6.23	0
4	2.64	.06	7.04	0
5	3.37	.01	7.54	0
6	4.07	-.07	8.03	0
7	3.53	.02	8.07	0
8	3.04	.09	5.38	0
9	1.98	.1	5.73	0
10	2.07	.12	6.04	0
11	2.24	.09	6.51	0

CONT.-

FR	CY	CX	LE	LP
12	2.49	.11	7.03	0
13	2.71	.09	7.54	0
14	3.09	.06	8.03	0
15	3.59	.03	8.7	0
16	3.82	-.01	8.97	0
17	4.26	-.07	9.44	0
18	4.8	-.08	9.88	0
19	5.31	-.13	10.29	0
20	5.95	-.2	10.73	0
21	6.58	-.25	10.99	2.23
22	7.14	-.26	11.12	3.38
23	7.86	-.32	11.09	4.5
24	8.35	-.42	11.13	5.66
25	8.97	-.65	11.09	6.57
26	9.51	-.87	12.11	7.67
27	11.51	-1.4	13.09	10.29

EXPERIMENTAL PARAMETERS :

$d = 1$ $\dot{m}_s = 1$ $V_s = 27871$ $P = 1.017$

$Ja = 45$ $\Delta T = 15$ $\Delta t = .79$ $CS = 1272$

$F = 27$ $Z = 40$ $T_p = 165$

EXPERIMENTAL RESULTS :

$t_g = 16.51$ $t_c = 5.5$ $t_t = 22.01$ $f_s = 64$

$R_o = 2.73$ $U = 650$ $h_c = 34227$

$R_m = 2.84$ $Pe_o = 21510$ $Nu_c = 155$

$Z_d = 6.58$ $Z_c = 11.51$ $Fo_c = 3.05E-05$

TEST NO : (8.4).3 FILM NO : 57-1/4

FR	TIME	VOLUME	AREA	RADIUS
1	.58	36.8	62.58	2.06
2	1.16	25.35	44.92	1.82
3	1.75	18.13	34.16	1.63
4	2.33	12.86	27.13	1.45
5	2.91	8.53	20.99	1.27
6	3.49	4.72	14.17	1.04
7	4.07	.56	4.02	.51
8	4.66	.03	.5	.18

FR	CY	CX	LE	LP
1	6.18	-.02	9.36	1.7
2	7	.03	9.23	3.44
3	7.49	.08	9.28	5.57
4	7.8	.14	9.22	6.45
5	8.12	.18	9.29	7.17
6	8.25	.12	9.24	7.51
7	8.7	-.04	9.51	8.33
8	9.29	.33	9.49	9.05

EXPERIMENTAL PARAMETERS :

$d = 1$	$\dot{m}_s = 1$	$V_s = 27871$	$P = 1.017$
$Ja = 60$	$\Delta T = 20$	$\Delta t = .58$	$CS = 1718$
$F = 8$	$Z = 40$	$T_p = 165$	

EXPERIMENTAL RESULTS :

$t_g = -$	$t_c = 3.6$	$t_t = -$	$f_s = -$
$R_o = 2.06$	$U = 547$	$h_c = 25525$	
$R_m = 2.06$	$Pe_o = 13740$	$Nu_c = 84$	
$Z_d = 6.18$	$Z_c = 9.29$	$Fo_c = 3.47E-05$	

TEST NO : (9.2).1 FILM NO : 58-2/1

FR	TIME	VOLUME	AREA	RADIUS
1	1.02	181.77	174.43	3.51
2	2.04	158.01	154.79	3.35
3	3.06	147.23	141.6	3.28
4	4.08	127.04	126.47	3.12
5	5.1	109.28	113.53	2.97
6	6.12	92.92	102.89	2.81
7	7.14	79.86	93.04	2.67
8	8.16	57.06	75.3	2.39
9	9.18	32.57	56.33	1.98
10	10.2	20.9	41.55	1.71
11	11.22	10.09	26.65	1.34
12	12.24	7.1	22.04	1.19
13	13.26	1.01	5.7	.62

FR	CY	CX	LE	LP
1	10.95	-.12	15.73	5.86
2	11.56	-.16	15.95	6.98
3	12.19	-.16	16.33	8.14
4	12.7	-.08	16.39	9.06
5	13.1	-.14	16.24	9.94
6	13.67	-.08	16.48	10.86
7	13.73	-.08	16	11.34
8	13.98	-.01	16.37	12.25
9	14.35	-.06	16.83	12.92
10	15.81	-.33	17.78	14.02
11	17.52	-.73	18.37	16.74
12	18.13	-1.02	18.76	17.53
13	18.26	-.86	18.67	17.84

EXPERIMENTAL PARAMETERS :

$d = 1$	$\dot{m}_s = 1.42$	$V_s = 39576$	$P = 1.003$
$Ja = 30$	$\Delta T = 10$	$\Delta t = 1.02$	$CS = 980$
$F = 13$	$Z = 40$	$T_p = 165$	

EXPERIMENTAL RESULTS :

$t_g = -$	$t_c = 12$	$t_t = -$	$f_s = -$
$R_o = 3.51$	$U = 627$	$h_c = 29663$	
$R_m = 3.51$	$Pe_o = 26520$	$Nu_c = 167$	
$Z_d = 10.95$	$Z_c = 18.26$	$Fo_c = 4.04E-05$	

TEST NO : (9.3).2 FILM NO : 59-1/2

FR	TIME	VOLUME	AREA	RADIUS
1	.79	9.8	24.24	1.33
2	1.57	19.66	38.22	1.67
3	2.36	33.22	54.64	1.99
4	3.14	45.5	69.67	2.21
5	3.93	53.48	79.49	2.34
6	4.72	63.89	90.67	2.48
7	5.5	67.84	96.29	2.53
8	6.29	76.6	102.98	2.63
9	7.07	80.28	105.37	2.68
10	7.86	86.37	109.9	2.74
11	8.65	93.12	114.29	2.81
12	9.43	96.87	117.09	2.85
13	10.22	100.12	119.17	2.88
14	11	106.51	123.46	2.94
15	11.79	106.04	123.86	2.94
16	12.58	109.93	127.79	2.97
17	13.36	109.53	129.22	2.97
18	14.15	113.44	134.07	3
19	14.93	115.6	135.49	3.02
20	15.72	92.42	112.13	2.8
21	16.51	75.93	96.27	2.63
22	17.29	61.64	79.54	2.45
23	18.08	48.86	66.81	2 27
24	18.86	39.98	57.88	2.12
25	19.65	29.51	48.7	1.92
26	20.44	18.08	37.47	1.63
27	21.22	4.4	15.94	1.02
28	22.01	.67	4.21	.54

FR	CY	CX	LE	LP
1	1.09	-.15	2.46	0
2	1.17	-.18	2.96	0
3	1.34	-.14	3.65	0
4	1.62	-.17	4.59	0
5	1.8	-.2	5.39	0
6	2.04	-.16	5.96	0
7	2.34	-.22	6.48	0
8	2.5	-.2	6.81	0
9	2.74	-.25	7.12	0
10	3	-.21	7.48	0

CONT.-

FR	CY	CX	LE	LP
11	3.23	-.25	7.93	0
12	3.6	-.25	8.62	0
13	4.02	-.21	9.01	0
14	4.47	-.2	9.54	0
15	4.91	-.17	9.99	0
16	5.28	-.21	10.39	0
17	5.66	-.25	10.73	0
18	5.96	-.25	10.95	0
19	6.32	-.22	11.24	0
20	7.2	-.22	11.4	2.63
21	8	-.09	11.5	3.49
22	8.78	-.03	11.69	5.61
23	9.19	-.04	11.8	6.66
24	9.49	-.01	11.82	7.62
25	9.91	-.04	11.7	8.1
26	10.4	-.14	12.12	8.68
27	10.95	-.66	12.4	9.77
28	11.91	-1.19	12.68	11.46

EXPERIMENTAL PARAMETERS :

$d = 1$	$\dot{m}_s = 1.42$	$V_s = 39576$	$P = 1.003$
$Ja = 45$	$\Delta T = 15$	$\Delta t = .79$	$CS = 1272$
$F = 28$	$Z = 40$	$T_p = 165$	

EXPERIMENTAL RESULTS :

$t_g = 15.72$	$t_c = 6.6$	$t_t = 22.32$	$f_s = 67$
$R_o = 2.8$	$U = 600$	$h_c = 29261$	
$R_m = 3.02$	$Pe_o = 20360$	$Nu_c = 132$	
$Z_d = 7.2$	$Z_c = 11.91$	$Fo_c = 3.47E-05$	

TEST NO : (9.4).3 FILM NO : 60-1/4

FR	TIME	VOLUME	AREA	RADIUS
1	.58	38.23	58.89	2.09
2	1.15	27.55	46.15	1.87
3	1.73	22.66	39.37	1.76
4	2.3	16.24	31.74	1.57
5	2.88	10.95	25.08	1.38
6	3.45	4.05	13.92	.99
7	4.03	.43	3.02	.47

FR	CY	CX	LE	LP
1	6.72	.02	9.51	3.31
2	7.22	-.01	9.46	4.88
3	7.56	-.06	9.52	5.81
4	7.85	-.11	9.42	6.44
5	8.21	-.08	9.42	7.13
6	8.54	.01	9.62	7.53
7	9.03	-.35	9.62	8.5

EXPERIMENTAL PARAMETERS :

$d = 1$	$\dot{m}_s = 1.42$	$V_s = 39576$	$P = 1.003$
$Ja = 60$	$\Delta T = 20$	$\Delta t = .58$	$CS = 1738$
$F = 7$	$Z = 40$	$T_p = 165$	

EXPERIMENTAL RESULTS :

$t_g = -$	$t_c = 3.5$	$t_t = -$	$f_s = -$
$R_o = 2.09$	$U = 587$	$h_c = 29328$	
$R_m = 2.09$	$Pe_o = 14960$	$Nu_c = 99$	
$Z_d = 6.72$	$Z_c = 9.03$	$Fo_c = 3.29E-05$	

TEST NO : (9.5).3 FILM NO : 61-1/6

FR	TIME	VOLUME	AREA	RADIUS
1	.46	18.75	35.78	1.65
2	.92	13.8	29.07	1.49
3	1.38	8.06	20.38	1.24
4	1.84	4.2	13.7	1
5	2.3	1.24	7.2	.67

FR	CY	CX	LE	LP
1	5.62	.03	7.79	3.28
2	5.94	.03	7.85	4.44
3	6.35	0	7.83	5.24
4	6.82	.01	7.8	6.18
5	6.96	0	7.62	6.61

EXPERIMENTAL PARAMETERS :

$d = 1$	$\dot{m}_s = 1.42$	$V_s = 39576$	$P = 1.003$
$Ja = 75$	$\Delta T = 25$	$\Delta t = .46$	$CS = 2177$
$F = 5$	$Z = 40$	$T_p = 165$	

EXPERIMENTAL RESULTS :

$t_g = -$	$t_c = 2.1$	$t_t = -$	$f_s = -$
$R_o = 1.69$	$U = 640$	$h_c = 29127$	
$R_m = 1.65$	$Pe_o = 13270$	$Nu_c = 82$	
$Z_d = 5.62$	$Z_c = 6.96$	$Fo_c = 3E-05$	

TEST NØ : (10.1).2 FILM NØ : 65-1/7

FR	TIME	VØLUME	AREA	RADIUS
1	1.99	76.09	91.94	2.63
2	3.98	68.65	85.23	2.54
3	5.97	51.63	69.97	2.31
4	7.96	43.51	63.58	2.18
5	9.95	39.66	59.86	2.12
6	11.93	36.78	57.23	2.06
7	13.92	33.21	55.31	1.99
8	15.91	28.87	54.38	1.9
9	17.9	12	37.4	1.42
10	19.89	10.37	34.11	1.35
11	21.88	4.78	15.11	1.04
12	23.87	4.7	14.81	1.04
13	25.86	2.16	8.51	.8
14	27.85	1.53	6.89	.71
15	29.84	.77	4.64	.57
16	31.82	.34	2.68	.43
17	33.81	.2	1.94	.36

FR	CY	CX	LE	LP
1	4.82	.13	8.87	.96
2	5.54	.15	9.05	2.56
3	6.27	.09	9.12	3.84
4	7.07	.09	9.3	5.33
5	7.6	.12	9.72	6.06
6	7.99	.14	9.97	6.6
7	8.3	.14	9.99	7.15
8	8.58	.16	9.99	7.65
9	9.15	.16	10.23	8.03
10	9.48	-.02	10.61	8.94
11	9.97	-.15	10.9	9.09
12	10.37	-.08	11.08	9.36
13	10.94	-.02	11.7	10.21
14	11.44	-.06	12.08	10.74
15	11.83	-.16	12.35	11.35
16	12.43	-.11	12.77	12.1
17	12.96	-.08	13.2	12.73

CONT.-

EXPERIMENTAL PARAMETERS :

$d = 1$	$\dot{m}_s = .45$	$V_s = 6643$	$P = 2.011$
$Ja = 15$	$\Delta T = 9.3$	$\Delta t = 1.99$	$CS = 503$
$F = 17$	$Z = 40$	$T_p = 165$	

EXPERIMENTAL RESULTS :

$t_g = -$	$t_c = 29.3$	$t_t = -$	$f_s = -$
$R_o = 2.63$	$U = 258$	$h_c = 16913$	
$R_m = 2.63$	$Pe_o = 7980$	$Nu_c = 68$	
$Z_d = 4.82$	$Z_c = 12.96$	$Fo_c = 1.8E-04$	

TEST NO : (10.2).1 FILM NO : 65-2/1

FR	TIME	VOLUME	AREA	RADIUS
1	.82	1.5	7.72	.71
2	1.64	3.13	11.24	.91
3	2.46	5.4	15.91	1.09
4	3.28	7.68	20.18	1.22
5	4.1	10.04	23.93	1.34
6	4.92	13.27	28.8	1.47
7	5.74	15.61	31.96	1.55
8	6.56	17.6	34.62	1.61
9	7.38	20.44	37.65	1.7
10	8.2	21.77	39.03	1.73
11	9.02	22.49	39.59	1.75
12	9.84	23.87	41.03	1.79
13	10.66	25.65	42.97	1.83
14	11.48	26.17	43.52	1.84
15	12.3	26.48	43.98	1.85
16	13.12	27.82	45.47	1.88
17	13.94	28.52	46.39	1.9
18	14.76	28.72	46.47	1.9
19	15.58	30.61	48.65	1.94
20	16.4	30.09	48.23	1.93
21	17.22	30.7	49.29	1.94
22	18.04	30.05	48.3	1.93
23	18.86	27.29	44.87	1.87
24	19.68	25.14	42.53	1.82
25	20.5	20.65	37.31	1.7
26	21.32	17.27	33.66	1.6
27	22.14	15.61	31.52	1.55
28	22.96	14.48	30.39	1.51
29	23.78	11.41	27.98	1.4
30	24.6	8.51	24.86	1.27
31	25.42	6.19	20.98	1.14
32	26.24	3.39	14.56	.93
33	27.06	.25	2.84	.39
34	27.88	.06	.88	.24

FR	CY	CX	LE	LP
1	.41	.07	.96	0
2	.62	.11	1.35	0
3	.76	.08	1.81	0
4	.87	.05	2.22	0

CONT.-

FR	CY	CX	LE	LP
5	1	.07	2.68	0
6	1.21	.07	3.22	0
7	1.31	.06	3.4	0
8	1.4	.02	3.69	0
9	1.5	.08	3.8	0
10	1.59	.12	3.88	0
11	1.65	.06	3.8	0
12	1.78	.05	3.91	0
13	1.94	.07	4.07	0
14	1.93	.07	4.1	0
15	2.02	.07	4.21	0
16	2.1	.06	4.37	0
17	2.19	.07	4.57	0
18	2.3	.09	4.67	0
19	2.41	.07	4.81	0
20	2.48	.02	4.92	0
21	2.77	.05	5.26	0
22	3.06	.02	5.54	.56
23	3.26	.03	5.55	1
24	3.5	.05	5.62	1.6
25	3.86	.04	5.65	2.33
26	3.99	.02	5.55	2.8
27	4.2	0	5.53	3.14
28	4.49	.03	5.69	3.49
29	4.62	.02	5.44	3.88
30	4.69	.01	5.3	4.12
31	4.83	-.01	5.3	4.37
32	4.99	.04	5.32	4.58
33	5.55	-.11	6.08	5.11
34	5.98	-.64	6.29	5.67

EXPERIMENTAL PARAMETERS :

$d = 1$ $\dot{m}_s = .45$ $V_s = 6643$ $P = 2.011$

$Ja = 30$ $\Delta T = 18.5$ $\Delta t = .82$ $CS = 1220$

$F = 34$ $Z = 40$ $T_p = 165$

EXPERIMENTAL RESULTS :

$t_g = 18.04$ $t_c = 9.3$ $t_t = 27.34$ $f_s = 58$

$R_o = 1.93$ $U = 285$ $h_c = 18618$

$R_m = 1.94$ $Pe_o = 6510$ $Nu_c = 58$

$Z_d = 3.06$ $Z_c = 5.98$ $Fo_c = 1.055E-04$

TEST NO : (11.1).1 FILM NO : 62-2/2

FR	TIME	VOLUME	AREA	RADIUS
1	1.74	40.96	72.59	2.14
2	3.48	48.76	80.25	2.27
3	5.22	53.88	84.99	2.34
4	6.96	54.22	87.62	2.35
5	8.7	56.44	94.42	2.38
6	10.44	53.34	87.85	2.34
7	12.18	48.57	83.58	2.26
8	13.92	39.04	69.09	2.1
9	15.66	31.78	56.08	1.97
10	17.4	26.41	46.49	1.85
11	19.14	19.36	37.14	1.67
12	20.88	10.53	26.66	1.36
13	22.62	3.98	14.03	.98
14	24.36	3.33	12.52	.93
15	26.1	.95	5.53	.61
16	27.84	.31	2.6	.42

FR	CY	CX	LE	LP
1	1.94	-.17	7.31	0
2	2.23	-.07	7.5	0
3	2.59	-.14	8.26	0
4	3.12	-.05	9.08	0
5	4.28	.01	10.42	0
6	5.69	.08	11.38	1.32
7	7.23	-.01	12.39	2.87
8	8.58	-.1	12.66	4.63
9	9.57	-.04	12.78	6.04
10	10.57	0	13.04	7.92
11	10.99	.02	12.8	9.62
12	11.58	-.08	12.8	10.73
13	13.14	.46	14.19	12.11
14	13.99	.47	14.73	13.35
15	14.57	.63	15.28	13.73
16	13.99	.79	14.54	13.46

CONT.-

EXPERIMENTAL PARAMETERS :

$d = 1$	$\dot{m}_s = .82$	$V_s = 12105$	$P = 2.011$
$Ja = 15$	$\Delta T = 9.3$	$\Delta t = 1.74$	$CS = 575$
$F = 16$	$Z = 40$	$T_p = 165$	

EXPERIMENTAL RESULTS :

$t_g = 10.44$	$t_c = 18$	$t_t = 28.44$	$f_s = 115$
$R_o = 2.33$	$U = 443$	$h_c = 26177$	
$R_m = 2.38$	$Pe_o = 12140$	$Nu_c = 94$	
$Z_d = 5.69$	$Z_c = 13.99$	$Fo_c = 1.409E-04$	

TEST NO : (11.2).3 FILM NO : 63-1/4

FR	TIME	VOLUME	AREA	RADIUS
1	.95	22.49	41.09	1.75
2	1.89	24.9	43.06	1.81
3	2.84	30.43	48.68	1.94
4	3.79	32.4	51.13	1.98
5	4.73	32.38	52.55	1.98
6	5.68	33.8	57.9	2.01
7	6.63	34.8	59.76	2.03
8	7.58	37.07	62.74	2.07
9	8.52	38.61	65.17	2.1
10	9.47	38.36	68.25	2.09
11	10.42	34.02	62.31	2.01
12	11.36	32.72	61.25	1.98
13	12.31	32.57	61.54	1.98
14	13.26	30.79	58.94	1.94
15	14.2	31.32	59.64	1.96
16	15.15	32.1	59.78	1.97
17	16.1	27.71	48.38	1.88
18	17.05	22.71	41.27	1.76
19	17.99	17.4	33.91	1.61
20	18.94	12.45	26.59	1.44
21	19.89	9.92	23.59	1.33
22	20.83	6	16.39	1.13
23	21.78	2.92	10.18	.89
24	22.73	1.35	6.3	.69
25	23.68	.56	3.52	.51
26	24.62	.23	2.13	.38

FR	CY	CX	LE	LP
1	1.65	-.01	4.13	0
2	1.82	-.03	4.23	0
3	1.96	-.03	4.5	0
4	2.25	.01	5.07	0
5	2.41	.03	5.33	0
6	2.51	.02	5.48	0
7	2.7	0	5.62	0
8	2.97	.01	5.8	0
9	3.2	-.03	6.26	0
10	3.31	-.01	6.62	0
11	3.3	-.09	6.9	0
12	3.37	-.05	7.1	0

CONT.-

FR	CY	CX	LE	LP
13	3.62	-.03	7.21	0
14	3.93	-.02	7.47	0
15	4.28	.01	7.73	0
16	4.83	-.01	8.2	0
17	5.71	.03	8.48	2.27
18	6.14	.08	8.58	3.69
19	6.55	.09	8.52	4.47
20	6.99	.23	8.59	5.58
21	7.46	.33	8.96	6.15
22	7.69	.43	8.85	6.75
23	7.69	.67	8.62	6.83
24	7.98	.76	8.72	7.29
25	8.78	0	9.25	8.22
26	9.27	-.49	9.53	8.99

EXPERIMENTAL PARAMETERS :

$d = 1$ $\dot{m}_s = .82$ $V_s = 12105$ $P = 2.011$
$Ja = 30$ $\Delta T = 18.5$ $\Delta t = .95$ $CS = 1056$
$F = 26$ $Z = 40$ $T_p = 165$

EXPERIMENTAL RESULTS :

$t_g = 16.1$ $t_c = 8$ $t_t = 24.1$ $f_s = 66$
$R_o = 1.88$ $U = 413$ $h_c = 23149$
$R_m = 2.1$ $Pe_o = 9190$ $Nu_c = 68$
$Z_d = 5.71$ $Z_c = 9.27$ $Fo_c = 9.56E-05$

TEST NO : (11.3).1 FILM NO : 63-2/1

FR	TIME	VOLUME	AREA	RADIUS
1	.74	1.71	8.9	.74
2	1.48	3.36	12.37	.93
3	2.22	6.5	18.86	1.16
4	2.96	10.7	25.63	1.37
5	3.7	13.98	31.1	1.49
6	4.44	18.3	37.15	1.63
7	5.18	21.43	40.93	1.72
8	5.92	24.34	44.97	1.8
9	6.66	25.28	46.18	1.82
10	7.4	25.54	46.45	1.83
11	8.14	25.07	46.44	1.82
12	8.88	23.89	45.46	1.79
13	9.62	22.22	44.22	1.74
14	10.36	22.78	45.49	1.76
15	11.1	20.18	41.3	1.69
16	11.84	15.77	35.98	1.56
17	12.58	10.72	27.55	1.37
18	13.32	7.84	22.79	1.23
19	14.06	5.32	17.77	1.08
20	14.8	1.82	8.67	.76
21	15.54	.26	2.28	.4

FR	CY	CX	LE	LP
1	.38	-.01	1.08	0
2	.51	.02	1.43	0
3	.7	0	1.8	0
4	.82	-.01	2.2	0
5	.92	-.03	2.56	0
6	1.06	-.02	2.99	0
7	1.23	0	3.47	0
8	1.36	.02	3.93	0
9	1.62	.05	4.57	0
10	1.84	.03	5.18	0
11	2	.01	5.36	0
12	2.33	.04	5.68	0
13	2.59	.01	6.03	0
14	2.95	.01	6.3	0
15	3.25	.01	6.31	.98
16	3.57	.06	6.34	1.51

CONT.-

FR	CY	CX	LE	LP
17	3.92	.1	6.36	2.11
18	4.33	.1	6.72	2.72
19	4.63	.06	6.72	3.3
20	4.76	.06	6.16	3.64
21	5.9	.32	6.27	5.54

EXPERIMENTAL PARAMETERS :

$d = 1$	$\dot{m}_s = .82$	$V_s = 12105$	$P = 2.011$
$Ja = 45$	$\Delta T = 27.6$	$\Delta t = .74$	$CS = 1351$
$F = 21$	$Z = 40$	$T_p = 165$	

EXPERIMENTAL RESULTS :

$t_g = 11.1$	$t_c = 4.6$	$t_t = 15.7$	$f_s = 97$
$R_o = 1.69$	$U = 420$	$h_c = 22474$	
$R_m = 1.83$	$Pe_o = 8500$	$Nu_c = 60$	
$Z_d = 3.25$	$Z_c = 5.9$	$Fo_c = 6.72E-05$	

TEST NO : (12.1).3 FILM NO : 66-2/3

FR	TIME	VOLUME	AREA	RADIUS
1	2.13	1.35	6.93	.69
2	4.26	24.37	46.4	1.8
3	6.39	63.66	93.13	2.48
4	8.52	79.62	111.99	2.07
5	10.65	95.13	136.65	2.83
6	12.78	116.8	144.54	3.03
7	14.91	132.03	156.71	3.16
8	17.04	136.16	157.17	3.19
9	19.17	137.18	159.67	3.2
10	21.3	156.81	177.3	3.35
11	23.43	162.03	183.24	3.38
12	25.56	171.3	186.55	3.45
13	27.69	148.65	153.71	3.29
14	29.82	119.68	131.59	3.06
15	31.95	104.57	115.75	2.92
16	34.08	97.31	112.94	2.85
17	36.21	86.07	98.69	2.74
18	38.34	63.83	81.27	2.48
19	40.47	49.17	72.82	2.27
20	42.6	33.38	57.37	2
21	44.73	26.06	52.01	1.84
22	46.86	15.55	41.97	1.55
23	48.99	5.47	19.16	1.09
24	51.12	4.27	13.92	1.01
25	53.25	2.28	9.02	.82
26	55.38	1.17	6.24	.65
27	57.51	.6	4	.52
28	59.64	.26	2.64	.39

FR	CY	CX	LE	LP
1	.51	-.06	1.22	0
2	1.08	-.03	2.67	0
3	1.6	-.1	5.19	0
4	2.11	-.12	7.05	0
5	2.67	-.26	8.29	0
6	3.35	-.24	9.37	0
7	4.21	-.19	10.73	0
8	5.17	-.2	11.88	0
9	6.2	-.21	12.78	0
10	7.04	-.2	13.81	0

CONT.-

FR	CY	CX	LE	LP
11	7.92	-.19	14.37	0
12	9.1	-.17	15.39	0
13	10.39	-.18	16.04	5.49
14	11.83	-.17	16.51	6.91
15	13.02	-.15	16.98	9.23
16	13.81	-.22	17.51	10.85
17	14.75	-.33	17.93	11.26
18	15.98	-.53	18.61	13.94
19	16.71	-.72	19.07	14.58
20	17.57	-.75	19.52	15.39
21	18.54	-.67	20.33	16.24
22	19.58	-.45	21.33	16.93
23	20.67	.08	21.84	20
24	21.83	.47	22.64	21.09
25	22.29	.95	23.01	21.56
26	22.94	1.58	23.73	22.29
27	23.55	2.14	23.92	23.14
28	24.4	2.38	24.55	24.24

EXPERIMENTAL PARAMETERS :

$d = 1$ $\dot{m}_s = 1.39$ $V_s = 20520$ $P = 2.011$
$Ja = 15$ $\Delta T = 9.3$ $\Delta t = 2.13$ $CS = 470$
$F = 28$ $Z = 40$ $T_p = 165$

EXPERIMENTAL RESULTS :

$t_g = 27.69$ $t_c = 28$ $t_t = 55.69$ $f_s = 39$
$R_o = 3.29$ $U = 471$ $h_c = 20883$
$R_m = 3.45$ $Pe_o = 18230$ $Nu_c = 107$
$Z_d = 10.39$ $Z_c = 24.4$ $Fo_c = 1.099E-04$

TEST NO : (12.2).2 FILM NO : 67-1/2

FR	TIME	VOLUME	AREA	RADIUS
1	1.17	2.64	11.3	.86
2	2.33	10.16	26.63	1.34
3	3.5	25.1	47.62	1.82
4	4.67	38.74	63.09	2.1
5	5.84	49.92	74.58	2.28
6	7	56.97	80.09	2.39
7	8.17	62.51	84.19	2.46
8	9.34	65.27	87.41	2.5
9	10.5	67.21	91.16	2.52
10	11.67	68.33	97.75	2.54
11	12.84	69.36	100.53	2.55
12	14	69.76	101.68	2.55
13	15.17	60.38	90.31	2.43
14	16.34	42.87	64.19	2.17
15	17.5	34.84	53.05	2.03
16	18.67	29.41	47.24	1.91
17	19.84	23.09	40.9	1.77
18	21.01	18.58	36.94	1.64
19	22.17	10.74	28.28	1.37
20	23.34	1.61	9.42	.73
21	24.51	.18	2.18	.35
22	25.67	.04	.7	.22

FR	CY	CX	LE	LP
1	.36	.01	.92	0
2	.65	.03	1.63	0
3	1.09	.03	2.92	0
4	1.46	.04	4.14	0
5	1.79	.07	5.1	0
6	2.17	-.03	5.71	0
7	2.57	.01	6.55	0
8	3.1	-.02	7.36	0
9	3.54	-.02	7.95	0
10	3.99	-.03	8.7	0
11	4.57	-.02	9.23	0
12	5.15	-.04	9.62	0
13	6.08	.08	10.21	2.31
14	7.54	.13	10.31	4.55
15	8.25	.18	10.58	6.12

CONT.-

FR	CY	CX	LE	LP
16	8.68	.16	10.77	6.89
17	9.11	.19	10.77	7.76
18	9.4	.24	10.65	8.4
19	9.69	.25	10.63	9.05
20	9.95	.47	10.37	9.56
21	10.15	.8	10.34	9.78
22	10.36	1.55	10.56	10.17

EXPERIMENTAL PARAMETERS :

$d = 1$	$\dot{m}_s = 1.39$	$V_s = 20520$	$P = 2.011$
$Ja = 30$	$\Delta T = 18.5$	$\Delta t = 1.17$	$CS = 857$
$F = 22$	$Z = 40$	$T_p = 165$	

EXPERIMENTAL RESULTS :

$t_g = 15.17$	$t_c = 9.5$	$t_t = 24.67$	$f_s = 71$
$R_o = 2.41$	$U = 447$	$h_c = 22186$	
$R_m = 2.55$	$Pe_o = 12750$	$Nu_c = 85$	
$Z_d = 6.08$	$Z_c = 10.36$	$Fo_c = 6.91E-05$	

TEST NO : (12.3).3 FILM NO : 67-2/5

FR	TIME	VOLUME	AREA	RADIUS
1	.77	17.87	36.42	1.62
2	1.54	22.87	43.31	1.76
3	2.32	28.45	50.02	1.89
4	3.09	32.42	55.5	1.98
5	3.86	35.12	59	2.03
6	4.63	37.05	60.98	2.07
7	5.4	40.24	64	2.13
8	6.18	40.9	64.67	2.14
9	6.95	42.25	66.11	2.16
10	7.72	40.85	64.87	2.14
11	8.49	35.8	57.73	2.04
12	9.26	29.45	50.07	1.92
13	10.04	21.72	40.51	1.73
14	10.81	16.99	34.01	1.59
15	11.58	10.7	24.7	1.37
16	12.35	4.84	17.74	1.05
17	13.12	.41	2.82	.46

FR	CY	CX	LE	LP
1	1.4	-.16	3.87	0
2	1.55	-.2	4.23	0
3	1.68	-.24	4.61	0
4	1.9	-.23	5.09	0
5	2.13	-.22	5.45	0
6	2.42	-.25	5.78	0
7	2.64	-.24	6.22	0
8	2.95	-.24	6.57	0
9	3.37	-.2	6.98	0
10	3.89	-.19	7.45	0
11	4.32	-.16	7.54	1.11
12	4.74	-.2	7.64	1.68
13	5.22	-.13	7.7	2.75
14	5.55	-.12	7.65	3.35
15	5.95	-.17	7.54	4.55
16	6.26	-.23	7.45	5.58
17	7.41	-.3	7.82	6.93

CONT.-

EXPERIMENTAL PARAMETERS :

$d = 1$	$\dot{m}_s = 1.39$	$V_s = 20520$	$P = 2.011$
$Ja = 45$	$\Delta T = 27.6$	$\Delta t = .77$	$CS = 1295$
$F = 17$	$Z = 40$	$T_p = 165$	

EXPERIMENTAL RESULTS :

$t_g = 8.49$	$t_c = 4.8$	$t_t = 13.29$	$f_s = 130$
$R_o = 2.04$	$U = 463$	$h_c = 27144$	
$R_m = 2.16$	$Pe_o = 11310$	$Nu_c = 89$	
$Z_d = 4.32$	$Z_c = 7.41$	$Fo_c = 4.82E-05$	

TEST NO : (12.4).3 FILM NO : 68-1/3

FR	TIME	VOLUME	AREA	RADIUS
1	.56	5.94	17.72	1.12
2	1.11	8.05	21.21	1.24
3	1.67	11.07	26.1	1.38
4	2.22	13.6	30.02	1.48
5	2.78	17.86	37.38	1.62
6	3.34	20.44	41.03	1.7
7	3.89	22.73	44.97	1.76
8	4.45	25.16	48.3	1.82
9	5	27.44	51.37	1.87
10	5.56	28.37	52.51	1.89
11	6.12	29.22	53.39	1.91
12	6.67	23.8	44.56	1.78
13	7.23	14.99	32.16	1.53
14	7.78	7.13	21.11	1.19
15	8.34	2.87	10.05	.88
16	8.9	1.16	5.77	.65
17	9.45	.45	3.27	.47
18	10.01	.21	2.06	.37

FR	CY	CX	LE	LP
1	1.09	-.11	2.87	0
2	1.28	-.17	2.95	0
3	1.42	-.19	3.41	0
4	1.56	-.16	3.95	0
5	1.74	-.12	4.47	0
6	2.01	-.09	4.89	0
7	2.35	-.04	5.2	0
8	2.62	.03	5.65	0
9	2.95	.13	6	0
10	3.25	.15	6.29	0
11	3.65	.15	6.8	0
12	4.16	.28	6.86	1.13
13	4.63	.27	6.88	2.28
14	5.12	.38	6.73	3.45
15	5.65	.57	6.68	4.55
16	5.92	.7	6.48	5.38
17	6.14	.7	6.49	5.81
18	6.14	.73	6.35	5.94

CONT.-

EXPERIMENTAL PARAMETERS :

$d = 1$	$\dot{m}_s = 1.39$	$V_s = 20520$	$P = 2.011$
$Ja = 60$	$\Delta T = 36.6$	$\Delta t = .56$	$CS = 1800$
$F = 18$	$Z = 40$	$T_p = 165$	

EXPERIMENTAL RESULTS :

$t_g = 6.68$	$t_c = 3$	$t_t = 9.68$	$f_s = 164$
$R_o = 1.78$	$U = 380$	$h_c = 25544$	
$R_m = 1.91$	$Pe_o = 8200$	$Nu_c = 72$	
$Z_d = 4.16$	$Z_c = 6.14$	$Fo_c = 3.91E-05$	

APPENDIX 5.

Bubble Shape Factor

The bubble shape factor, as defined in section 5.4 is

$$\psi = \frac{\text{Measured bubble surface area}}{4.\pi.R^2} \qquad (A\ 1.1)$$

where R is the radius of a sphere of volume equal to the measured bubble volume. This means that ψ will have a value greater than or equal to unity, the higher the value is, giving an indication of the level of bubble distortion.

Some examples of bubble shape factor are given as a function of radius ratio (β) in Figs. A 5.1 and A 5.2.

The values of ψ (β) generally oscillated with a value always greater than unity, as shown, for test 11.2, in Fig. A 5.1. In a few cases, a near spherical bubble detached from the orifice and while condensing, became hemispherical then spherical-cap shaped, and finally collapsed as spherical. In such cases as illustrated, for test 4.2, in Fig. A 5.1, the shape factor increased until condensation was about 87% complete and then decreased towards unity in the later stages of collapse. In two or three cases, the shape factor continued to increase throughout collapse, indicating that, in these cases, bubble distortion continued throughout the entire collapse process. An example of this type of collapse occurs in test 6.3 as shown in Fig. A 5.2. In a few cases, the bubble, which was distorted at detachment, became near spherical, before again becoming slightly distorted as collapse continued. An example of this type of collapse occurs in test 11.1 as shown in Fig. A 5.2.

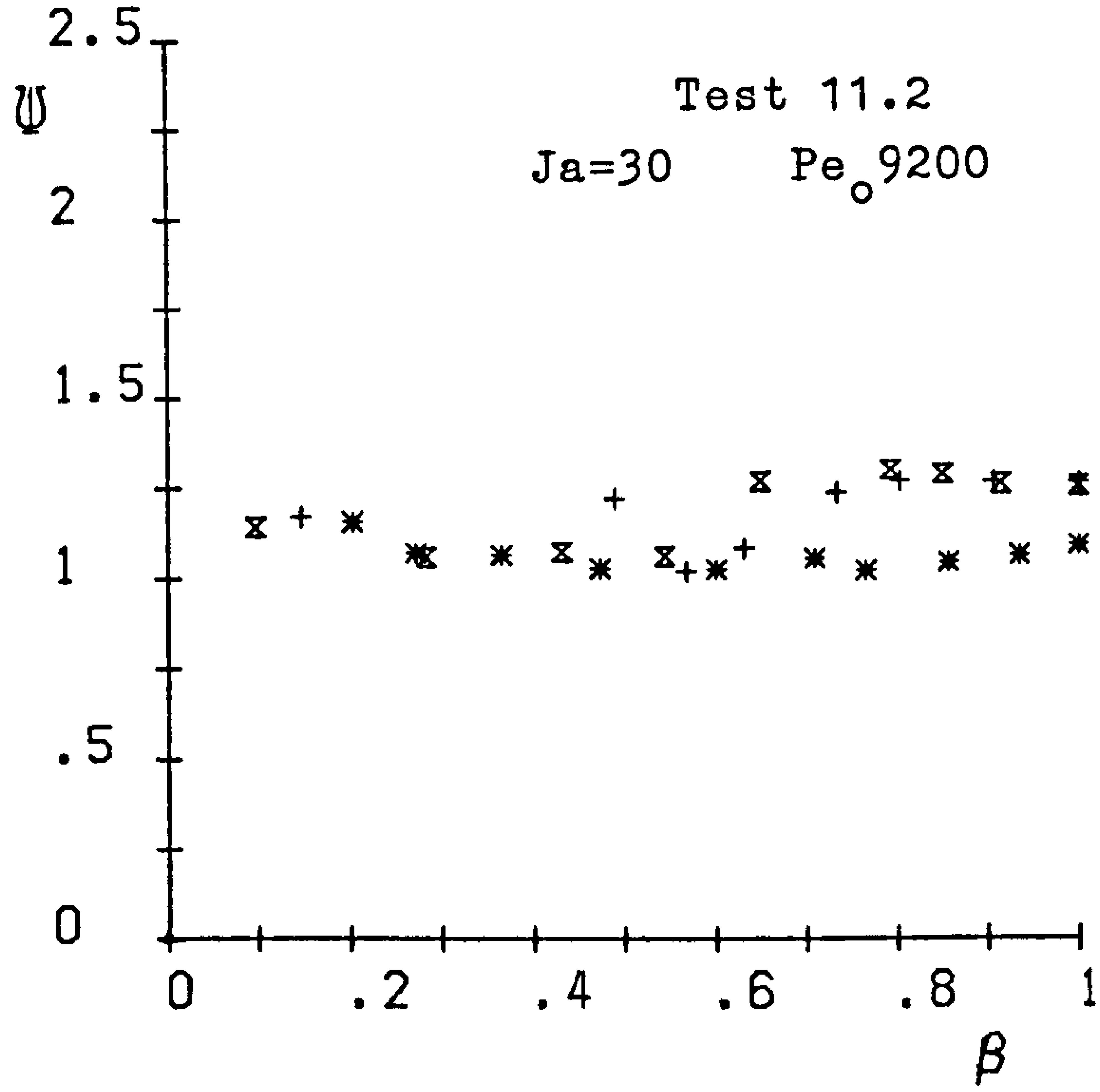

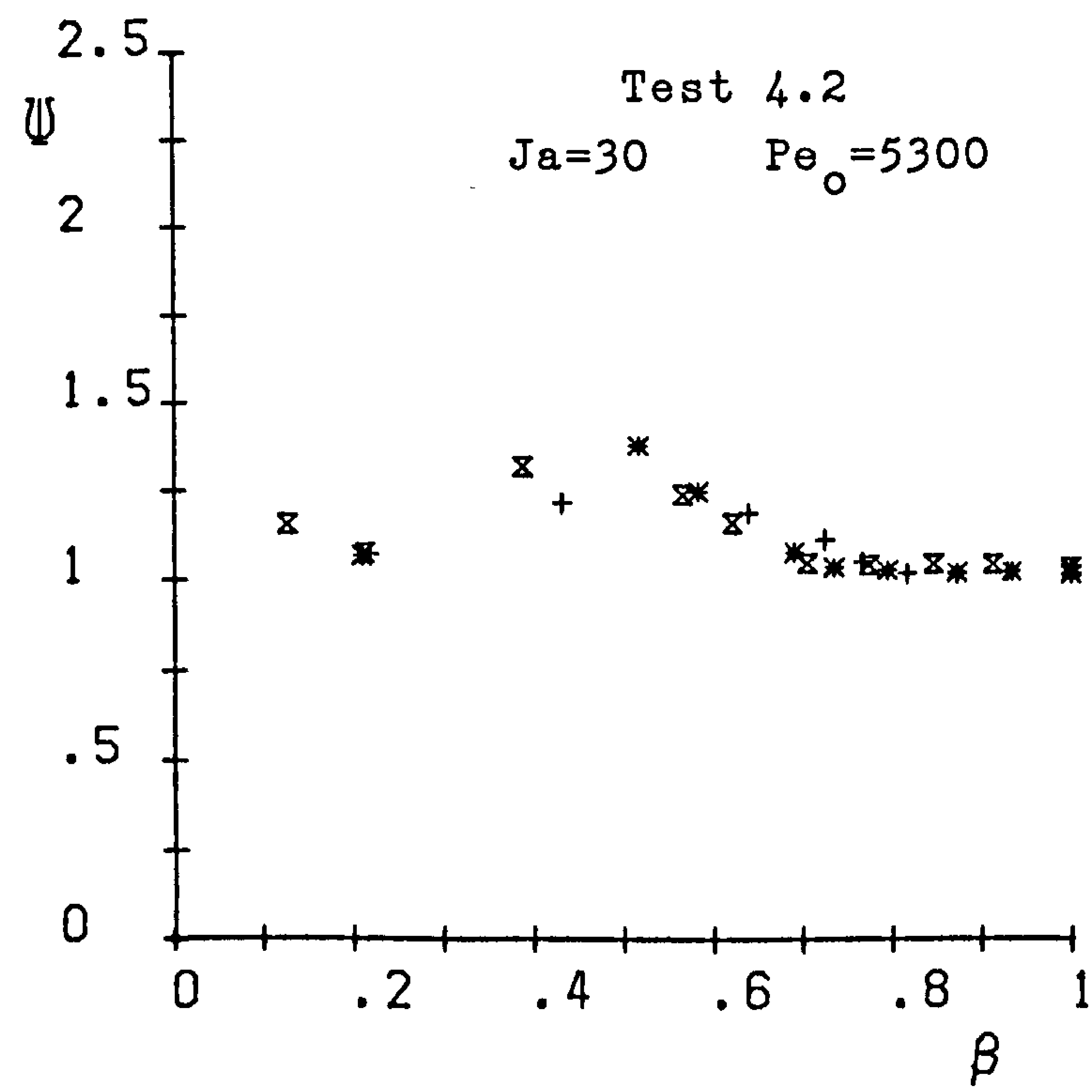

Fig.A5.1 Bubble shape factor as function of radius ratio

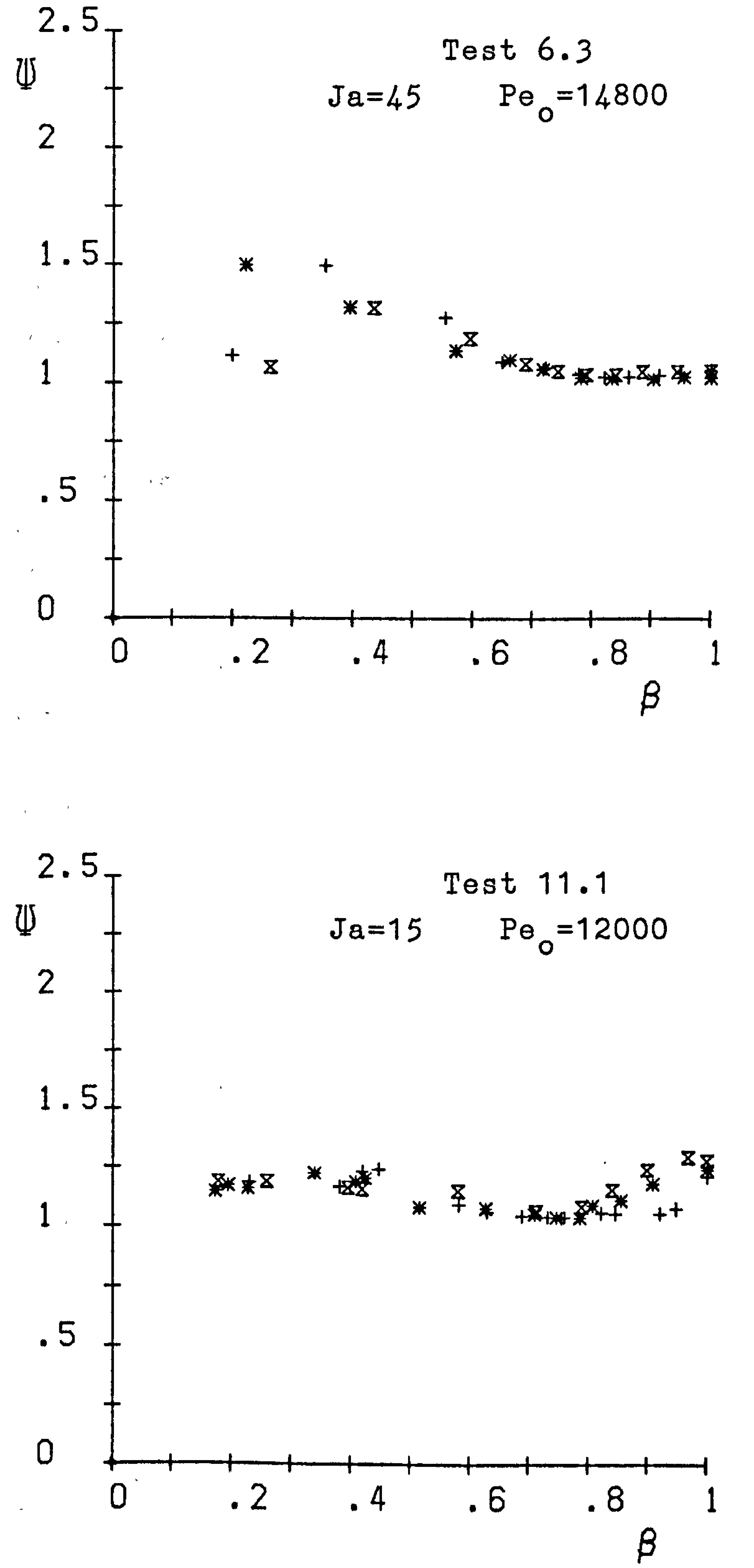

Fig A5.2 Bubble shape factor as function of radius ratio

A simple average of ψ values calculated for all the data points (N) in any test is given by

$$\psi_m = \frac{\sum_{1}^{N} \psi}{N} \qquad \text{(A 5.2)}$$

The values obtained for each experimental condition are listed in table A 5.1. A mean average value for all the data was calculated to be 1.134.

In section 5.4 the effect of bubble distortion has been analysed and equation (5.55) was derived using the simplified bubble collapse equation.

Using a simulation program, TUTSIM, the values of ψ corresponding to four different functions have been plotted in Figs. A 5.3 and A 5.4 for test conditions corresponding to those shown in Figs. A 5.1 and A 5.2. In each case the program also gives a plot of equation (5.55) for the corresponding ψ function. In addition, curves for equation (5.48) corresponding to $\psi = 1$ are also plotted.

In all cases the bubbles collapse faster when ψ has values greater than unity.

Information about TUTSIM is given in Appendix 3. The block diagram and the listing of the model for the bubble shape factor function being $\psi = 1 + a\,(1-\beta)^b$, are given in Fig. A 5.5 in the attached portfolio and in table A 5.2, respectively. For $\psi = a + b\cos(2\pi\beta)$, the block diagram and the listing are presented in Fig. A 5.6 in the attached portfolio and in table A 5.3.

Test No.	ψ_m	Test No.	ψ_m
1.1	1.312	7.1	1.127
1.2	1.165	7.2	1.121
2.1	1.187	7.3	1.139
2.2	1.142	8.1	1.136
2.3	1.070	8.2	1.135
3.1	1.146	8.3	1.110
3.2	1.137	8.4	1.080
3.3	1.120	9.2	1.103
3.4	1.135	9.3	1.097
		9.4	1.065
		9.5	1.080
4.1	1.133	10.1	1.138
4.2	1.100	10.2	1.118
5.1	1.143	11.1	1.139
5.2	1.190	11.2	1.150
5.3	1.120	11.3	1.177
6.1	1.162	12.1	1.143
6.2	1.168	12.2	1.151
6.3	1.111	12.3	1.101
6.4	1.091	12.4	1.144

Table A 5.1 Average values of shape factors for each experimental condition

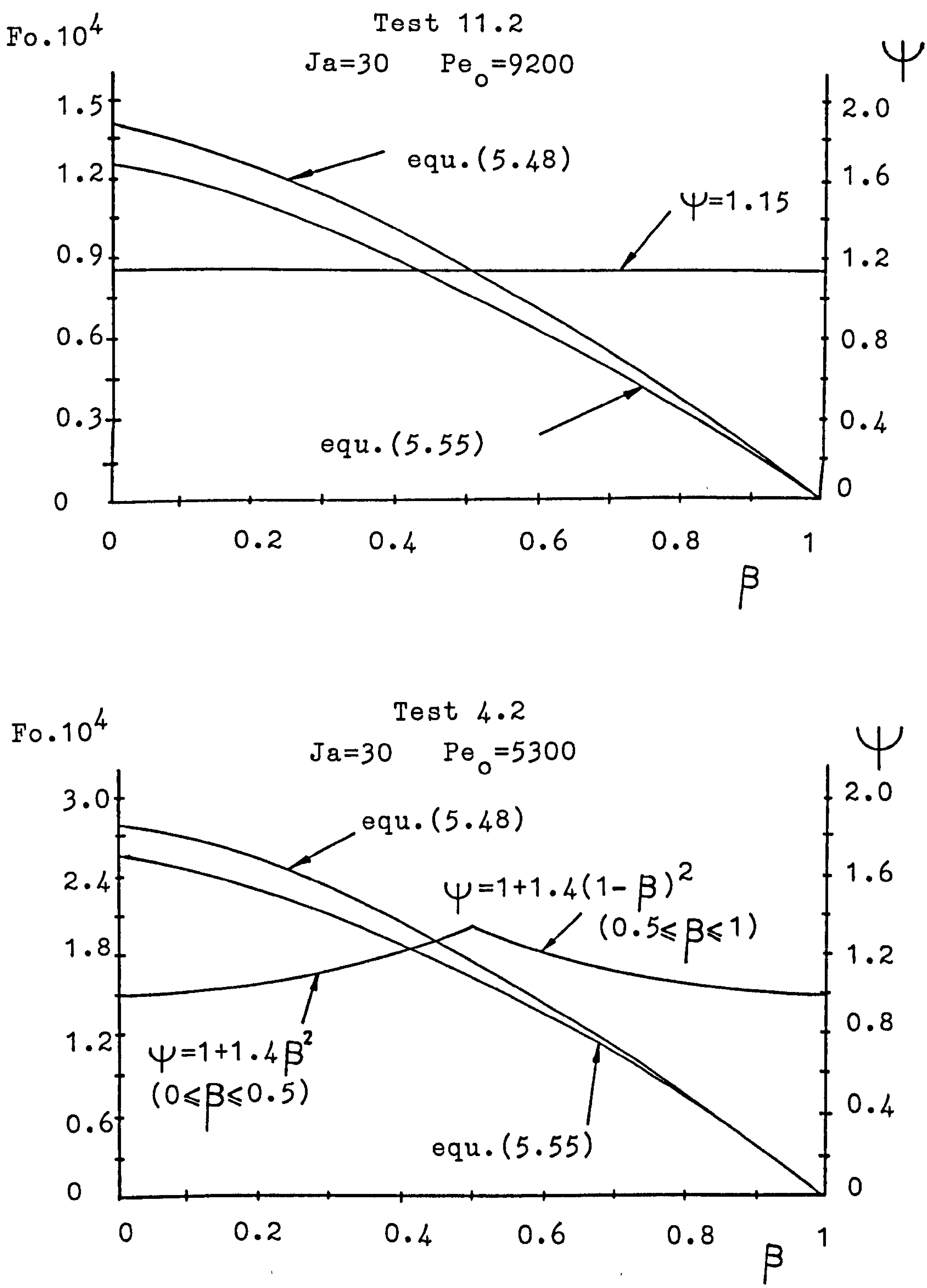

Fig.A5.3 Shape factor and Fourier number versus radius ratio for different values of shape factor function

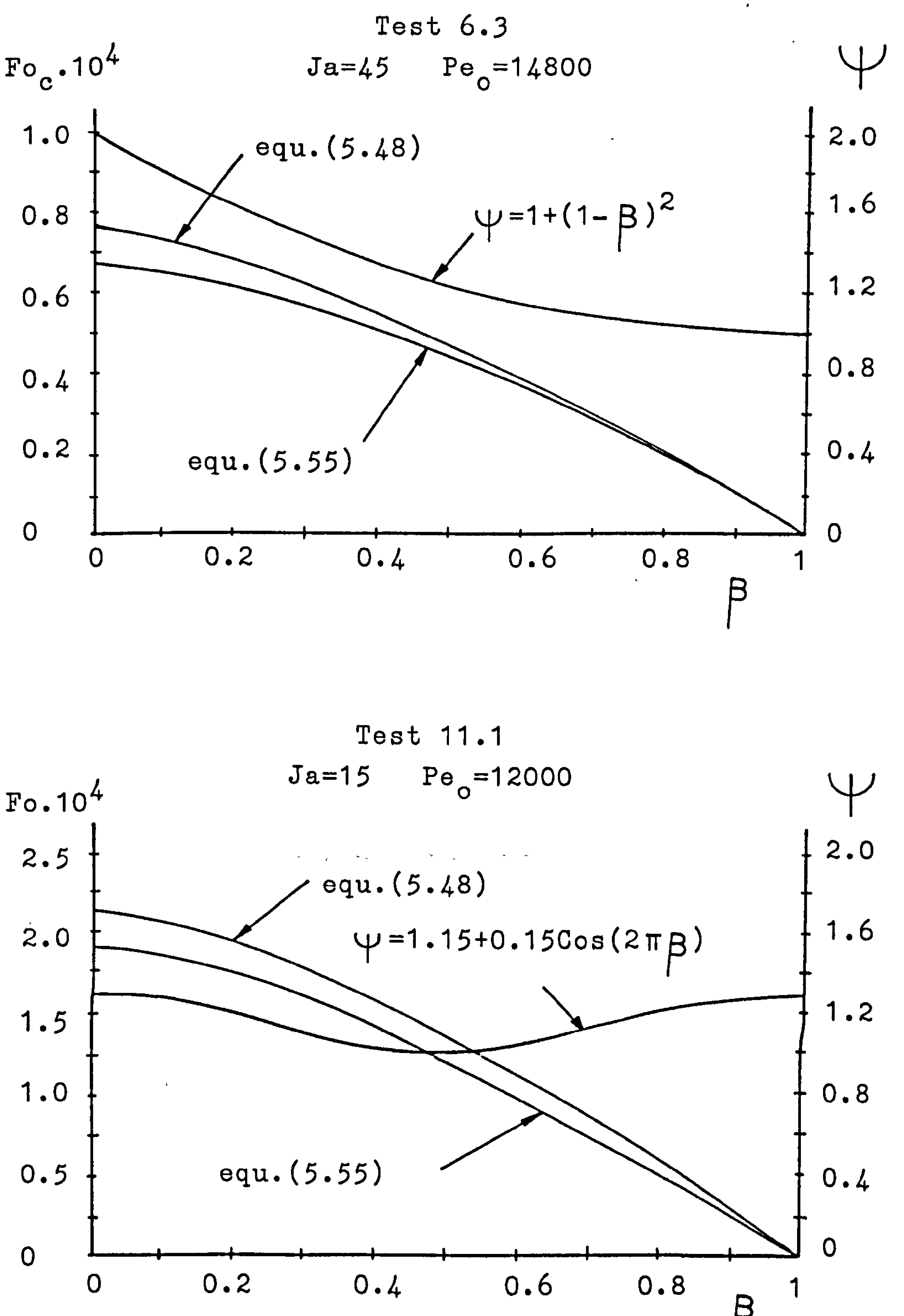

Fig.A5.4 Shape factor and Fourier number versus radius ratio for different values of shape factor function

```
TIMING
 0.10000E-01   0.10000E+01

OUTPUTBLOCKS AND RANGES
X1:    21       0.00000E+00   0.10000E+01
Y1:    27       0.00000E+00   0.25000E-03
Y2:    23       0.00000E+00   0.20000E+01

MODEL
                   1 TIM
 0.00000E+00       2 REL     1     7     1     1
 0.50000E+00       3 REL    21     2     2     1
 0.20000E+01       4 PWR     3
 0.00000E+00       5 REL     4     9     4     1
                   6 MUL     5     8
 0.10000E+01       7 CON
 0.16000E+01       8 CON
 0.00000E+00       9 CON
                  10 SUM     7     6
                  11 DIV    22    23
 0.00000E+00      12 INT    11
                  13 DIV    12    20
 0.10000E+05      14 CON
                  15 SQT    14
 0.15000E+02      16 CON
                  17 TIM
                  18 TIM
 0.21220E+01      19 CON
                  20 MUL    15    16    19
                  21 SUM     7    -1
                  22 SQT    21
 0.10000E+01      23 GAI    10
 0.28800E+00      24 CON
                  25 DIV    24    14
                  26 MUL     1    25
                  27 SUM    13    26
```

Table A5.2 The listing of the model for the bubble collapse equation(5.55) with $\psi = 1 + a(1-\beta)^b$

```
TIMING
 0.10000E-01   0.10000E+01

OUTPUTBLOCKS AND RANGES
X1:    21        0.00000E+00   0.10000E+01
Y1:    27        0.00000E+00   0.25000E-03
Y2:    23        0.00000E+00   0.20000E+01

MODEL
                          1 TIM
                          2 SUM     1
 0.62832E+01              3 CON
                          4 MUL    21      3
                          5 COS     4
 0.25000E+00              6 CON
 0.10000E+01              7 CON
                          8 MUL     5      6
 0.00000E+00              9 CON
                         10 SUM     7      6      8
                         11 DIV    22     23
 0.00000E+00             12 INT    11
                         13 DIV    12     20
 0.10000E+05             14 CON
                         15 SQT    14
 0.15000E+02             16 CON
                         17 TIM
                         18 TIM
 0.21220E+01             19 CON
                         20 MUL    15     16     19
                         21 SUM     7     -1
                         22 SQT    21
 0.10000E+01             23 GAI    10
 0.28800E+00             24 CON
                         25 DIV    24     14
                         26 MUL     1     25
                         27 SUM    13     26
```

Table A5.3 The listing of the model for calculation of the bubble collapse equation(5.55) with $\psi = a + b\cos(2\pi\beta)$

APPENDIX 6

Collapse of spherical-cap bubbles

When a spherical-cap bubble rises, with a constant velocity U, through a subcooled liquid, heat transfer will take place from the top of the bubble and in addition some heat transfer may take place by conduction into the wake.

If we consider that the spherical-cap bubble shown in Fig. A 6.1 has a constant radius, R_o and an angle γ, which decreases as collapse continues, we can, by assuming simplified potential flow over the spherical surface, determine the heat transfer from the top surface of the bubble. If we neglect bubble radial velocity (i.e. $\dot{R} = 0$), the velocities u_r and u_θ can be written from equations (5.4) and (5.5) as

$$u_r \simeq -3U\frac{y}{R_o}\cos\theta \qquad \text{(A 6.1)}$$

$$u_\theta \simeq \frac{3}{2}U.\sin\theta \qquad \text{(A.6.2)}$$

For these conditions, Ruckenstein [8] gave the heat flux through the liquid boundary layer at angle θ as

$$q_\theta = c_p.\rho_l.\Delta T.\frac{\frac{3}{2}.U.R_o\alpha.\sin^2\theta}{\sqrt{\frac{3}{2}.\pi.\alpha U.R_o^3\left(\frac{2}{3}-\cos\theta+\frac{\cos^3\theta}{3}\right)}} \qquad \text{(A 6.3)}$$

Thus, the heat transferred at the upper (front) surface, between $\theta = 0$ and $\theta = \gamma$, is given as

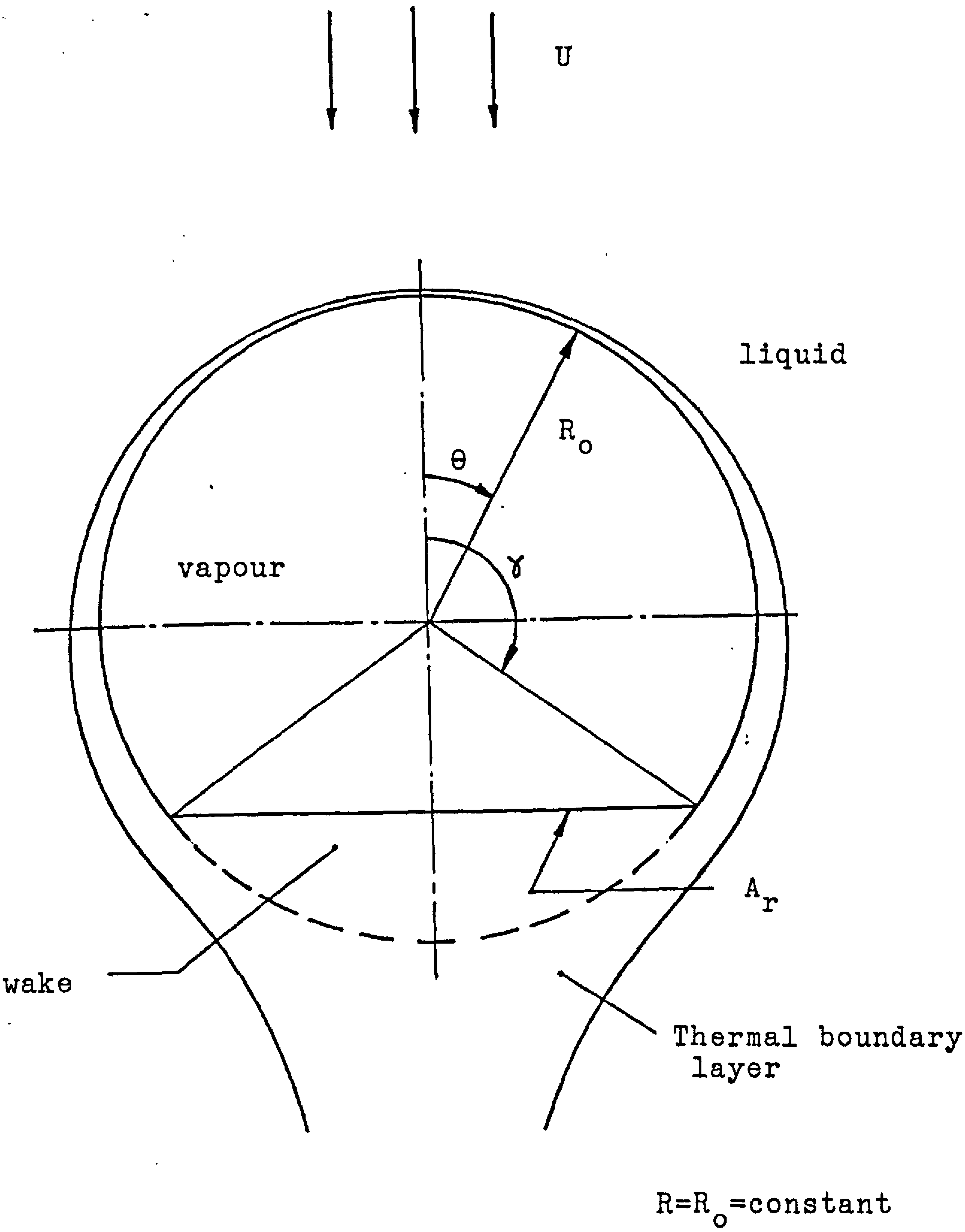

Fig.A6.1 Theoretical model for collapse of spherical-cap bubbles

$$Q_{\gamma f} = \int_0^{\gamma} 2\pi R_o^2 \sin\theta . \, q_{\theta} . d\theta$$

$$= \frac{2\pi R_o^2 c_p \rho_1 . \Delta T . \frac{3}{2} . U R_o \alpha}{\sqrt{\frac{3}{2}} \; \pi . \alpha U R_o^3} . \int_0^{\gamma} \frac{\sin^3\theta}{(\frac{2}{3} - \cos\theta + \frac{1}{3}\cos^3\theta)^{\frac{1}{2}}} \, d\theta$$

$$= 3\sqrt{\frac{2\pi}{3}} . \frac{R_o^3 c_p . \rho_1 . \Delta T . U . \alpha}{\sqrt{\alpha . U . R_o^3}} \int_0^{\gamma} \frac{\sin^3\theta}{(\frac{2}{3} - \cos\theta + \frac{1}{3}\cos^3\theta)^{\frac{1}{2}}} \, d\theta \tag{A 6.4}$$

Let $y = \frac{2}{3} - \cos\theta + \frac{1}{3}\cos^3\theta$

$$\therefore \; dy = [\sin\theta - \cos^2\theta \sin\theta] \, d\theta = \sin^3\theta \, d\theta$$

$$\therefore \int_0^{\gamma} \frac{\sin^3\theta}{(\frac{2}{3} - \cos\theta + \frac{1}{3}\cos^3\theta)^{\frac{1}{2}}} \, d\theta = \int_0^{y_\gamma} \frac{dy}{y^{\frac{1}{2}}} = 2y^{\frac{1}{2}} \Big|_0^{y_\gamma}$$

$$= 2(\frac{2}{3} - \cos\theta + \frac{1}{3}\cos^3\theta)^{\frac{1}{2}} \Big|_0^{\gamma} = 2(\frac{2}{3} - \cos\gamma + \frac{1}{3}\cos^3\gamma)^{\frac{1}{2}} \tag{A 6.5}$$

Therefore,

$$Q_{\gamma f} = 3\sqrt{\frac{2\pi}{3}} . \frac{R_o^3 c_p . \rho_1 . \Delta T . U . \alpha}{\sqrt{\alpha . U . R_o^3}} . 2 . [\frac{2}{3} - \cos\gamma + \frac{1}{3}\cos^3\gamma]^{\frac{1}{2}}$$

$$= 3\sqrt{\frac{2\pi}{3}} . (c_p . \rho_1 . \Delta T) . (U . \alpha \, R_o^3)^{\frac{1}{2}} . 2[\frac{2}{3} - \cos\gamma + \frac{1}{3}\cos^3\gamma]^{\frac{1}{2}}$$

$$= 3\sqrt{\frac{2\pi}{3}} \cdot (c_p \cdot \rho_l \cdot \Delta T) \cdot \left(\frac{2UR_o}{\alpha}\right)^{1/2} \cdot \sqrt{2} \cdot \alpha \cdot R_o \left[\frac{2}{3} - \cos\gamma + \frac{1}{3}\cos^3\gamma\right]^{1/2}$$
(A 6.6)

$$Q_{\gamma f} = 6\sqrt{\frac{\pi}{3}} \cdot (c_p \cdot \rho_l \cdot \Delta T) Pe_o^{1/2} \cdot \alpha R_o \left[\frac{2}{3} - \cos\gamma + \frac{1}{3}\cos^3\gamma\right]^{1/2}$$
(A 6.7)

In addition to this heat transferred at the top surface of the bubble, heat may also be conducted into the water in the wake, and this can be determined by using a method similar to that of Coppus [50], who employed Danckwert's [51] surface renewal model for mass transfer at the wake of a spherical-cap bubble in the form

$$k_m \sim \sqrt{D \cdot s} \qquad \text{(A 6.8)}$$

where D is the diffusion coefficient and s is the surface renewal rate. Lamont and Scott [53], assuming that mass transfer is controlled by small eddies, obtained a value of average mass transfer coefficient as

$$k_m \sim \left(\frac{D}{\nu}\right)^{0.5} \cdot (\varepsilon\nu)^{0.25} \qquad \text{(A 6.9)}$$

where ε is the rate of energy dissipation by turbulence per unit mass.

Coppus [50] estimated ε from the total energy dissipation rate of the bubble, Γ as follows :

$$\Gamma = \text{Drag} \cdot U = (\rho_l \cdot g \cdot V_b) \cdot U \qquad \text{(A 6.10)}$$

He assumed that all the energy is dissipated in the closed wake behind the bubble and determined the total energy dissipation rate per unit mass as

$$\varepsilon_T = \frac{\Gamma}{\rho_l V_w} = \frac{g\ V_b . U}{V_w} = \frac{g\ U}{V_w/V_b} \tag{A 6.11}$$

where V_b is the volume of the bubble and V_w is the volume of the wake.

Coppus suggested that the energy dissipated by turbulence was equal to the total energy dissipation rate times a function of the Reynolds number or

$$\varepsilon = \varepsilon_T . f(Re) = \frac{g\ U}{V_w/V_b} . f(Re) \tag{A 6.12}$$

where for a low value of Reynolds number (laminar wake flow) f(Re) = 0 and for a high value of Reynolds number (turbulent wake flow) f(Re) = 1.

Since we have turbulent flow,

$$\varepsilon = \frac{g\ U}{V_w/V_b} \tag{A 6.13}$$

Substituting this in equation (A 6.9) and inserting a constant of proportionality of 0.30 (Coppus suggested a value between 0.20 and 0.40) gives,

$$k_m = 0.30\left(\frac{D}{\nu}\right)^{0.5} . \left(\frac{gU\nu}{V_w/V_b}\right)^{0.25} = 0.30\left(\frac{D}{\nu}\right)^{0.5} . \left(\frac{V_b}{V_w}\right)^{0.25} (gU\nu)^{0.25}$$

$$\therefore \frac{k_m . R}{D} = 0.30\left(\frac{\nu}{D}\right)^{0.5} . \left(\frac{gR}{U^2} . \frac{U^3 R^3}{\nu^3}\right)^{0.25} . \left(\frac{V_b}{V_w}\right)^{0.25}$$

$$= 0.30\ \left(\frac{\nu}{D}\right)^{0.5} . \left(\frac{gR}{8U^2}\right)^{0.25} . \left(\frac{2UR}{\nu}\right)^{0.75} . \left(\frac{V_b}{V_w}\right)^{0.25}$$

$$= 0.30 \left(\frac{\nu}{D}\right)^{0.5} \cdot \left(\frac{gR}{8U^2}\right)^{0.25} \cdot Re^{0.75} \cdot \left(\frac{V_b}{V_w}\right)^{0.25} \qquad (A\ 6.14)$$

By using an analogous heat transfer relationship which substitutes $\frac{h}{\rho_l c_p}$ for the mass transfer coefficient k_m and the thermal diffusivity α for the diffusion coefficient D, we can write

$$\frac{\frac{h}{\rho_l c_p}.R}{\alpha} = 0.30\left(\frac{\nu}{\alpha}\right)^{0.5} \cdot \left(\frac{gR}{8U^2}\right)^{0.25} \cdot Re^{0.75} \cdot \left(\frac{V_b}{V_w}\right)^{0.25}$$

or

$$\frac{\frac{h}{\rho_l c_p}.R}{\alpha} = C_b.Pr^{0.5}.Re^{0.75}.\left(\frac{V_b}{V_w}\right)^{0.25}$$

$$= C_b.Pe^{0.50}.Re^{0.25}.\left(\frac{V_b}{V_w}\right)^{0.25} \qquad (A\ 6.15)$$

where $C_b = 0.30 \left(\frac{gR}{8U^2}\right)^{0.25}$ (A 6.16)

Assuming a closed spherical wake,

$$\frac{V_b}{V_w} = \frac{\pi R^3\left[\frac{2}{3} - \cos\gamma + \frac{\cos^3\gamma}{3}\right]}{\frac{4}{3}\pi R^3 - \pi R^3\left[\frac{2}{3} - \cos\gamma + \frac{\cos^3\gamma}{3}\right]} \qquad (A\ 6.17)$$

$$\therefore \frac{V_b}{V_w} = \frac{\left[\frac{2}{3} - \cos\gamma + \frac{\cos^3\gamma}{3}\right]}{\frac{4}{3} - \left[\frac{2}{3} - \cos\gamma + \frac{\cos^3\gamma}{3}\right]} = \frac{C_1}{\frac{4}{3} - C_1} \qquad (A\ 6.18)$$

where $C_1 = \frac{2}{3} - \cos\gamma + \frac{\cos^3\gamma}{3}$ (A 6.19)

Hence, equation (A 6.15) can be written as

$$\frac{\frac{h}{\rho_L c_p} . R}{\alpha} = C_b \, Pe^{\frac{1}{2}} . Re^{1/4} . \left[\frac{C_1}{\frac{4}{3} - C_1}\right]^{1/4}$$

Thus, heat transferred to the wake at the rear of the bubble is expressed as

$$Q_{\gamma r} = h.A_r.\Delta T = h.\Delta T.\pi \, (R \sin\gamma)^2$$

where A_r is the surface area at the rear of the bubble.

$$\therefore Q_{\gamma r} = C_b \rho_L c_p.\pi.\Delta T.R^2.\sin^2\gamma.\frac{\alpha}{R}.Pe^{\frac{1}{2}}.Re^{1/4} . \left[\frac{C_1}{\frac{4}{3} - C_1}\right]^{1/4}$$

Since $R = R_o$ = constant, $Pe \equiv Pe_o$, $Re \equiv Re_o$,

$$Q_{\gamma r} = \pi C_b.(c_p \rho_L \Delta T).R_o.\alpha.Pe_o^{\frac{1}{2}}.Re_o^{1/4}.\sin^2\gamma\left[\frac{C_1}{\frac{4}{3} - C_1}\right]^{1/4} \quad \text{(A 6.20)}$$

Combining equations (A 6.7) and (A 6.20) to obtain the total heat transfer from the bubble,

$$Q_\gamma = Q_{\gamma f} + Q_{\gamma r} = 6\sqrt{\frac{\pi}{3}}.(c_p.\rho_L\ .\Delta T).Pe_o^{1/2}.\alpha.R_o.\left[\frac{2}{3} - \cos\gamma + \frac{\cos^3\gamma}{3}\right]^{1/2} +$$

$$\pi C_b.(c_p\rho_L\ \Delta T)Pe_o^{1/2}Re_o^{1/4}.R_o.\alpha.\sin^2\gamma.\left[\frac{C_1}{\frac{4}{3} - C_1}\right]^{1/4}$$

$$\therefore\ Q_\gamma = (c_p\rho_L\ \Delta T)Pe_o^{1/2}.R_o\alpha\left[6\sqrt{\frac{\pi}{3}}\ C_1^{1/2} + \pi C_b.Re_o^{1/4}.\sin^2\gamma.\frac{C_1^{1/4}}{(\frac{4}{3} - C_1)^{1/4}}\right]$$

Using a similar method to that adopted in section 5.2.2, to determine the collapse rate of the bubble, equation (5.25) can now be written as

$$Q_\gamma = -\rho_v.h_{fg}.\frac{dV}{dt}$$

$$\therefore\ \frac{dV}{dt} = -\left(\frac{c_p.\rho_L\ .\Delta T}{\rho_v.h_{fg}}\right).Pe_o^{1/2}.R_o.\alpha.\left[6\sqrt{\frac{\pi}{3}}.C_1^{1/2} + \pi C_b Re_o^{1/4}.\sin^2\gamma.\frac{C_1^{1/4}}{(\frac{4}{3} - C_1)^{1/4}}\right]$$

$$\therefore\ \frac{dV}{dt} = -4Ja.Pe_o^{1/2}.\frac{\alpha}{4R_o^2}\left[6\sqrt{\frac{\pi}{3}}\ R_o^3 C_1^{1/2} + \pi C_b.Re_o^{1/4}.R_o^3.\sin^2\gamma.\frac{C_1^{1/4}}{(\frac{4}{3} - C_1)^{1/4}}\right]$$

$$\therefore \frac{dV}{dFo} = -4JaPe_o^{\frac{1}{2}}\left[6\sqrt{\frac{\pi}{3}}.R_o^3C_1^{\frac{1}{2}} + \pi.C_b.Re_o^{\frac{1}{4}}.R_o^3.\sin^2\gamma.\frac{C_1^{\frac{1}{4}}}{(\frac{4}{3}-C_1)^{\frac{1}{4}}}\right] \quad \text{(A 6.21)}$$

$$\text{Let } Z = \frac{V}{V_o} = \frac{V}{\frac{4}{3}\pi R_o^3} = \frac{\pi R_o^3[\frac{2}{3}-\cos\gamma+\frac{\cos^3\gamma}{3}]}{\frac{4}{3}.\pi.R_o^3} \quad \text{(A 6.22)}$$

$$\therefore Z = \frac{3}{4}\left[\frac{2}{3} - \cos\gamma + \frac{\cos^3\gamma}{3}\right] = \frac{3}{4}C_1 \quad \text{(A 6.23)}$$

$$\text{and } dZ = \frac{1}{\frac{4}{3}\pi R_o^3}.dV$$

Hence, equation (A 6.21) can be written as

$$\frac{dZ}{dFo} = -4JaPe_o^{\frac{1}{2}}\left[6\sqrt{\frac{\pi}{3}}.\frac{C_1^{\frac{1}{2}}}{\frac{4}{3}.\pi} + \pi C_b Re_o^{\frac{1}{4}}.\frac{1}{\frac{4}{3}.\pi}.\sin^2\gamma.\frac{C_1^{\frac{1}{4}}}{(\frac{4}{3}-C_1)^{\frac{1}{4}}}\right]$$

$$= -4JaPe_o^{\frac{1}{2}}\left[6\sqrt{\frac{\pi}{3}}.\frac{(\frac{4}{3}Z)^{\frac{1}{2}}}{\frac{4}{3}.\pi} + C_b.Re_o^{\frac{1}{4}}.\frac{1}{\frac{4}{3}}\sin^2\gamma\frac{(\frac{4}{3}Z)^{\frac{1}{4}}}{(\frac{4}{3}-\frac{4}{3}Z)^{\frac{1}{4}}}\right]$$

$$= -4JaPe_o^{\frac{1}{2}}\left[6.\sqrt{\frac{\pi}{3}}.\sqrt{\frac{3}{4}}.\frac{Z^{\frac{1}{2}}}{\pi} + \frac{3}{4}.C_b.Re_o^{\frac{1}{4}}.\sin^2\gamma.\frac{Z^{\frac{1}{4}}}{(1-Z)^{\frac{1}{4}}}\right]$$

Hence,

$$\frac{dZ}{dFo} = -4Ja.Pe_o^{1/2}.\left[\frac{3}{\sqrt{\pi}}.Z^{1/2}+\left(\frac{3}{4}C_bRe^{1/4}\right).\sin^2\gamma.\frac{Z^{1/4}}{(1-Z)^{1/4}}\right]$$

(A 6.24)

Integrating gives,

$$Fo = -\frac{1}{4.Ja.Pe_o^{1/2}}.\int_{Z_o}^{Z}\frac{dZ}{\frac{3}{\sqrt{\pi}}.Z^{1/2}+\left(\frac{3}{4}C_b.Re_o^{1/4}\right)\sin^2\gamma.\frac{Z^{1/4}}{(1-Z)^{1/4}}}$$

(A 6.25)

where $Z = \frac{3}{4}\left[\frac{2}{3}-\cos\gamma+\frac{\cos^3\gamma}{3}\right]$

From equation (A 6.23),

$$\frac{dZ}{d\gamma} = \frac{3}{4}\frac{d}{d\gamma}\left(\frac{2}{3} - \cos\gamma + \frac{\cos^3\gamma}{3}\right)$$

$$\therefore dZ = \frac{3}{4}\left(\sin\gamma - \sin\gamma.\cos^2\gamma\right)d\gamma = \frac{3}{4}\sin^3\gamma.d\gamma$$

(A 6.26)

Therefore, equation (A 6.25) can be written in terms of γ as

$$Fo = -\frac{1}{4JaPe_o^{1/2}}.\int_{\pi}^{\gamma}\frac{\frac{3}{4}.\sin^3\gamma.d\gamma}{\frac{3}{\sqrt{\pi}}.\frac{\sqrt{3}}{2}.C_1^{1/2}+\left(\frac{3}{4}C_bRe_o^{1/4}\right).\sin^2\gamma.\frac{\left(\frac{3}{4}\right)^{1/4}.C_1^{1/4}}{\left(1-\frac{3}{4}C_1\right)^{1/4}}}$$

$$\therefore Fo = -\frac{3}{16JaPe_o^{1/2}}.\int_{\pi}^{\gamma}\frac{\sin^3\gamma\, d\gamma}{\frac{3}{2}.\frac{\sqrt{3}}{\pi}.C_1^{1/2}+\left(\frac{3}{4}.C_b.Re_o^{1/4}\right).\left(\frac{3}{4}\right)^{1/4}.\frac{\sin^2\gamma.C_1^{1/4}}{\left(1-\frac{3}{4}C_1\right)^{1/4}}}$$

(A 6.27)

From the definition of Z in equation (A 6.22), the dimensionless radius, β can be calculated as

$$\beta = \left(\frac{V}{V_o}\right)^{1/3} = Z^{1/3} \qquad \text{(A 6.28)}$$

$$\therefore \; \beta = \left[\frac{3}{4}\left[\frac{2}{3} - \cos\gamma + \frac{\cos^3\gamma}{3}\right]\right]^{1/3} \qquad \text{(A 6.29)}$$

For a given experimental condition the Jakob number, Peclet number, Reynolds number and C_b are known. For a given angle, γ, equation (A 6.27) gives the value of Fourier number (Fo) and equation (A 6.29) determines the value of β.

A simulation program, TUTSIM was used to calculate and draw β versus Fo curve according to the above equations. The block diagram and the listing of the model are given in Fig. A 6.2 in the attached portfolio and table A 6.1,respectively. Information about TUTSIM is given in Appendix 3. The comparison of this theoretical analysis with the experimental data is given in Chapter 6.

Equation (A 6.24) can be rewritten as

$$\frac{dZ}{dFo} = -4JaPe_o^{1/2}\left[\frac{3}{\sqrt{\pi}}.Z^{1/2} + A.\sin^2\gamma.\left(\frac{Z}{1-Z}\right)^{1/4}\right] \qquad \text{(A 6.30)}$$

where $A = \frac{3}{4}\,C_bRe_o^{1/4}$.

When heat transfer at the rear of the bubble is neglected, A = 0 and equation (A 6.30) reduces to

```
TIMING
 0.50000E-01  0.31416E+01

OUTPUTBLOCKS AND RANGES
X1:     26       0.00000E+00   0.10000E-03
Y1:     24       0.00000E+00   0.10000E+01

MODEL
                            1  TIM
                            2  COS    22
                            3  MUL     2     2     2
 0.50000E+00                4  GAI     3
 0.15000E+01                5  GAI     2
                            6  SUM    -4     5     7
 0.10000E+01                7  CON
                            8  SUM     7    -9
 0.50000E+00                9  GAI     6
                           10  DIV     9     8
 0.50000E+00               11  PWR     9
 0.25000E+00               12  PWR    10
 0.16926E+01               13  GAI    11
 0.00000E+00               14  CON
                           15  MUL    14    12    17    17
                           16  SUM    13    15
                           17  SIN    22
                           18  MUL    17    17    17
 0.75000E+00               19  GAI    18
                           20  DIV    19    16
 0.00000E+00               21  INT    20
 0.00000E+00               22  REL     1    23    23     1
 0.50000E-01               23  CON
 0.33333E+00               24  PWR     9
                           25  SUM   -24     7
                           26  DIV    21    31
 0.15000E+02               27  CON
 0.40000E+01               28  CON
 0.86000E+04               29  CON
 0.50000E+00               30  PWR    29
                           31  MUL    30    27    28
```

Table A6.1 The listing of the model for the collapse of spherical-cap bubbles

$$\frac{dZ}{dFo} = -\frac{12}{\sqrt{\pi}} JaPe_o^{\frac{1}{2}} Z^{\frac{1}{2}} \qquad \text{(A 6.31)}$$

Hence,

$$\frac{dZ}{Z^{\frac{1}{2}}} = -\frac{12}{\sqrt{\pi}}.Ja\ Pe_o^{\frac{1}{2}}\ dFo$$

Integrating gives,

$$2Z^{\frac{1}{2}} = -\frac{12}{\sqrt{\pi}}.JaPe_o^{\frac{1}{2}} Fo + c$$

at $\Upsilon = \pi$, $Z = \frac{3}{4}\left(\frac{2}{3} + 1 - \frac{1}{3}\right) = 1$ and $Fo = 0$

$\therefore C = 2$

Therefore,

$$2\ Z^{\frac{1}{2}} = -\frac{12}{\sqrt{\pi}}.\ JaPe_o^{\frac{1}{2}} Fo + 2$$

$$\therefore\ Z = \left(1 - \frac{6}{\sqrt{\pi}} Ja\ Pe_o^{\frac{1}{2}} Fo\right)^2$$

or

$$\beta = \left(1 - \frac{6}{\sqrt{\pi}} Ja\ Pe_o^{\frac{1}{2}} Fo\right)^{2/3} \qquad \text{(A 6.32)}$$

which is equation (2.29) given by Isenberg et al. [23] for the collapse of spherical bubbles rising freely with negligible bubble radial velocity.

REFERENCES

1) S.J.D. van Stralen and R. Cole, Boiling Phenomena, Hemisphere Publishing Corporation, 1979.

2) S. Sideman, D. Moalem-Maron, Direct contact condensation, Advances in Heat Transfer, Vol.15, pp.227-281, 1982.

3) Lord Rayleigh, On the pressure developed in a Liquid during the collapse of a spherical cavity, Phil. Mag.,Vol. 34, pp. 94-98, 1917.

4) H.K. Forster and N. Zuber, Growth of a vapour bubble in a superheated liquid, J. Appl. Phys., Vol. 25, pp. 474-478, 1954.

5) M.S. Plesset and S.A. Zwick, The growth of vapour bubbles in superheated liquids, J. Appl. Phys., Vol. 25, pp. 493-500, 1954.

6) L.E. Scriven, On the dynamics of phase growth, Chem. Eng. Sci., Vol. 10, pp. 1-13, 1959.

7) S.G. Bankoff, Diffusion-controlled bubble growth, Adv. Chem. Eng., Vol. 6, pp. 1-60, 1966.

8) E. Ruckenstein, On heat transfer between vapour bubbles in motion and the boiling liquid from which they are generated, Chem. Eng. Sci., Vol. 10, pp. 22-30, 1959.

9) V.G. Levich, Physicochemical Hydrodynamics, Prentice-Hall, Inc., Englewood Cliffs, N.J., 1962.

10) L.W. Florschuetz, B.T. Chao, On the mechanics of vapour bubble collapse, J. of Heat Transfer, ASME Transactions, Vol. 87, P209, 1965.

11) D.D. Wittke and B.T. Chao, Collapse of vapour bubbles with translatory motion, J. of Heat Transfer, ASME trans., Vol. 89, P.17, 1967.

12) G.G. Brucker, E.M. Sparrow, Direct contact condensation of steam bubbles in water at high pressure, Int. J. Heat Mass Transfer, Vol. 20, No.4, pp.371-381, 1977

13) D. Nordmann, Temperature, pressure and heat transfer in the proximity of condensing bubbles, Ph.D. thesis (in German), 1980, University of Hannover.

14) H. Gröber, S. Erk, Fundamentals of Heat Transfer, revised by U. Grigull, McGraw-Hill, 1961.

15) F. Mayinger, Y.M. Chen, Heat transfer at the phase boundaries of condensing bubbles, European Two-Phase Flow Group Meeting, paper G12, Zurich-Switzerland, 1983, 17pp.

16) J. Denekamp, A. Kogan and A. Solan, On the condensation of an injected vapour bubble in a subcooled liquid stream, Progress in Heat and Mass Transfer, Vol. 6, P.179, 1972.

17) H. Delmas and H. Angelino, Experimental study of the influence of non-condensable gases on condensation of steam bubbles, Rev. Gen. Therm., No 198-199, pp. 525-533, 1978.

18) S.G. Bankoff and J.P. Mason, Heat transfer from the surface of a steam bubble in turbulent subcooled liquid stream, A.I.Ch.E. Journal, Vol. 8(1), pp. 30-33, 1962.

19) M. Dimić, Collapse of one-component vapour bubble with translatory motion, Int. J. Heat Mass Trans., Vol. 20, p.1325, 1977.

20) A.A. Voloshko, A.V. Vurgaft, Study of condensation of single vapour bubbles in a layer of subcooled liquid, Heat Transfer-Soviet Research, Vol. 3, No.2, pp. 160-164, March-April 1971.

21) O. Levenspiel, Collapse of steam bubbles in water, Industrial and Engineering Chemistry, Vol. 51, No. 6, pp. 787-790, 1959.

22) V.F. Prisnyakov, Condensation of vapour bubbles in liquid, Int. Heat Mass Trans., Vol. 14, pp. 353-356, 1971.

23) J. Isenberg, D. Moalem, S. Sideman, Direct contact heat transfer with change of phase: bubble collapse with translatory motion in single and two component systems, 4th Int. Heat Trans. Conf. Paris, Vol.5, Paper B 2.5, 11pp., 1970

24) J. Isenberg and S. Sideman, Direct contact heat transfer with change of phase: bubble condensation in immiscible liquids, Int. J. Heat Mass Trans., Vol. 13, pp. 997-1010, 1970.

25) D. Moalem and S. Sideman, Bubble condensation with non-homogeneous distribution of non-condensables, Int. J. Heat Mass Transfer, Vol. 14, pp. 2152-2156, 1971.

26) D. Moalem and S. Sideman, The effect of motion on bubble collapse, Int. J. Heat Mass Transfer, Vol. 16, pp. 2321-2329, 1973.

27) A.H. Abdelmessih, F.C. Hooper and S. Nangia, Flow effects on bubble growth and collapse in surface boiling, Int. J. Heat Mass Transfer, Vol. 15, pp. 115-125, 1972.

28) J. Isenberg and S. Sideman, Flow field around collapsing bubble trains: Theoretical analysis, Appl. Sci. Res., Vol. 24, pp. 53-64, 1971.

29) D. Moalem, S. Sideman, A. Orell and G. Hestroni, Condensation of bubble trains: An approximate solution, Progress in Heat and Mass Transfer, Vol. 6, pp.155-177, 1972.

30) D. Moalem, S. Sideman, A. Orell and G. Hetsroni, Direct contact heat transfer with change of phase: Condensation of a bubble train, Int. J. Heat Mass Transfer, Vol. 16, pp. 2305-2319, 1973.

31) E. Ruckenstein and E.J. Davis, The effects of bubble translation on vapour bubble growth in a superheated liquid, Int. J. Heat Mass Transfer, Vol. 14, pp. 939-952, 1971.

32) W.H. Hughes and J.A. Brighton, Theory and problems of fluid dynamics, Schaum's Outline Series in Engineering, McGraw-Hill Book Company, 1967.

33) D.W. Holder and R.J. North, Schlieren Methods, National Physical Laboratory, Dept. of Scientific and Industrial Research, No. 31, HMSO, 1963.

34) H. Schmidt, Bubble formation and heat transfer during dispersion of superheated steam in saturated water - I: Bubble size and bubble detachment at single orifices, Int. J. Heat Mass Transfer, Vol. 20, pp. 635 - 646, 1977.

35) H. Schmidt, Bubble formation and heat transfer during dispersion of superheated steam in saturated water - II: Heat transfer from superheated steam bubbles to saturated water during bubble formation, ibid, Vol. 20, pp.647-654, 1977.

36) M. Akiyama, Bubble collapse in subcooled boiling, Bulletin of the JSME, Vol. 16, No 93, pp. 570-575, 1973.

37) U. Grigull, Die Grundsetze der Warmeubertragung, Springer, 1955.

38) F. Bošnjakovic, Verdampfung und Flussigkeitsuberhitzung, Tech. Mech. Thermodyn. Berl., Vol. 1, pp.358-362, 1930.

39) G. Birkhoff, R.S. Margulies, and W.A. Horning, Spherical bubble growth, Phys. Fluids, Vol.1, No.3., pp.201-204, 1958.

40) L.W. Florschuetz, C.L. Henry and A.R. Khan, Growth rates of free vapour bubbles in liquids at uniform superheats under normal and zero gravity conditions, Int. J. Heat Mass Transfer, Vol. 12, pp. 1465-1489, 1969.

41) H.C. Hewitt and J.D. Parker, Bubble growth and collapse in liquid nitrogen, Journal of Heat Transfer, Trans. ASME, Vol. 90 (C), No.1, pp.22-26, 1968.

42) L.S. Tong and J. Weisman, Thermal Analysis of Pressurised Water Reactors, American Nuclear Society, 2nd ed., 1979.

43) F.C. Gunther, Progress Report No 4-75, Jet Propulsion Laboratory, California Institute of Technology, Pasadena, California, June 1950.

44) L.A. Skinner and S.G. Bankoff, Dynamics of vapour bubbles in spherically symmetric temperature fields of general variation, Phys. Fluids, Vol. 7, No.1, pp.1-6, 1964.

45) Y.R. Mayhew and G.F.C. Rogers, Thermodynamic and Transport Properties of Fluids, Basil Blackwell, 2nd edition, 1978.

46) Peebles, F.N., Garber, H.J., Studies on the motion of gas bubbles in liquids, Chem. Eng. Progr., Vol. 49, 2 (Feb., 1953), pp. 88-97.

47) Davies, R.M., Taylor, G.I., Proc. Royal Soc. (London), 200A, 1950, pp. 375-390.

48) Mendelson, H.D., The prediction of bubble terminal velocities from wave theory, A.I.Ch.E.J., Vol. 13, No.2 (March 1967), pp. 250-253.

49) K. Pearson, Tables of incomplete beta function, Biometrica Office, University College, London, 1934.

50) J.H.C. Coppus, The structure of the wake behind spherical cap bubbles and its relation to the mass transfer mechanism, Ph.D thesis, 1977, Eindhoven University of Technology.

51) P.V. Danckwerts, Ind. Engng. Chem., Vol. 43, P.1400, 1953.

52) J.D. Parker, J.H. Boggs, E.F. Blick, Introduction to fluid mechanics and heat transfer, Addison-Wesley, 1969.

53) J.C. Lamont, D.S. Scott, An eddy cell model of mass transfer into the surface of a turbulent liquid, AIChE J., Vol.16, pp.513-519, 1970.